Progressive Collapse Assessment of Intact and Damaged Ship Structures under Combined Bending and Torsional Loading

Maria Syrigou

Submitted for the degree of Doctor of Philosophy

School of Marine Science and Technology

Faculty of Science, Agriculture and Engineering

Newcastle University

May 2017

School of Marine Science and Technology

Armstrong Building

Newcastle University

NE1 7RU

United Kingdom

Abstract

The Simplified Progressive Collapse Method is a quick and well-established method recommended by International Association of Classification Societies (IACS) for the evaluation of a ship's ultimate strength due to longitudinal bending. However, in the case which the torsional rigidity of the structure is reduced i.e. containerships, longitudinal bending may not be the dominant reason for failure. Torsion and shear forces may influence the global strength and therefore the effect of combined loading needs to be investigated.

The current research aims to understand hull girder failure modes under these combined loads both for intact and damage case scenarios and incorporate torsional loading effect into the existing method. A hull girder which is subjected to longitudinal bending moment and torsional loading generates compressive/tensile and shear stresses on its plates and stiffened panels. Therefore, a thorough investigation of plates under these combined loads has been carried out. The outcome of this study is interaction diagrams of compression/tension and shear for steel and aluminium plates. The ultimate strength of the structure is then estimated for an applied amount of torsion calculating the shear flow distribution of the plates in the cross section and using the results of the previous study. The same procedure is repeated for different amounts of torsion and the interaction diagram of vertical/horizontal bending moment and torsional moment is derived.

For validation, the proposed method is applied to a number of different intact box girders and to a hull girder of a 10000 TEU containership. The effect of damage on the ultimate strength is examined only under bending due to the current representation of damage in the simplified method. The results are compared with the results of non-linear finite element models which have been generated and analysed for this purpose.

The results for all studies show very good correlation, however the simplified method provides a sufficient advantage of time estimation and simplicity in comparison with the existing methods. It can be used in both concept and preliminary design to provide accurate estimation of hull girder strength. This extension of the Simplified Progressive Collapse Method, which accounts for combined load effects, is particularly useful in cases which require quick estimate of ultimate strength.

To my parents,

Sotiris and Anna

Acknowledgements

Above all, I would like to express my deep gratitude to Professor Bob Dow, my research supervisor. Firstly, I would like to thank him for choosing me in this project, believing in me from day one and for being such an exceptional supervisor. Prof Dow excels in academia with his knowledge and experience and is always willing to share this. He is a very busy person, but he always had time for me. His valuable and patient guidance, his support and encouragement and his unique manner to make me calm or "furious" undoubtedly influenced my research. My gratitude, my respect and how special he became to me will never change. A simple but extremely heartfelt thank you is the least I can say to him. Thank you, Bob!

Furthermore, I would like to express my appreciation to Dr Simon Benson, my second supervisor, for his advice and assistance in my project. My grateful thanks are also extended to the Office of Naval Research (ONR) for its continuous financial support over the years.

In addition, I would like to express my gratitude to Dr Elizabeth Lewis from the Department of Civil Engineering and Geoscience of Newcastle University for organizing the code club and helping me learn Python. My special thanks are also due to Dr Emmanuel Alfred Mohammed for providing me with the results of his thesis and to Dr Richard Villavicencio for providing me with the executable program from Lloyd's for the calculation of torsional constant.

Furthermore, I am thankful to my officemates for sharing countless hours of studying and 'living' together in the same office; I wish them all the best for their future. My best wishes also to all the PhD students of the marine technology department in Newcastle University. Moreover, I would like to take the opportunity to thank friends who I felt were always thinking of me and I apologise for not spending as much time as I wanted with you.

Last but not least, I would like to thank my family. My dad and mum who always support me, love me and believe in me, without any doubts, without asking for anything back, with all their heart. Many thanks to my brother and his wonderful family too for being so supportive and Phaedra who belongs to our family and is always at our side.

Contents

List of Figures

List of Tables

Nomenclature

A	Enclosed area of the mean periphery of the cell
E	Young's Modulus
G	Shear Modulus
K_n	Knock down factor
M_T, T	Torsional moment
M_{TU}, T_{max}	Ultimate torsional moment
M_V, BM	Vertical bending moment
M_{VU}, BM_{max}	Ultimate vertical bending moment
$R_{plate(u)}$	Plate resistance
$R_{stiff(u)}$	Stiffener resistance
$R_{L(u)}$	Panel resistance (interframe calculation)
$R_{PO(u)}$	Panel resistance (orthotropic calculation)
$R_{OVERALL(u)}$	Minimum panel resistance, min($R_{L(u)}$, $R_{PO(u)}$)
$T_{applied}$	Applied torsional moment
T_{max}	Maximum torsional moment
T_o	Maximum torsional moment in the elastic area
a	Plate Length
a/b	Plate aspect ratio
a_t	Width of the tensile residual stress zone in x-axis
b	Plate width
b_t	Width of the tensile residual stress zone in y-axis
d_s	Periphery of the cell/loop
h_w	Stiffener web height
k_n	Knock down factor for Load Shortening Curve (LSC)
n_{sy}	Number of transverse frames in an orthogonally stiffened panel
q	Shear flow
t, t_p	Plate thickness
v_{os}	Maximum side imperfection amplitude in the stiffener
w_o	Maximum out of plane imperfection amplitude of the plate
w_{oc}	Maximum column imperfection amplitude of the panel
w_{os}	Maximum imperfection eccentricity of the stiffener
w_{ow}	Maximum web imperfection
β	Plate slenderness ratio
γ	Material shear strain
γ_o	Material shear yield strain
ε	Material strain
ε_0	Material yield strain
ϑ	Angular twist
λ	Column slenderness ratio
ν	Poison Ratio
σ_E	Elastic Yield stress
σ_{cr}	Critical elastic buckling stress
$\sigma_{0.2}$	0.2% proof stress (aluminium)
$\sigma_{0.2(HAZ)}$	Reduced proof yield stress in the HAZ

σ	Ultimate strength compressive/tensile strength of the plate
$\sigma_{0,}\ \sigma_Y$	Yield stress for steel
σ_{rcx}	Compressive residual stress in x-axis
σ_{rcy}	Compressive residual stress in y-axis
σ_{rtx}	Tensile residual stress in x-axis
σ_{rty}	Tensile residual stress in y-axis
$\tau_{applied}$	Applied shear stress
τ_E	Critical elastic shear stress
τ_{cr}	Elastic shear bucking stress with plasticity correction
$\tau_{u,}\ \tau$	Ultimate shear stress
$\tau_o,\ \tau_Y$	Yield shear stress

Abbreviations

A.R.E.	Admiralty Research Establishment
HAZ	Heat Affected Zone
IACS	International Association of Classification Societies
LSC	Load Shortening Curve
NFEM	Nonlinear Finite Element Method
ProColl	Compartment Level Progressive Collapse Program

Chapter 1

Introduction

1.1. Research Overview

The progressive collapse assessment of ship structures under longitudinal bending moment has been thoroughly investigated the last decades. The longitudinal bending moment either in sagging or in hogging condition is the principle load which ship structures have to withstand. Therefore, several methods have been developed and introduced in the literature. Among these, the most well-established methods are the simplified progressive collapse method (Smith, 1977), known also as the incremental-iterative method in some classification rules, and the nonlinear finite element method (NLFEM). The simplified progressive collapse method is recommended by the ISSC Committee (Yao, 2000) and its main advantages over the nonlinear finite element method are its simplicity in modelling (user-friendly) and its extremely short computational time for the analysis, providing good accuracy when compared to the NLFEM (S. Benson et al., 2013), (Alfred Mohammed et al., 2016) and experimental results (Dow, 1991).

Both methods consider pure longitudinal bending moment as the principle load case. However, in the case where the torsional rigidity of the hull girder is low due to large openings on it, torsional load might have a considerable effect on the strength of the structure. Large openings on the structure usually occur due to its design e.g. the design of containerships is marked by lack of primary deck structure or due to damage e.g. collision, grounding, fire (Figure 1.1). Therefore, a quick and reliable strength assessment of the ship structure which takes into account the effect of torsion is required, either in the preliminary design or in the case of damage for the purpose of recoverability assessment. Furthermore, the frequency and the magnitude of these loads, as well as the potential severity of the damaged caused, can be influenced by the decisions taken during the structural design.

In the literature, the effect of torsion on ship structures has been investigated with: the experimental and theoretical results of rectangular box girders under combined bending, shear and torsional loads by Ostapenko (Ostapenko and Chen, 1982); the mathematical model of differential equations for further development of the beam theory to represent the

torsional and horizontal bending response of ship hulls by Pedersen (Pedersen, 1991); the ultimate strength assessment of 4,300 TEU containership under combined torsion and bending using a special purpose nonlinear finite element program, ALPS/HULL by Paik (Paik et al., 2001b); the prediction of the maximum torsional load of a ship hull by Hu and Chen (Hu and Chen, 2001); the experimental and theoretical analysis (NLFEM) of models with open cross- section by Sun and Soares (Sun and Soares, 2003); and the progressive collapse assessment of a 10,000 TEU containership under combined torsion and vertical and horizontal bending moment with non-linear finite element analysis by Alfred Mohammed (Alfred Mohammed, 2014).

Figure 1.1: The fire operation of Safmarine Meru after her collision with Northern Jasper, a German containership, in the waters of Ningbo, China, on 7th May 2016.

However, none of the aforementioned studies has introduced a quick and reliable methodology for the progressive collapse assessment of ship structures under torsion and bending. Recently, Tanaka (Tanaka et al., 2015) investigated a 5,250 TEU containership under torsion and bending loadings, both experimentally and theoretically (NLFEM), and he proposed a methodology in which warping and shear stresses are taking into account using the Smith method. Further validation of the proposed methodology is required though, since

there is not a particularly good agreement between the experimental and the theoretical results; the latter are overestimated by 10%. In a later study, Tanaka (Tanaka et al., 2016) presents the results of his proposed methodology including also the effect of the transverse bulkheads for the same model i.e. 5,250 TEU containership. The proposed methodology predicts a value of ultimate strength 13.4% less than the F.E. results under pure bending. Finally, only the results of the proposed methodology under combined torsion and bending are presented without any comparison with the F.E. results, though. At this point, it should be mentioned that the simplified progressive collapse method as defined by Smith (Smith, 1977) is limited to the strength assessment of ship structures under bending only in the case which the collapse occurs between the transverse frames (interframe). It is not able to predict the progressive collapse in case its collapse occurs overall the structure and this effect seems to be totally ignored in Tanaka's study.

On the contrary, the extended simplified progressive collapse method by Benson and Dow (Benson, 2011) which is based on the original simplified progressive collapse method by Smith (Smith, 1977), overcomes this limitation. A nonlinear orthotropic plate theory approach is incorporated into the methodology which is implemented in a computer program (ProColl) and allows the estimation of the progressive collapse of structures subjected to bending modelling both interframe and overall collapse.

1.2. Research Aim and Objectives

The current study incorporates the effect of torsion into the extended simplified progressive collapse method and investigates the progressive collapse of structures with low torsional rigidity either due to the design of the structure or due to damage on it. Therefore, the proposed methodology allows the strength assessment of ship structures subjected to combined torsional and bending loads and can model:

- Interframe collapse;
- Overall collapse extending to more than single frame space;
- Stiffener tripping;
- Plate buckling;

In parallel, the proposed methodology by the author is implemented into the existing computer program, ProColl, for the strength assessment of ship structures according to the extended simplified progressive collapse method. The program remains quick and reliable, but also takes into account the effect of combined bending and torsion on the analysis.

In Chapter 2, the relevant literature review to the current research is presented. The main loads on ship structures are categorized and the existing methodologies for the strength assessment of ship structures subjected to bending are discussed. Previous studies which investigated the behaviour of hull and box girders under torsion are presented and analysed. A thorough investigation in the literature for the behaviour of steel and aluminium plates under compression/tension, pure shear and combined compressive/tensile and shear stresses is carried out and presented.

In Chapter 3, the approach of the proposed methodology is described and analysed giving further insight into the incorporation of torsion into the extended simplified progressive collapse method and the reasons which an extensive investigation of steel and aluminium plates under compression/tension, pure shear and combined these loads was carried out.

In Chapter 4, the nonlinear finite element analysis of steel and aluminium plates is presented. In the first part, the progressive collapse behaviour of steel and aluminium plates with aspect ratio 1 to 5 is investigated under pure shear loading. The outcome of this study, allows the investigation of square steel and aluminum plates under axial compression/tension and pure shear. The results are compared with theoretical and empirical formulas in the literature. This comparison validates the boundary conditions of the plates which remain the same under pure compression, pure shear and combined compression/tension and shear. The analysis of the plates under these combined loads takes part and the interaction diagram of compressive/tensile and shear stresses for typical ship steel and aluminium plating are generated.

In Chapter 5, a series of box girders with four (4) different types of cross- sections which alter the torsional rigidity is investigated under torsion using the nonlinear finite element method. In each case, the torsional capacity is estimated and combined loads of torsional and sagging bending moment are applied for the strength assessment of the structure. Both methodologies, the nonlinear finite element method and the proposed method are applied.

The results are compared and show good agreement. Two of the above models are also subjected to combined torsional and hogging bending moment and are analysed according to both methods. Relevant comparison of the results occurs showing a good correlation.

In Chapter 6, the progressive collapse assessment of a 10,000 TEU containership under combined torsional and vertical sagging and hogging moment is presented according to the nonlinear finite element method and the proposed methodology. The finite element results which are presented, are taken from an existing study in the literature (Alfred Mohammed, 2014). The torsional capacity of the structure is already known from the F.E. analysis and in this study, the equivalent model is built in ProColl and analysed under combined torsional and bending loads. The interaction diagrams of torsional and hogging/sagging bending moment according to the results of both methodologies are presented and compared showing a very good agreement.

In Chapter 7, the progressive collapse of an intact box girder, Box Girder E, under combined torsional and bending loads is analysed according to the nonlinear finite element analysis and the proposed methodology. The comparison of these results show good agreement. Two types of damage cases are applied to Box Girder E whose sizes vary along the width of the structure or along its length. The damaged box girders are subjected to pure torsion and then to combined torsional and bending moment using the nonlinear finite element method. The interaction diagrams of the damaged box girders are generated and compared with the interaction diagram of the intact box girder. The graphs provide useful information and understanding of the behaviour of the damaged box girders under combined torsional and bending loads, as well the effect on the residual strength of the structure due to different type and size of damage extent. The damaged box girders subjected only to vertical bending moment are analysed with the proposed method due to limitations of the method which are related to the representation of the damage in the proposed methodology and are the subjected of a separate PhD research project. The results of the damaged box girders under pure bending according to both methodologies are compared and they agree very well.

In Chapter 8, the conclusions of the current study are discussed and recommendations for future research are introduced.

1.3. Research Scope and Contributions

The scope of the current research is to develop further the extended simplified progressive collapse method in order to take into account the torsional effect on the hull girder. The final outcome is a methodology for the progressive collapse assessment of ship structures under combined torsional and bending loads which is fast, reliable, efficient and able to model any type of collapse mode of the structure i.e. interframe, overall, stiffener tripping or plate buckling.

The novelty of this research is that no equivalent method has been introduced before. The application of the proposed methodology may be extremely useful in the preliminary of design ship structures with low torsional rigidity or in the residual strength assessment of damaged ships, where torsional load might has a significant effect on the progressive collapse of the structure.

Chapter 2

Literature Review

2.1. Introduction

This chapter presents a review of the literature on ultimate strength and progressive collapse of ship structures. Initially, the definition of limit state design and ultimate strength are provided and the different groupings of limit state design are presented. Then, the existing methodologies for the progressive collapse assessment of ship hull girders under bending loads are presented. The research to date concerning the effect of torsion on the progressive collapse follows. Finally, an extensive research on the behaviour of steel and aluminium plates under axial compression/tension, pure shear and combined compressive/tensile and shear loads was carried out and is presented.

2.2. Limit State Design

A particular point of interest over the last few decades has been the limit state design of ship structure. “In a limit state design, the design is checked for all groups of limit states to ensure that the safety margin between the maximum likely loads and the weakest possible resistance of the structure is large enough and that fatigue damage is tolerable.” (Dow, 2007a)

Limit states are divided in the following groups:

a. Ultimate limit state due to buckling or plastic collapse of the structural components (i.e. columns, beam columns, plates, shells, stiffened panels and shells, structural connections and hull girders) (Dow, 2007a)

b. Fatigue limit state due the effect of cyclic loads on critical structural details

c. Accidental limit state due to collision, grounding, fire or freak waves

d. Serviceability limit state due to deterioration or loss of less vital functions (e.g. deformations which may spoil the aesthetic appearance of the structure, vibration or noise which are unpleasant to people) (Paik et al., 2002)

In the ultimate limit state, the strength of the structure has been shifted from point A (Figure 2.1) which is the elastic buckling strength adjusted by a plasticity correction to point B. Point

B represents the ultimate strength of the structure which takes into account the post collapse behaviour of all the structural components and their interactions. (Paik et al., 2002)

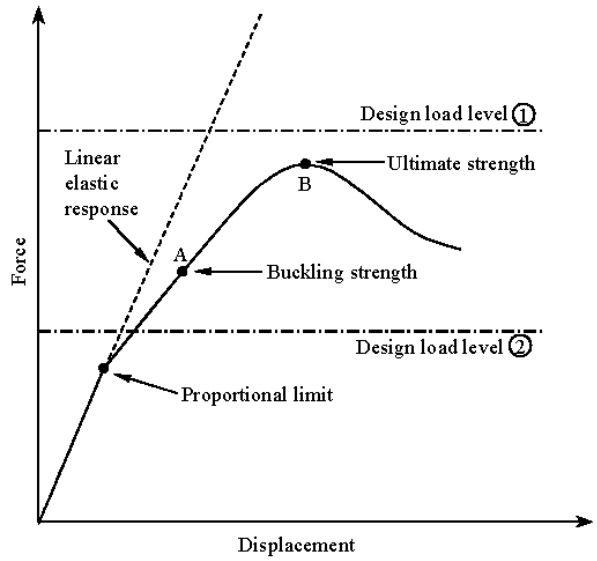

Figure 2.1: Structural design considerations based on the ultimate limit state (Paik et al., 2002)

2.3. Ultimate Strength Assessment

The International Association of Classification Societies (IACS) recommends the following methods for the ultimate strength assessment of intact ship structures under vertical and horizontal bending moment:

a. The Incremental-iterative Procedure, known also as the Simplified Progressive Collapse Method (Smith Method), developed by Smith and Dow in the 1970's.

b. The Non-Linear Finite Element Method (NLFEM).

c. The Idealized Structural Unit Method (ISUM).

2.3.1. The Simplified Progressive Collapse Method (Smith Method)

The simplified progressive collapse method was introduced by Smith (Smith, 1977) in 1977. Smith extended Caldwell's study (Caldwell, 1965) and developed a methodology for the evaluation of the ultimate strength of ship structure. Since then, this methodology has been validated with experimental data (Dow, 1991) and other studies (Paik, 2010) and it is one of the most well- established methods for ship's ultimate strength assessment. The main advantages of the Smith Method are that it provides an accurate estimation of the ultimate strength of the structure very quickly and it demands only the cross section of the ship for the set-up which is simple and straight forward.

According to the method, the ship cross section is divided into elements. Every element consists of a plate with its associated stiffener. The progressive collapse behavior of the element under axial compression/tension is described either by its stress-strain curve (Figure 2.2) which is also called Load Shortening Curve (LSC) or by perfectly elastic-plastic behaviour.

Then, the vertical curvature is applied incrementally to the ship's cross-section and the following iterative procedure occurs in each increment:

- The strain of each element is calculated assuming that the cross section remains plane and bending occurs around an instantaneous neutral axis of the cross section.
- The incremental stress of each element is calculated using the slope of the LSC for the corresponding instantaneous strain.
- The incremental stresses are summed to give element total stresses.
- The total stress values of all elements are integrated over the cross section in order to calculate the total bending moment. (Figure 2.3)

The main assumptions of the method are:

a. The plane-sections remain plane.

b. The behaviour of each element is independent from the adjacent element.

c. The collapse of the section occurs between the frames (interframe).

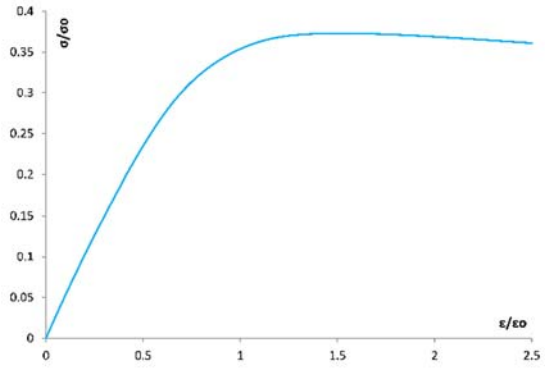

Figure 2.2: Load Shortening Curve

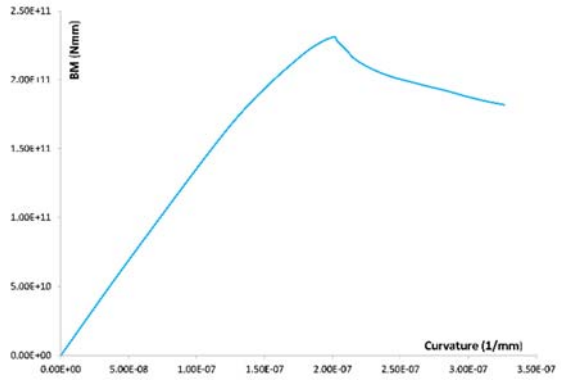

Figure 2.3 Moment-Curvature graph of the structure

2.3.2. The Non-Linear Finite Element Method (NLFEM)

The Non-Linear Finite Element Method (NLFEM) is also a well-established method which was initially introduced by Courant (Cook et al., 2002) in 1943, calculating the torsional rigidity of a hollow shaft. The cross section was divided into triangles and the stress values at the nodes were used for the linear interpolation of the stress function over each triangle. Later, in the 1950s the same approach was applied in aeronautical industry and the method was developed further mainly by Turner, Taig and Argyris in the United States, England and Germany, respectively. In 1963, the FEA was recognised as a form of Rayleigh-Ritz method by academia but it was the development of digital computers in the late 1970s which established the method in the actual design (Cook et al., 2002).

The method provides numerical solution of field problems which are described by differential equations or by an integral expression (Cook et al., 2002). According to the Non-Linear Finite Element Method (Dow, 2007b) the following procedure has to be applied:

- The structure is divided into pieces (elements and nodes);
- The behaviour of the physical quantities of each element are described;
- The elements are assembled at the nodes to form an approximate system of equations for the whole structure;
- The system of equations which involve unknown quantities (e.g. displacements) at the nodes is solved;

- The desired quantities (e.g. stress, strains, moments) at the selected elements are then calculated;

The main advantage of NLFEM is able to estimate the ultimate strength of the structure under any type of load or combinations of loads applied simultaneously or sequentially. There is no restriction on the boundary conditions, the geometric representation of the structure and the behaviour of the materials. In fact, the model can resemble the actual structure or part of it (Cook et al., 2002). However, it's a very complicated method and time consuming relating to the user involvement in modelling and the computational time. It requires a detailed geometry of the structure and its accuracy depends on a high level of expertise because there are many parameters which have to be checked and evaluated simultaneously.

2.3.3. The Extended Simplified Progressive Collapse Method

The extended simplified progressive collapse method introduced by Benson and Dow (Benson et al., 2015) is based on the simplified progressive collapse method (section 2.3.1) and calculates the ultimate strength of intact structures under vertical and horizontal bending moment.

A similar methodology to the simplified progressive collapse method is followed replacing the stress-strain curve of the element with the stress-strain curve of the panel. This approach overcomes two of the main assumptions of the initial methodology; independent behaviour of each element and only interframe collapse. The cross section still has to remain plain, but this time at compartment ends. The structure is divided into panels instead of elements (plate-stiffener) and an example is shown in Figure 2.4.

The stress-strain curve of each panel is calculated using the orthotropic plate theory as described by Benson and Dow (Benson et al., 2015). The main concept of the orthotropic plate approach is that estimates the strength of a stiffened panel assuming its stiffeners are 'smeared' to the plate and only overall collapse mode occurs. Therefore, its strength should be compared with the interframe strength of the panel. The minimum value of these two defines not only the ultimate strength of it but also the mode of its collapse and its load shortening curve.

This approach can model:

- Interframe collapse;
- Overall collapse extending to more than a single frame space;
- Stiffener tripping;
- Plate buckling;

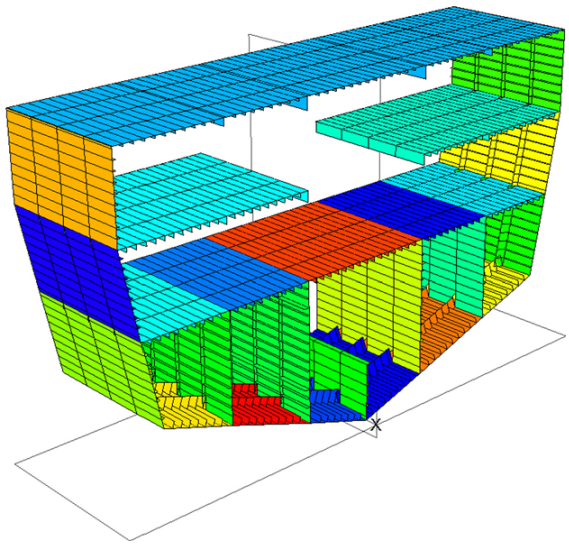

Figure 2.4: Example panel sets for a prismatic hull girder (Benson et al., 2015)

This methodology has been implemented in the computer program ProColl (Progressive Collapse). The flow diagram in Figure 2.5 provides further explanation for the sequence of calculations which ProColl follows and generates the final stress-strain curve for the simplified method (Smith method). In the first pass, the stress-strain curves of the plates and stiffeners of each panel are recalled from the F.E. database. For each panel, both interframe and overall strength are calculated and the minimum of these defines its buckling mode, its ultimate strength and generates the stress-strain curve for an equivalent plate. In the second pass, the same procedure is repeated but now panels have been replaced by their equivalent plates and the deep longitudinal stiffeners are having the role of simple plate stiffeners. The final stress-strain curve which derives is used to the progressive simplified method as described in section 2.3.1.

This methodology efficiently calculates the instantaneous stiffness of the stiffened panel at all levels and uses this to evaluate the failure mode and load/shortening curve for the panel.

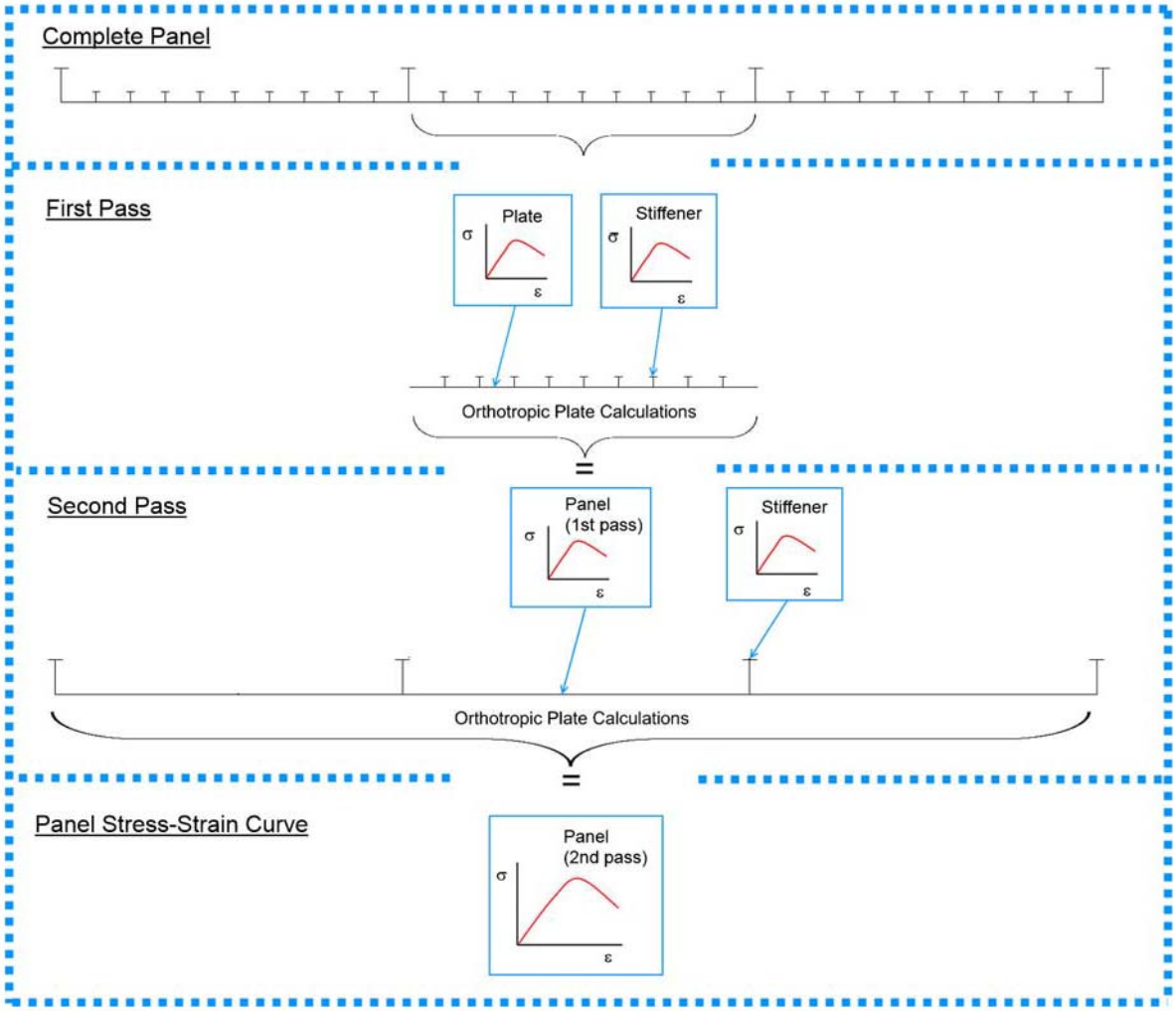

Figure 2.5: Irregular panel calculation flow diagram (Benson et al., 2015)

2.3.4. The Idealized Structural Unit Method (ISUM)

The Idealized Structural Unit Method (ISUM) was initially introduced by Ueda and Rashed (Ueda and Rashed, 1974) in 1974 analyzing the progressive collapse behaviour of a transverse framed structure of a tanker. The approach of this methodology was to reduce the number of degrees of freedom in the elements of the conventional finite element analysis modelling large-sized structural members as structural units (ISUM elements). The aim was to reduce the computation time in comparison with the N.L.F.E. analysis and keep the accuracy of the results at reasonable level (Hughes and Paik, 2010).

The formulation of ISUM element is critically important in the methodology, therefore theoretical, experimental and numerical studies have been conducted/carried out in order to define its structural behaviour and reduce any limitations. Ueda, Paik and Yao have proposed different types of ISUM elements represented them; as a beam-column element with two nodal points (Ueda and Rashed, 1974), as a rectangular plate element with four nodal points (Ueda et al., 1984) (Paik, 1995), as a rectangular plate element whose deflection is represented by eigen-functions (Ueda and Masaoka, 1995) or as a rectangular plate element with new lateral shape function (Fujikubo et al., 2000). These are some of the most representative studies for the ISUM element in the literature and each representation of it attempts to overcome different issues in the analysis (e.g. large number of different formulations, consideration of initial imperfections, local failures of individual structural components and overall failure of the system).

Over the years, the Idealized Structural Unit Method has been applied, with varying number of success, to a number of different ship collapse problems e.g. (Hughes and Paik, 2010), (Paik et al., 1996), (Paik et al., 2001b), (Paik, 2007), (Kim et al., 2013), (Pei et al., 2015).

Finally, the Idealized Structural Unit Method (ISUM) is incorporated by the rules of the International Association of Classification Societies (IACS) (2008) for the progressive collapse assessment of ships under vertical bending moment (Hughes and Paik, 2010) along with the Smith Method which is used in this research.

2.4. Torsional Effect on Ship Structures

Although, the development of torsional analysis started in the 1850's with Saint-Venant's classical torsional theory for pure torsion, it was only in the 1980's when Ostapenko (Ostapenko and Vaucher, 1980), (Ostapenko, 1981), (Ostapenko and Moore, 1982), (Ostapenko and Chen, 1982) investigated the torsional effect on ship structures ultimate strength. Ostapenko' s research aimed to develop a methodology which takes into account the effects of bending, shear and torque for the ultimate strength assessment of ship hulls. Until then, there was extensive research on the collapse behaviour of individual ship hull components (i.e. plates, stiffeners, panels, grillages etc.) under compression/tension and combined bending and shear loads, and it was only Smith's method (Smith, 1977) which could estimate the progressive collapse of the whole ship structure under bending loading. Therefore, Ostapenko investigated the ultimate strength of box girders under bending, shear and torsion both theoretically and experimentally. The theoretical results of his initially study (Ostapenko, 1981) show a good agreement with the experimental results only in the case of bending and shear loads. Ostapenko' s later studies (Ostapenko and Chen, 1982) show a better correlation of experimental and theoretical results for box girders with rectangular cross section under combined bending, shear and torsional loads. The main conclusions of his study were 'that warping was insignificant for the cross sections which analysed'; 'the effects of shear lag are negligible'; and 'the overall failure mode collapse was not considered in the proposed method'. Finally, there is no further studies in the literature of Ostapenko's method applied to ship structures whose their size and cross section are very different from the tested rectangular box girders of his study.

In the 1980's, Pedersen also investigated the torsional and horizontal bending moment response of ship hulls (Pedersen, 1983) and containerships (Pedersen, 1985), (Pedersen, 1991). In his study, a mathematical model of differential equations is proposed for further development of the beam theory to represent the torsional and horizontal bending response of ship hulls. Warping stresses, shear deflections, rotatory inertia, cross-sectional discontinuities are included to the model and a baseline for the ship loading is defined which takes into account the effect of the combined moments (i.e. torsional and horizontal bending moment).

In the 2000's, the size of the containerships and the demand of container transport were increased leading to further investigation of the torsional effect on ship's strength. Paik (Paik et al., 2001b) develop a special purpose non-linear finite element program, ALPS/HULL, based on the Idealized Structural Unit Method (ISUM) for the analysis of the ultimate strength of ship hulls under torsion, vertical shear, horizontal shear, vertical and horizontal bending moment and lateral pressure loads. The ultimate strength of a 4300TEU containership was analysed investigating the effect of warping stresses. According to his research, although warping stresses affect the torsional stiffness of the structure, their effect on its ultimate torsional strength is small. Paik also proposed interaction formulations of vertical bending moment and torsional moment in hogging and sagging condition based on regression analysis of his results. Both formulations show high insensitivity of vertical bending moment to torsional loads and they are described by Equation 2.1 and Equation 2.2:

$$\left(\frac{M_V}{M_{VU}}\right)^{3.7} + \left(\frac{M_T}{M_{TU}}\right)^{3.7} = 1, \qquad for\ hogging$$

Equation 2.1

$$\left(\frac{M_V}{M_{VU}}\right)^{3.1} + \left(\frac{M_T}{M_{TU}}\right)^{3.1} = 1, \qquad for\ sagging$$

Equation 2.2

Hu and Chen (Hu and Chen, 2001) developed a methodology for the prediction of the maximum torsional load of a ship hull in the limit state ignoring the warping stresses. The plastic shear flow distribution of the cross section was defined by the upper-bound and lower-bound theorem. The limit torsional moment was calculated for three containerships of 300, 1600 and 4000 TEU. These results were compared with the values which derive from the relevant rule equations of the main classification societies (i.e. DNV, GL, ABS, BV and LR). The comparison showed that very low safety factor is taken into account by the classification societies for large containerships with respect to the ultimate torsional capacity of the structure.

Furthermore, Sun and Soares (Sun and Soares, 2003) investigated both experimentally and theoretically, the torsional capacity of two models with the same open cross section under pure torsion. The effect of different parameters concerning the boundary conditions, initial deformations and residual stresses was also studied. The experimental results showed different collapse modes between the two models but the same value of ultimate torque. The theoretical results were analysed using the non-linear finite element method (ANSYS) and two cases of boundary conditions were considered; full and partially restrained unloaded end. The partially restrained end was representing the real boundary conditions in the test, therefore the results of this analysis show better agreement with the experimental torque value. The partially restrained F.E. model at its end was also investigated under different initial imperfections, residual stresses and warping stresses. The effect of the initial deformation on the ultimate torque is small while residual stresses clearly affect torsional capacity of the stucture. Finally, the incorporation of the warping strain into the model led to a good agreement between the experimental and theoretical results. The main outcome of this study is that ultimate torque exceeds the initial yielding torque and the boundary conditions have very large effect on the results.

Alfred Mohammed's study (Alfred Mohammed, 2014) was divided into two parts. In the first part, Alfred Mohammed develops a method to define the maximum wave load combinations taking into account the sea state for a certain route and the response amplitude operators (RAOs) of a 10,000 TEU OL185 containership. In the second part, the progressive collapse analysis of this containership takes part under combined torsional and bending loads using the non-linear finite element analysis and the interaction diagram of torsional and bending loads is defined. Finally, the extreme global wave-induced loads which derived from the first part of the study are inserted to the interaction diagram and the strength of the structure is checked under these combined loads. Further details about Alfred Mohammed's study are given in chapter 6, as the same model was analysed with the proposed methodology in the current study and it has been used for the validation of the method.

Finally, Tanaka et al. (Tanaka et al., 2015) investigated the ultimate strength of a 5250 TEU containership under combined vertical bending and torsion, experimentally and theoretically. Three 1/13 scaled models were subjected to combined bending and torsion (M/T=0.5), only

to torsional loading and only to vertical bending, respectively. In each model, its aft-end was totally fixed and the load was applied to each side at the other end using hydraulic jacks which were generating opposite or in the same direction vertical forces. In the finite element model, the load was applied though a rigid supporter at the same position at both sides of the model with a predefined vertical velocity. These boundary conditions were selected in order to generate maximum warping stresses in the model although this not a realistic representation of the combined torsional and bending loading in actual ship structures. An actual ship structure is partially restrained against warping (Alfred Mohammed, 2014) and the accuracy of the actual stress distribution depends on the degree of the torsional restraint at its ends (Ostapenko and Moore, 1982). In Tanaka et al. study, the F.E. model and the model of each experiment present similar collapse mode, however the experimental results differ with the F.E. results which predict higher stresses (i.e. F.E. analysis) and further investigation is needed. Additionally, a methodology is proposed by Tanaka et al. (Tanaka et al., 2015) for the estimation of the progressive collapse under combined torsional and bending loads. According to the proposed methodology, torsional load which satisfies the torsional elasticity of the structure is applied to it. The hull girder is divided into beam elements and the cross sections of each beam element are subdivided into straight-line elements. The effect of the torsional load and warping stresses is taken into account in an iterative procedure according to Smith method (Smith, 1977). The results of this methodology present good correlation with the F.E. results and further investigation follows in order to take into account the effect of the bulkheads.

The effect of the transverse bulkheads is taken into account using an orthotropic plate approach and it is incorporated into the proposed methodology (Tanaka et al., 2016). In the second part of this study, the F.E. results are compared with the results of the proposed methodology when the model is subjected only to vertical bending and the ultimate strength according to the F.E. analysis is 13.4% higher. Finally, the bending moment- curvature relationship according to the proposed methodology is presented for vertical bending load only and two cases of combined torsional and bending load without a comparison with the F.E. results though.

2.5. Strength of steel and aluminium alloy ship plating under axial compression/tension, pure shear and combined loads of compression/tension and shear.

Torsional loads in ship hull girders induce shear stresses (called St. Venant's torsional shear stresses) on the plating which is one of the main structural components for structural strength. In parallel, vertical bending loads generate compressive/ tensile loads on the plates. Therefore, particular interest on the behaviour of plates under these combined loads is given due to the approach of the proposed methodology for the progressive collapse assessment of ship hull girders under combined torsion and bending (chapter 3).

The background material of plates under axial compression/tension, pure shear and combined loads of compression/tension and shear was investigated for both, steel and marine aluminium alloys (5083-H116 and 6082-T6), materials. In the literature there are many extensive studies on steel and aluminium plates under axial compression/tension. Some studies have been carried out for plates under pure shear, mostly for slender plates and very little data is available on plates under combined loads of shear and compression/tension in order to establish the design criteria for plates under combined loads.

Material properties of steel and aluminium show different characteristic behaviour and need to be investigated separately to define their progressive collapse behaviour. Typical stress-strain curves for aluminium and steel are depicted in Figure 2.6. The yield point and the plastic area of steel are well-defined and its behaviour could be assumed as simple elastic-perfectly plastic without significantly altering the strength assessment of the structure. On the contrary, this is not the case for aluminium alloys in which the yield point lies in a rounded area of the stress-strain curve and the plasticity area smoothly follows.

However, it is not only the stress-strain curves which are different for these materials but also some particularities which have to be taken into account. During welding, a tensile stress zone is introduced in both steel and aluminium plates. The width and tensile stresses in this zone is defined by Equation 2.9 - Equation 2.11. A Heat Affected Zone (HAZ) is additionally introduced to aluminium alloy plates due to welding. It could be assumed that its width is equal to the width of residual stresses zone (Benson, 2011). This heat affected zone has as effect to reduce the apparent yield stress (0.2% proof stress) and ultimate stress of the material in the HAZ, especially for 6000-series, hence the stress-strain curve of aluminium alloy in the HAZ differs

significantly from the parent material and has to be considered during the strength assessment of the structure (Figure 2.7).

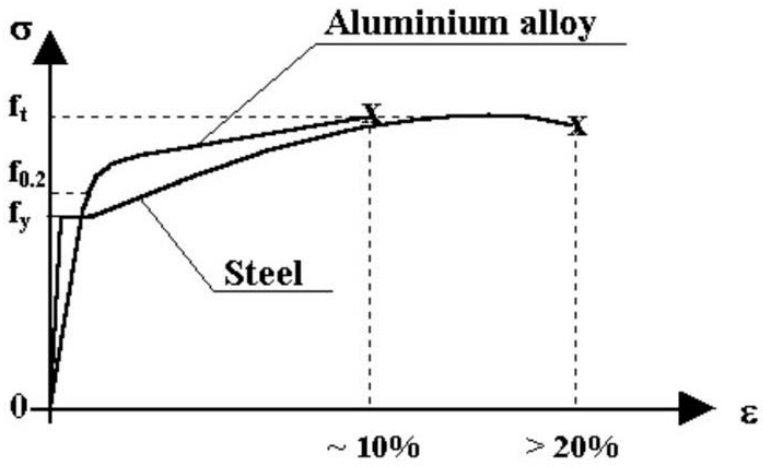

Figure 2.6: Comparison between typical stress-strain curves for aluminium and mild steels (Mazzolani, 1995)

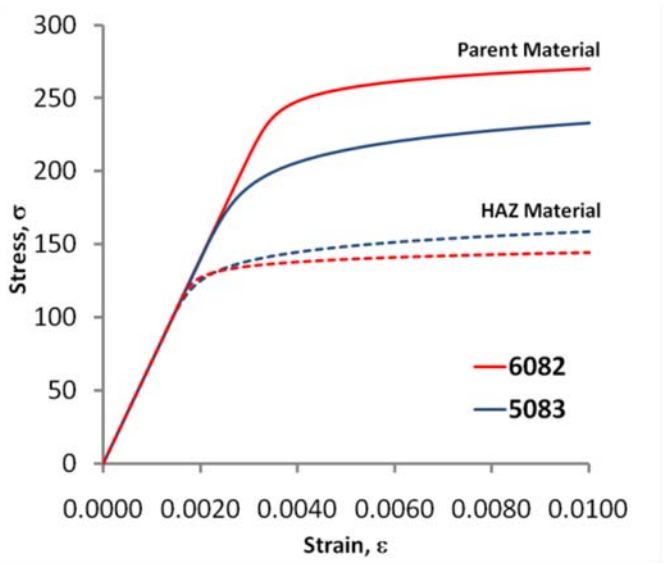

Figure 2.7: Comparative HAZ material properties for 5083-H116 and 6082-T6 aluminium alloys (Benson, 2011)

2.5.1. Plates under axial compression/tension

The ultimate strength of steel and aluminium plates under axial compression/tension has been thoroughly investigated in literature by different numerical approaches and experimental data. The main parameters which affect the ultimate strength of a plate under compressive/ tensile loads are its geometric characteristics, slenderness ratio (β) and aspect ratio (a/b), its material properties, the boundary conditions of both the loaded and the unloaded edges, the level of the initial imperfections (w/w_o) and the level of residual stresses (σ_{rc}/σ_o). The above parameters affect the progressive collapse of the plate.

2.5.1.1. Steel plates

The elastic buckling stress formula as described by (Bleich, 1952) and (Timoshenko and Gere, 1982) is given by Equation 2.3., even though this formula has "relatively little meaning in practical terms" (Faulkner, 1975). The slenderness ratio (β) of ships plating ranges between 1 and 5. So, very stocky plates (β=1-2) collapse close to the yield stress (σ_Y) of the material and less stocky plates (β=2-5) collapse at values higher than the theoretical elastic buckling load given by Equation 2.3. and lower than the yield stress of the material.

$$\sigma_E = \frac{k\pi^2}{12(1-v^2)}\left(\frac{t}{b}\right)^2 \qquad \text{Equation 2.3}$$

$$\mathrm{k} = [a/(m_o b) + m_o b/a]^2, \; where \; m_o = 1 \; for \; 1 \le a/b \le \sqrt{2} \qquad \text{Equation 2.4}$$

In the above formula, plasticity correction can be applied using Johnson-Ostenfeld formula and the critical stress (ultimate) is defined as:

$$\sigma_{cr} = \begin{Bmatrix} \sigma_E, & for\ \sigma_E \le 0.5\sigma_F \\ \sigma_F\,[1-\sigma_F/(4\sigma_E)], & for\ \sigma_E > 0.5\sigma_F \end{Bmatrix}, \begin{Bmatrix} \sigma_F = \sigma_Y \\ \sigma_{E,\ \text{Equation 2.3}} \end{Bmatrix} \qquad \text{Equation 2.5}$$

However, the ultimate strength of plates has also been assessed by semi-analytical and empirical approaches, experimental data and non-linear finite element simulations.

One of the most established and well-known empirical formula for predicting the collapse of steel plates in the literature and industry is Faulkner's formula (Equation 2.6). In Faulkner's study (Faulkner, 1975), the effect of initial geometric imperfections, lateral pressure, residual

stresses due to welding and boundary conditions of unloaded edges was investigated taking into account a wide range of experimental data and previous studies. Faulkner evaluated the measurements of three hundred plates with an average level of central plate distortion equal to $0.12\beta^2$ and the proposed formulation was based on simply supported unwelded plates with no constraints on the unloaded edges.

$$\frac{\sigma}{\sigma_o} = \frac{2}{\beta} - \frac{1}{\beta^2}, \qquad \beta \geq 1$$

$$\frac{\sigma}{\sigma_o} = 1, \qquad \beta < 1$$

Equation 2.6

where:

σ = ultimate strength of the plate

β = plate slenderness ratio defined as:

$$\beta = \frac{b}{t}\sqrt{\sigma_o / E}$$

Equation 2.7

b = plate width over which uniform compression is applied

t = plate thickness

σ_o or σ_Y = material yield stress; *E* = Young's modulus and *v* = Poison's ratio

Frieze (Frieze et al., 1977) also examined the behaviour of steel plates under compression using the finite difference dynamic relaxation method and compared his results with experimental data and Faulkner's results. In his study, Frieze compares the buckling strength of square very stocky and less stocky plates (β=0.691 and 2.074 respectively) with unrestrained and constrained unloaded edges for two different levels of initial distortions. The boundary conditions of the unloaded edges have a direct impact on the ultimate strength of plates under compressive loading. Restrained edges (clamped) may increase the elastic stress limit up to 75% (Faulkner, 1975), but not its ultimate strength, as experimental studies have shown (Ractliffe, 1966), (Moxham, 1970). However, the longitudinal stiffeners along the sides of the plates provide negligible rotational restraint on plating and no further investigation of plates with clamped edges is needed. An actual representation of the boundary conditions on

the unloaded edges allows free in-plane translation with unloaded edges remaining straight (constrained edges). An additional case is investigated though for comparison, without constraining the edges (unrestrained edges), in which according to Frieze's study "the slender plates with their unloaded edges constrained to remain straight carry significant higher loads than corresponding plates with edges unrestrained in-plane" (Frieze et al., 1977).

In the 1980s, a thorough investigation of ship platting under compressive and tensile loading was conducted by Admiralty Research Establishment (A.R.E.) at Dunfermline, which also formulated the progressive collapse method (Smith Method).

Initially, Dow (Dow and Smith, 1984) examined the effect of fourteen different shapes for various levels of initial deformation on the buckling stress of plates with the aspect ratio (a/b) 4.0, 1.0, 0.8 and 0.67. The plates were analysed using ASAS-NL, a non-linear finite element program whose results were validated with Crisfield's computer program, Frieze's dynamic relaxation procedure results and with experimental values. This study shows that the initial distortions embedded in the plate due to the manufacturing process have particular significance to buckling strength as the plate loses some of its stiffness. For long plates (a/b>1), the worst case scenario is that the plate may be governed by the lowest buckling mode, in which case the shape of the initial distortions is half-sine wave and equal to plate's breadth. The buckling behaviour is similar to this of square plates, which is assumed to be the most severe and conservative estimate for a plate's ultimate strength assessment. In this study, plates with constrained edges were mainly examined without taking into account residual stresses.

However, in later studies by the same authors (Smith et al., 1987), (Dow, 1997), the stress-strain curves of plates with constrained edges were investigated taking into account the effect of geometric imperfections and residual stresses. In these studies, a series of stress-strain curves for plates under longitudinal compressive/tensile load are presented applying three levels for the maximum amplitude of initial distortions which are described in Equation 2.8 :

$$\frac{w_0}{t} = \begin{Bmatrix} 0.025\beta^2, & slight \\ 0.1\beta^2, & average \\ 0.3\beta^2, & severe \end{Bmatrix} \qquad \text{Equation 2.8}$$

The residual stresses are formulated due to high temperature during the welding procedure; a zone of tensile stress is introduced by this process to the plate along each side, separating it to tensile and compressive blocks (Figure 2.8). The value of tensile stresses is equal to the yield stress of the material (σ_Y). The width of the tensile zone is given by Equation 2.9 & Equation 2.10 and three levels of residual stress can be taken into account according to Equation 2.11. Smith's and Dow's studies (Smith et al., 1987), (Dow, 1997) as well as other studies e.g. (Ractliffe, 1966), (Little, 1973), (Faulkner, 1975), (Frieze et al., 1977) have also investigated the effect of residual stresses on the bucking strength and the stiffness of the plates.

$$2b_t = \frac{\sigma_{rcx}}{\sigma_{rcx} - \sigma_{rtx}} \text{ b} \qquad \text{Equation 2.9}$$

$$2a_t = \frac{\sigma_{rcy}}{\sigma_{rcy} - \sigma_{rty}} a \qquad \text{Equation 2.10}$$

$$\frac{\sigma_{rcx}}{\sigma_Y} = \begin{Bmatrix} -0.05, & slight \\ -0.15, & average \\ -0.3, & severe \end{Bmatrix} \qquad \text{Equation 2.11}$$

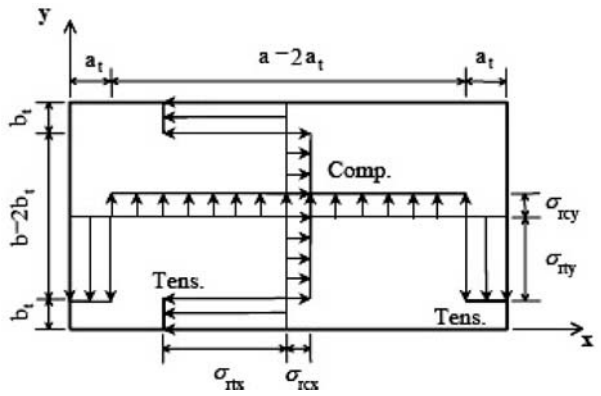

Figure 2.8: Idealised residual stress distribution in x and y direction (Paik et al., 2008)

Chalmers used the results by A.R.E. in his book (Chalmers, 1993) which included stress-strain curves of plates under compressive/tensile, transverse, biaxial and lateral loadings by Dow and Smith. A series of data, which has been validated with experimental results, is presented for plates with slenderness ratio (β) 1 to 4, column slenderness ratio (λ) 0.2 to 1.2, As/A=0.2 and aspect ratio (a/b) equal to 1 under slight, average and severe level of initial imperfections and residual stresses as described by Equation 2.8 until Equation 2.11. This database from

A.R.E. which Smith initially used in his method has been validated (Dow, 1991) and is well-established, thus it was chosen to help in the validation of the results in the present study.

Since then, many studies have been conducted in this field e.g. (Paik and Thayamballi, 2003), (Zhang et al., 2008a) etc. because finite element software programs became more useable and more widely applied. Benson (Benson, 2011) conducted a thorough investigation into the effect of geometric imperfections for steel and aluminium unstiffened and stiffened plates subjected to axial compression. In his study, the ultimate strength of plates and panels subjected to compressive loads was investigated under different levels and modes of initial distortions, different levels of residual stresses and boundary conditions. Then, a database of stress-strain curves was generated and incorporated in the computer code ProColl (see 2.4.3). Benson applied residual stresses provided by Equation 2.9 to Equation 2.11. An average level of initial imperfections was assumed according to Equation 2.8 and their shape is described by a three mode Fourier series equation:

$$\frac{w}{w_o} = \left(0.8\sin\left(\frac{\pi x}{a}\right) + 0.2\sin\left(\frac{m\pi x}{a}\right) + 0.01\sin\left(\frac{(m+1)\pi x}{a}\right)\right)\sin\left(\frac{\pi y}{b}\right), \qquad \text{Equation 2.12}$$

$$m = int\left(\frac{a}{b}\right) + 1$$

According to Benson's research a ratio of 80% to 20% single half wave to square half wave (square mode =m) provides a realistic representation of the shape of the imperfections without being particularly optimistic or conservative. This realistic characterisation also gives enough of an imperfection in the preferred buckling mode to nucleate the minimum failure mode.

An additional higher mode (m+1) is added in order to ensure that nucleation will occur only in one region and imperfection distribution will be unsymmetrical. Finally, imperfections are implemented to the plate using trigonometric functions which are defined with the direct node translation method.

2.5.1.2. Aluminium plates

In the literature, recent studies are more useful to the current research concerning aluminium plates because their material properties are closer to those which are defined today. The properties of the marine aluminium alloys have been improved during the 1980s in order to increase their resistance to corrosion from seawater. The main studies which carried out for marine aluminium alloys plates are these of Little (Little, 1982), Mofflin and Dwight (Mofflin and Dwight, 1984), and more recently by Eurocode 9 (Eurocode 9 EN 1997-1-1, 2007), Hopperstad (Hopperstad et al., 1999), Kristensen (Kristensen, 2001), Paik and Duran (Paik and Duran, 2004) and Benson (Benson, 2011).

Little (Little, 1982) investigated the collapse behaviour of aluminium plates with different slenderness ratio (β) under axial compression taking into account their initial distortions, but not heat affected zones (HAZ). Mofflin and Dwight (Mofflin and Dwight, 1984) produced a series of experimental data for aluminium plates subjected to in-plane loads considering geometric imperfections and HAZ. Both studies consisted of the main background for Eurocode 9 (Eurocode 9 EN 1997-1-1, 2007) which provides guidelines for the structural design of aluminium plates. In Hopperstad's study (Hopperstad et al., 1999), the ultimate strength of aluminium alloys was investigated experimentally under compression taking into account initial distortions, residual stresses and HAZ. These results were compared with numerical simulations showing a very good correlation.

Kristensen (Kristensen, 2001) also analysed the ultimate strength of 6082-T6 aluminium alloy plates under multiple loads (axial compression, transverse, biaxial, shear loads, combined shear and compressive loadings) using nonlinear finite element analysis (NLFEM) and including geometric imperfections, residual stresses and HAZ.

Paik and Duran (Paik and Duran, 2004) investigated 5083-H116 aluminium plates with NLFEM taking into account all the pre-mentioned parameters and proposed a formulation (Equation 2.21). Finally, Benson (Benson, 2011) compared Mofflin's results to empirical formulas suggested by Faulkner, Johnson-Ostenfeld, Eurocode 9 EN1997-1-1 and Paik & Duran. A very good correlation of all results was found for low (less than 1) and intermediate (1 to 2.3) values of slenderness ratio (β).

The formulas which may be used for aluminium plate's ultimate strength assessment under axial compressive loadings are:

- Faulkner's formulation (Faulkner, 1975) in which the yield stress (σ_o) in Equation 2.6 should be replaced by the proof yield stress at 0.2% offset strain.
- Johnson-Ostenfeld formula (Equation 2.5) in which the yield stress (σ_Y) should be replaced by the proof yield stress at 0.2% offset strain.
- Eurocode 9 class 4 (Eurocode 9 EN 1997-1-1, 2007) for marine alloys suggests the design value the compression force (N_{ED}) to be equal to:

$$\frac{N_{ED}}{N_{Rd}} \leq 1.0 \qquad \text{Equation 2.13}$$

Where:

N_{ED} = design value of the compression force; N_{RA}= design resistance to normal forces equal to:

$$N_{Rd} = \frac{A_{eff \cdot \sigma_o}}{\gamma_{M1}} \qquad \text{Equation 2.14}$$

If we assume N_{ED}= N_{Rd} and safety factor to account for design uncertainties (γ_{M1}) equal to 1, the design resistance N_{Rd} derives from:

$$N_{Rd} = A_{eff} \cdot \sigma_o \qquad \text{Equation 2.15}$$

Where:

σ_o = proof yield stress at 0.2% offset strain; A_{eff} = overall effective area equal to:

$$A_{eff} = 2b_{HAZ}\rho_{o_{HAZ}}t + (b - 2b_{HAZ})\rho_c t \qquad \text{Equation 2.16}$$

Where:

b_{HAZ} = width of the Heat Affected Zone; t = plate thickness.

The reduced factors of the yield stress in the HAZ and of the proof yield stress are:

$$\rho_{o_{HAZ}} = \frac{\sigma_{o_{HAZ}}}{\sigma_o}$$ Equation 2.17

$$\beta = \frac{C_1}{\left(\frac{\beta}{\varepsilon}\right)} - \frac{C_2}{\left(\frac{\beta}{\varepsilon}\right)^2}$$ Equation 2.18

Where:

$C_1 = 29$; $C_2 = 198$

$$\beta = \frac{b}{t}$$ Equation 2.19

$$\varepsilon = \sqrt{250/\sigma_o}$$ Equation 2.20

- According to Paik and Duran's formulations (Paik and Duran, 2004), the ultimate strength of aluminium plates derives from:

$$\frac{\sigma}{\sigma_o} = \begin{Bmatrix} -0.13\beta + 0.921, \beta < 3 \\ -0.07\beta + 0.741, \beta \geq 3 \end{Bmatrix}$$ Equation 2.21

β = plate slenderness ratio, defined in Equation 2.7

2.5.2. Plates under pure shear

Plates which are subjected to shear loadings have been investigated by aeronautical, naval and civil engineers in order to provide deeper insight to buckling and post-buckling behaviour of plates under these loads. Due to different applications, the boundary conditions, geometric characteristics and the material properties of plates may differ. In aeronautical engineering, very slender aluminium plates are usually examined, which are high unlikely to be applied in marine structures. Typical ship plates are steel and marine aluminium alloys of the 5000 and 6000 series in order to have high resistance in corrosion; their slenderness ratio (β) usually ranges between 1 and 5 and their edges are simply supported but constrained to remain straight. In civil engineering studies, steel plates of similar thickness to ship plates are investigated, but the boundary conditions of the edges differ examining only two cases in which plates are simply supported or clamped. However, all studies have been taken into account as each of them contributes in a different way to the current study.

2.5.2.1. Steel plates

The critical elastic shear stress formula for simply supported plate equivalent to elastic buckling stress formulation (Equation 2.3) is given by Equation 2.22.

$$\tau_E = \frac{k_s \pi^2 E}{12(1-v^2)} \left(\frac{t}{b}\right)^2, \qquad k_s = 5.3 + 4(a/b)^2 \ \& \ a/b \geq 1 \qquad \text{Equation 2.22}$$

However, the elastic shear buckling stress with plasticity correction can be used instead applying the Jonson-Ostenfeld formula which is described in Equation 2.23.

$$\tau_{cr} = \begin{cases} \tau_E, & for\ \tau_E \leq 0.5\sigma_F \\ \sigma_F\,[1-\sigma_F/(4\tau_E)], & for\ \tau_E > 0.5\sigma_F \end{cases}, \begin{cases} \sigma_F = \tau_Y = \sigma_Y/\sqrt{3} \\ \tau_{E,\ \text{Equation 2.22}} \end{cases} \qquad \text{Equation 2.23}$$

Initially, Rutherford (Rutherford, 1983) introduced a semi-analytical formula for the ultimate shear stress based on design curves from the aircraft industry. In 2008, Zhang and Rutherford (Zhang et al., 2008) proposed a simpler formulation (Equation 2.24) for the estimate of ultimate shear stress of ship plating without residual stresses.

In Zhang's study, plates with aspect ratio (a/b) equal to 4.45 and slenderness ratio (β) 1.19-3.91 are modelled using ABAQUS and then they are compared against Rutherford's initial equation, Nara's (Equation 2.25), Eurocode 3 (Equation 2.27), Paik's (Equation 2.28) and his proposed equation (Equation 2.24). In this case, it shows particularly good correlation with Rutherford's, Nara's and Zhang's N.F.E.M results. However, in the case of slender plates with different aspect ratio (a/b) equal to 1, 2, 3 the proposed formula agrees constantly only with Rutherford's equation.

$$\frac{\tau_u}{\tau_Y} = \begin{Bmatrix} 1, & for\ \beta_\tau < 1 \\ \dfrac{2}{\sqrt{\beta_\tau}} - \dfrac{1}{\beta_\tau}, & for\ \beta_\tau \geq 1 \end{Bmatrix}, \begin{Bmatrix} \beta_\tau = \dfrac{\beta}{1 + (b/a)^{3/2}} \\ \tau_Y = \sigma_Y/\sqrt{3} \\ \beta, \text{ Equation 2.7} \end{Bmatrix} \quad \text{Equation 2.24}$$

Nara's equation (Equation 2.25) is based on N.F.E.M. results, where steel plates of aspect ratio (a/b) 1 to 1.5 and thickness (b/t) 50.6 to 196.9 are examined taking into account average initial distortions and residual stresses. The proposed formulation derives by regression analysis of the F. E. results and it is described as:

$$\frac{\tau_u}{\tau_Y} = \left(\frac{0.486}{\lambda}\right)^{1/3}, for\ 0.486 \leq \lambda \leq 2 \quad \text{Equation 2.25}$$

$$\lambda = \left(\tau_y/\tau_E\right)^{1/2} \quad \text{Equation 2.26}$$

Another empirical formulation is suggested by Eurocode 3 (Eurocode 3 ENV 1993-1-1, 2005) as follows:

$$\frac{\tau_u}{\tau_Y} = \begin{Bmatrix} 1, & \lambda \leq 0.8 \\ 1 - 0.625(\lambda - 0.8), & 0.8 \leq \lambda \leq 1.2 \\ 0.9/\lambda, & \lambda \geq 1.2 \end{Bmatrix}, \{\lambda\ as\ defined\ by \text{ Equation 2.26}\} \quad \text{Equation 2.27}$$

In addition, Paik (Paik et al., 2001a) investigated the ultimate shear stress (τ_u) using F.E. analysis for a series of steel plates with aspect ratio (a/b) 1, 3, 5, varying thickness, average

initial distortions (Equation 2.8) and constrained edges which allow the sides to remain straight. The proposed empirical formula is:

$$\frac{\tau_u}{\tau_Y} = \begin{cases} 1.324\left(\frac{\tau_E}{\tau_y}\right), & for\ 0 < \frac{\tau_E}{\tau_y} < 0.5 \\ 0.039\left(\frac{\tau_E}{\tau_y}\right)^3 - 0.274\left(\frac{\tau_E}{\tau_y}\right)^2 & \\ +0.676\left(\frac{\tau_E}{\tau_y}\right) + 0.388, & for\ 0.5 < \frac{\tau_E}{\tau_y} \leq 2 \\ 0.956, & for\ \frac{\tau_E}{\tau_y} > 2 \end{cases} \quad \text{Equation 2.28}$$

Where, τ_E is the elastic critical shear stress and it is given by Equation 2.22.

In Paik's and Nara's research, critical shear stress values seem to be independent from the aspect ratio of the plates, which agrees also with Santos Rizzo's results (Rizzo et al., 2014). Santos Rizzo (Rizzo et al., 2014) has modelled steel plates with aspect ratio (a/b) 1 to 4 using N.F.E.M. and his Von-Mises contour plots show that long plates under shear behave like multiple square plates. In Paik's graph (Paik and Thayamballi, 2003) the proposed critical stress formulation follows the same pattern with Eurocode 3 (Equation 2.27) and shows good correlation with the elastic buckling strength formula with plasticity correction (Equation 2.23). In the same graph, Nara's equation results (Equation 2.25) are also depicted and seem to agree with Equation 2.23.

In civil engineering, Alinia's research (Alinia et al., 2009) in which simply supported and clamped thin plates subjected to shear, show that the through thickness bending stress and yield pattern of the plates have not been significantly affected by the support conditions. However, the plates in this study are perfectly flat which is not the case in the current study.

2.5.2.2. Aluminium plates

Marine aluminium alloy plates (6082-T6) subjected to shear have been analysed by Kristensen (Kristensen, 2001) using NLFEM examining the effect of residual stresses and heat affected zone (25mm) along all edges of the plate. In Figure 2.9, the necessity to include HAZ in the ultimate shear strength assessment of aluminium plates is shown, but not also the residual stresses which may have a minor effect.

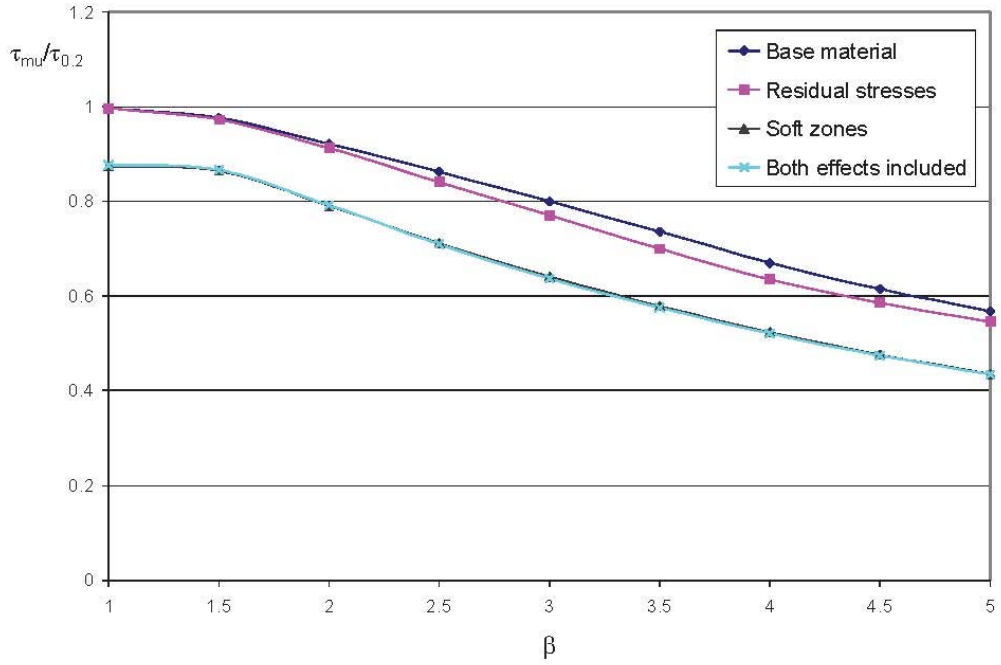

Figure 2.9: Ultimate capacities of plates made of alloy 6082-T6 exposed to pure shear load (Kristensen, 2001)

The Jonson-Ostenfeld formula (Equation 2.23) for steel plates under shear can be used for the critical shear load estimate of aluminium plates replacing the yield stress (σ_Y) with the proof yield stress at 0.2% offset strain.

Also, Eurocode 9 EN 1997-1-1 (Eurocode 9 EN 1997-1-1, 2007, p. 9) provides the following formulations for the estimation of critical shear stress of aluminium plates:

$$V_{ED} \leq V_{Rd}$$ Equation 2.29

Where:

V_{ED} = design value of the shear force at the cross section; V_{Rd} = design shear resistance of the cross section.

If we assume $V_{ED} = V_{Rd}$ and safety factor to account for design uncertainties (γ_{M1}) equal to 1, the design shear resistance of the cross section (V_{Rd}) derives from:

- For non-slender plates $\beta \leq 39\varepsilon$, where β is defined by Equation 2.19 and ε by Equation 2.20, a yielding check is required using the following formula:

$$V_{Rd} = A_{net} \cdot \sigma_o / \left(\gamma_{M1}\sqrt{3}\right) \quad \text{Equation 2.30}$$

Where:

A_{net} = net effective area, equal to:

$$A_{net} = 2b_{HAZ}\frac{\sigma_{HAZ}}{\sigma_o}t + (b - 2b_{HAZ})\frac{\sigma_o}{\sigma_o}t \quad \text{Equation 2.31}$$

- Slender plates $\beta > 39\varepsilon$, where β is defined by Equation 2.19 and ε by Equation 2.20, a yielding check is required the Equation 2.30 and a buckling check using the following formula:

$$V_{Rd} = v_1 \cdot b \cdot t \cdot \sigma_o / \left(\gamma_{M1}\sqrt{3}\right) \quad \text{Equation 2.32}$$

Where:

$$v_1 = v_1 \cdot t \cdot \varepsilon \cdot \sqrt{k_t}/b < k_\tau \frac{430 \cdot t^2 \cdot \varepsilon^2}{b^2} \leq 1 \quad \text{Equation 2.33}$$

b = plate's breadth; a = plate's length;

$$k_\tau = 5.34 + 4.00 \cdot (b/a)^2, \qquad for\ a/b \geq 1 \quad \text{Equation 2.34}$$

2.5.3. Plates under combined loads of compression/tension and shear

In the literature, the studies which examine plates subjected to compression/tension and shear are very limited. Both loads should occur simultaneously in order to be an actual representation of ship's loading, therefore an important point of interest during this study is the applied boundary conditions. In addition, the effect of initial distortions and residual stresses was investigated. It should also be mentioned that aluminium plates are more complicated than steel plates as the defined material properties may differ in each study.

2.5.3.1. Steel plates

In aeronautics, Batdorf's (Batdorf and Stein, 1947) research was focused on simply supported flat rectangular plates (a/b = 1, 2 and 4) under combined loads of shear and longitudinal direct stress. The critical shear and direct stress were computed by an energy method and the following formulation was proposed:

$$\left(\frac{\tau}{\tau_{cr}}\right)^2 + \frac{\sigma}{\sigma_{cr}} = 1 \qquad \text{Equation 2.35}$$

Bleich (Bleich, 1952) also studied simply supported plates under these combined loads and created a design chart solving an energy method. Ueda (Ueda et al., 1985), much later, derived an empirical formula based on Bleich's interaction curves for plates subjected to combined shear and compressive loads. The proposed formulation provides the elastic shear and buckling stress values as it follows:

$$\left(\frac{\tau}{\tau_E}\right)^{a_{11}} + \frac{\sigma}{\sigma_E} = 1 \qquad \text{Equation 2.36}$$

where:

τ, σ are the elastic values of shear and compressive stress respectively under combined loads;

τ_E, elastic shear stress under pure shear as described by Equation 2.22

σ_E, elastic direct stress under pure compression as described by Equation 2.3 and Equation 2.4

$$a_{11} = \begin{cases} -0.16(a/b)^2 + 1.080(a/b) + 1.082, & 1 \le a/b \le 3.2 \\ 2.90, & a/b > 3.2 \end{cases}$$ Equation 2.37

Paik (Paik and Thayamballi, 2003) also provides a formulation in his book for shear and buckling strength of plates subjected to combined loads taking into account the plasticity correction by Johson-Ostenfeld formula. The general formula modified for combined compressive (-) /tensile (+) and shear loads becomes:

$$\left(\frac{\sigma}{\sigma_{cr}}\right)^2 + \left(\frac{\tau}{\tau_{cr}}\right)^2 = 1, \qquad \begin{cases} \sigma_{cr}, using \text{ Equation 2.5} \\ \tau_{cr}, using \text{ Equation 2.23} \end{cases}$$ Equation 2.38

However, the ultimate strength of steel plates under shear and axial compression/tension seems to investigated initially by Harding (Harding et al., 1977) using multi-layer/DR finite difference analysis. In his extensive research, the effect of the constraints at the unloaded edges (unrestrained and constrained edges), the level of initial imperfections (slight, average, severe) and residual stresses (in longitudinal and transverse direction) were taken into account. Plates with aspect ratio (a/b) equal to 1 and slenderness ratio (β) equal to 2.075, 4.149 and 6.224 were subjected simultaneously to shear and compressive/tensile loadings. Their strength assessment provides an informative data of series of direct stress, shear stress/strain curves and interaction curves under these combined loads giving insight into the effect of the pre-mentioned parameters on the behaviour of a plate.

2.5.3.2. Aluminium plates

Limited research has been carried out for aluminium marine alloys plates under combined loads of axial compression/ tension and shear. Dier (Adrian F. Dier, 1987) compared the behaviour of steel and 5083 aluminium alloy square plates with slenderness ratio (β) equal to 4.149, average level of initial geometric imperfections, without residual stresses and constrained edges. In his study, dynamic relaxation method was used for the analysis and aluminium's alloy properties were based on the kinematic model with multilinear representations of the material stress/strain curves.

Compressive and shear loads were combined applying a constant ratio of shear to in-plane displacement (0:1, 1/2:2, 1:1, 1:1/2, and 1:0) for the plates. The results show similar behaviour of steel and aluminium alloy 5083 plates under the aforementioned ratios and the interaction diagrams of shear and compressive loads for both materials are presented in Figure 2.10.

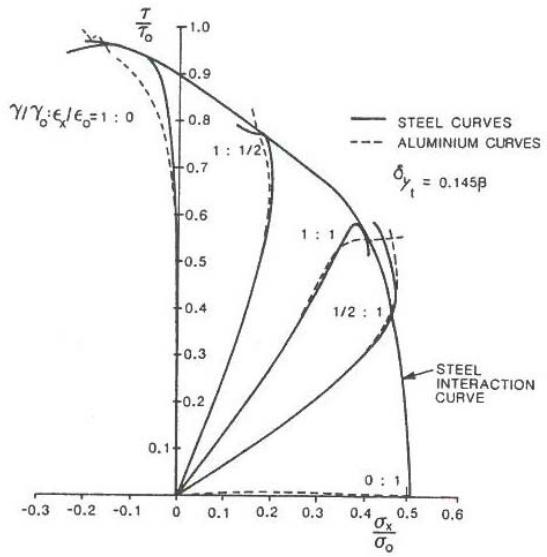

Figure 2.10: Stress paths and interaction curve: shear and compression, a/b=1, β=4.149 (Adrian F. Dier, 1987)

Another study which examines aluminium plates under combined loads of shear and compression is Kristensen's study (Kristensen, 2001). In his research, 6082-T6 aluminium alloy plates (a/b=3) with a width heat affected zone of 25mm along all their edges are subjected to shear and compressive loadings and they are analysed using NLFEM. The interaction curves of these plates with slenderness (β) 1 to 5 are shown in Figure 2.11.

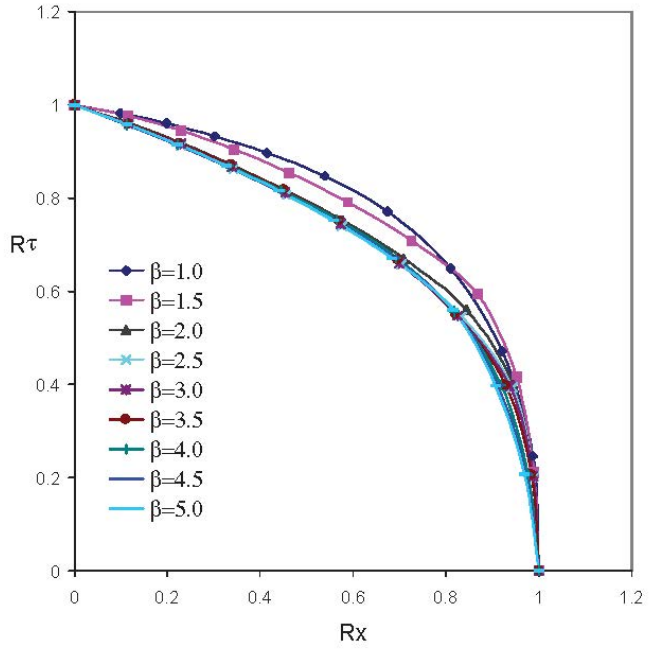

Figure 2.11: Interaction curves for plates exposed to axial compression in combination with shear loads. The plates have heat affected zones along all edges. (Kristensen, 2001)

2.6. Summary

This chapter first categorises the types of loads which a ship might be subjected and the limit state design of ship structures is also defined. Then, the existing methodologies for the progressive collapse assessment of ship hull girders under the most dominant load which is the bending load, are presented. Furthermore, the effect of torsional loads on ship's strength assessment is investigated in the literature, discussed and analysed. In the end, an extensive investigation in the behaviour of steel and aluminium plates under pure axial compressive/tensile loads, pure shear loads and combined compressive/tensile and shear loads takes part due to the approach which the author follows on the proposed methodology.

Chapter 3

Methodology

3.1. Introduction

In this chapter, the methodology for the incorporation of torsional effect into the extended simplified progressive collapse method is described. Initially, a brief description of the extended simplified progressive collapse method is given. Then, the main assumptions of the proposed methodology by the author are presented. The calculation of the shear flow distribution in the cross section is also explained and finally the flow chart of this part of the code is presented and analysed.

3.2. Background

As has been mentioned, the proposed methodology is incorporated in the extended simplified progressive collapse method in order to take into account the torsion effect into the progressive collapse assessment. The extended simplified progressive collapse method by Benson and Dow (Benson, 2011) estimates the progressive collapse of intact structures under vertical and horizontal bending moment. It is based on the simplified progressive collapse method by Smith and Dow (Smith et al., 1987), which is a well-established methodology and recommended by the classification societies of IACS and the ISSC 2000 committee VI.2 (Ultimate Hull Strength Girder).

The extended simplified progressive collapse method has already been discussed in section 2.3.3 and the simplified progressive collapse method is described in section 2.3.1. The main advantage of the extended simplified progressive collapse method over the initial methodology (Smith method) is its ability to model not only the interframe collapse but also the overall collapse of the structure. This is achieved by using the nonlinear orthotropic plate theory approach which Benson (Benson, 2011) implemented in ProColl. The instantaneous overall panel resistance, $R_{OVERALL(u)}$, according to Benson is the lesser value of $R_{L(u)}$ (interframe calculation) and $R_{PO(u)}$ (overall calculation) at each increment.

The calculation of the $R_L(u)$ of the panel, at a given panel end displacement, u, derives from the following equations, using the representative load shortening curve (LSC) which is generated by the NLFEM datasets:

$$R_L\,(u) = \frac{R_{plate(u)} \cdot b \cdot t + R_{stiff(u)} \cdot (h_w \cdot t_w + b_f \cdot t_f)}{b \cdot t + h_w \cdot t_w + b_f \cdot t_f} \quad \text{Equation 3.1}$$

Where:

$$R_{plate}\,(u) = \sigma'_s(u) \cdot \sigma_o \cdot b \cdot t_p \quad \text{Equation 3.2}$$

$$\mathrm{u} = \varepsilon' \cdot \varepsilon_o \cdot \alpha \quad \text{Equation 3.3}$$

$$R_{stiff}\,(u) = \sigma'_s(u) \cdot \sigma_o \cdot (h_w \cdot t_w + b_f \cdot t_f) \quad \text{Equation 3.4}$$

The calculation of the $R_{PO}(u)$ of the panel, at a given panel end displacement, u, derives from the orthotropic plate calculations which are presented in the flow chart in Figure 124 in Benson's study and they are analysed in detail at the same section (Benson, 2011).

The resistance of the panel according to both interframe ($R_{L(u)}$) and orthotropic ($R_{PO(u)}$) calculation is calculated in each iteration and the min value of the above (i.e. $R_{L(u)}$, $R_{PO(u)}$) is selected as the resistance of the panel, $R_{OVERALL(u)}$.

However, the components of the plate and stiffener resistance, $R_{plate}(u)$ and $R_{stiff}(u)$ respectively, are taking into account separately in the calculations for R_L and R_{PO}. Shear stresses affect only the plates, not the stiffeners of the structure. Therefore, the aim is to develop a methodology which incorporates the effect of shear into the resistance of the plates ($R_{plate}(u)$) during the calculation. The stiffener spacing provides the plating aspect ratio and slenderness.

3.3. Main assumptions

The main assumption of the approach is that the structure fails due to bending and that torsion has a secondary load effect. The proposed methodology is based on the simplified progressive collapse method which estimates the strength of a ship structure under vertical

and horizontal bending moment. The vertical bending moment is the dominant load of the structure in most cases. Torsion may affect its strength in some cases where the torsional rigidity of the structure is low, but it is not the dominant load even in these cases.

In addition, the cross section has to remain plane at the compartment ends, likewise in the extended simplified progressive collapse method. The ends of the structure are free to move in transverse direction (x-axis), so no warping stresses are generating into the structure.

Since the structure does not develop warping stresses, the applied torsion to the structure generates St. Venant's torsional shear stresses which affect only the plates of the structure, not its stiffeners.

Finally, the shear stresses due to standard bending theory are currently ignored in this approach. Previous studies showed these are small compared to the shear stresses due to torsional loads.

3.4. Approach of the proposed methodology

The approach of the proposed methodology initially investigates the behaviour of ship's plating subjected only to compressive/tensile loads, to shear loads and to simultaneously combined shear and compressive/tensile loads. The outcome of this investigation provides interaction diagrams of compressive/tensile and shear stresses for typical ship plates (β=1-6). These interaction diagrams are then digitised and programmed into ProColl.

Within ProColl, the shear flow distribution in the cross section is calculated due to an amount of applied torque. Since, the amount of shear stress on each plate is known and the interaction diagram of shear and compressive/tensile stresses is known too, from the prior investigation, a knock down factor, Kn, can be defined for each plate. This factor is applied to the associated load shortening curve of the plate in the extended simplified progressive collapse methodology. In this way, the effect of shear is taken into account into the $R_{plate}(u)$ value and the iterative procedure of the methodology occurs, estimating the progressive collapse in its end. The maximum value in the bending moment-curvature defines its ultimate strength value for this amount of applied torsion to the structure.

Thereinafter, a different amount of torsion is assumed and the above procedure is repeated estimating the progressive collapse of the structure and its ultimate strength under this

amount of torsional load. The iteration of the procedure stops when the applied value of torsion reaches the maximum value of its torsional load.

In the end of the analysis, the bending moment curvature relationship of the structure under each applied amount of torsional load is provided, while, an interaction diagram of torsion and bending moment is generated in parallel. This interaction diagram defines a safe limit of combined torsional and bending loads in which the strength of the structure is sufficient.

The flow chart diagram for the incorporation of torsion into the extended simplified progressive collapse method is depicted in Figure 3.1.

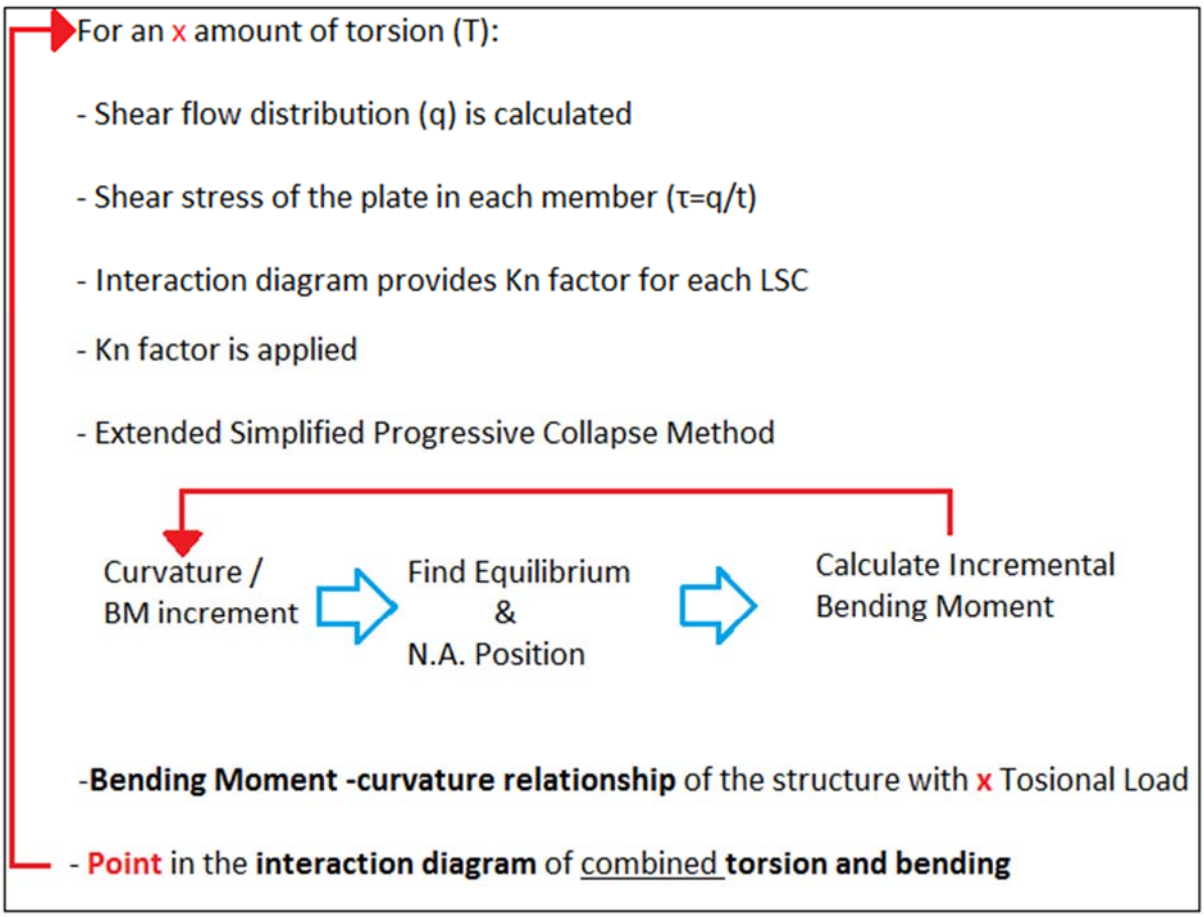

Figure 3.1: Flow chart diagram for the incorporation of torsion into the Extended Simplified Progressive Collapse Method

3.5. Shear flow distribution

The torsional shear flow distribution of any closed section can be calculated based on the method of successive corrections as described by Bruhn (Bruhn, 1973). This method is usually applied to aero-structures; for example, the cross sections of their wings are consisted by multiple numbers of cells which are subjected to torsional loads.

According to the method, initially it is assumed that each cell of the cross section acts independently and it is subjected to a shear flow q which makes Gθ equal to 1 in Equation 3.5.

$$\mathrm{G} \cdot \vartheta = \frac{qL}{2A} \oint \frac{d_s}{t} \qquad \text{Equation 3.5}$$

Where:

$G = \frac{E}{2(\nu+1)}$, shear modulus

ϑ, angular twist

q, shear flow of the cell

d_s, periphery of the cell

t, thickness of plate

For $G \cdot \vartheta = 1$, Equation 3.5 for each cell of the cross section becomes:

$$\mathrm{q} = \frac{2A}{\oint \frac{d_s}{t}} \; per\ unit\ length \qquad \text{Equation 3.6}$$

Recalculating $G \cdot \vartheta$ for each cell using Equation 3.5 and the shear flow from Equation 3.6, results to $G \cdot \vartheta < 1$, but ϑ value should be the same for all cells, otherwise distortion of the original shape of the cross section occurs. Therefore, correction of the assumed shear flow (q) in each cell is needed due the resultant shear flow in the common plates between the cells.

The correction of the resultant shear flow in the common plates takes part adding a shear flow to the cell which cancels the negative twist due to the shear flow of the other cell in the common plate.

For example, we are taking two cells with shear flow q_1, q_2 and we assumed that there is only one common plate between them which has $\frac{d_s}{t} = \delta_{12}$.

Additionally, for cell 1 and cell 2 we assume $\frac{d_s}{t} = \delta_1$ and $\frac{d_s}{t} = \delta_2$, respectively.

Therefore, for cell 1:

$$\mathrm{G} \cdot \vartheta = \frac{1}{2A_1}[q_1 \cdot (\delta_1 - \delta_{12}) + (q_1 - q_2) \cdot \delta_{12}] < 1 \qquad \text{Equation 3.7}$$

And for cell 2:

$$\mathrm{G} \cdot \vartheta = \frac{1}{2A_2}[q_2 \cdot (\delta_2 - \delta_{12}) + (q_2 - q_1) \cdot \delta_{12}] < 1 \qquad \text{Equation 3.8}$$

The adding shear flow (q') in order to cancel the influence of the other cell to the common plate can be written as:

For cell 1:

$$q_1' \cdot \delta_1 - q_2 \cdot \delta_{12} = 0 \qquad \text{Equation 3.9}$$

The carry over factor from cell 2 to cell 1 is:

$$COF_{21} = \frac{\delta_{12}}{\delta_1} \qquad \text{Equation 3.10}$$

And Equation 3.9 due to Equation 3.10 becomes:

$$q_1' = COF_{21} \cdot q_2 \qquad \text{Equation 3.11}$$

Respectively for cell 2:

$$q_2{}' \cdot \delta_2 - q_1 \cdot \delta_{12} = 0 \qquad \text{Equation 3.12}$$

The carry over factor from cell 1 to cell 2 is:

$$COF_{12} = \frac{\delta_{12}}{\delta_2} \qquad \text{Equation 3.13}$$

And Equation 3.12 due to Equation 3.13 becomes:

$$q_2{}' = COF_{12} \cdot q_1 \qquad \text{Equation 3.14}$$

Applying $q_1{}'$ and $q_2{}'$ to Equation 3.7 and Equation 3.8, we calculate a $G \cdot \vartheta$ value which is less than 1 but closer to it than before, due to the corrected shear flow:

For cell 1:

$$\mathrm{G} \cdot \vartheta = \frac{1}{2A_1}[q_1{}' \cdot (\delta_1 - \delta_{12}) + (q_1{}' - q_2{}') \cdot \delta_{12}] < 1 \qquad \text{Equation 3.15}$$

And for cell 2:

$$\mathrm{G} \cdot \vartheta = \frac{1}{2A_2}[q_2{}' \cdot (\delta_2 - \delta_{12}) + (q_2{}' - q_1{}') \cdot \delta_{12}] < 1 \qquad \text{Equation 3.16}$$

Therefore, additional correction of the shear flow (q'') is needed which based on Equation 3.11 and Equation 3.14 is:

For cell 1:

$$q_1{}'' = COF_{21} \cdot q_2{}' \qquad \text{Equation 3.17}$$

For cell 2:

$$q_2{}'' = COF_{12} \cdot q_1{}' \qquad \text{Equation 3.18}$$

The corrected shear flow q_1'' and q_2'' for cell 1 and 2 are applied to Equation 3.15 and Equation 3.16 calculating:

For cell 1:

$$\mathrm{G} \cdot \vartheta = \frac{1}{2A_1}[q_1'' \cdot (\delta_1 - \delta_{12}) + (q_1'' - q_2'') \cdot \delta_{12}] \qquad \text{Equation 3.19}$$

And for cell 2:

$$\mathrm{G} \cdot \vartheta = \frac{1}{2A_2}[q_2'' \cdot (\delta_2 - \delta_{12}) + (q_2'' - q_1'') \cdot \delta_{12}] \qquad \text{Equation 3.20}$$

If the result in Equation 3.19 and Equation 3.20 is not equal to 1, we apply another correction updating Equation 3.17 - Equation 3.20, until they result $\mathrm{G} \cdot \vartheta = 1$.

The final shear flow in each cell is:

$$q_{1_{corrected}} = q_1 + q_1' + q_1'' + q_1''' \qquad \text{Equation 3.21}$$

And

$$q_{2_{corrected}} = q_2 + q_2' + q_2'' + q_2''' \qquad \text{Equation 3.22}$$

Additionally, it is known that torsion in the elastic area for closed sections is calculated by:

$$\mathrm{T} = 2 \cdot \sum A \cdot q \qquad \text{Equation 3.23}$$

A= the enclosed area of the mean periphery of the cell

q= the shear flow of the cell

In the above example of the two cells, Equation 3.23 becomes:

$$\mathrm{T} = 2 \cdot \left(A_1 \cdot q_{1_{corrected}} + A_2 \cdot q_{2_{corrected}}\right) \qquad \text{Equation 3.24}$$

3.6. Knock down Factor (Kn)

The calculation described in section 3.5 provides the shear flow distribution on the plates of each cell in the cross section for an arbitrary amount of torsion T. In continue the values of shear on the plates are normalized with respect to the value of the shear yield stress which is equal to:

$$\tau_Y = \frac{\sigma_Y}{\sqrt{3}}$$ Equation 3.25

This shear distribution corresponds to an amount of torsion which is called T_o and after this point which shear yield occurs, the shear flow in the cells remain constant. The shear flow of a cell whose one plate has reached its critical shear stress value, cannot be increased even though the applied torsional load is increasing. The additional torsional load (i.e. beyond T_o) will cause redistribution of the initial shear flow to the other cells. However, this effect is not taken into account in the current methodology due to its perceived small effect in the results.

Therefore, fractions of T_o are applied in each iteration calculating corresponding fractions of the maximum shear stress in each plate. If the user defines a torsional load $T_{max} > T_o$, the shear stress of each plate for $T_{applied} > T_o$ is equal to the shear stress value of the plate in the case of $T_{applied} = T_o$.

Then, the interaction diagram of shear and compressive/tensile stresses provides a factor for each plate for a known amount of shear (e.g. $\tau_{applied}$) which is applied during the iteration. This factor is applied to both the values of stress and strain in the initial load shortening curve (LSC). The applied factor (k_n) results in an updated LSC equal to the LSC which derives from the F.E. analysis for plates under combined compression/tension and the amount of applied shear load ($\tau_{applied}$) (Figure 3.2). Therefore, torsion is incorporated into the extended simplified progressive collapse method as a reduction factor on the initial strength of the plates. This will also have a direct effect on the orthotropic plate theory for computation of overall collapse.

The procedure continues until torsion becomes equal to T_o or when it reaches the maximum value of torsion T_{max}, which the user has defined.

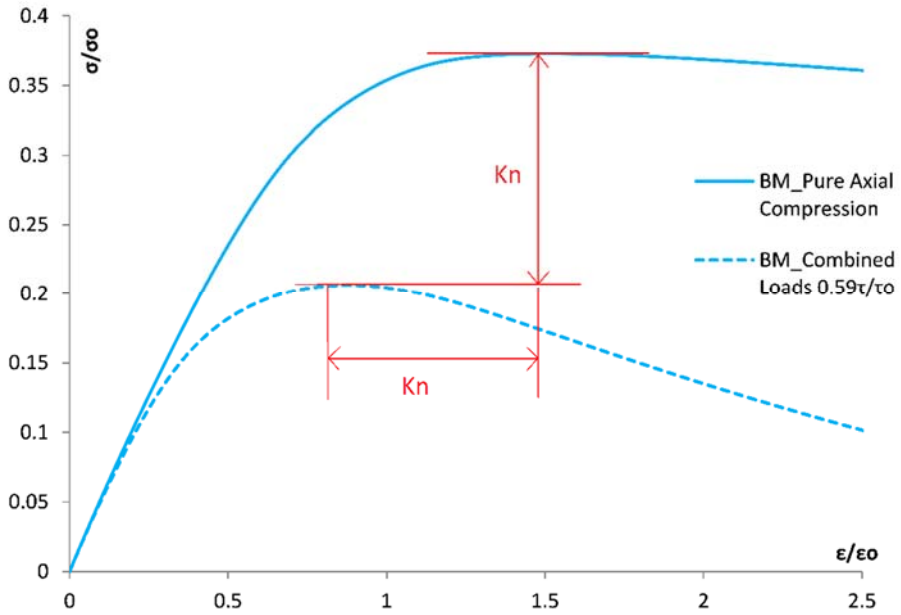

Figure 3.2: Knock down factor (kn) is applied to the LSC in order to derive an updated LSC with the effect of shear load.

3.7. Summary

This chapter describes the methodology for the incorporation of torsion to the extended simplified progressive collapse method. First, the method for incorporating the effect of torsion into the simplified method is described. Then, the main assumptions and a flow chart diagram of the proposed methodology are presented. An extensive description of the shear flow calculation in the cross section follows. Finally, the incorporation of torsional effect to the simplified method using reduction factors to the load shortening curves of the plates is explained.

Chapter 4

Strength of steel and aluminium alloy ship plating under combined shear and compression/tension

4.1. Introduction

This chapter presents the results of an extensive study of the strength of steel and aluminium alloy plating under combined loads of shear and compression/tension investigated, by the author, using the Non-Linear Finite Element Method (NLFEM). Initially, the settings for NLFEM modelling are described. Therefore, the material properties of steel and aluminium alloy 5083-H116 and 6082-T6, the mesh of the model, the initial geometric imperfections, residual stresses and the boundary conditions of the plates are discussed in detail.

Previous work for steel and aluminium plates subjected to axial loads has shown that the collapse of square plates will give an excellent estimate of the strength of long plates subjected to axial loads. The results presented are divided to two parts. In part 1, steel and aluminium plates with aspect ratio (a/b) 1 to 4 and slenderness ratio (β) 1 to 5 which are subjected to pure shear are presented. The results are shown similar behaviour for the plates with different aspect ratio under pure shear. In part 2, only square steel and aluminum plates (1000x1000mm) are examined since their behaviour under shear remains independent from the aspect ratio. A series of steel, aluminium alloy 5083-H116 and 6082-T6 plates with aspect ratio (a/b) equal to 1 and slenderness ratio (β) 1 to 6 is investigated under axial compression/tension, pure shear and combined compressive/tensile and shear loads. Finally, a summary of the prior investigation is discussed, pointing out the main outcome.

4.2. NLFEM modelling

4.2.1. Material properties

The stress-strain curves of steel, aluminium alloy 5083-H116 and aluminium alloy 5083-H116 in the heat affected zone (HAZ) are depicted in Figure 4.1. An elastic-perfectly plastic material behaviour was assumed for steel with yield stress $\sigma_o = 245MPa$, Young's Modulus $E = 207GPa$ and Poisson's number $v = 0.3$. The material behaviour of aluminium was described based on Ramberg-Osgood model approximation for the stress/strain curve, using Equation

4.1 and 'knee factor' (n) equal to 15 and 30 for aluminium alloy 5083-H116 and 6082-T6 respectively. The 0.2% proof stress is $\sigma_{0.2} = 215MPa$ (5083-H116) and $\sigma_{0.2} = 260MPa$ (6082-T6), Young's Modulus $E = 70GPa$ and Poisson's number $v = 0.33$.

$$\varepsilon = \frac{\sigma}{E} + 0.002\left(\frac{\sigma}{\sigma_{0.2}}\right)^{n} \qquad \text{Equation 4.1}$$

The stress/strain curve of both alloys in the Heat Affected Zone (HAZ) is described also by the same equation (Equation 4.1), but using a reduced proof yield stress ($\sigma_{0.2_{(HAZ)}}$) instead (Benson, 2011). Therefore, the reduced proof yield stress was taken equal to:

5083-H116: $\sigma_{0.2_{(HAZ)}} = 0.67 \cdot \sigma_{0.2} = 0.67 \cdot 215 = 144.05MPa$

6082-T6: $\sigma_{0.2_{(HAZ)}} = 0.53 \cdot \sigma_{0.2} = 0.53 \cdot 260 = 130.91MPa$

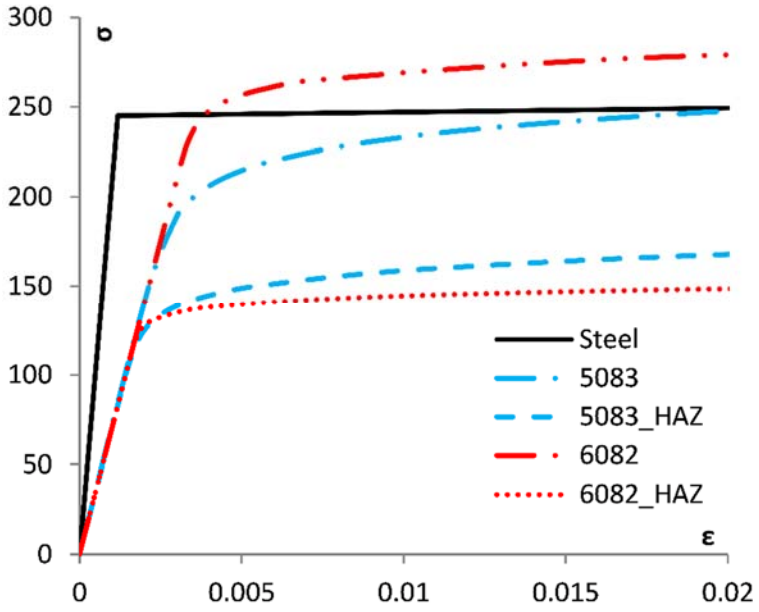

Figure 4.1: Stress/strain curves of steel, aluminium alloy 5083-H116, 6082-T6 and 5083-H116 & 6082-T6 in the HAZ

4.2.2. Mesh convergence study

All plates were modelled in ABAQUS using quadrilateral shell elements (S4R) with reduced integration which is valid for both thick and thin shell problems as previous studies have shown (Alinia et al., 2009), (Kristensen, 2001), (Benson, 2011). A mesh convergence study was conducted to select the element size. A square steel plate of slenderness ratio (β) equal to 3 and mesh size of 50mm, 20mm, 10mm and 5mm was examined under axial compression and pure shear. Its ultimate strength and critical shear stress are depicted in Figure 4.2 and Figure 4.3 respectively and both of them show to converge for mesh size less than 20mm. Therefore, an element size of 10mm is suitable to balance for computational time and accuracy.

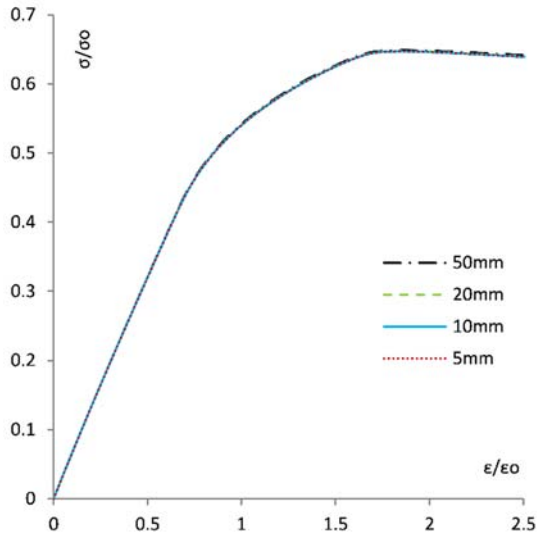

Figure 4.2: Mesh convergence study for steel constrained plate (β=3) under axial compression

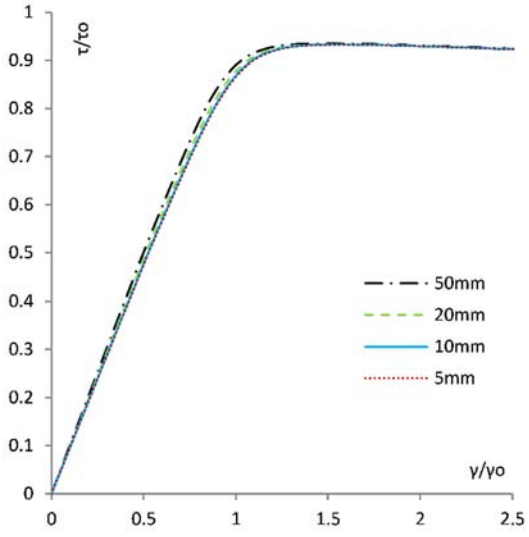

Figure 4.3: Mesh convergence study for steel constrained plates (β=3) under pure shear

4.2.3. Initial geometric imperfections

Previous studies (Frieze et al., 1977), (Smith et al., 1987), (Benson, 2011) have proved the influence of initial geometric imperfections to the ultimate strength of ship plating. Hence, an average level of initial imperfections with maximum amplitude $w_o = 0.1\beta^2 t$ and Fourier series imperfection shape described by Equation 2.8 and Equation 2.12 were taken into account according to Dow's (Dow and Smith, 1984) and Benson's research ((Benson, 2011). A typical representation combining 80% of a single half sine wave and 20% of a square half sine wave has been used along plate's length and a single half sine wave along its width, in order to incorporate a realistic distortion of critical elastic buckling mode. However, in the case where aspect ratio of the plate is equal to 1, the shape of the imperfections is single half sine wave along in both directions as it is the most conservative case and it's described by Equation 2.8 and the following equation:

$$\frac{w}{w_o} = \sin\left(\frac{\pi x}{a}\right)\sin\left(\frac{\pi y}{b}\right), \qquad for\ a/b = 1 \qquad \text{Equation 4.2}$$

4.2.4. Residual stresses/ Heat Affected Zone (HAZ)

The ultimate strength of steel plates under compression is affected by the tensile residual stress zone which is introduced to the plate due to welding (Frieze et al., 1977), (Smith et al., 1987), (Paik and Thayamballi, 2003), (Benson, 2011). Therefore, this zone is modelled along the unloaded sides of the plate. The width of the tensile zone for steel was calculated in order to achieve equilibrium between the tensile area of stress equal to $0.95\sigma_o$ and the compressive area with average level of longitudinal residual stresses equal to $\sigma_{rc}/\sigma_o = -0.15$ (Smith et al., 1987).

The width of the Heat Affected Zone (HAZ) for aluminium plates was taken 25mm along the unloaded sides of the plate according to Benson's research (Benson, 2011), (Kristensen, 2001). The tensile stress was assumed equal to $0.95 \cdot \sigma_{0.2_{(HAZ)}}$ and the compressive stresses were calculated as described in (Benson, 2011) in order to achieve equilibrium of the stresses on the plate.

4.2.5. Boundary conditions

A complex set of boundary conditions was developed in order to be valid not only for plates subjected to shear or axial compression/tension, but also in both loads simultaneously.

In the first part, the aim is to apply shear load as displacement in x direction on edge 3 (Figure 4.4). Therefore, all edges are simply supported. All nodes of edge 3 should have the same displacement in x direction, so they are constrained in x-direction. Additionally, edge 1 is fixed in x and z direction in order to fix the plate in the space and the unloaded edges (2 and 4) are constrained to remain straight but free to move in-plane. To clarify the boundary conditions of the unloaded edges, 'straight' means that all nodes e.g. at edge 2, retain the linearity of their displacement in x-direction between the corner nodes i.e. RP1 and RP4. The in-plane movement is free; however the nodes of the unloaded edges displace linearly in z direction between the corner nodes which depicts a realistic behaviour of the edges.

Thence, a relaxation step without load follows in order to obtain self-equilibrating residual stress distribution on the plate due to the initial distortions. In the first part, where only pure shear occurs, the load is applied as displacement in x direction on edge 3 using the Riks arc length and defining a particularly small step for each increment.

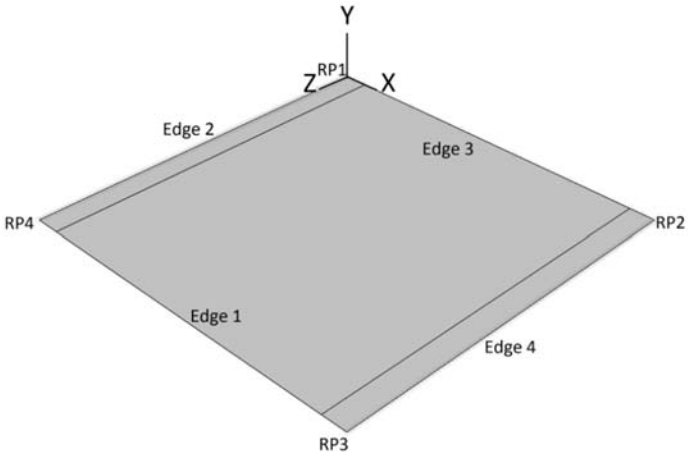

Figure 4.4: Finite element model of plate

In the second part, where the shear and axial compression/tension are applied simultaneously, the boundary conditions were kept the same. However, the case of

unrestrained unloaded edges was also investigated in which the edges 2 and 4 (Figure 4.4) are not constrained to remain straight. A relaxation step was applied again before the load in order to self-equilibrate the stresses on the plate due to initial distortions. The load is applied as displacement on edge 3 in:

- Z direction for axial compression/tension
- X direction for shear
- Z and x direction simultaneously for combined loads of axial compression/ tension and shear

4.3. Results Part I: Ship plating with aspect ratio (a/b) 1 to 4 under pure shear

The progressive collapse of steel and aluminium alloy 5083-H116 plates of slenderness ratio (β) 1 to 5 under pure shear is presented in Figure 4.5-Figure 4.14. Plates with constrained unloaded edges and slenderness ratio (β) 1 to 5 are examined for a range of aspect ratio (a/b) 1 to 4. The shear stress-shear strain curves of steel plates are presented in Figure 4.5-Figure 4.9 and aluminium alloy 5083-H116 plates in Figure 4.10-Figure 4.14, respectively.

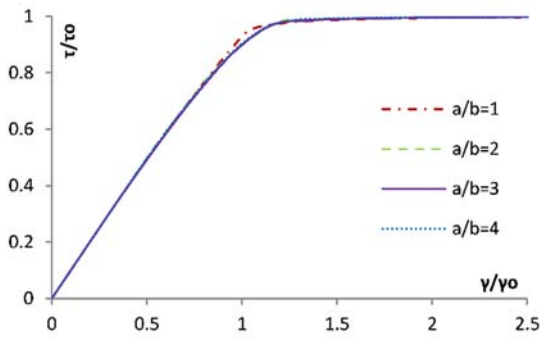

Figure 4.5: Steel plates with β=1 and a/b=1-4 under pure shear.

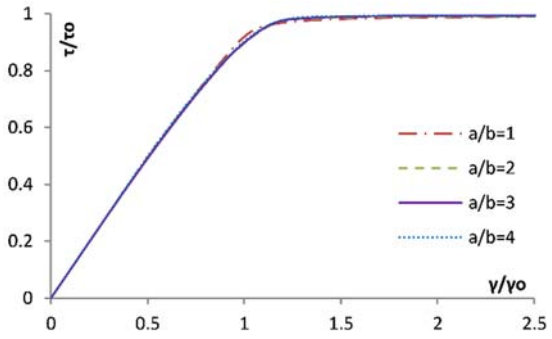

Figure 4.6: Steel plates with β=2 and a/b=1-4 under pure shear

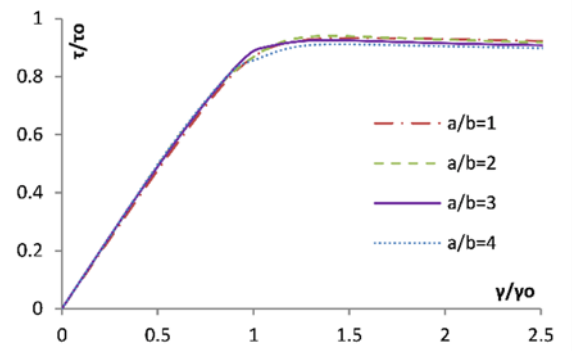

Figure 4.7: Steel plates with β=3 and a/b=1-4 under pure shear

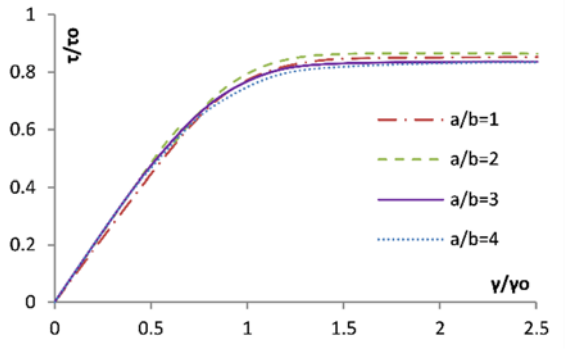

Figure 4.8: Steel plates with β=4 and a/b=1-4 under pure shear

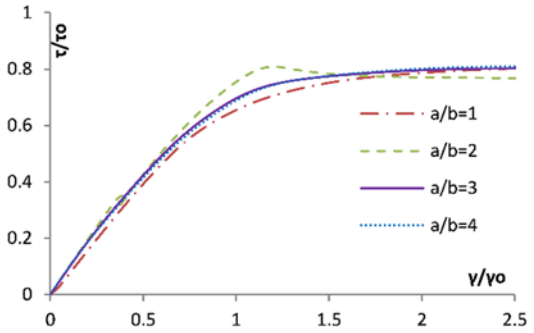

Figure 4.9: Steel plates with β=5 and a/b=1-4 under pure shear

The progressive collapse behaviour of constrained plates under shear seems to be independent of the aspect ratio (a/b) of plates with slenderness ratio (β) 1 to 4 for both steel and aluminum alloys, Figure 4.5 - Figure 4.9 and Figure 4.10 - Figure 4.14, respectively. Figure 4.15 and Figure 4.16 show Von-Mises contour plots for steel and aluminium plates of slenderness ratio (β) equal to 3 and aspect ratio (a/b) 1 to 4.

Figure 4.9 & Figure 4.14 show that only very slender plates with slenderness ratio (β) equal to 5 seem to be quite affected by aspect ratio. However, these plates (β=5) are very slender and they are not particularly used as ship plating (Chalmers, 1993). Their application is more common in aerospace structures for plates of this aspect ratio and higher.

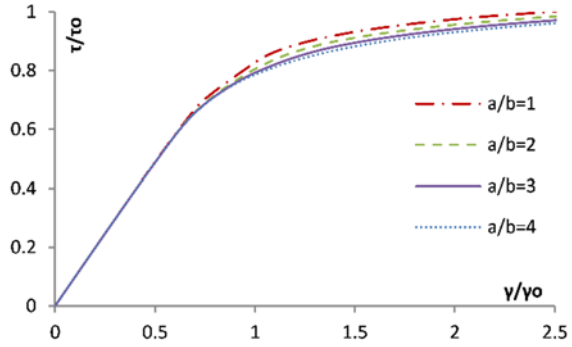

Figure 4.10: Aluminium alloy 5083-H116 plates with β=1 and a/b=1-4 under pure shear

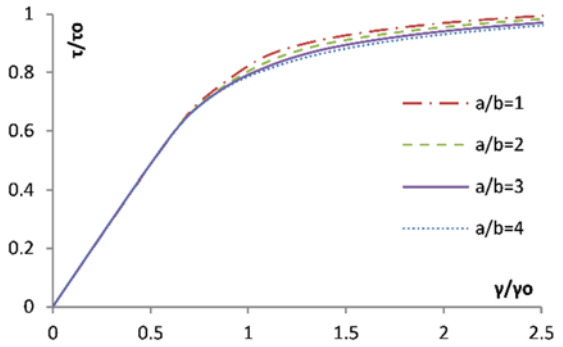

Figure 4.11: Aluminium alloy 5083-H116 plates with β=2 and a/b=1-4 under pure shear

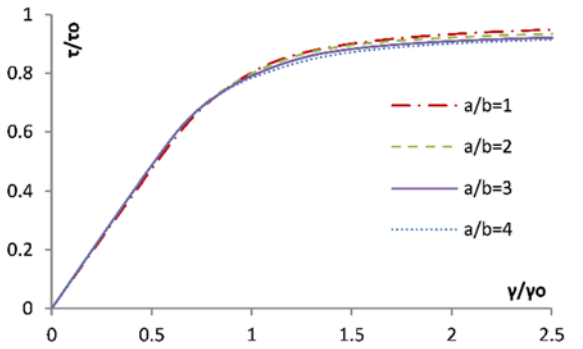

Figure 4.12: Aluminium alloy 5083-H116 plates with β=3 and a/b=1-4 under pure shear

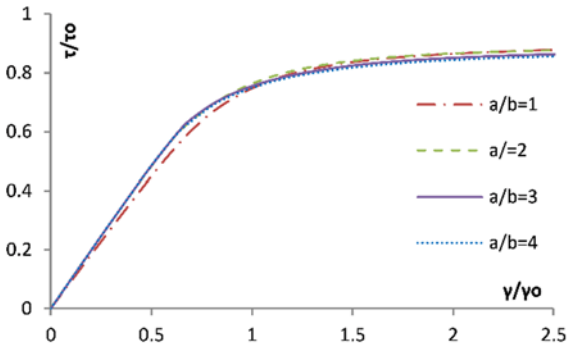

Figure 4.13: Aluminium alloy 5083-H116 plates with β=4 and a/b=1-4 under pure shear

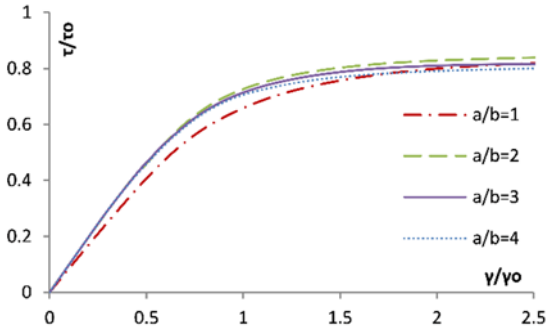

Figure 4.14: Aluminium alloy 5083-H116 plates with β=5 and a/b=1-4 under pure shear

The contour plots of Von-Mises equivalent stresses for steel and aluminium alloy 5083-H116 plates with typical slenderness value (β=3) and aspect ratio 1-4 subjected to pure shear are presented in Figure 4.15 and Figure 4.16 respectively. In the case of steel plates (Figure 4.15), all plates present approximately the same maximum shear stress value and the pattern of the shear stress distribution of the plate with aspect ratio equal to 1 is repeated twice, three and four times respectively to plates with aspect ratio 2, 3 and 4. The same pattern follows the aluminium plates under pure shear (Figure 4.16) but with lower values of maximum shear stress than in steel plates. Furthermore, the reduced 0.2% proof strain stress in the HAZ clearly depicted in the Von-Mises contour plots of aluminium plates.

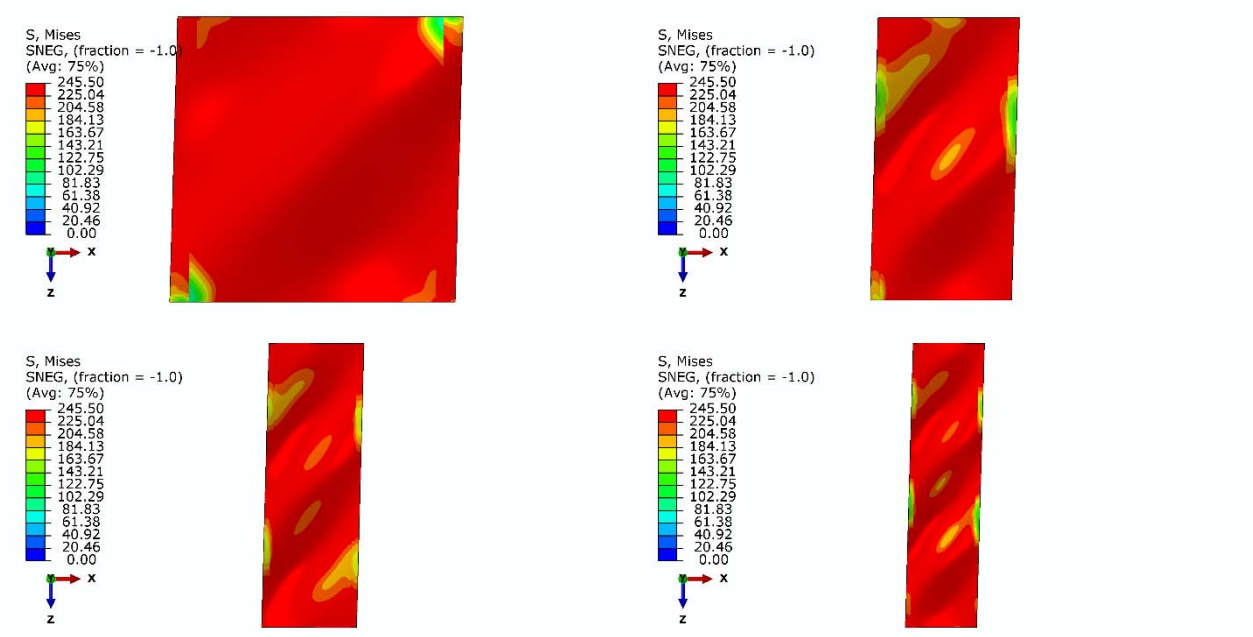

Figure 4.15: Von-Mises contour plots of restrained steel plates (β=3) under pure shear at collapse and $\gamma/\gamma_o \leq 2.5$, with a/b=1-4 magnify x10

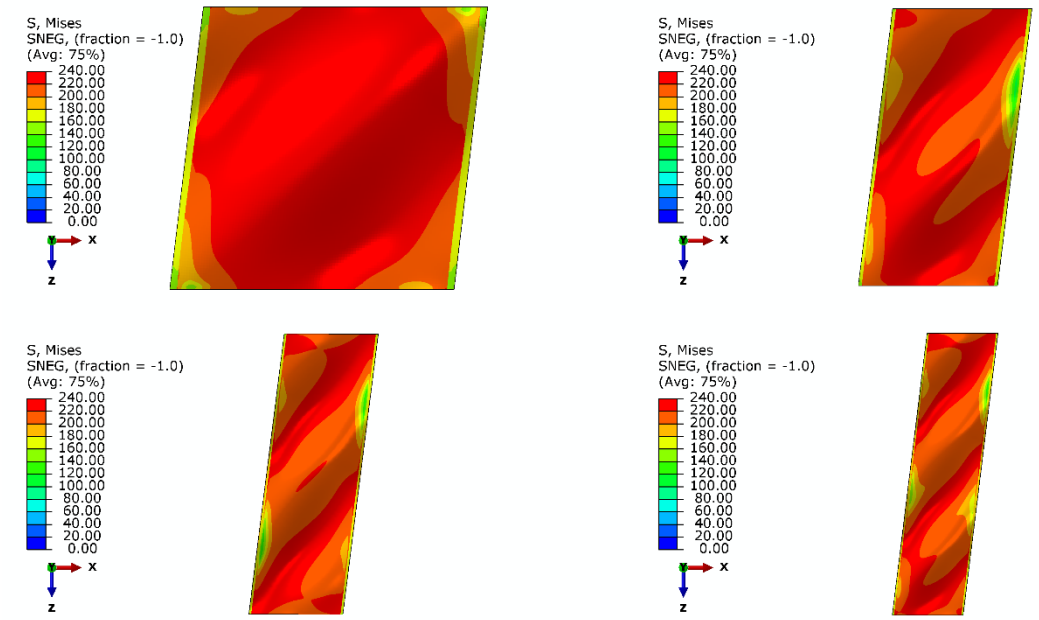

Figure 4.16: Von-Mises contour plots of restrained aluminium alloy 5083-H116 (β=3) under pure shear at collapse and $\gamma/\gamma_o \leq 2.5$, with a/b=1-4 magnify x10

4.4. Results Part II: Square ship plating under combined loads of axial compression/tension and shear

In this study, the progressive collapse behaviour of square (1000x1000mm) steel and aluminium alloy plates (5083-H116 and 6082-T6) under axial compression/tension, pure shear and combined loads of axial compression/tension and shear is investigated using finite element analysis. Initially, the plates are subjected only to axial compression/tension and to pure shear in order to investigate the effect of the constrained and unrestrained unloaded edges on the progressive collapse of the plate. The stress-strain curves of both cases are presented and the results are compared to well-known theoretical formulas which are mentioned in the literature review (section 2.5). These comparisons are shown in section 4.4.3 for steel, aluminium alloy 5083-H116 and aluminium alloy 6082-T6.

Finally, the interaction diagrams of axial compressive/tensile and shear loads for steel, aluminium alloy 5083-H116 and 6082-T6 plates and for slenderness ratio (β) 1 to 6 are presented in section 0. Each point in these diagrams depicts the maximum value of shear and compressive/tensile load which a plate may sustain. Therefore, these diagrams are used for the incorporation of torsion effect in the Simplified Progressive Collapse Method.

4.4.1. Steel, aluminium alloy 5083-H116 and 6082-T6 plates under axial compression/tension

A series of steel, aluminium alloy 5083-H116 and 6082-T6 plates with slenderness ratio (β) 1 to 6 is subjected to in-plane compression and tension. As it has already mentioned, two cases are examined for unloaded edges; one in which are free to move in plane (unrestrained) and another one in which are constrained to remain straight (constrained). The stress-strain curves of these plates under pure compression/tension are presented in Figure 4.17 to Figure 4.22 for a range of slenderness ratio (β) 1 to 6.

The load shortening curves of steel square plates are depicted in Figure 4.17 and Figure 4.18 for unrestrained and constrained edges, respectively. It seems that constrained plates become stiffer than unrestrained due to the constraints of unloaded edges which is expected and their ultimate strength increases too. However, this is not the case for very stocky plates (β=1)

which fail though plastic yielding and their ultimate strength is independent from the boundary conditions on the unloaded edges.

Similar pattern to steel plates under direct in-plane compression and tension seems to follow aluminium alloy 5083-H116 and 6082-T6 plates (Figure 4.19 to Figure 4.22). Non-stocky constrained aluminium plates present higher values of compressive and tensile stress which may sustain and become stiffer in comparison to unrestrained plates. In addition, there are no particular differences in the behaviour between alloy 5083-H116 and 6082-T6 plates with the same boundary conditions, unrestrained (Figure 4.19 and Figure 4.21) and constrained (Figure 4.20 and Figure 4.22) under compression/ tension.

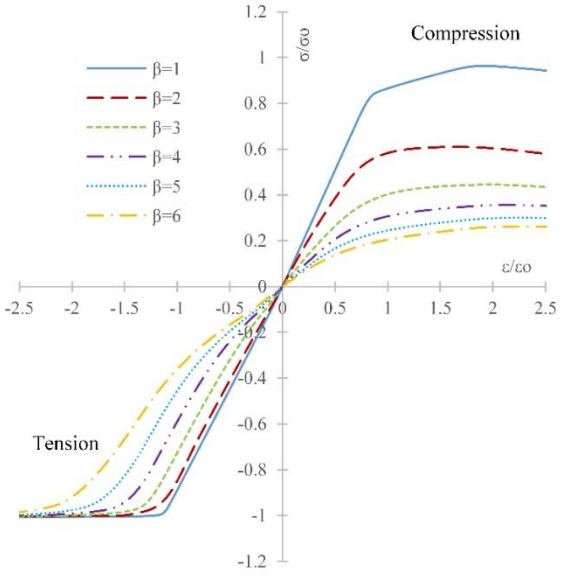

Figure 4.17: Stress-strain curves of unrestrained steel plates under axial compression/tension

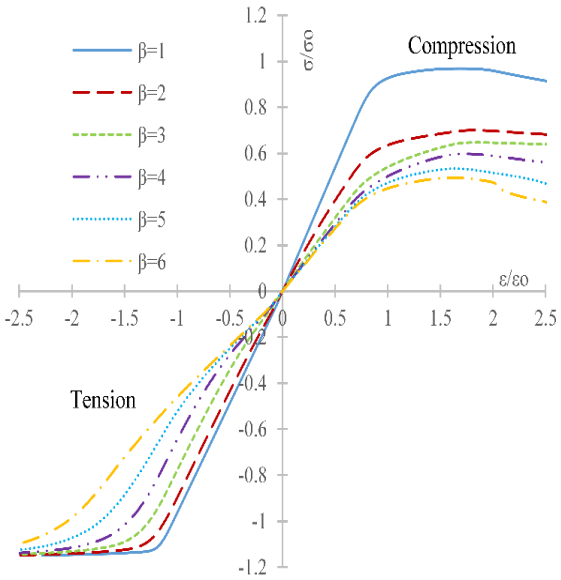

Figure 4.18: Stress-strain curves of constrained steel plates under axial compression/tension.

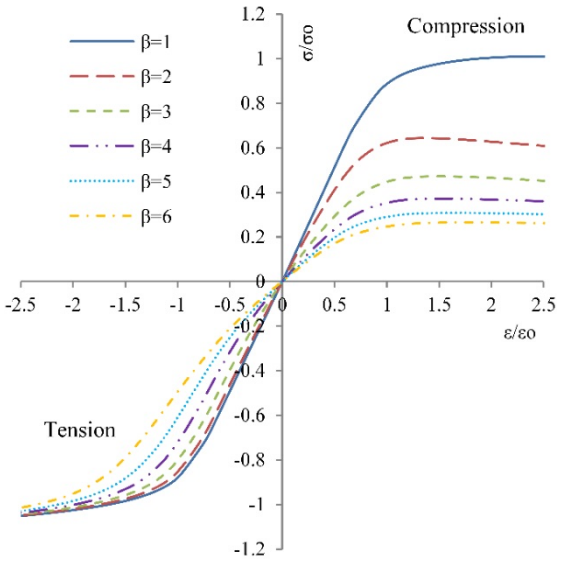

Figure 4.19: Unrestrained aluminium alloy 5083-H116 plates under axial compression/tension

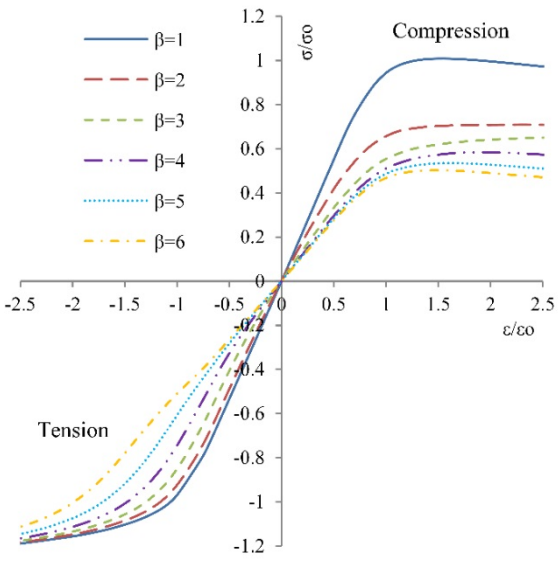

Figure 4.20: Constrained aluminium alloy 5083-H116 plates under axial compression/tension

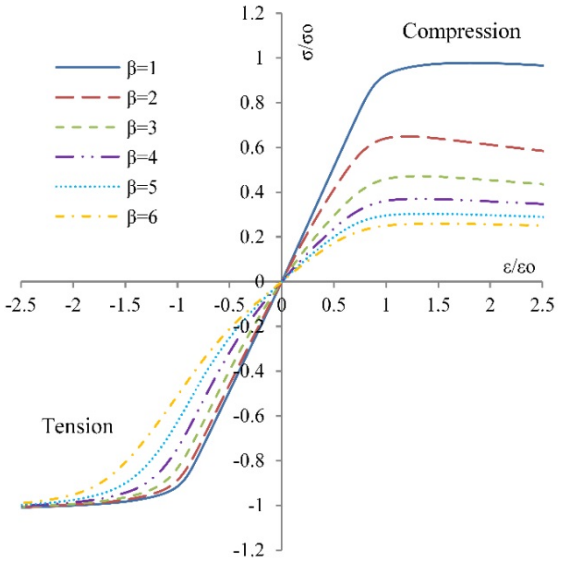

Figure 4.21: Unrestrained aluminium alloy 6082-T6 plates under axial compression/tension

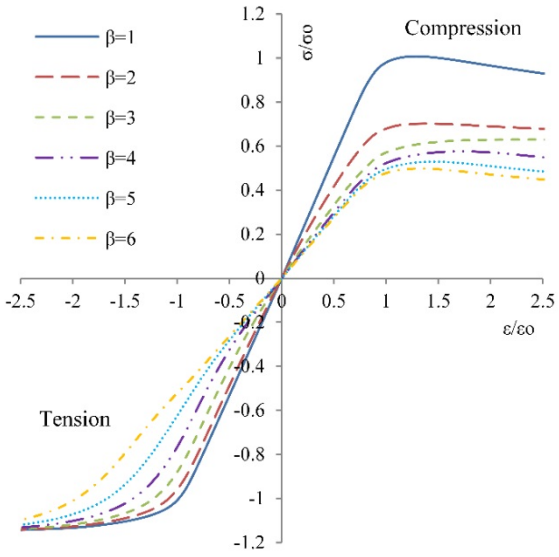

Figure 4.22: Constrained aluminium alloy 6082-T6 plates under axial compression/tension

4.4.2. Steel, aluminium alloy 5083-H116 and 6082-T6 plates under pure shear

The same series of steel and aluminium plates which was investigated under compression/shear in section 4.4.1 was also subjected to pure shear. The critical shear stress-shear strain curves of this series are presented in Figure 4.23 to Figure 4.28. The behaviour of stocky (β=1, 2) steel unrestrained plates remains unaffected by the boundary conditions of unloaded edges and failure occurs due to shear yielding (Figure 4.23). Critical shear stress decreases as plate becomes more slender and shear buckling occurs. The shear stress-strain curves of constrained steel plates (Figure 4.24) follow similar pattern but slender plates (β>2) show increased critical shear stress and stiffness in comparison with unrestrained plates.

The behaviour of aluminium alloy 5083-H116 (Figure 4.25 & Figure 4.26) and 6082-T6 (Figure 4.27 & Figure 4.28) plates does not differ from this of steel plates under pure shear. The shear stress- strain curves show shear stress to increase as plate becomes more slender, stocky plates not to be affected by the boundary conditions of unloaded edges and only slender plates are affected becoming stiffer and increasing their critical shear stress.

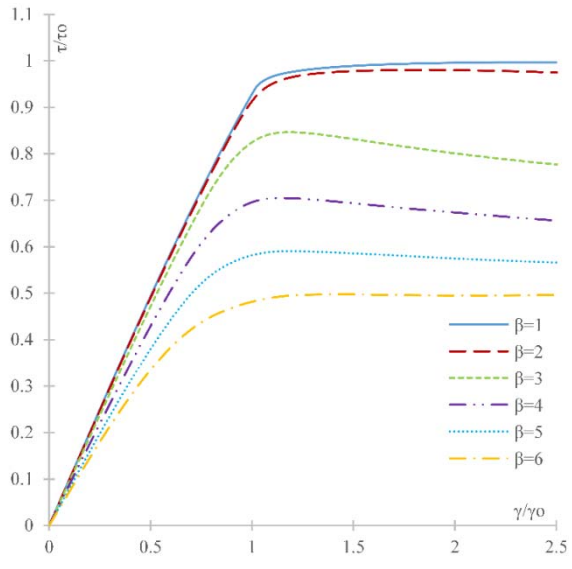

Figure 4.23: Shear stress-shear strain curves of unrestrained plates under pure shear

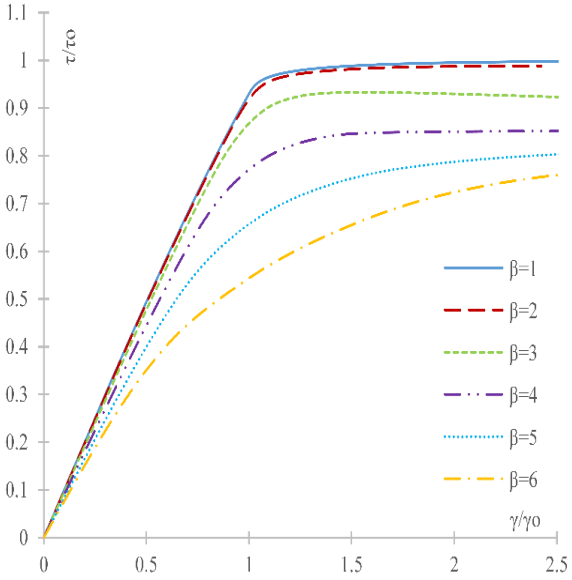

Figure 4.24: Shear stress-shear strain curves of constrained plates under pure shear.

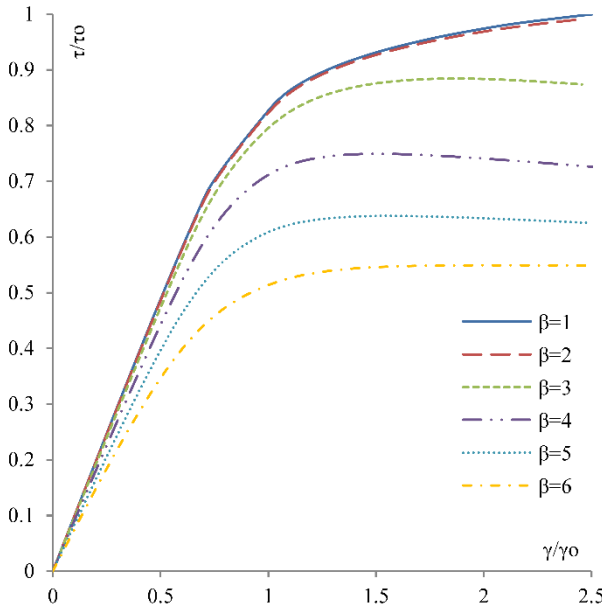

Figure 4.25: Unrestrained aluminium alloy 5083-H116 plates under pure shear

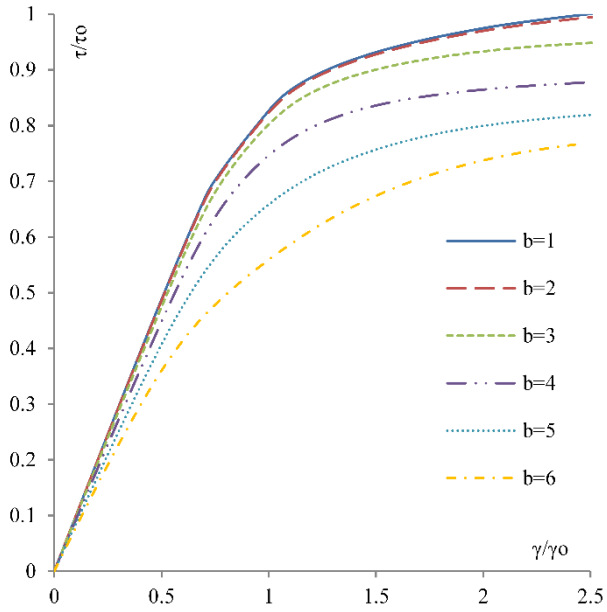

Figure 4.26: Constrained aluminium alloy 5083-H116 plates under pure shear

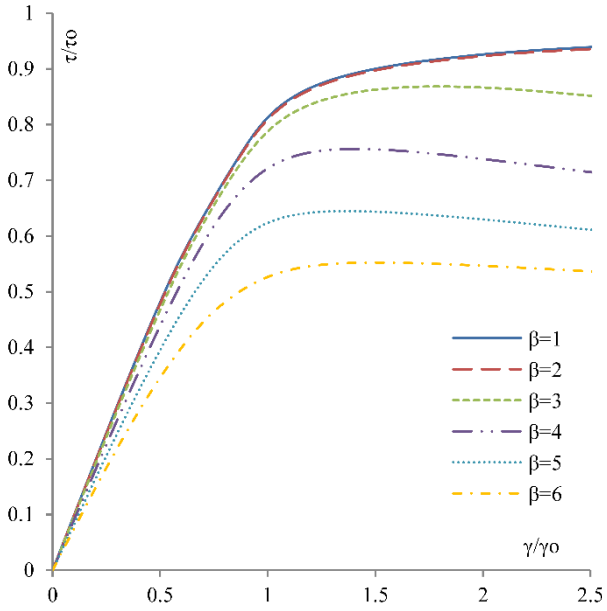

Figure 4.27: Unrestrained aluminium alloy 6082-T6 plates under pure shear.

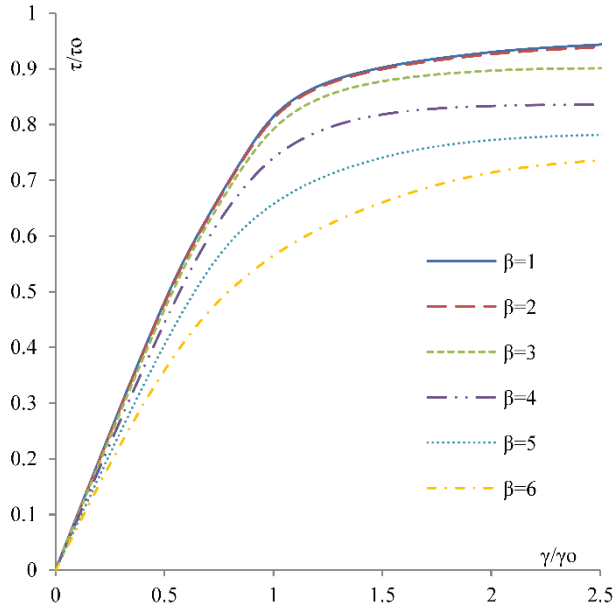

Figure 4.28: Constrained aluminium alloy 6082-T6 plates under pure shear.

4.4.3. Comparison of ultimate strength and critical shear stress of steel, aluminium alloy 5083-H116 and 6082-T6 plates with theoretical formulas and previous studies

A comparison of the nonlinear finite element results of ultimate strength of plates under pure axial compression and pure shear with relevant theoretical formulas and other studies was taken part. The purpose of this comparison is to validate the boundary conditions which are applied to plate models under combined loads of compression/ tension and shear, since are the same with these of separate load cases of axial compression and pure shear.

The direct stress of unrestrained steel plates under axial compression is compared with Chalmers' results, Faulkner's theoretical formula (Equation 2.6) and critical elastic stress formulation with corrected plasticity by Johnson-Ostenfeld (Equation 2.5) in Figure 4.29. All of these formulas/studies are referring or have been applied to unrestrained plates. The graph of the F.E. results for unrestrained plates shows a good correlation with Faulkner's theoretical values and Chalmers's results as it follows the same pattern and does not overestimate plates' ultimate strength. Differences are expected as we compare F.E. results with theoretical values (Faulkner) and a different study (Chalmers') in which all parameters and analysis are not exactly the same.

The critical elastic stress formulation with corrected plasticity by Johnson-Ostenfeld estimates critical elastic direct stress which is much lower than plate's ultimate strength when buckling occurs in the elasto-plastic area for slender plates ($\beta>2$). However, in the case of stocky plates ($\beta<2$) which yield in plasticity region, Johnson-Ostenfeld formulation agrees well with the rest studies and formulas.

The nonlinear finite element results of plates with constrained edges are also presented in Figure 4.29. Stocky plates ($b<2$) which their ultimate strength is not affected by constraints on the unloaded edges show good correlation with the compared formulas and studies which are referring to unrestrained plates. The direct stress of slender plates ($\beta>2$) is higher due to the constrained edges which provide additional strength to the plate. However, the reason of including the F.E. results of these plates in the graph (Figure 4.29.) is not in order to validate their boundary conditions but to obtain an estimation of their difference in ultimate strength.

In addition, these findings agree with Frieze's study on the ultimate load behaviour of plates in compression (Frieze et al., 1977).

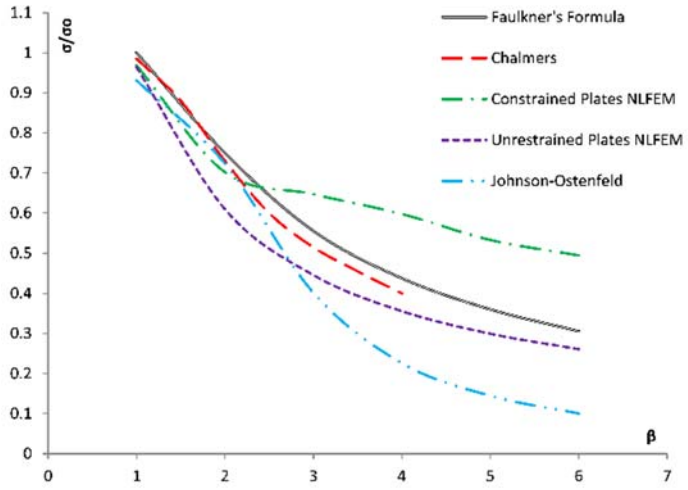

Figure 4.29: Comparison of N.L.F.E. results of the current study with other studies and theoretical values of the ultimate strength of steel plates under axial compression.

The critical shear stress of both unrestrained and constrained steel plates under pure shear is compared with theoretical formulas proposed by Nara (Equation 2.25), Johnson-Ostenfeld (Equation 2.23), Paik and Thayamballi (Equation 2.28), Zhang (Equation 2.24) and Eurocode 3 (Equation 2.27) in Figure 4.30. All formulations are referred to constrained plates and provide the critical shear stress except Johnson-Ostenfeld's formulation. This formulation estimates the elastic shear stress of plates with correction due to plasticity which is lower than ultimate shear stress. The ultimate shear stress of stocky plates ($\beta<2$) according to all formulations and F.E. results does not particularly differ. Unrestrained slender plates ($\beta>2$) are affected by the boundary conditions of unloaded edges and its critical shear stress is decreasing much more than this of constrained plates. The graph of slender constrained plates follows similar pattern to Zhang's, Nara's, Paik and Thayamballi's and Eurocode 3 formulations. The critical shear stress for plates with slenderness ratio (β) equal to 3 show very good agreement with the developed empirical formula by Paik and Thayamballi (Equation 2.28) and for plates with slenderness ratio (β) more than 4 with Nara's formulation (Equation 2.25).

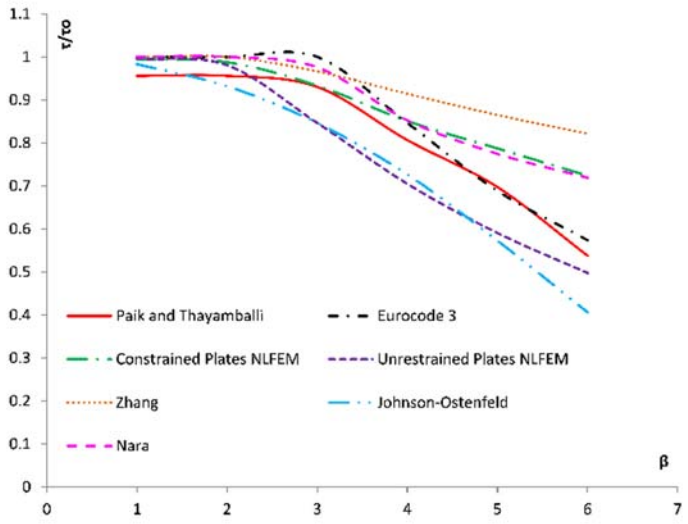

Figure 4.30: Comparison of N.L.F.E. results of the current study with other studies and theoretical values of the critical shear stress of steel plates under pure shear.

Aluminium alloys 5083-H116 and 6082-T6 plates under axial compression are compared with theoretical formulations in Figure 4.31 and Figure 4.32, respectively. Both aluminium alloys 5083-H116 and 6082-T6 present similar behaviour under axial compression, therefore only the behaviour of 5083-H116 is analysed in detail and any difference which occurs with 6082-T6 is commented.

The ultimate strength of unrestrained and constrained aluminium alloy plates is compared with Faulkner's formula (Equation 2.6), Eurocode 9 (Equation 2.13 - Equation 2.20) and Paik and Duran's formulation (Equation 2.21) in Figure 4.31 and Figure 4.32. The graph of unrestrained plates presents similar pattern to Faulkner's empirical formula for unrestrained plates and Eurocode 9 results. The ultimate strength of stocky constrained plates ($\beta<2$) is not affected by the boundary conditions of the unloaded edges and it decreases as the plate becomes more slender but much less than in the case of unrestrained edges. Paik and Duran's graph for slender plates ($\beta>2$) is close to Faulkner's, Eurocode 9 and the F.E. graph for unrestrained plates but following different slope.

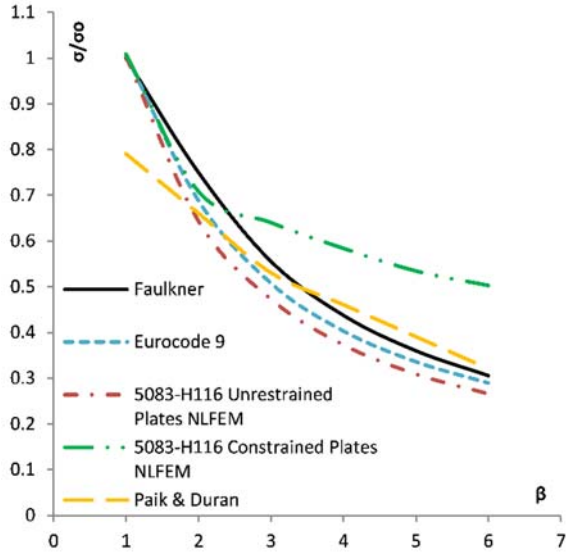

Figure 4.31: Comparison of NFEM results of the current study with theoretical values of the ultimate strength of aluminium alloy 5083-H116 plates under axial compression.

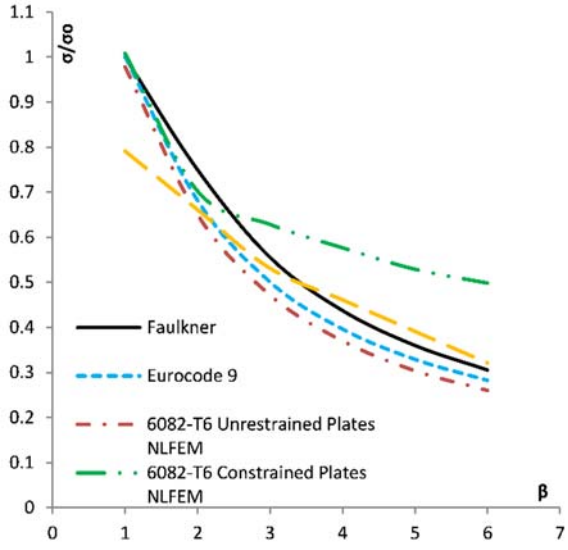

Figure 4.32: Comparison of F.E. results of the current study with other theoretical values of the ultimate strength of aluminium alloy 6082-T6 plates under axial compression.

The critical shear stress of aluminium alloys 5083-H116 and 6082-T6 plates under pure shear is compared with Eurocode 9 formulas (Equation 2.29 - Equation 2.34) in Figure 4.33 and Figure 4.34 respectively. Stocky plates (β<2) subjected to shear are also independent from the boundary conditions at the edges. Constrained slender plates withstand higher levels of critical shear stress than unrestrained plates. However, the graphs in both cases have similar curvature.

Eurocode's 9 formulations for non-slender plates estimate critical shear stress due to yield and an additional buckling check is required for slender plates. The estimated critical shear stress for non-slender plates (β<2) according to Eurocode's 9 formulations is higher than the non-linear finite element results but both graphs follow the same pattern, a straight horizontal line. The buckling shear stress of slender plates (β>2) shows similar tendency with the non-linear finite element results.

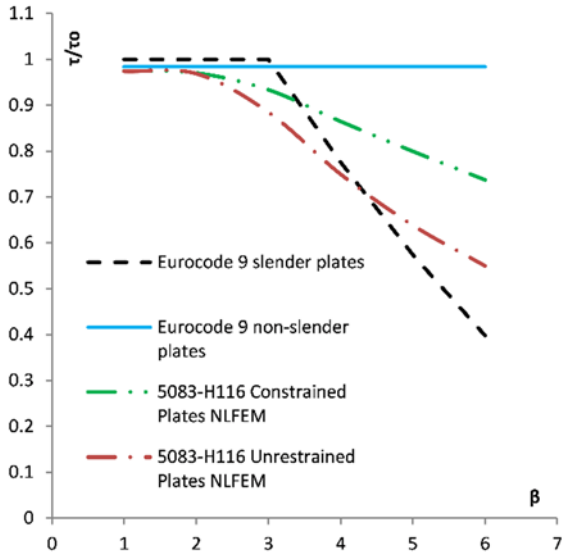

Figure 4.33: Comparison of NFEM results of the current with theoretical values of the critical shear stress of aluminium alloy 5083-H116 plates under pure shear.

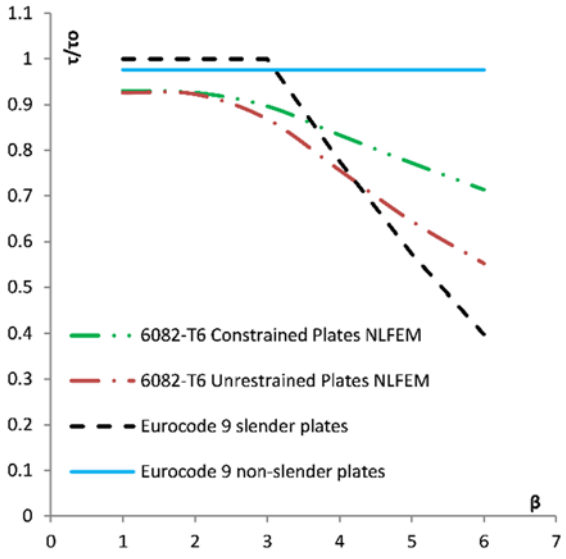

Figure 4.34: Comparison of F.E. results of the current study with other theoretical values of the critical shear stress of aluminium alloy 6082-T6 plates under pure shear.

4.4.4. Interaction diagrams of axial compressive/tensile and shear loads for steel, aluminium alloy 5083-H116 and 6082-T6 plates

The interaction diagram of axial compressive and shear loads for steel and aluminium alloy 5083-H116 and 6082-T6 plates with unrestrained and constrained edges are presented in Figure 4.37 - Figure 4.42. Each point depicts the peak direct stress and the peak shear stress of plates under these combined loads. In cases where either the direct or shear stress components have failed to reach a peak value, limitations have been set for the interaction relationship. In this case, values of either direct or shear stress at strain values of ε/εo=2 or γ/γo=2 are used to define the failure stresses for the interaction diagram (Figure 4.35 & Figure 4.36).

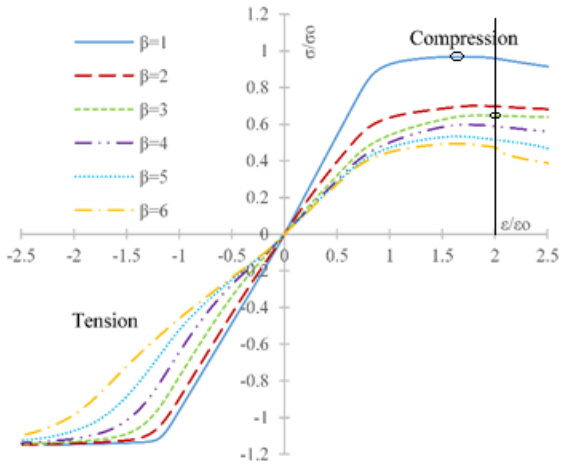

Figure 4.35: Strain limit of ε/εo = 2 and examples of direct axial stress values for the interaction diagram

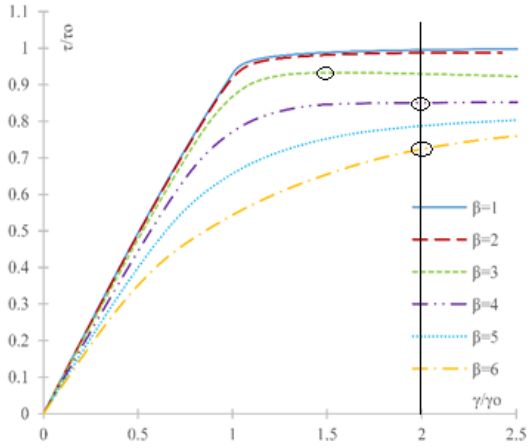

Figure 4.36: Shear strain limit of γ/γo = 2 and examples of direct shear stress values for the interaction diagram

The interaction diagrams of steel plates with unrestrained and constrained edges are depicted in Figure 4.37 and Figure 4.38, respectively. Figure 4.37 shows that very stocky unrestrained steel plates (β=1) follows the Mises yield criterion, according to which $(\sigma/\sigma_o)^2 + (\tau/\tau_o)^2 = 1$ and slender unrestrained plates present high insensitivity of compressive strength to shear for proportions up to $0.5\tau_o$. In the case of constrained steel plates (Figure 4.38), very stocky (β=1) and less stocky plates (β=2, 3) behave in a similar manner to the Mises criterion. The

insensitivity of the compressive strength to applied shear remains, but for lower proportions of shear and for very slender plates (β=4, 5, 6). The ultimate and critical shear strength of constrained plates with slenderness ratio (β) higher than 2 under pure axial compression/tension and pure shear is increased in comparison with these of unrestrained plates, as already it has been mentioned in previous sections.

The interaction diagrams of aluminium alloy 5083-H116 plates with unrestrained and constrained edges are depicted in Figure 4.39 and Figure 4.40, respectively. Similar pattern occurs between steel (Figure 4.37) and aluminium alloy 5083-H116 (Figure 4.39) with unrestrained edges where stocky plates (β=1) follows the Mises yield criterion and very slender plates (β>2) develop high insensitivity to shear. Buckling remains the dominate reason of failure for low proportions of shear to axial compressive load and shear starts to affect plate's strength when it reaches approximately the 50% of shear yield stress. The behaviour of plates with slenderness ratio β=2 is similar to the behaviour of stocky plates but without verifying the Mises yield criterion. The interaction diagram of the constrained aluminium alloy 5083-H116 plates in Figure 4.40 does not present particular differences from this of steel constrained plates (Figure 4.38). Very stocky plates (β=1) comply with Mises criterion and less stocky plates (β=2, 3) behave in a similar manner. The influence of shear load to the axial compressive strength is greater in the case of slender plates (β=4, 5, 6) and shear buckling occurs for low proportions of shear to direct stress. However, the behaviour of aluminium constrained plates under combined tensile and shear loadings seems to differ from this of steel plates, especially for very slender plates (β=6).

The interaction diagrams of aluminium alloy 6082-T6 plates with unrestrained and constrained edges are depicted in Figure 4.41 and Figure 4.42, respectively. There no particular differences between the interaction diagrams of aluminium alloys 5083-H116 and 6082-T6. Only, in the case of very slender (β=5, 6), unrestrained aluminium alloy 6082-T6 plates, shear insensitivity occurs for lower proportions of shear than in the same case for aluminium alloy 5083-H116.

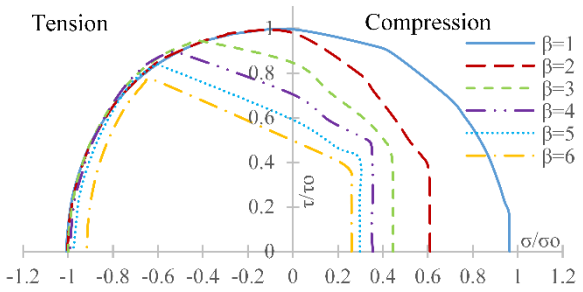

Figure 4.37: Interaction diagram of axial compressive/tensile and shear loads for unrestrained steel plates.

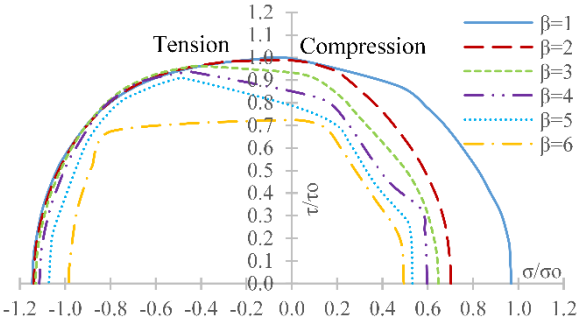

Figure 4.38: Interaction diagram of axial compressive/tensile and shear loads for restrained steel plates.

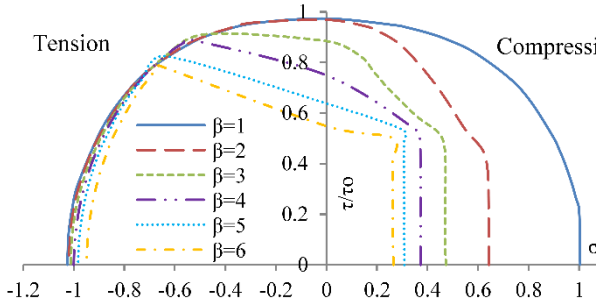

Figure 4.39: Interaction diagram of axial compressive/tensile and shear loads for unrestrained aluminium alloy 5083-H116 plates.

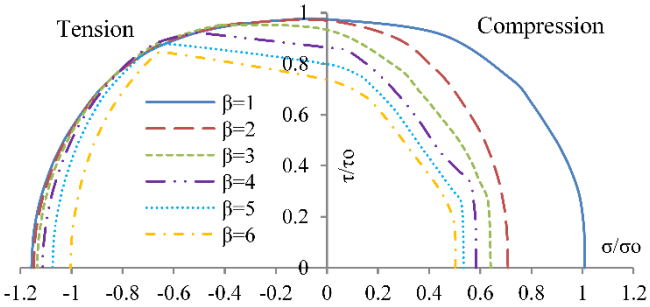

Figure 4.40: Interaction diagram of axial compressive/tensile and shear loads for restrained aluminium alloy 5083-H116 plates.

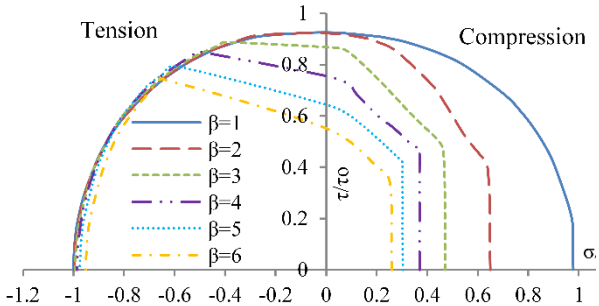

Figure 4.41: Interaction diagram of axial compressive/tensile and shear loads for unrestrained 6082-T6 plates.

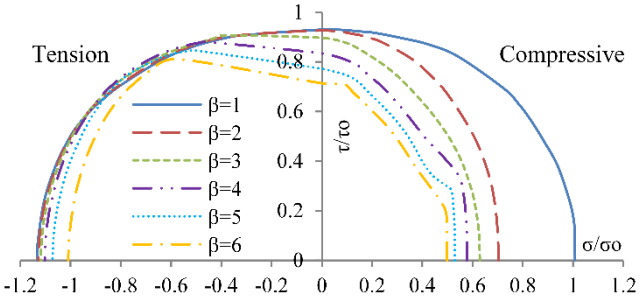

Figure 4.42: Interaction diagram of axial compressive/tensile and shear loads for restrained 6082-T6 plates.

4.5. Summary

The strength of steel and aluminium ship plating under axial compression/tension, shear and combined compressive/tensile and shear loadings was investigated in this chapter. Initially, all parameters for setting up the plate model of non-linear finite element analysis are described analytically. Then, the study was divided to two parts.

In the first part, steel and aluminium plates with constrained edges, aspect ratio (a/b) 1 to 4 and slenderness ratio (β) 1 to 5 are subjected to pure shear. The results show that the progressive collapse behaviour of plates under pure shear is not affected by the aspect ratio (a/b) of the plates. Therefore, only square plates (a/b=1) were investigated further in the second part.

In the second part, square plates with slenderness ratio (β) 1 to 6 are subjected to axial compressive/tensile, shear and combined compressive/tensile and shear loads, applying the same boundary conditions. The effect of constraining unloaded edges, keeping them straight, was also investigated. Initially, axial compressive/ tensile and shear loads are applied separately. Then, the results are compared with theoretical formulas and previous studies in order to validate the boundary conditions which are applied to the plate. Finally, the plates are subjected to combined loads of axial compression/tension and shear and their interaction diagrams are generated. These diagrams show the ultimate strength which a plate may sustain under a certain/ defined amount of critical shear stress. The results show that the constraints of unloaded edges enhance the ultimate strength of slender plates but not also the strength of stocky plates. Slender constrained plates are more susceptible to shear than unrestrained plates which show high shear insensitivity and buckle due to axial compressive loadings. Finally, steel, aluminium alloy 5083-H116 and 6082-T6 plates of the same slenderness ratio and with the same constraints applied to the unloaded edges follow similar pattern in their interaction diagrams without the material causing particular differences.

Chapter 5

Progressive Collapse Assessment of Intact Box Girders under Combined Bending and Torsional Loads

5.1. Introduction

This chapter presents the results of four intact box girders under combined bending and torsion. The size of the box girder remains the same in each case but its cross section alters in order to investigate the effect of torsional rigidity on the structure. Initially, the geometric characteristics and the material properties of these box girders are presented. Then, all models are subjected to pure torsion using the nonlinear finite element method and defining the torsional capacity of each box girder. Since their torsional ultimate strength is known, each box girder is then subjected to combined torsional and bending loads, applying first different fractions of its maximum torsional load followed by vertical bending moment (sagging) until collapse. Each analysis is conducted using the nonlinear finite element method and the proposed extended progressive collapse method. An interaction diagram of these combined loads is derived for each box girder, defining the limit of the ultimate strength and a safe zone in which the structure may sustain these loads. The same procedure is repeated for box girders under combined torsional loads and vertical bending moment (hogging), but only the most critical cases have been examined due to time limitations. Finally, a comparison of these results from both nonlinear FEA and the simplified method follows.

5.2. Geometric characteristics of intact box girders

5.2.1. Types of intact box girders

A relatively large box girder of **12.6m width, 8.4m height and 12.6m** length was selected to be modelled for the purpose of this study. Its material is steel with yield stress of **245Mpa** and Young's modulus **207GPa** with linearly elastic- perfectly plastic stress-strain curve. The model was chosen based on the results of previous studies (Syrigou, 2012) and (S. D. Benson et al., 2013) in which two intact box girders of different size, a small one (W=4.8m, H=4.2m, L=9.0m) and a large one (W=12.6m, H=8.4m, L=12.6m), with the same plate slenderness ratio (β) and column slenderness ratio (λ) are initially subjected to vertical bending moment. Then,

different level of damage was applied to them and their behaviour under vertical bending moment was investigated. The results of this study showed that in most cases (i.e. intact and damage), overall collapse occurs to the large box girder but not also to the small box girder which fails between its transverse frames (interframe collapse).

Therefore, a large steel size box girder (**12.6m width, 8.4m height and 12.6m length**) was assumed to be more suitable for further investigation and closer to a more realistic representation of a ship hull girder. Additionally, four different types of cross sections were selected for investigation in order to understand the behaviour of the box girder as its St. Venant torsional constant (k) alters. These cross sections are described as follows in sections 5.2.1.1 - 5.2.1.4.

5.2.1.1. Box Girder A

The cross section of the Box Girder A is depicted in Figure 5.1. Standard tee bar stiffeners whose dimensions are shown in Figure 5.2, were used throughout the Box Girder A and they are spaced **600mm** apart. Each plate has a transverse frame spacing of **1800mm**, therefore according to Equation 2.7 the slenderness ratios (β) of top/bottom (t=8mm) and side (t=10mm) flanges are 2.58 and 2.064 respectively. The section of 1800mm length consists a bay and the whole model consists of 7 bays (total length of model **12600mm**) which are separated by transverse frames. The size of the transverse frames is the double of the longitudinal stiffeners size and their dimensions are shown in Figure 5.2.

Additionally, the torsional constant (k) of this cross section was calculated according to the described methodology in chapter 3 and the result was validated against Lloyd's program (see appendix A). Its torsional constant (**k**) is equal to $\mathbf{9.27 \times 10^{12}\ mm^4}$.

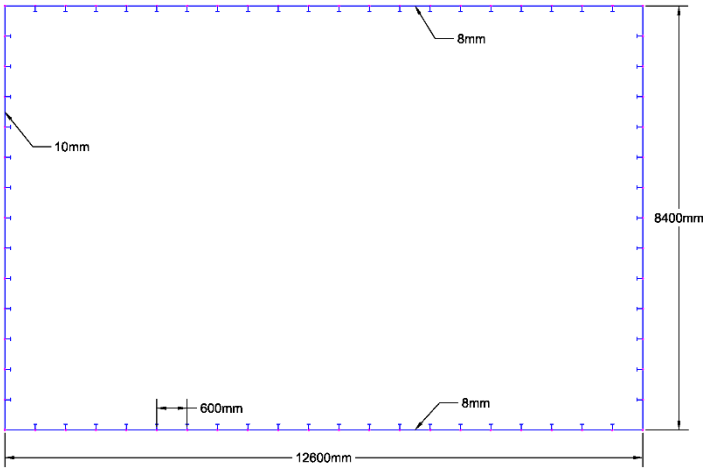

Figure 5.1: The cross-section of Box Girder A

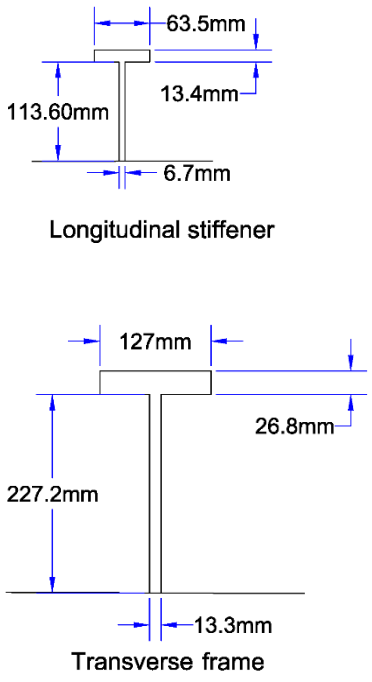

Figure 5.2: Dimensions of longitudinal stiffener and transverse frame

5.2.1.2. Box Girder B

The cross section of Box Girder B was derived from the cross section of Box Girder A adding a double bottom (t=10mm) in a distance of **1800mm** above the baseline (BL). This cross section is shown in Figure 5.3 and it was selected in order to increase the torsional rigidity of Box Girder A creating cells in the cross section. The longitudinal stiffeners are the same with those of Box Girder A and the slenderness ratios (β) of the double bottom (t=10mm) and inner side (t=8) flanges are 2.064 and 2.58 respectively. The rest of the structure remains the same with that of Box Girder A, consisting by 7 bays of 1800mm length each, which are separated by transverse frames as depicted in Figure 5.2.and without any solid floors in the double bottom.

Finally, the torsional constant (k) of Box Girder B was calculated and validated against Lloyd's program (see appendix A). Its value is slightly increased in comparison to the k value of Box Girder A due to the added cells. The torsional constant (k) of Box Girder B is equal to $\mathbf{9.95 \times 10^{12} mm^4}$.

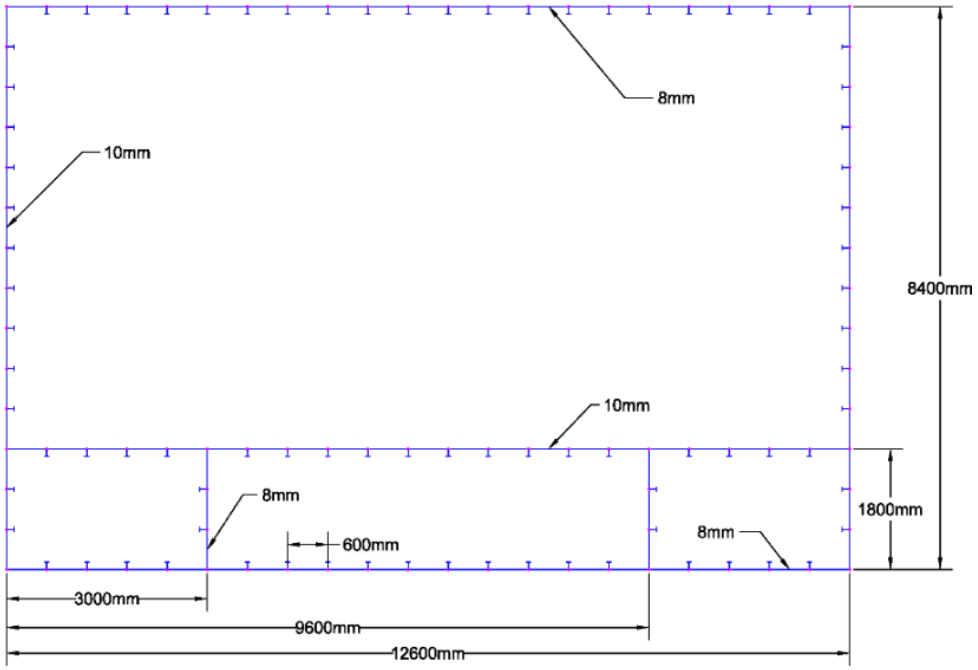

Figure 5.3: The cross-section of Box Girder B

5.2.1.3. Box Girder C

A cross section which resembles more to a ship's cross section was also modelled. Inner doubled sides and an intermediate deck (4800mm above BL) were added in the cross section of Box Girder B. This cross section is depicted in Figure 5.4 and the slenderness ratios (β) of the inner side shell (8mm) and intermediate deck (10mm) flanges are 2.58 and 2.064, respectively. The longitudinal stiffeners remain the same throughout the cross section and the structure is consisted by 7 bays of 1800mm length each, which are separated by transverse frames as depicted in Figure 5.2.

The torsional constant (k) of Box Girder C was also calculated and validated against Lloyd's program (see appendix A). Its torsional rigidity is obviously increased in comparison to the k value of Box Girder A and it is equal to $\mathbf{10.55 \times 10^{12}\ mm^4}$.

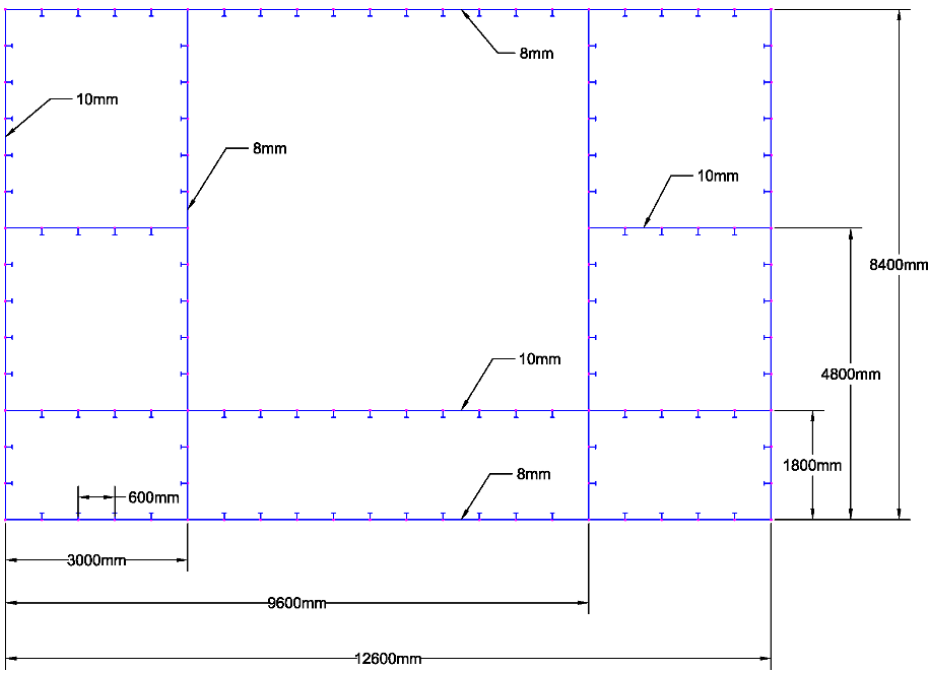

Figure 5.4: The cross-section of Box Girder C

5.2.1.4. Box Girder D

Torsion might become critical for the case where the torsional rigidity of the structure is low, due to a non-continuous main deck, as it has already mentioned (section 2.3.4). This occurs in case where there are large openings in the structure due to its design or as result of damage. Therefore, a model with a large opening, called Box Girder D, was examined which was created from Box Girder C removing its upper deck. Its cross section is depicted in Figure 5.5.

The structure of Box Girder D is facsimile of Box Girder C structure, with exception of the removed upper deck. It is consisted by 7 bays of 1800mm length each, separated by transverse frames (Figure 5.2). At this point, it should be mentioned that the thickness of the plates in the first and last bay of this model were thickened up. Their thickness was doubled in order to keep the same boundary conditions in all boxes for the F.E. analysis and apply the torsional load between the bulkheads. Further explanation is given in the relevant section (5.3.3).

The torsional constant (k) of Box Girder D is significantly reduced due to the existence of the open deck and it is equal to $\mathbf{2.5 \times 10^{12}\ mm^4}$.

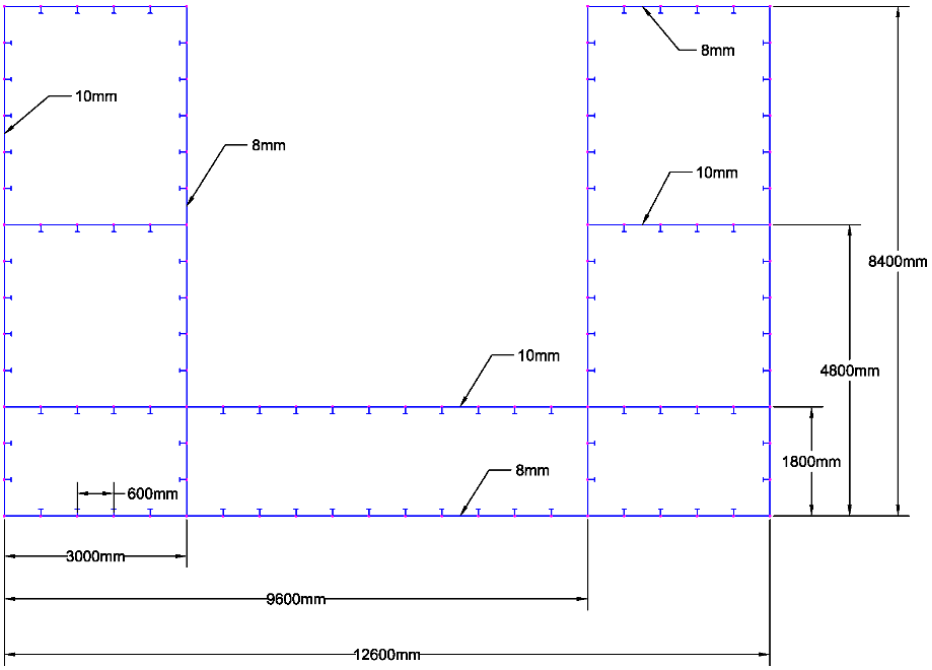

Figure 5.5: The cross-section of Box Girder D

5.2.2. Initial geometric imperfections

The geometric imperfections which are introduced to the stiffened panels during their construction process were taken into account for the analysis and their distribution was assumed as multi-mode Fourier half sine which must be zero at the transverse frames. The plate and stiffener imperfections of a stiffened panel are described according to Benson's study (Benson, 2011) and they are defined in the following sections.

5.2.2.1. Plate imperfections

The plate imperfections are described by Equation 5.1 re-arranging Equation 2.12 for the axis system which is shown in Figure 5.9 and they are depicted in Figure 5.6. An average level of maximum amplitude equal to $w_o = 0.1\beta^2 t$ is assumed according to Equation 2.8. Therefore, plate imperfections are defined as:

$$\frac{w_{pl}}{w_o} = \left(0.8\sin\left(\frac{\pi u}{a}\right) + 0.2\sin\left(\frac{m\pi u}{a}\right) + 0.01\sin\left(\frac{(m+1)\pi u}{a}\right)\right)\sin\left(\frac{\pi v}{b}\right), \quad \text{Equation 5.1}$$

$$m = int\left(\frac{a}{b}\right) + 1$$

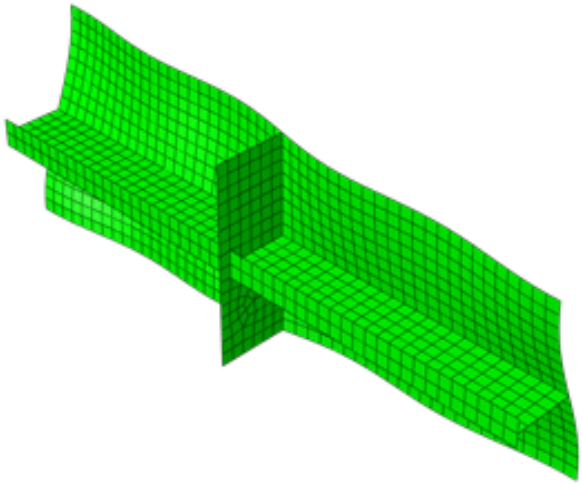

Figure 5.6: Plate imperfection combine 80/20 single mode to square mode (m) (Benson, 2011)

The shape of plate imperfections along the width of the plate is a half sine wave equal to the width of the plate. The shape of plate imperfections along plate's length is a combination of 80% of single half sine wave (Figure 5.7), 20% of a "square" mode half sine wave (m) (Figure 5.8) and 1% of a higher mode (m+1) according to Equation 5.1. The first two modes incorporate an initial distortion distribution which provides a realistic buckling mode of the plate. The last mode (m+1) ensures the nucleation of collapse only to one part of the plate.

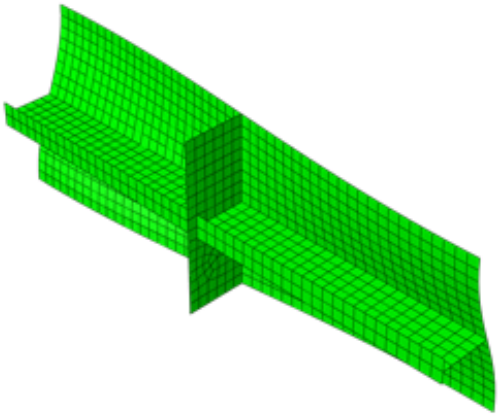

Figure 5.7: Plate imperfections single mode (Benson, 2011)

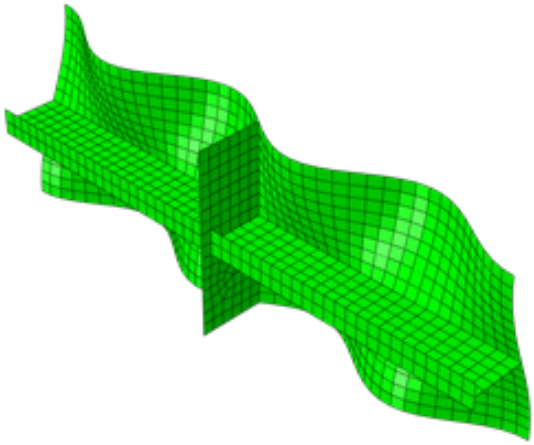

Figure 5.8: Plate imperfections square mode(m) (Benson, 2011)

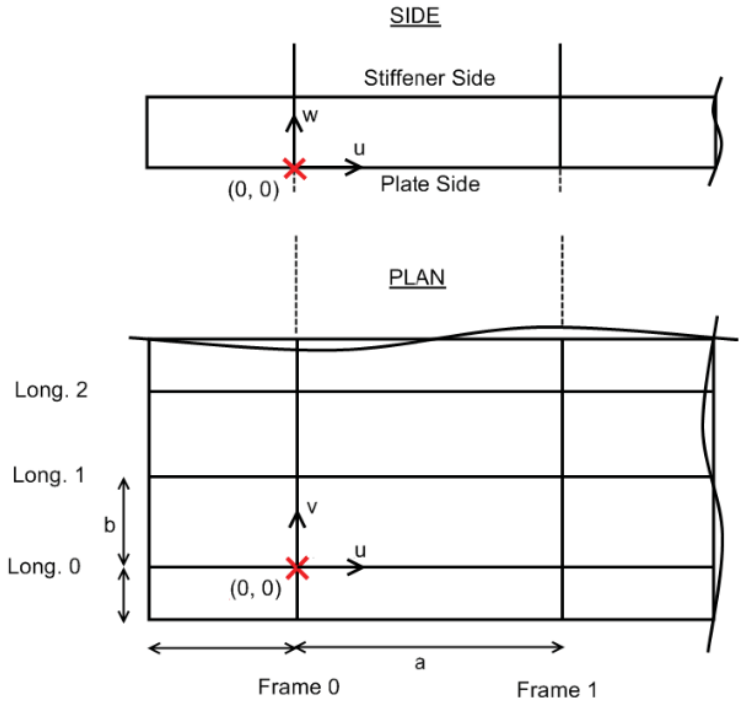

Figure 5.9: Panel coordinate system (Benson, 2011)

5.2.2.2. Stiffener imperfections

Three types of stiffener imperfections, as well as the plate imperfections described in section 5.2.2.1, were considered according to Benson's research (Benson, 2011) which are:

- ***Stiffener side imperfection***

Stiffener's side imperfection is the eccentricity of the whole stiffener from its vertical position as it is depicted in Figure 5.10. The initial distortions due to eccentricity are given by the following equation:

$$\frac{v_s}{w_{os}} = \frac{w}{h_w}\left(0.8\sin\left(\frac{\pi u}{a}\right) + 0.2\sin\left(\frac{i\pi u}{a}\right)\right), i = int(a/h_w) + 1 \qquad \text{Equation 5.2}$$

Where:

- $w_{os} = 0.002a$, w = coordinate in z-axis (Figure 5.11)
- a = plate length; h_w = web height

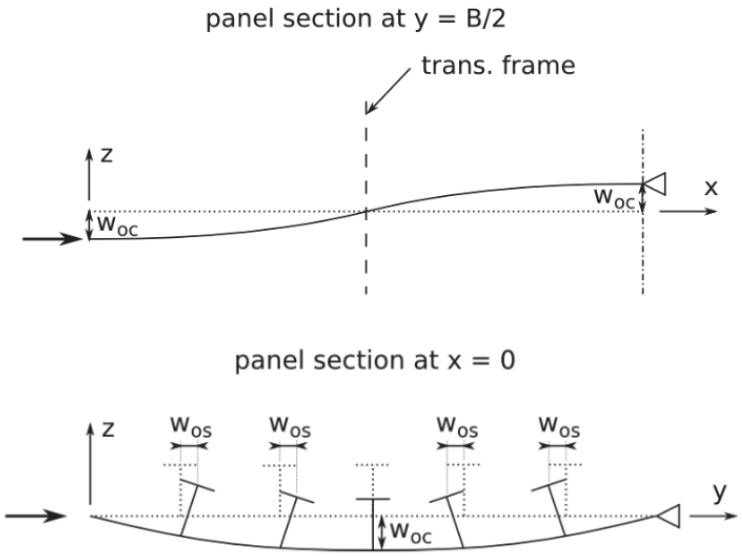

Figure 5.10: Stiffener side and column imperfection (Benson, 2011)

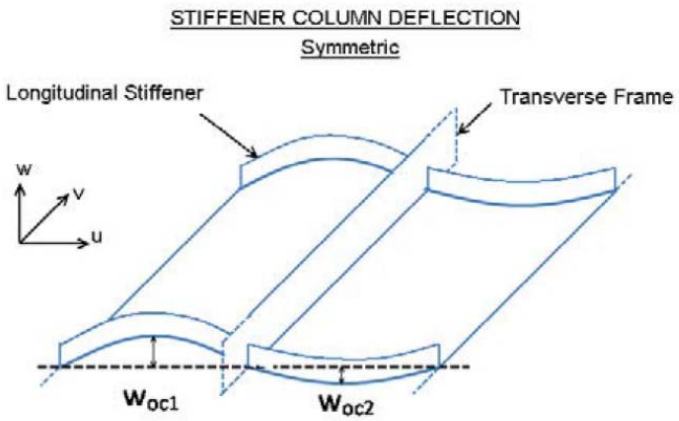

Figure 5.11: Stiffener column deflection (Benson, 2011)

- ***Stiffener web imperfection***

The stiffener web imperfection was considered as the out of flatness of the web stiffener which is depicted in Figure 5.12 and it is calculated by the following equation:

$$\frac{w_{web}}{w_{ow}} = \left(0.8\sin\left(\frac{\pi u}{a}\right) + 0.2\sin\left(\frac{i\pi u}{a}\right)\right), i = int(a/h_w) + 1 \qquad \text{Equation 5.3}$$

Where:

- $w_{ow} = 0.001a$, a = plate length; h_w = web height

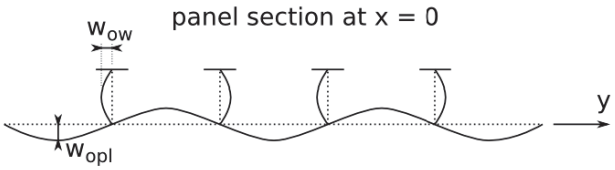

Figure 5.12: Stiffener web imperfection (Benson, 2011)

- ***Column imperfection***

The column imperfection is the "out of flatness of the entire panel" (Benson, 2011) in the longitudinal direction of the panel between its transverse frames (Figure 5.10). The shape of a single half wave which alters its direction at each transverse frame (Figure 5.11) represents the distribution of column distortions and it is described as:

$$\frac{w_c}{w_{oc}} = \sin\left(\frac{\pi u}{a}\right) \qquad \text{Equation 5.4}$$

The ratio of the deflection between transverse frames is given by Equation 5.5 and their magnitudes by Equation 5.6:

$$\frac{w_{oc2}}{w_{oc1}} = -0.25 \qquad \text{Equation 5.5}$$

$$w_{oc} = \begin{Bmatrix} 0.0008a, & \lambda < 0{,}2 \\ 0.0012a, & 0.2 < \lambda < 0.6 \\ 0.0015a, & \lambda > 0.6 \end{Bmatrix} \qquad \text{Equation 5.6}$$

The total initial distortions which are applied to each node with the method of direct node translation are given by Equation 5.7. The new coordinates of the node (u', v', w') are:

$$u' = u, \qquad v' = v + v_s, \qquad w' = w + w_{pl} + w_{web} + w_c \qquad \text{Equation 5.7}$$

5.2.3. Residual stresses

Residual stresses which are introduced to the structure due to welding were also taken into consideration. A tensile residual zone along each longitudinal side of the plate was considered with tensile stress equal to 95% of yield stress (245MPa). The width of each zone was calculated according to Equation 2.9 and for average level of residual stresses (Equation 2.11).

5.3. Intact box girders under torsion using NLFEM

5.3.1. Introduction

In this section, a mesh convergence study and sensitivity analysis of Box Girder A under torsional load is presented. Then, the boundary conditions and solution methods which applied to all box girders are discussed and explained thoroughly. Finally, the F.E. results of each box girder under pure torsion are presented separately, showing the torsional moment-angle relationship and the contour plots of Von-Misses stresses, shear stresses and displacement.

5.3.2. Mesh convergence and sensitivity analysis

Initially, a conventional four node shell element (S4R) with reduced integration (5 points) was chosen for the Nonlinear Finite Element Analysis. This type of element is commonly used in the literature e.g. (Alinia et al., 2009), (Zhang et al., 2008b), (Benson, 2011) as it is capable of solving non-linear problems with large-strain formulations and it satisfactory handles thick and slender plates. Each node has six degrees of freedom (three translational and three rotational).

A mesh convergence study for Box Girder A was carried out for elements of 330mm and 50mm size as it is shown in Figure 5.13. A previous mesh convergence study of 100mm, 50mm, 35mm and 25mm element size has been carried out for a smaller size box girder (**4.8m width, 4.2m height and 9.0 m length)** (Syrigou, 2012) showing convergence for size element less than 50mm. Since the size of the current model is larger than the size of the model in the previous study, it was assumed that a mesh element size of 50mm provides reliable results. In addition, the prohibitive computational time for the analysis with smaller size element (more than 2 weeks for a model of 25mm element size subjected only one load) plus the instability of the analysis led to this decision.

Different types of solution were selected due to the fact that F.E. analysis was extremely unstable. Their differences are covered in the relevant sections (section 5.3.3 & 5.3.4). Initially, a very coarse mesh size of 330mm (S4R) was chosen using Riks analysis, in order to obtain a rough estimate of the torsional capacity of Box Girder A. Then, every attempt to reduce the mesh size failed and a 50mm shell element size without reduced integration (S4) was selected.

This type provided satisfactory results for the analysis of this model under pure torsional load but did not work for all cases.

In cases where high geometric non-linearity occurred or high torsional loads were applied to the model, this element type (S4) was not suitable for the convergence of Riks analysis. Therefore, an element type (S4R) of 50mm size was finally selected for both static implicit analysis using Riks and dynamic explicit analysis.

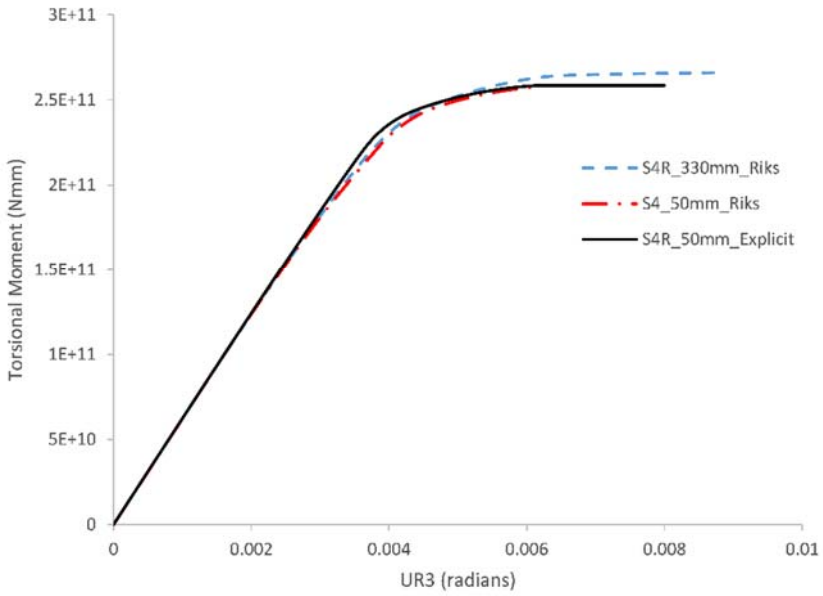

Figure 5.13: Mesh convergence study for Box Girder A

5.3.3. Boundary conditions

The described box girders were modelled in ABAQUS adding two robust transverse bulkheads (of 30mm thickness) to each F.E. model. The position of these bulkheads is at the end of the 1st bay and at the beginning of the 7th (last) bay of the model and their purpose is to ensure that the structure collapses between these bulkheads.

As it has already mentioned in section 5.2.1.4, the thickness of the plates in 1st and 7th bay for Box Girder D was doubled. This was carried out because the model of Box Girder D without increased plate thickness (in the 1st & 7th bay) under torsion, was failing outside the region of these two bulkheads. Therefore, their thickness was increased preventing shear stresses to dominate the plates outside of this region.

The boundary conditions depend also on the selected computational method. In this study, static Riks analysis and explicit dynamic analysis are used and explained thoroughly in section 5.3.4. Therefore, the boundary conditions slightly differ due to the requirements of each method and their differences are discussed in the following sub-sections.

5.3.3.1. Initial boundary conditions

The initial settings and constrains which applied to Box Girder B are shown in Figure 5.14 and similar settings and constraints were applied to every model. The aim is to apply the same rotational displacement in all nodes of End-1 and retain End-2 fixed. As stated before each node has 6 degrees of freedom (3 translational and 3 rotational). Therefore, all nodes in End-2 need to be constrained in all degrees of freedom in order to fix End-2.

A controlled rotational displacement in z axis (UR3) should be applied for torsion in all nodes at End-1 and at the same time their rotational displacement in x axis (UR1) should be zero in order to keep End-1 plane. For this purpose, all nodes at End-1 are tied to RP-1 which is a reference point in the space, with a rigid body constraint. In this way, any constraint or load which is applied to RP-1 is automatically transmitted to all nodes of End-1. Thus, both rotational displacements in z axis (UR3) and x axis (UR1) are constrained in the initial step.

5.3.3.2. Relaxation step

A relaxation step takes place before the load step in the case where the latter step is solved using static analysis. The relaxation step aims to self-equilibrate the residual stresses on the structure, therefore static analysis without any load is applied. This will ensure the equilibrium between applied residual stresses and initial distortions.

In the case which dynamic explicit analysis is applied, this step (relaxation) is omitted and the load during the dynamic explicit analysis is applied extremely slowly, allowing to the model to self-equilibrate its residual stresses.

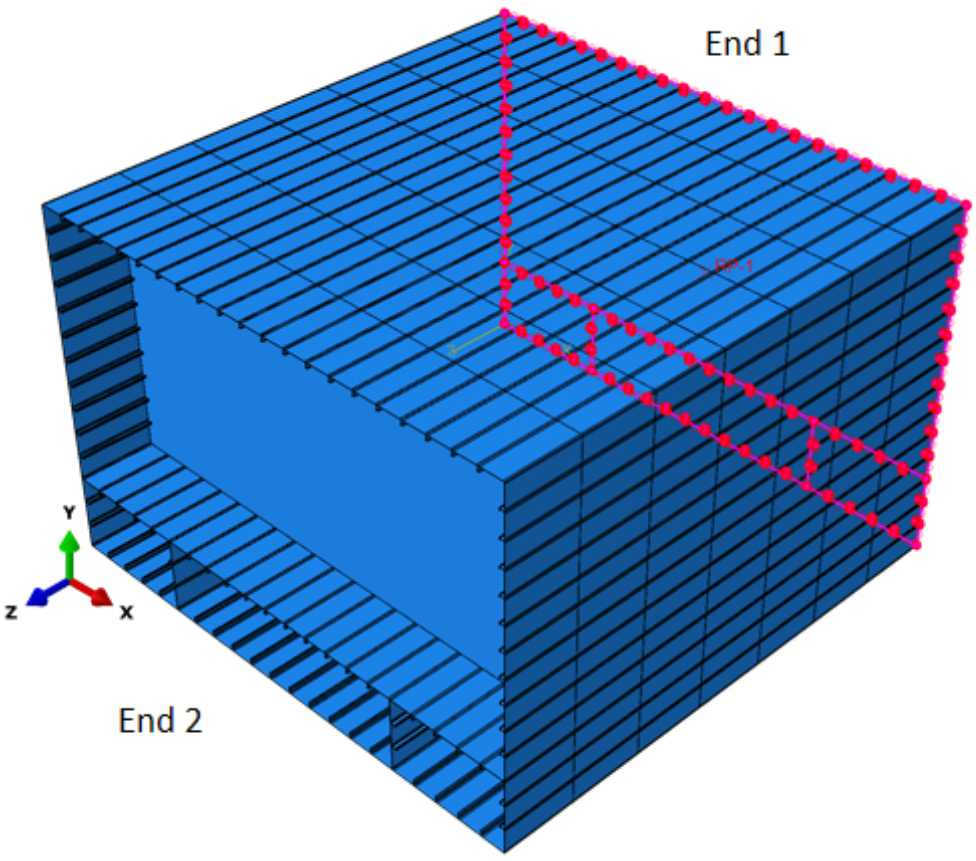

Figure 5.14: Boundary conditions for Box Girder B

5.3.3.3. Torsional load

In both solution methods, static and dynamic explicit analysis, the load is applied as controlled rotational displacement in z axis (UR3) to RP-1 point. This displacement generates an incremental torsional moment at End-1 which leads the model to collapse. How the displacement is applied depends on the selected computational method and it is described in detail in the following section (5.3.4).

5.3.4. Solution methods

Both geometric and material nonlinearity are modelled in the analysis of the four box girders. Geometrically nonlinear behaviour occur due to large rotation and large displacement (buckling) in the structure. Any large deformation of the structure may change the load direction, therefore the deformed structural geometry should be taken into account. Furthermore, material nonlinearity is introduced due to the nonlinear stress-strain relationship of the material (e.g. elastic-plastic behaviour of steel). The recommended solution methods for nonlinear problems are:

5.3.4.1. Riks Analysis

Riks analysis is an arc length incremental method which performs particularly well for static problems susceptible to snap through behaviour during the analysis (e.g. buckling analysis). Therefore, rotational moment is applied as controlled rotational displacement (UR3) to RP-1 and the maximum arc length increment is defined with a small value in order to ensure the reliability of the solution.

However, static solution (Riks) fails to converge in many cases of this study and convergence is achieved only in some cases where the mesh size of the model is very coarse (330mm). In these cases, dynamic explicit analysis is used despite the fact that the problem is considered to be quasi-static in nature.

5.3.4.2. Dynamic Explicit Analysis

A time independent problem (static problem) may be solved using dynamic analysis if the load is applied very slowly to the structure achieving a quasi-static analysis. The criterion to assume

a dynamic analysis as quasi-static according to ABAQUS manual, is a percentage up to 5% of kinetic (ALLKE) to strain (ALLIE) energy in the model.

An extensive parametric study was carried out in the case of Box Girder A under pure bending due to the fact that its static solution was available for comparison and it is presented in section (5.4.2.1). In this study, load is applied in different time periods using dynamic explicit analysis and the results are compared to these of its equivalent static solution. Convergence is achieved when the percentage of kinetic to internal energy is less than 0.5%. Therefore, this percentage is checked in every dynamic explicit analysis for Box Girder A and it should be less than 0.5% in order to assume the analysis as quasi-static and its results valid.

In the other cases i.e. Box Girder C and Box Girder D which explicit dynamic analysis is required, the percentage of ALLKE/ALLIE is calculated by running a 200sec and 300sec time step for the explicit analysis of each model under pure torsion and pure vertical bending.

The load is applied to the reference point RP-1 point as controlled rotational displacement (UR3) using the *smooth step* ABAQUS CAE command and subsequently is transferred to all the nodes of End-1 generating rotational moment. The *smooth step* ABAQUS CAE command defines a quadratic relationship between applied load and time steps and it eliminates the oscillations which dynamic analysis introduces to the model.

5.3.5. Torsional capacity of Box Girder A

The progressive collapse strength assessment of Box Girder A under torsional load is depicted in Figure 5.15. Its strength was assessed using Riks analysis with S4R shell element type and a coarse mesh size of 330mm. This analysis provides a rough estimation of its torsional strength, but a finer mesh is essential for avoiding the overestimation of its strength.

Therefore, the mesh size was reduced to 50mm, but Riks analysis failed to converge. Hence, the same type of shell element but without reduced integration (S4) and mesh size 50mm was selected using Riks analysis. This analysis provides satisfying results for Box Girder A, however it fails to converge in other cases (i.e. Box Girder C and Box Girder D). A comparison of the torsional capacity of all box girders under the same settings is preferable, therefore the option of the dynamic explicit analysis was investigated.

A parametric study for the settings of dynamic analysis was carried out for Box Girder A under pure bending and is presented in the relevant section (5.4.2.1). The outcome of this parametric study suggests a S4R element with mesh size 50mm and its load should be applied in a *smooth load step* of 200sec in order to achieve a quasi-static analysis. The results of the dynamic analysis of Box Girder A under torsion using these settings seems to agree with the static Riks analysis results for S4 element of 50mm size (Figure 5.15).

The torsional capacity of Box Girder A is:

- $\mathbf{2.5 \times 10^{11} Nmm}$

The contour-plots of Von-Misses equivalent stresses, shear stresses and displacement for Box Girder A under torsion at the collapse are shown in Figure 5.16, Figure 5.17 and Figure 5.18, respectively. All graphs which depict the same contour plot are under the same scale in order to allow their comparison between the four box girders.

Figure 5.16 shows the Von-Mises equivalent stresses in the structure and the pattern of diagonal stresses on its plates due to shear.

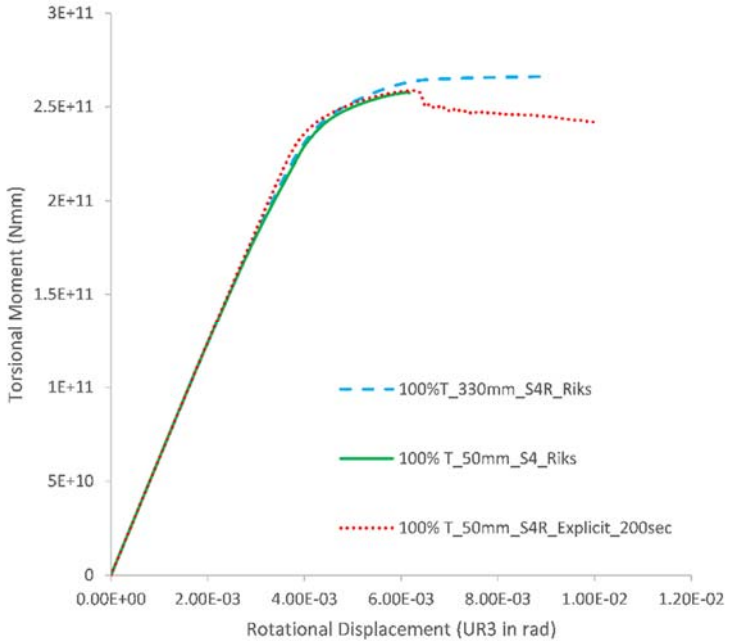

Figure 5.15: Progressive collapse strength assessment of Box Girder A under torsion

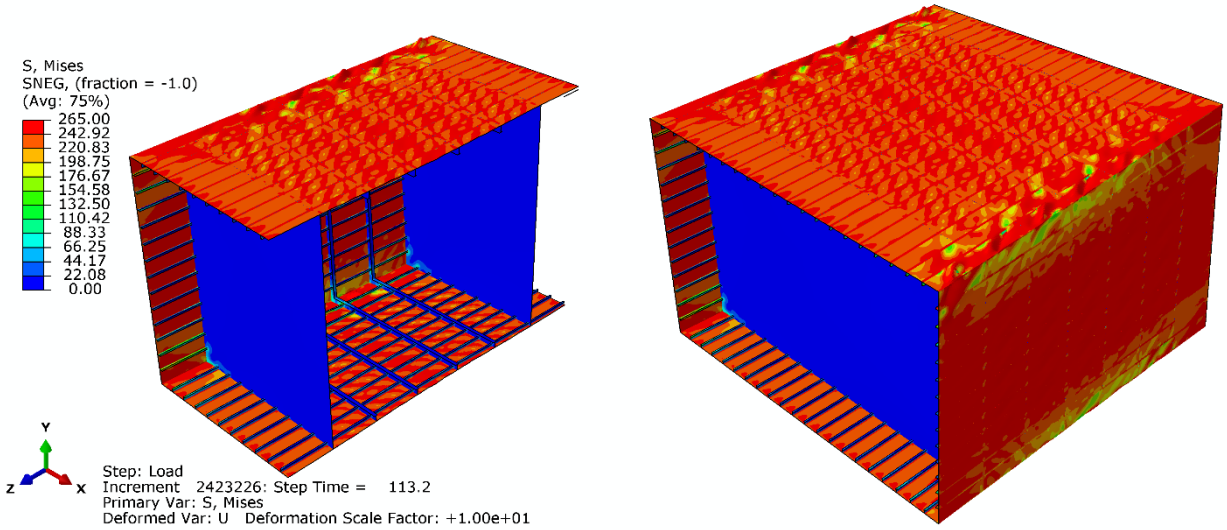

Figure 5.16: Contour plots of Von Misses equivalent stresses for Box Girder A at the collapse under torsion (magnify x10)

The direction of shear stresses is shown in Figure 5.17, with positive sign of shear stresses on the side plates and negative sign of shear stresses on the deck and bottom plates. The contour plot of the displacement in Figure 5.18 shows a displacement of 40mm for the transverse frames and the side plates of the structure close to the End-1, in which the torsional load was applied. Therefore, the collapse of Box Girder A due to torsion is overall.

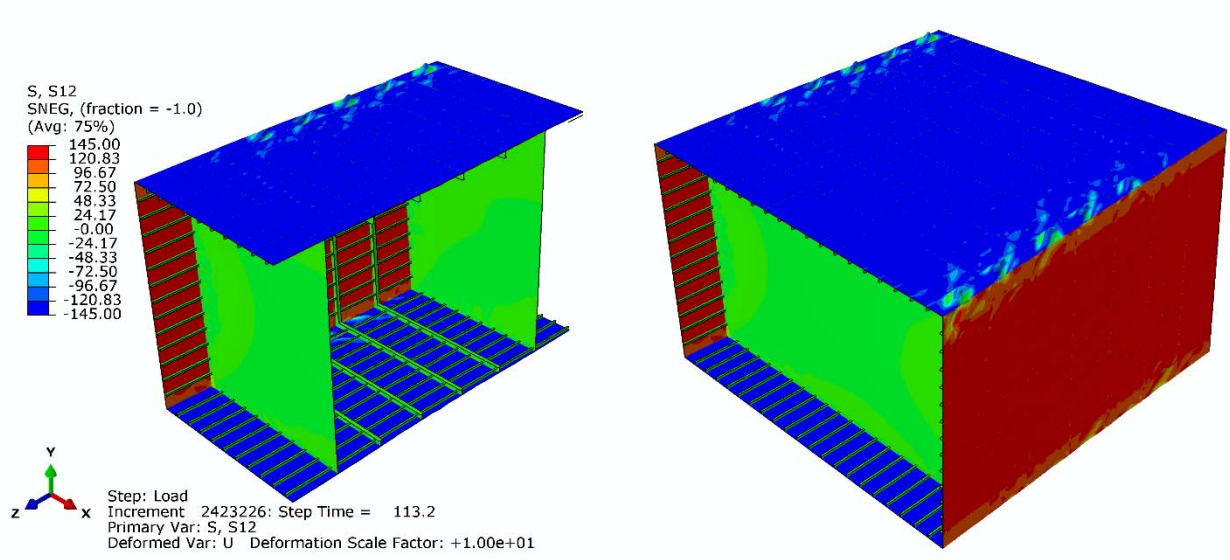

Figure 5.17: Contour plots of shear stresses for Box Girder A at the collapse under torsion (magnify x10)

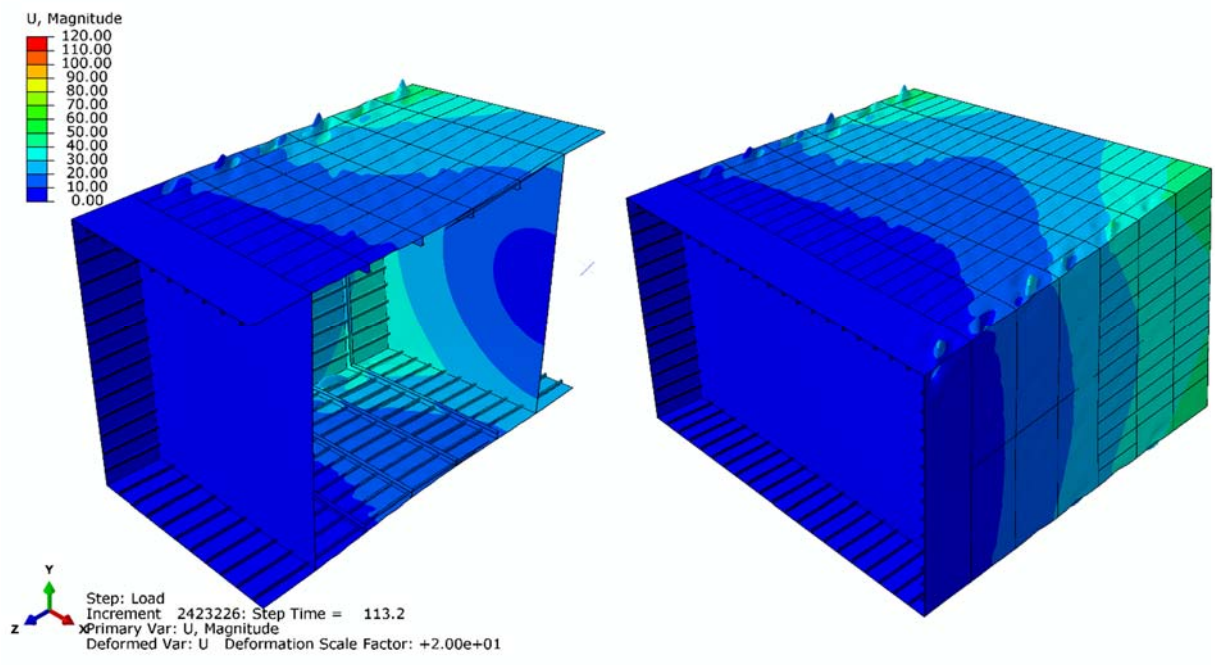

Figure 5.18: Contour plots of displacement for Box Girder A at the collapse under torsion (magnify x20)

5.3.6. Torsional capacity of Box Girder B

The progressive collapse strength assessment of Box Girder B under torsional load is depicted in Figure 5.19. The same types of analyses as described in the case of Box Girder A under torsion (section 5.3.5) were carried out. The Riks analysis with coarse mesh (330mm) overestimates the torsional strength of the structure. However, the results of the explicit and Riks analysis with a fine mesh size of 50mm present good agreement.

The torsional capacity of Box Girder B is:

- $\mathbf{2.5 \times 10^{11} Nmm}$

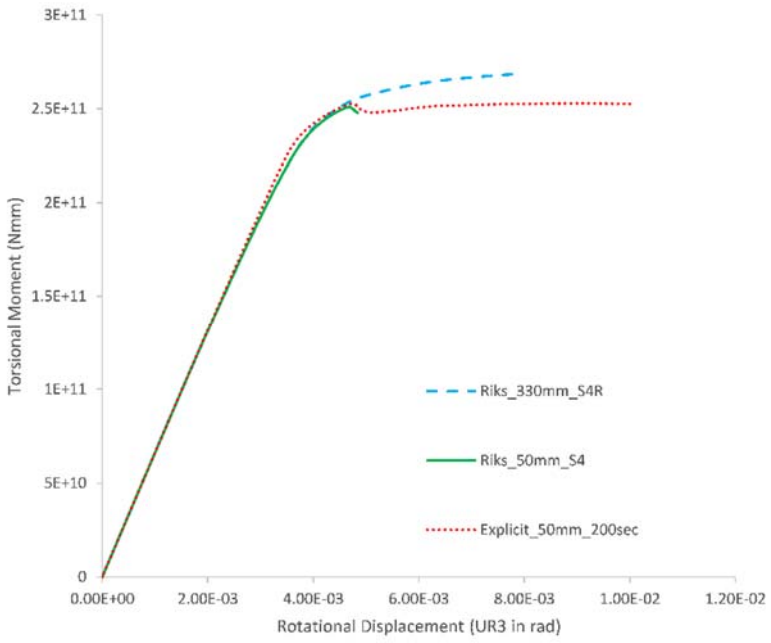

Figure 5.19: Progressive collapse strength assessment of Box Girder B under torsion

The contour-plots of Von-Misses equivalent stresses, shear stresses and displacement for Box Girder B under torsion at the collapse are shown in Figure 5.20, Figure 5.21 and Figure 5.22, respectively.

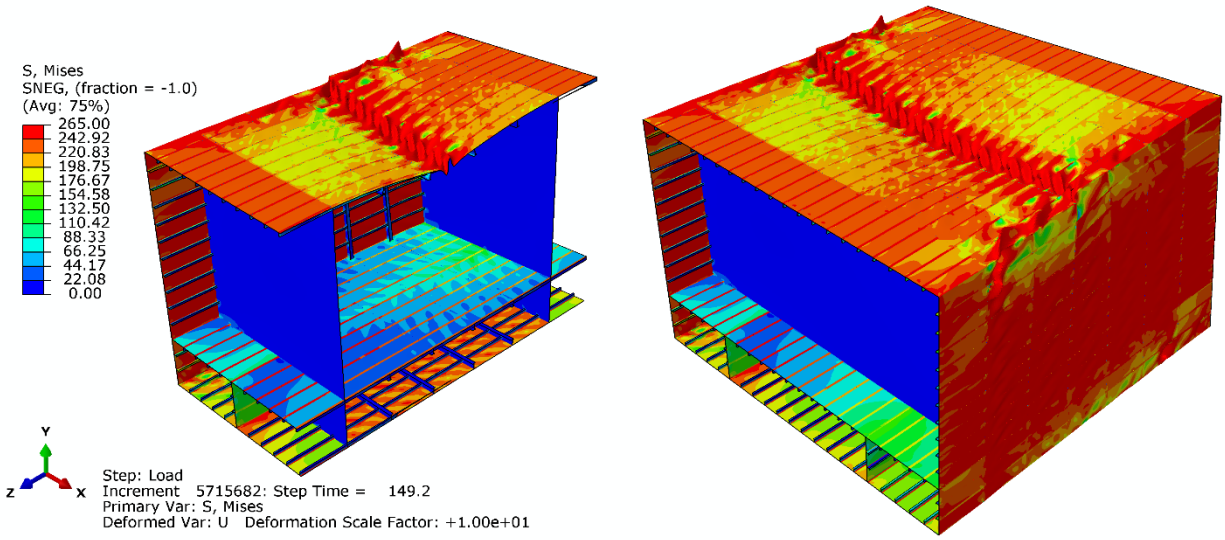

Figure 5.20: Contour plots of Von Misses equivalent stresses for Box Girder B at the collapse under torsion (magnify x10)

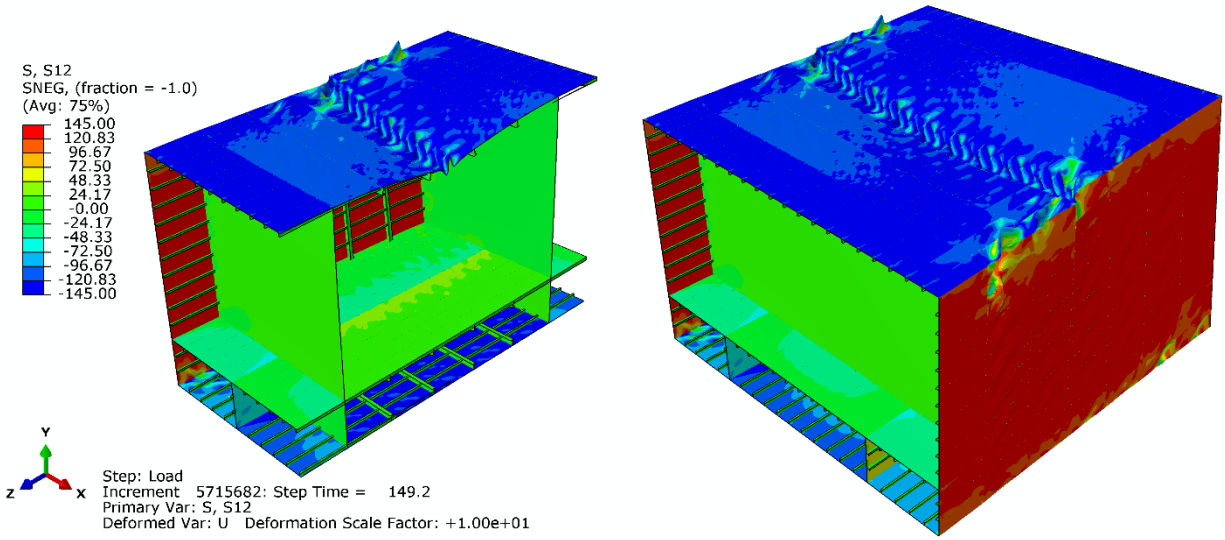

Figure 5.21: Contour plots of shear stresses of Box Girder B at the collapse under torsion (magnify x10)

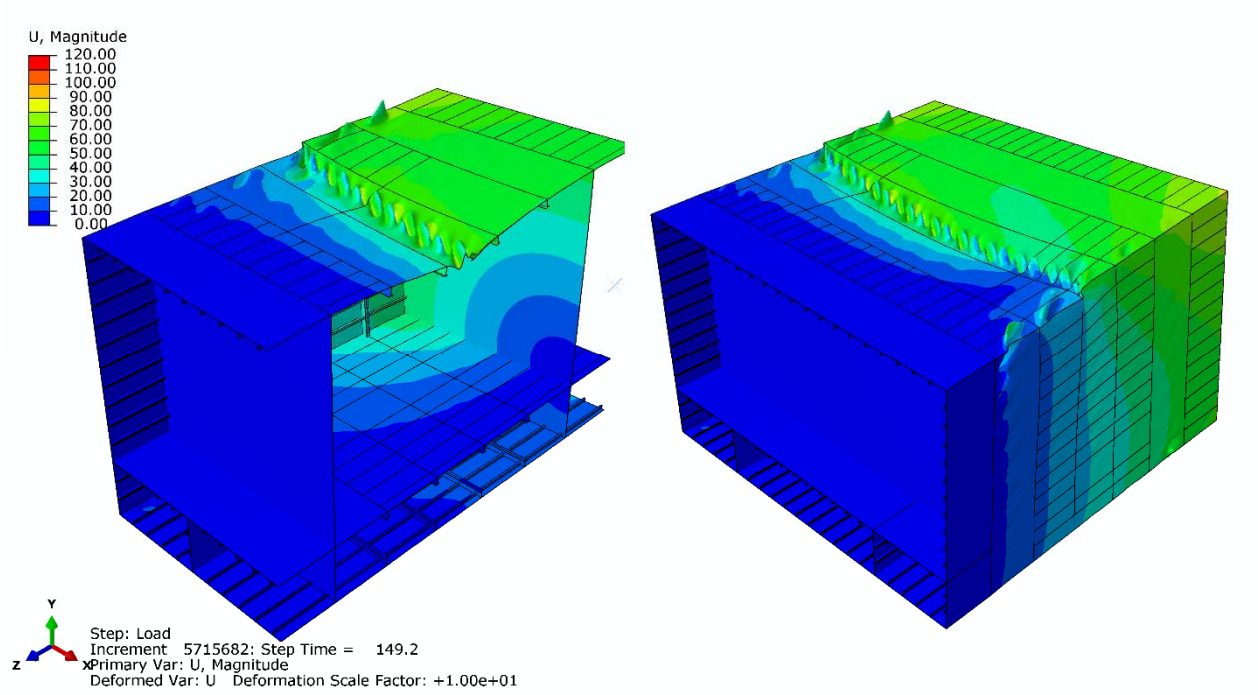

Figure 5.22: Contour plots of displacement for Box Girder B at the collapse under torsion (magnify x10)

The contour plots of Von-Mises stresses of Box Girder B under torsion in Figure 5.20 show high stresses on the deck and side plates of the structure. The collapse occurs in the middle of the deck and Figure 5.22 shows overall deformation of the side, deck plates and transverse frames. Furthermore, opposite direction of the shear stresses between the side and the deck/bottom plates is depicted in Figure 5.21.

5.3.7. Torsional capacity of Box Girder C

The progressive collapse strength assessment of Box Girder C under torsional load is depicted in Figure 5.23. The same types of analysis as described in the case of Box Girder A under torsion (section 5.3.5) were carried out. However, once again, Riks analysis with S4R element type and mesh size 50mm fails to converge. Therefore, explicit analyses with 200sec and 300sec load application times were carried out, showing very strong correlation in their results.

The torsional capacity of the box girder is:

- $\mathbf{3.028 \times 10^{11} Nmm}$

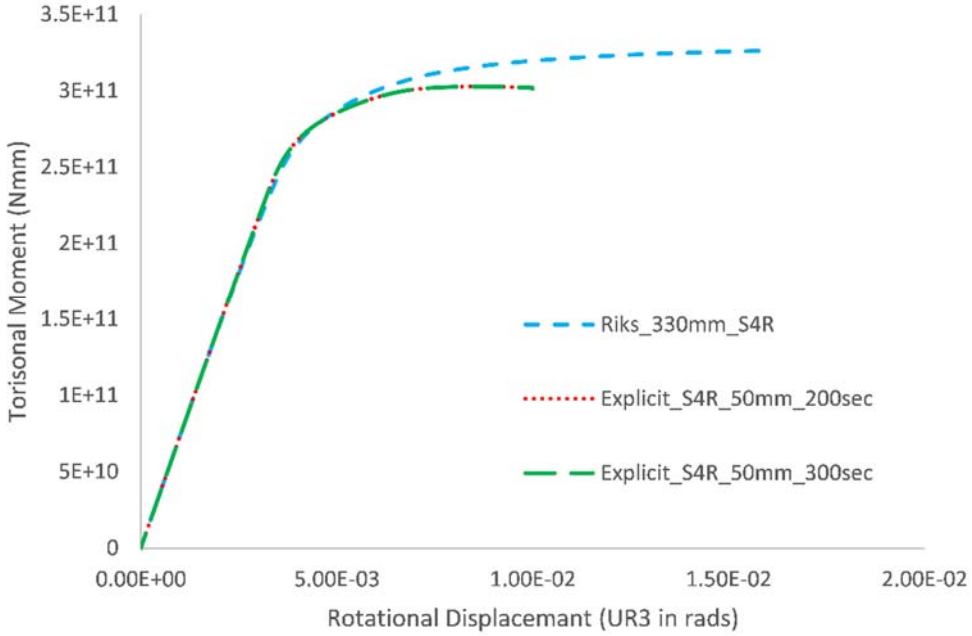

Figure 5.23: Progressive collapse strength assessment of Box Girder C under torsion

The contour-plots of Von-Misses equivalent stresses, shear stresses and displacement for Box Girder C under torsion at the collapse are shown in Figure 5.24, Figure 5.25 and Figure 5.26, respectively.

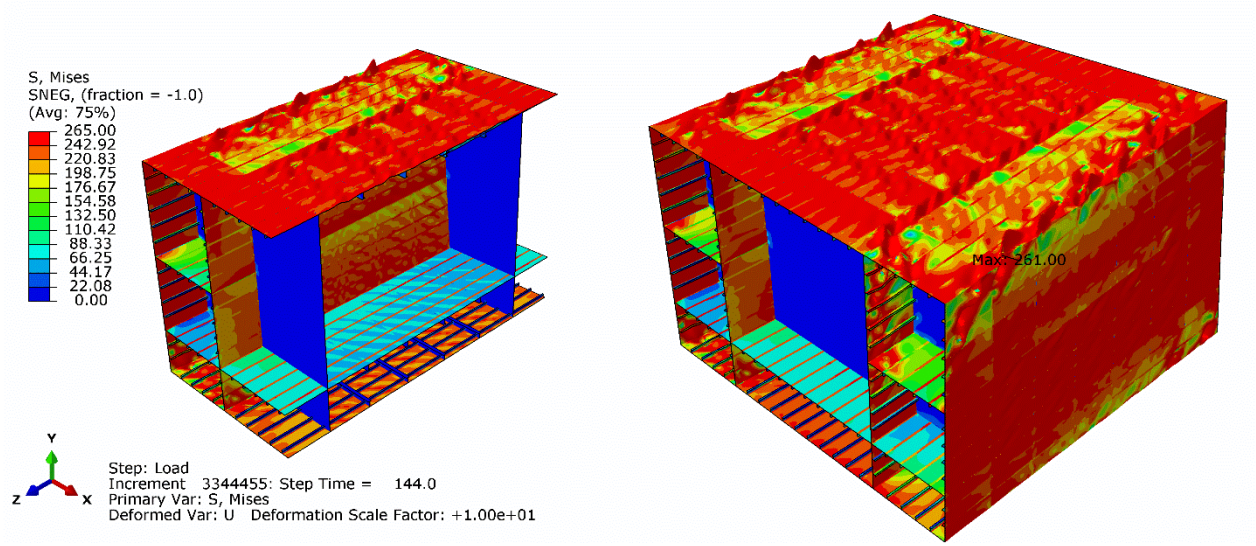

Figure 5.24: Contour plots of Von Misses equivalent stresses for Box Girder C at the collapse under torsion (magnify x10)

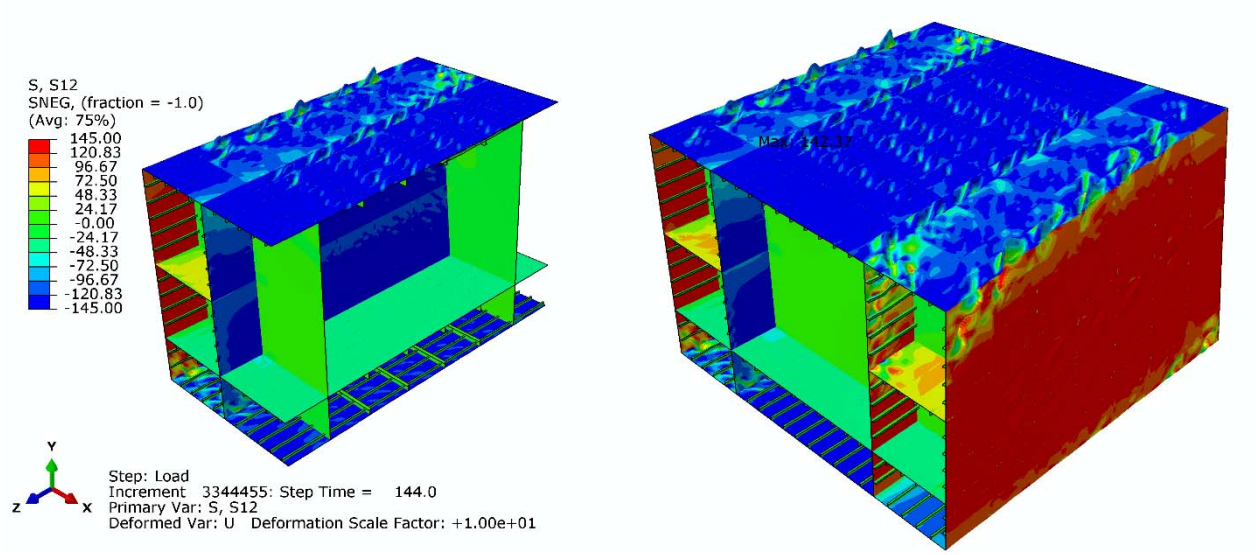

Figure 5.25: Contour plots of shear stresses for Box Girder C at the collapse under torsion (magnify x10)

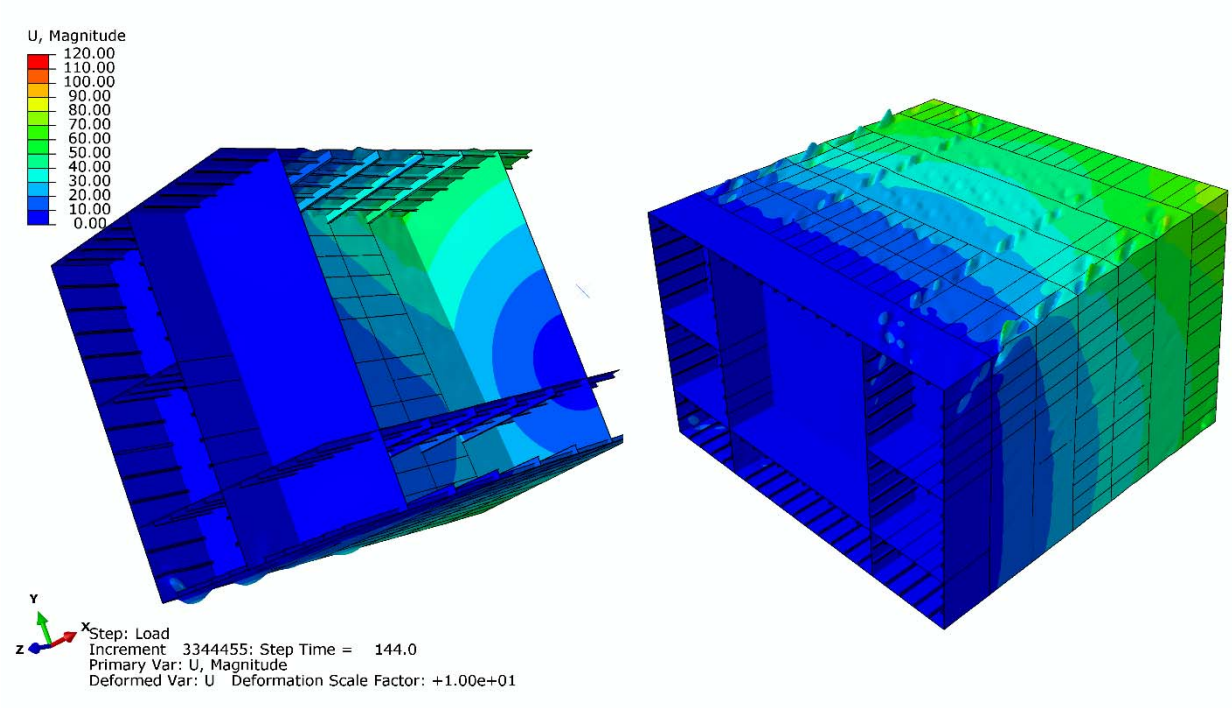

Figure 5.26: Contour plots of displacement for Box Girder C at the collapse under torsion (magnify x10)

The deck, bottom, side and inner side plates of the Box Girder C are dominated by high values of Von-Mises stresses (Figure 5.24). High deformation occurs to the deck plates with overall collapse mode, i.e. transverse frames and plates, in Figure 5.26. The maximum values of shear stresses occur in the deck, bottom, side and inner side plates with different directions which are depicted in Figure 5.25. In the same figure, there are no shear stresses in the transverse frames and longitudinal stiffeners of the structure, showing that shear stresses affect only the plates.

5.3.8. Torsional capacity of Box Girder D

The progressive collapse strength assessment of Box Girder D under torsional load is depicted in Figure 5.27. In this case, no static analysis achieved its convergence, therefore only dynamic analysis was carried out. Explicit dynamic analyses were carried out with 200sec and 300sec time steps whose results show very good agreement between them. The graph of torsional moment-rotational displacement (Figure 5.27) is a smooth curve in the elastic-plastic area without a peak and a clearly defined point for the collapse of the structure.

The torsional capacity of the open box is:

- $\mathbf{2.47 \times 10^{11} Nmm}$

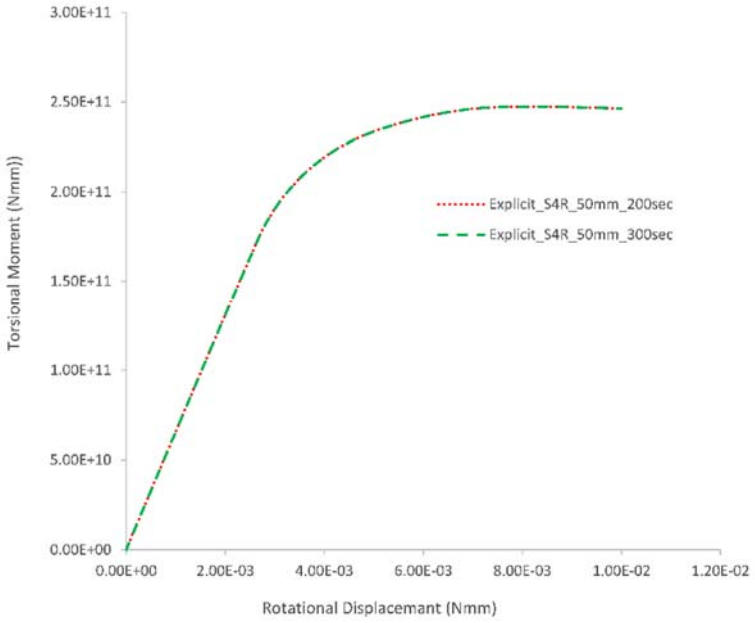

Figure 5.27: Progressive collapse strength assessment of Box Girder D under torsion

The contour-plots of Von-Misses equivalent stresses, shear stresses and displacement for Box Girder D at the collapse are depicted in Figure 5.28, Figure 5.29 and Figure 5.30, respectively. The plates in the 1st and 7th bay of this model have doubled thickness in comparison with the plates of the other bays. This occurs in order to avoid the collapse of Box Girder D due to torsion outside of the region of the two bulkheads. This case is shown in Figure 5.31, Figure 5.32 and Figure 5.33, but it is not preferable as the torsional capacity of the structure is

underestimated and not the same boundary conditions are applied in comparison with the other box girders.

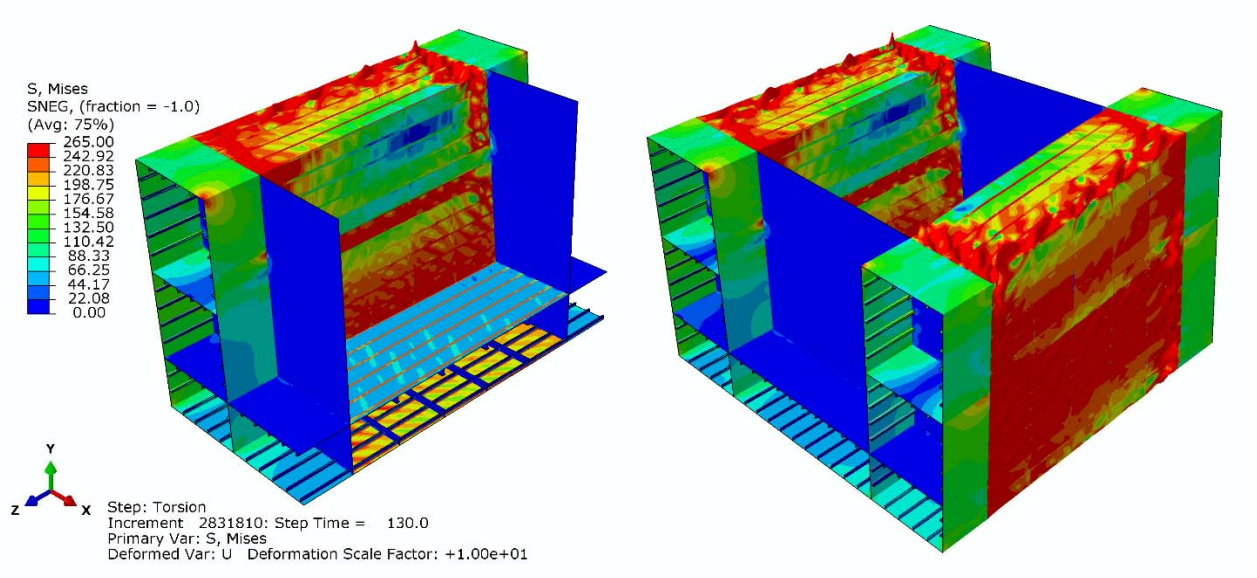

Figure 5.28: Contour plots of Von Misses equivalent stresses for Box Girder D at the collapse under torsion (magnify x10)

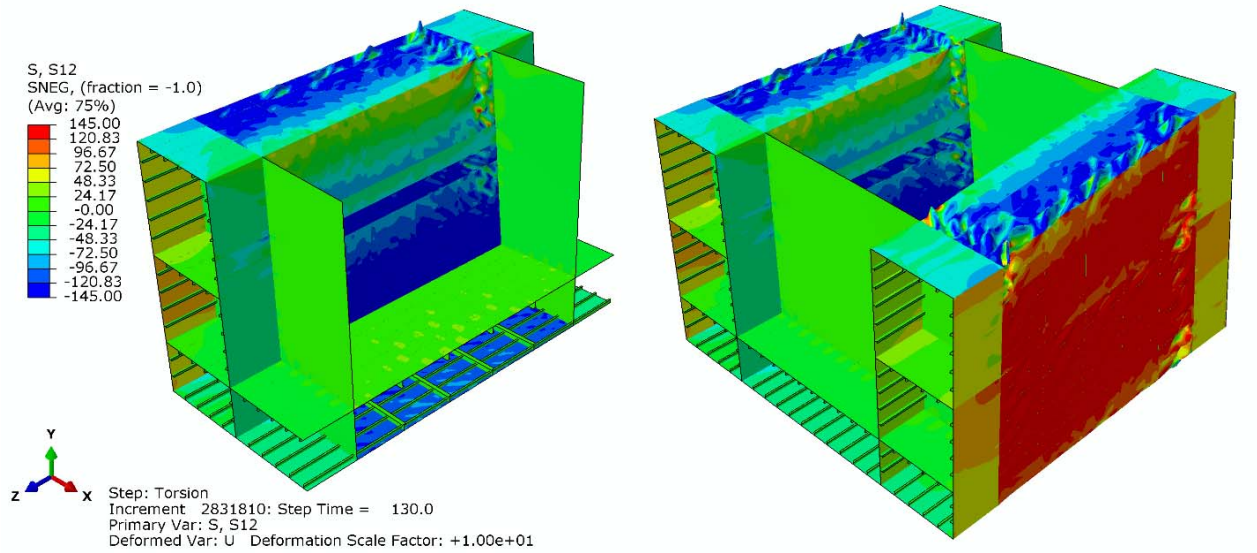

Figure 5.29: Contour plots of shear stresses for Box Girder D at the collapse under torsion (magnify x10)

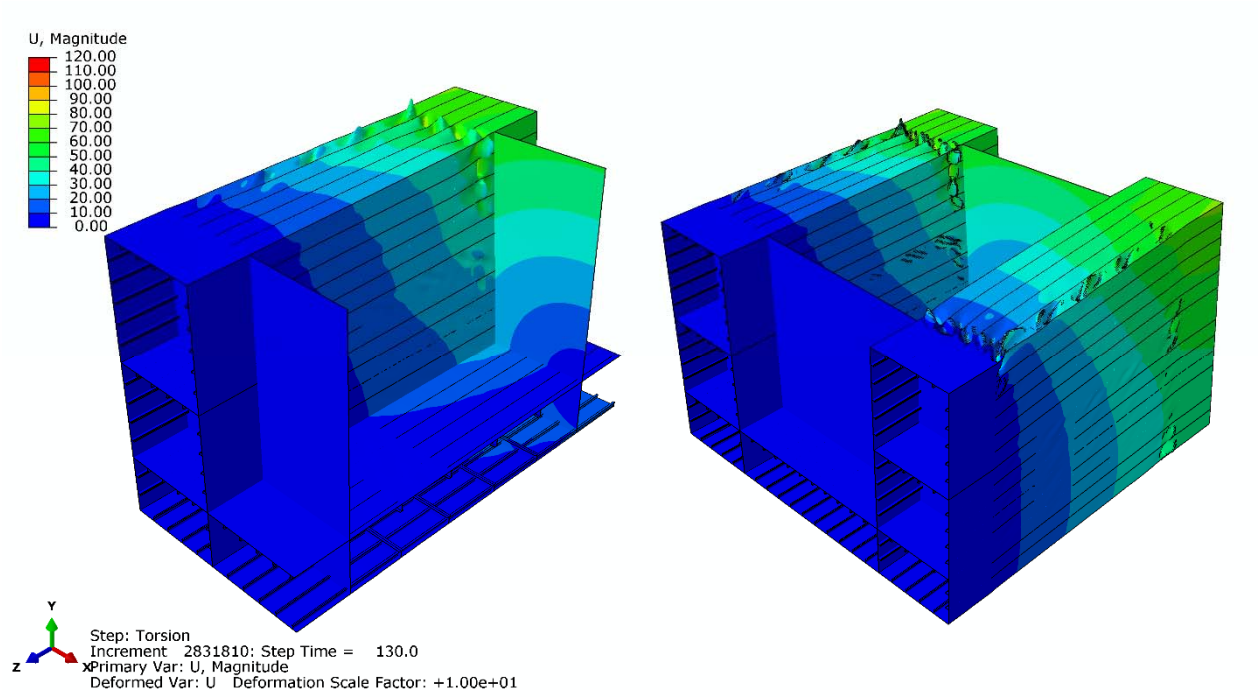

Figure 5.30: Contour plots of displacement for Box Girder D at the collapse under torsion (magnify x10)

The contour plots of Von-Misses stresses (Figure 5.28) show high stresses on the side plates and on the deck/bottom plates close to the bulkheads. Additionally, the deformation is anti-symmetrical around the centerline of Box Girder D and overall collapse mode occurs (Figure 5.30). High values of shear stresses are presented particularly on the side, inner side, bottom and deck plates whose sign and direction are shown in Figure 5.29.

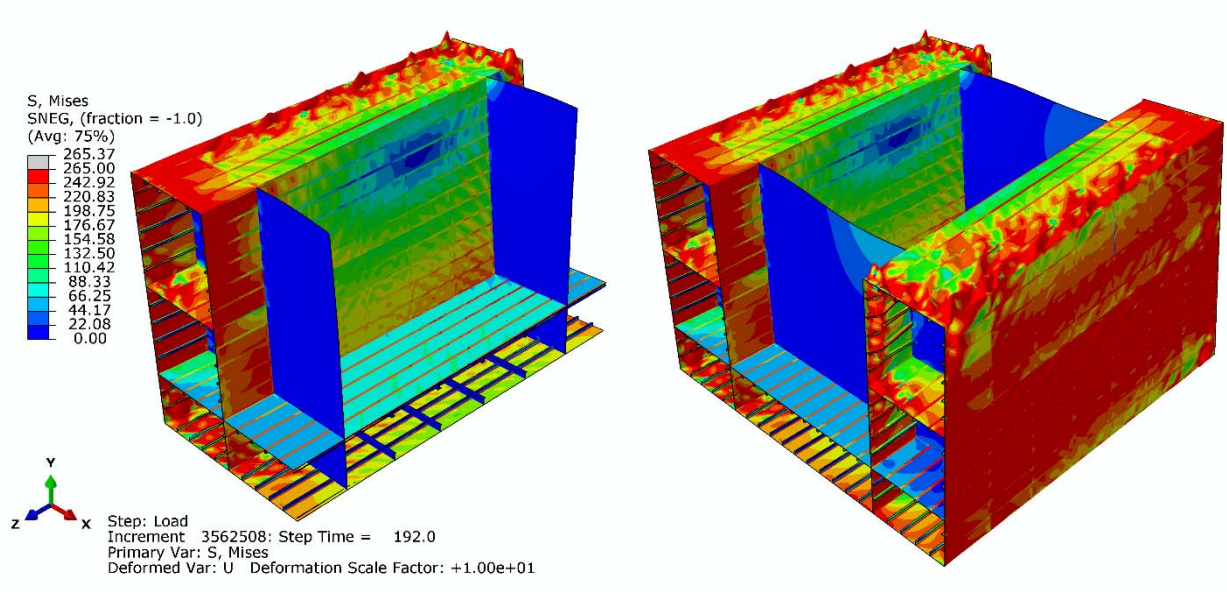

Figure 5.31: Contour plots of Von Misses equivalent stresses for Box Girder D without doubled thickened plates in the end bays at the collapse under torsion (magnify x10)

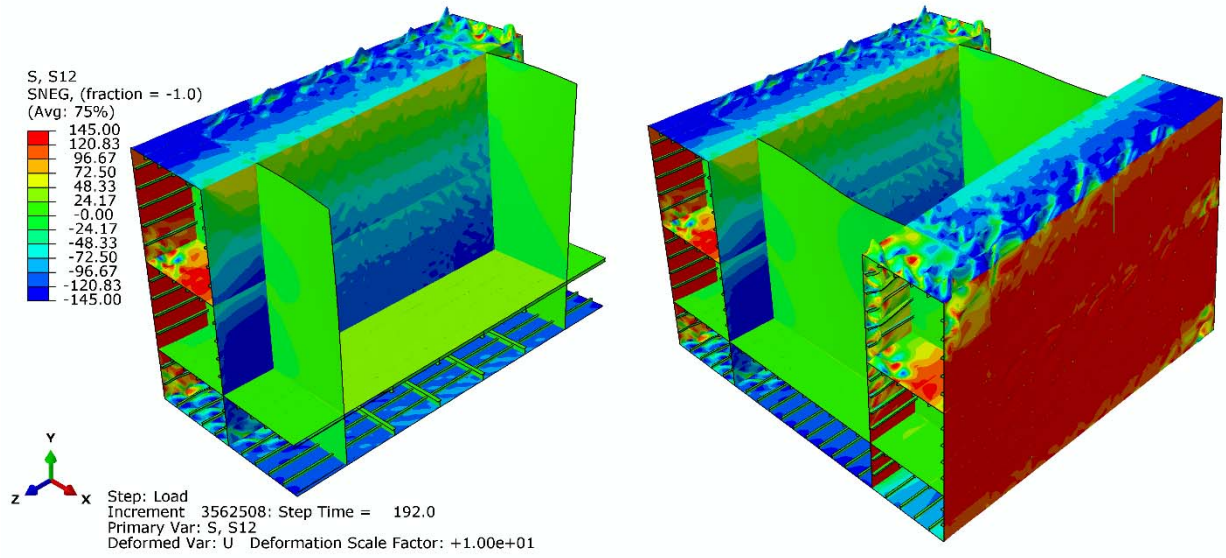

Figure 5.32: Contour plots of shear stresses for Box Girder D' without doubled thickened plates in the end bays at the collapse under torsion (magnify x10)

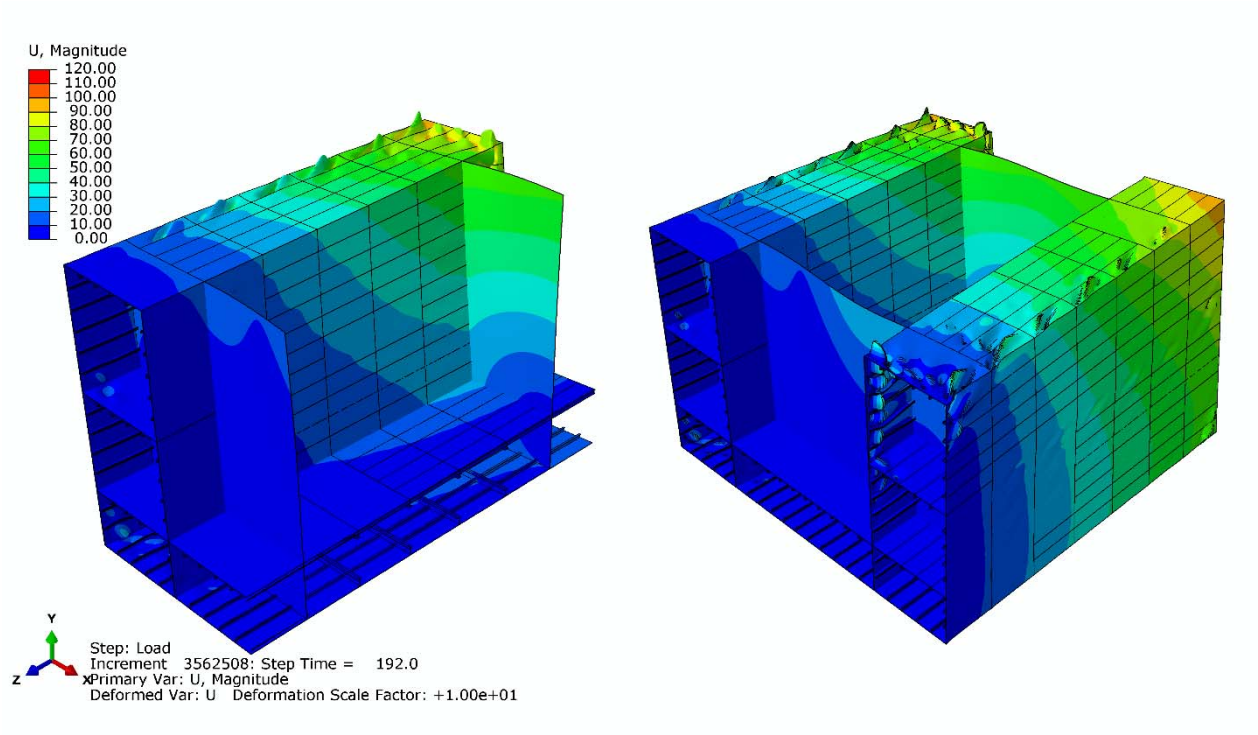

Figure 5.33: Contour plots of displacement for Box Girder D without doubled thickened plates in the end bays at the collapse under torsion (magnify x10)

As it was mentioned before, Figure 5.31, Figure 5.32 and Figure 5.33 show the contour plots of Von-Misses stresses, shear stresses and displacement for Box Girder D without thickened plates in the end bays. The collapse of this structure occurs outside of the examined area, i.e. the area between the bulkheads, which is not the case and led to the decision to increase the thickness of the plates in the end bays. The stresses and deformations in the model are significantly affected by the boundary conditions, which is not the case when the end bays are stiffened up.

5.4. Intact box girders under combined vertical sagging bending and torsion using the Nonlinear Finite Element Method

In this section, the four box girders are analysed under combined torsional and bending loads using the nonlinear finite element method. The maximum torsional load of each box girder is known, so fractions of it are applied first to each model and then vertical bending moment is applied until the collapse of the structure.

5.4.1. Boundary Conditions

The initial boundary conditions remain the same to these which are applied to the box girders under torsional load (section 5.3.3.1). In the following loading steps, for the case which the torsional load is zero and the structure is subjected only to bending moment, the boundary conditions are as described in section 5.3.3 and 5.3.4, but the rotational displacement at End-1 (Figure 5.14) is applied in x axis (UR1) instead of z axis (UR3). It should be mentioned that these boundary conditions always allow the End-1 to move axially (free U3), so no stretching of the neutral axis occurs.

In all other cases which combined torsion and bending loads are applied to the structure, the boundary conditions are defined based on the computational method as follows:

5.4.1.1. Static analysis (Riks)

A relaxation step (General Static) without any load is applied at End-1 (Figure 5.14) in order to self-equilibrate the residual stresses and initial distortions in the structure (same as in section 5.3.3.2). Then, the selected amount of torsion is applied to RP-1 as torsional moment (CM3) using the general static method. Thereinafter, the propagated torsional load remains to the structure and positive rotational displacement in axis (UR1) is applied to RP-1, thus the box girder is subjected to sagging bending moment up to its collapse.

5.4.1.2. Explicit Dynamic analysis

In the cases which dynamic explicit analysis was carried out, the relaxation step is omitted. The aim is to achieve a quasi-static analysis applying the load extremely slowly to the model in order to reduce the oscillations and the percentage of kinetic to internal energy to be less

than a certain value. This value is different for each model and is defined by the results of the explicit analysis for 200sec and 300sec time step.

The results of the dynamic explicit analysis under pure torsional load are completed and provide the amount of torsional moment which is applied in every time interval. Therefore, the selected amount of torsional moment is applied to RP-1 in specific time which ensures quasi-static analysis. After this step is completed, positive/negative rotational displacement in x axis is applied to End-1 via RP-1 (Figure 5.14) in 200sec load application time and the whole structure is subjected to sagging/hogging bending moment until the collapse.

5.4.2. Box Girder A

The results of Box Girder A under bending and under combined torsional and bending moment are presented in this section. A parametric study for the time step in dynamic analysis was previously carried out and is presented to define the time interval which the load should be applied in order to achieve quasi-static analysis.

5.4.2.1. Parametric Study (Pure Bending)

The simple geometry of Box Girder A allows Riks and general static analysis to complete without any convergence issues. Therefore, this model was selected to carry out a parametric study for dynamic explicit analysis and validate its results. A quasi-static analysis is characterised by negligible inertia forces, very small velocity of the material and negligible kinetic energy. These may be achieved controlling the mass density and/or applying the load very slowly (*smooth load step*) during a long period of time.

In this study, the mass density is constant in all cases. A smooth step of rotational displacement equal to 0.01rad is applied to End-1 (Figure 5.14) in a period of time which is investigated. The aim is to define this period of time of application of the load in which the kinetic energy is negligible and minimum oscillations occur to the model.

ABAQUS notes define kinetic energy as negligible when the percentage of kinetic to internal energy (ALLKE/ALLIE) is between 1- 5% throughout the whole analysis. However, the results of dynamic analyses seem to converge with the results of Riks and general static analysis when the percentage of kinetic to internal energy (ALLKE/ALLIE) is equal or less than 0.5% (Figure 5.34 and Table 5.1). This occurs for a time period equal or more than 200sec (i.e. in the cases of 200sec, 300sec).

Therefore, a smooth step with period time 200sec and ALLKE/ALLIE% equal or less than 0.5% was assumed suitable for the set-up of the quasi-static analysis for Box Girder A and providing results in reasonable time. The results of this parametric study are shown below in Table 5.1 and Figure 5.34.

Type of analysis	Period of Time (sec)	Mesh size (mm)	Max Percentange of ALLKE/ALLIE %	Max Bending Moment (Nmm)	Results vs Riks %
Riks	N.A.	50	-	2.32E+11	0.00%
Riks	N.A.	25	-	2.30E+11	-0.79%
Gerenal Static	N.A.	50	-	2.32E+11	0.05%
Dynamic Explicit	3	50	6.34%	2.79E+11	20.47%
Dynamic Explicit	13	50	1.45%	2.70E+11	16.73%
Dynamic Explicit	30	50	1.30%	2.67E+11	15.14%
Dynamic Explicit	100	50	0.80%	2.45E+11	5.68%
Dynamic Explicit	200	50	0.50%	2.41E+11	4.02%
Dynamic Explicit	300	50	0.38%	2.39E+11	3.32%

Table 5.1: Dynamic and static analysis results of Box Girder A under bending load

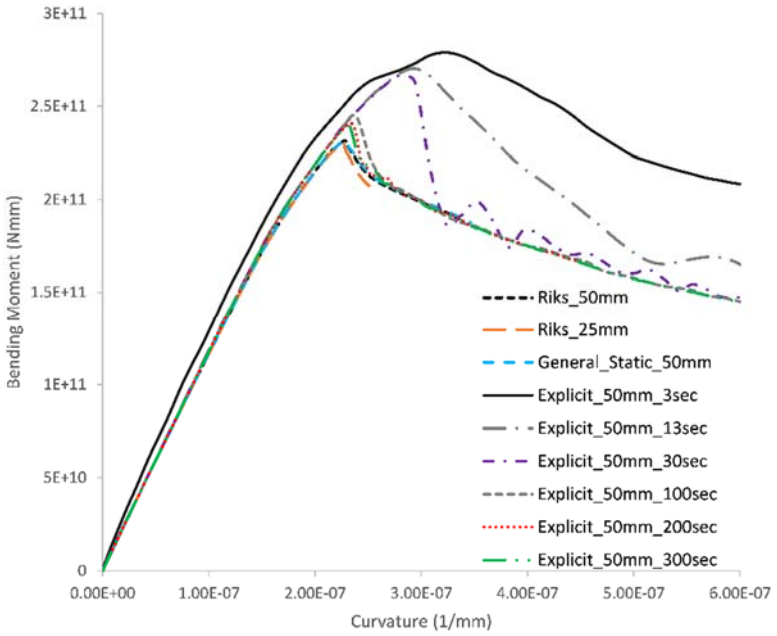

Figure 5.34: Moment-curvature relationship of Box Girder A under bending moment according to different parameters of static and dynamic explicit analysis.

5.4.2.2. Under combined torsional and sagging bending moment

The results of Box Girder A under combined torsional (%Tmax) and bending loads are shown in Figure 5.35. In each case, different fraction of its torsional capacity (Tmax) is applied to the model and then the model is subjected to bending moment up and further to its collapse. Figure 5.35 shows the bending moment-curvature relationship in each case. The structure retains its stiffness while its ultimate strength decreases with the increase of the torsional load.

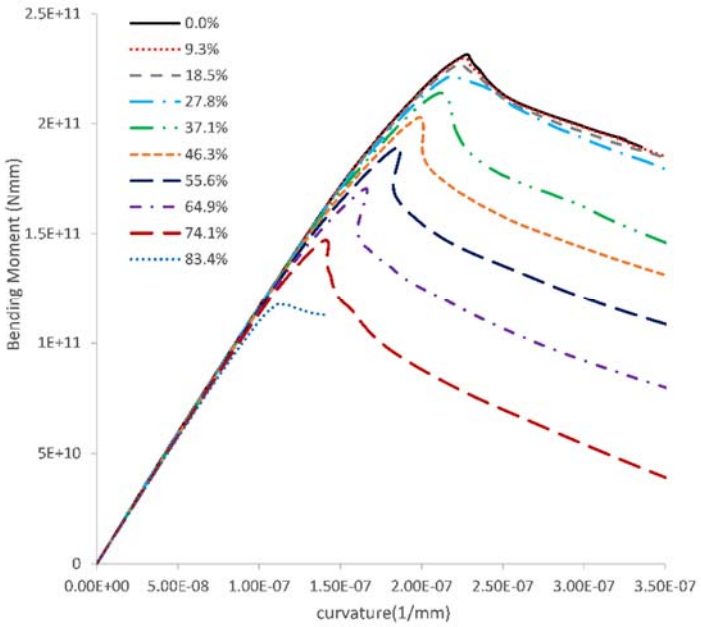

Figure 5.35: Bending moment-curvature relationship of Box Girder A under combined torsional and bending loads

The contour plots of displacement and equivalent Von Mises stresses for Box Girder A under pure bending, combined torsional load 9.3%, 37.1%, 74.1% of Tmax and bending moment at the collapse are depicted in Figure 5.36 - Figure 5.39. Overall collapse occurs to the structure in all cases since the transverse frames deform.

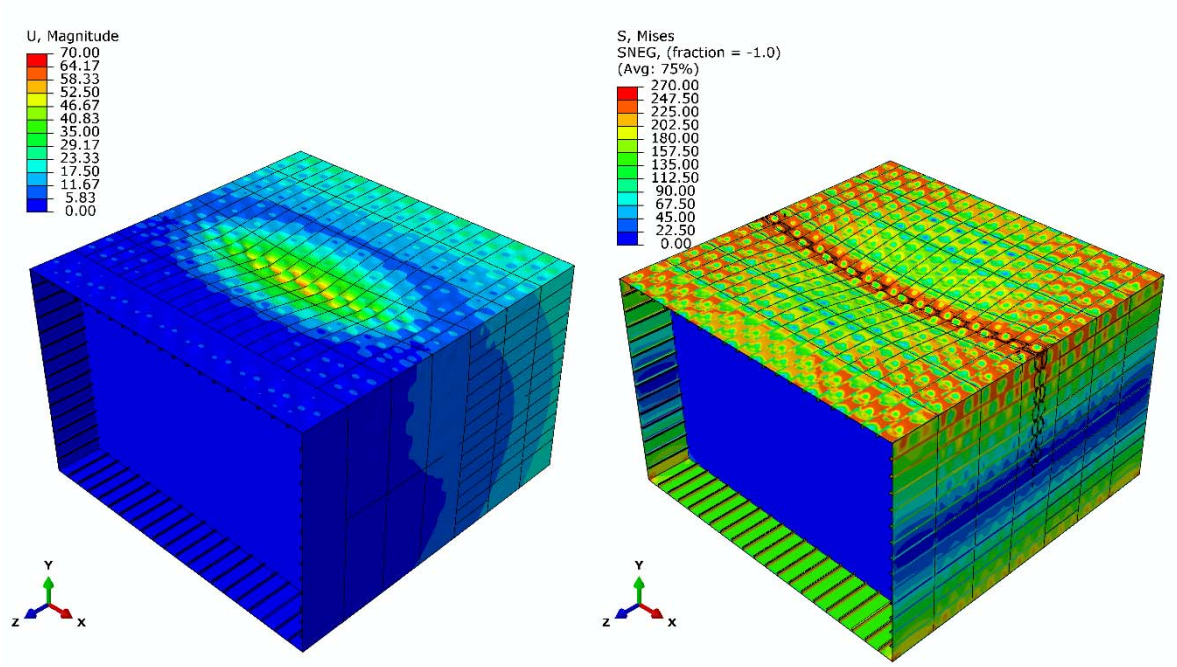

Figure 5.36: Contour plots of displacement and Von Mises equivalent stresses for Box Girder A at collapse under only bending moment (magnify x10) (Riks)

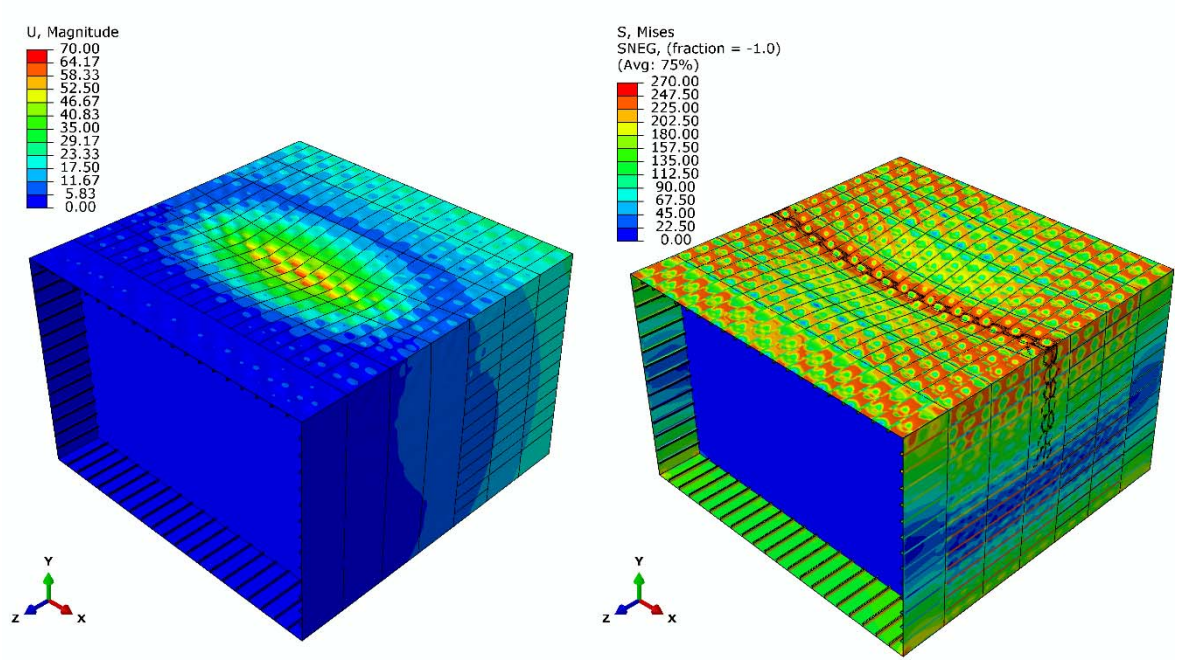

Figure 5.37: Contour plots of displacement and Von Mises equivalent stresses for Box Girder A at collapse under torsional load 2.40E+010Nmm (9.3%Tmax) and bending moment (magnify x10) (Riks)

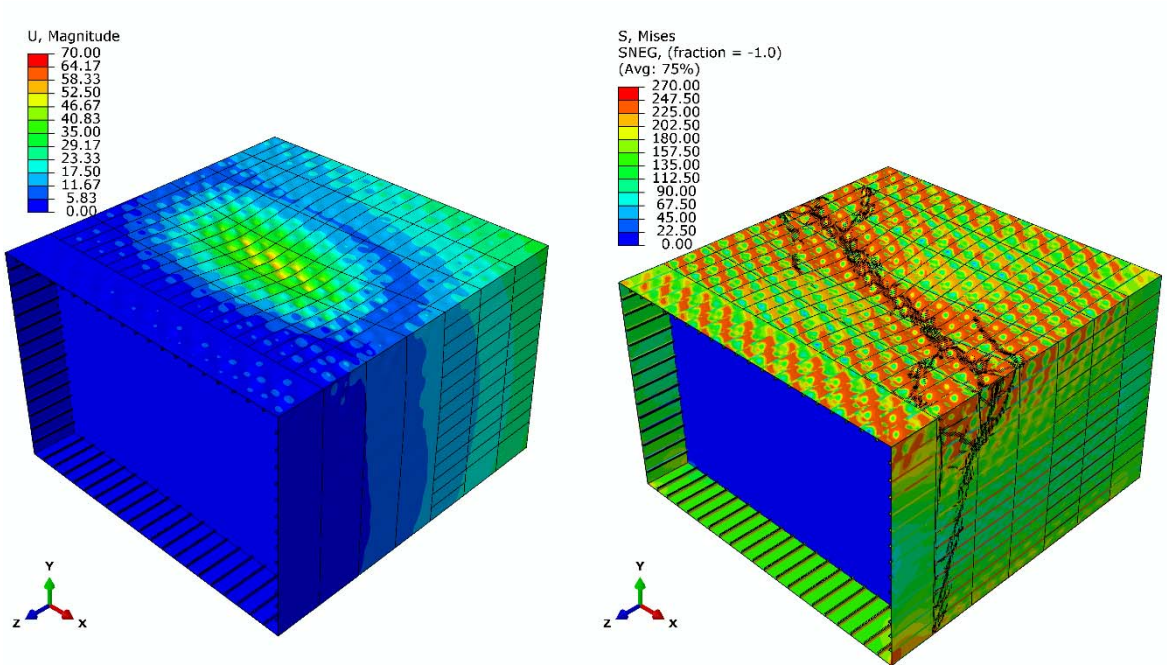

Figure 5.38: Contour plots of displacement and Von Mises equivalent stresses for Box Girder A at collapse under torsional load 9.5812E+010Nmm (37.1%Tmax) and bending moment (magnify x10) (Riks)

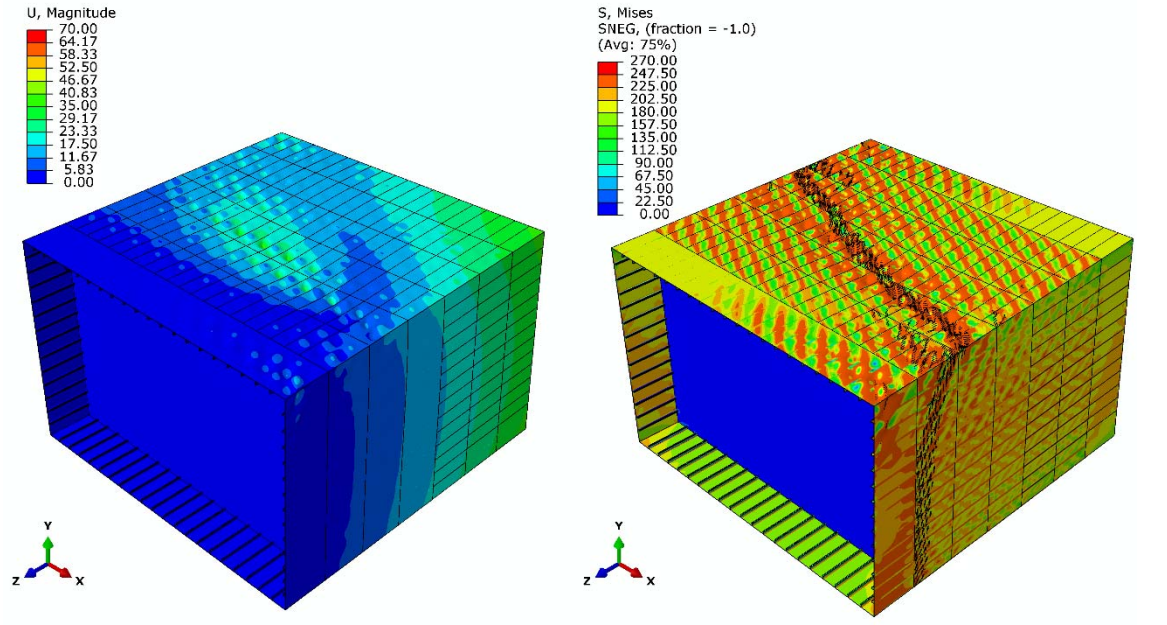

Figure 5.39: Contour plots of displacement and Von Mises equivalent stresses for Box Girder A at collapse under torsional load 1.92E+011Nmm (74.1%Tmax) and bending moment (magnify x10) (Riks)

Figure 5.36 and Figure 5.37 show that high values of displacement and Von-Misses stresses occur in the deck plates of the central bays of Box Girder A in the cases which the model is subjected only to vertical sagging bending moment and/or low amounts of torsional loads combined with bending. As the torsional load increases (Figure 5.38) the displacement of the deck plates in the centre decreases in comparison with the previous case, Von-Misses stresses appear along the diagonal of each plate on the deck and deformation of the structure occurs along its diagonal. This pattern becomes stronger as the torsional load increases (Figure 5.39), dominating also to the side plates and the maximum displacement appears close the end bay which the torsional load is applied i.e. End-1.

The interaction diagram of torsional and bending moment is depicted in Figure 5.40 defining an area within any combination of torsional and bending load is safe. The shape of the graph is close to this of a circle quadrant form. The ultimate strength of the structure decreases as the torsional load increases.

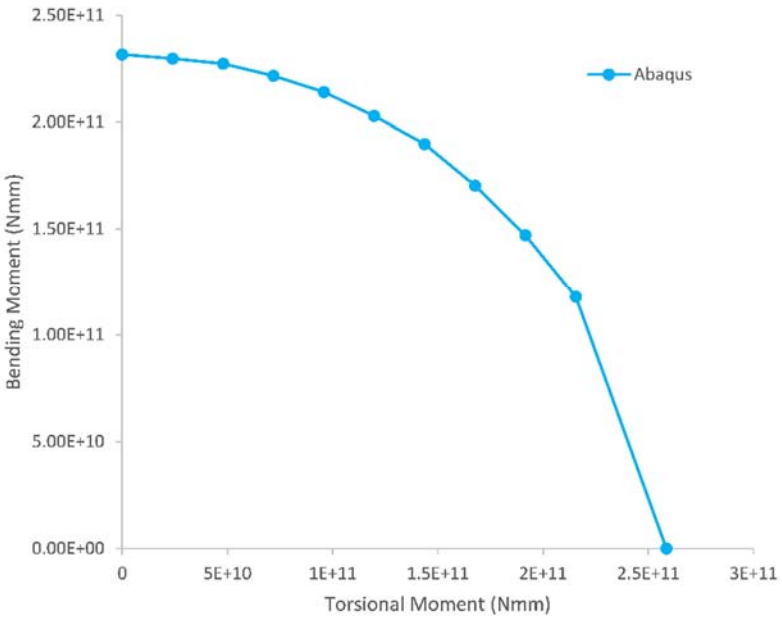

Figure 5.40: Interaction diagram of torsional and bending moment for Box Girder A

5.4.3. Box Girder B

The results of Box Girder B under combined torsional (%Tmax) and bending loads are shown in Figure 5.41. Different fractions of its torsional capacity (Tmax) are applied to the model in each case and then it is subjected to bending sagging moment until the collapse. Figure 5.41 shows the bending moment-curvature relationship of the structure in each case. The structure retains its stiffness while its ultimate strength decreases with the increase of the torsional load.

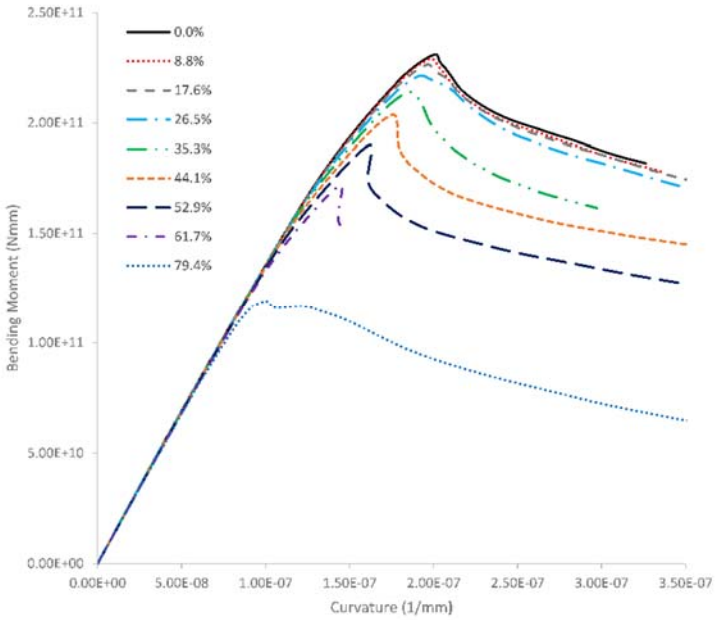

Figure 5.41: Bending moment- curvature relationship of Box Girder B under combined torsional and bending loads

The contour plots of displacement and equivalent Von Mises stresses of the Box Girder B under pure bending, combined torsional load 8.8%, 35.3%, 79.4% of Tmax and bending moment at the collapse are depicted in Figure 5.42 - Figure 5.45. Overall collapse occurs to the structure in all cases since the transverse frames deform.

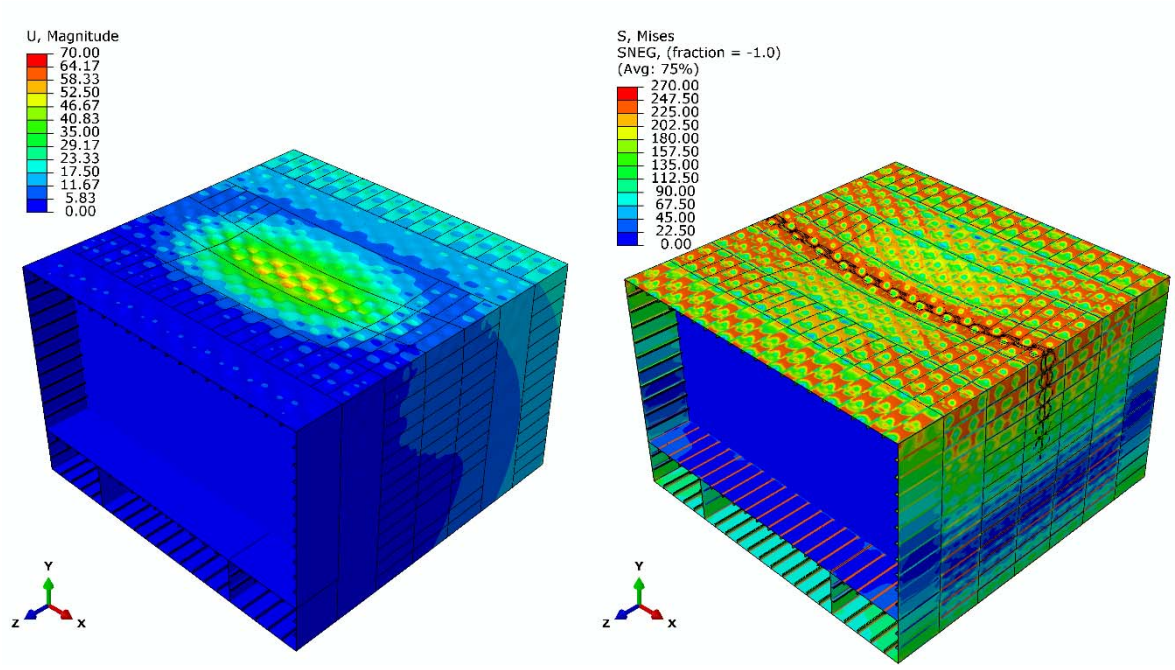

Figure 5.42: Contour plots of displacement and Von Mises equivalent stresses for Box Girder B at collapse under only bending moment (magnify x10) (Riks)

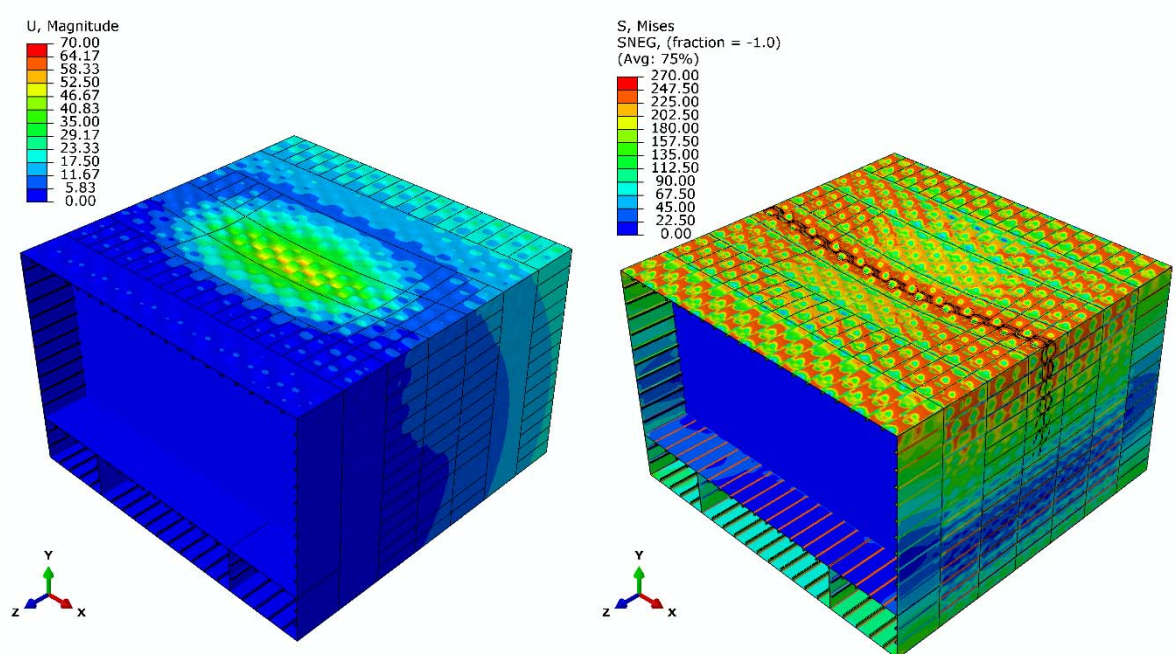

Figure 5.43: Contour plots of displacement and Von Mises equivalent stresses for Box Girder B at collapse under torsional load 2.23E+010Nmm (8.8%Tmax) and bending moment (magnify x10) (Riks)

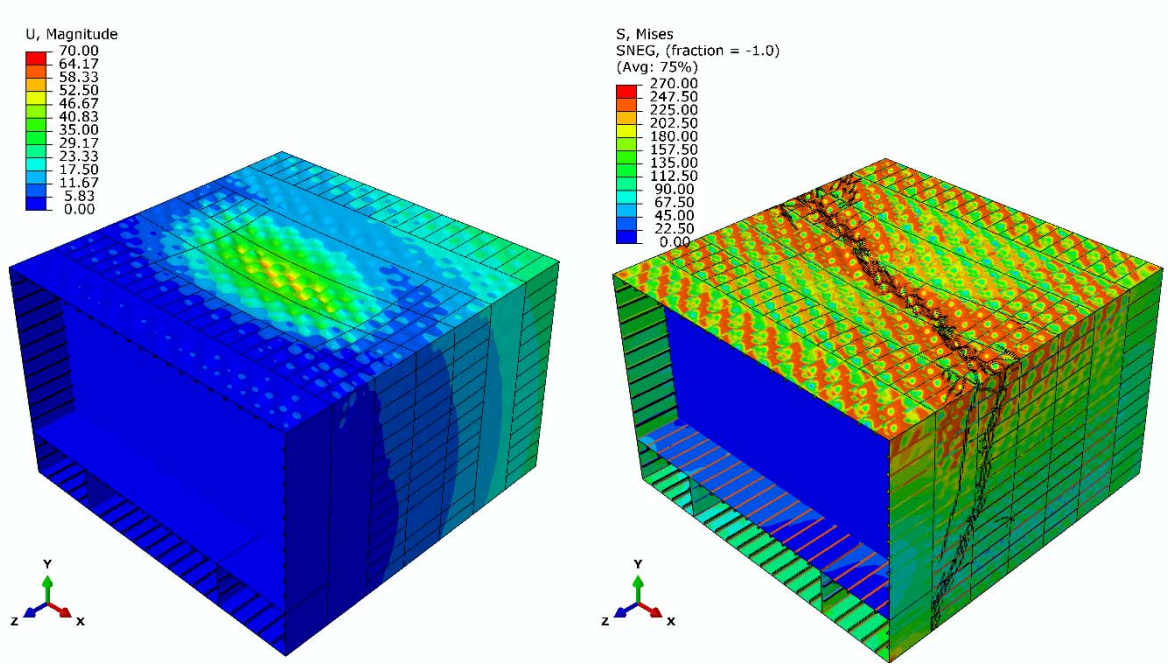

Figure 5.44: Contour plots of displacement and Von Mises equivalent stresses for Box Girder B at collapse under torsional load 8.92E+010Nmm (35.3%Tmax) and bending moment (magnify x10) (Riks)

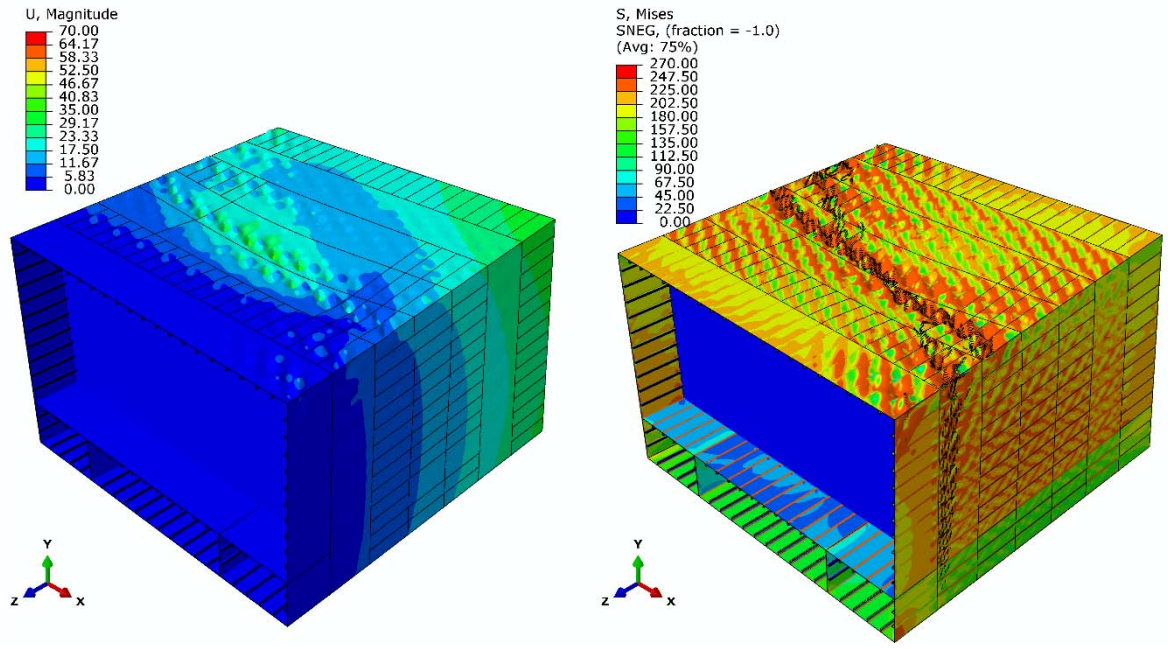

Figure 5.45: Contour plots of displacement and Von Mises equivalent stresses for Box Girder B at collapse under torsional load 2.01E+011Nmm (79.4%Tmax) and bending moment (magnify x20) (Riks)

The behaviour of Box Girder B under pure bending and combined torsional and bending loads in sagging is similar to this of Box Girder A under equivalent loads. Therefore, Box Girder B presents high values of displacement and Von-Misses stresses on its deck in the central bays under pure bending (Figure 5.42) and low amounts of torsional load combined with vertical sagging bending moment (Figure 5.43). As the torsional load increases (Figure 5.44), Von-Misses stresses form a diagonal shape on the deck plates, the collapse occurs along the diagonal of the structure and the displacement in the centre of the structure decreases. Finally, the tendency of the described pattern becomes stronger for higher values of torsional load combined with bending (Figure 5.45) and this pattern appears also on the sides of the structure.

The interaction diagram of torsional and bending moment is depicted in Figure 5.46 defining an area within any combination of torsional and bending load is permissible. The ultimate strength of the structure decreases as the torsional load increases, following a circle quadrant form.

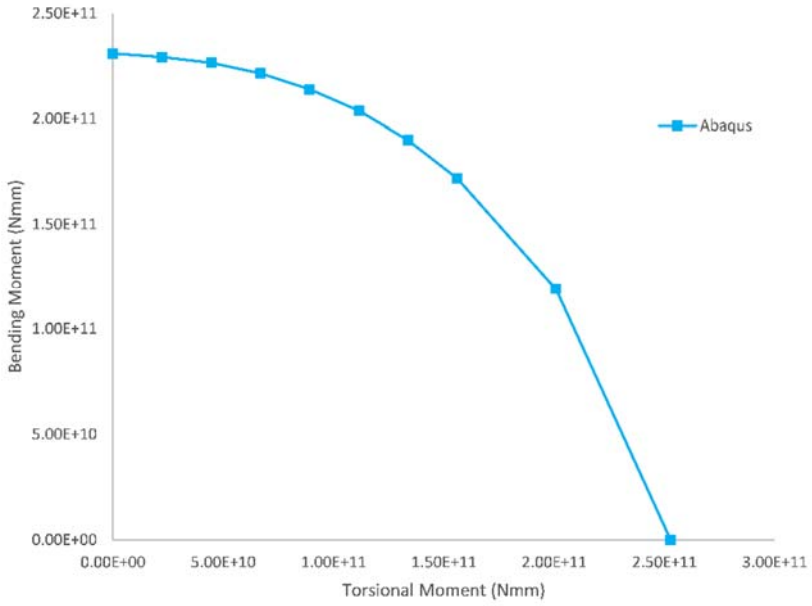

Figure 5.46: Interaction diagram of torsional and bending moment for Box Girder B

5.4.4. Box Girder C

The previous cases, i.e. Box Girder A and Box Girder B which are subjected to combined torsional and bending sagging moment, were analysed using static Riks analysis. However, the analysis of the Box Girder C under combined torsional and bending moment using Riks analysis fails to converge in some cases (e.g. high amount of torsional load) and dynamic explicit analysis is required. Therefore, a parametric study was carried out first in order to define the time for the application of the load in explicit analysis. Dynamic analysis with 200sec provides valid results in the case which the model is subjected only to torsional moment (Figure 5.23). Box Girder C subjected only to bending moment is analysed with static Riks and dynamic explicit analysis with 200sec time interval. The results of both analyses show convergence in Figure 5.47. So, dynamic explicit analysis with 200sec time interval will be used for the cases of combined torsion and bending, in which static Riks analysis fails to converge.

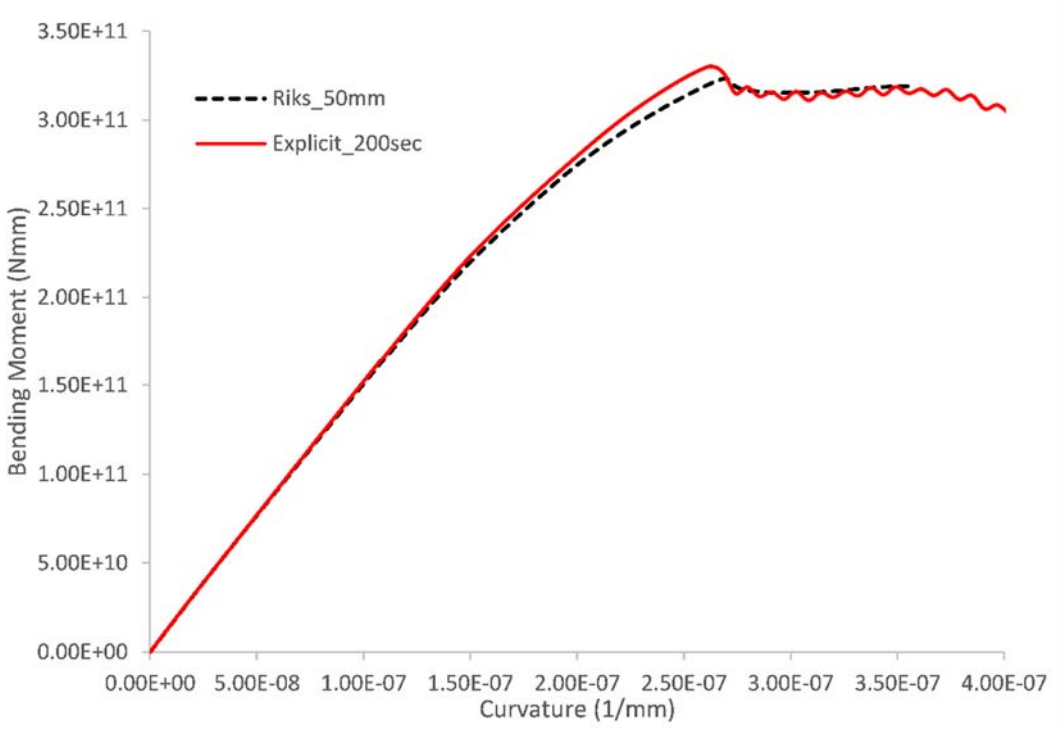

Figure 5.47: Bending moment-curvature relationship of Box Girder C subjected only to bending moment according to static Riks and explicit dynamic analysis

The results of Box Girder C under combined torsional (%Tmax) and bending loads are shown in Figure 5.48. Different fractions of its torsional capacity (Tmax) are applied to the model in each case and then it is subjected to bending sagging moment until the collapse. Figure 5.48 shows the bending moment-curvature relationship of Box Girder C in each case. The strength of the structure decreases as the torsional load increases and the same stiffness is presented approximately in all cases.

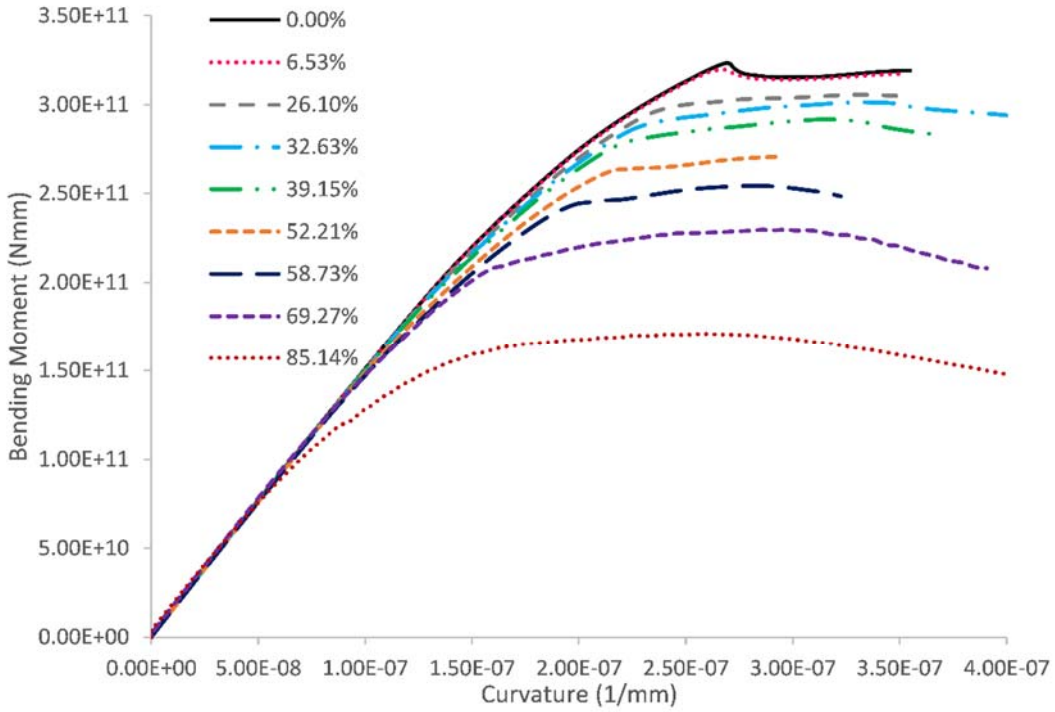

Figure 5.48: Bending moment-curvature relationships of Box Girder C under combined torsional and bending loads

The contour plots of displacement and equivalent Von Mises stresses for Box Girder C under pure bending, combined torsional loads 26.10%, 39.15%., 58.73% and 85.14% of Tmax and bending moment at the collapse are depicted in Figure 5.49 - Figure 5.53. In all cases the transverse frames deform, therefore overall collapse occurs.

In the case which Box Girder C is subjected only to bending moment, high values of compressive stresses appear on the deck of the structure (Figure 5.49) with maximum values close to the bulkhead of End-2. Box girder C presents similar behaviour when is subjected to

low amount of torsion combined with bending (Figure 5.50), but the values of Von-Misses stresses and displacement are higher than these under pure bending.

As the amount of the applied torsion increases (Figure 5.51 and Figure 5.52), high values of Von-Misses stresses appear in the diagonal direction of the deck and the sides of the structure. The contour plot of the displacement presents high deformation at the bays close to the bulkhead at End-2.

In the case which very high amount of torsional load is applied combined with bending (Figure 5.53), high values of Von-Misses stresses are presented all over the structure and the collapse of the deck plates occurs in the bay close to the bulkhead at End-1, where the torsional load is applied.

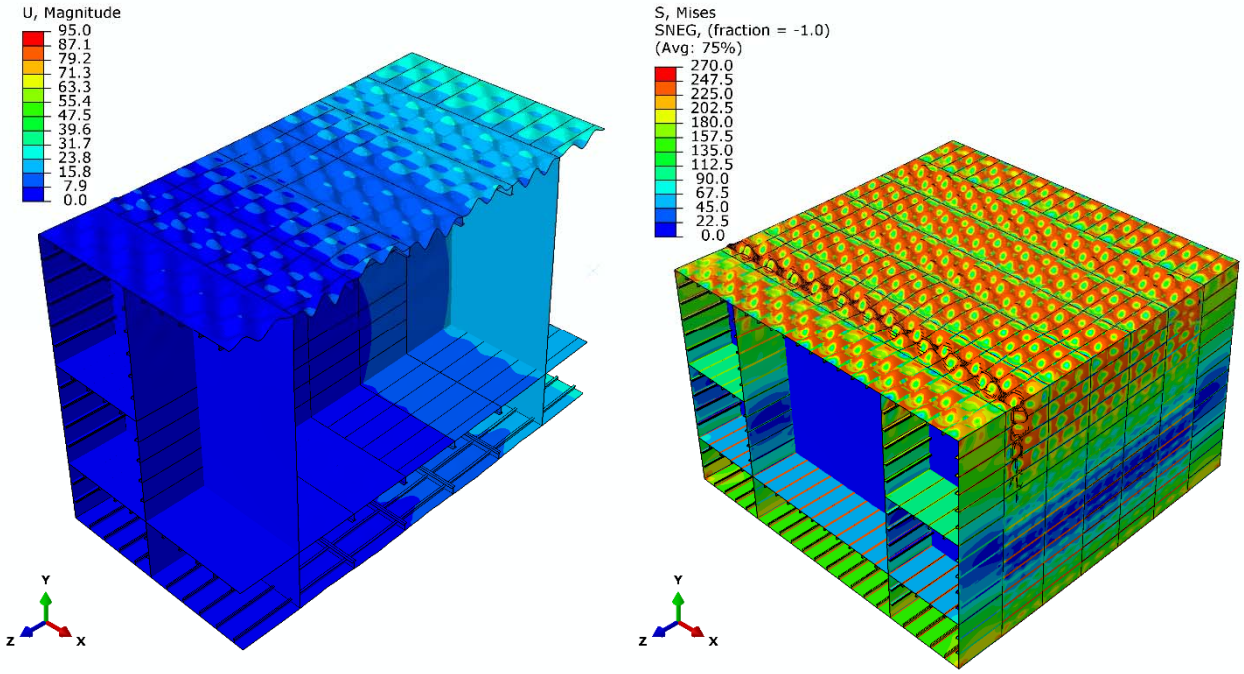

Figure 5.49: Contour plots of displacement and Von Mises equivalent stresses for Box Girder C at collapse subjected only to bending moment (magnify x20) (Riks)

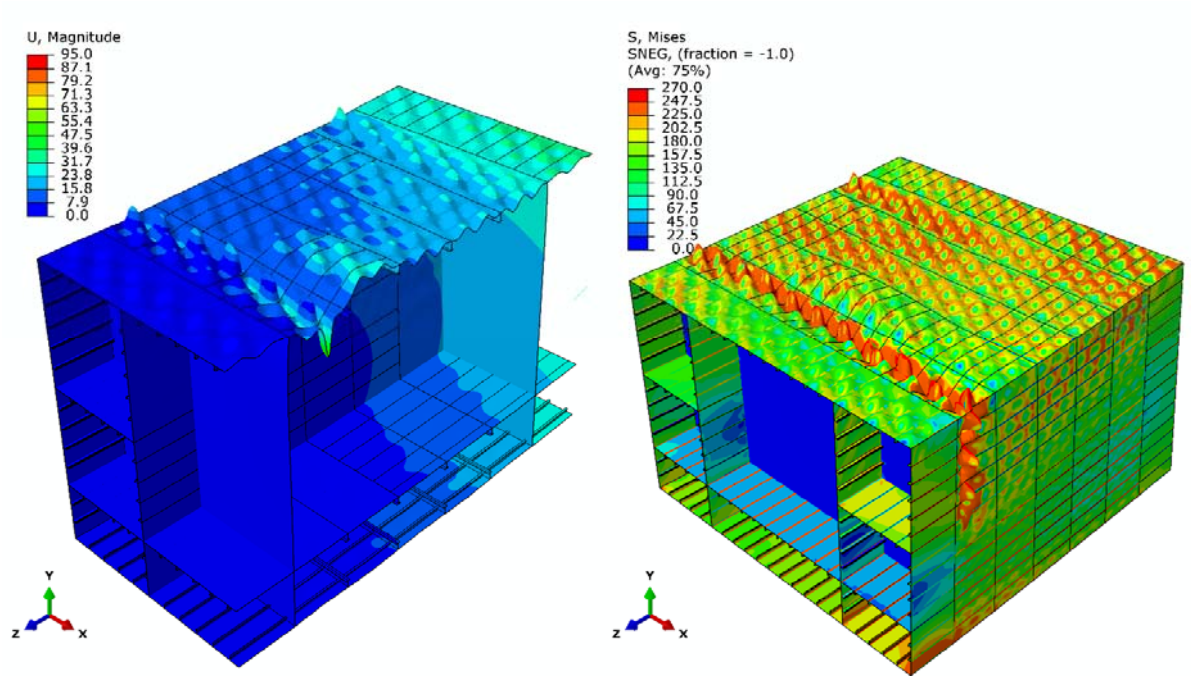

Figure 5.50: Contour plots of displacement and Von Mises equivalent stresses for Box Girder C at collapse under torsional load 7.90E+010Nmm (26.10%Tmax) and bending moment (magnify x20) (Riks)

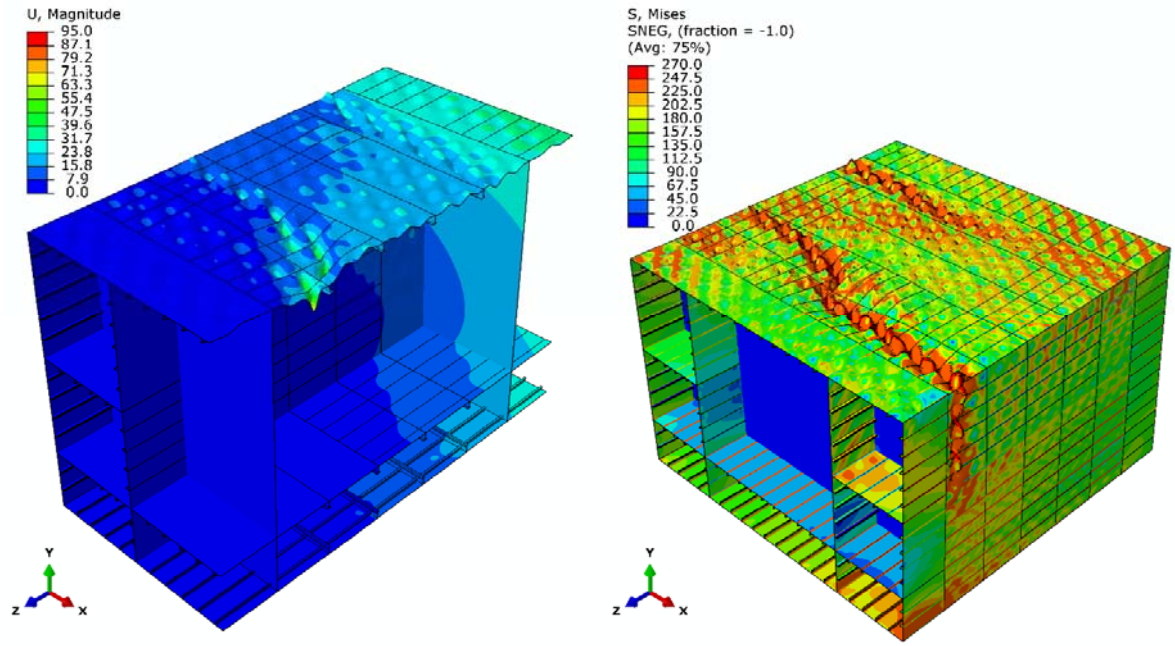

Figure 5.51: Contour plots of displacement and Von Mises equivalent stresses for the Box Girder C at collapse under torsional load 1.19E+011Nmm (39.15%Tmax) and bending moment (magnify x10) (Riks)

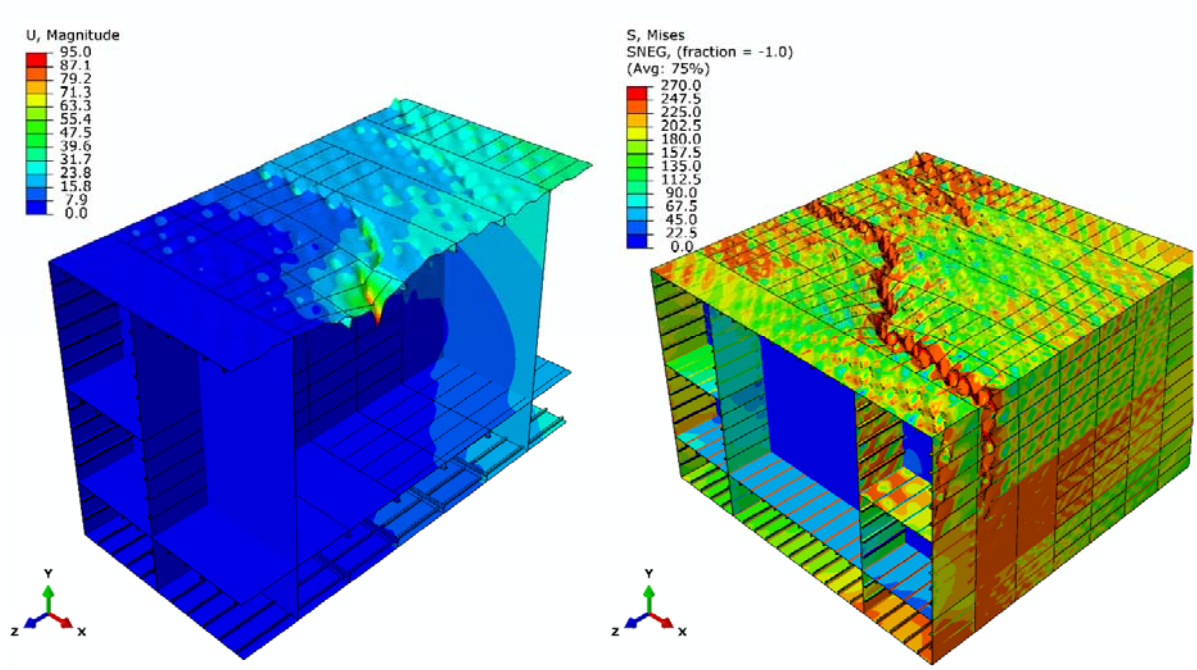

Figure 5.52: Contour plots of displacement and Von Mises equivalent stresses for Box Girder C at collapse under torsional load 1.78E+011Nmm (58.73%Tmax) and bending moment (magnify x10) (Riks)

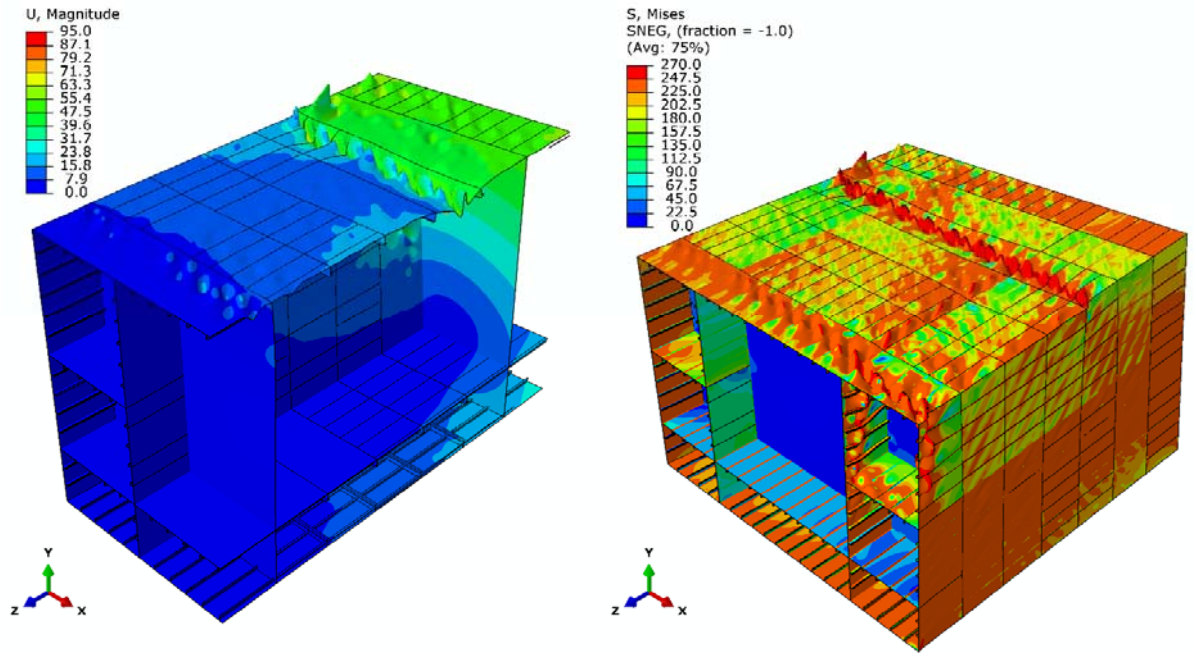

Figure 5.53: Contour plots of displacement and Von Mises equivalent stresses for Box Girder C at collapse under torsional load 2.57E+011Nmm (85.14%Tmax) and bending moment (magnify x10) (Dynamic Explicit Analysis)

The interaction diagram of torsional and bending moment is depicted in Figure 5.54 defining an area within any combination of torsional and bending load is safe. The ultimate bending load decreases as the torsional load increases and the graph has circle quadrant shape.

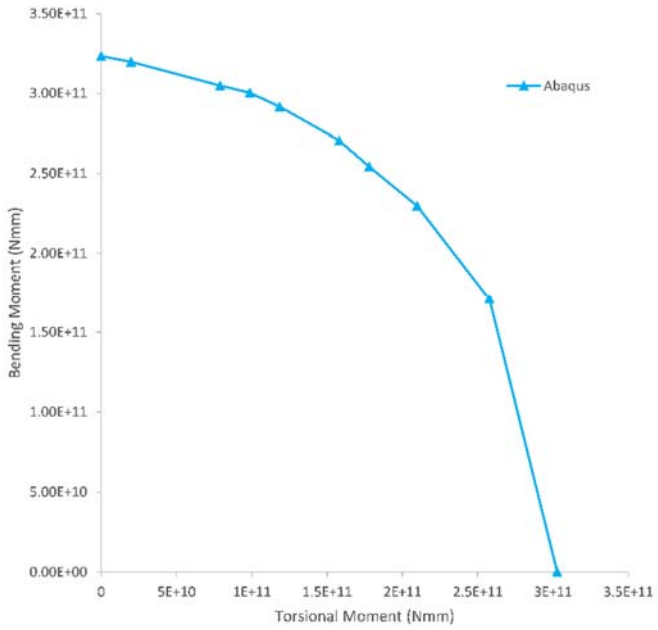

Figure 5.54: Interaction diagram of torsional and bending moment for Box Girder C

5.4.5. Box Girder D

Initially, a parametric study for the explicit dynamic analyses with 200sec and 300sec time interval was carried out when Box Girder D is subjected only to bending moment. These results are depicted in Figure 5.55 and both analyses show very good correlation. Good correlation show also the results of the explicit analysis with 200sec and 300sec for Box Girder D subjected only to torsional load in Figure 5.27. Therefore, an explicit analysis with 200sec time interval is applied in all cases of Box Girder D due to the fact that Riks analysis fails to converge.

As it has already mentioned, the plates of both end bays of this model are thicker in order to avoid the collapse of the structure in this area. The bending moment-curvature relationships of Box Girder D with combined torsional load are shown in Figure 5.56. The stiffness remains approximately the same in all cases and the strength decreases as the torsional load increases.

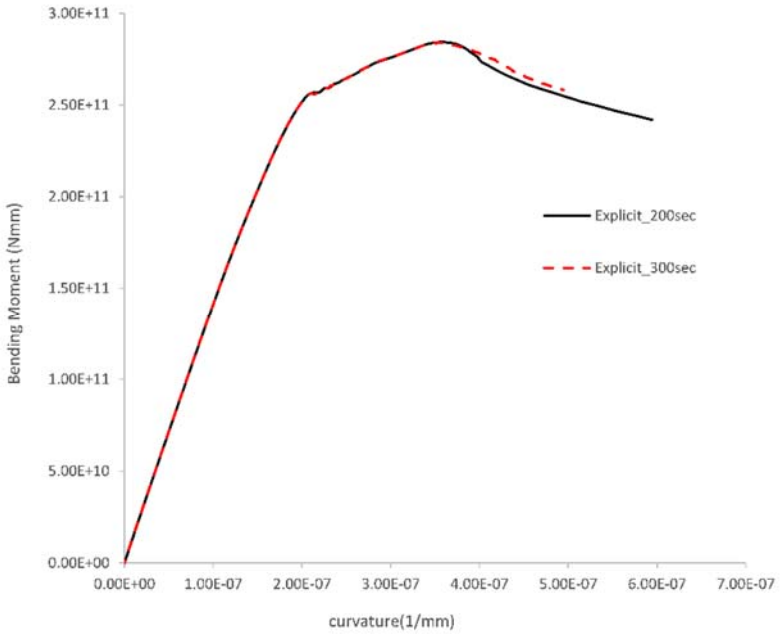

Figure 5.55: Bending moment-curvature relationship of Box Girder D subjected only to bending moment according to explicit dynamic analyses with 200sec and 300sec time interval

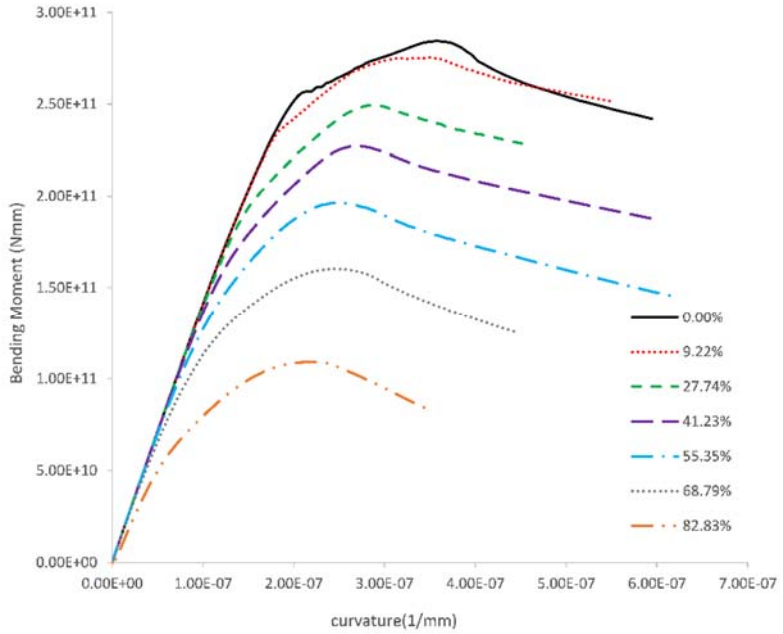

Figure 5.56: Bending moment – curvature relationships of Box Girder D under combined torsional and bending loads

The contour plots of the displacement and equivalent Von Mises stresses for Box Girder D under pure bending, combined torsional load 27.74%, 55.35%, 82.83% of Tmax and bending moment at the collapse are depicted in Figure 5.57 - Figure 5.60. In all cases the transverse frames deform, therefore overall collapse occurs.

The contour plots of Von-Misses stresses and displacement for Box Girder D under pure bending show high values of stresses and displacement at the bays close to both bulkheads (Figure 5.57).

The effect of low amounts of torsional load with combined bending (Figure 5.58 and Figure 5.59) shifts the previous described pattern of Von-Misses stresses and displacement to the diagonal direction of the structure i.e. anti-symmetrical along z-axis.

In cases which the applied torsional load is very high, e.g. 82.83%Tmax, (Figure 5.60), high values of Von-Misses stresses appear also to the sides of the structure.

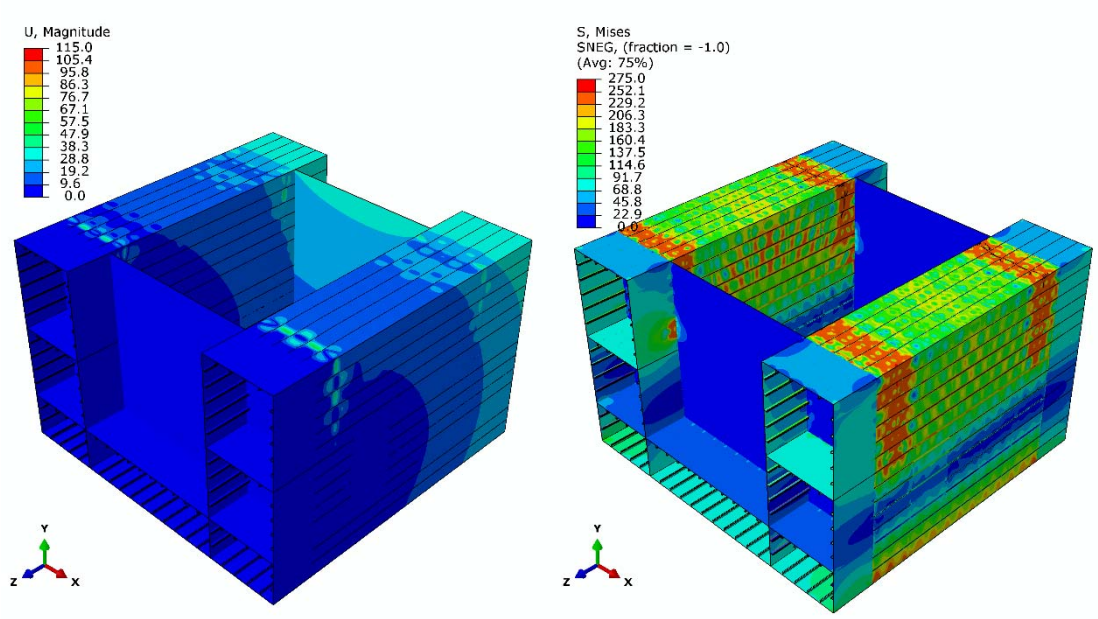

Figure 5.57: Contour plots of displacement and Von Mises equivalent stresses for Box Girder D at collapse subjected only to bending moment (magnify x1) (Dynamic Explicit)

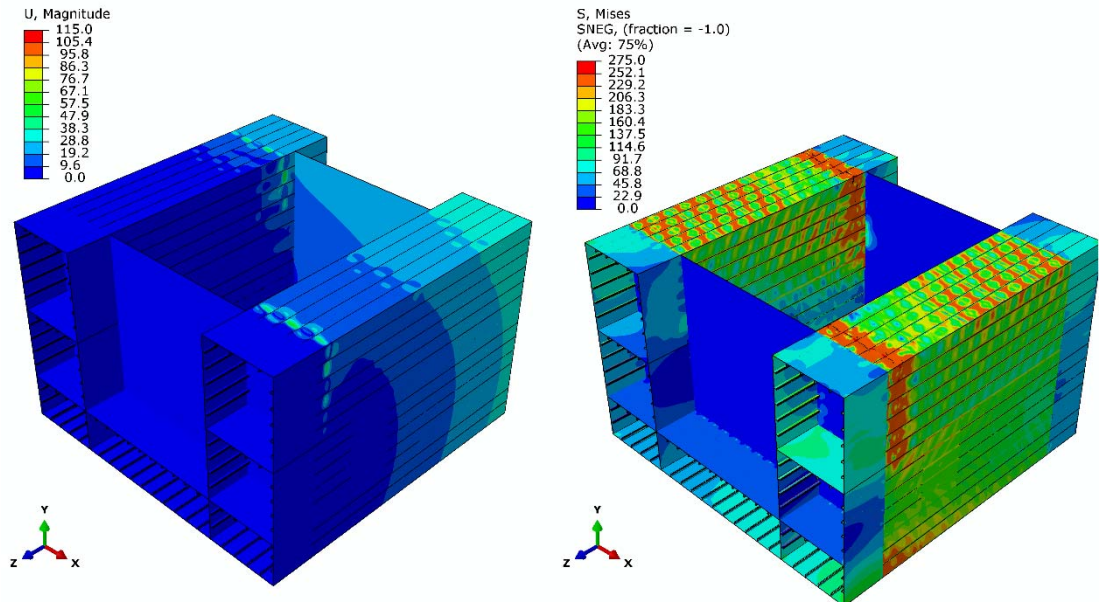

Figure 5.58: Contour plots of displacement and Von Mises equivalent stresses for Box Girder D at collapse under torsional load 6.86E+010Nmm (27.74%Tmax) and bending moment (magnify x1) (Dynamic Explicit)

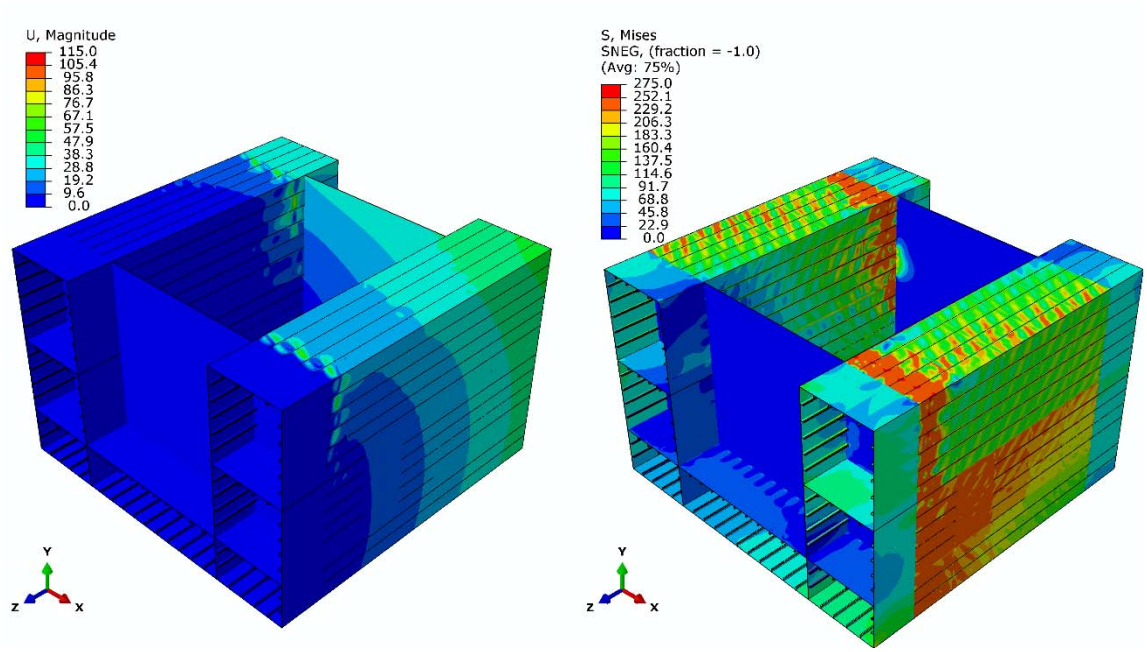

Figure 5.59: Contour plots of displacement and Von Mises equivalent stresses for Box Girder D at collapse under torsional load 1.369E+011Nmm (55.35%Tmax) and bending moment (magnify x1) (Dynamic Explicit)

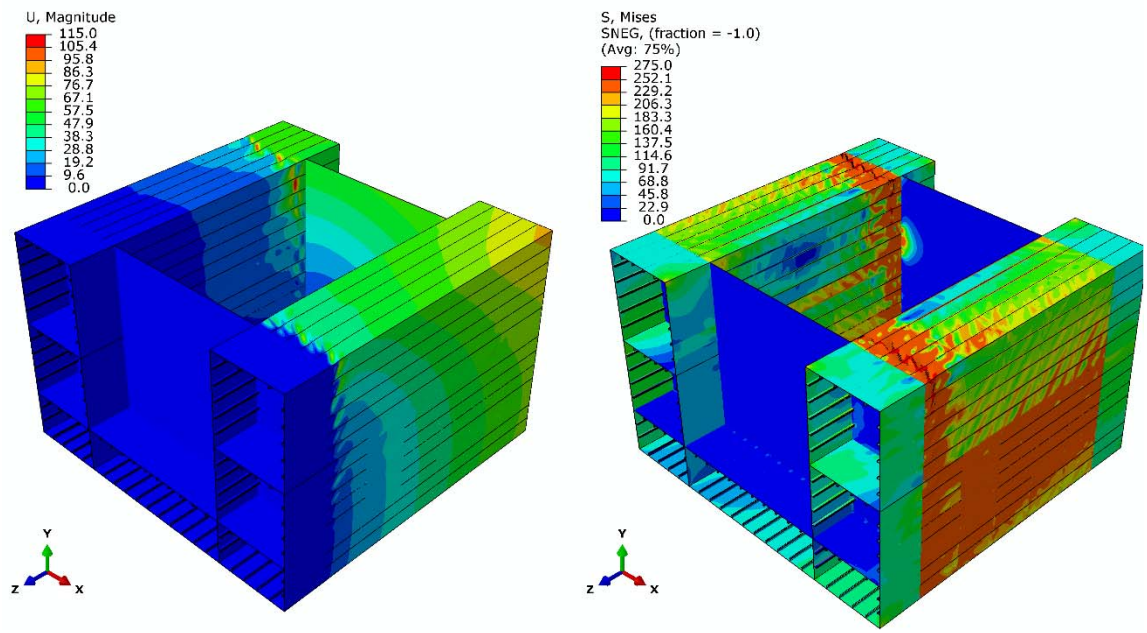

Figure 5.60: Contour plots of displacement and Von Mises equivalent stresses for Box Girder D at collapse under torsional load 2.049E+011Nmm (82.83%Tmax) and bending moment (magnify x1) (Dynamic Explicit)

The interaction diagram of torsional and bending moment is depicted in Figure 5.61 defining an area within any combination of torsional and bending load is safe. The ultimate bending load decreases as the torsional load increases.

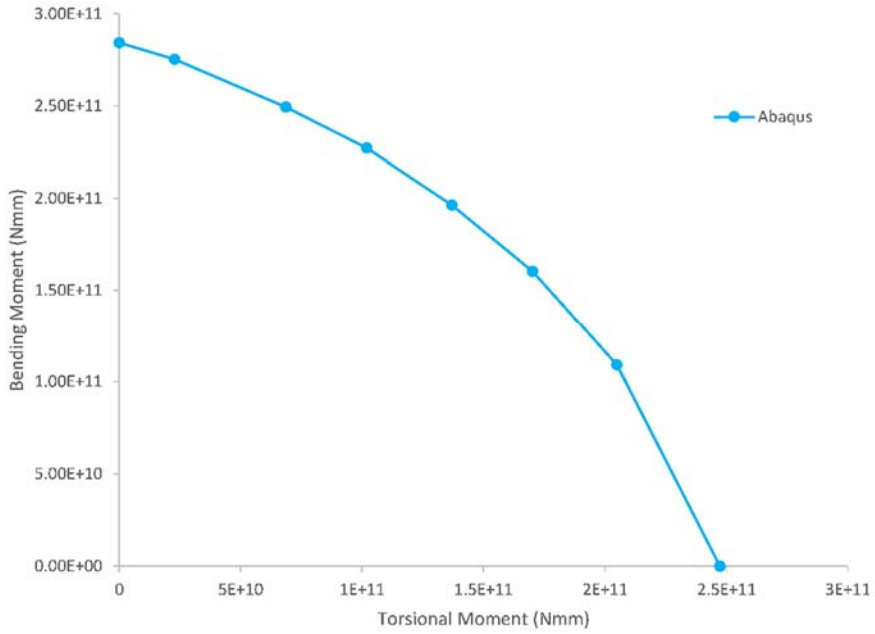

Figure 5.61: Interaction diagram of torsional and bending moment for Box Girder D

5.5. Intact box girders under combined vertical hogging bending and torsion using the Nonlinear Finite Element Method

The progressive collapse of Box Girder C and Box Girder D were also investigated under combined torsional and vertical hogging bending moment. The boundary conditions remain the same as these of combined torsional and vertical sagging bending moment case in section 5.4.1 but instead of applying positive rotation (UR1) in axis x, negative rotation UR1 is applied for the hogging condition. At this point, it should be also mentioned that all the analyses were solved with explicit dynamic analysis cause Riks analysis failed to converge in all hogging cases. The selected time interval in which the load was applied was 200sec for all cases. This is the same time interval which provided reliable results in the previous study of combined torsional and vertical sagging bending loads.

5.5.1. Box Girder C

Initially, Box Girder C is subjected only to vertical hogging bending moment and then to combined torsional loads of 32.65%Tmax, 58.67%Tmax and 85.14%Tmax and vertical hogging bending moment up to collapse. The results of the bending moment – curvature in hogging are shown in Figure 5.62. The elastic stiffness of Box Girder C does not significantly alter due to torsional load; however its strength obviously decreases as the torsional load increases.

The contour plots of displacement and equivalent Von Mises stresses of Box Girder C under pure bending in hogging is depicted in Figure 5.63, and under combined torsional load 32.65%Tmax and hogging bending moment in Figure 5.64.

Figure 5.64 shows that the maximum bending load occurs in the end bays of the model and the same pattern follow all the rest cases of combined torsional and bending loads in hogging. This probably leads to underestimate its strength and the thickness of plates in this area should be increased in order to avoid maximum stresses outside of the area of the bulkheads. However, remodeling the finite element model and rerunning these analyses is very time consuming (minimum a month), plus the fact that these results are not crucial for the validation of the code. Therefore, they were included with the purpose to define the pattern for the interaction graph of torsion and bending moment in the hogging condition which is depicted in Figure 5.65.

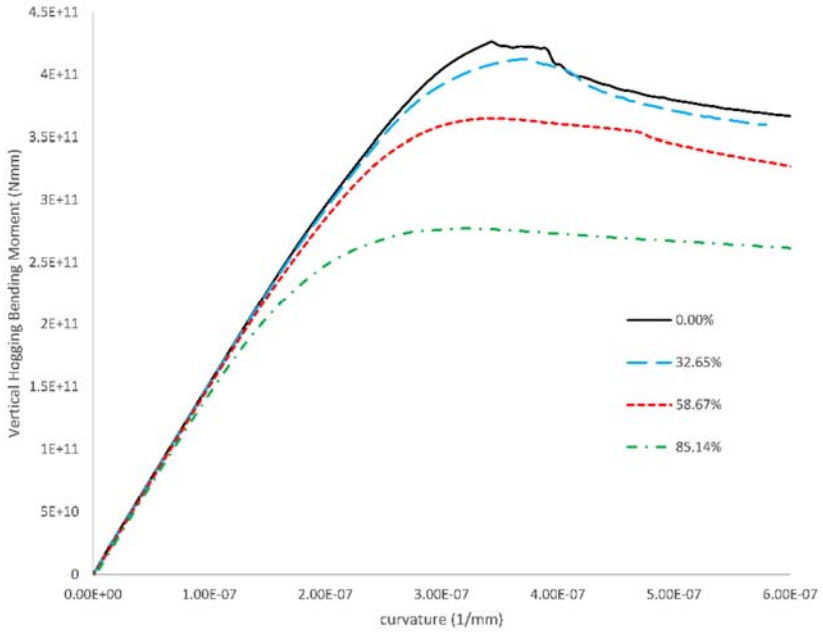

Figure 5.62: Bending Moment – curvature relationships of Box Girder C under combined torsional and bending loads in hogging

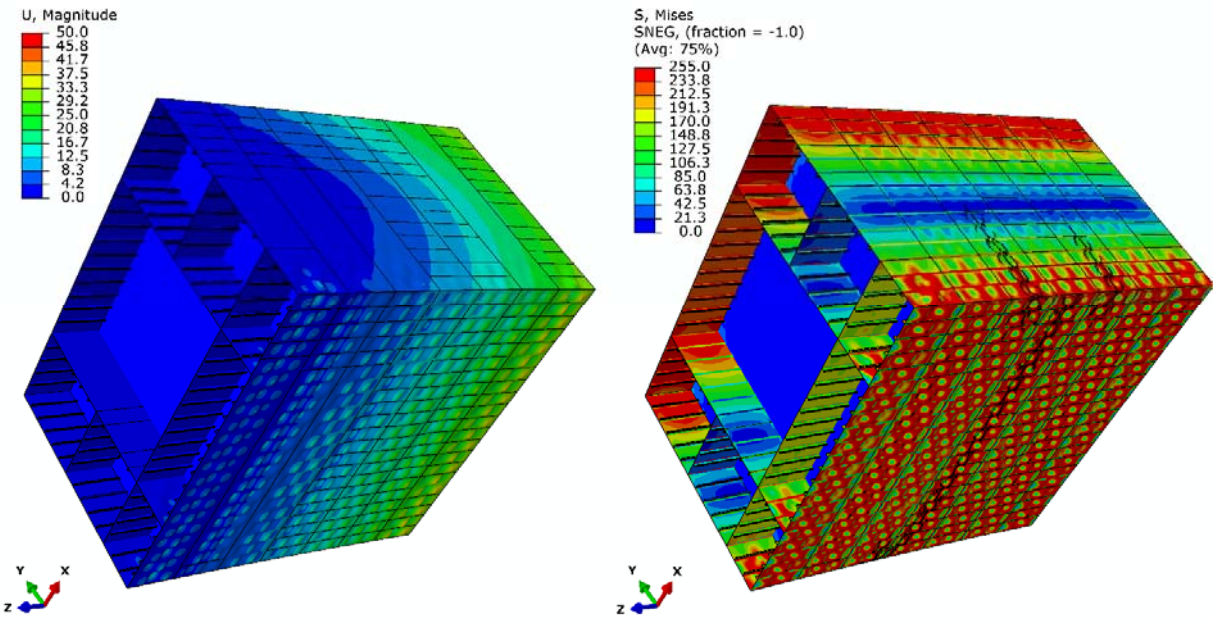

Figure 5.63: Contour plots of displacement and Von Mises equivalent stresses for Box Girder C at collapse under bending moment in hogging condition (magnify x10) (Dynamic Explicit)

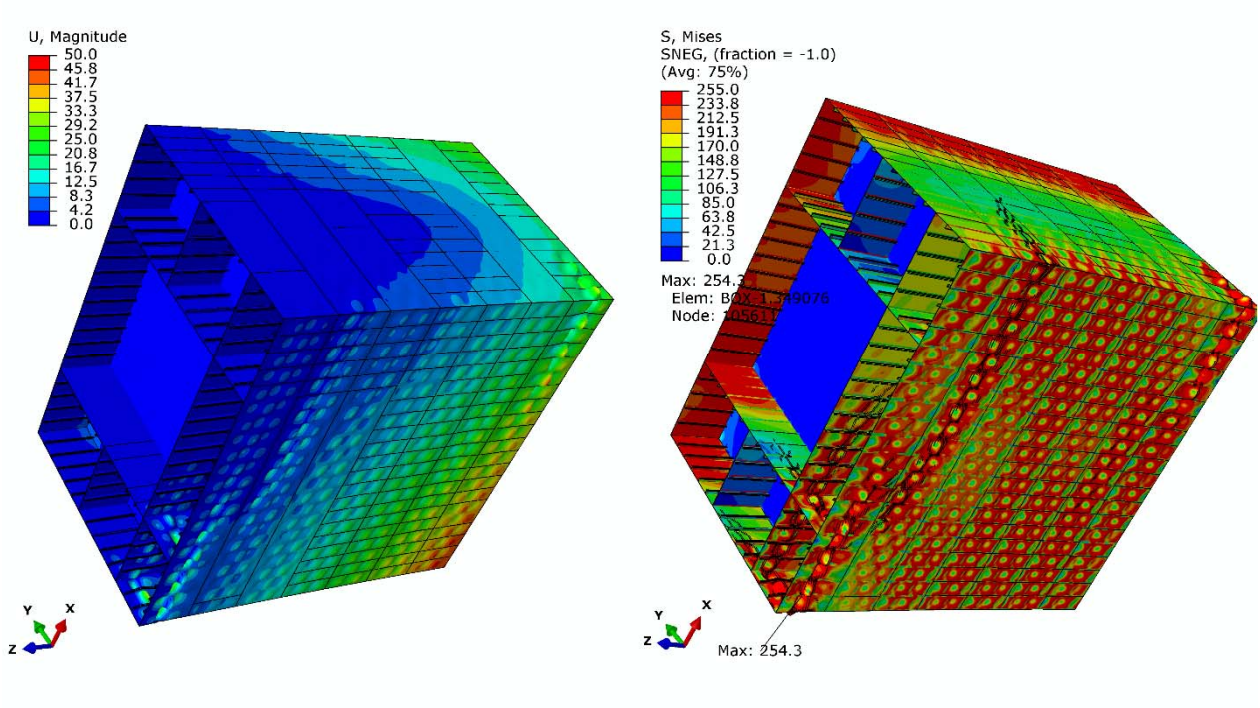

Figure 5.64: Contour plots of displacement and Von Mises equivalent stresses for Box Girder C at collapse under torsional load 9.89E+010Nmm (32.65%Tmax) and hogging bending moment (magnify x10) (Dynamic Explicit)

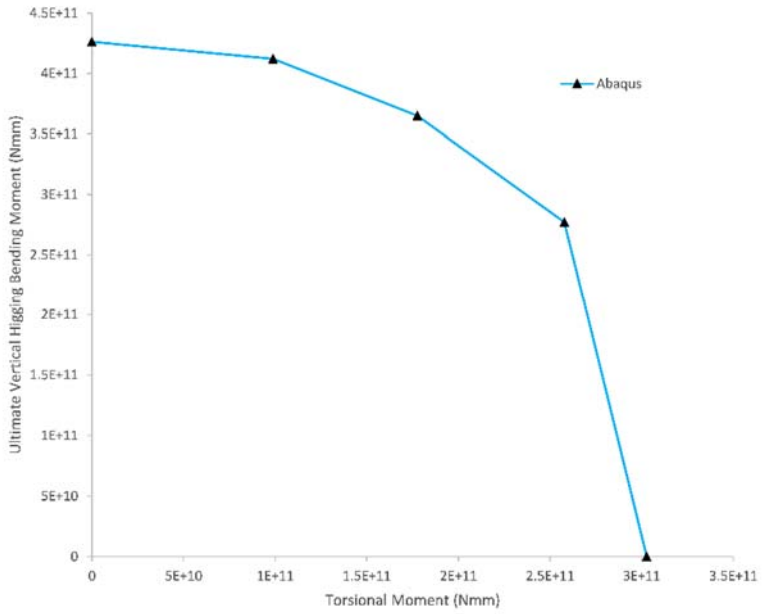

Figure 5.65: Interaction diagram of torsional and bending moment for Box Girder C in hogging

5.5.2. Box Girder D

Box Girder D is subjected only to vertical hogging bending moment and to combined torsional loads of 27.74%Tmax, 55.35%Tmax and 82.83%Tmax and vertical hogging bending moment up to collapse.

The bending moment – curvature relationships of Box Girder D are shown in Figure 5.66. The graphs show that the strength of Box Girder D decreases as the torsional load increases. Its stiffness does not significantly changes due to torsion and the post collapse behaviour presents smooth steady reduction of its ultimate strength.

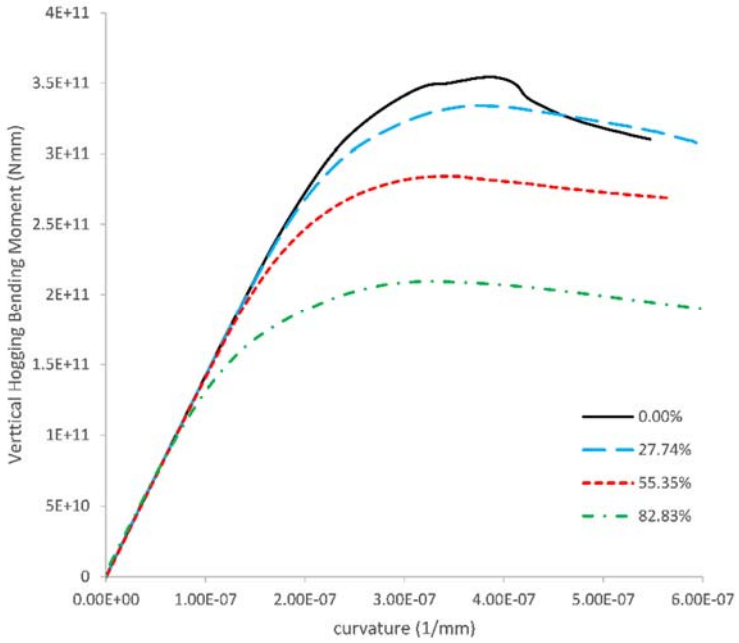

Figure 5.66: Bending Moment – curvature relationship of Box Girder D under combined torsional and bending loads in hogging

The contour plots of displacement and equivalent Von Mises stresses of Box Girder D under pure bending in hogging and under combined torsional loads of 27.74%Tmax, 55.35%Tmax and 82.83%Tmax and vertical hogging bending moment are depicted in Figure 5.67 - Figure 5.70. Overall collapse occurs in all cases in hogging condition.

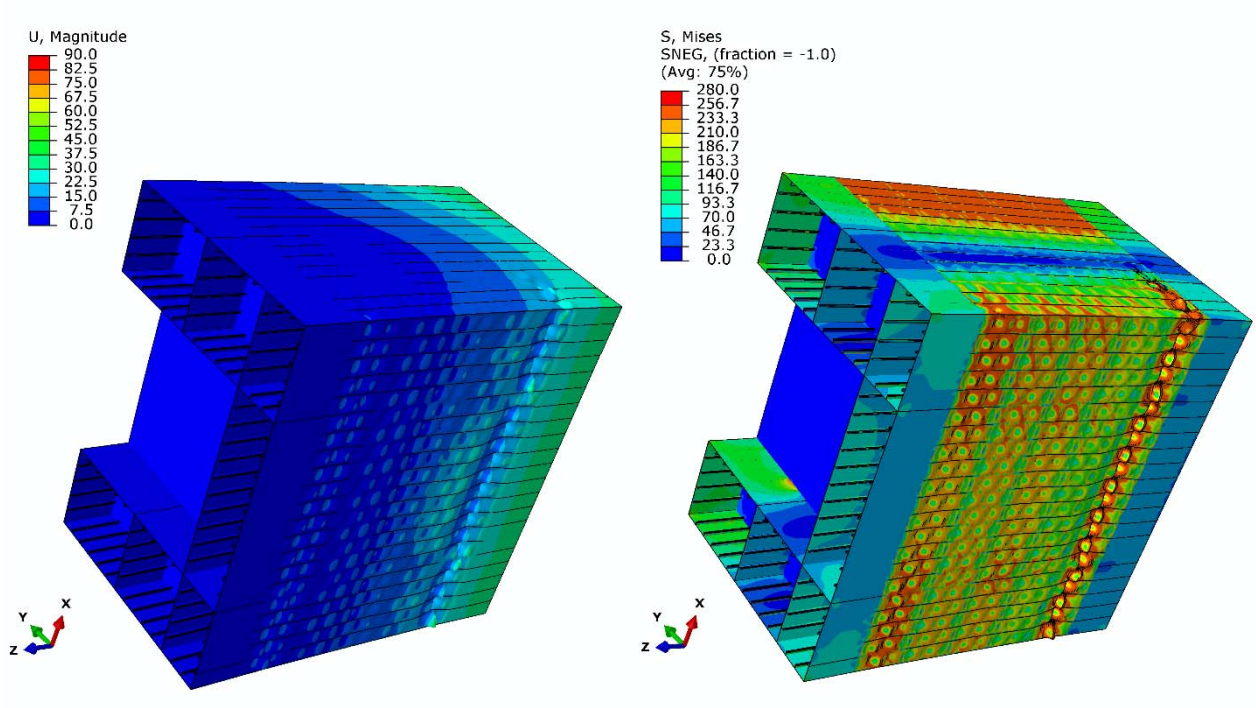

Figure 5.67: Contour plots of displacement and Von Mises equivalent stresses for Box Girder D at collapse under bending moment in hogging condition (magnify x10) (Dynamic Explicit)

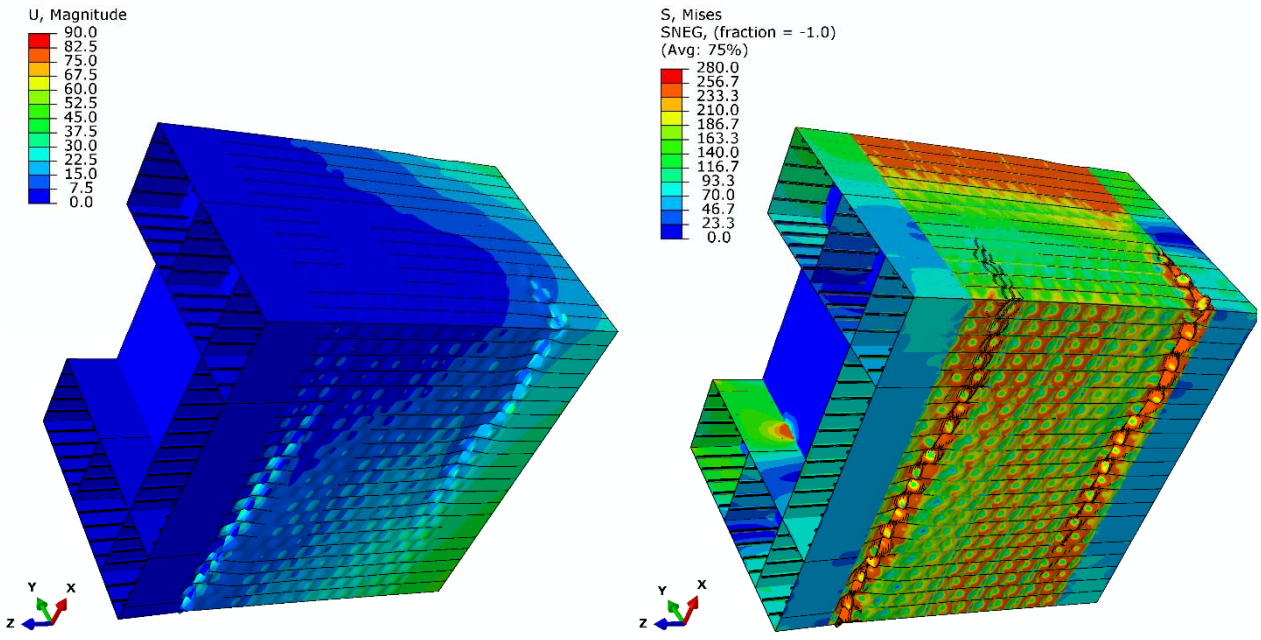

Figure 5.68: Contour plots of displacement and Von Mises equivalent stresses for Box Girder D at collapse under torsional load 6.86E+010Nmm (27.74%Tmax) and hogging bending moment (magnify x10) (Dynamic Explicit)

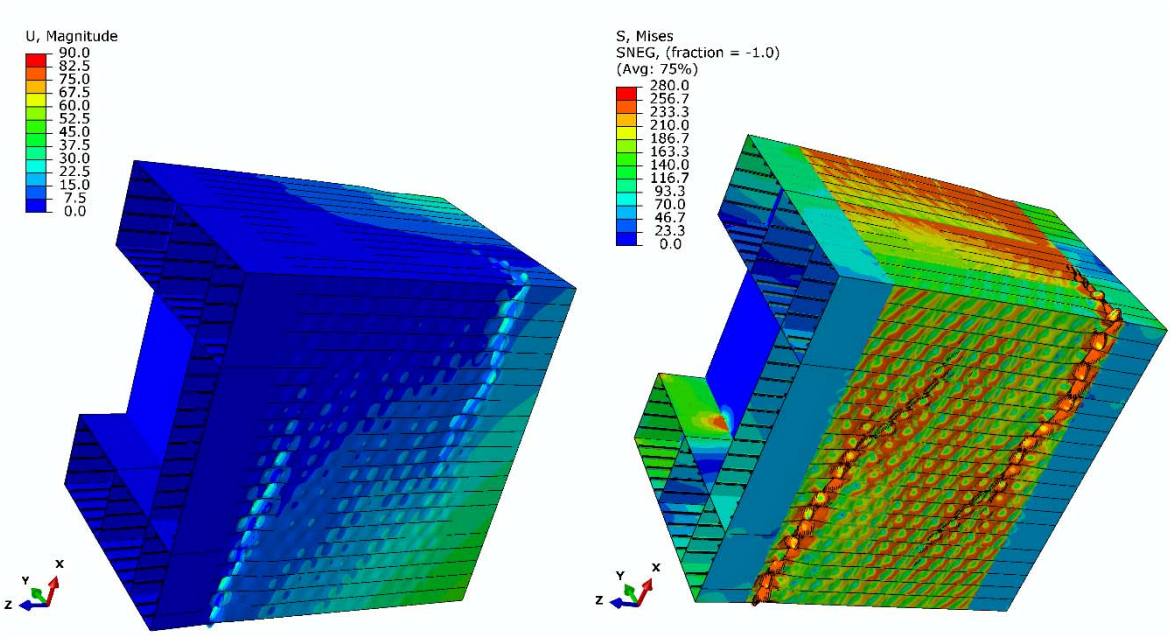

Figure 5.69: Contour plots of displacement and Von Mises equivalent stresses for Box Girder D at collapse under torsional load 1.37E+011Nmm (55.35%Tmax) and hogging bending moment (magnify x10) (Dynamic Explicit)

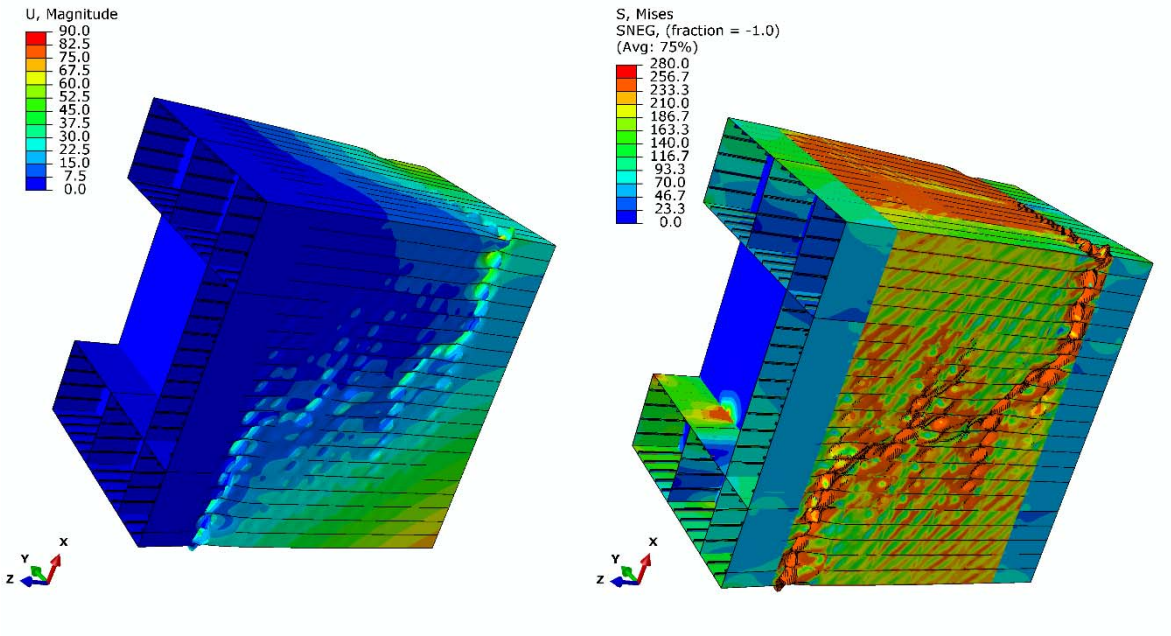

Figure 5.70: Contour plots of displacement and Von Mises equivalent stresses for Box Girder D at collapse under torsional load 2.049E+011Nmm (82.83%Tmax) and hogging bending moment (magnify x10) (Dynamic Explicit)

The contour plots of the displacement and Von-Misses stresses for Box Girder D subjected only to vertical hogging bending moment show high deformation and stresses along the bay close to the bulkhead at End-1, in which the load is applied. For low amount of torsional load, e.g. 27.74%Tmax (Figure 5.68), high stresses and displacement occur along the bays close to the two bulkheads. As the torsional load increases (Figure 5.69 and Figure 5.70), the bottom plates of Box Girder D yield along the diagonal of the structure.

The interaction diagram of torsional and bending moment of Box Girder D in hogging is shown in Figure 5.71. The ultimate strength of the structure decreases as the torsional load increases. An area of quadrant shape is formed within the strength of the structure is adequate under these combined loads.

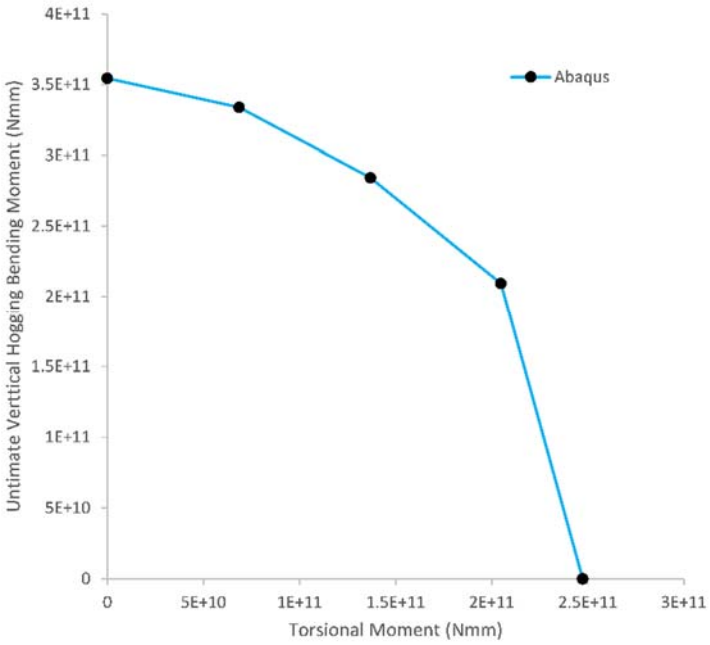

Figure 5.71: Interaction diagram of torsional and ultimate vertical bending moment of Box Girder D in hogging condition

5.6. Intact box girders under combined vertical sagging bending and torsion using the Extended Simplified Progressive Collapse Method

The same box girders are analysed with the proposed methodology described in chapter 3, using ProColl. The set up in ProColl and the results of their analyses are presented in the following sections.

5.6.1. Box Girder A

The model of Box Girder A in ProColl was created based on the provided data from section 5.2.1.1 and its ProColl file is presented in Appendix B. The same initial imperfections to the NLFE model were incorporated also to ProColl model. The cross section of Box Girder A is consisted only by one loop; therefore all plates belong to loop number 1 (Figure 5.72). In this case, four (4) load shortening curves were defined, each for each side of the rectangular and the corresponding plates are associated with their load shortening curve. Additionally, the model is consisted by five bays (i.e. nsy=5), which is the number of bays between the bulkheads. The model was analysed under combined torsional and vertical sagging bending moment.

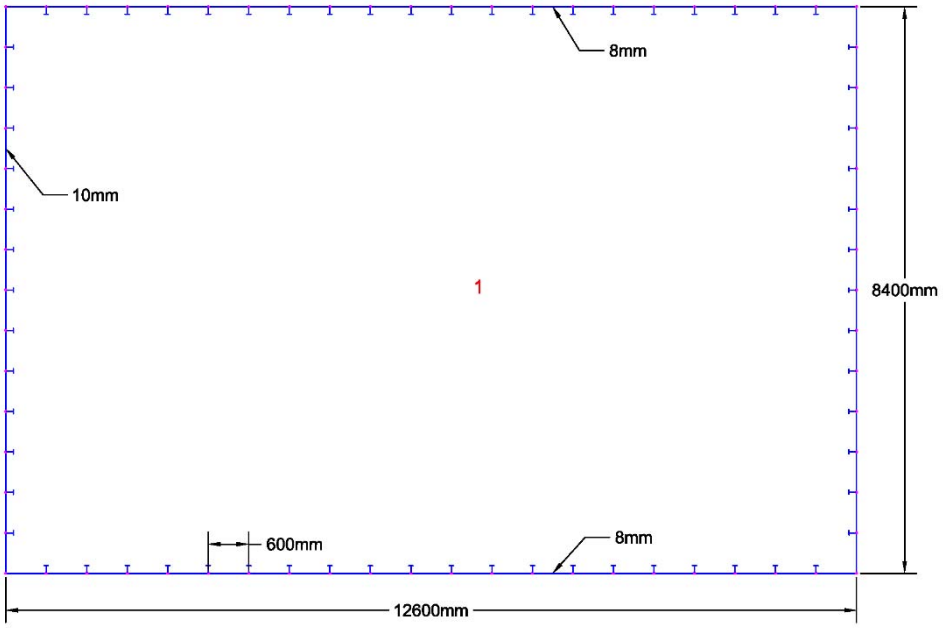

Figure 5.72: The cross-section of Box Girder A with its defined numbered loops/cells in ProColl

The moment-curvature relationships of Box Girder A subjected to combined torsional load (Nmm) and vertical sagging bending moment are shown in Figure 5.73. Different amounts of torsional load are applied to the structure up to $T_o$and its progressive collapse decreases as the torsional load increases. The post collapse pattern of the graph for low amount of torsion (i.e. 0Nmm and 2.40E+10Nmm) is different than this for higher amount of applied torsion. This occurs due to the way which the extended simplified progressive collapse method generates the inclination of the curve in the post collapse area and it extensively explained in Benson's thesis (Benson, 2011).

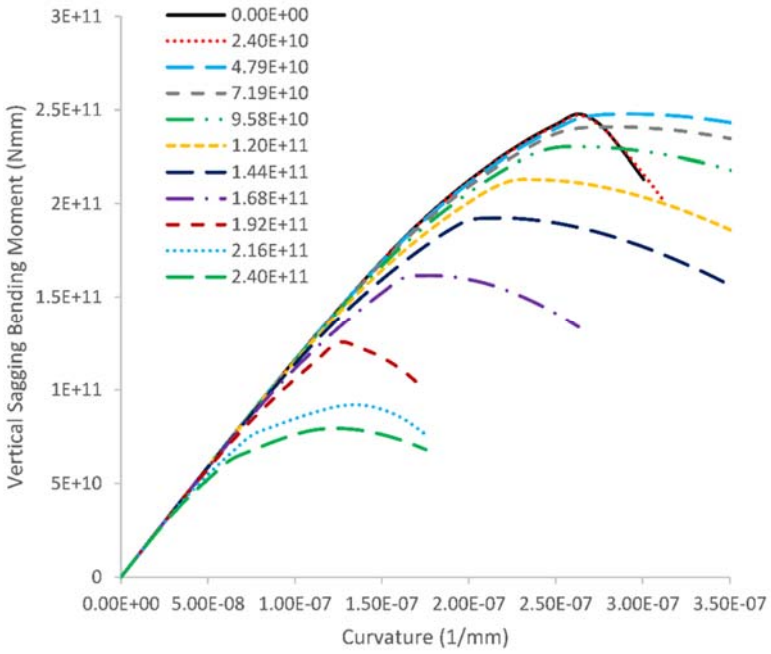

Figure 5.73: Bending moment-curvature relationships of Box Girder A under combined torsional moment (in Nmm) and sagging bending moment

The interaction diagram of torsion and bending moment according to the proposed methodology is presented in Figure 5.74. The bending moment decreases as the torsional load increases defining an area within the strength of the structure is sufficient under these combined loads. As maximum torsional load was assumed the value of T_o, which is calculated by the program and the graph shows no results under pure torsion which is one of the main assumptions of the proposed methodology.

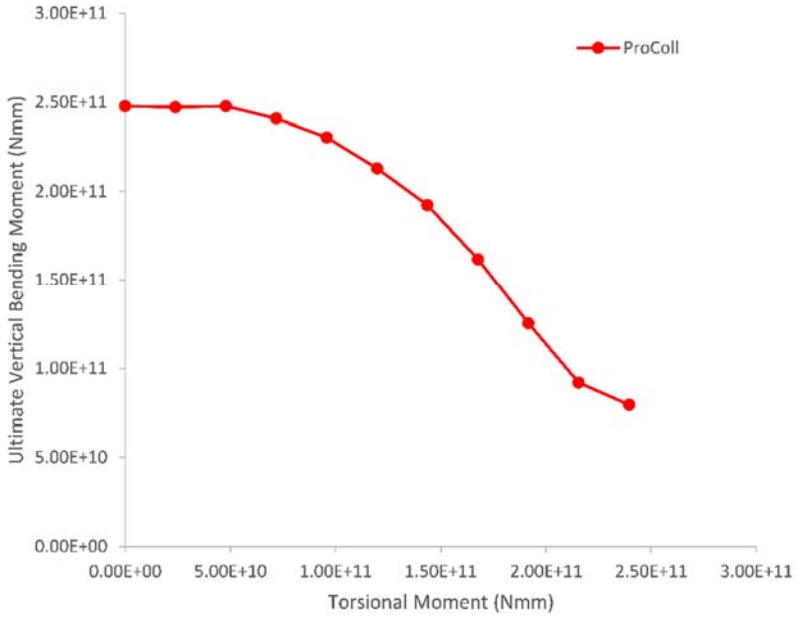

Figure 5.74: Interaction diagram of vertical bending moment and torsion for Box Girder A according to the proposed methodology

5.6.2. Box Girder B

The model of Box Girder B in ProColl was created based on the provided data from section 5.2.1.2 and its file is presented in Appendix B. The same initial imperfections to the NLFE model were incorporated also to ProColl model. The cross section of Box Girder B is consisted only by four (4) loops which are shown in Figure 5.75. The defined load shortening curves and their associated plates are shown in the ProColl file in Appendix B. Additionally, the model is consisted by five bays (i.e. nsy=5), which is the number of bays between the bulkheads. The model was analysed under combined torsional and vertical sagging bending moment.

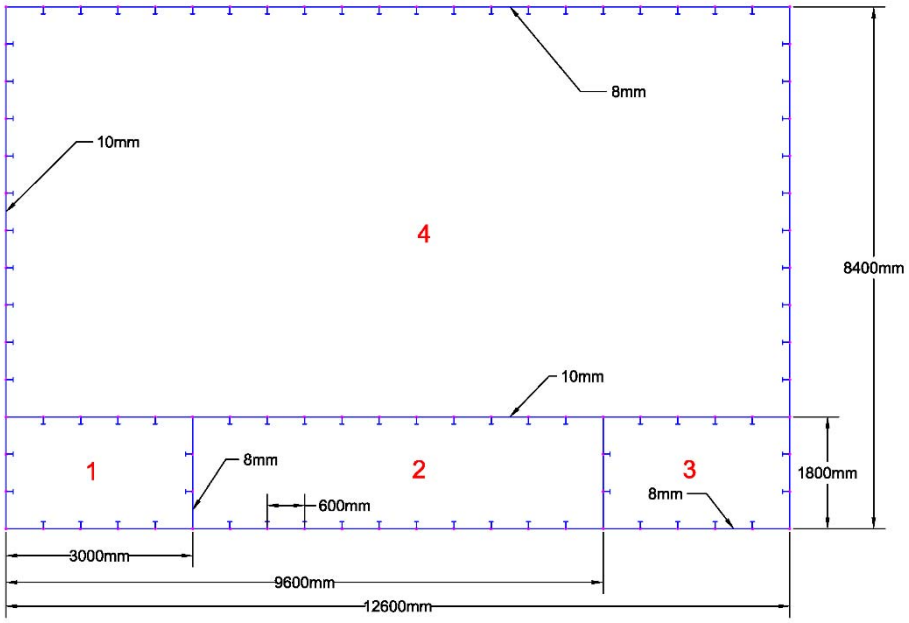

Figure 5.75: The cross-section of Box Girder B with its defined numbered loops/cells in ProColl

The moment-curvature relationships of Box Girder B subjected to combined torsional load (Nmm) and vertical sagging bending moment are shown in Figure 5.76. Different amounts of torsional load are applied to the structure up to T_o and its progressive collapse decreases as the torsional load increases.

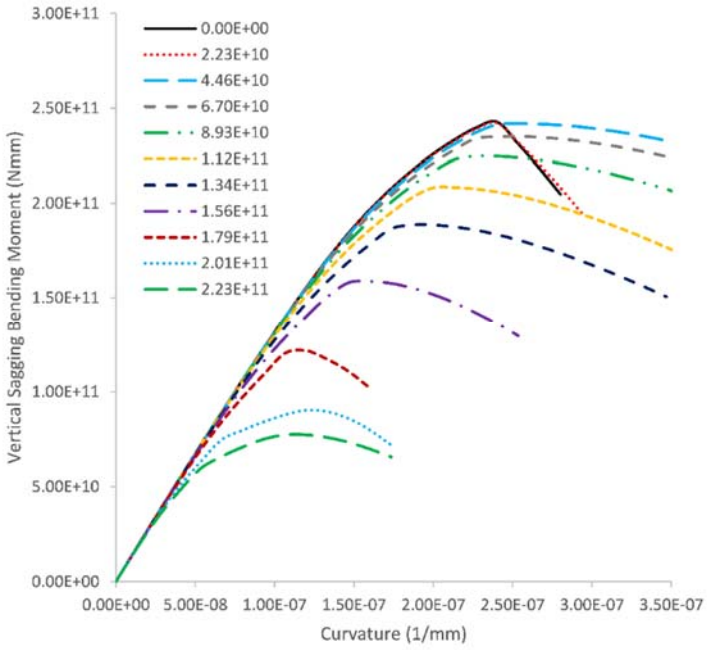

Figure 5.76: Bending moment-curvature relationships of Box Girder B under combined torsional moment (in Nmm) and sagging bending moment

The interaction diagram of torsion and bending moment according to the proposed methodology is presented in Figure 5.77. The bending moment decreases as the torsional load increases defining an area within the strength of the structure is sufficient under these combined loads. The value of T_o which is calculated by the program was assumed as the maximum torsional load and the graph shows no results under pure torsion.

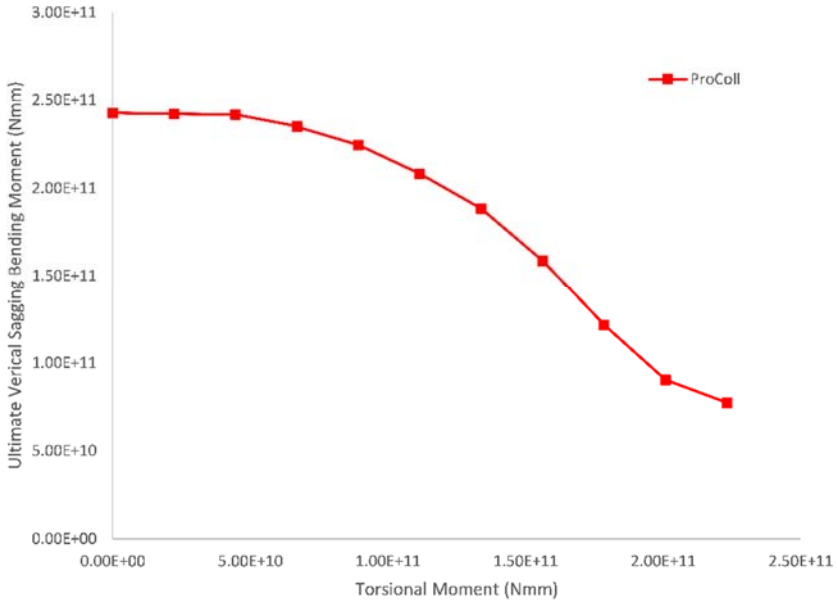

Figure 5.77: Interaction diagram of vertical bending moment and torsion for Box Girder B according to the proposed methodology

5.6.3. Box Girder C

The model of Box Girder C in ProColl was created based on the provided data from section 5.2.1.3 and its file is presented in Appendix B. The same initial imperfections to the NLFE model were incorporated also to ProColl model. The cross section of Box Girder C is consisted by eight (8) loops which are shown in Figure 5.78. The defined load shortening curves and their associated plates are shown in the file of ProColl in Appendix B. Additionally, the model is consisted by five bays (i.e. nsy=5), which is the number of bays between the bulkheads. The model was analysed under combined torsional and vertical sagging bending moment.

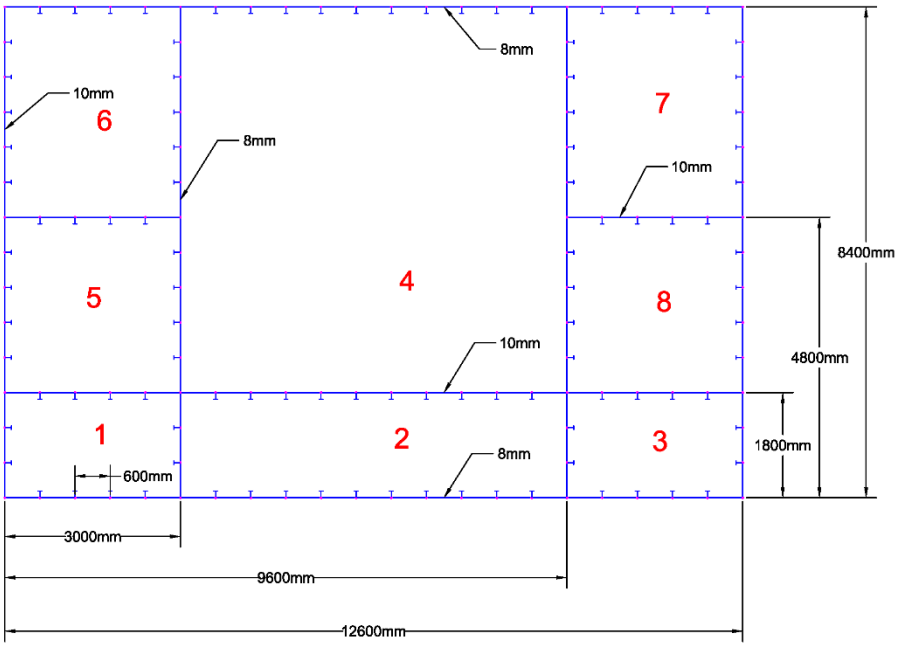

Figure 5.78: The cross-section of Box Girder C with its defined numbered loops/cells in ProColl

The moment-curvature relationships of Box Girder C subjected to combined torsional load (Nmm) and vertical sagging bending moment are shown in Figure 5.79. Different amounts of torsional load are applied to the structure up to $T_o$and its progressive collapse decreases as the torsional load increases.

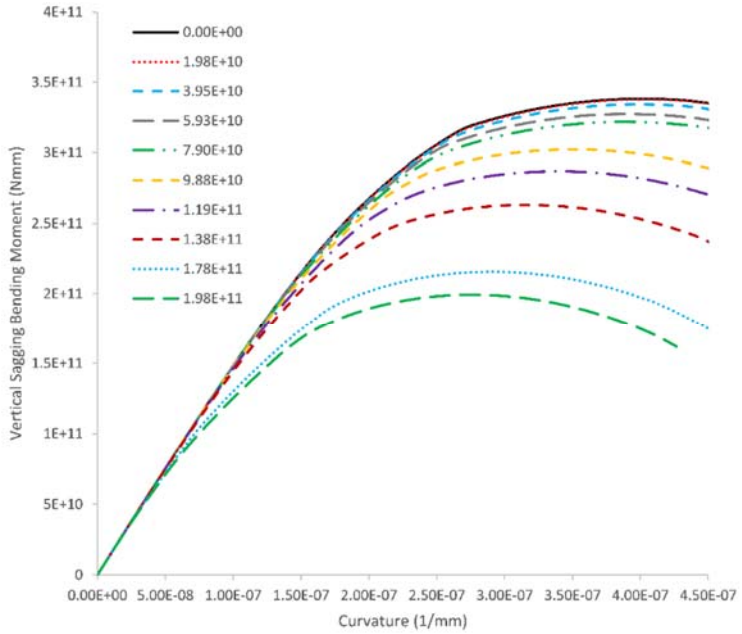

Figure 5.79: Bending moment-curvature relationships of Box Girder C under combined torsional moment (in Nmm) and sagging bending moment

The interaction diagram of torsion and bending moment according to the proposed methodology is presented in Figure 5.80. The bending moment decreases as the torsional load increases defining an area within the strength of the structure is sufficient under these combined loads. The value of T_o which is calculated by the program was assumed as the maximum torsional load and the graph shows no results under pure torsion.

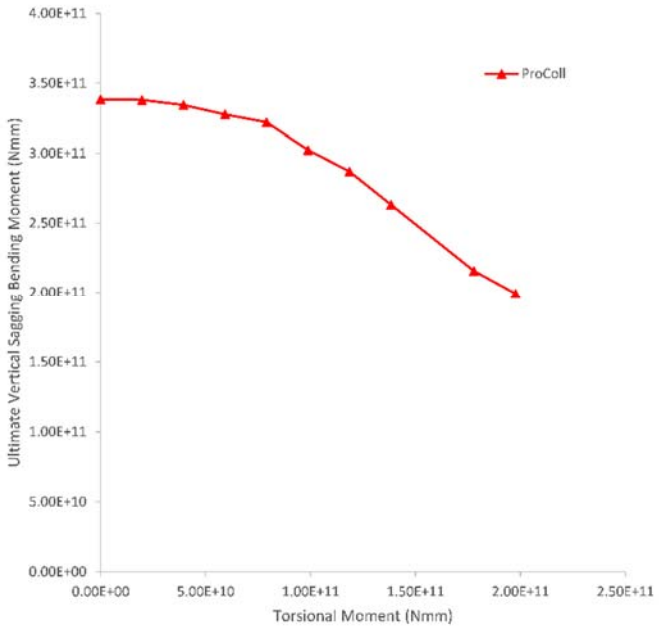

Figure 5.80: Interaction diagram of vertical bending moment and torsion for Box Girder C according to the proposed methodology

5.6.4. Box Girder D

The model of Box Girder D in ProColl was created based on the provided data from section 5.2.1.4 and its file is presented in Appendix B. The same initial imperfections to the NLFE model were incorporated also to ProColl model. The cross section of Box Girder D is consisted by seven (7) loops which are shown in Figure 5.81. The defined load shortening curves and their associated plates are shown in the file of ProColl in Appendix B. Additionally, the model is consisted by five bays (i.e. nsy=5), which is the number of bays between the bulkheads. The model was analysed under combined torsional and vertical sagging bending moment.

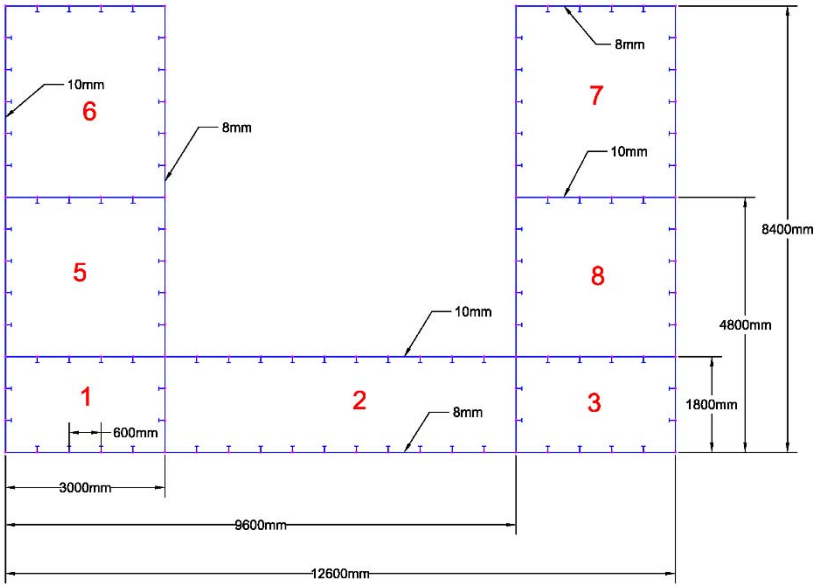

Figure 5.81: The cross-section of Box Girder D with its defined numbered loops/cells in ProColl

The moment-curvature relationships of Box Girder D subjected to combined torsional load (Nmm) and vertical sagging bending moment are shown in Figure 5.82. Different amounts of torsional load are applied to the structure up to T_o and its progressive collapse decreases as the torsional load increases.

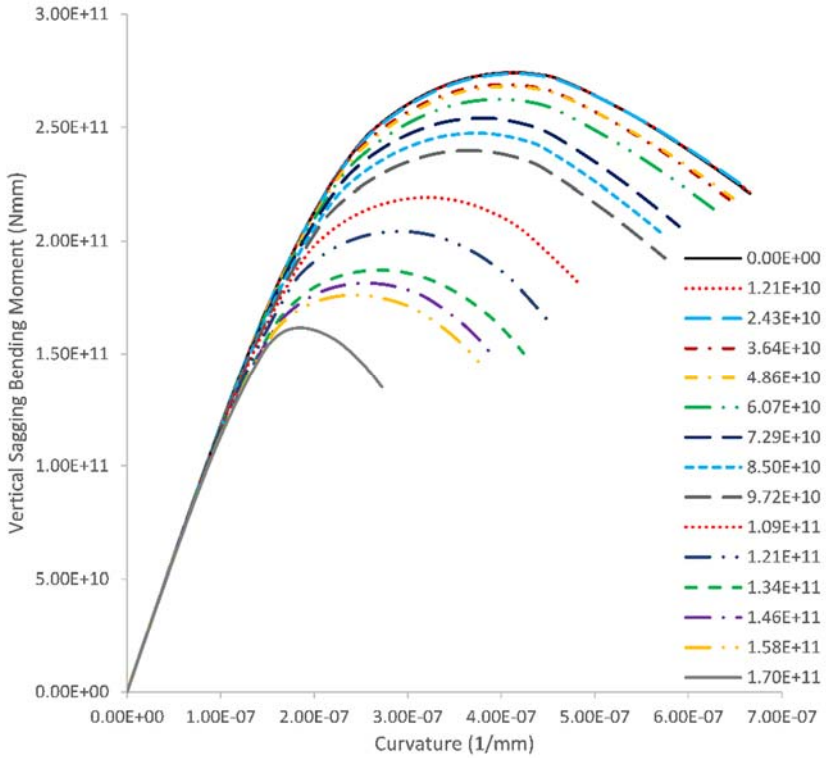

Figure 5.82: Bending moment-curvature relationships of Box Girder D under combined torsional moment (in Nmm) and sagging bending moment

The interaction diagram of torsion and bending moment according to the proposed methodology is presented in Figure 5.83. The bending moment decreases as the torsional load increases defining an area within the strength of the structure is sufficient under these combined loads. The value of T_o which is calculated by the program was assumed as the maximum torsional load and the graph shows no results under pure torsion.

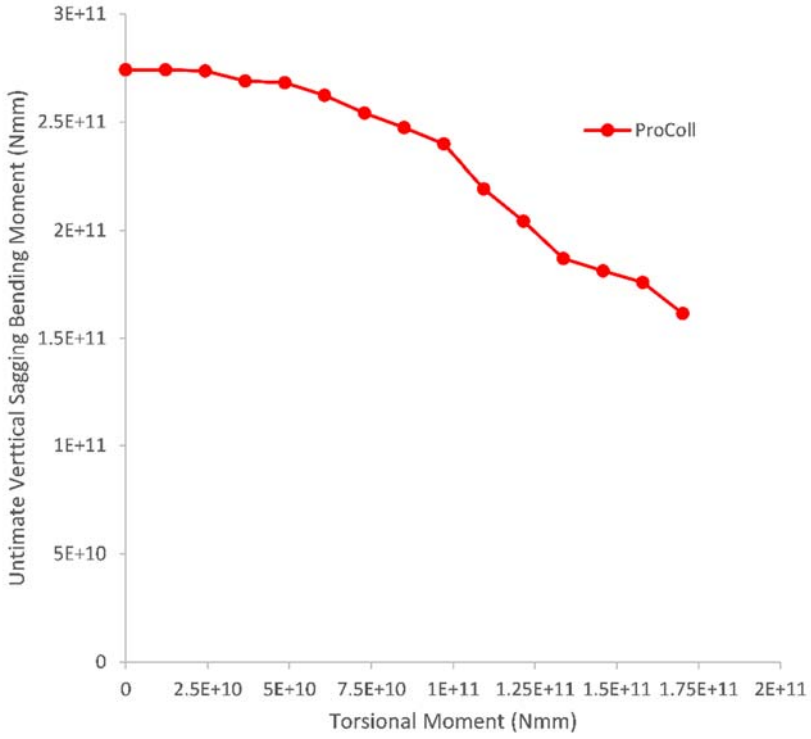

Figure 5.83: Interaction diagram of vertical bending moment and torsion for Box Girder D according to the proposed methodology

5.7. Intact box girders under vertical hogging bending and torsion using the Extended Simplified Progressive Collapse Method

The results of Box Girder C and Box Girder D under combined torsion and vertical hogging bending moment according to the proposed methodology are presented in this section.

5.7.1. Box Girder C

The set-up of the model under combined torsional and vertical hogging bending moment in ProColl is the same with this which is described in section 5.6.3. The user needs to select the option of "torsion with vertical hogging" instead of "torsion with vertical sagging" in the GUI of ProColl in order to run the aforementioned model under these combined loads. The vertical bending-curvature relationships of Box Girder C under combined torsion and vertical hogging bending moment are presented in Figure 5.84. The progressive strength of the structure decreases evenly at the peak and post collapse area, as the applied torsion increases. All graphs present the same slope in the pre-collapse area, showing that the stiffness of the structure is not affected by the applied torsion.

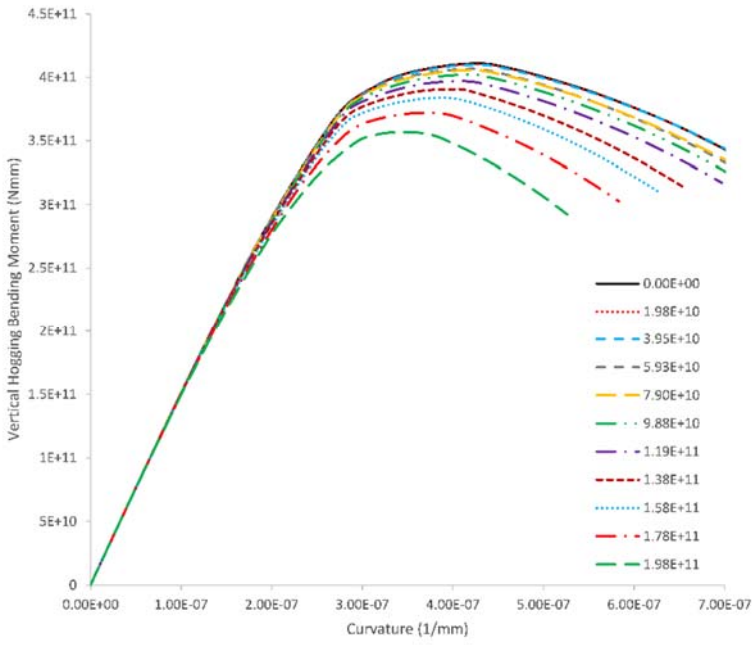

Figure 5.84: Vertical bending moment-curvature relationships of Box Girder C under combined torsional moment (in Nmm) and hogging bending moment

The interaction diagram of the torsional and vertical bending moment of Box Girder C in hogging according to the proposed methodology for the incorporation of torsion into the extended simplified progressive collapse method is shown in Figure 5.85. The strength of the structure decreases as the applied torsion increases. The graph defines the limit which beneath it the strength of the structure is adequate under these combined loads.

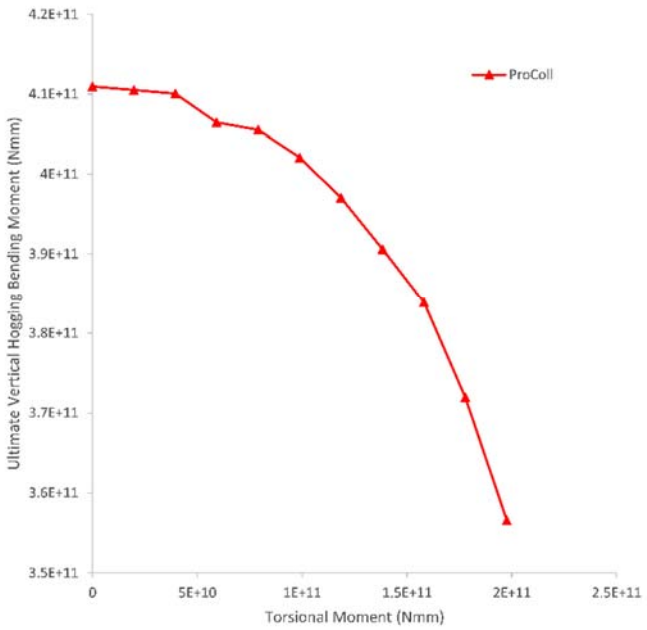

Figure 5.85: Interaction diagram of vertical hogging bending moment and torsion for Box Girder C according to the proposed methodology

5.7.2. Box Girder D

The set-up of the model under combined torsion and vertical hogging bending moment is the same with this which is described in section 5.6.4. The user needs to select the option of "torsion with vertical hogging" in the GUI of ProColl in order to run the file under these loads. The vertical bending-curvature relationships of Box Girder D under combined torsional and vertical hogging bending moment are presented in Figure 5.86. The progressive strength of the structure smoothly decreases as the amount of torsion increases. All graphs present the same slope in the pre-collapse area, showing that the stiffness of the structure is not affected by the applied torsion.

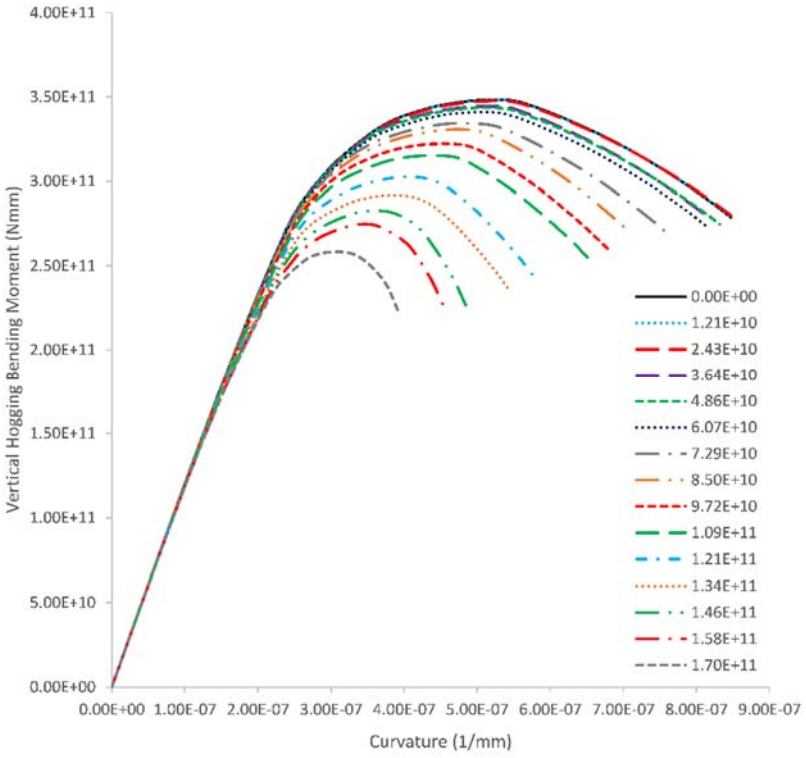

Figure 5.86: Vertical bending moment-curvature relationships of Box Girder D under combined torsional moment (in Nmm) and hogging bending moment

The interaction diagram of the torsional and vertical bending moment of Box Girder D in hogging according to the proposed methodology is shown in Figure 5.87. The strength of the structure decreases as the applied torsion increases and the graph defines an area within the strength of the structure is adequate under these combined loads.

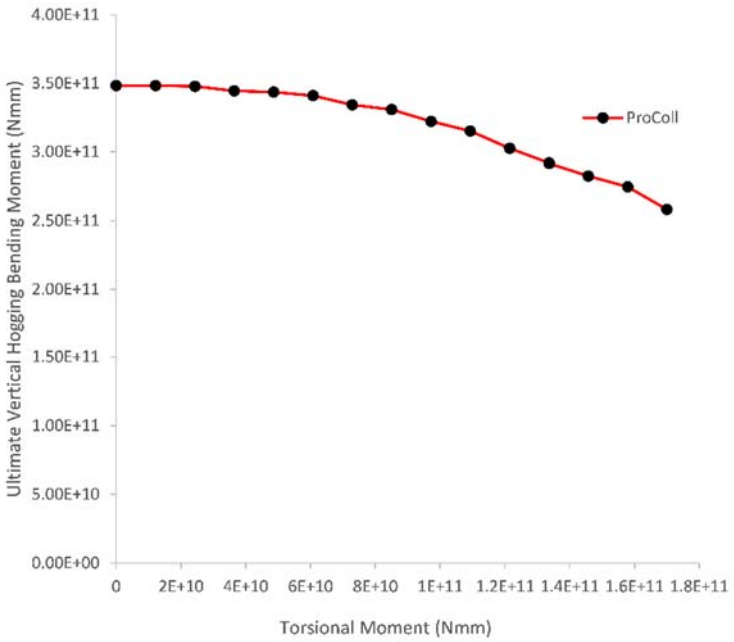

Figure 5.87: Interaction diagram of vertical hogging bending moment and torsion for Box Girder D according to the proposed methodology

5.8. Comparison of the results

In this section, the results of the nonlinear finite element method and the extended simplified progressive collapse method are compared. In the comparison, the results of the theoretical interaction of torsion and bending (Equation 5.8) are also included. All graphs are normalised by the values of the F.E. results.

$$\left(\frac{T}{T_{max}}\right)^2 + \left(\frac{B}{B_{max}}\right)^2 = 1 \qquad \text{Equation 5.8}$$

5.8.1. Box Girder A

The results of Box Girder A subjected to combined torsion and vertical bending moment are presented in Figure 5.88 according to the nonlinear F.E. method, the proposed methodology and the theoretical interaction of torsion and bending (Equation 5.8). All values are normalised by the values of $BM_{max}$and T_{max} of the F.E. results which in this case are:

$\boldsymbol{T_{max} = 2.59 \times 10^{11} Nmm}$ and $\boldsymbol{BM_{max} = 2.32 \times 10^{11} Nmm}$

The theoretical results show extremely good correlation with the F.E. results and their graphs follow the shape of quadrant circle. Similar shape follows the interaction graph according to the proposed methodology and good agreement is achieved. The ultimate strength of Box Girder A for low amount of applied torsion has less than 0.1BMmax difference between the two methodologies.

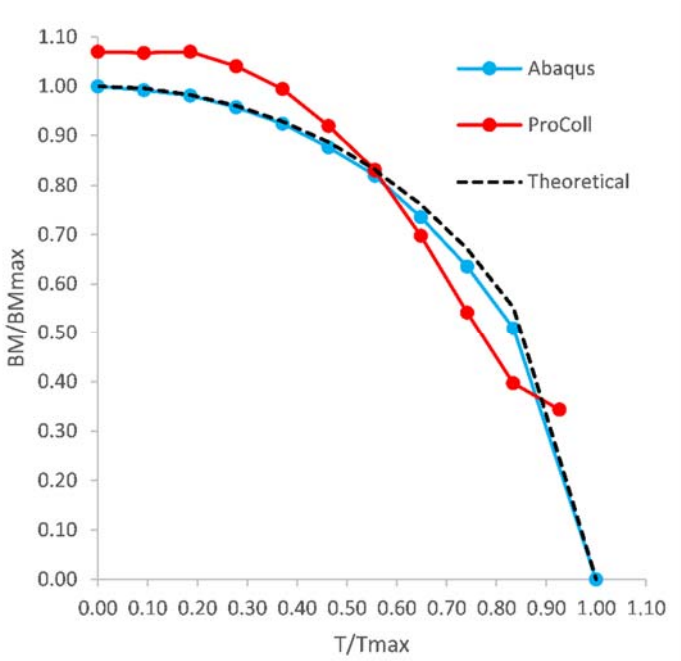

Figure 5.88: Comparison between the results of the NLFEM, the proposed methodology and the theoretical relationship of torsion and bending (Equation 5.8) for Box Girder A

5.8.2. Box Girder B

The results of Box Girder B subjected to combined torsion and vertical bending moment are presented in Figure 5.89 according to the nonlinear F.E. method, the proposed methodology and the theoretical interaction of torsion and bending (Equation 5.8). All values are normalised by the values of $BM_{max}$and T_{max} of the F.E. results which in this case are:

$\boldsymbol{T_{max} = 2.52 \times 10^{11} Nmm}$ and $\boldsymbol{BM_{max} = 2.31 \times 10^{11} Nmm}$

The theoretical results show extremely good correlation with the F.E. results and their graphs follow the shape of quadrant circle. Similar shape follows the interaction graph according to the proposed methodology and good agreement is achieved. The ultimate strength of Box Girder B for low amount of applied torsion has approximately 0.05BMmax difference between the two methodologies.

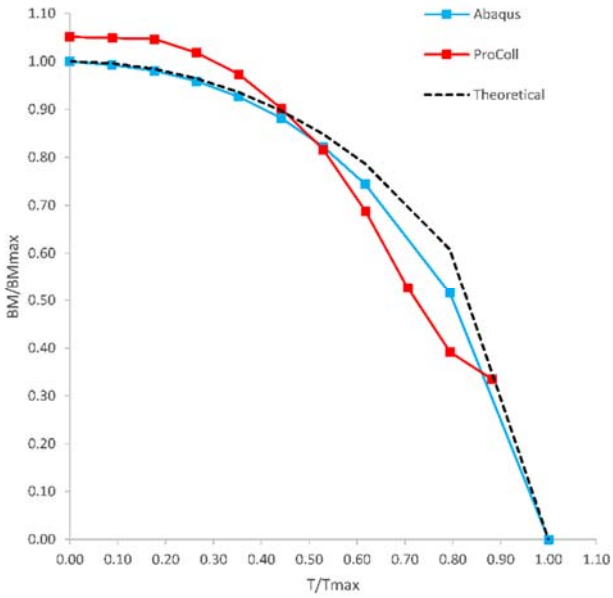

Figure 5.89: Comparison between the results of the NLFEM, the proposed methodology and the theoretical relationship of torsion and bending (Equation 5.8) for Box Girder B

5.8.3. Box Girder C

The results of Box Girder C subjected to combined torsion and vertical hogging/sagging bending moment are presented in Figure 5.90 according to the nonlinear F.E. method, the proposed methodology and the theoretical interaction of torsion and bending (Equation 5.8). All values are normalised by the values of $BM_{max}$and T_{max} of the F.E. results which in this case are:

$$\boldsymbol{T_{max} = 3.028x10^{11}Nmm,\ BM_{max_{sag}} = 3.23x10^{11}Nmm,}$$

$$\boldsymbol{BM_{max_{hog}} = 4.26x10^{11}Nmm}$$

The theoretical results show extremely good correlation with the F.E. results and their graphs follow the shape of quadrant circle. The interactions graphs according to the proposed methodology show good agreement too. The structure present higher stress in hogging condition than in sagging and both graphs have similar pattern. The proposed methodology predicts a torsional capacity (To) less than the Tmax of the F.E. method which is expected as this value, i.e. To, corresponds to torsion of the structure in the end of its elastic behaviour.

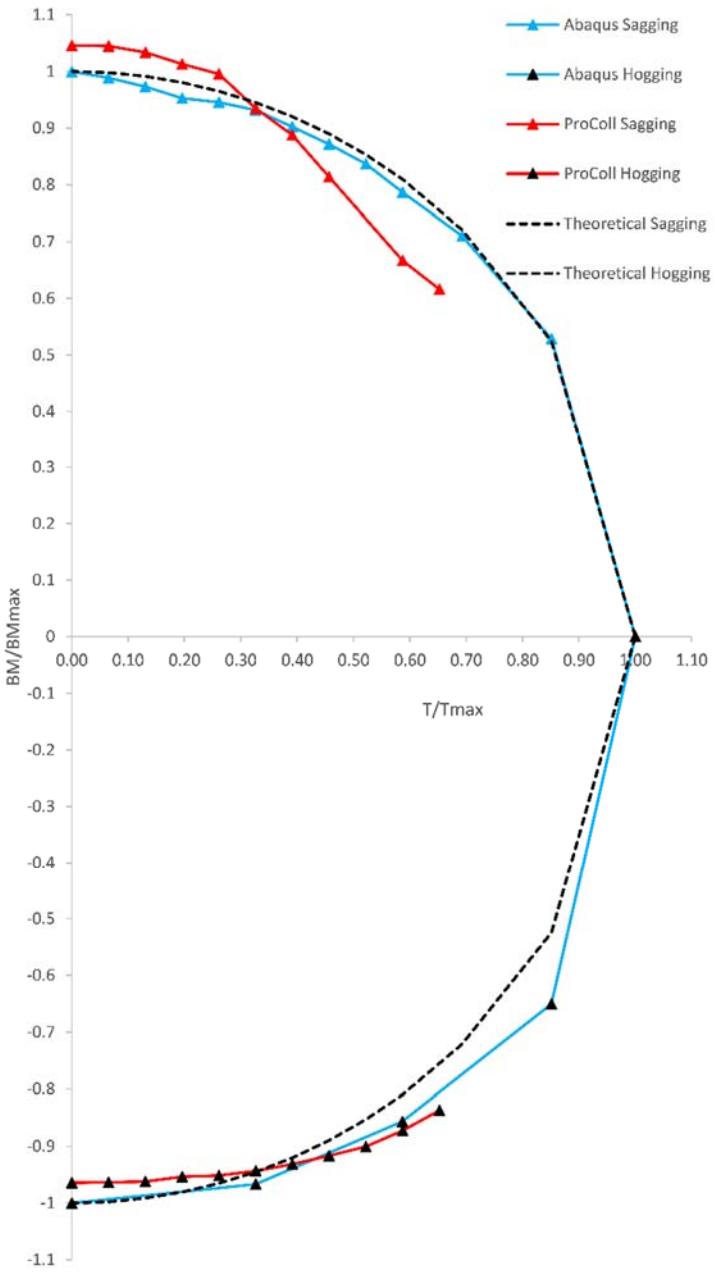

Figure 5.90: Comparison between the results of the NLFEM, the proposed methodology and the theoretical relationship of torsion and bending (Equation 5.8) for Box Girder C

5.8.4. Box Girder D

The results of Box Girder D subjected to combined torsion and vertical hogging/sagging bending moment are presented in Figure 5.91 according to the nonlinear F.E. method, the proposed methodology and the theoretical interaction of torsion and bending (Equation 5.8). All values are normalised by the values of $BM_{max}$and T_{max} of the F.E. results which in this case are:

$$\boldsymbol{T_{max} = 2.4x10^{11}Nmm,} \qquad \boldsymbol{BM_{max_{sag}} = 2.28x10^{11}Nmm,}$$

$$\boldsymbol{BM_{max_{hog}} = 3.54x10^{11}Nmm}$$

The theoretical results of Box Girder D show good correlation with the F.E. results and their graphs follow the shape of quadrant circle. The interactions graphs according to the proposed methodology show good agreement with the F.E. results and the theoretical formulation too.

The torsional capacity (To) according to the proposed methodology is less than the Tmax of the F.E. method and it is expected because value To corresponds to the torsional capacity of the structure in the end of its elastic behaviour.

Finally, Box Girder D presents higher strength in hogging condition than in sagging and both graphs have similar pattern despite of the existence of the open deck.

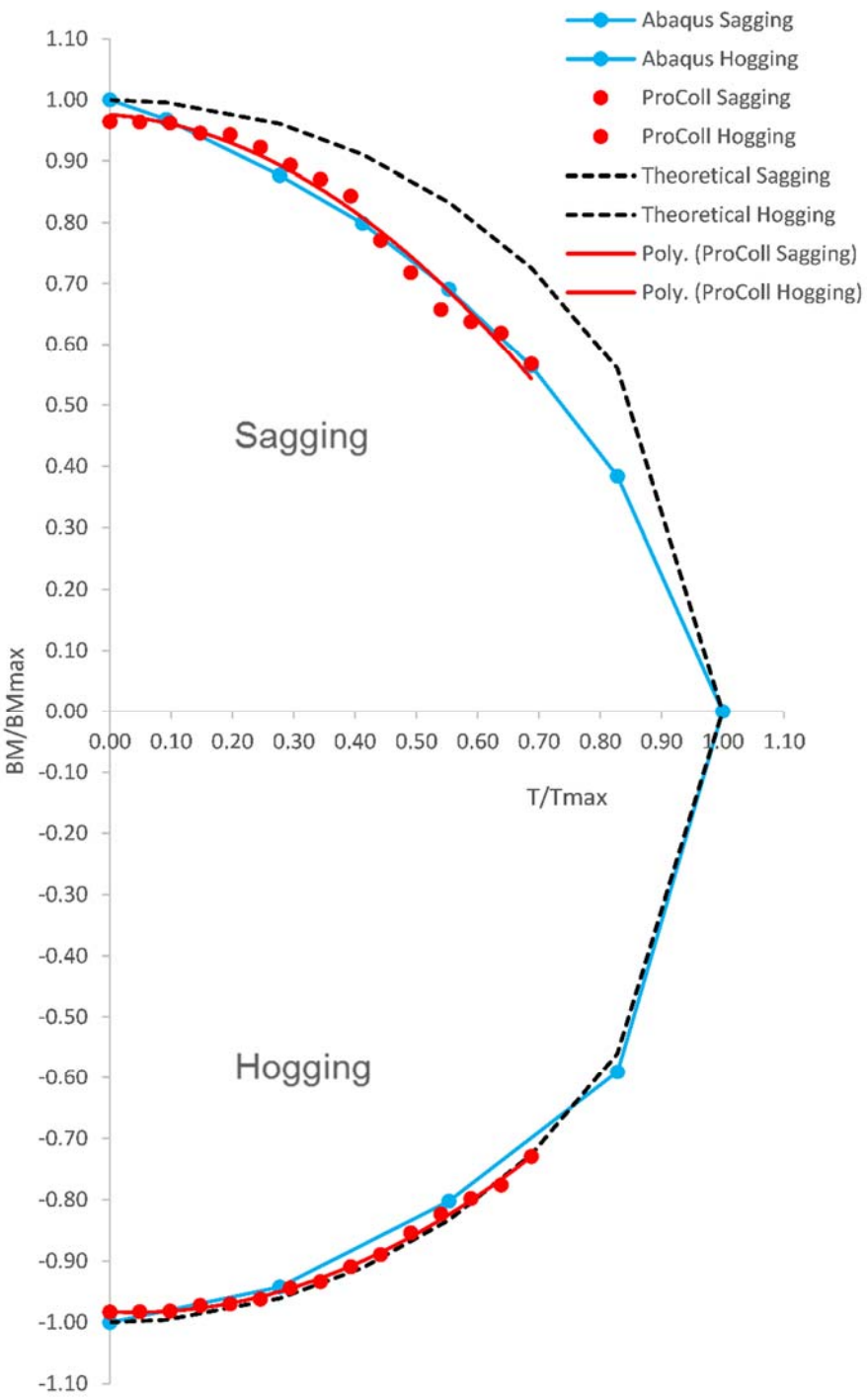

Figure 5.91: Comparison between the results of the NLFEM, the proposed methodology and the theoretical relationship of torsion and bending (Equation 5.8) for Box Girder D

5.9. Summary

This chapter investigates the behaviour of four box girders of the same size but with different cross sections and torsional constant values (k) under combined torsional and bending loads. Initially, the behaviour of the box girders subjected to pure torsion is investigated using the nonlinear F.E. analysis. The results show how the geometry affects the torsional behaviour of the structure and how the structure collapses under pure torsional load.

Then, all boxes are subjected to torsional and vertical sagging bending moment using the nonlinear F.E. method and the proposed methodology for the incorporation of torsion into the extended simplified progressive collapse method. The bending moment-curvature relationships under different amounts of applied torsional load are generated for each structure. The interaction diagrams of torsion and vertical sagging bending moment define the area in which the structure has adequate strength under these combined loads.

Furthermore, two of these models, Box Girder C and Box Girder D, are investigated under combined torsion and vertical hogging bending moment using both methodologies, the nonlinear F.E. analysis and the proposed methodology. Their results show similar pattern of progressive collapse to this under combined torsion and vertical sagging bending moment. However, the strength of these structures in combined torsion and hogging bending moment is higher than this in combined torsion and sagging bending moment.

In the end, the results according to the nonlinear F.E. method, the proposed methodology and the theoretical interaction of torsion and bending (Equation 5.8) are compared for each model. In general, the comparison shows very good agreement between the results of the two methodologies and the theoretical formulation in all cases.

Chapter 6

Progressive collapse assessment of 10,000 TEU container ship under combined bending and torsional loads

6.1. Introduction

In the previous chapter, the progressive collapse of four box girders was investigated using both methodologies; the finite element method and the extended progressive collapse method. Their results showed very good agreement. Afterwards, a reasonable question should be; what is the value of torsional load which floating structures should sustain in reality and how this compares with the torsional limit of the proposed methodology. Additionally, although the investigated box girders have cross sections similar to ship cross sections, their size differs significantly from the size of a real ship structure. Therefore, an analysis of a ship structure according to the proposed methodology and its validation are essential for the establishment of the extended simplified progressive collapse method.

6.2. Containership 10,000 TEU container ship

A 10,000 TEU container ship was selected in this case study based on the available data in the literature. Alfred Mohammed (Alfred Mohammed, 2014) carried out his research for a 10,000 TEU container ship OL185 based on data provided by Lloyd's Register. In his study, Alfred Mohammed follows and validates a methodology in order to define the maximum wave load combinations taking into account the sea state for a certain route and the response amplitude operators (RAOs) of the ship. Since the extreme global wave-induced loads are known, the maximum still water bending moment is selected based on the worst loading condition on the ship.

Then, a three-compartment finite element model of the containership is designed for structural analysis under combined loads of vertical bending moment, horizontal bending moment and torsional moment. In the current study, the model of this containership was designed in ProColl. The results of the proposed methodology under combined vertical hogging/sagging bending moment and torsion are compared with the finite element results from Alfred Mohammed's study (Alfred Mohammed, 2014). Finally, the extreme global wave

combined loads for the worst loading case (i.e. maximum bending moment) are depicted in the interaction diagram of combined torsional and bending loads.

6.2.1. Maximum wave load combinations and maximum still vertical bending moment

The most severe global wave load combinations according to Alfred Mohammed's study occur at 160.742m from the A.P. and the values of torsional and vertical bending moment are $\mathbf{2.901x10^8 Nm}$ and $\mathbf{1.366x10^{10} Nm}$ respectively. These values are depicted in Table 6.1 as F_4 (torsional moment) and F_5 (vertical bending moment) for the long-term analysis. Therefore, the case (P1') which describes only the combined extreme loads is define as follows:

- Case P1' (only extreme global combined loads):

  Torsional moment = $\mathbf{2.901x10^8 Nm}$

  Vertical Bending Moment = $\mathbf{1.366x10^{10} Nm}$

	F_1 (N)	F_2 (N)	F_3 (N)	F_4 (Nm)	F_5 (Nm)	F_6 (Nm)
C_5 $(short\text{-}term)$	4.800×10^7	3.278×10^7	6.805×10^7	2.769×10^8	1.174×10^{10}	4.407×10^9
C_5 $(long\text{-}term)$	5.231×10^7	3.292×10^7	6.794×10^7	2.901×10^8	1.366×10^{10}	4.193×10^9

Table 6.1: Global wave loads combinations at 160.742m from the A.P. for short-term and long-term analyses using the cross-spectral probabilistic method at the most extreme design vertical bending moment (Alfred Mohammed, 2014)

The worst loading condition according to the loading manual of the OL185 containership is L12.3 (Table 6.2) in which the maximum still water bending moment is equal to $657154t \cdot m$ *or* $6.29x10^9 Nm$.

The distribution of still water bending moments according to the hydrostatic analysis is shown in Figure 6.1. The maximum still water bending moment does not occur at 160.742m from the A.P., where the extreme combined loads occur. However, two cases will be taken into account examining also the more conservative case in which extreme loads and maximum vertical bending moment occur at the same longitudinal distance from the A.P. Therefore, the

ultimate strength of the containership should sustain the following torsional and vertical bending load combinations in hogging condition:

- Case P1 at 160.742m from A.P.:

  Torsional moment = $\mathbf{2.901x10^8 Nm}$

  Vertical Bending Moment = $\mathbf{1.366x10^{10} + 4.46x10^9 Nm = 1.812x10^{10} Nm}$

- Case P2 (maximum vertical moments along the length of the container ship):

  Torsional moment = $\mathbf{2.901x10^8 Nm}$

  Vertical Bending Moment = $\mathbf{1.366x10^{10} + 5.69x10^9 Nm = 1.935x10^{10} Nm}$

Loading condition	Loading description	Max. Bending Moment (t-m)
L00.0	Light ship	445428
L10.0	Docking - No payload - 55% bunker	521420
L14.0	Docking - 25% payload - 55% bunker	208317
L01.1	Operating ballast - departure	492653
L01.3	Operating ballast - arrival	414242
L03.1	Homogeneous loading - 11t/TEU - departure	393855
L03.3	Homogeneous loading - 11t/TEU - arrival	536486
L04.1	Homogeneous loading - 14t/TEU - departure	510826
L04.3	Homogeneous loading - 14t/TEU - arrival	564101
L11.1	Hom. loading - 8.5t/TEU - No WB - departure	458066
L11.3	Hom. loading - 8.5t/TEU - No WB - arrival	579340
L12.1	Hom. loading - 8.5t/TEU - departure	448763
L12.3	Hom. loading - 8.5t/TEU - arrival	657154

Table 6.2: Loading conditions from loading manual for OL185 containership (Alfred Mohammed, 2014)

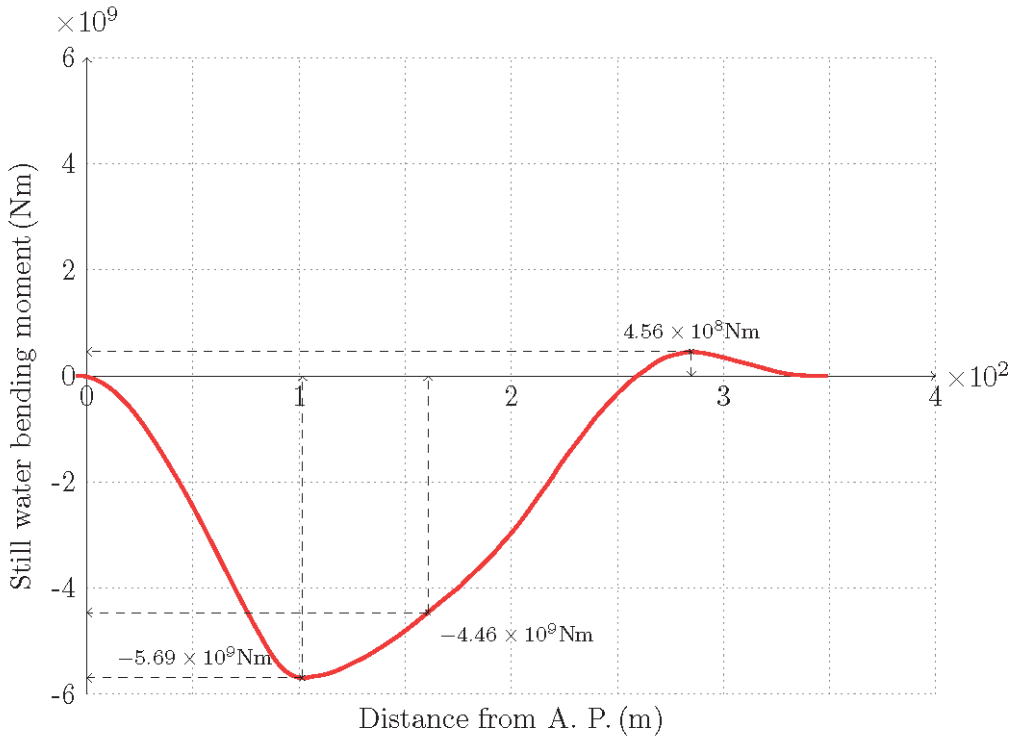

Figure 6.1: Distribution of still water bending moment along the length of the container ship showing the maximum and minimum moments (Alfred Mohammed, 2014)

6.2.2. Geometric characteristics and material properties

The midship section of the OL185 container ship is depicted in Figure 6.2 and further details about its scantlings are given in Table 6.3, Table 6.4 and Table 6.5.

The material properties of steel are:

- HT36 with $\sigma_Y = 355N/mm^2$, for scantlings given as XH;
- HT40 with $\sigma_Y = 390N/mm^2$, for scantlings given as XH40;

  Where X represents the letters A, D and E.

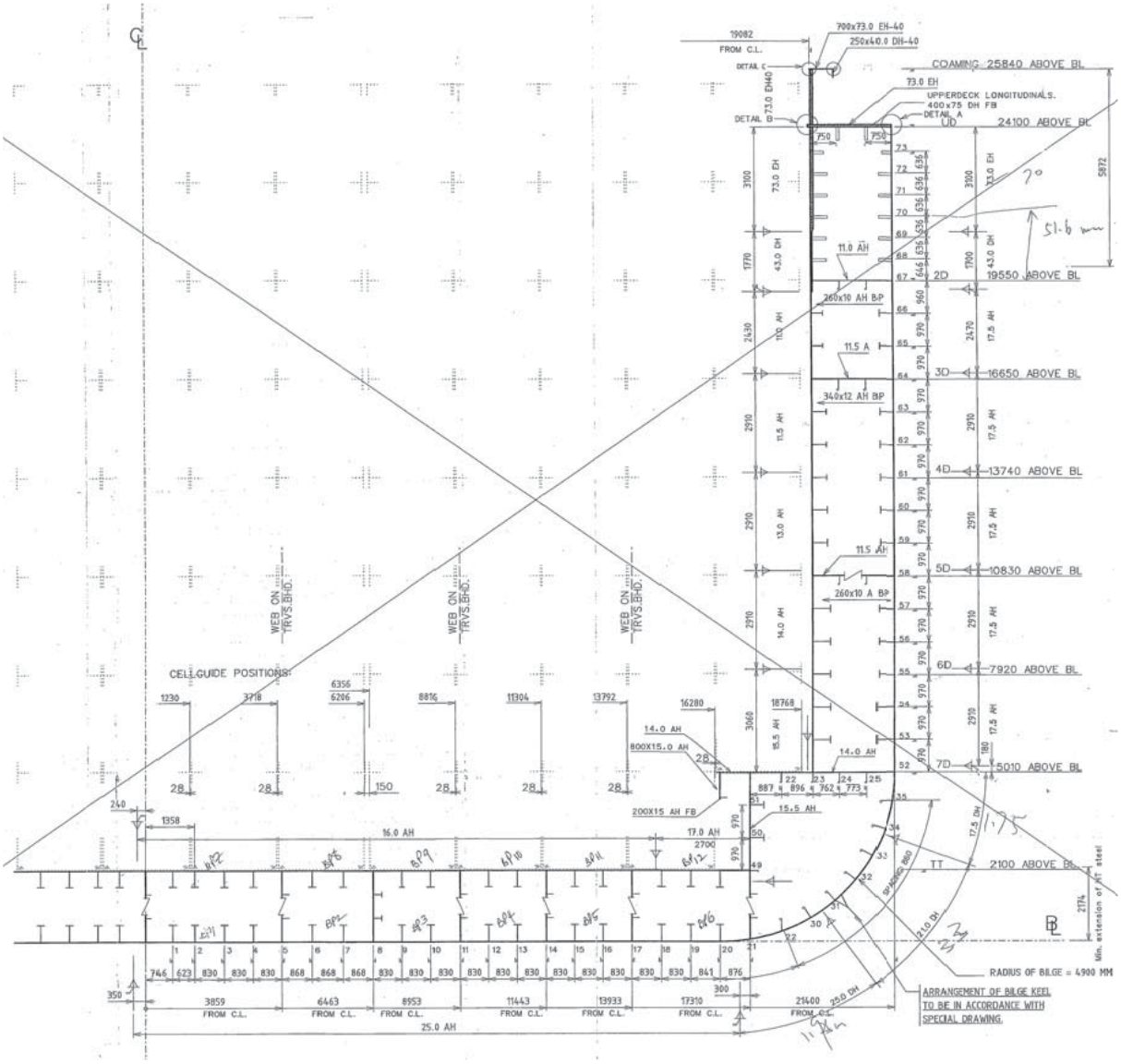

Figure 6.2: The midship section of the OL185 container ship (Alfred Mohammed, 2014)

Long. No.	L.Bhd. 17310 Off CL	L.Bhd. 19082 Off CL	Side Shell
73		300x75 DH FB	300x75 DH FB
72		400x75 DH FB	400x75 DH FB
71		400x75 DH FB	400x75 DH FB
70		400x75 DH FB	400x75 DH FB
69		400x75 DH FB	400x75 DH FB
68		400x75 DH FB	400x75 DH FB
67		**Deck 2**	**Deck 2**
66		320x11/130x15 AH	400x11/150x20 AH
65		320x11/130x15 AH	400x11/150x20 AH
64		**Deck 3**	**Deck 3**
63		400x11/150x20 AH	400x11/200x25 AH
62		400x11/150x20 AH	400x11/200x25 AH
61		400x11/150x20 AH	400x11/200x25 AH
60		400x11/200x20 AH	400x11/200x25 AH
59		400x11/200x20 AH	400x11/200x25 AH
58		**Deck 5**	**Deck 5**
57		480x11/200x20 AH	440x11/200x25 AH
56		480x11/200x20 AH	440x11/200x25 AH
55		480x11/200x20 AH	440x11/200x25 AH
54		500x11/200x25 AH	500x11/200x30 AH
53		500x11/200x25 AH	500x11/200x30 AH
52	**Deck 7**		
51	400x11/200x20 AH		
50	400x11/200x20 AH		
49	240x12 AH BP		

Table 6.3: Longitudinal bulkheads and side shell longitudinals (Alfred Mohammed, 2014)

Girder	Plating	Stiffener
Girder in center line (CL)	16.5 AH	150x15 AH FB
Girder 3859 off CL	16.5 AH	200x15 AH FB
Girder 6463 off CL	16.5 AH	240x11/150x15 AH
Girder 8953 off CL	16.5 AH	200x15 AH FB
Girder 11443 off CL	16.5 AH	200x15 AH FB
Girder 13933 off CL	16.5 AH	200x15 AH FB
Girder 17310 off CL	16.5 AH	200x15 AH FB

Table 6.4: Double bottom girders (Alfred Mohammed, 2014)

Deck 7 Longitudinals	
Stiffener	Description
No. 22-23	300x11 AH BP
No. 24-25	320x12 AH BP
Inner Bottom Longitudinals	
No. 2-3-4 , 6-7, 10, 12-13, 15-16, 18-19	480x11/200x30 AH
No. 1	480x11/200x15 AH
No. 9	480x11/130x15 AH
No. 20	500x11/200x30 AH
Bottom and Bilge Longitudinals	
No. 1-4, 6-7, 9-10, 12-13, 15-16, 18-19	500x22/200x30 AH
No. 20	500x25/200x30 AH
No. 22, 30-35	370x13 AH BP

Table 6.5: Other longitudinals (Alfred Mohammed, 2014)

6.2.3. Non-linear finite element model of OL185 container ship

A three compartment model with two bulkheads was modelled in ABAQUS CAE and there are 54 bays between the bulkheads with frame spacing 791mm. Approximately 1 million number of linear quadrilateral (S4R) and triangular (S3) elements were used in the model and their size was varied from 200mm to 800mm depending on the area of the structure. Therefore, a coarse mesh size (800mm) was applied to the transverse bulkheads and a finer mesh size (200mm) to the plates, stiffeners, decks and longitudinal bulkheads. More detailed description

of the mesh and the mesh convergence study is provided in Alfred Mohammed's study (Alfred Mohammed, 2014).

The initial geometric imperfections of the container ship were modelled exactly as the initial geometric imperfections of the box girders which are described in section 5.2.2. In addition, the same boundary conditions were applied to the OL185 finite element model and the box girder models (section 5.3.3 and section 5.4.1). In Figure 6.3, it is shown how the end nodes of the F.E. model of the container ship are tied to a reference point RP-1. The other end of the structure is fully constrained (Figure 6.4) and the load is applied as smooth step via this reference point. Therefore, angular displacement is applied to the axes according to Figure 6.5:

- x axis (UR1), positive or negative, for vertical sagging or hogging bending moment
- z axis (UR3) for torsional moment
- z axis (UR3) up to a certain amount of torsional moment; then, the model is held and angular displacement in x axis (UR1) is applied to the model up to its collapse

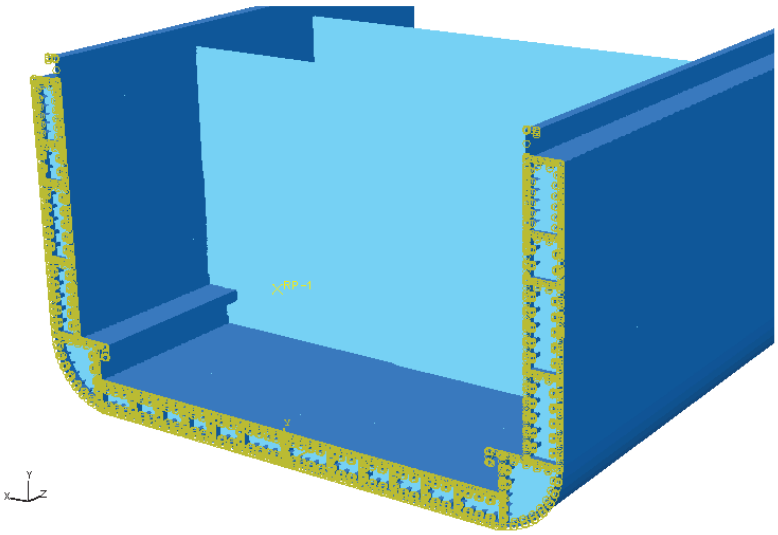

Figure 6.3: OL185 showing an end whose nodes are tied to an individually created reference point RF-1 in ABAQUS model (Alfred Mohammed, 2014)

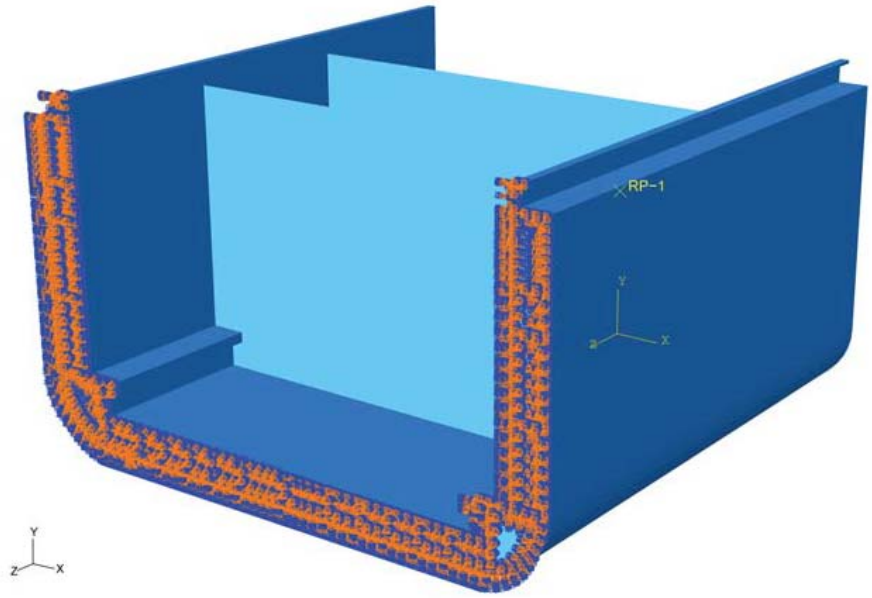

Figure 6.4: F.E. model of OL185 showing the edge modes fully constrained against all six degrees of freedom with the applied boundary conditions (Alfred Mohammed, 2014)

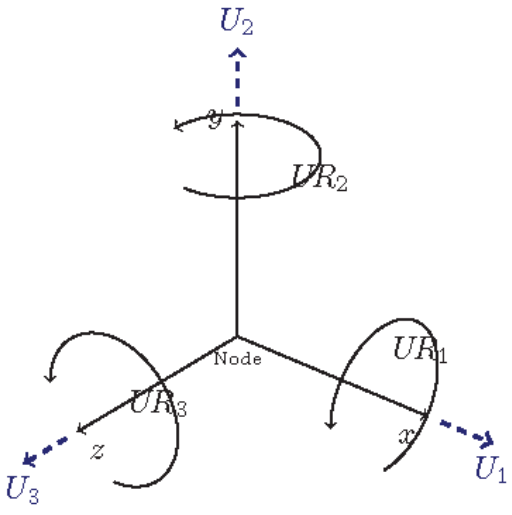

Figure 6.5: Orientation of displacements and rotations in model space (six degrees of freedom) (Alfred Mohammed, 2014)

6.2.4. ProColl model of OL185 container ship

The model of the OL185 container ship in ProColl was created based on the provided data from the midship section (Figure 6.2) and the scantlings (Table 6.3, Table 6.4 and Table 6.5). The same initial imperfections to the NLME model were incorporated in the ProColl model. Figure 6.6 shows the graphic representation of the ProColl model and its file is also attached in Appendix B. The midship section of the OL1855 containership has 22cells/loops, therefore each plate was associated with the number of the cell/loop which belongs. The common plates i.e. the plates which belong to two cells/loops were associated to both of them. The length F.E. model is consisted by 54 bays (791mm each) between the transverse bulkheads, therefore the same number on frames (nsy) was also set in ProColl (nsy=54). The model was analysed under combined torsional and vertical sagging/hogging bending loads.

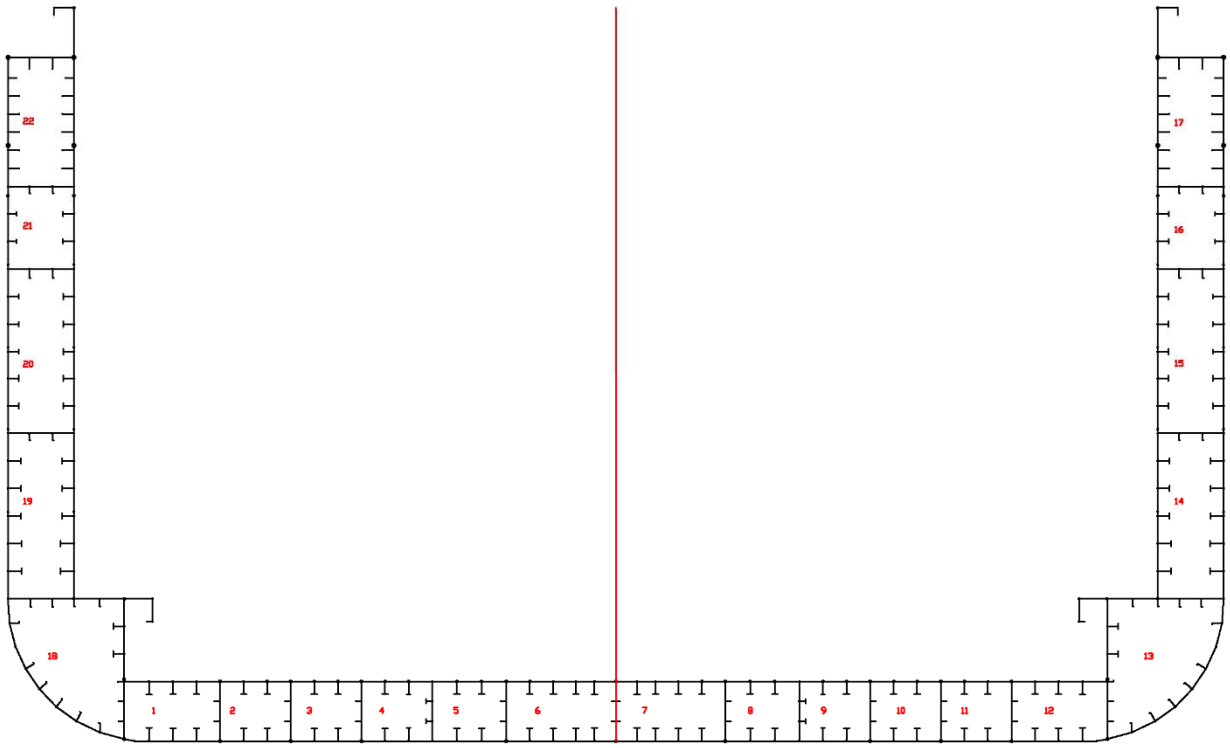

Figure 6.6: Graphical representation of OL185 container ship in ProColl and its numbered cells/loops.

6.3. Ultimate strength assessment of the OL185 container ship

The ultimate strength of the OL185 container ship was investigated under combined torsional and bending loads in both hogging and sagging condition. The analyses carried out using the non-linear finite element method by Alfred Mohammed (Alfred Mohammed, 2014) and the extended simplified progressive collapse method for combined torsional and bending loads which is proposed in the current study. The aim is to validate the results of the proposed methodology with the NLFE results and check if the structure may sustain the maximum combined torsional and bending loads which were defined in section 6.2.1.

6.3.1. Non- linear finite element results (ABAQUS)

In this subsection, the finite results of the OL185 container ship from Alfred Mohammed's study (Alfred Mohammed, 2014) are briefly presented in order to be available for comparison with the results of the proposed methodology.

6.3.1.1. Under torsional load

The maximum torsional capacity of the OL185 container ship is $\boldsymbol{T_{max} = 7.684x10^{9}Nm}$

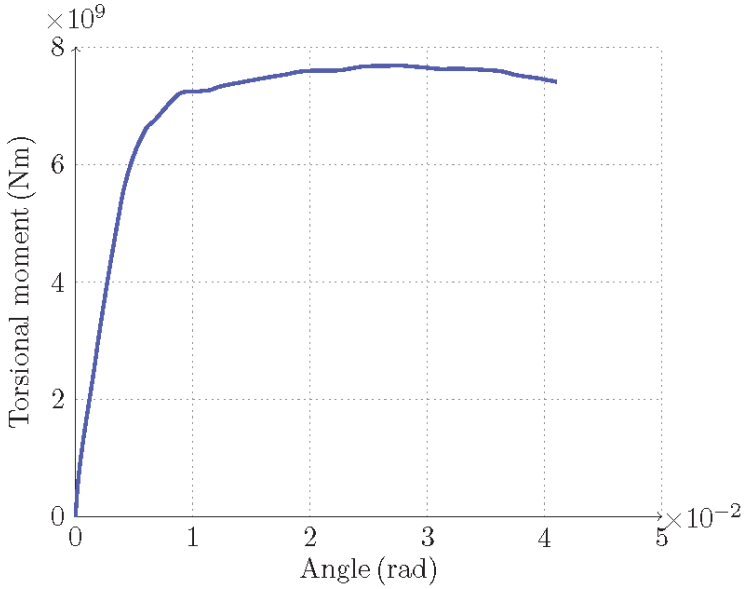

Figure 6.7: A moment-curvature relationship for progressive collapse of OL185 under torsion according to ABAQUS results (Alfred Mohammed, 2014)

6.3.1.2. Under combined torsional and vertical bending moment

The moment-curvature relationships of the OL185 container ship under torsional and vertical sagging or hogging bending moment are depicted in Figure 6.8 and Figure 6.9 respectively.

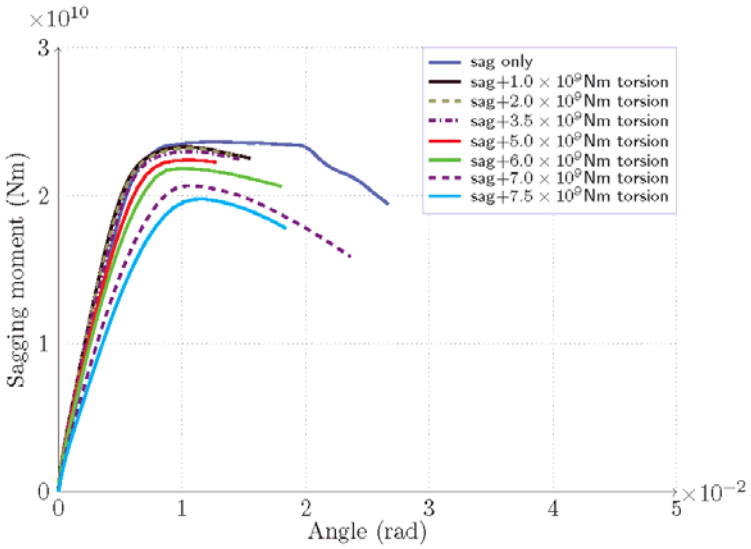

Figure 6.8: Moment-curvature relationships for sagging moment and torsion for the midship section of OL185 container ship according to ABAQUS results (Alfred Mohammed, 2014)

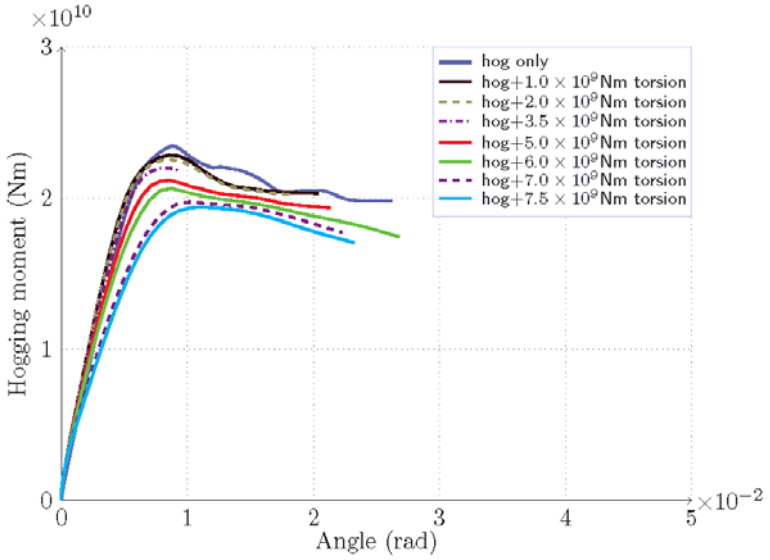

Figure 6.9: Moment-curvature relationships for hogging moment and torsion for the midship section of OL185 container ship according to ABAQUS results (Alfred Mohammed, 2014)

6.3.1.3. Interaction diagram of torsional and bending loads

A non-dimensioned interaction diagram of the ultimate sagging/hogging vertical bending moment and the torsional load of the OL185 container ship based on the previous presented NLFE results is depicted in Figure 6.10.

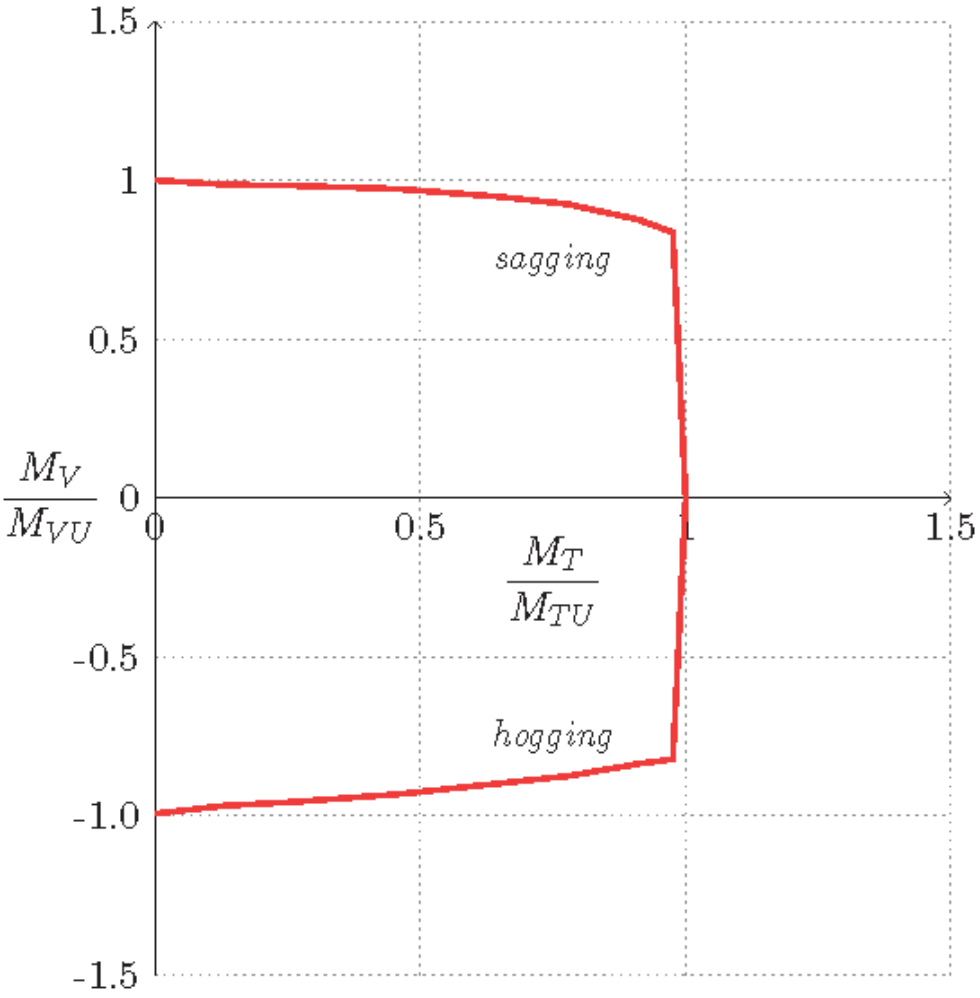

Figure 6.10: Ultimate strength relationship between vertical bending moment and torsion for the midship section of OL185 container ship (Alfred Mohammed, 2014)

6.3.2. Extended Simplified Progressive Collapse Method (ProColl)

6.3.2.1. Under torsional load

As it was mentioned in chapter 3, the user has the option to define the maximum torsional capacity of the structure. In this case, the maximum torsional load (T_{max}) is known from the N.L.F.E. analysis and it is equal to $\mathbf{7.684x10^9 Nm.}$ Since $T_{max} > T_o$, the shear flow distribution in the cells for applied torsion greater than T_o is not increased (section 3.6).

6.3.2.2. Under combined torsional and vertical bending moment

The moment-curvature relationships for torsional and vertical sagging/hogging bending moment are presented in Figure 6.11/Figure 6.12 respectively.

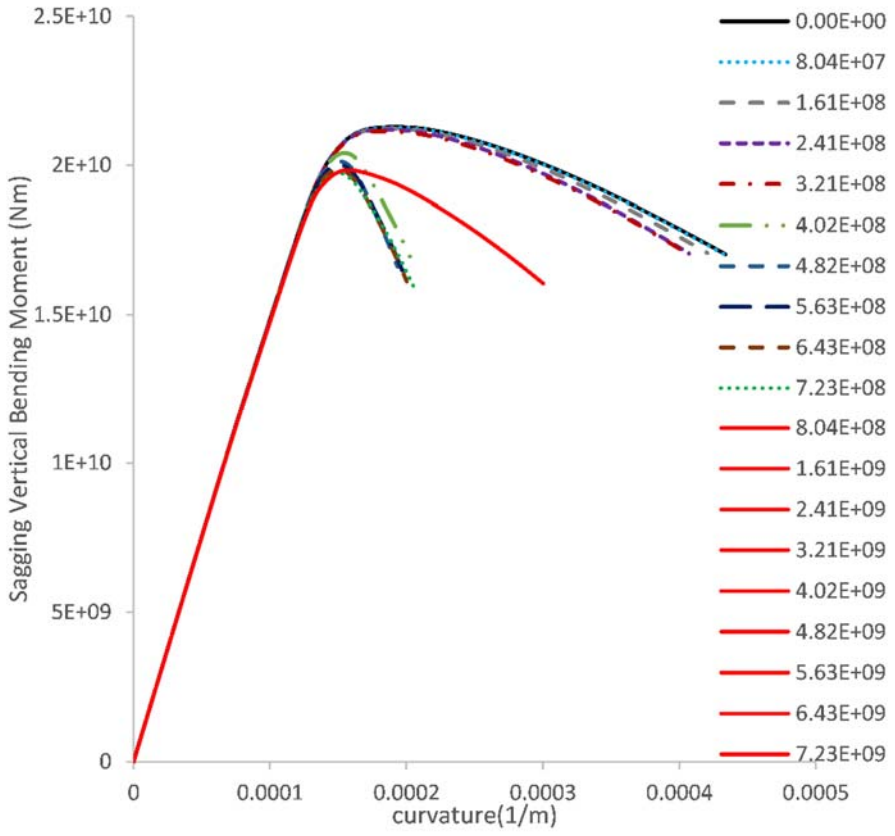

Figure 6.11: Moment-curvature relationships for sagging moment and torsion (Nm) according to ProColl

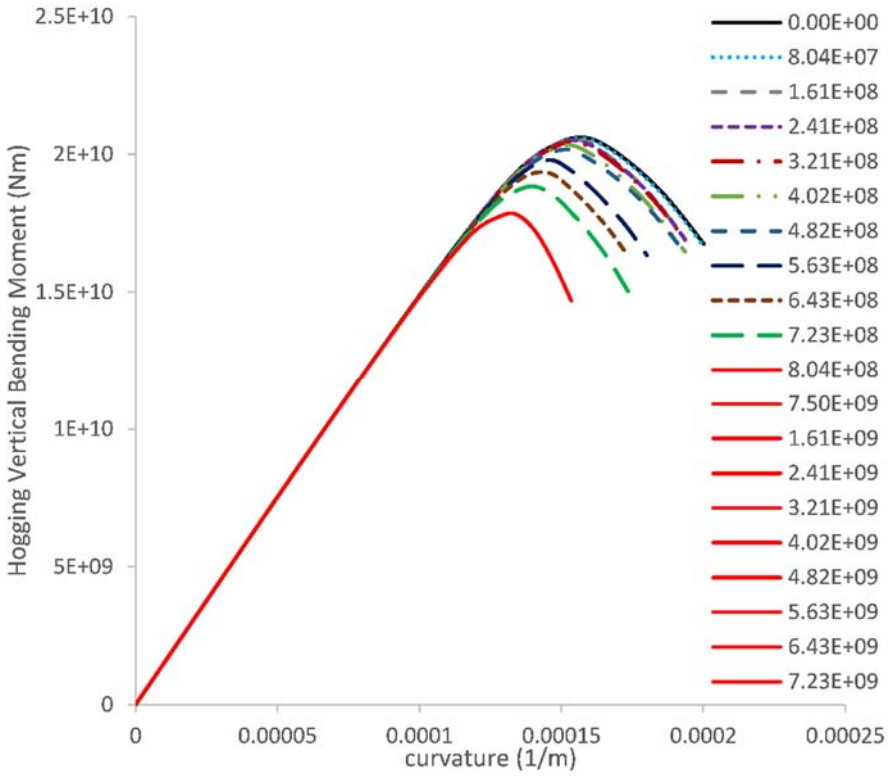

Figure 6.12: Moment-curvature relationships for hogging moment and torsion (Nm) according to ProColl

Both figures depict the vertical bending moment-curvature relationship of the structure under different amount of torsional moment. In both conditions, sagging and hogging, the stiffness of the structure is not affected by the torsional load. However, its strength decreases as the applied torsional load increases but only up to a certain value (8.04E+08 Nm) equal to T_o. Above this amount of torsion, no further decrease in the strength of the OL185 container ship is presented. As it is explained in section 3.6, once a plate reaches its shear yield stress value, the shear distribution in the cells currently remains constant for any increase in the applied torsional load (i.e. $T_o < T_{applied} \leq T_{max}$).

6.3.2.3. Interaction diagram of torsional and bending loads

The interaction diagram of combined torsional and vertical sagging/hogging bending moment is shown in Figure 6.13. The graph provides the upper limit of the vertical bending moment (ultimate strength) in sagging and hogging condition for any amount of torsion up to its maximum torsional capacity. The structure collapses before this maximum torsional load is applied to the structure due to the fact that torsion is not the dominant load in a ship structure. However, this will be analysed afterwards in section 6.3.3 in which the extreme combined torsional and vertical bending loads for the container ship are taken into account.

The interaction diagram presents the peaks values of vertical bending moment from Figure 6.11 and Figure 6.12. The structure displays a constant bending strength above $T_o = 8.04E + 08Nm$ (Figure 6.13), which is the shear yield torsional load and no further shear load is carried by the plates. As the collapse load under pure torsion is reached, the theory behind the approach used here is not applicable and the analysis stops.

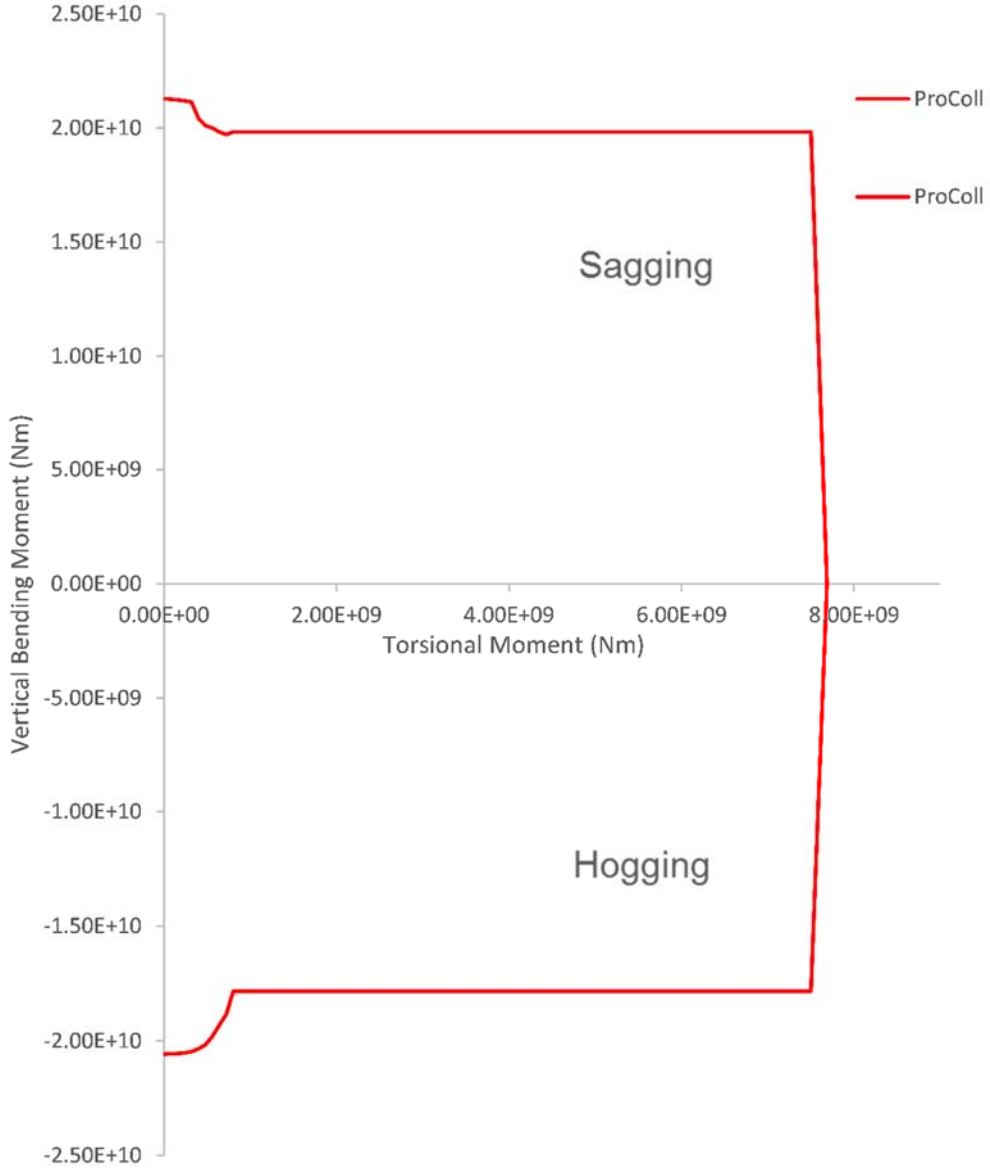

Figure 6.13: Interaction diagram of torsional and vertical bending load in sagging and hogging condition of the OL185 container ship according to ProColl

6.3.3. Comparison of NLFEM and Extended Simplified Progressive Collapse Method

In this section, the results of the non-linear finite element and the extended simplified progressive collapse method are compared in Figure 6.14, Figure 6.15 taking also into account the extreme combined loads of torsion and vertical bending moment which defined in section 6.2.1.

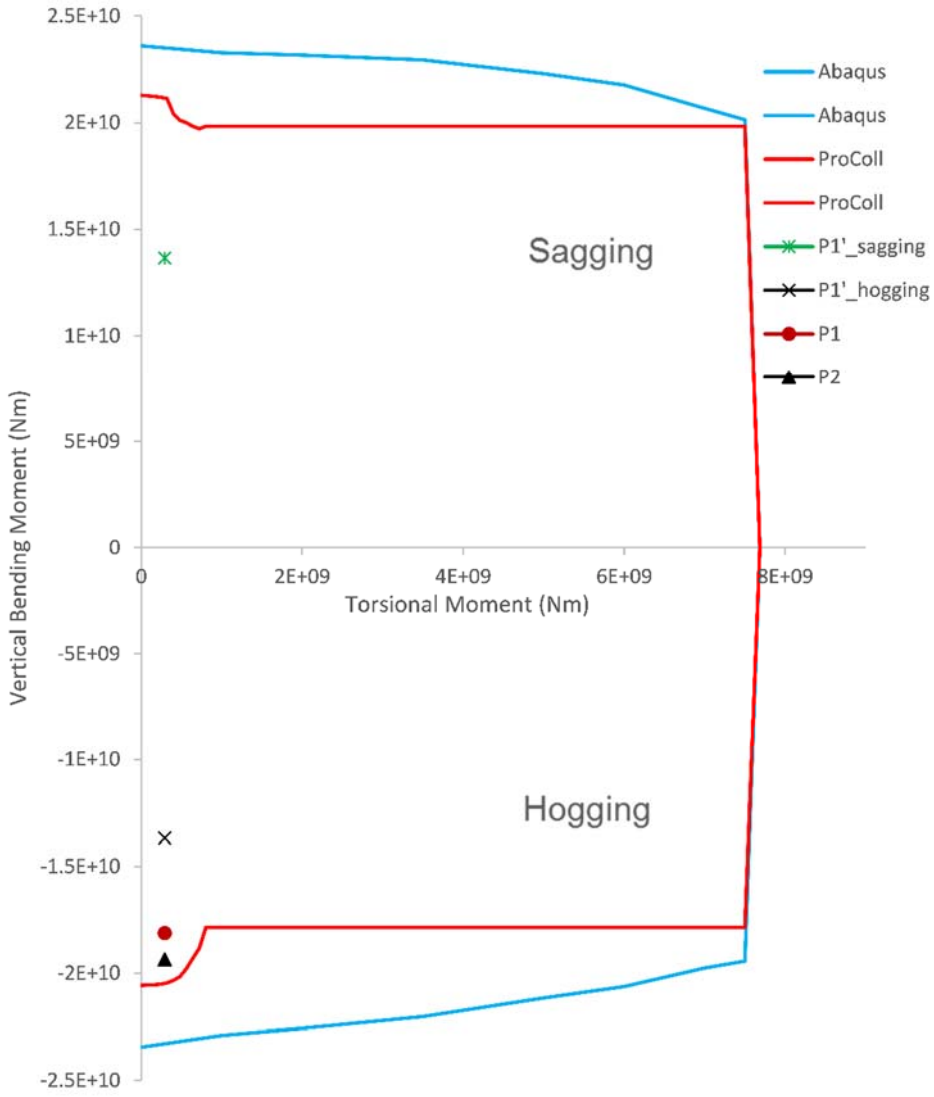

Figure 6.14: Interaction diagram of combined torsional and bending loads according to NLFEM and ProColl and its associated wave-induced torsional moment with i) the most extreme wave-induced vertical bending moment (P1') ii) the P1'value plus the still water bending moment at 160.742m from the A.P. (P1) iii) the P1' value plus the maximum still water bending moment along its length (P2)

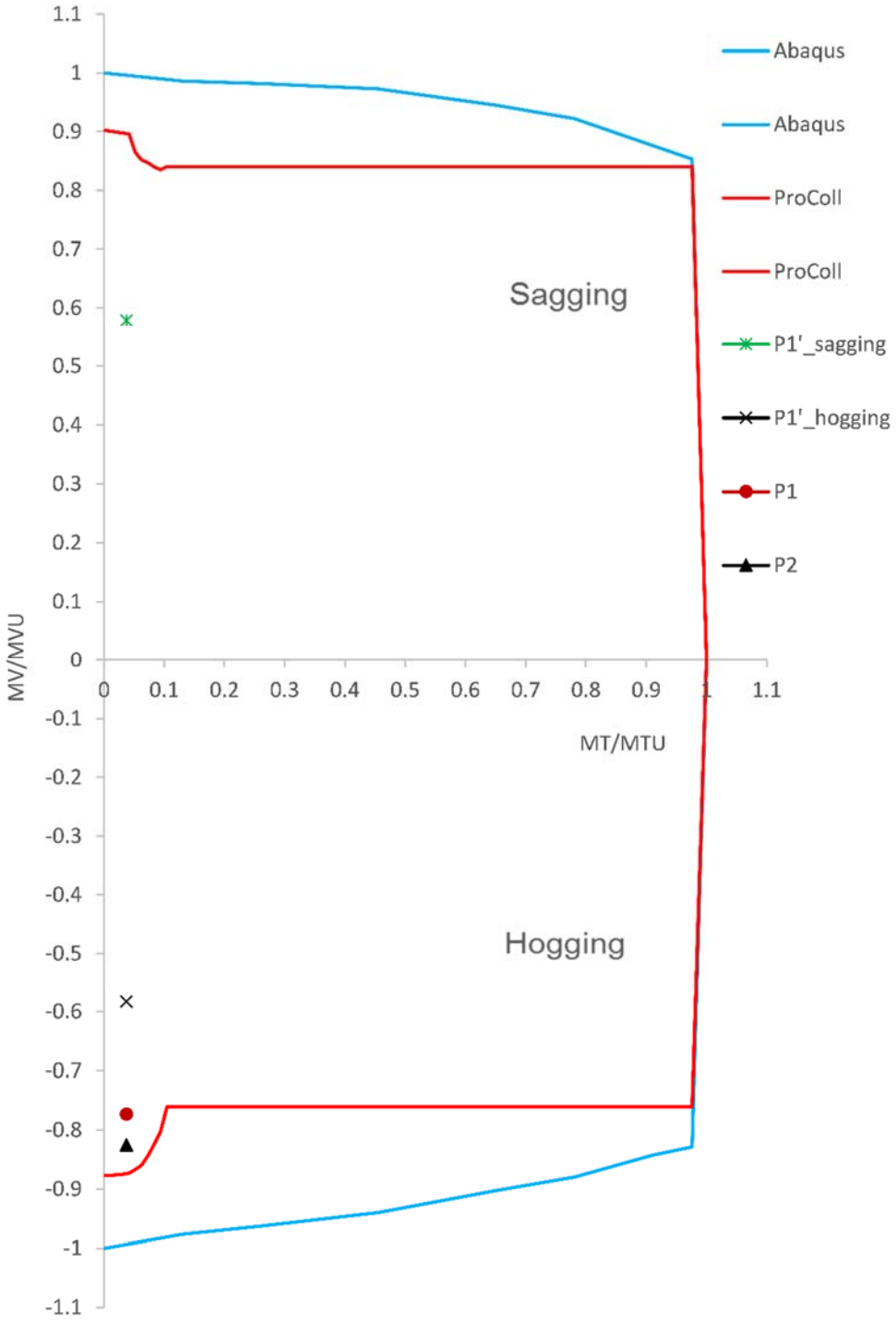

Figure 6.15: Non-dimensioned interaction diagram of combined torsional and bending loads according to NLFEM and ProColl and its associated wave-induced torsional moment with i) the most extreme wave-induced vertical bending moment (P1') ii) the P1'value plus the still water bending moment at 160.742m from the A.P. (P1) iii) the P1' value plus the maximum still water bending moment along its length (P2)

The interaction diagrams of torsional and vertical sagging/hogging bending moment according to NLFEM and the proposed methodology are presented in Figure 6.14. The results show a good agreement and both graphs present similar pattern. The extended simplified progressive collapse method seems more conservative in its results than the non-linear finite element method. Furthermore, the estimate strength by both methodologies may sustain the most extreme-wave induced vertical bending moment and the maximum still water bending moment along the length of the ship with its associated wave induced torsional moment (point P2). P2 case is the most severe and conservative case scenario after P1 case which is the worst load combination at the frame 160.742m from the A.P. and may occur once in the life-time (25 years) of the OL185 container ship (P2 case). P1 case is the most extreme wave-induced vertical bending moment and its associated wave-induced torsional moment without taking into account the still water bending moment.

Figure 6.15 presents the normalised values of Figure 6.15 based on the maximum bending moment in sagging and hogging and maximum torsional moment of the NLFE results which are $2.36x10^{10}Nm$, $2.34x10^{10}Nm$ and $7.684x10^{9}Nm$ respectively. Figure 6.15 shows that the maximum wave-induced torsional load for the OL185 container ship is less than the 10% (3.7%Tmax) of its maximum torsional capacity.

6.4. Summary

In chapter 6, the case study of a 10000TEU OL185 container ship is investigated under combined torsional and vertical bending moment in sagging and hogging condition. The ultimate strength of the structure under these combined loads was analysed using the non-linear finite element method and the extended simplified progressive collapse method. The results and the modelling of the finite element analysis are briefly presented and discussed because they have been carried out in another study (Alfred Mohammed, 2014). The same study provides also useful data about the extreme wave-induced vertical bending moment and its associated wave-induced torsional moment for the OL185 container ship. The OL185 containership is also modelled in ProColl and the results of the proposed methodology are presented and compared with the finite element results.

The interaction diagrams of torsional and vertical bending moment in sagging and hogging conditions according to both methodologies show good agreement with this of the extended simplified progressive collapse method to be more conservative than the non-linear finite element method. Finally, both sets of results show that the structure may sustain the most extreme predicted combined loads and that the wave-induced torsional load of the container ship is less than the 10% of its maximum torsional capacity.

Chapter 7

Progressive collapse of intact and damaged box girder under bending, torsion and combined bending and torsional loads

7.1. Introduction

This chapter presents a case study for the progressive collapse of damaged box girders when subjected to combined bending and torsional loads. In the first part, the geometric characteristics of the intact Box Girder E are presented along with the results of its progressive collapse assessment under torsional loads (using the NLFEM) and under combined torsional and bending loads (using the NLFEM & the extended simplified progressive collapse method).

In the second part, Box Girder E is subjected to different damage case scenarios and the damage extent alters either across the width or along the length of the structure. The strength assessment of these damaged box girders follows under torsional loading and under combined torsional and bending loads according to the nonlinear finite element analysis. Furthermore, the damaged box girders under bending load were analysed using the extended simplified progressive collapse method. The progressive collapse behaviour of the damaged box girders under combined torsion and bending was also investigated with the proposed methodology. However, the effect of torsion to local damage is not incorporated yet into the proposed methodology. The reasons are explained in section 7.3.4 and ongoing investigation occurs on this area.

7.2. Part I: Intact Box Girder E

7.2.1. Introduction

In this section, first the geometric characteristics of intact Box Girder E are presented and then its progressive collapse is analysed under pure bending, pure torsion and combined bending and torsional loads. Both methods, the nonlinear finite element method and the extended progressive collapse method are applied. The modelling procedure of both methodologies is described and their results are presented. In the end of this part, a comparison of the above results is presented.

7.2.2. Geometric characteristics

A simple box girder of **4.8m width, 4.2m height and 9.0m length,** called Box Girder E, was selected to be modelled for the purpose of this study. Box Girder E has also been examined in previous study by the author (Syrigou, 2012) under pure bending, investigating its progressive collapse and residual strength under different damage case scenarios with both methods; the nonlinear finite element analysis and the extended simplified progressive collapse method. The results of this study had shown that the residual strength of the damaged structure is highly dependent on the size of transverse damage extent and different sizes of longitudinal damage extent have almost the same effect on the strength of the structure.

In the current study, the strength of the same box girder, Box Girder E, is investigated under combined bending and torsional loadings. The size of this model allows a rigorous study to be carried out without significant computational penalties and provides a satisfactory amount of results for better understanding of its behaviour under these combined loads.

The geometry of Box Girder E is shown in Figure 7.1 (& in Appendix C) and standard tee bar stiffeners were used throughout the box girder which are spaced **600mm** apart. Each plate has a length of **1800mm**, therefore according to Equation 2.7 the slenderness ratio (β) of top/bottom and side flanges is 2.58 and 2.064 respectively. Each section is 1800mm long and it consists one bay. The whole model is consisted by five (5) bays (i.e. total length of model **9000mm**) which are separated by transverse frames. The size of transverse frames is doubled the size of the longitudinal stiffeners.

The material properties of steel are Young's modulus **207GPa** and yield stress of **245Mpa** with linearly elastic-perfectly plastic stress-strain behaviour (Figure 4.1).

Average level of geometric imperfections were taken into account for plates and stiffeners exactly as they are described in 5.2.2 paragraph. Additionally, tensile stresses equal to 95% of yield stress (245MPa) were considered in a tensile zone of 50mm width along each longitudinal side of the plates. The value of the residual stresses was calculated according to Equation 2.9.

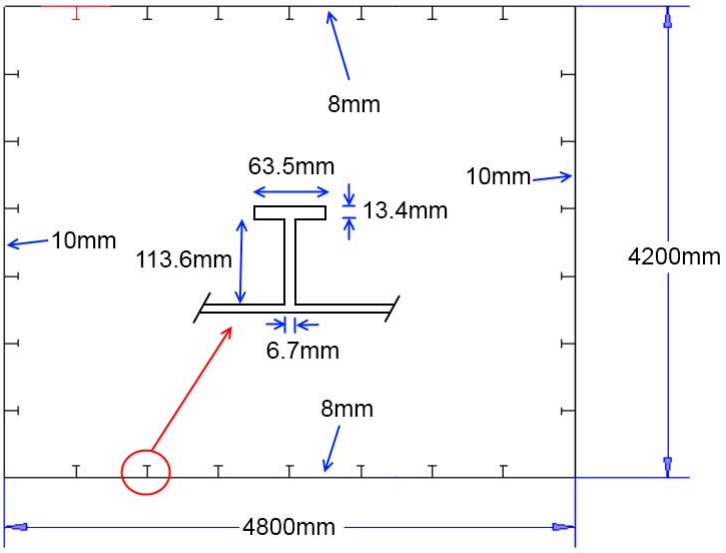

Figure 7.1: The cross-section of Box Girder E

7.2.3. Progressive collapse of intact box girder with the NLFEM.

In this section, the progressive collapse of Box Girder E subjected to pure bending, pure torsion and combined bending and torsional loads is analysed with the Nonlinear Finite Element Method using static (Riks) analysis. At this point, it should be mentioned that the nonlinearity of this model did not cause any convergence issues using static analysis, therefore Riks analysis was applied to all cases.

7.2.3.1. NLFEM Modelling

The set-up of the F.E. model in ABAQUS is very similar to this of the four box girders solved with static analysis and already it has been described in Chapter 5. A conventional four node shell element (S4R) with reduced integration (5 points) was used for the modelling and each node has six degrees of freedom (i.e. three translational and three rotational).

A mesh convergence study was carried out for the case which the model is subjected to pure bending with element size equal to 100mm, 50mm, 35mm and 25mm, showing a satisfactory convergence for an element size of less than 50mm (Figure 7.2).

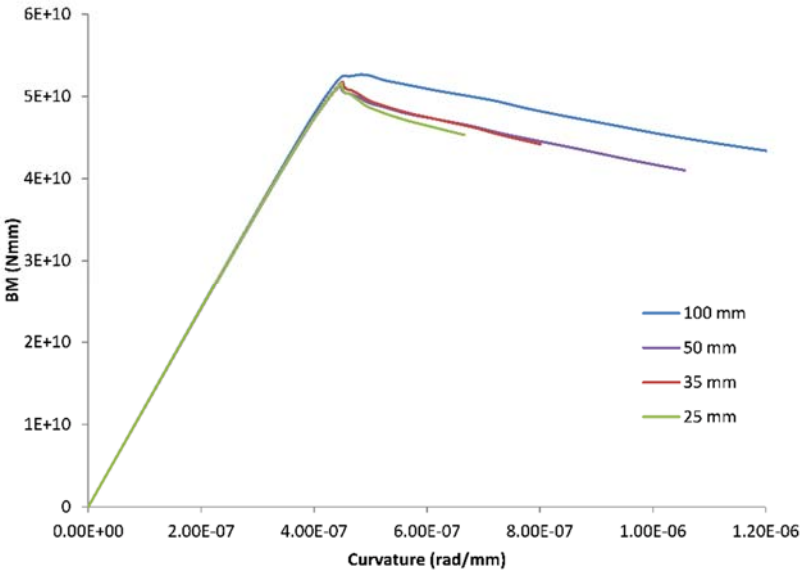

Figure 7.2: Mesh convergence study for Box Girder E subjected to pure bending

The boundary conditions of Box Girder E are shown in Figure 7.3. Initially, all nodes of End2 are fixed in all degrees of freedom and the nodes of End1 are tied with a rigid body constraint to the reference point RF-1. This point, RF-1, does not belong to the geometry of the model but in the space and any constraint which is applied to it, is automatically transferred to all nodes of End1.

Therefore, rotational constraint in x-axis (UR1) is applied to RF-1 in order End1 to remain in plane. Then, a relaxation step follows without any load in order to self-equilibrate residual stresses in the model. Finally, the load is applied via the reference point RF-1 and in the case of:

i) Pure bending, is applied as rotational displacement in x-axis (UR1) using the Riks analysis;

ii) Pure torsion, is applied as rotational displacement in z-axis (UR3) using the Riks analysis;

iii) Combined torsion and bending loads, is applied initially as rotational moment in z-axis (CM3) with known percentage (%) of applied torsion using the general static analysis. Then, the model is held and rotational displacement is applied to RF-1 in x-axis (UR1) using the Riks method. At this point, it should be mentioned that the

Riks solution can be used only once during the analysis in ABAQUS and not in multiple steps. Therefore, this the reason why the general static analysis was used for the torsional load and the Riks analysis for the bending load.

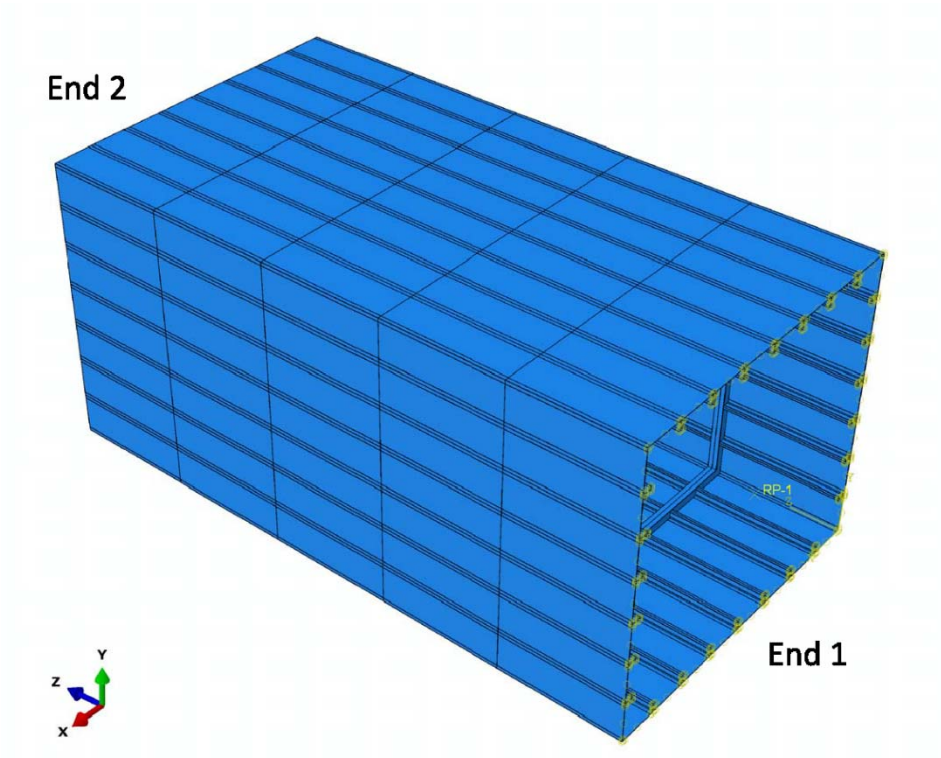

Figure 7.3: Boundary conditions of Box Girder E

7.2.3.2. Results: Under Vertical Bending Moment

The progressive collapse strength assessment of Box Girder E under vertical bending moment is depicted in Figure 7.4. Initially, the structure was modelled with and without residual stresses, but including initial imperfections, in order to investigate their effect on its progressive collapse. The stiffness of the structure is mainly affected by the presence of residual stresses (Figure 7.4) and the box girder becomes less stiff.

The values of ultimate strength under pure bending according to the nonlinear finite element analysis with and without residual stresses are:

- $\mathbf{5.30 \times 10^{10} Nmm}$, including residual stresses to the model
- $\mathbf{5.19 \times 10^{10} Nmm}$, without residual stresses to the model

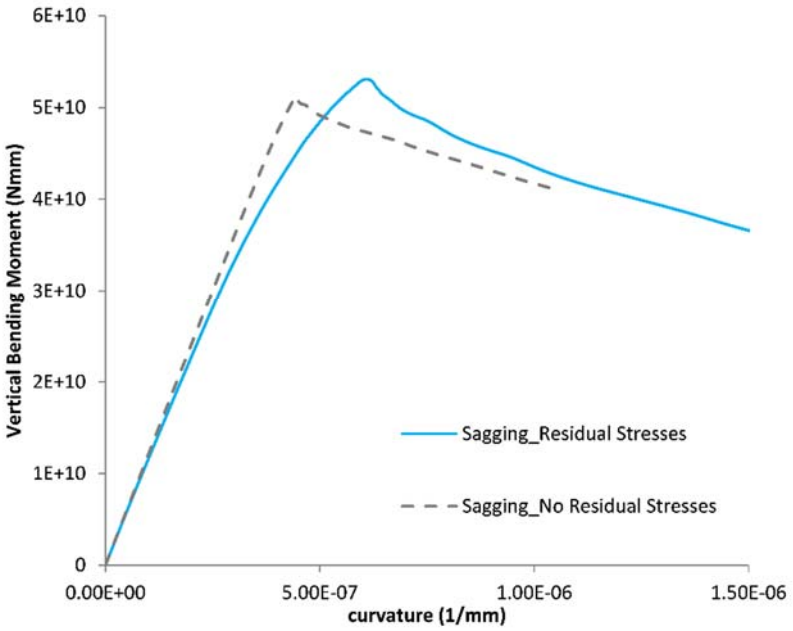

Figure 7.4: Vertical bending moment-curvature of intact Box Girder E under bending (NLFEM)

The contour plots of equivalent Von-Mises stresses at collapse and post-collapse of the intact Box Girder E with residual stresses are presented in Figure 7.5, in the left-hand side and the right-hand side respectively. The compressive stresses are generated on the deck plates, because the structure is subjected to sagging. Furthermore, the collapse occurs between the transverse frames (i.e. interframe) which it is shown in the contour plots of the displacement (Figure 7.6).

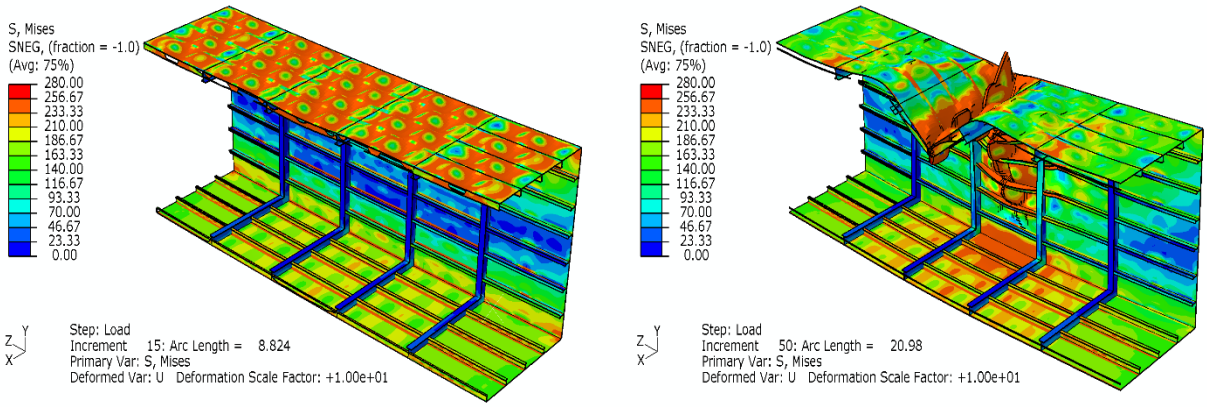

Figure 7.5: Contour plot of equivalent Von-Misses stresses at collapse and post-collapse of the intact Box Girder E with residual stressed under bending moment (magnify x10)

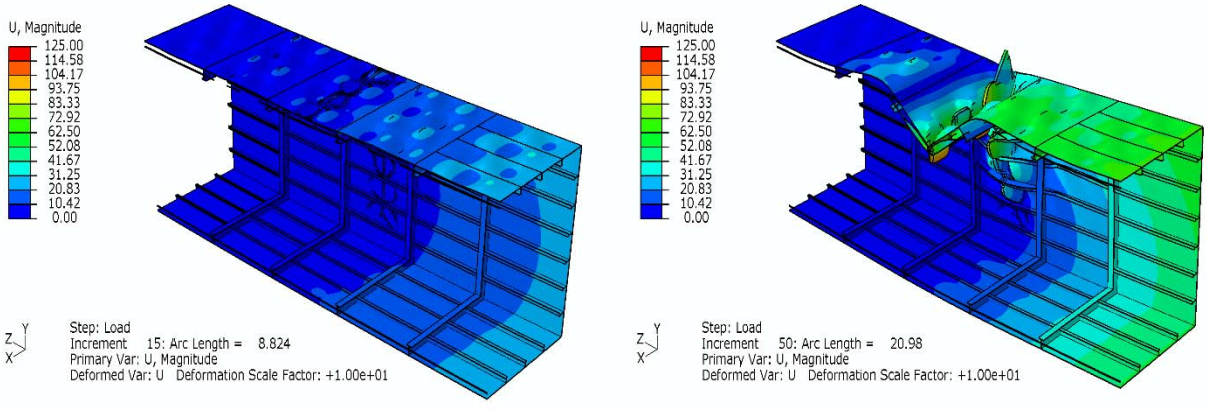

Figure 7.6: Contour plot of displacement at collapse and post collapse of the intact Box Girder E with residual stresses under bending moment (magnify x10)

7.2.3.3. Results: Under Torsion

The progressive collapse of Box Girder E under torsional load is depicted in Figure 7.7. Both cases, with and without residual stresses in the model including initial distortions, were examined and the results of their torsional moment-rotational displacement relationship show slightly different response in the nonlinear area. The stiffness of Box Girder E with residual stresses is increased in comparison with the stiffness of the box girder without residual stresses.

The values of the torsional capacity (i.e. maximum torsional moment) of Box Girder E with and without residual stresses according to the nonlinear finite element method are:

- $\mathbf{4.75 \times 10^{10} Nmm}$, including residual stresses to the model
- $\mathbf{4.88 \times 10^{10} Nmm}$, without residual stresses to the model

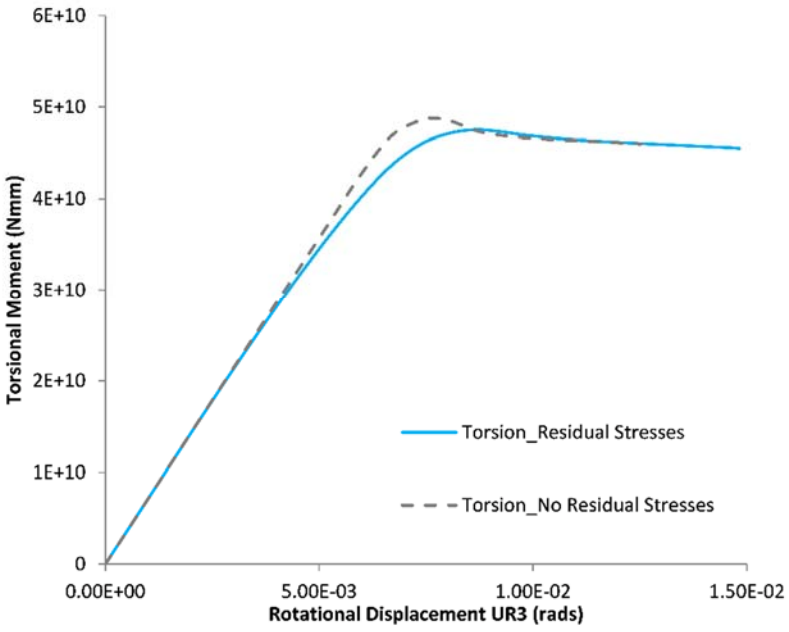

Figure 7.7: Torsional moment- angle relationship of intact Box Girder E under torsion

The contour plots of equivalent Von-Mises stresses at collapse and post-collapse of the intact Box Girder E with residual stresses under torsion are presented in Figure 7.8, in the left and right hand side respectively. High stresses are generated in the bays which are close to the constrained end (End 2). The collapse of the intact Box Girder E occurs between its transverse frames and it is shown in the contour plots of the displacement (Figure 7.9).

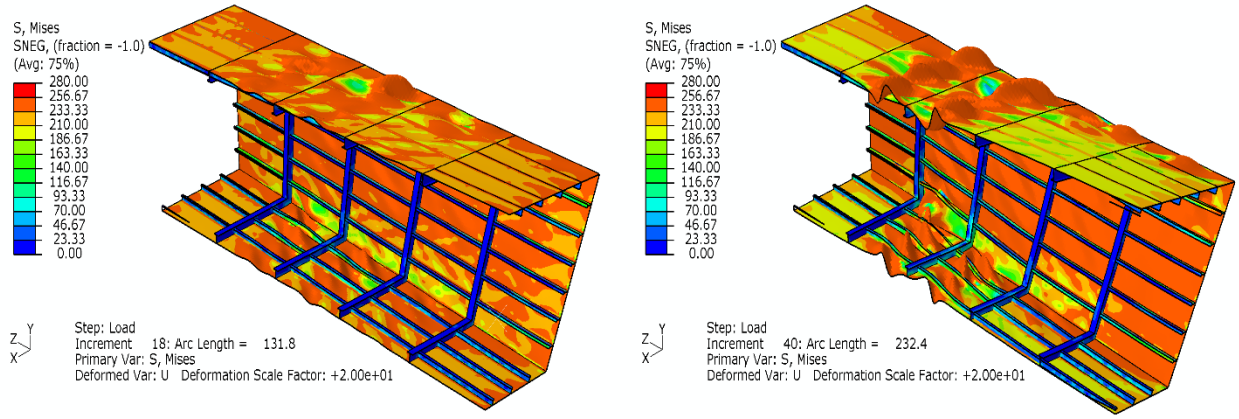

Figure 7.8: Contour plot of equivalent Von-Misses stresses at collapse and post-collapse of intact Box Girder E under torsional moment (magnify x20)

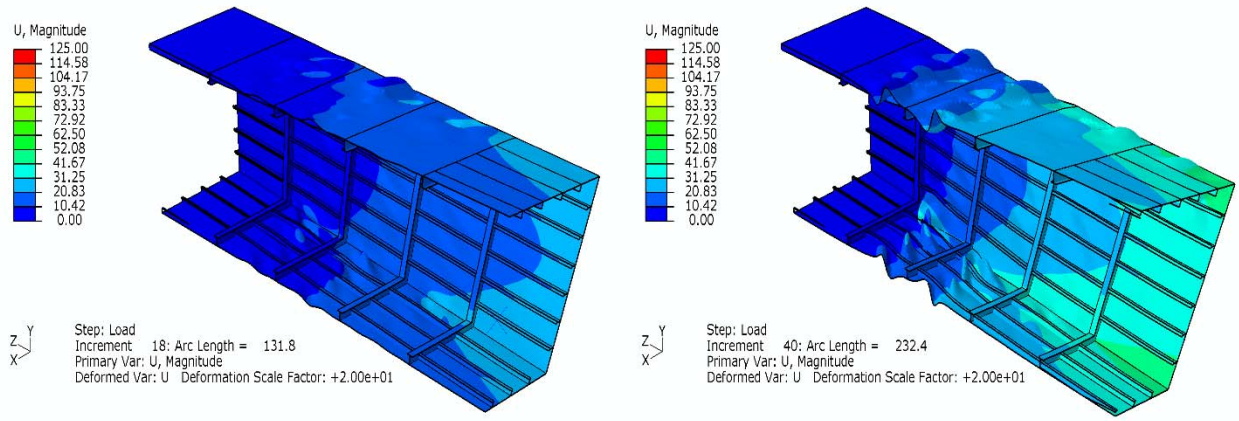

Figure 7.9: Contour plot of displacement at collapse and post collapse of intact Box Girder E under torsional moment (magnify x20)

7.2.3.4. Results: Under combined Torsion and Bending

In this section, the results of Box Girder E with residual stresses subjected to combined torsional and vertical bending loads are presented. The effect of residual stress was taken into account representing the actual behaviour of Box Girder E.

The torsional capacity of Box Girder E has already been estimated in the previous section. Therefore, fractions of the maximum torsional moment may be applied to the model in each case study during the first step of the analysis. When this analysis step is completed, rotational displacement (UR1) is applied to all nodes of End1 via the reference point RF-1. This displacement causes controlled bending moment to the model until its collapse and further steps of it (i.e. post-collapse).

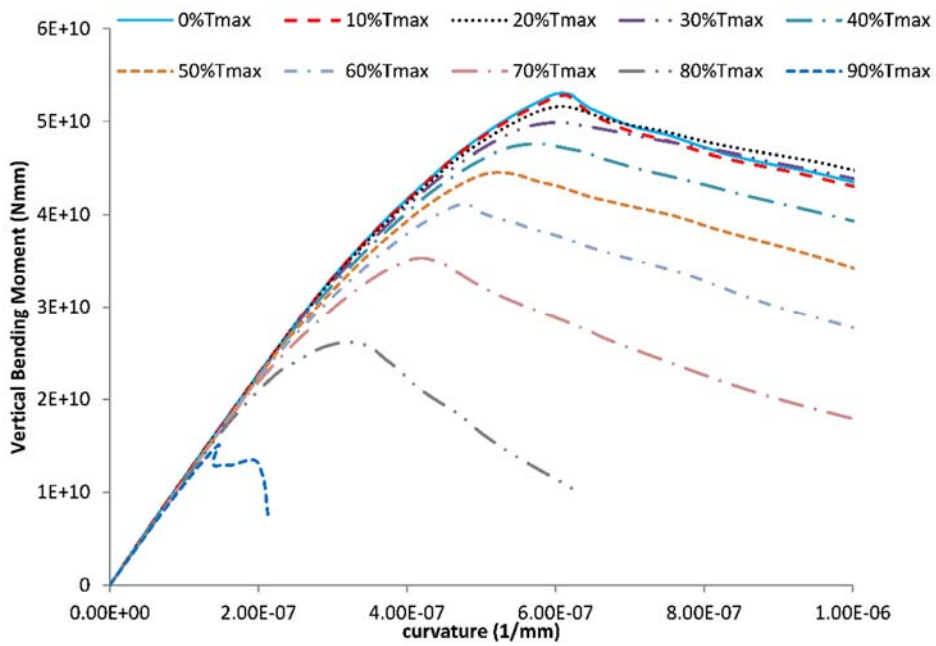

Figure 7.10: Moment-curvature curves of intact Box Girder E including residual stresses under combined torsional and bending loads

The progressive collapse assessment of the intact Box Girder E with residual stresses under combined torsional and bending loads is presented in Figure 7.10. The stiffness of the structure before the collapse (pre-collapse) is not particularly affected by the applied amount of torsional moment to the structure. However, the ultimate strength (peak point of each curve) is constantly decreases as the amount of torsional load increases. This decrease is quite

insignificant for low percentages of torsional moment (i.e. 10%, 20%), but it becomes higher as the amount of torsional load increases.

The progressive collapse behaviour of the structure is similar in each of the following ranges of applied torsional load; 10%-20% 30%-50% and 60%-90%Tmax and bending moment. Therefore, only one representative case from each range is presented. The contour plots of Von-Mises stresses and displacement for Box Girder E under 10%Tmax and bending are shown in Figure 7.11 and Figure 7.12. The collapse occurs between the transverse frames of the middle bay (interframe collapse).

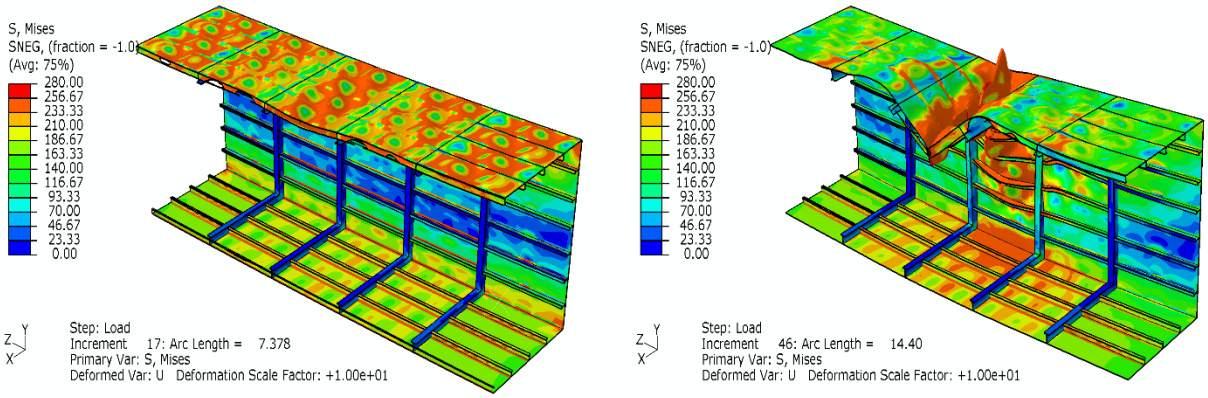

Figure 7.11: Contour plot of equivalent Von-Misses stresses at collapse and post-collapse for the intact Box Girder E under 10% of torsional capacity applied and bending (magnify x1)

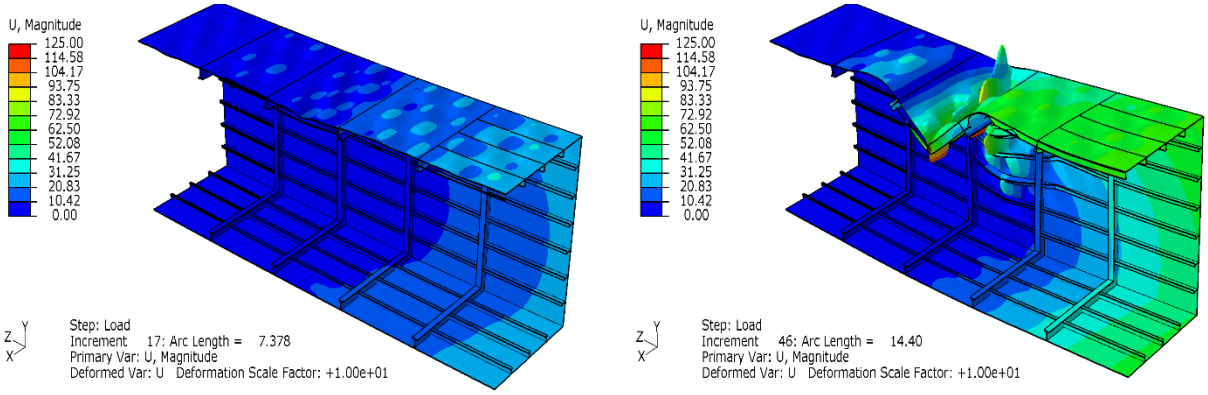

Figure 7.12: Contour plot of the displacement at collapse and post-collapse for the intact Box Girder E under 10% of torsional capacity applied and bending (magnify x1)

The contour plots of the equivalent Von-Misses stresses and displacement at collapse and post-collapse for Box Girder E under 30%Tmax and bending are shown in Figure 7.13 and Figure 7.14, respectively. In this case, the collapse occurs between the transverse frames not in the middle bay of the structure but in the bay close to the restrained end of it.

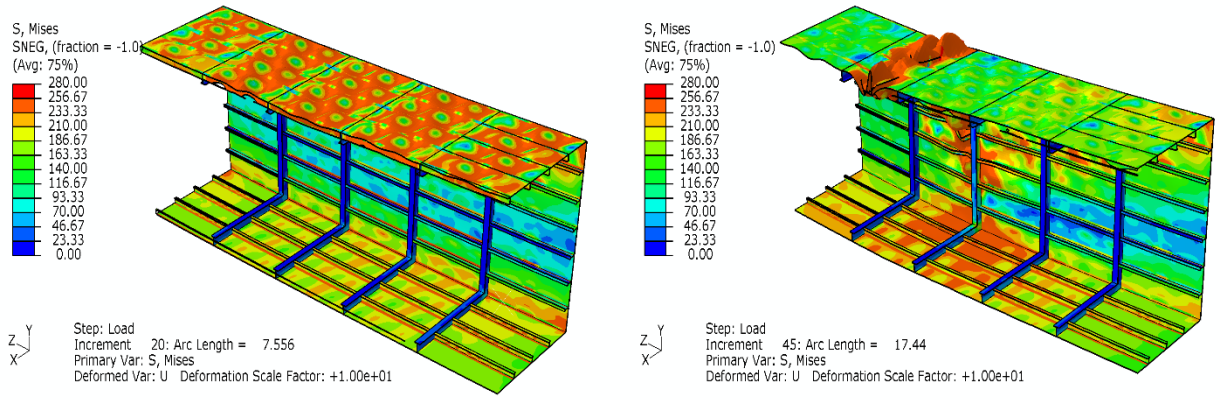

Figure 7.13: Contour plot of equivalent Von-Misses stresses at collapse and post-collapse for the intact Box Girder E under 30% of torsional capacity applied and bending (magnify x1)

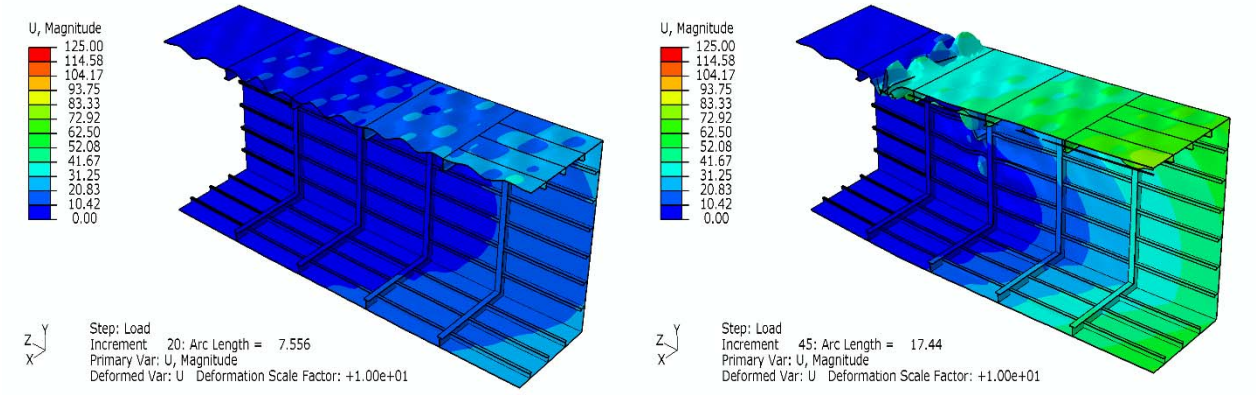

Figure 7.14: Contour plot of the displacement at collapse and post-collapse for the intact Box Girder E under 30% of torsional capacity applied and bending (magnify x1)

The contour plots of the equivalent Von-Misses stresses and displacement at collapse and post-collapse for Box Girder E under 60%Tmax and bending are shown in Figure 7.15 and Figure 7.16, respectively. In this case, the structure fails in the middle bay between the transverse frames.

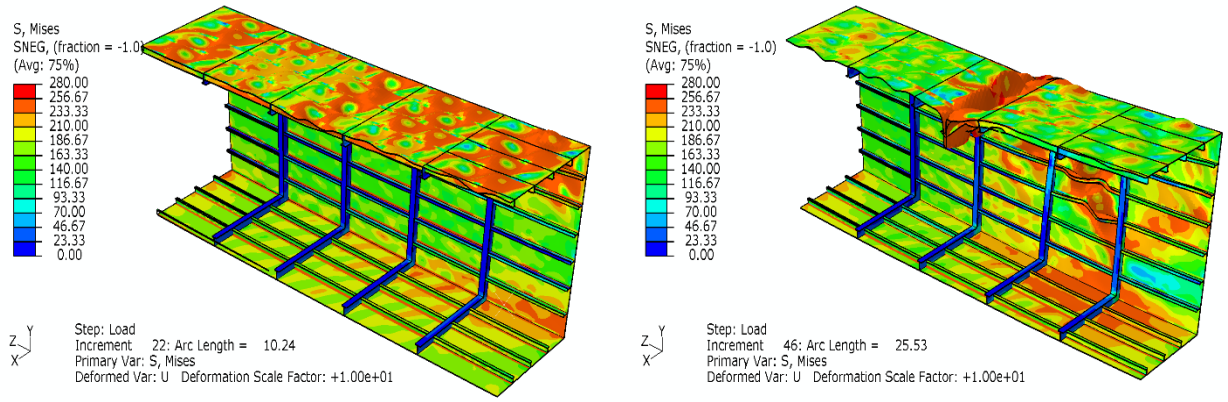

Figure 7.15: Contour plot of equivalent Von-Misses stresses at collapse and post-collapse for the intact Box Girder E under 60% of torsional capacity applied and bending (magnify =x1)

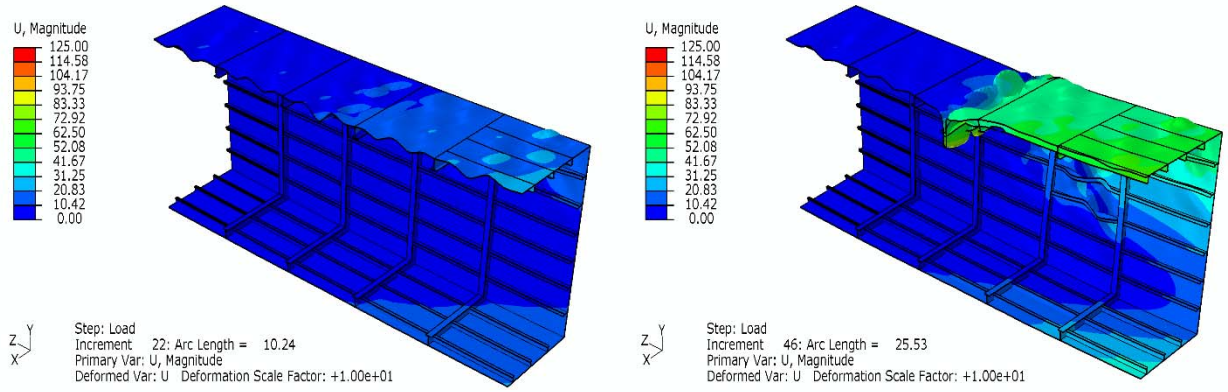

Figure 7.16: Contour plot of the displacement at collapse and post-collapse for the intact Box Girder E under 60% of torsional capacity applied and bending (magnify x1)

The interaction diagram of torsional moment and maximum bending moment which the intact Box Girder E may sustain is presented in Figure 7.17. The graph defines a safe limit in the area below it in which any combination of these loads is permissible. A non-dimensional interaction graph of these combined torsional and bending loads is presented in Figure 7.18. This plot includes also the theoretical graph which derives applying Equation 5.8 for the same values of torsional moment. Both graphs show very good correlation, especially for low amounts of torsion, and follow the theoretical formulation for torsion and bending.

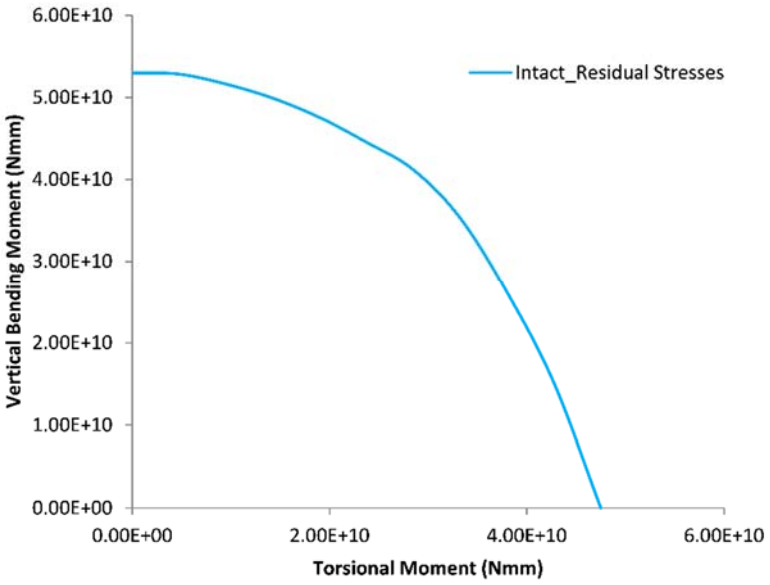

Figure 7.17: Interaction diagram of torsional and bending moment for the intact Box Girder E (ABAQUS)

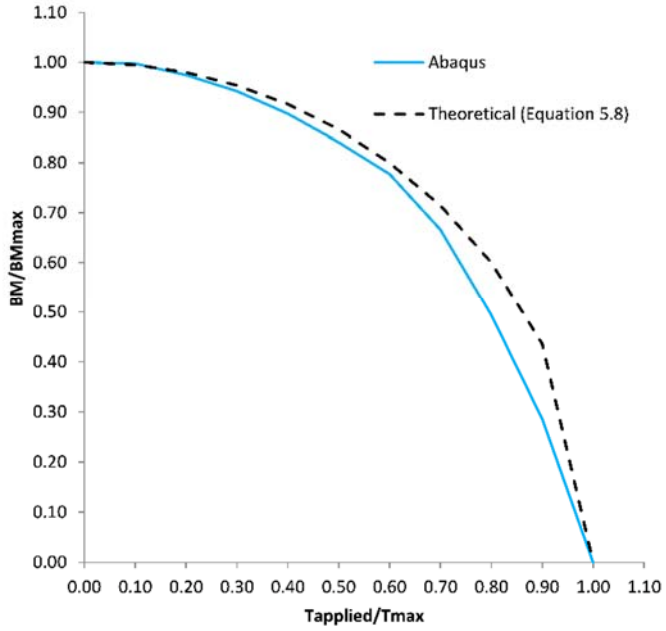

Figure 7.18: Non-dimensional interaction diagram of combined torsional and bending loads for the intact Box Girder E

7.2.4. Progressive Collapse of intact box girder with the Extended Progressive Collapse Method (ProColl)

In this section, the progressive collapse of the intact Box Girder E including the residual stresses effect is investigated under pure bending and combined bending and torsional loads, using the proposed extended simplified progressive collapse method. Initially, the modelling of the intact Box Girder E in ProColl is described and then the results of the analyses under the aforementioned loads are presented.

7.2.4.1. Extended Progressive Collapse Method modelling

The set-up of the model in the extended progressive collapse method requires the description of the cross-section of the structure. The geometry of the cross-section is described by plates and stiffeners placed in the right coordinates. Each plate with its associated stiffener consists an element and every element belongs to a load shortening curve (LSC) and a numbered loop.

In this case, the shape of the cross section of Box Girder E is a simple rectangular which is depicted in Figure 7.1. and Appendix C. It is consisted only by one (1) loop, therefore all plates are assigned to the same numbered loop e.g. number 1. Furthermore, four (4) LSC are defined in the model, one for each side. Finally, the length of the structure is defined as the length of each bay, 1800mm, multiply be the total number of transverse frames, 5 (i.e. total length 9000mm).

The material properties of steel with Young's modulus **207GPa** and yield stress **245Mpa** are assumed. The width of the residual stresses zone was taken equal to 50mm only along the length of the plate and the stresses were calculated according to Equation 2.8. An average level of initial imperfections was assumed according to Equation 2.8, with their shape described by Equation 2.12. The ProColl data file is presented in Appendix B.

In the case where only vertical bending moment occurs, incremental curvature is applied directly to the model and the extended progressive collapse method is implemented as described in section 2.3.3. In the case where torsional load is applied with combined vertical bending moment, the numbered loop of each plate is taken into account into the analysis in order to calculate shear flow distribution on the plates and torsional load and the proposed methodology is implemented according to the flow chart diagram in Chapter 3.

7.2.4.2. Results: Under Vertical Bending Moment

The progressive collapse of the intact Box Girder E under vertical bending moment in sagging is depicted in Figure 7.19. The value of its ultimate strength according to the extended progressive collapse method is:

- $\mathbf{5.17 \times 10^{10} Nmm}$, including residual stress and initial deformations to the model

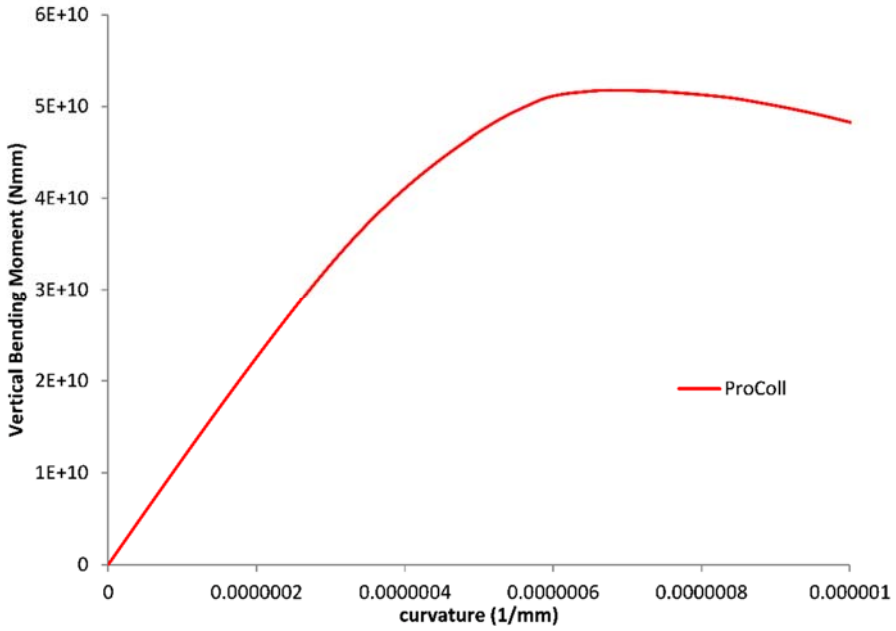

Figure 7.19: Vertical bending moment-curvature relationship of the intact Box Girder E under vertical bending moment (ProColl)

7.2.4.3. Results: Under combined Bending and Torsion

The bending moment-curvature relationships of the intact Box Girder E with applied torsion according to the proposed methodology (Chapter 3) are presented in Figure 7.20. The strength of Box Girder E decreases as the amount of the applied torsional moment increases, without particularly affecting its stiffness though. Finally, similar pattern of bending moment-curvature relationship is presented up to high amounts of applied torsional moment (i.e. 3.65E+10Nmm).

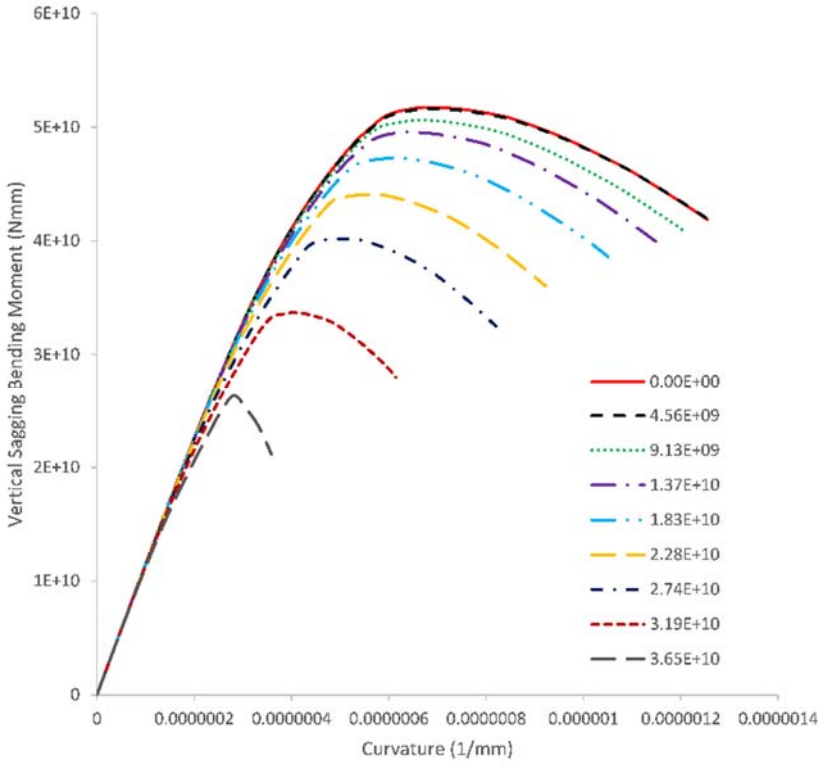

Figure 7.20: Bending moment-curvature relationship of the intact Box Girder E subjected to different amount of torsional moment (Nmm) and vertical bending moment (in sagging condition)

The interaction diagram of torsional moment and vertical bending moment according to the proposed extended simplified progressive collapse method is depicted in Figure 7.21. The graph defines a safe limit for the strength of intact Box Girder E when is subjected to combined torsional and bending loads.

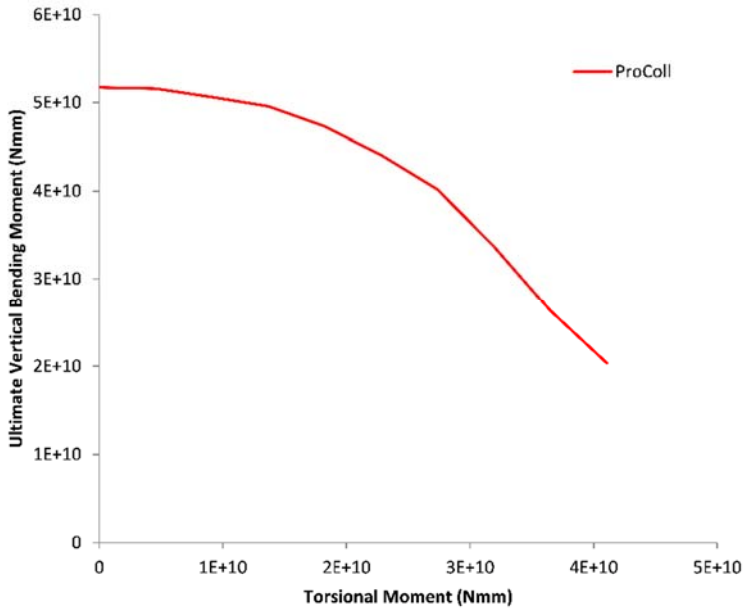

Figure 7.21: Interaction of torsional and vertical bending moment of intact Box Girder E according to the proposed extended simplified progressive collapse method (ProColl)

7.2.5. Comparison of the results for intact box girder under combined torsion and bending

The normalised interaction diagram of torsional and bending moment with respect to the F.E. values, $\boldsymbol{Tmax = 4.75 \times 10^{10} Nmm}$ and $\boldsymbol{BMmax = 5.30 \times 10^{10} Nmm}$, is presented in Figure 7.22.

The results of the intact Box Girder E according to both methodologies, the NLFEM and the proposed methodology, are compared in the same graph and show very good correlation.

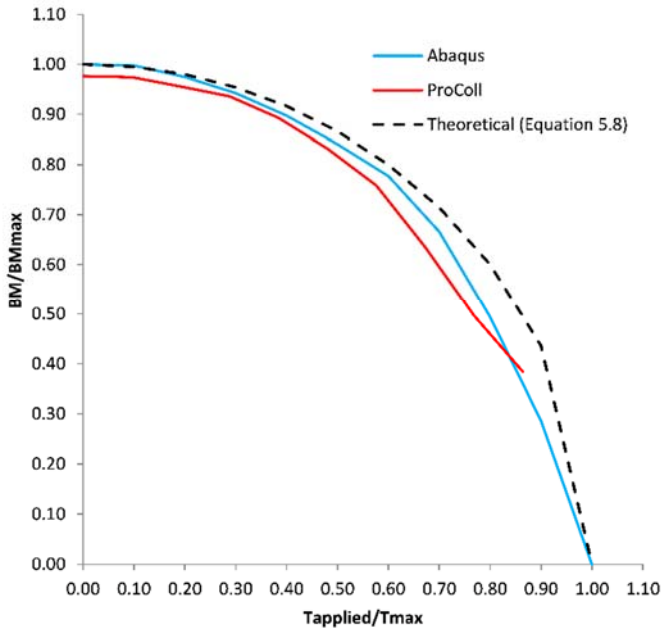

Figure 7.22: Normalised interaction diagram of torsion and bending of the intact Box Girder E according to the NLFEM (ABAQUS) and the proposed extended simplified progressive collapse method (ProColl).

7.3. Part II: Trans. & Long. Damage Cases of Box Girder E

7.3.1. Introduction

In this section, the residual strength of Box Girder E is investigated for different damage case scenarios under pure bending, torsion and combined torsional and bending loads. Damage is represented as a cut-out of the damaged structure without taking into account any effect which the released energy from the collision may cause. Both methodologies, the nonlinear finite element method and the proposed extended progressive collapse method are applied. The residual strength of damaged structures is presented and a comparison of these results follows aiming to show the differences between the two methodologies.

This analysis has been carried out to investigate the effects of damage when combined bending and torsional loads are present. This will also be used to validate the future damage model to be incorporated in ProColl for the effect of combined loads.

7.3.2. Damage Cases

The criterion according to which the damage case scenarios were selected, was to examine the effect of the longitudinal and transverse damaged extent. Therefore, initially the longitudinal damage extent is constant and the size of the transverse damaged extent varies. In each case, the structure is subjected to pure bending, torsion and combined torsional loads and bending.

Then, the longitudinal size of the damaged extent varies keeping the transverse damaged extent constant and the structure is subjected to the same pattern of loads (i.e. bending, pure torsion, combined torsion and bending).

7.3.2.1. Different size of transverse damage extent

Three cases of different size of transverse damage extent were examined (Figure 7.23 & Appendix C). Initially, a very narrow elliptical damage extent of 64mm width (Trans. Damage Case I) in which the central stiffener is actually removed. Then, a circular cut-out of c=0.3B=1440mm (Trans. Damage Case II) and an elliptical cut-out with the length of its major axis equal to 2c=2880mm (Trans. Damage Case III) were examined. The damage is always

applied to the center of the central bay of Box Girder E, therefore it is symmetrical. Finally, the length of the damage extent is constant and equal to 1440mm in all cases.

7.3.2.2. Different size of longitudinal damage extent

Two cases of different size of longitudinal damage extent were investigated (Figure 7.24 & Appendix C). Initially, a circular cut-out of 0.3B=c=1440mm (Long. Damage Case I) was examined and afterwards an elliptical cut-out 2c=2880mm long (Long. Damage Case II) which causes the loss of two transverse frames. The damage is also symmetrical as it is always applied to the center of the central bay of the box girder. Finally, the width of the damage extent is constant and equal to 1440mm in both damage cases.

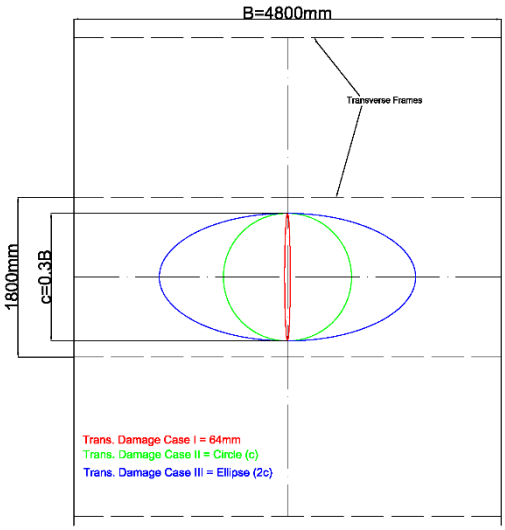

Figure 7.23: Sketch of different transverse cut-outs damage extents

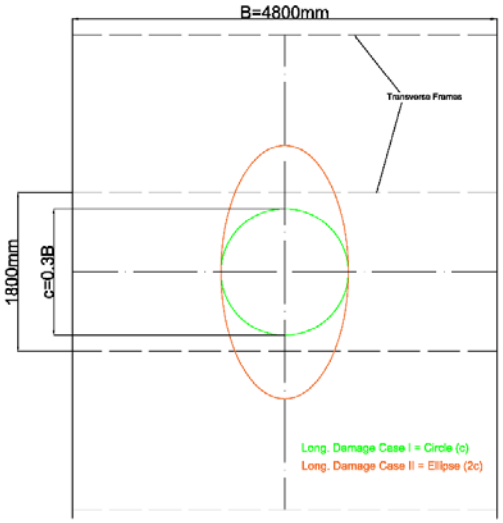

Figure 7.24: Sketch of different longitudinal cut-outs damage extents

These damage scenarios are not able to be modelled accurately in the current version of ProColl since this requires the removal of the damaged elements for the full length of the compartment. However, in the future with the implementation of the new damaged element into ProColl this should be able to be modelled more accurately.

7.3.3. Damaged box girders with different transverse damage extent (NLFEM)

The NLFE modelling of the damaged box girders is very similar to this of the intact Box Girder E, as described in section 7.2.3.1. The only difference is in the geometry of the models in which the damage extents are represented as cut-outs. Their size is depicted in Figure 7.23 and further details about the set-up of the model are referred in section 7.3.2.1.

Initially, all damaged box girders were subjected to vertical bending moment, then they were examined under pure torsion and finally under combined torsional and bending loads using the nonlinear finite element method.

7.3.3.1. Under vertical bending moment

The contour plots of the equivalent Von-Misses stresses and the displacement at collapse and post-collapse for Trans. Damage Case I, II and III of Box Girder E subjected only to vertical bending moment are shown in Figure 7.25 - Figure 7.30.

In Figure 7.25, the compressive stresses on the deck plates are shown for Trans. Damage Case I of Box Girder E under pure bending. The contour plots of the displacement in Figure 7.26 show the collapse of the structure between its transverse frames (interframe) in the middle bay of it.

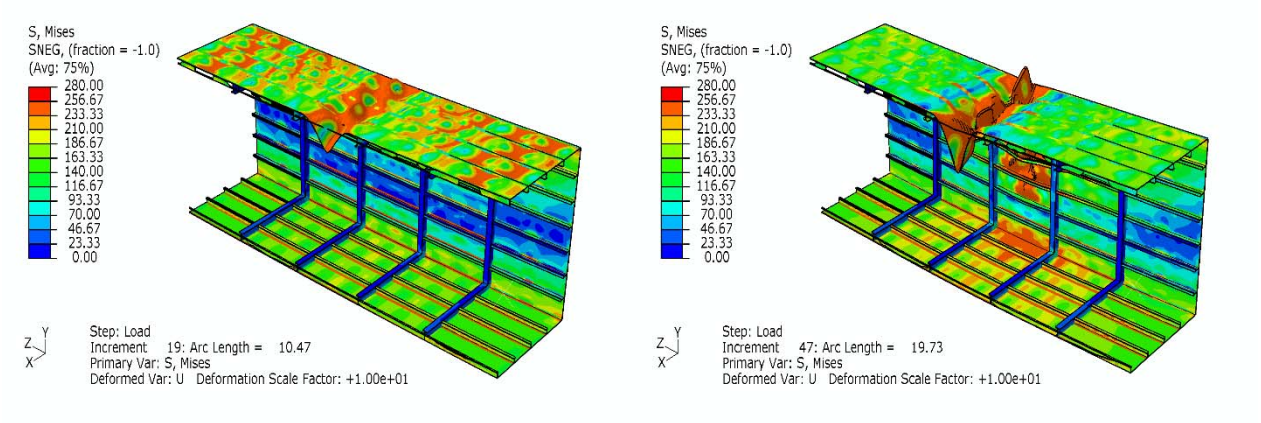

Figure 7.25: Contour plot of equivalent Von-Misses stresses at collapse and post-collapse for Trans. Damage Case I of Box Girder E under bending moment (magnify x10)

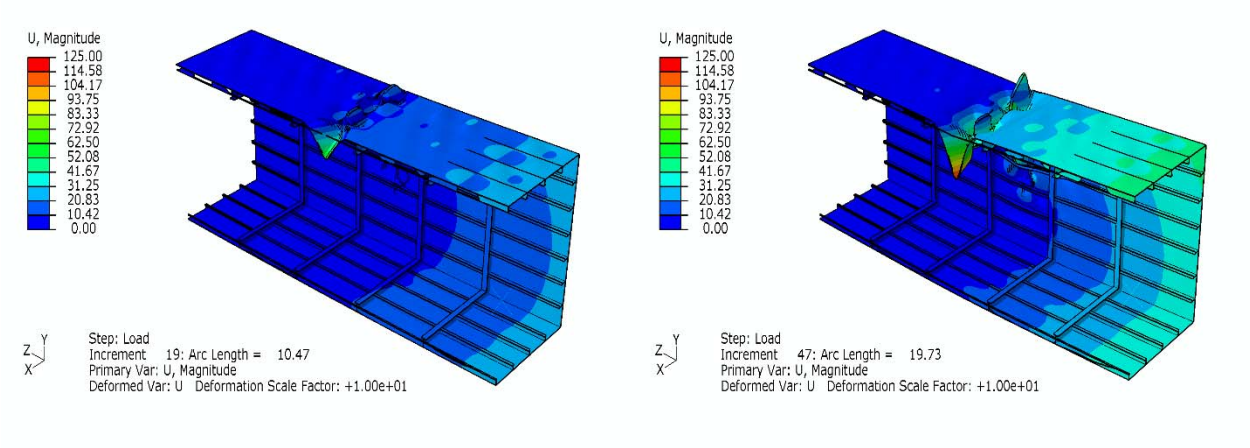

Figure 7.26: Contour plot of the displacement at collapse and post-collapse for Trans. Damage Case I of Box Girder E under bending moment (magnify x10)

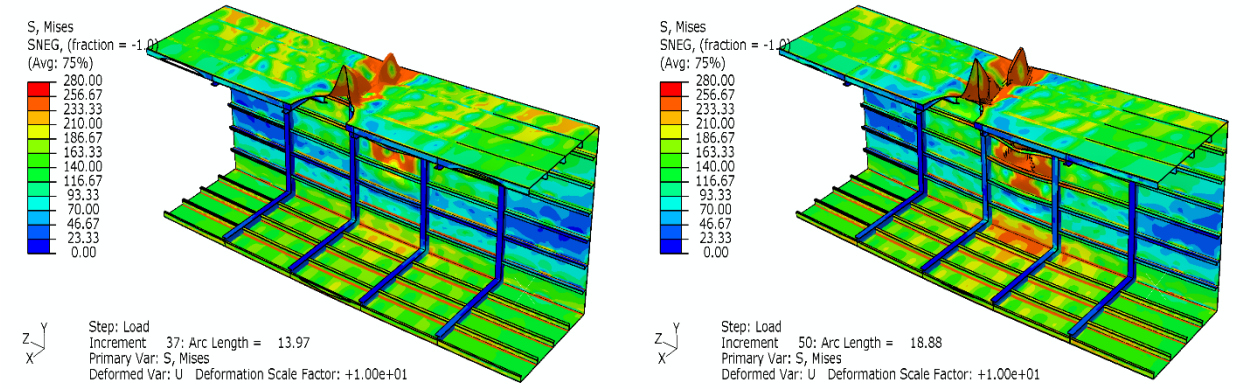

Figure 7.27: Contour plot of equivalent Von-Misses stresses at collapse and post-collapse for Trans. Damage Case II of Box Girder E under bending moment (magnify x10)

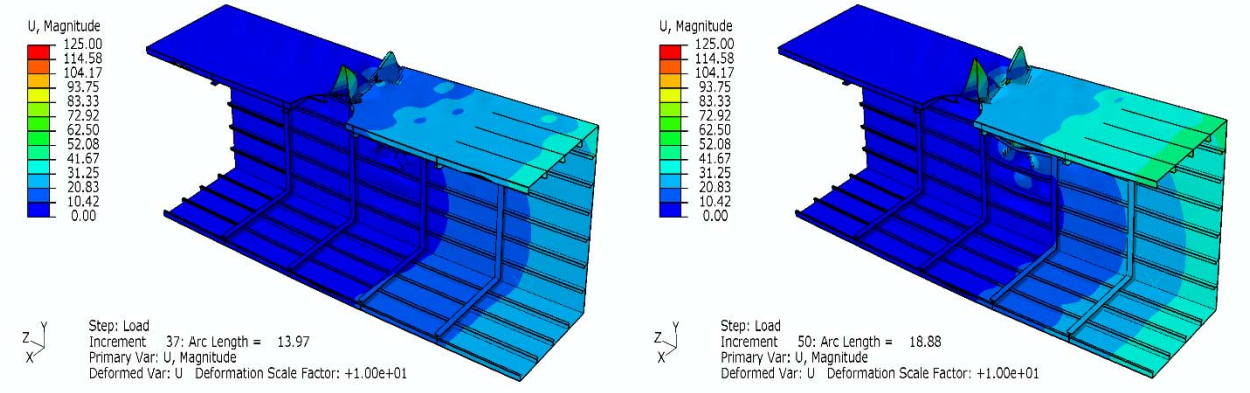

Figure 7.28: Contour plot of the displacement at collapse and post-collapse for Trans. Damage Case II of Box Girder E under bending moment (magnify x10)

The contour plots of the Von-Mises stresses and the displacement for Trans. Damage Case II of Box Girder E subjected only to bending are shown in Figure 7.27 and Figure 7.28, respectively. In this case, interframe collapse mode occurs due to the bending load. Similar behaviour presents also Box Girder E in Trans. Damage Case III, in which the size of the transverse damage extent is larger and its contour plots of Von-Mises and displacement are shown in Figure 7.29 and Figure 7.30, respectively.

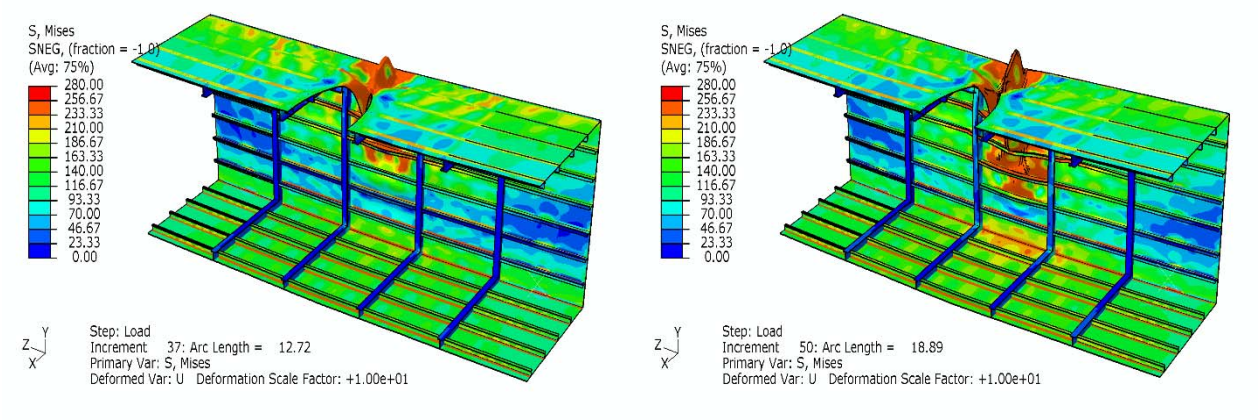

Figure 7.29: Contour plot of equivalent Von-Misses stresses at collapse and post-collapse for Trans. Damage Case III of Box Girder E under bending moment (magnify x10)

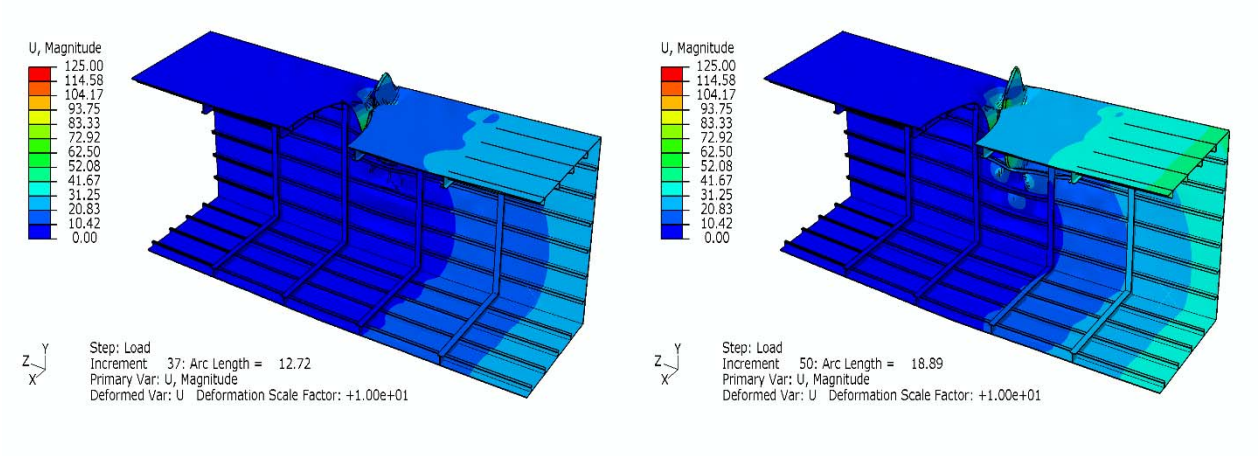

Figure 7.30: Contour plot of the displacement at collapse and post-collapse for Trans. Damage Case III of Box Girder E under bending moment (magnify x10)

The progressive collapse for the Trans. Damage Case I, II and III of Box Girder E subjected to vertical bending moment is presented in Figure 7.31. The strength and the stiffness of Box Girder E decrease as the damage extent increases. The post-collapse strength of the structure in the damage cases presents a smoother drop than this in the intact.

The ultimate strength in each case is:

- $\mathbf{5.30 \times 10^{10} Nmm}$, for intact Box Girder E
- $\mathbf{4.75 \times 10^{10} Nmm}$, for Trans. Damage Case I of Box Girder E
- $\mathbf{4.05 \times 10^{10} Nmm}$, for Trans. Damage Case II of Box Girder E
- $\mathbf{3.34 \times 10^{10} Nmm}$, for Trans. Damage Case III of Box Girder E

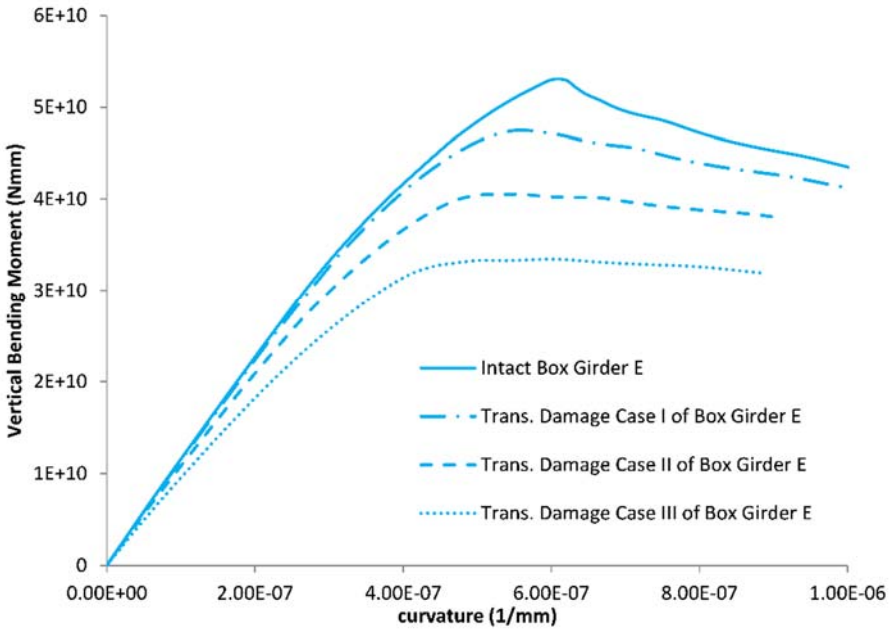

Figure 7.31: Moment-Curvature relationships of intact Box Girder E and Trans. Damage Cases I, II and III of Box Girder E subjected to vertical bending moment (NLFEM)

7.3.3.2. Under pure torsion

The contour plots of the equivalent Von-Misses stresses and the displacement at collapse and post-collapse of the Trans. Damage Cases I, II and III of Box Girder E under torsional load are shown in Figure 7.32 -Figure 7.37.

The contour plots of the Von-Mises stresses and the displacement for the Trans. Damage Case I of Box Girder E under pure torsion, Figure 7.32 and Figure 7.33, show an interframe collapse of the structure in the middle bay of the model.

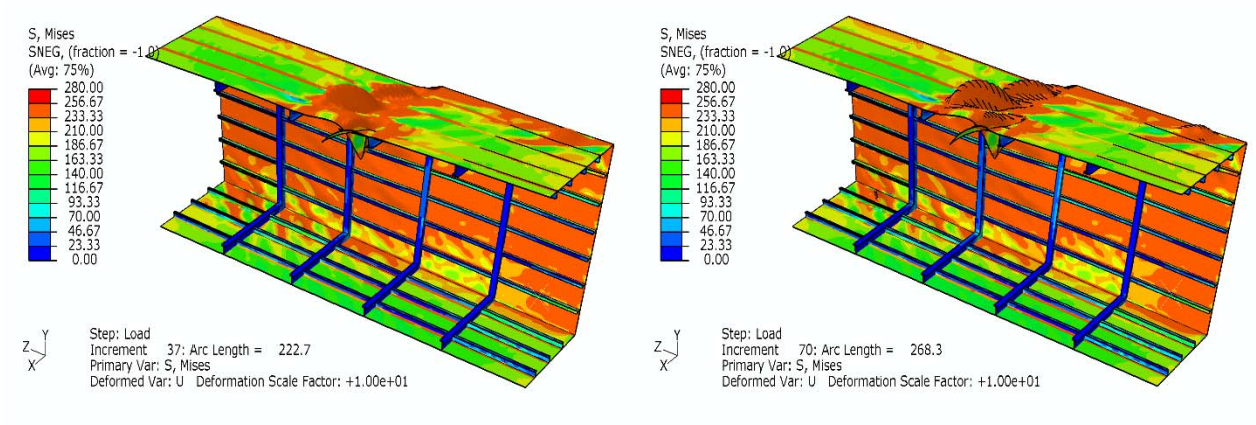

Figure 7.32: Contour plot of equivalent Von-Misses stresses at collapse and post-collapse for Trans. Damage Case I of Box Girder E under torsional moment (magnify x10)

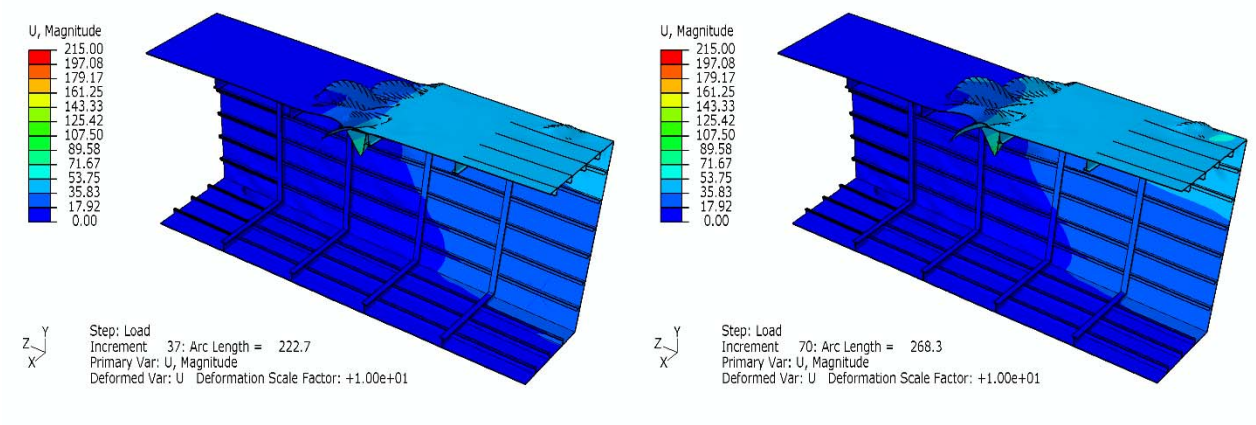

Figure 7.33: Contour plot of displacement at collapse and post-collapse for Trans. Damage Case I of Box Girder E under torsional moment (magnify x10)

In the cases which the transverse damage extent is increased, i.e. Trans. Damage Case II and III, the contour plots of the Von-Mises stresses and the displacement, Figure 7.34 - Figure 7.37, show an interframe collapse mode for these damaged structures.

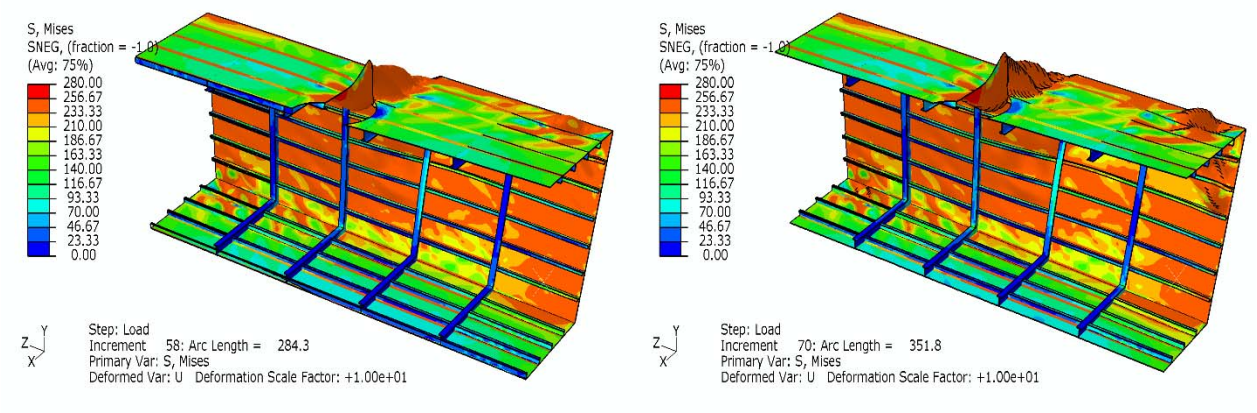

Figure 7.34: Contour plot of equivalent Von-Misses stresses at collapse and post-collapse for Trans. Damage Case II of Box Girder circle E under torsional moment (magnify x10)

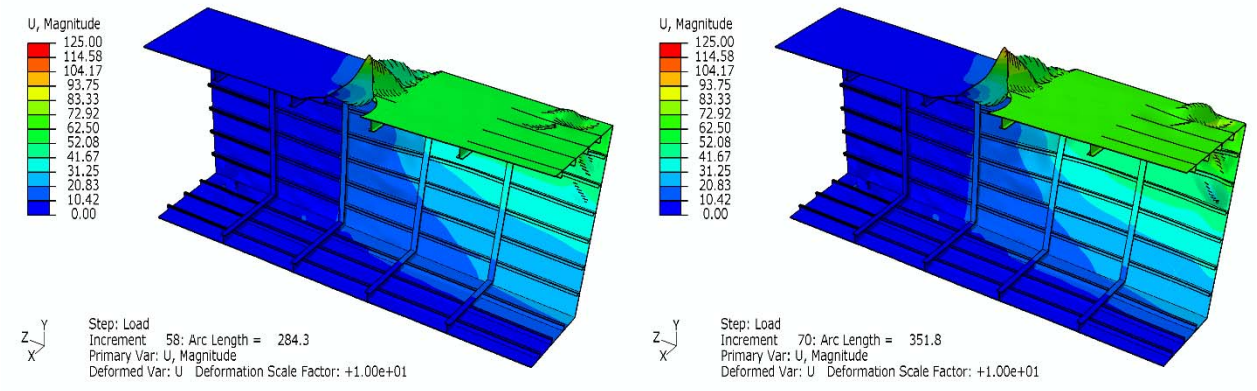

Figure 7.35: Contour plot of displacement at collapse and post-collapse for Trans. Damage Case II of Box Girder E under torsional moment (magnify x10)

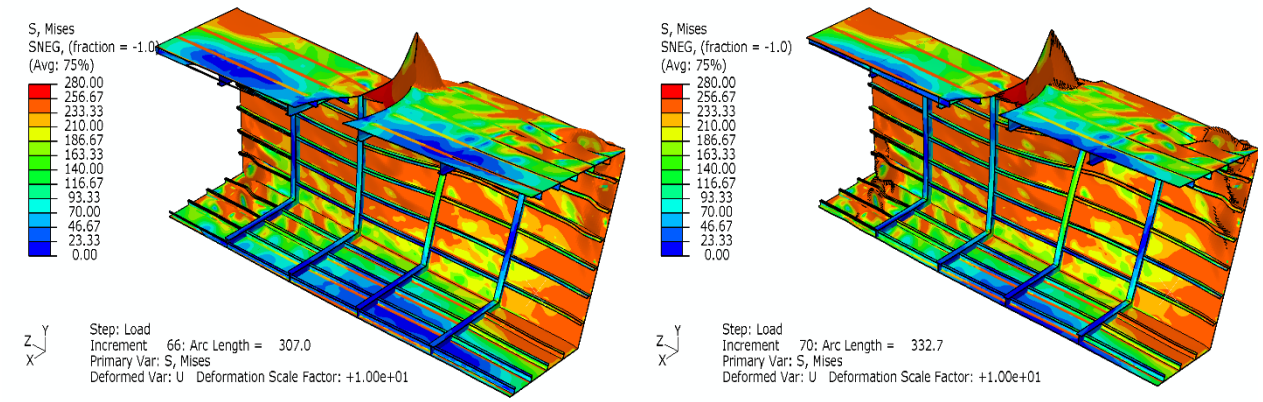

Figure 7.36: Contour plot of equivalent Von-Mises stresses at collapse and post-collapse for Trans. Damage Case III of Box Girder E under torsional moment (magnify x10)

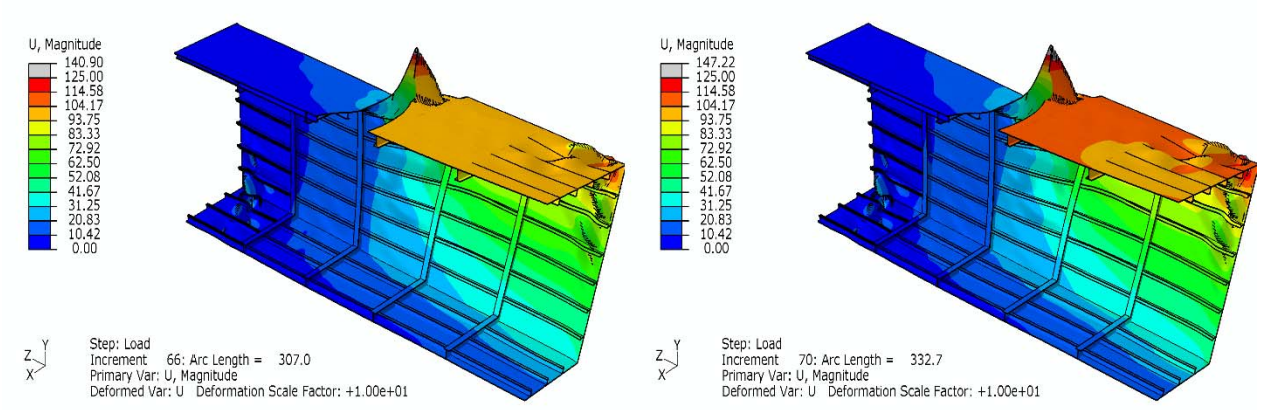

Figure 7.37: Contour plot of equivalent Von-Mises stresses at collapse and post-collapse for Trans. Damage Case III of Box Girder E under torsional moment (magnify x10)

The torsional moment-angle relationships for Trans. Damage Case I, II and III of Box Girder E subjected only to torsional load are presented in Figure 7.38. The torsional moment which Box Girder E may sustain, decreases as the damage extent increases.

The ultimate strength in each case is:

- $\mathbf{4.75 \times 10^{10} Nmm}$, for intact Box Girder E
- $\mathbf{4.18 \times 10^{10} Nmm}$, for Trans. Damage Case I of Box Girder E
- $\mathbf{3.68 \times 10^{10} Nmm}$, for Trans. Damage Case II of Box Girder E
- $\mathbf{3.01 \times 10^{10} Nmm}$, for Trans. Damage Case III of Box Girder E

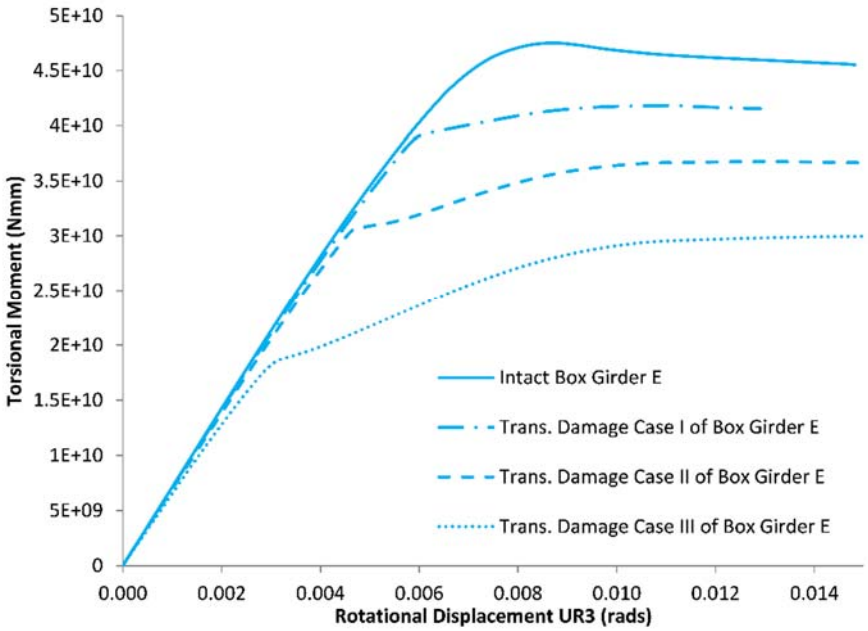

Figure 7.38: Torsional Moment- Angle relationships of intact Box Girder E and Trans. Damage Case I, II and III of Box Girder E subjected to torsional load (NLFEM)

7.3.3.3. Under combined torsional loads and bending

In this section, the bending moment-curvature relationships for Trans. Damage Case I, II and III of Box Girder E subjected to different amounts of torsional load and then bending are presented in Figure 7.39, Figure 7.40 and Figure 7.41, respectively. In each case, the strength of the damaged box girder gradually decreases as the applied torsion increases. Their stiffness though is not particularly affected by low amounts of applied torsion and it is obviously changing only for high amounts of torsion (more than 70%Tmax).

The maximum value of each bending moment-curvature for the applied amount of torsion is plotted in Figure 7.42, generating the interaction diagram of applied torsion and ultimate/residual strength which the intact and damaged structure may sustain. Figure 7.42 show a gradual decrease of the values in the intact case as the size of the transverse damage extent increases, Trans. Damage Case I, II and III.

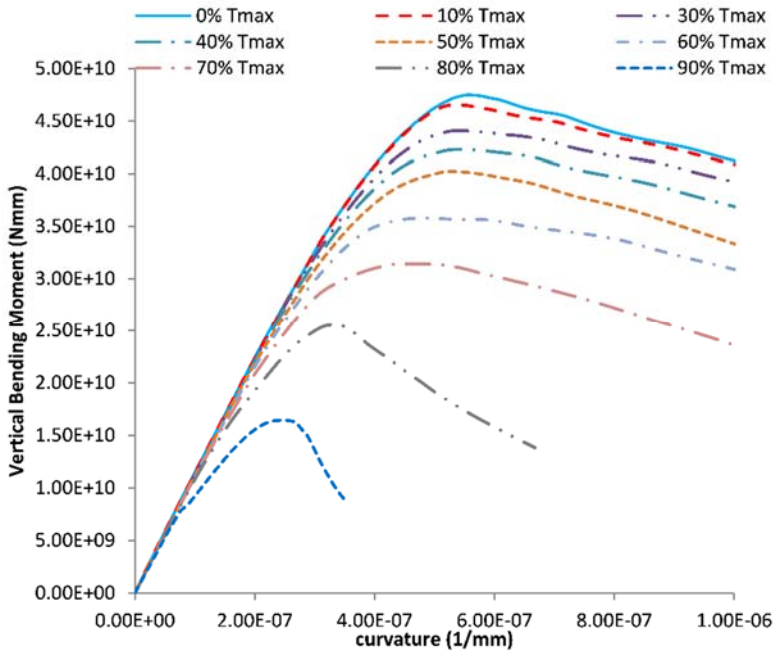

Figure 7.39: Moment-Curvature relationships for the Trans. Damage Case I of Box Girder E subjected to combined torsional loads and bending (NLFEM)

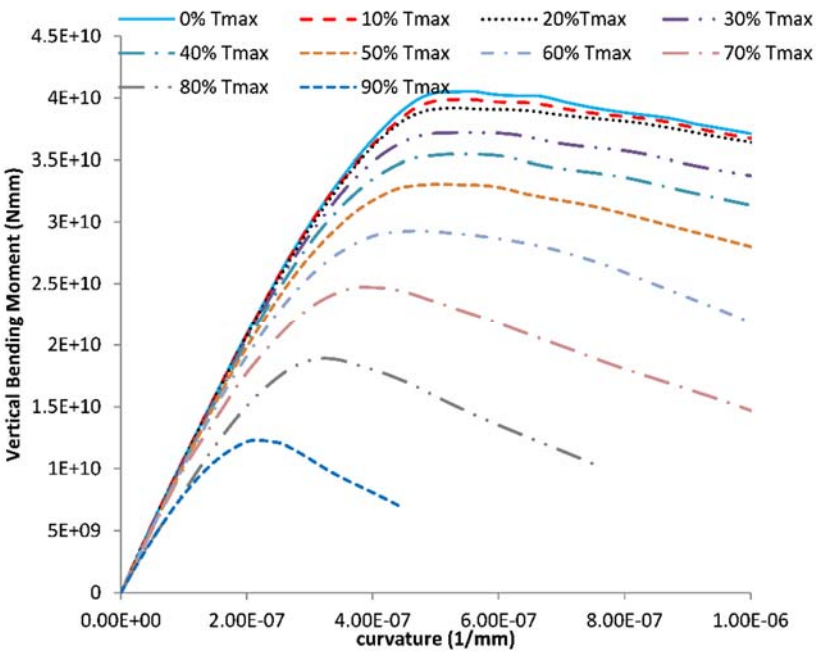

Figure 7.40: Moment-Curvature relationships for Trans. Damage Case II of Box Girder E subjected to combined torsional loads and bending (NLFEM)

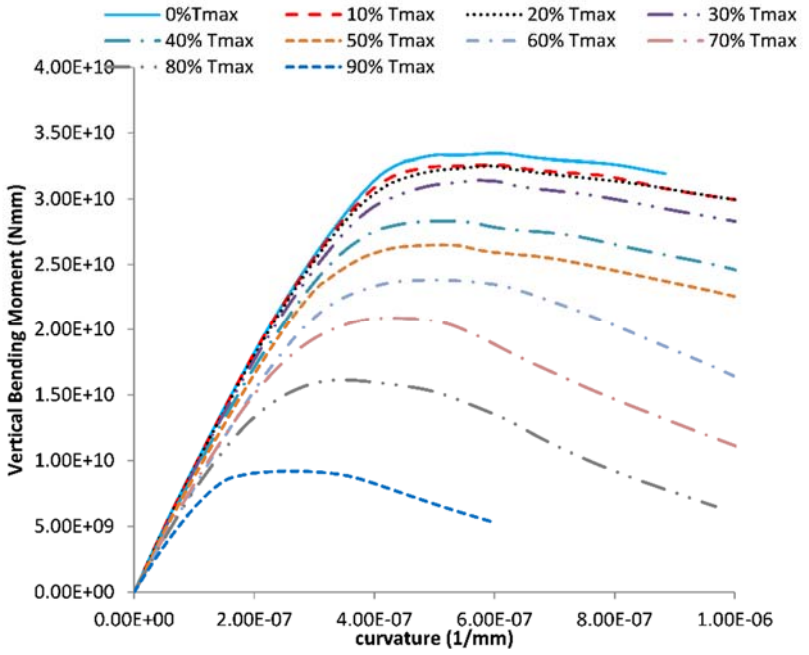

Figure 7.41: Moment-Curvature relationships for Trans. Damage Case III of Box Girder E subjected to combined torsional loads and bending (NLFEM)

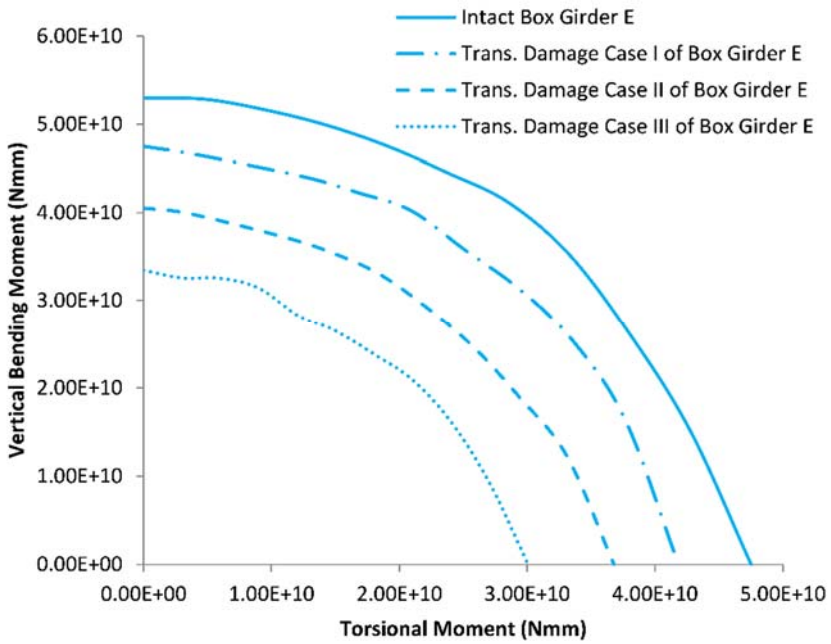

Figure 7.42: Interaction Diagram of torsional and bending load for the intact and Trans. Damage Case I, II and III of Box Girder E.

The contour plots of the equivalent Von-Misses stresses and the displacement at collapse and post collapse are shown in Figure 7.43 - Figure 7.46 for Trans. Damage Case I of Box Girder E, in Figure 7.47 - Figure 7.50 for Trans. Damage Case II of Box Girder E and in Figure 7.51 - Figure 7.54 for Trans. Damage Case III of Box Girder E under combined torsional load and bending.

The purpose is to show how the failure mode of the damaged structure is affected by the amount of applied torsion in each damage case. The collapse behaviour of the damaged box girders without any torsional load has already been presented in Figure 7.26, Figure 7.28 and Figure 7.30 showing that interframe collapse mode occurs in all cases.

In the case of Trans. Damage Case I of Box Girder E, the structure fails between its transverse frames under any amount of applied torsion and bending, e.g. for 50%Tmax and bending load (Figure 7.43 & Figure 7.44), for 60%Tmax and bending load (Figure 7.45 & Figure 7.46).

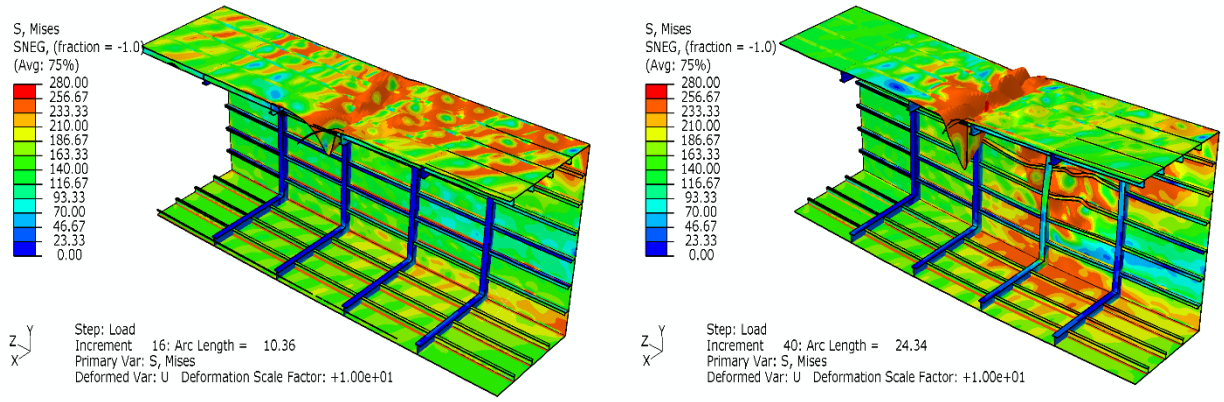

Figure 7.43: Contour plot of equivalent Von-Misses stresses at collapse and post-collapse for Trans. Damage Case I of Box Girder E under 50% of torsional capacity applied and bending (magnify x10)

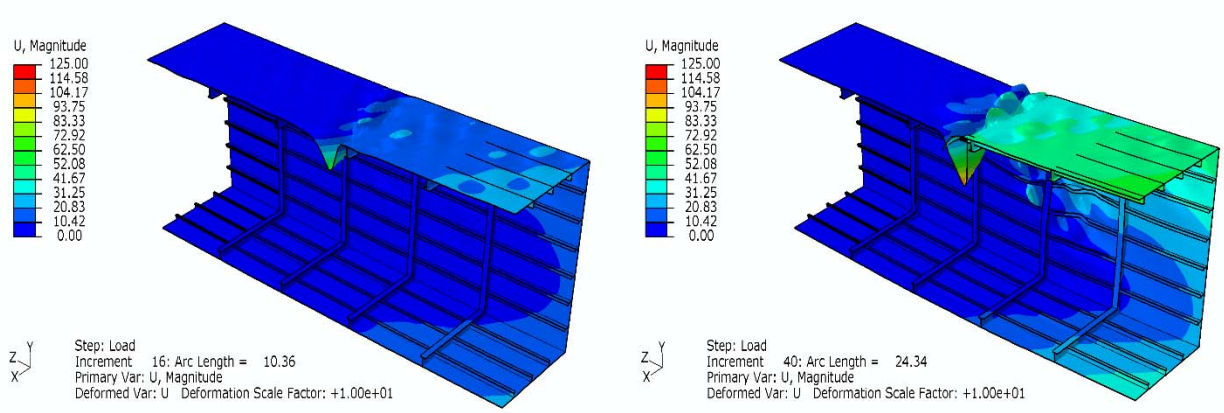

Figure 7.44: Contour plot of the displacement at collapse and post-collapse for Trans. Damage Case I of Box Girder E under 50% of torsional capacity applied and bending (magnify x10)

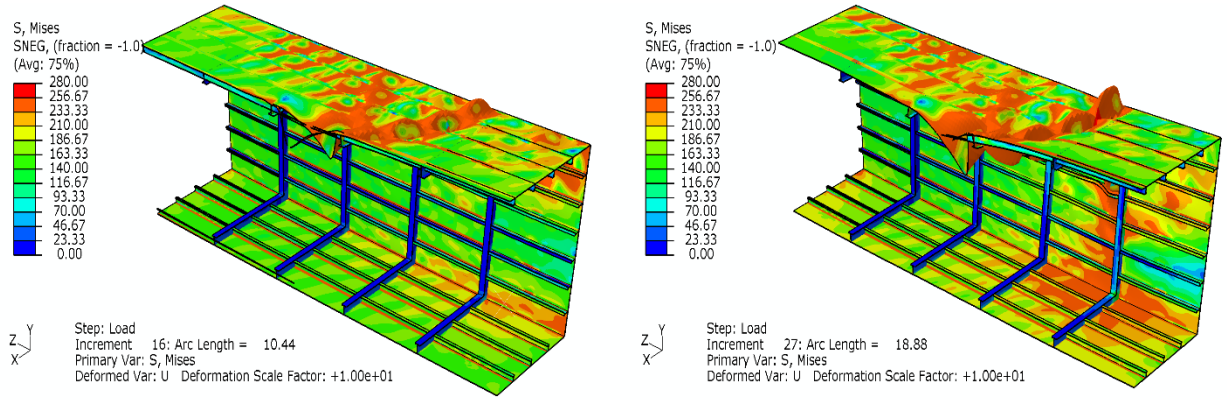

Figure 7.45: Contour plot of equivalent Von-Misses stresses at collapse and post-collapse for Trans. Damage Case I of Box Girder E under 60% of torsional capacity applied and bending (magnify x10)

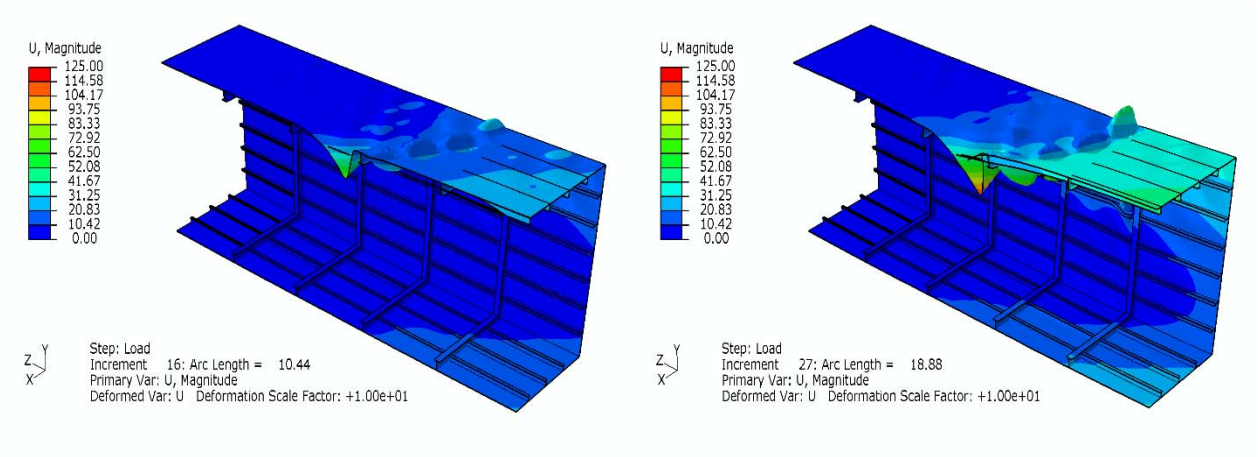

Figure 7.46: Contour plot of the displacement at collapse and post-collapse for Trans. Damage Case I of Box Girder E under 60% of torsional capacity applied and bending (magnify x10)

Similarly, in Trans. Damage Case II of Box Girder E, interframe collapse mode occurs to the structure under any amount of applied torsion and bending, e.g. for 60%Tmax and bending load (Figure 7.47 &Figure 7.48), for 90%Tmax and bending load (Figure 7.49 &Figure 7.50).

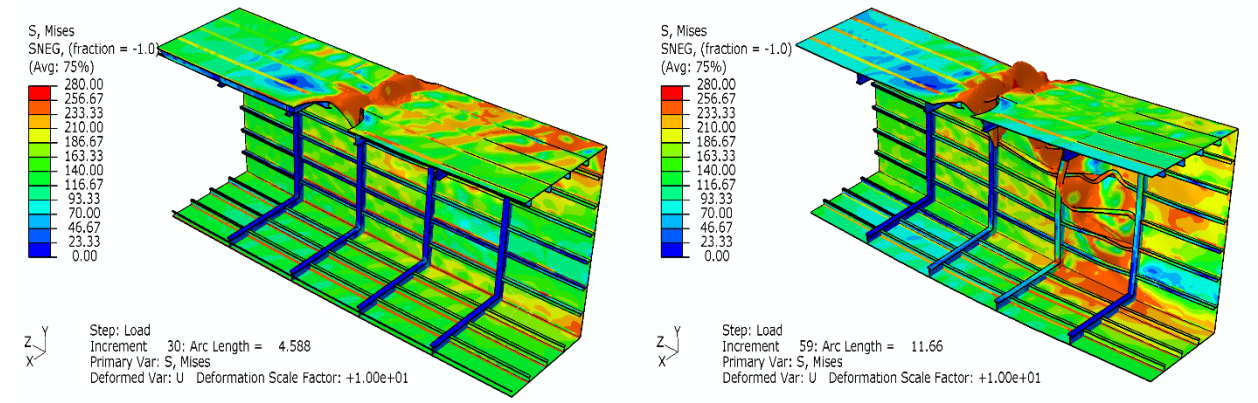

Figure 7.47: Contour plot of equivalent Von-Misses stresses at collapse and post-collapse for Trans. Damage Case II of Box Girder E under 60% of torsional capacity applied and bending (magnify x10)

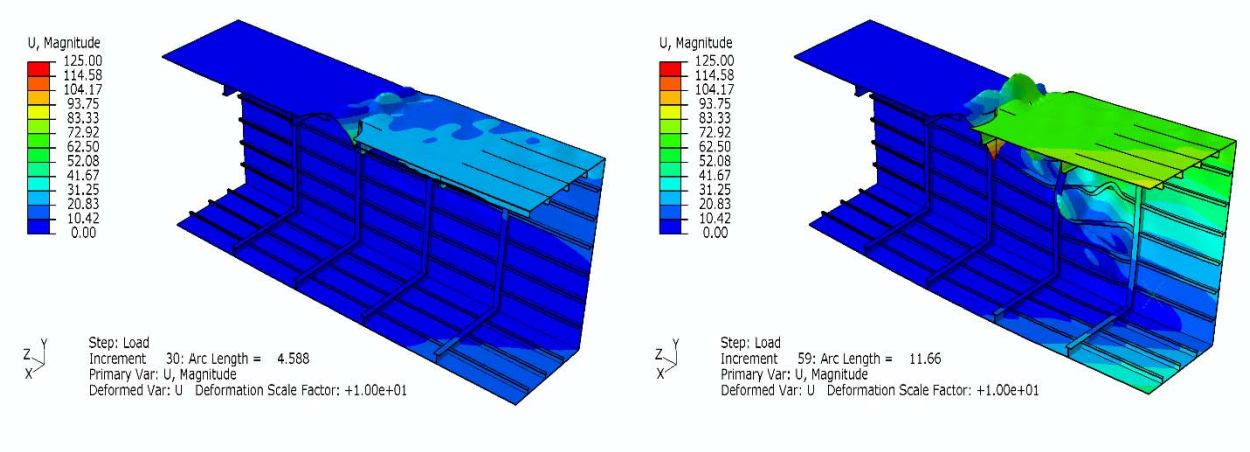

Figure 7.48: Contour plot of the displacement at collapse and post-collapse for Trans. Damage Case II of Box Girder E under 60% of torsional capacity applied and bending (magnify x10)

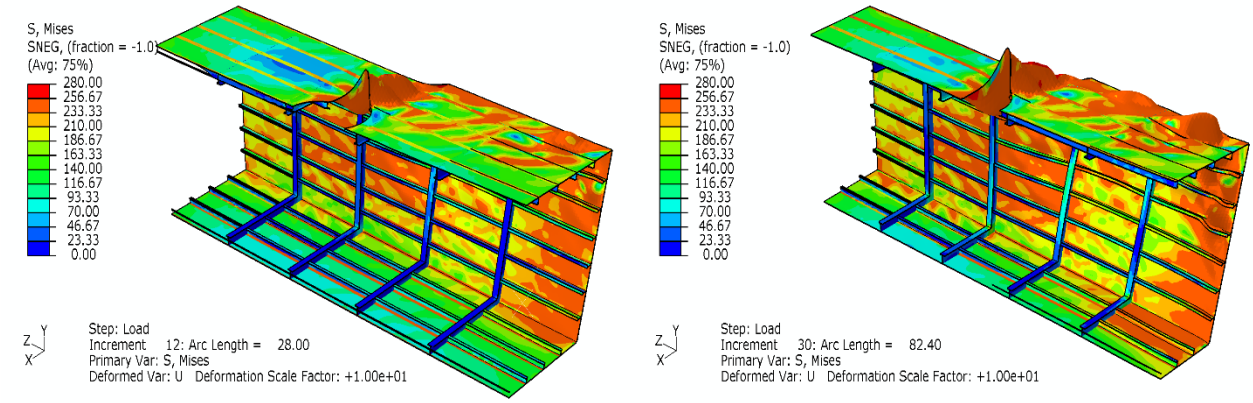

Figure 7.49: Contour plot of equivalent Von-Misses stresses at collapse and post-collapse for Trans. Damage Case II of Box Girder E under 90% of torsional capacity applied and bending (magnify x10)

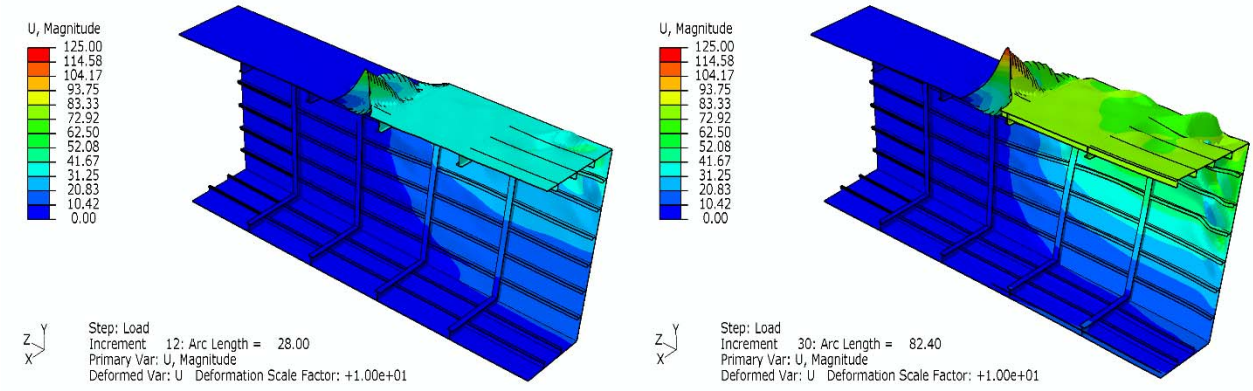

Figure 7.50: Contour plot of the displacement at collapse and post-collapse for Trans. Damage Case II of Box Girder E under 90% of torsional capacity applied and bending (magnify x10)

In Trans. Damage Case III of Box Girder E, interframe collapse mode of failure is shown for the structure under any amount of applied torsion and bending, e.g. for 60% & 90%Tmax and bending (Figure 7.51 - Figure 7.54).

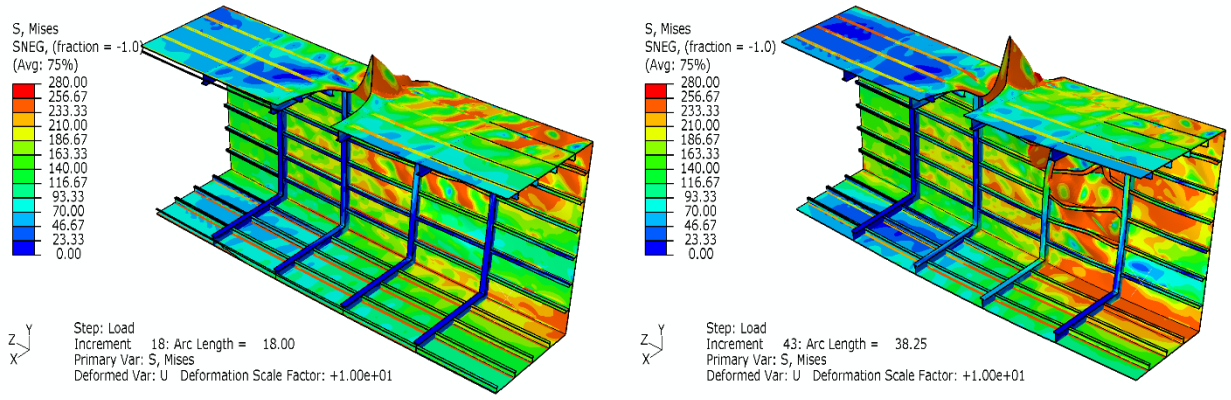

Figure 7.51: Contour plot of equivalent Von-Misses stresses at collapse and post-collapse for Trans. Damage Case III of Box Girder E under 60% of torsional capacity applied and bending (magnify x10)

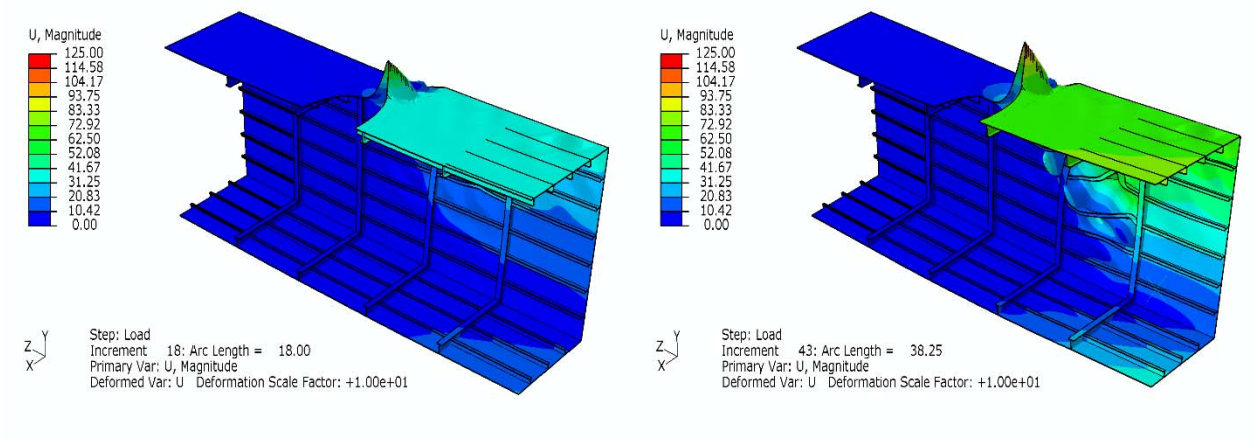

Figure 7.52: Contour plot of the displacement at collapse and post-collapse for Trans. Damage Case III of Box Girder E under 60% of torsional capacity applied and bending (magnify x10)

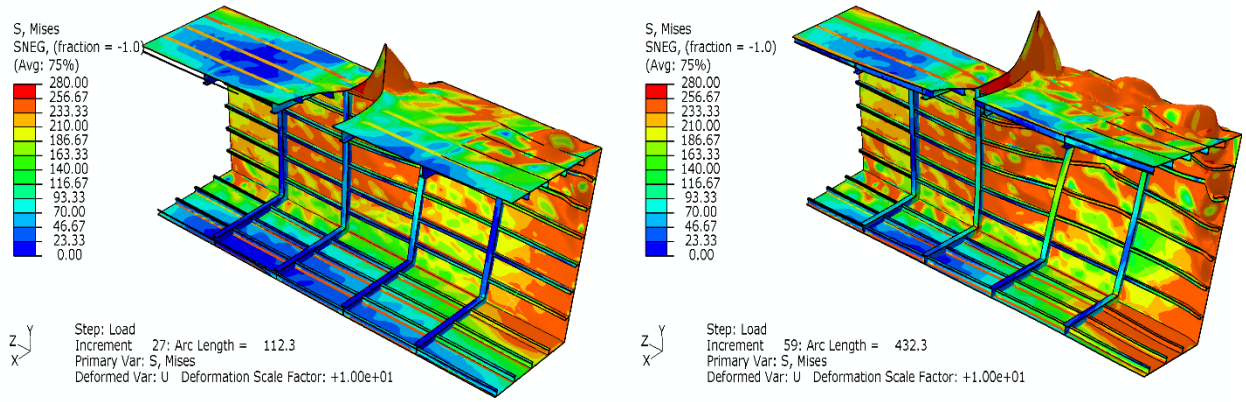

Figure 7.53: Contour plot of equivalent Von-Misses stresses at collapse and post-collapse for Trans. Damage Case III of Box Girder E under 90% of torsional capacity applied and bending (magnify x10)

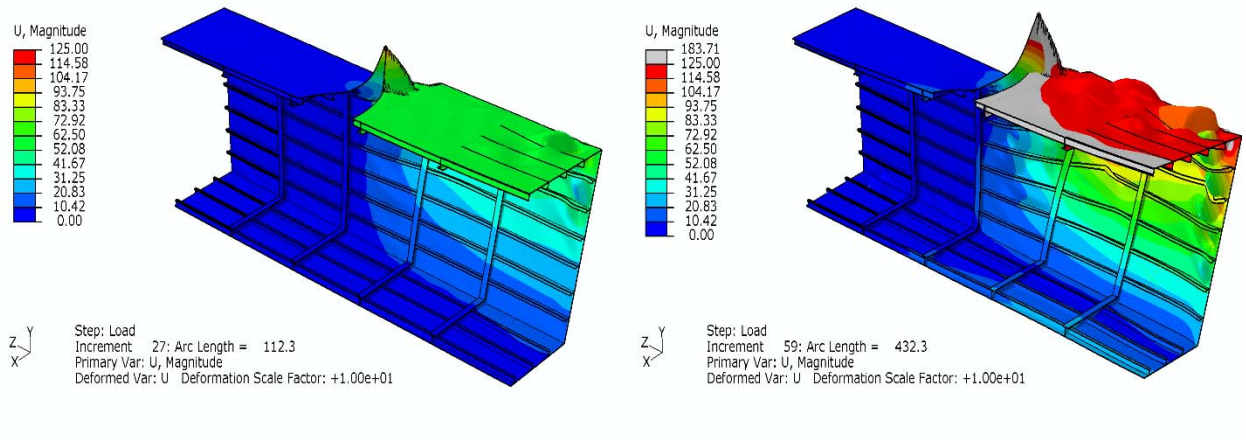

Figure 7.54: Contour plot of the displacement at collapse and post-collapse for Trans. Damage Case III of Box Girder E under 90% of torsional capacity applied and bending (magnify x10)

7.3.4. Damaged box girders with different transverse damage extent (ProColl)

In this section, Trans. Damage Case I, II and III of Box Girder E are examined using the extended simplified progressive collapse method. The initial aim of the current study was to investigate the progressive collapse of these damaged box girders under vertical bending and combined torsion and bending using the proposed methodology. A part of this aim was achieved, i.e. the progressive collapse assessment of the damaged box girders under bending moment.

However, as it has already mentioned the strength assessment of the damaged box girders under combined torsional and bending loads using the proposed methodology cannot be currently achieved. The reason is that the current representation of damage in the methodology, leads to the removal of the damaged area from the model along its whole length.

This representation even though provides valid results when the damaged box girder is subjected to bending loads (see next section), it is not valid under combined loads. A simple explanation is that the torsional rigidity of the same damaged model according to NFEM and the proposed simplified methodology is completely different and this leads eventually to the comparison of two different models, which currently invalidates this approach.

Therefore, the research for the representation of damage in the proposed methodology continues and in this study the progressive collapse of the damaged box girders is examined only under bending.

7.3.4.1. Under pure bending

The progressive collapse of the intact and for Trans. Damage Case I, II and III of Box Girder E subjected only to vertical bending moment is depicted in Figure 7.55. The bending moment-curvature relationships of these damaged box girders have similar pattern with this of the intact Box Girder E. However, the strength of the structure decreases as the transverse damage extent increases.

The ultimate strength according to the simplified extended progressive collapse method is:

- $\mathbf{5.17} \times \mathbf{10^{10}}\boldsymbol{Nmm}$, for intact Box Girder E
- $\mathbf{5.06} \times \mathbf{10^{10}}\boldsymbol{Nmm}$, for Trans. Damage Case I of Box Girder E
- $\mathbf{4.31} \times \mathbf{10^{10}}\boldsymbol{Nmm}$, for Trans. Damage Case II of Box Girder E
- $\mathbf{3.46} \times \mathbf{10^{10}}\boldsymbol{Nmm}$ for Trans. Damage Case III of Box Girder E

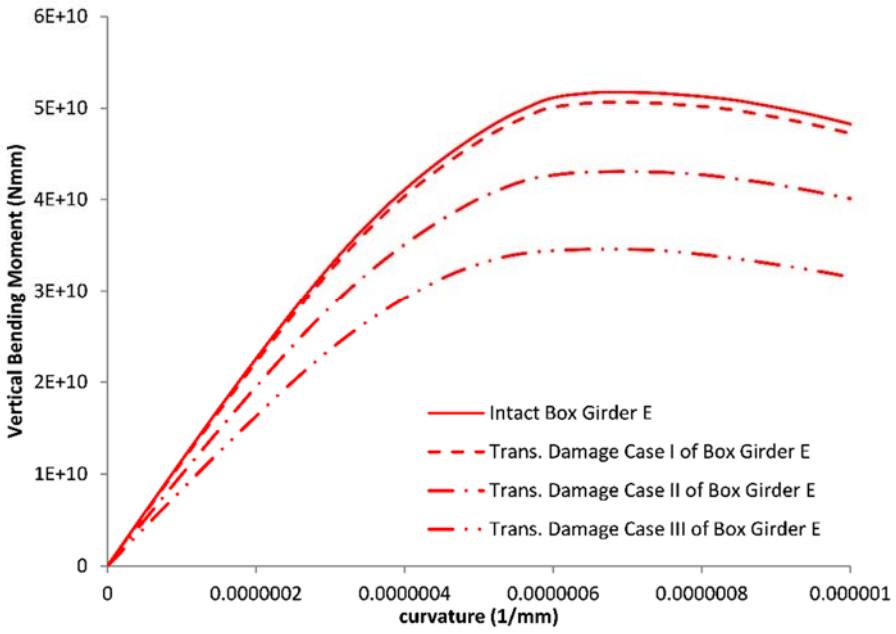

Figure 7.55: Moment-Curvature relationship of the intact and for Trans. Damage Case I, II and III of Box Girder E subjected to vertical bending moment (ProColl)

7.3.5. Comparison of the results for damaged box girders with varying size of transverse damage extent under vertical bending loading

The ultimate strength of the box girders with different size of transverse damage extent subjected only to vertical bending moment (sagging) is presented in Figure 7.56 according to the NLFEM and the extended simplified progressive collapse method. Both graphs are plotted against to the percentage (%) of the size of damage extent to the width of Box Girder E. Both methods show very good correlation in their results and their graphs have the same tendency.

It should be noticed that for very small size of transverse damage extent (Trans. Damage Case I), the drop of the residual strength is not the same in both methods. In this damage case, all the stiffeners in the cross-section are intact and only a part of the central plate is damaged. This kind of damage is predicted differently by ProColl and ABAQUS, probably due to the different representations of the boundary conditions around the hole in ProColl, and further investigation is required for this case.

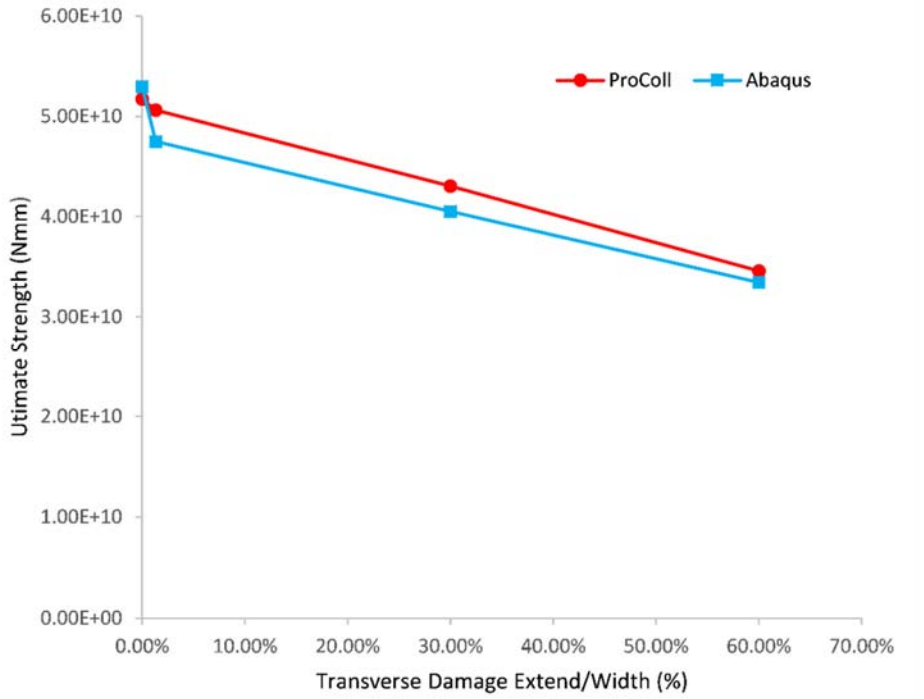

Figure 7.56: Comparison of the ultimate strength according to the NLFEM and the extended progressive collapse method for box girders with varying % of transverse damage extent

7.3.6. Damaged box girders with different longitudinal damage extent (NLFEM)

Almost the same modelling with the intact Box Girder E (section 7.2.3.1) and Trans. Damage Case I, II and III of Box Girder E (section 7.3.3) in the N.L.F.E.M. was followed for Long. Damage Case I and II of Box Girder E. The damage is represented as a cut-out in model's geometry. The sizes of the longitudinal damage extents are varying in each case and they were taken according to Figure 7.24 (see also Appendix C). Detailed description of Long. Damage Case I and II is given in section 7.3.2.1.

All damaged box girders are subjected to vertical bending moment, then to torsional loading in order to estimate their torsional capacity and finally to combined torsional and bending loads.

7.3.6.1. Under vertical bending moment

The contour plots of the equivalent Von-Misses stresses at collapse and post-collapse for Long. Damage Case I and II of Box Girder E under vertical bending moment are shown in Figure 7.27 - Figure 7.28 and Figure 7.57 - Figure 7.58, respectively. The collapse of the damaged structures with varying size of longitudinal damage extent occurs between their transverse frames in all examined cases of this study.

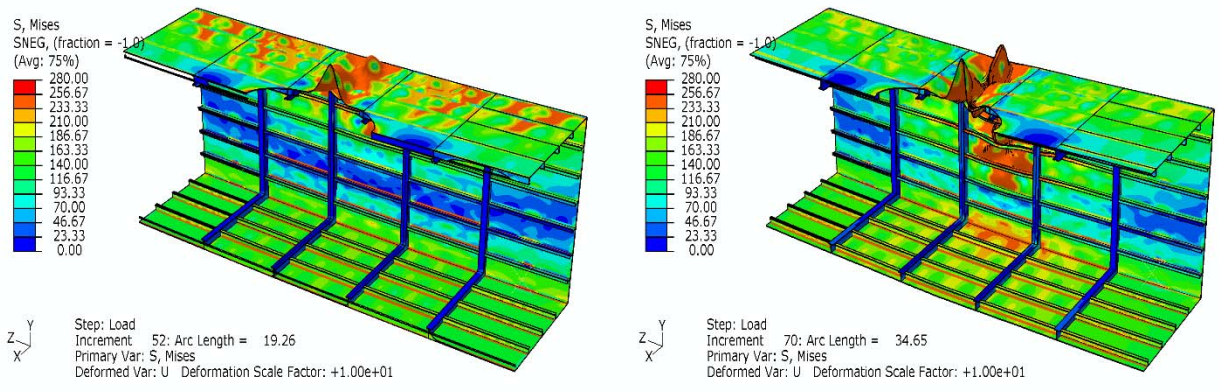

Figure 7.57: Contour plot of equivalent Von-Misses stresses at collapse and post-collapse for Long. Damage Case II of Box Girder E under bending moment (magnify x10)

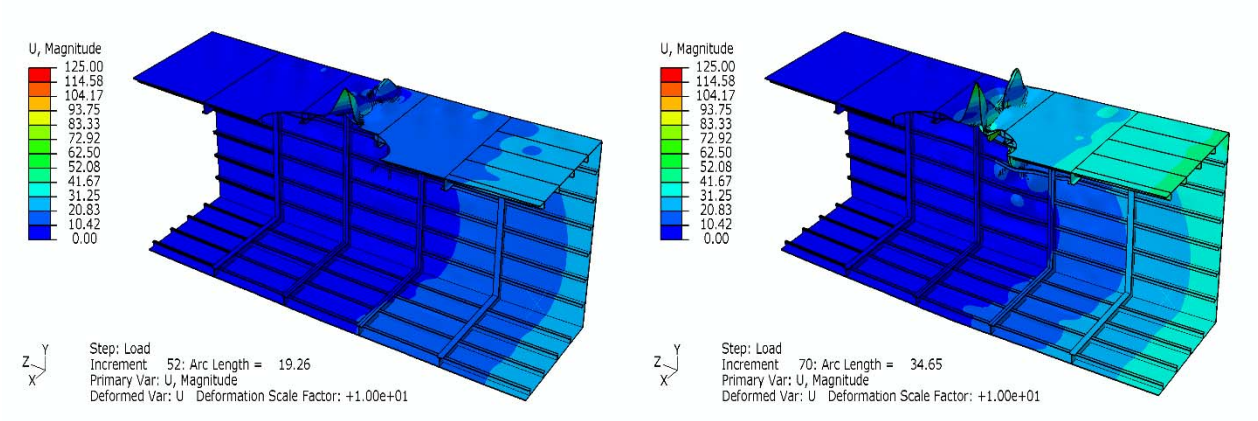

Figure 7.58: Contour plot of the displacement at collapse and post-collapse for Long. Damage Case II of Box Girder E under bending moment (magnify x10)

Figure 7.57 and Figure 7.58 show interframe collapse mode in the middle bay for Long. Damage Case II of Box Girder E subjected only to vertical bending moment.

The bending moment-curvature relationships of the damaged box girders with different longitudinal size of damage extent, subjected to vertical bending moment are presented in Figure 7.59. Their strength is reduced in comparison to the strength of the intact Box Girder E. However, the reduction is approximately the same in both damage cases, Long. Damage Case I and II, independently from the length of the damage extent. Therefore, in the case which interframe collapse occurs, it is probably the size of the transverse damage extent which defines the residual strength of the damaged structure.

The ultimate strength in each case according to the nonlinear finite element method is:

- $\mathbf{5.30} \times \mathbf{10^{10}}\boldsymbol{Nmm}$, for intact Box Girder E
- $\mathbf{4.05} \times \mathbf{10^{10}}\boldsymbol{Nmm}$, for Long. Damage Case I of Box Girder E
- $\mathbf{4.03} \times \mathbf{10^{10}}\boldsymbol{Nmm}$, for Long. Damage Case II of Box Girder E

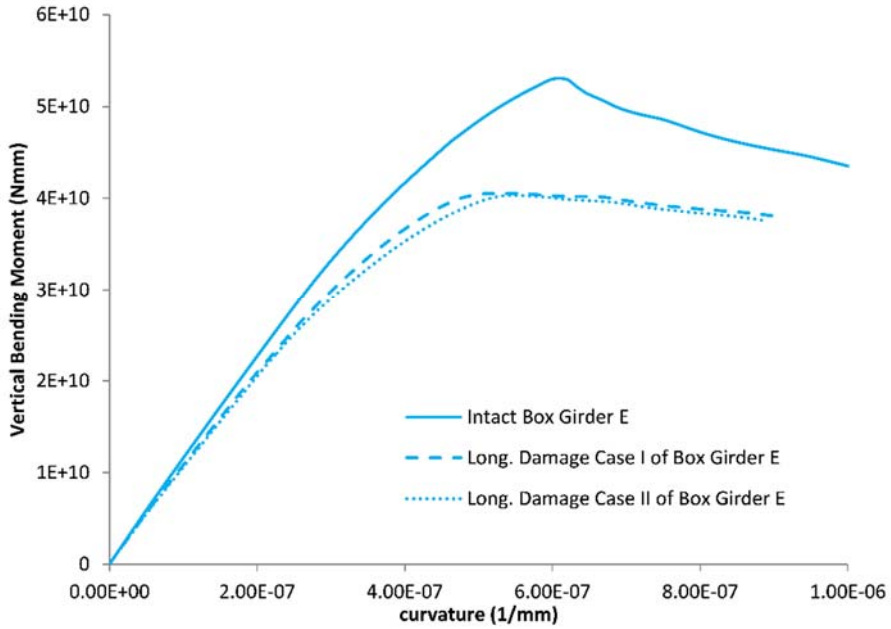

Figure 7.59: Moment-Curvature relationships of the intact and Long. Damage Case I and II of Box Girder E subjected to vertical bending moment (NLFEM)

7.3.6.2. Under pure torsion

The contour plots of the equivalent Von-Misses stresses and the displacement at collapse and post-collapse for Long. Damage Case I and II of Box Girder E under torsional load are shown in Figure 7.34 - Figure 7.35 and Figure 7.60 - Figure 7.61, respectively. Both structures fail between their transverse frames under pure torsion.

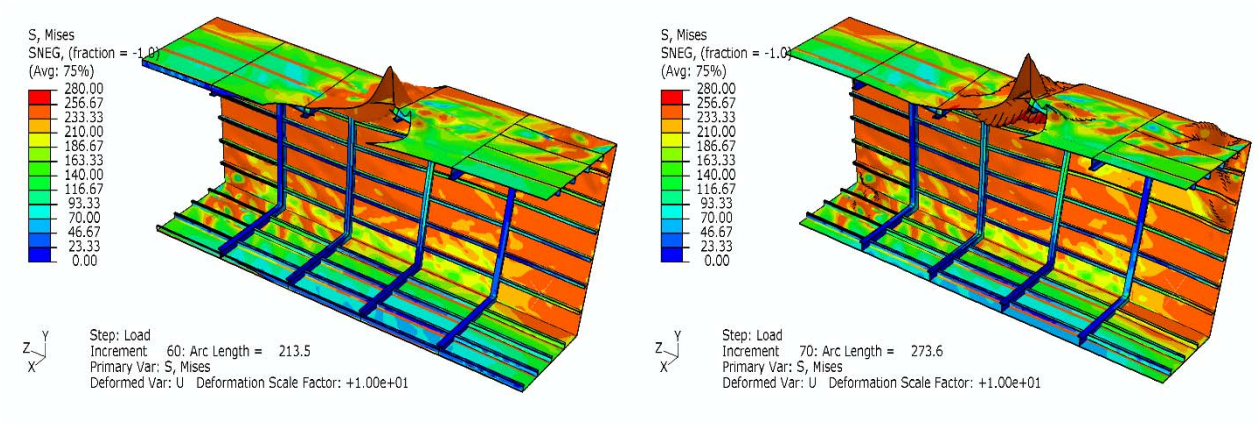

Figure 7.60: Contour plot of equivalent Von-Misses stresses at collapse and post-collapse for Long. Damage Case II of Box Girder E under torsional moment (magnify x10)

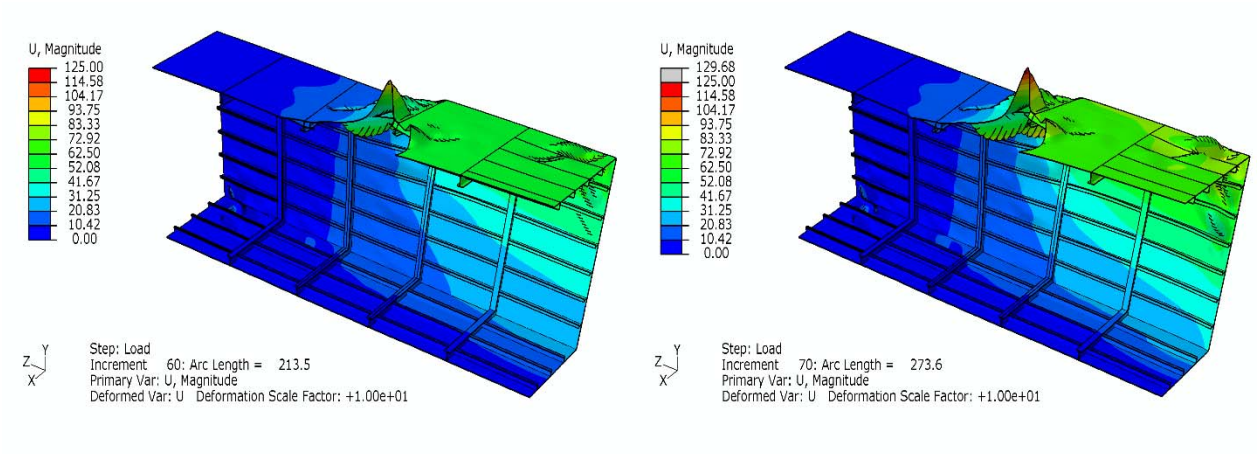

Figure 7.61: Contour plot of the displacement at collapse and post-collapse for Long. Damage Case II of Box Girder Long. E under torsional moment (magnify x10)

The torsional moment-angle relationships of the intact and Long. Damage Case I and II of Box Girder E subjected to torsional load is presented in Figure 7.62. The torsional moment which Box Girder E may sustain, decreases due to damage. However, approximately the same reduction in their torsional capacity is presented in both cases damage cases, Long. Damage Case I and II, independently from the size of the longitudinal damage extent.

The torsional capacity in each case according to the nonlinear finite element method is:

- $\mathbf{4.75 \times 10^{10} Nmm}$, for intact Box Girder E
- $\mathbf{3.68 \times 10^{10} Nmm}$, for Long. Damage Case I of Box Girder E
- $\mathbf{3.54 \times 10^{10} Nmm}$, for Long. Damage Case II of Box Girder E

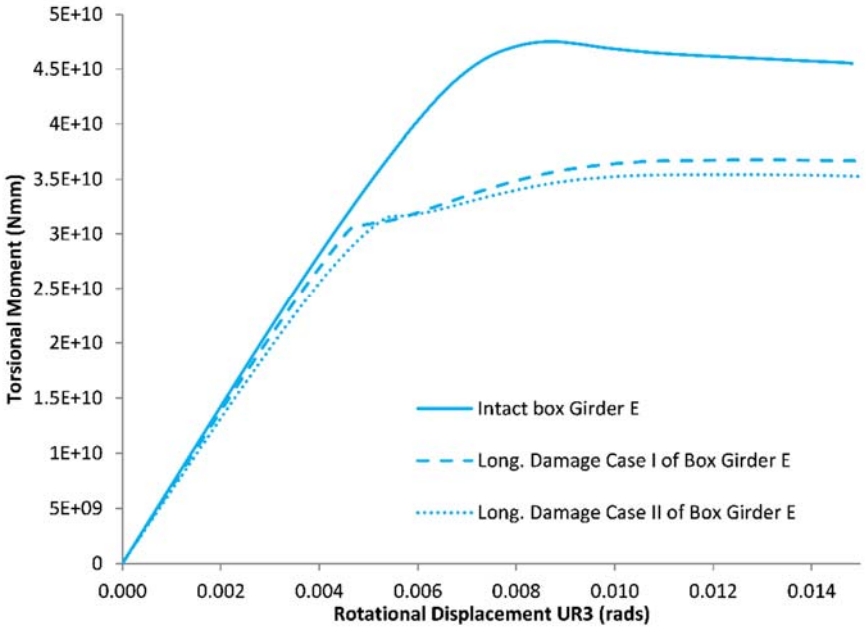

Figure 7.62: Torsional Moment-Angle relationships of the intact and for Long. Damage Case I and II of Box Girders E subjected to torsional load (NLFEM)

7.3.6.3. Under combined torsional loads and bending moment

The results of damaged box girders with different size of longitudinal damage extent under torsional and bending loads are shown in this section.

Figure 7.40 and Figure 7.63 are shown the moment-curvature relationships for Long. Damage Case I and II of Box Girder E under these combined loads, respectively. The strength of both damaged box girders decreases as the applied torsion increases. Their stiffness in the pre-collapse area slowly decreases too, but it is obviously changing for high values of applied torsion (more than 70%Tmax).

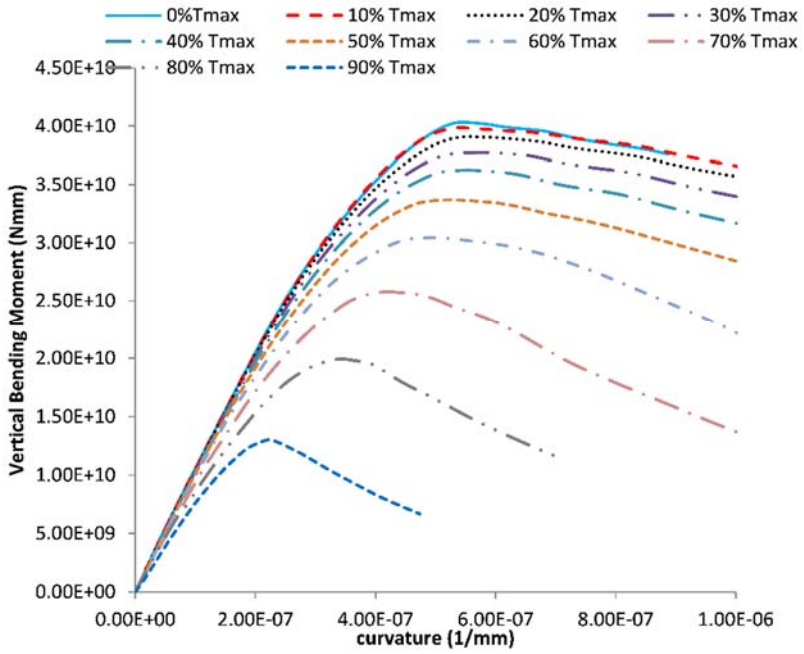

Figure 7.63: Moment-Curvature relationships for Long. Damage Case II of Box Girder E under combined torsional loads and bending (NLFEM)

The interaction diagram of torsional and bending load for these cases is presented in Figure 7.64. The plot shows that these damaged box girders may sustain approximately the same amount of combined torsional and bending loads even though the length of the damaged extent in Long. Damage Case II is twice the length than this in Long. Damage Case I. All graphs present similar pattern.

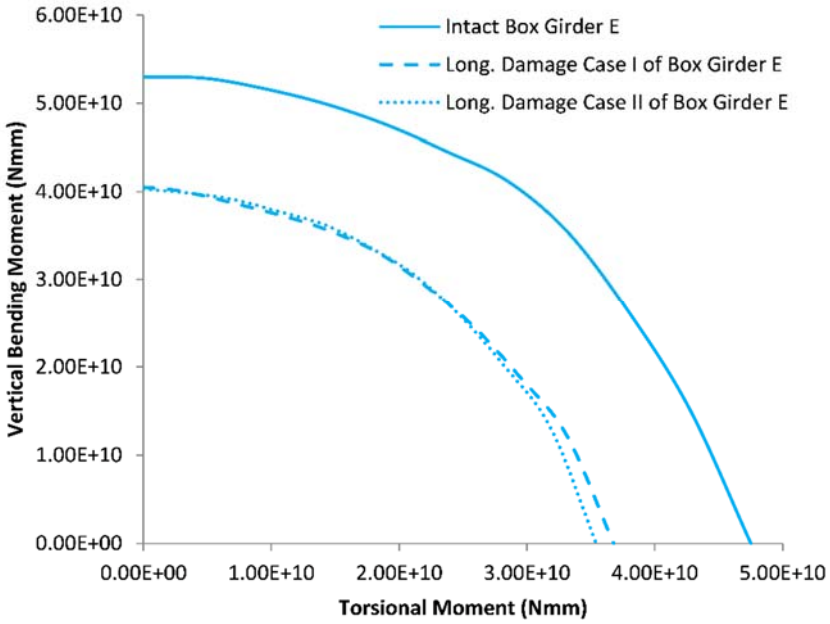

Figure 7.64: Interaction Diagram of torsional and bending loads for the intact Box Girder E and Long. Damage Case I and II of Box Girder E

The contour plots of the equivalent Von-Misses stresses and the displacement at collapse and post collapse for Long. Damage case I of Box Girder E under combined loads are shown in Figure 7.47 - Figure 7.50 (interframe collapse mode) and for Long. Damage case II of Box Girder E under combined loads in Figure 7.65 - Figure 7.68 (interframe collapse mode).

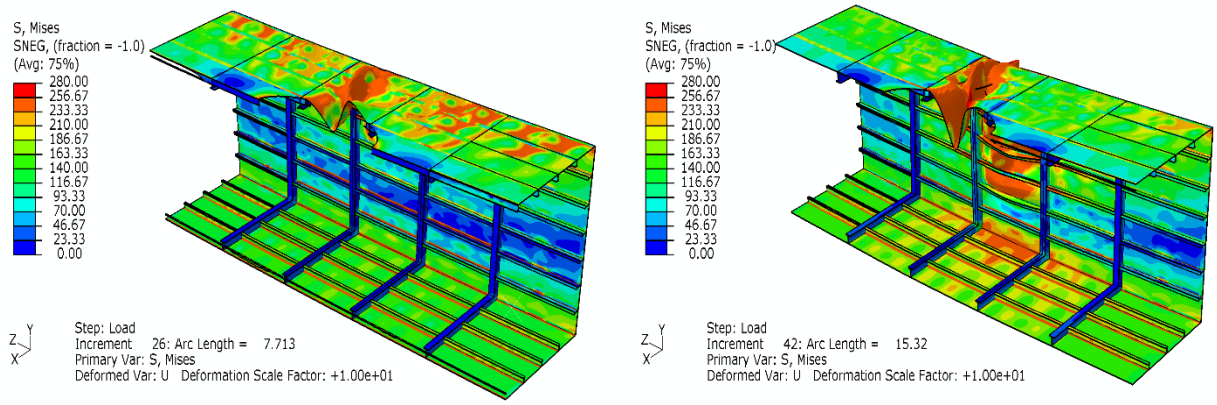

Figure 7.65: Contour plot of equivalent Von-Misses stresses at collapse and post-collapse for Long. Damage Case II of Box Girder E under 10%Tmax and bending (magnify x10)

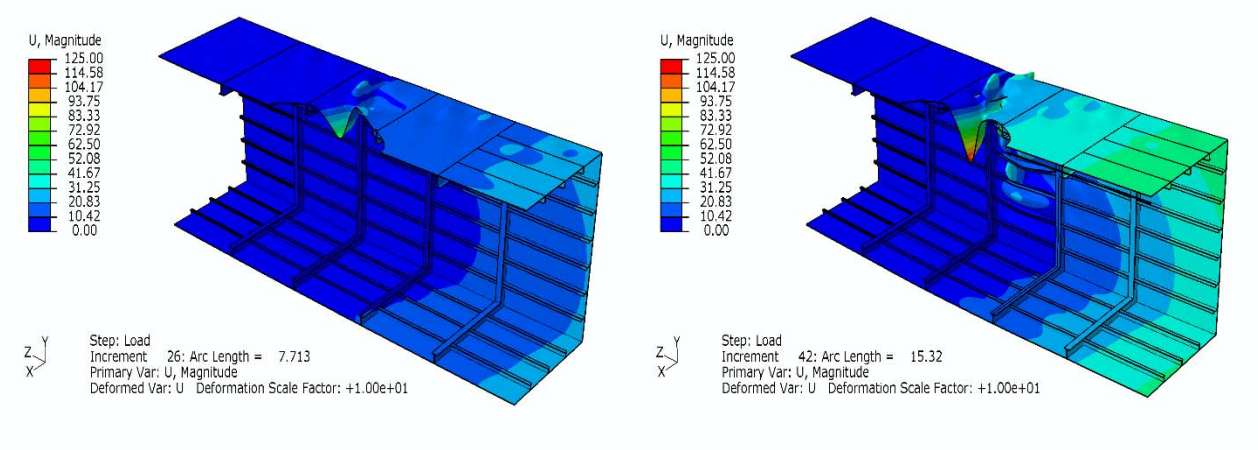

Figure 7.66: Contour plot of the displacement at collapse and post-collapse for Long. Damage Case II of Box Girder E under 10%Tmax and bending (magnify x10)

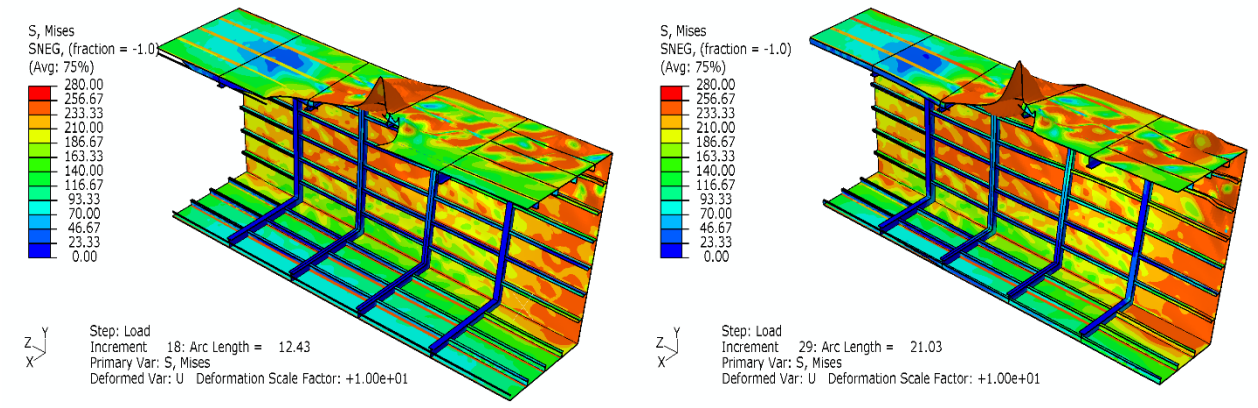

Figure 7.67: Contour plot of equivalent Von-Misses stresses at collapse and post-collapse for Long. Damage Case II of Box Girder E under 90%Tmax and bending (magnify x10)

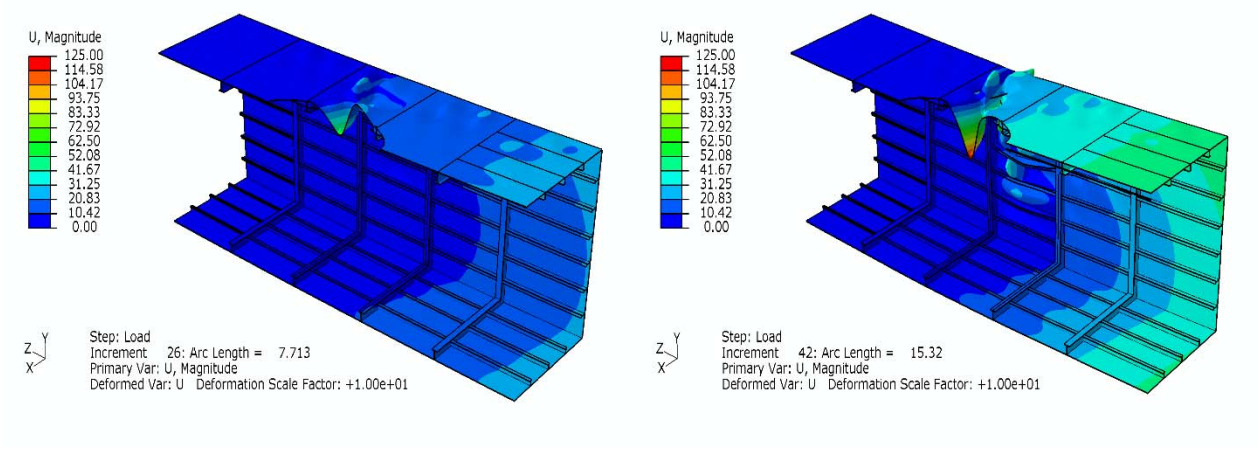

Figure 7.68: Contour plot of the displacement at collapse and post-collapse for Long. Damage Case II of Box Girder E under 90%Tmax and bending (magnify x10)

7.3.7. Damaged box girders with longitudinal damage extent (ProColl)

In this section, the progressive collapse of damaged box girders with different size of longitudinal damage extent using the proposed methodology was investigated only under vertical bending moment for the same reasons which were mentioned and discussed in section 7.3.4.

7.3.7.1. Under vertical bending

The progressive collapse of the damaged structures with varying longitudinal damage extent subjected only to vertical bending moment are depicted in Figure 7.69. The bending moment-curvature relationships of these damaged box girders have similar pattern with the intact Box Girder E and present identical reduced progressive collapse. Their ultimate strength according to the simplified extended progressive collapse method is:

- $\mathbf{5.17} \times \mathbf{10^{10}}\boldsymbol{Nmm}$, for intact Box Girder E
- $\mathbf{4.31} \times \mathbf{10^{10}}\boldsymbol{Nmm}$, for Long. Damage Case I of Box Girder E
- $\mathbf{4.31} \times \mathbf{10^{10}}\boldsymbol{Nmm}$, for Long. Damage Case II of Box Girder E

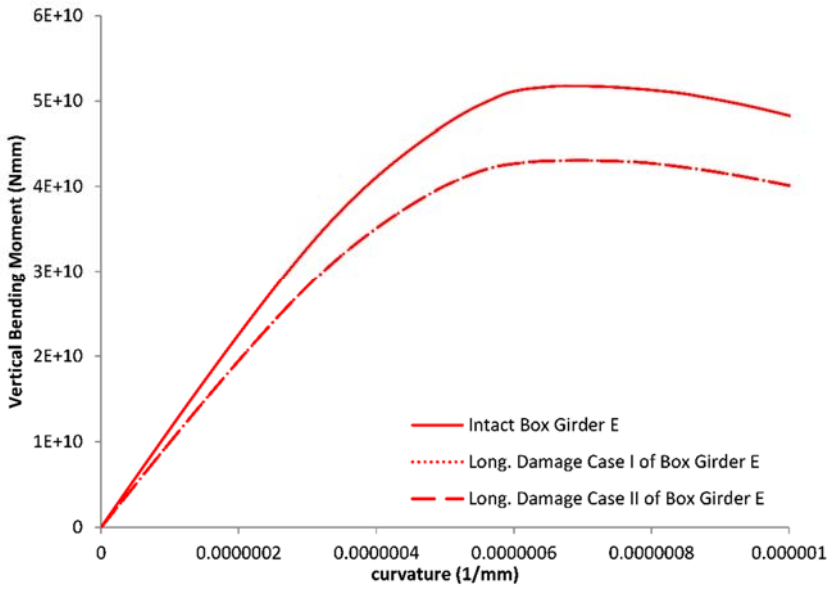

Figure 7.69: Moment-Curvature relationships of the intact and Long. Damage Case I and II of Box Girder E subjected to vertical bending moment (ProColl)

7.3.8. Comparison of the results for damaged box girders with varying size of longitudinal damage extent under vertical bending loading

The ultimate strength of the box girders with different size of longitudinal damage extent subjected only to vertical bending moment (sagging) is presented in Figure 7.70 according to the NLFEM and the extended simplified progressive collapse method. Both graphs are plotted against to the percentage (%) of the size of the damage extent to the length of Box Girder E and their results show very good correlation. Both graphs have the same tendency and predict almost no further reduction in the residual strength of the structure for a size of longitudinal damage extent for more than 16% of structure's length. This is interpreted as the same progressive collapse behaviour of the box girder with and without its main transverse frame but with the same loss of transverse extend, setting the size of the transverse damage extent the dominant factor which affects the residual strength of Box Girder E in case of damage.

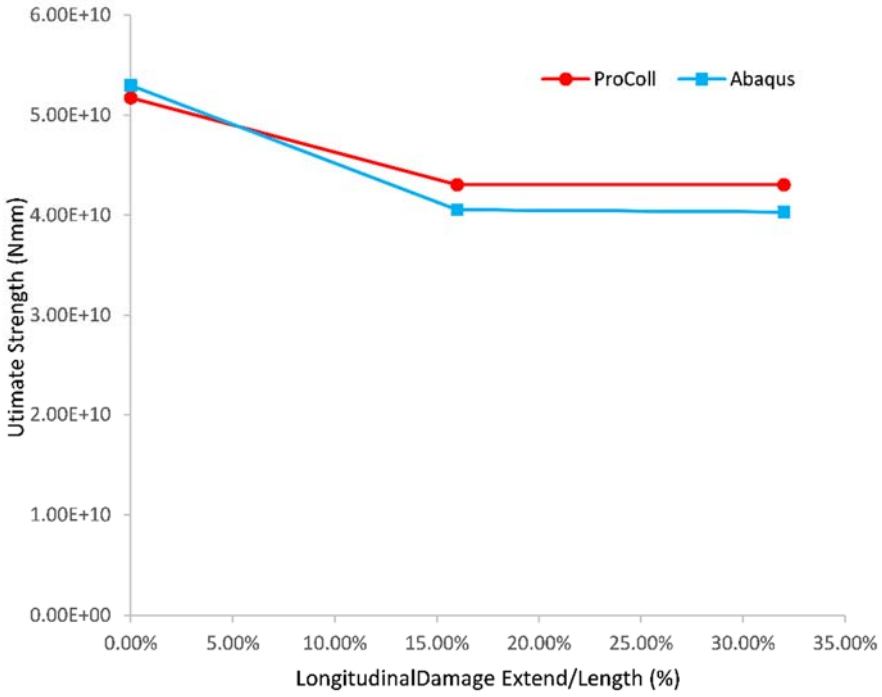

Figure 7.70: Comparison of the ultimate strength according to the NLFEM and the extended progressive collapse method for box girders with varying % of longitudinal damage extent

7.4. Summary

This chapter presents a case study for the effect of damage on the progressive collapse of box girders subjected to combined loading of bending and torsion. Initially, the progressive collapse behaviour of the intact Box Girder E under the aforementioned loads is examined using the nonlinear finite element analysis and the proposed extended simplified progressive collapse method by the author. Both methods show good correlation in their results.

Then, two kind of damage cases are decided for the investigation. In the first, the size of the damage extent varies along the width of the box girder, but its length remains constant in all cases. In the second, the size of the damage extent varies along the length of the structure and its width remain the same. Both sets of damaged cases are applied to Box Girder E as a cut-out of its model.

The damaged box girders are subjected to bending, torsion and combinations of these loads and they are analysed using the nonlinear finite element method. The results of the damaged box girders show continuous decrease of their progressive collapse with the increase of the size of their transverse damage extent. However, in the case which the size of the longitudinal damage increases, the same reduction in the strength of the structure occurs in all cases. This leads to the conclusion, that the residual strength of the damaged box girder is highly depended on the size of its transverse damage extent in case of damage. In addition, all the interactions diagrams of torsion and bending present similar pattern to the interaction diagram of the intact Box Girder E which follows the theoretical interaction of torsion and bending (Equation 5.8).

In parallel, the same damaged box girders are subjected to vertical bending moment and they analysed with the extended simplified progressive collapse method. These results are compared with the nonlinear finite element method's results and present good agreement.

Finally, the proposed methodology by the author is not applied to the damaged box girders under combined loads of torsion and bending due to the need of different representation of the damage in the existing methodology as it was explained and extension of the simplified method is currently under development to cover this combined load case for damaged box girders.

Chapter 8

Conclusions and Recommendations

8.1. Discussion and conclusions

This thesis proposes a methodology for the strength assessment of ship structures under combined torsional and bending loads by incorporating the effect of torsion into the simplified progressive collapse method. The latter methodology is a well-established method for the strength assessment of ship structures under bending and it is simple, quick and reliable. In the literature, there are no other methodologies for the strength assessment of ships which combine all the above characteristics.

Although the longitudinal strength of hull girders is critical for the structure, there are cases in which the torsional rigidity of the structure is low, e.g. containerships and ships with damage, torsional loads may affect the strength of the structure. Therefore, the proposed methodology aims to incorporate the effect of torsional loads into the simplified progressive collapse methodology.

An extensive investigation of the literature provides valuable knowledge of the existing methodologies for the strength assessment of ship structures under bending, studies for the torsional effect on ship structures and the behaviour of steel and aluminium plates under pure shear, pure compression/ tension and combined shear and compressive/tensile loads.

The investigation for the behaviour of steel and aluminium plates under these loads is essential in this study due to their contribution into the simplified methodology and the approach for the incorporation of torsion by the proposed methodology. The proposed methodology applies a knock down factor to the load shortening curves of the plates, due to the effect of torsion which is carried as shear in the plating, reducing their strength characteristics. The shear stresses on the plates come from pure torsional load on the structure (St. Venant's torsional shear stresses); therefore torsion is incorporated into the progressive collapse methodology as a reduction factor on the bending strength. This methodology assumes that the dominant load effect is always the longitudinal bending and the torsional loading is a secondary loading effect.

The investigation of steel and aluminium plates under pure shear provides some very useful outcomes such as the aspect ratio of the plate does not affect the critical shear stress of the plate. Therefore after establishing this conclusion the study can be continued by investigating only square steel and aluminum plates under pure shear, pure compression/tension and combined shear and compression/tension. The boundary conditions to achieve simultaneous shear and compressive/tensile loading are very important. Thus, steel and aluminium plates are subjected to pure shear and to pure compression applying the boundary conditions of the simultaneous combined loading. The results are compared against theoretical formulas and results of other studies and they present good agreement. Then, simultaneous loads of shear and compression/tension are applied to plates with slenderness ratio (β) 1 to 6 and the interaction diagrams of these combined loads are generated for steel plates and aluminium alloys 5083-H116 and 6082-T6 plates. In general, stocky plates demonstrate tendency to fail due primary yielding, where slender plates are more likely to demonstrate a combination of buckling and yielding characteristics.

In order to validate the proposed methodology the progressive collapse of four (4) box girders subjected to combined torsion and bending is investigated using the non-linear finite element method and the proposed methodology. All box girders have the same size but different cross-sections which provide different torsional rigidity to each model. Initially, all box girders are subjected to pure torsion using the nonlinear F.E. analysis. The results show that the torsional capacity of the structure is clearly affected by the torsional rigidity of the structural cross-section. During the study, all boxes are subjected to torsional and vertical sagging bending moment using the nonlinear F.E. method and the proposed methodology for the incorporation of torsion into the extended simplified progressive collapse method. The bending moment-curvature relationships under different amounts of applied torsional load are generated for each structure according to both methodologies. The progressive collapse of all structures in bending reduces as the applied amount of torsion increases. In all cases, torsion does not affect the stiffness of the structure in the pre-collapse area. The contour plots of the displacement and Von-Mises stresses show an overall collapse mode of failure in all the examined cases.

Furthermore, two of these models, Box Girder C and Box Girder D, are subjected to combined torsion and vertical hogging bending moment using both methodologies. These results have similar pattern with these of the corresponding models subjected to torsion and vertical sagging bending moment, but the strength of the structure in the former case (i.e. torsion and hogging) is higher than the strength in the latter (i.e. torsion and sagging). Finally, in this case study, a comparison of all results takes place for each model. In the comparison, the interaction diagrams of torsion and vertical hogging/sagging bending moment according to the nonlinear F.E. method, the proposed methodology and the theoretical interaction of torsion and bending (Equation 5.8) are compared for each model. The results of the F.E. analysis, the simplified method and the interaction equation show good agreement with each other for all models and cases. Finally, the interaction diagrams of torsion and vertical bending moment define an envelope for each structure within its strength is adequate under these combined loads.

A case study of a 10000TEU OL185 container ship is also investigated under combined torsional and vertical bending moment in sagging and hogging condition using the nonlinear F.E. method and the proposed methodology. The F.E. analysis has been carried out by Alfred Mohammed's study (Alfred Mohammed, 2014) and his study provides also data for the extreme wave-induced vertical bending moment and its associated wave-induced torsional moment for the OL185 container ship. Therefore, the proposed methodology is applied to the model of a real structure whose size is much bigger than the examined box girders and also the amount of the maximum wave-induced torsional load of the structure is known. The comparison of the results between the two methodologies show very good correlation with the extended simplified progressive collapse method results which are shown to be more conservative than the nonlinear F.E. method results. In addition, both sets of results show that the structure may sustain the extreme predicted combined loads and that the wave-induced torsional load of the container ship is less than the 10% of its maximum torsional capacity. Finally, it should be commented that the interaction diagram of torsion and bending of the containership significantly alters from the corresponding diagram of the examined box girders. In the case of the containership, the design of the structure is such that the cross-section maintains its bending strength when subjected to large torsional loads. The box girders demonstrate a more gradual elastic-plastic collapse behaviour than the containership, this is

shown by presenting more rounded interaction curves. These curves also demonstrate better agreement with the simplified interaction curve according to Equation 5.8.

The effect of damage in the progressive collapse assessment of box girders under vertical bending moment, torsion and combined torsional and bending load is investigated in chapter 7. Initially, the intact Box Girder E is examined under these loads using the non-linear F.E. method and the proposed methodology. Both methods show good correlation in their results. Then, two kinds of damage cases are used for further investigation. In the first case, the size of the damage extent varies across the width of the box girder, but its length remains constant in all cases. In the second case, the size of the damage extent varies along the length of the structure and its width remain the same. Both sets of damaged cases are applied to Box Girder E by removal of elements of the cross section.

The results of the damaged box girders under pure bending according to both methodologies show continuous decrease of their progressive collapse with the increase of the size of their transverse damage extent. However, in the case that the width of the damage extent remains constant, the increase of the longitudinal damage extent does not significantly alter the progressive collapse response of the damaged structure. This leads to the conclusion, that the residual strength of the damaged box girder is highly depended on the extent of the transverse damage.

The damaged box girders under combined torsion and bending were analysed only with the non-linear F.E. method. The results of the analyses show all the interactions diagrams of torsion and bending to present similar pattern to this of the intact box girder and they follow the theoretical formulation for the interaction of torsion and bending (Equation 5.8).

Finally, the simplified method is not used to analyse the damaged box girders under combined loads of torsion and bending due to the damage element model, which is under development in ProColl, not yet being fully implemented.

8.2. Recommendations

Future work in this area could be performed in the incorporation of combined torsion and horizontal bending moment into the extended simplified progressive collapse methodology. The horizontal bending moment is not critical for the structure but torsional loads are higher in oblique seas. Therefore, further investigation of the progressive collapse of ship structures is needed under combined torsional and horizontal bending loads.

Furthermore, the representation of damage in the extended simplified progressive collapse method should be investigated. At the present time, damage is represented as a cut-out of the structure which is not always efficient in the simplified progressive collapse methodology. If part of the structure is removed from the cross section, the current methodology assumes that it has been removed from the whole length of it which is might not be the case. Therefore, the representation of damage in the structure as a reduction factor of its initial strength may be a more efficient approach. Then, the combination of torsional and bending loads would be feasible for damaged structures according to the proposed methodology in the extended simplified progressive collapse method.

Finally, improvements in the code, ProColl, may occur in order to reduce the amount of the work which the user needs for the set-up of the model. For example, an automatic identification of the loops/cells in the cross-section will reduce time and effort during the set-up of the model in ProColl.

Chapter 9

References

Adrian F. Dier, 1987. Comparisons of Steel and Aluminium Plate Strengths, in: Proceeding of the International Conference on Steel and Aluminium Structures. Cardiff, UK.

Alfred Mohammed, E., 2014. Reliability based methodolody for the assessment of cumulative life-time hydrodynamic loads and structural capacity. Newctle. Univ. PhD Thesis.

Alfred Mohammed, E., Benson, S.D., Hirdaris, S.E., Dow, R.S., 2016. Design safety margin of a 10,000 TEU container ship through ultimate hull girder load combination analysis. Mar. Struct. 46, 78–101. doi:10.1016/j.marstruc.2015.12.003

Alinia, M.M., Habashi, H.R., Khorram, A., 2009. Nonlinearity in the postbuckling behaviour of thin steel shear panels. Thin-Walled Struct. 47, 412–420.

Batdorf, S.B., Stein, M., 1947. Critical Combinations of Shear and Direct Stress for Simply Supported Rectangular Flat Plates (No. 1223). National Advisory Committee For Aeronautics, Washington.

Benson, S., 2011. Progressive Collapse Assessment of Lightweight Ship Structures. Newcastle University.

Benson, S., AbuBakar, A., Dow, R.S., 2013. A comparison of computational methods to predict the progressive collapse behaviour of a damaged box girder. Eng. Struct. 48, 266–280. doi:10.1016/j.engstruct.2012.09.031

Benson, S., Downes, J., Dow, R.S., 2015. Overall buckling of lightweight stiffened panels using an adapted orthotropic plate method. Eng. Struct. 85, 107–117.

Benson, S.D., Syrigou, M.S., Dow, R.S., 2013. Longitudinal strength assessment of damaged box girders. Presented at the International Conference on Collision and Grounding of Ships and Offshore Structures, Trondheim, pp. 305–314.

Bleich, F., 1952. Buckling Strength of Metal Structures. McGraw-Hill, New York.

Bruhn, 1973. Analysis and design of flight vehicle structures.

Caldwell, J.B., 1965. Ultimate longitudinal strength, in: Trans. RINA. pp. 411–430.

Chalmers, D.W., 1993. Design of Ships' Structures. HMSO, London.

Cook, R.D., Malkus, D.S., Plesha, M.E., Witt, R.J., 2002. Concepts and Applications of Finite Element Analysis, 4th ed. Wiley.

Dow, R.S., 2007a. Lecture Notes: Structural Design Principles, Newcastle University.

Dow, R.S., 2007b. Lecture Notes: Advanced Structural Analysis, Newcastle University.

Dow, R.S., 1997. Structural Redundancy and Damage Tolerance in Relation to Ultimate Ship Hull Strength. Adv. Mar. Struct. 3.

Dow, R.S., 1991. Testing and Analysis of a 1/3 Scake Frigate Model, in: Advances in Marine Structures. Elsevier, Dunfermline, Scotland, pp. 749–773.

Dow, R.S., Smith, C.S., 1984. Effects of Localized Imperfections on Compressive Strength of Long Rectangular Plates. J. Constr. Steel Res. 4, 51–76.

Eurocode 3 ENV 1993-1-1, 2005. Design of steel structures, part 1.1 General rules and rules for buildings. British Standard Institution, London.

Eurocode 9 EN 1997-1-1, 2007. Design of Aluminium Structures, part 1.1 General structural rules. British Standard Institution, London.

Faulkner, D., 1975. A review of effective plating for use in the analysis of stiffened plating in bending and compression. J. Ship Res. 19, 1–17.

Frieze, P.A., Dowling, P.J., Hobbs, R.E., 1977. Ultimate Load Behaviour of Plates in Compression, in: Steel Plated Structures. Crosby Lockwood Staples, London, pp. 24–50.

Fujikubo, M., Kaeding, P., Yao, T., 2000. ISUM recatngular plate element with new lateral function. Longitudinal and transverse thrust. J. Soc. Nav. Archit. Jpn. 209–219.

Harding, J.E., Hobbs, R.E., Neal, B.G., 1977. Ultimate Load Behaviour of Plates under Combined Direct and Shear In-plane Loading, in: Steel Plated Structures. Crosby Lockwood Staples, London, pp. 369–404.

Hopperstad, O.S., Langseth, M., Tryland, T., 1999. Ultimate strength of aluminium alloy outstands in compression: experiments and simplified analysis. Thin-Walled Struct. 34, 279–294.

Hu, Y., Chen, B., 2001. Limit State of Torsion of Ship Hulls with Large Hatch Openings. J. Ship Res. 45, 95–102.

Hughes, O.F., Paik, J.K., 2010. Ship structural analysis and design. Society of Naval Architects and Marine Engineers., Jersey City, N.J.

Kim, D.K., Park, D.H., Kim, H.B., Kim, B.J., Seo, J.K., Paik, J.K., 2013. Lateral pressure effects on the progressive hull collapse behaviour of a Suezmax-class tanker under vertical bending moments. Ocean Eng. 63, 112–121. doi:10.1016/j.oceaneng.2012.12.040

Kristensen, O.H.H., 2001. Ultimate Capacity of Aluminium Plates under Multiple Loads, considering HAZ Properties. NTNU, Trondheim.

Little, G.H., 1982. Collapse behaviour of aluminium plates. Int. J. Mech. Sci. 24, 37–45.

Little, G.H., 1973. Plate failure in stiffened steel compression panels. CUED, Cambridge.

Mazzolani, F.M., 1995. Aluminium alloy structures, 2nd ed. London ; New York : E & FN Spon.

Mofflin, D.S., Dwight, J.B., 1984. BUCKLING OF ALUMINIUM PLATES IN COMPRESSION. pp. 397–427.

Moxham, K.E., 1970. Compression in welded web plates. Cambridge University.

Ostapenko, A., 1981. Effect of torsion on strength of ship hulls. SNAME.

Ostapenko, A., Chen, Y., 1982. Effect of torsion on strength of ship hulls (No. 468.11). Lehigh University.

Ostapenko, A., Moore, T.., 1982. Maximum strength of ship hulls subjected to moment and shear (No. 497.5). Lehigh University.

Ostapenko, A., Vaucher, A., 1980. Ultimate strength of ship hulls girders under moment, torque and shear (No. 453.6). Lehigh University.

Paik, J., Duran, A., 2004. Ultimate Strength of Aluminium Plates and Stiffened Panels for Marine Applications. Mar. Technol. Vol.41, 108–121.

Paik, J., Thayamballi, A., 2003. Ultimate limit state design of steel-plated structures. John Wiley & Sons Ltd, Chichester, UK.

Paik, J.K., 2010. Ultimate Strength of Ship Hulls, in: Ship Structural Analysis and Design. SNAME, Jersey City, p. 16.1-16.21.

Paik, J.K., 2007. Ultimate limit state performance of oil tanker structures designed by IACS common structural rules. Thin-Walled Struct. 45, 1022–1034.

Paik, J.K., 1995. Advanced idealized structural unit considering excessive tension-deformation effects. J. Hydrosp. Technol. 1, 125–145.

Paik, J.K., Thayamballi, A.K., Che, J.S., 1996. Ultimate strength of ship hulls under combined vertical bending, horizontal bending and shearing forces. SNAME 104, 31–59.

Paik, J.K., Thayamballi, A.K., Kim, B.J., 2001a. Advanced ultimate strength formulations for ship plating under combined biaxial compression/tension, edge shear, and lateral pressure loads. Mar. Technol. 38, 9–25.

Paik, J.K., Thayamballi, A.K., Pedersen, P.T., Park, Y.I., 2001b. Ultimate strength of ship hulls under torsion. Ocean Eng. 28, 1097–1133.

Paik, J.K., Wang, G., Kim, B.J., Thayamballi, A.K., 2002. Ultimate Limit State Design of Ship Hulls (ABS Technical Papers). ABS.

Pedersen, P.T., 1991. Beam Theories for torsional-bending response of ship hulls. J. Ship Res. 35, 254–265.

Pedersen, P.T., 1985. Torsional Response of container ships. J. Ship Res. 29, 194–205.

Pedersen, P.T., 1983. A beam model for the torsional bending response of ship hulls. Trans RINA 125, 171–182.

Pei, Z., Iijima, K., Fujikubo, M., Tanaka, S., Okazawa, S., Yao, T., 2015. Simulation on progressive collapse behaviour of whole ship model under extreme waves using idealized structural unit method. Mar. Struct. 40, 104–133. doi:10.1016/j.marstruc.2014.11.002

Ractliffe, A.T., 1966. The strength of plates in compression. Cambridge University.

Rizzo, N.A. dos S., Amante, D. do A., Estefen, S., 2014. Ultimate shear strength of stiffened panels for offshore structures, in: ASME 2014 33rd International Conference on Ocean, Offshore and Arctic Engineering. Presented at the OMAE 2014, San Francisco, California, USA.

Rutherford, S.E., 1983. Hull strength under bending and shear (Hull Structures Report No. No. 83/19). Lloyd's Register, London.

Smith, C.S., 1977. Influence of local compressive failure on ultimate longitudinal strength of a ship's hull, in: Practical Design of Ships and Other Floating Structures. Presented at the Internatinal Symposium on Practical Design of Ships and Other Floating Structures., Tokyo, Japan.

Smith, C.S., Davidson, P.C., Chapman, J.C., Dowling, P.J., 1987. Strength and stiffness of ships plating under in-plane compression and tension. R. Inst. Nav. Archit.

Sun, H.-H., Soares, C.G., 2003. An experimental study of ultimate torsional strength of a ship-type hull girder with a large deck opening. Mar. Struct. 16, 51–67.

Syrigou, M.S., 2012. The Residual Ultimate Strength of Damaged Ships. Newcastle University, U.K.

Tanaka, Y., Hashizume, Y., Ogawa, H., Tatsumi, A., Fujikubo, M., 2016. Analysis method of ultimate strength of ship hull girder under combined loads - Application to an existing container ship. Presented at the Proceedings of the International Conference on Offshore Mechanics and Arctic Engineering - OMAE.

Tanaka, Y., Ogawa, H., Tatsumi, A., Fujikubo, M., 2015. Analysis method of ultimate hull girder strength under combined loads. Ships Offshore Struct. 10, 587–598.

Timoshenko, S.P., Gere, J.M., 1982. Theory of elastic stability. McGraw-Hill, New York.

Ueda, Y., Masaoka, K., 1995. Ultimate strength analysis of thin plated structures using Eigen-function. Rectangular plate element with initial imperfection. J. Soc. Nav. Archit. Jpn. 463–471.

Ueda, Y., Rashed, S.M.H., 1974. An ultimate transverse strength analysis of ship structure. J. Soc. Nav. Archit. Jpn. 309–324.

Ueda, Y., Rashed, S.M.H., Paik, J.K., 1985. NEW INTERACTION EQUATION FOR PLATE BUCKLING. Trans. JWRI Jpn. Weld. Res. Inst. 14, 159–173.

Ueda, Y., Rashed, S.M.H., Paik, J.K., 1984. Plate and stiffened plate units of the idealized structural unit method under in-plane loading. J. Soc. Nav. Archit. Jpn. 366–376.

Yao, T., 2000. Ultimate hull girder strength. Proc. 14th Int. Ship Offshore Struct. Congr. 2, 321–391.

Zhang, S., Kumar, P., Rutherford, S.E., 2008a. Ultimate shear strength of plates and stiffened panels. Ships Offshore Struct. 3, 105–112.

Zhang, S., Kumar, P., Rutherford, S.E., 2008b. Ultimate shear strength of plates and stiffened panels. Ships Offshore Struct. 3, 105–112.

Appendix A

Calculation of torsional constant (k) according to Lloyd's Register program

The calculations of torsional constant (k) according to Lloyd's program for:

a. Box Girder A;

```
1

     C O N T R O L   D A T A


          NUMBER OF NODAL POINT ...........    4

          NUMBER OF ELEMENT ...............    3

          NUMBER OF MATERIAL ..............    1

          SYMETRY CONDITION ( NSYM ) ......    1

               IF NSYM.EQ.0 NOT SYMETRIC
               IF NSYM.EQ.1 SYMMETRIC ABOUT Y AXIS
               IF NSYM.EQ.2 SYMMETRIC ABOUT X AXIS
               IF NSYM.EQ.4 SYMMETRIC ABOUT X AND Y AXIS

          SECTION TYPE ....................    0

               IF NSEC.EQ.0 CLOSED SECTION
               IF NESC.NE.0 OPEN   SECTION


1

     N O D A L   P O I N T   D A T A


      NODE    BOUNDARY COND.              COORDINATE
    NUMBER      Y-SYM    X-SYM           -X             -Y
         1          1        0         0.000          0.000
         2          0        0      6300.000          0.000
         3          0        0      6300.000       8400.000
         4          1        0         0.000       8400.000
1

     M A T E R I A L   D A T A


          MATERIAL NO.  1     SHEAR MODULUS =    0.100E+01


     E L E M E N T   D A T A


  ELEM. NO.   NODE-I    NODE-J   MAT. NO.     THICKNESS
         1         1         2         1         8.000
         2         2         3         1        10.000
         3         3         4         1         8.000
1
```

```
 WARPING FN  OR SECTORIAL COOR (CENTROID)

 NODE        WARPING FN    NODE        WARPING FN    NODE        WARPING
FN
    1     0.00000E+00        2     8.05304E+06        3    -8.05304E+06
    4     0.00000E+00


 WARPING FN OR SECTORIAL COOR (SHEAR CENTER)

 NODE        WARPING FN    NODE        WARPING FN    NODE        WARPING
FN
    1     0.00000E+00        2     8.05304E+06        3    -8.05304E+06
    4     0.00000E+00


 SHEAR STRESS DUE TO PURE TORSION

 ELEM           TAU-S    ELEM           TAU-S    ELEM           TAU-S
    1     0.54783E+04        2     0.43826E+04        3     0.54783E+04


 SHEAR STRESS BY S.FORCE

 ELEM          TAU(Y-DIR SF)  SFLOW(Y-SF)  TAU(X-DIR SF)  SFLOW(X-SF)
    1            -0.2911E-05   -0.2329E-04    0.4960E-05    0.3968E-04
    2            -0.5952E-05   -0.5952E-04    0.0000E+00    0.0000E+00
    3            -0.2911E-05   -0.2329E-04   -0.4960E-05   -0.3968E-04


 SHEAR STRESS BY S.FORCE (Unit Force * UNIT**3)

 ELEM          TAU(Y-DIR SF)  SFLOW(Y-SF)  TAU(X-DIR SF)  SFLOW(X-SF)
    1            -0.2911E-05   -0.1058E+09    0.4960E-05    0.3704E+09
    2            -0.5952E-05   -0.2705E+09    0.0000E+00    0.0000E+00
    3            -0.2911E-05   -0.1058E+09   -0.4960E-05   -0.3704E+09

 SHEAR STRESS BY S.FORCE (Unit Force / UNIT**2)

 ELEM          TAU(Y-DIR SF)  SFLOW(Y-SF)  TAU(X-DIR SF)  SFLOW(X-SF)
    1            -0.2911E-05   -0.2911E-05    0.4960E-05    0.4960E-05
    2            -0.5952E-05   -0.5952E-05    0.0000E+00    0.0000E+00
    3            -0.2911E-05   -0.2911E-05   -0.4960E-05   -0.4960E-05
1

 Box Girder A

     P R O P E R T I E S   O F   B E A M   S E C T I O N
```

```
       COORDINATE OF CENTROID (      0.000,   4200.000 )
   COORDINATE OF SHEAR CENTER (      0.000,   4200.000 )

                SECTIONAL AREA   =  0.3696000E+06
 MOMENT OF INERTIA( ABOUT Y-AXIS )=  0.9335088E+13
 MOMENT OF INERTIA( ABOUT X-AXIS )=  0.4544064E+13

WARPING CONSTANT (SHEAR CENTER) =  0.7989706E+19
WARPING CONSTANT   ( CENTROID ) =  0.7989706E+19
                           IWX =  0.0000000E+00
                           IWY =  0.0000000E+00
           TORTIONAL CONSTANT =  0.9277106E+13

 SHEAR COEFF. OF CROSS SECTION
                 KX( IN X-DIR ) =  0.5454545E+00
                 KY( IN Y-DIR ) =  0.3531552E+00
            WARPING TORSION KZ  =  0.6823457E-01
```

b. Box Girder B;

```
1

     C O N T R O L   D A T A


          NUMBER OF NODAL POINT ...........    8

          NUMBER OF ELEMENT ...............    8

          NUMBER OF MATERIAL ..............    1

          SYMETRY CONDITION ( NSYM ) ......    1

               IF NSYM.EQ.0 NOT SYMETRIC
               IF NSYM.EQ.1 SYMMETRIC ABOUT Y AXIS
               IF NSYM.EQ.2 SYMMETRIC ABOUT X AXIS
               IF NSYM.EQ.4 SYMMETRIC ABOUT X AND Y AXIS

          SECTION TYPE ....................    0

               IF NSEC.EQ.0 CLOSED SECTION
               IF NESC.NE.0 OPEN   SECTION


1

     N O D A L   P O I N T   D A T A


      NODE    BOUNDARY COND.               COORDINATE
    NUMBER      Y-SYM    X-SYM            -X             -Y
         1          1        0         0.000          0.000
         2          0        0      3300.000          0.000
         3          0        0      6300.000          0.000
         4          0        0      6300.000       1800.000
         5          0        0      3300.000       1800.000
         6          0        0      6300.000       8400.000
         7          1        0         0.000       1800.000
         8          1        0         0.000       8400.000
1

     M A T E R I A L   D A T A

          MATERIAL NO.  1     SHEAR MODULUS =    0.100E+01

     E L E M E N T   D A T A


  ELEM. NO.   NODE-I    NODE-J   MAT. NO.     THICKNESS
         1         1         2         1          8.000
         2         2         3         1          8.000
         3         3         4         1         10.000
         4         4         5         1         10.000
         5         5         7         1         10.000
         6         2         5         1          8.000
```

```
         7         4         6         1         10.000
         8         6         8         1          8.000
1
```

WARPING FN OR SECTORIAL COOR (CENTROID)

NODE	WARPING FN	NODE	WARPING FN	NODE	WARPING FN
1	0.00000E+00	2	3.84663E+06	3	5.40655E+06
4	-2.28062E+05	5	-9.31163E+05	6	-8.50357E+06
7	0.00000E+00	8	0.00000E+00		

WARPING FN OR SECTORIAL COOR (SHEAR CENTER)

NODE	WARPING FN	NODE	WARPING FN	NODE	WARPING FN
1	0.00000E+00	2	4.90255E+06	3	7.42240E+06
4	1.78779E+06	5	1.24759E+05	6	-6.48772E+06
7	0.00000E+00	8	0.00000E+00		

SHEAR STRESS DUE TO PURE TORSION

ELEM	TAU-S	ELEM	TAU-S	ELEM	TAU-S
1	0.46077E+04	2	0.39621E+04	3	0.31697E+04
4	-0.18765E+04	5	-0.13599E+04	6	0.64567E+03
7	0.50461E+04	8	0.63077E+04		

SHEAR STRESS BY S.FORCE

ELEM	TAU(Y-DIR SF)	SFLOW(Y-SF)	TAU(X-DIR SF)	SFLOW(X-SF)
1	-0.1074E-05	-0.8589E-05	0.3466E-05	0.2773E-04
2	-0.2113E-05	-0.1691E-04	0.2190E-05	0.1752E-04
3	-0.2955E-05	-0.2955E-04	0.6892E-06	0.6892E-05
4	0.2990E-05	0.2990E-04	-0.2530E-05	-0.2530E-04
5	0.5122E-06	0.5122E-05	-0.3533E-05	-0.3533E-04
6	-0.1494E-05	-0.1195E-04	0.1226E-06	0.9805E-06
7	-0.6444E-05	-0.6444E-04	0.1785E-06	0.1785E-05
8	-0.2952E-05	-0.2362E-04	-0.3243E-05	-0.2594E-04

SHEAR STRESS BY S.FORCE (Unit Force * UNIT**3)

ELEM	TAU(Y-DIR SF)	SFLOW(Y-SF)	TAU(X-DIR SF)	SFLOW(X-SF)
1	-0.1074E-05	-0.4544E+08	0.3466E-05	0.3138E+09
2	-0.2113E-05	-0.8943E+08	0.2190E-05	0.1983E+09
3	-0.2955E-05	-0.1563E+09	0.6892E-06	0.7798E+08
4	0.2990E-05	0.1582E+09	-0.2530E-05	-0.2863E+09
5	0.5122E-06	0.2709E+08	-0.3533E-05	-0.3998E+09
6	-0.1494E-05	-0.6321E+08	0.1226E-06	0.1109E+08
7	-0.6444E-05	-0.3409E+09	0.1785E-06	0.2020E+08
8	-0.2952E-05	-0.1249E+09	-0.3243E-05	-0.2935E+09

SHEAR STRESS BY S.FORCE (Unit Force / UNIT**2)

ELEM	TAU(Y-DIR SF)	SFLOW(Y-SF)	TAU(X-DIR SF)	SFLOW(X-SF)
1	-0.1074E-05	-0.1074E-05	0.3466E-05	0.3466E-05
2	-0.2113E-05	-0.2113E-05	0.2190E-05	0.2190E-05
3	-0.2955E-05	-0.2955E-05	0.6892E-06	0.6892E-06
4	0.2990E-05	0.2990E-05	-0.2530E-05	-0.2530E-05
5	0.5122E-06	0.5122E-06	-0.3533E-05	-0.3533E-05
6	-0.1494E-05	-0.1494E-05	0.1226E-06	0.1226E-06
7	-0.6444E-05	-0.6444E-05	0.1785E-06	0.1785E-06
8	-0.2952E-05	-0.2952E-05	-0.3243E-05	-0.3243E-05

1

Box Girder B

P R O P E R T I E S O F B E A M S E C T I O N

COORDINATE OF CENTROID (0.000, 3442.105)

COORDINATE OF SHEAR CENTER (0.000, 3122.129)

SECTIONAL AREA = 0.5244000E+06

MOMENT OF INERTIA(ABOUT Y-AXIS)= 0.1131570E+14

MOMENT OF INERTIA(ABOUT X-AXIS)= 0.5290014E+13

WARPING CONSTANT (SHEAR CENTER) = 0.6332272E+19

WARPING CONSTANT (CENTROID) = 0.7490828E+19

IWX = -0.3620755E+16

IWY = 0.0000000E+00

TORTIONAL CONSTANT = 0.9953219E+13

SHEAR COEFF. OF CROSS SECTION

KX(IN X-DIR) = 0.6045724E+00

KY(IN Y-DIR) = 0.2519949E+00

WARPING TORSION KZ = 0.4278060E-01

c. Box Girder C;

```
1

     C O N T R O L   D A T A


          NUMBER OF NODAL POINT ...........   11

          NUMBER OF ELEMENT ...............   13

          NUMBER OF MATERIAL ..............    1

          SYMETRY CONDITION ( NSYM ) ......    1

               IF NSYM.EQ.0 NOT SYMETRIC
               IF NSYM.EQ.1 SYMMETRIC ABOUT Y AXIS
               IF NSYM.EQ.2 SYMMETRIC ABOUT X AXIS
               IF NSYM.EQ.4 SYMMETRIC ABOUT X AND Y AXIS

          SECTION TYPE ....................    0

               IF NSEC.EQ.0 CLOSED SECTION
               IF NESC.NE.0 OPEN   SECTION


1

     N O D A L   P O I N T   D A T A


      NODE    BOUNDARY COND.               COORDINATE
    NUMBER      Y-SYM    X-SYM            -X             -Y
         1          1        0          0.000          0.000
         2          0        0       3300.000          0.000
         3          0        0       6300.000          0.000
         4          0        0       6300.000       1800.000
         5          0        0       3300.000       1800.000
         6          0        0       6300.000       4800.000
         7          0        0       3300.000       4800.000
         8          0        0       6300.000       8400.000
         9          0        0       3300.000       8400.000
        10          1        0          0.000       8400.000
        11          1        0          0.000       1800.000
1

     M A T E R I A L   D A T A


          MATERIAL NO.  1     SHEAR MODULUS =    0.100E+01


     E L E M E N T   D A T A

  ELEM. NO.   NODE-I    NODE-J   MAT. NO.     THICKNESS
```

1	1	2	1	8.000
2	2	3	1	8.000
3	3	4	1	10.000
4	4	5	1	10.000
5	2	5	1	8.000
6	4	6	1	10.000
7	6	7	1	10.000
8	7	5	1	8.000
9	6	8	1	10.000
10	8	9	1	8.000
11	9	7	1	8.000
12	9	10	1	8.000
13	5	11	1	10.000

1

WARPING FN OR SECTORIAL COOR (CENTROID)

NODE	WARPING FN	NODE	WARPING FN	NODE	WARPING FN
1	0.00000E+00	2	4.07242E+06	3	4.69815E+06
4	-8.49464E+05	5	-2.17013E+04	6	-4.88151E+06
7	-5.83519E+06	8	-1.21255E+07	9	-9.80451E+06
10	0.00000E+00	11	0.00000E+00		

WARPING FN OR SECTORIAL COOR (SHEAR CENTER)

NODE	WARPING FN	NODE	WARPING FN	NODE	WARPING FN
1	0.00000E+00	2	6.40001E+06	3	9.14174E+06
4	3.59413E+06	5	2.30589E+06	6	-4.37921E+05
7	-3.50760E+06	8	-7.68187E+06	9	-7.47691E+06
10	0.00000E+00	11	0.00000E+00		

SHEAR STRESS DUE TO PURE TORSION

ELEM	TAU-S	ELEM	TAU-S	ELEM	TAU-S
1	0.50480E+04	2	0.40225E+04	3	0.32180E+04
4	-0.17380E+04	5	0.10255E+04	6	0.49560E+04
7	0.66819E+03	8	-0.13622E+04	9	0.42878E+04
10	0.53597E+04	11	-0.21974E+04	12	0.75572E+04
13	-0.20073E+04				

SHEAR STRESS BY S.FORCE

ELEM	TAU(Y-DIR SF)	SFLOW(Y-SF)	TAU(X-DIR SF)	SFLOW(X-SF)
1	-0.1053E-05	-0.8420E-05	0.3431E-05	0.2745E-04
2	-0.9587E-06	-0.7670E-05	0.1849E-05	0.1479E-04
3	-0.2016E-05	-0.2016E-04	0.6134E-06	0.6134E-05
4	0.6163E-06	0.6163E-05	-0.1832E-05	-0.1832E-04
5	-0.2587E-05	-0.2070E-04	0.6423E-06	0.5138E-05
6	-0.3786E-05	-0.3786E-04	0.7848E-06	0.7848E-05
7	-0.8363E-07	-0.8363E-06	-0.1015E-05	-0.1015E-04
8	0.4486E-05	0.3588E-04	-0.1602E-05	-0.1281E-04
9	-0.2800E-05	-0.2800E-04	-0.2691E-06	-0.2691E-05
10	-0.1075E-05	-0.8601E-05	-0.1929E-05	-0.1543E-04
11	0.3626E-05	0.2901E-04	0.1031E-05	0.8247E-05
12	-0.1266E-05	-0.1013E-04	-0.4113E-05	-0.3290E-04
13	0.5558E-06	0.5558E-05	-0.3781E-05	-0.3781E-04

SHEAR STRESS BY S.FORCE (Unit Force * UNIT**3)

ELEM	TAU(Y-DIR SF)	SFLOW(Y-SF)	TAU(X-DIR SF)	SFLOW(X-SF)
1	-0.1053E-05	-0.5034E+08	0.3431E-05	0.3813E+09
2	-0.9587E-06	-0.4586E+08	0.1849E-05	0.2055E+09
3	-0.2016E-05	-0.1205E+09	0.6134E-06	0.8523E+08
4	0.6163E-06	0.3685E+08	-0.1832E-05	-0.2545E+09
5	-0.2587E-05	-0.1237E+09	0.6423E-06	0.7139E+08
6	-0.3786E-05	-0.2263E+09	0.7848E-06	0.1090E+09
7	-0.8363E-07	-0.5000E+07	-0.1015E-05	-0.1410E+09
8	0.4486E-05	0.2145E+09	-0.1602E-05	-0.1780E+09
9	-0.2800E-05	-0.1674E+09	-0.2691E-06	-0.3738E+08
10	-0.1075E-05	-0.5142E+08	-0.1929E-05	-0.2144E+09
11	0.3626E-05	0.1734E+09	0.1031E-05	0.1146E+09
12	-0.1266E-05	-0.6054E+08	-0.4113E-05	-0.4571E+09
13	0.5558E-06	0.3323E+08	-0.3781E-05	-0.5253E+09

SHEAR STRESS BY S.FORCE (Unit Force / UNIT**2)

ELEM	TAU(Y-DIR SF)	SFLOW(Y-SF)	TAU(X-DIR SF)	SFLOW(X-SF)
1	-0.1053E-05	-0.1053E-05	0.3431E-05	0.3431E-05
2	-0.9587E-06	-0.9587E-06	0.1849E-05	0.1849E-05
3	-0.2016E-05	-0.2016E-05	0.6134E-06	0.6134E-06
4	0.6163E-06	0.6163E-06	-0.1832E-05	-0.1832E-05
5	-0.2587E-05	-0.2587E-05	0.6423E-06	0.6423E-06
6	-0.3786E-05	-0.3786E-05	0.7848E-06	0.7848E-06
7	-0.8363E-07	-0.8363E-07	-0.1015E-05	-0.1015E-05
8	0.4486E-05	0.4486E-05	-0.1602E-05	-0.1602E-05
9	-0.2800E-05	-0.2800E-05	-0.2691E-06	-0.2691E-06
10	-0.1075E-05	-0.1075E-05	-0.1929E-05	-0.1929E-05
11	0.3626E-05	0.3626E-05	0.1031E-05	0.1031E-05
12	-0.1266E-05	-0.1266E-05	-0.4113E-05	-0.4113E-05

```
   13             0.5558E-06    0.5558E-06   -0.3781E-05   -0.3781E-05
1

Box Girder C

     P R O P E R T I E S   O F   B E A M   S E C T I O N

        COORDINATE OF CENTROID (      0.000,   3813.913 )

    COORDINATE OF SHEAR CENTER (      0.000,   3108.581 )

                  SECTIONAL AREA   =  0.6900000E+06

  MOMENT OF INERTIA( ABOUT Y-AXIS )=  0.1389308E+14

  MOMENT OF INERTIA( ABOUT X-AXIS )=  0.5978842E+13

 WARPING CONSTANT (SHEAR CENTER) =  0.1415516E+20

 WARPING CONSTANT   ( CENTROID ) =  0.2106687E+20

                            IWX = -0.9799234E+16

                            IWY =  0.0000000E+00

              TORTIONAL CONSTANT =  0.1055812E+14

  SHEAR COEFF. OF CROSS SECTION

                   KX( IN X-DIR ) =  0.4370571E+00

                   KY( IN Y-DIR ) =  0.3841334E+00

               WARPING TORSION KZ  =  0.7320152E-01
```

d. Box Girder D;

```
1

     C O N T R O L   D A T A


          NUMBER OF NODAL POINT ...........   10

          NUMBER OF ELEMENT ...............   12

          NUMBER OF MATERIAL ..............    1

          SYMETRY CONDITION ( NSYM ) ......    1

               IF NSYM.EQ.0 NOT SYMETRIC
               IF NSYM.EQ.1 SYMMETRIC ABOUT Y AXIS
               IF NSYM.EQ.2 SYMMETRIC ABOUT X AXIS
               IF NSYM.EQ.4 SYMMETRIC ABOUT X AND Y AXIS

          SECTION TYPE ....................    0

               IF NSEC.EQ.0 CLOSED SECTION
               IF NESC.NE.0 OPEN   SECTION


1

     N O D A L   P O I N T   D A T A


      NODE    BOUNDARY COND.               COORDINATE
    NUMBER      Y-SYM    X-SYM            -X             -Y
         1          1        0          0.000          0.000
         2          0        0       3300.000          0.000
         3          0        0       6300.000          0.000
         4          0        0       6300.000       1800.000
         5          0        0       3300.000       1800.000
         6          0        0       6300.000       4800.000
         7          0        0       3300.000       4800.000
         8          0        0       6300.000       8400.000
         9          0        0       3300.000       8400.000
        10          1        0          0.000       1800.000
1

     M A T E R I A L   D A T A


          MATERIAL NO.  1     SHEAR MODULUS =    0.100E+01



     E L E M E N T   D A T A

  ELEM. NO.   NODE-I    NODE-J   MAT. NO.     THICKNESS
```

1	1	2	1	8.000
2	2	3	1	8.000
3	3	4	1	10.000
4	4	5	1	10.000
5	2	5	1	8.000
6	4	6	1	10.000
7	6	7	1	10.000
8	7	5	1	8.000
9	6	8	1	10.000
10	8	9	1	8.000
11	9	7	1	8.000
12	5	10	1	10.000

1

WARPING FN OR SECTORIAL COOR (CENTROID)

NODE	WARPING FN	NODE	WARPING FN	NODE	WARPING FN
1	0.00000E+00	2	-4.34652E+06	3	-7.14186E+06
4	-1.48788E+07	5	-1.09801E+07	6	-2.67707E+07
7	-2.96403E+07	8	-4.25154E+07	9	-5.01894E+07
10	0.00000E+00				

WARPING FN OR SECTORIAL COOR (SHEAR CENTER)

NODE	WARPING FN	NODE	WARPING FN	NODE	WARPING FN
1	0.00000E+00	2	1.06999E+07	3	2.15831E+07
4	1.38462E+07	5	4.06627E+06	6	1.95428E+06
7	-1.45939E+07	8	-1.37904E+07	9	-3.51430E+07
10	0.00000E+00				

SHEAR STRESS DUE TO PURE TORSION

ELEM	TAU-S	ELEM	TAU-S	ELEM	TAU-S
1	0.21168E+04	2	0.25021E+04	3	0.20017E+04
4	-0.33434E+03	5	-0.38535E+03	6	0.23360E+04
7	0.40957E+03	8	0.29200E+04	9	0.19265E+04
10	0.24081E+04	11	0.24081E+04	12	0.16934E+04

SHEAR STRESS BY S.FORCE

ELEM	TAU(Y-DIR SF)	SFLOW(Y-SF)	TAU(X-DIR SF)	SFLOW(X-SF)
1	-0.1186E-05	-0.9490E-05	0.4994E-05	0.3995E-04
2	-0.1087E-05	-0.8697E-05	0.2661E-05	0.2129E-04
3	-0.2266E-05	-0.2266E-04	0.1251E-05	0.1251E-04
4	0.7084E-06	0.7084E-05	-0.2583E-05	-0.2583E-04
5	-0.2898E-05	-0.2318E-04	0.1380E-05	0.1104E-04
6	-0.4108E-05	-0.4108E-04	0.2150E-05	0.2150E-04
7	0.1315E-06	0.1315E-05	-0.8953E-06	-0.8953E-05
8	0.4685E-05	0.3748E-04	-0.3837E-05	-0.3070E-04
9	-0.2728E-05	-0.2728E-04	0.9474E-06	0.9474E-05

10	-0.7683E-07	-0.6146E-06	-0.4305E-06	-0.3444E-05
11	0.2902E-05	0.2322E-04	-0.1335E-05	-0.1068E-04
12	0.5644E-06	0.5644E-05	-0.5746E-05	-0.5746E-04

SHEAR STRESS BY S.FORCE (Unit Force * UNIT**3)

ELEM	TAU(Y-DIR SF)	SFLOW(Y-SF)	TAU(X-DIR SF)	SFLOW(X-SF)
1	-0.1186E-05	-0.4533E+08	0.4994E-05	0.5474E+09
2	-0.1087E-05	-0.4154E+08	0.2661E-05	0.2916E+09
3	-0.2266E-05	-0.1083E+09	0.1251E-05	0.1713E+09
4	0.7084E-06	0.3383E+08	-0.2583E-05	-0.3539E+09
5	-0.2898E-05	-0.1107E+09	0.1380E-05	0.1513E+09
6	-0.4108E-05	-0.1962E+09	0.2150E-05	0.2945E+09
7	0.1315E-06	0.6282E+07	-0.8953E-06	-0.1227E+09
8	0.4685E-05	0.1790E+09	-0.3837E-05	-0.4206E+09
9	-0.2728E-05	-0.1303E+09	0.9474E-06	0.1298E+09
10	-0.7683E-07	-0.2936E+07	-0.4305E-06	-0.4719E+08
11	0.2902E-05	0.1109E+09	-0.1335E-05	-0.1463E+09
12	0.5644E-06	0.2696E+08	-0.5746E-05	-0.7873E+09

SHEAR STRESS BY S.FORCE (Unit Force / UNIT**2)

ELEM	TAU(Y-DIR SF)	SFLOW(Y-SF)	TAU(X-DIR SF)	SFLOW(X-SF)
1	-0.1186E-05	-0.1186E-05	0.4994E-05	0.4994E-05
2	-0.1087E-05	-0.1087E-05	0.2661E-05	0.2661E-05
3	-0.2266E-05	-0.2266E-05	0.1251E-05	0.1251E-05
4	0.7084E-06	0.7084E-06	-0.2583E-05	-0.2583E-05
5	-0.2898E-05	-0.2898E-05	0.1380E-05	0.1380E-05
6	-0.4108E-05	-0.4108E-05	0.2150E-05	0.2150E-05
7	0.1315E-06	0.1315E-06	-0.8953E-06	-0.8953E-06
8	0.4685E-05	0.4685E-05	-0.3837E-05	-0.3837E-05
9	-0.2728E-05	-0.2728E-05	0.9474E-06	0.9474E-06
10	-0.7683E-07	-0.7683E-07	-0.4305E-06	-0.4305E-06
11	0.2902E-05	0.2902E-05	-0.1335E-05	-0.1335E-05
12	0.5644E-06	0.5644E-06	-0.5746E-05	-0.5746E-05

1

Box Girder D

P R O P E R T I E S O F B E A M S E C T I O N

COORDINATE OF CENTROID (0.000, 3433.898)

COORDINATE OF SHEAR CENTER (0.000, -1125.620)

SECTIONAL AREA = 0.6372000E+06

```
  MOMENT OF INERTIA( ABOUT Y-AXIS )=  0.1370142E+14
  MOMENT OF INERTIA( ABOUT X-AXIS )=  0.4776324E+13

 WARPING CONSTANT (SHEAR CENTER) =  0.1169579E+21
 WARPING CONSTANT   ( CENTROID ) =  0.4017995E+21
                             IWX = -0.6247187E+17
                             IWY =  0.0000000E+00
              TORTIONAL CONSTANT =  0.2507933E+13

  SHEAR COEFF. OF CROSS SECTION
                   KX( IN X-DIR ) =  0.2824834E+00
                   KY( IN Y-DIR ) =  0.4244598E+00
               WARPING TORSION KZ  =  0.4169768E+00
```

Appendix B

ProColl Files

a. Box Girder A

##
ProColl Template
##
Filename | Length | Units
Box Girder A | 1800 | mm
##

##	ELEMENT DESCRIPTORS		COORDINATES:				PLATE DIMRIMARY LONGITUDINAL DIMENSIONS:								FRAME DIMENSIONS:								MATERIAL DEFINITIONS:								LOAD SHORTENING CURVE:			
ID	Type	Description	Mirror	angle	ycoord	zcoord	b	tp	hwx	twx	bfx	tfx	nsx	loop	hwx2	twx2	bfx2	tfx2	nsx2	hwy	twy	bfy	tfy	framespacin	nsy	HAZ	Pmat	Smat	strDeq	E	v	Imp	LSCurve	Clone	Sname
1	LSC		N				600	8	113.6	6.65	63.5	13.4	20							227.2	13.3	127	26.8		5	40,909	Steel	Steel	245	207000	0.3	A	1		
2	LSC		N				600	10	113.6	6.65	63.5	13.4	13							227.2	13.3	127	26.8		5	40,909	Steel	Steel	245	207000	0.3	A	1		
3	LSC		N				600	8	113.6	6.65	63.5	13.4	20							227.2	13.3	127	26.8		5	40,909	Steel	Steel	245	207000	0.3	A	1		
4	LSC		N				600	10	113.6	6.65	63.5	13.4	13							227.2	13.3	127	26.8		5	40,909	Steel	Steel	245	207000	0.3	A	1		
5	E	Horz. Plate_1	N	0	0	0	600	8						1												40,909	Steel	Steel	245	207000	0.3	A	2	1	
6	E	Horz. Plate_2	N	0	600	0	600	8						1												40,909	Steel	Steel	245	207000	0.3	A	2	1	
7	E	Horz. Plate_3	N	0	1200	0	600	8						1												40,909	Steel	Steel	245	207000	0.3	A	2	1	
8	E	Horz. Plate_4	N	0	1800	0	600	8						1												40,909	Steel	Steel	245	207000	0.3	A	2	1	
9	E	Horz. Plate_5	N	0	2400	0	600	8						1												40,909	Steel	Steel	245	207000	0.3	A	2	1	
10	E	Horz. Plate_6	N	0	3000	0	600	8						1												40,909	Steel	Steel	245	207000	0.3	A	2	1	
11	E	Horz. Plate_7	N	0	3600	0	600	8						1												40,909	Steel	Steel	245	207000	0.3	A	2	1	
12	E	Horz. Plate_8	N	0	4200	0	600	8						1												40,909	Steel	Steel	245	207000	0.3	A	2	1	
13	E	Horz. Plate_9	N	0	4800	0	600	8						1												40,909	Steel	Steel	245	207000	0.3	A	2	1	
14	E	Horz. Plate_10	N	0	5400	0	600	8						1												40,909	Steel	Steel	245	207000	0.3	A	2	1	
15	E	Horz. Plate_11	N	0	6000	0	600	8						1												40,909	Steel	Steel	245	207000	0.3	A	2	1	
16	E	Horz. Plate_12	N	0	6600	0	600	8						1												40,909	Steel	Steel	245	207000	0.3	A	2	1	
17	E	Horz. Plate_13	N	0	7200	0	600	8						1												40,909	Steel	Steel	245	207000	0.3	A	2	1	
18	E	Horz. Plate_14	N	0	7800	0	600	8						1												40,909	Steel	Steel	245	207000	0.3	A	2	1	
19	E	Horz. Plate_15	N	0	8400	0	600	8						1												40,909	Steel	Steel	245	207000	0.3	A	2	1	
20	E	Horz. Plate_16	N	0	9000	0	600	8						1												40,909	Steel	Steel	245	207000	0.3	A	2	1	
21	E	Horz. Plate_17	N	0	9600	0	600	8						1												40,909	Steel	Steel	245	207000	0.3	A	2	1	
22	E	Horz. Plate_18	N	0	10200	0	600	8						1												40,909	Steel	Steel	245	207000	0.3	A	2	1	
23	E	Horz. Plate_19	N	0	10800	0	600	8						1												40,909	Steel	Steel	245	207000	0.3	A	2	1	
24	E	Horz. Plate_20	N	0	11400	0	600	8						1												40,909	Steel	Steel	245	207000	0.3	A	2	1	
25	E	Horz. Plate_21	N	0	12000	0	600	8						1												40,909	Steel	Steel	245	207000	0.3	A	2	1	
26	E	Vert. Plate_R_1	N	90	12600	0	600	10						1												40,909	Steel	Steel	245	207000	0.3	A	2	2	
27	E	Vert. Plate_R_2	N	90	12600	600	600	10						1												40,909	Steel	Steel	245	207000	0.3	A	2	2	
28	E	Vert. Plate_R_3	N	90	12600	1200	600	10						1												40,909	Steel	Steel	245	207000	0.3	A	2	2	
29	E	Vert. Plate_R_4	N	90	12600	1800	600	10						1												40,909	Steel	Steel	245	207000	0.3	A	2	2	
30	E	Vert. Plate_R_5	N	90	12600	2400	600	10						1												40,909	Steel	Steel	245	207000	0.3	A	2	2	
31	E	Vert. Plate_R_6	N	90	12600	3000	600	10						1												40,909	Steel	Steel	245	207000	0.3	A	2	2	
32	E	Vert. Plate_R_7	N	90	12600	3600	600	10						1												40,909	Steel	Steel	245	207000	0.3	A	2	2	
33	E	Vert. Plate_R_8	N	90	12600	4200	600	10						1												40,909	Steel	Steel	245	207000	0.3	A	2	2	
34	E	Vert. Plate_R_9	N	90	12600	4800	600	10						1												40,909	Steel	Steel	245	207000	0.3	A	2	2	
35	E	Vert. Plate_R_10	N	90	12600	5400	600	10						1												40,909	Steel	Steel	245	207000	0.3	A	2	2	
36	E	Vert. Plate_R_11	N	90	12600	6000	600	10						1												40,909	Steel	Steel	245	207000	0.3	A	2	2	
37	E	Vert. Plate_R_12	N	90	12600	6600	600	10						1												40,909	Steel	Steel	245	207000	0.3	A	2	2	
38	E	Vert. Plate_R_13	N	90	12600	7200	600	10						1												40,909	Steel	Steel	245	207000	0.3	A	2	2	
39	E	Vert. Plate_R_14	N	90	12600	7800	600	10						1												40,909	Steel	Steel	245	207000	0.3	A	2	2	
40	E	Horz. Plate_Top_1	N	180	12600	8400	600	8						1												40,909	Steel	Steel	245	207000	0.3	A	2	3	
41	E	Horz. Plate_Top_2	N	180	12000	8400	600	8						1												40,909	Steel	Steel	245	207000	0.3	A	2	3	
42	E	Horz. Plate_Top_3	N	180	11400	8400	600	8						1												40,909	Steel	Steel	245	207000	0.3	A	2	3	
43	E	Horz. Plate_Top_4	N	180	10800	8400	600	8						1												40,909	Steel	Steel	245	207000	0.3	A	2	3	
44	E	Horz. Plate_Top_5	N	180	10200	8400	600	8						1												40,909	Steel	Steel	245	207000	0.3	A	2	3	
45	E	Horz. Plate_Top_6	N	180	9600	8400	600	8						1												40,909	Steel	Steel	245	207000	0.3	A	2	3	
46	E	Horz. Plate_Top_7	N	180	9000	8400	600	8						1												40,909	Steel	Steel	245	207000	0.3	A	2	3	
47	E	Horz. Plate_Top_8	N	180	8400	8400	600	8						1												40,909	Steel	Steel	245	207000	0.3	A	2	3	
48	E	Horz. Plate_Top_9	N	180	7800	8400	600	8						1												40,909	Steel	Steel	245	207000	0.3	A	2	3	
49	E	Horz. Plate_Top_10	N	180	7200	8400	600	8						1												40,909	Steel	Steel	245	207000	0.3	A	2	3	
50	E	Horz. Plate_Top_11	N	180	6600	8400	600	8						1												40,909	Steel	Steel	245	207000	0.3	A	2	3	
51	E	Horz. Plate_Top_12	N	180	6000	8400	600	8						1												40,909	Steel	Steel	245	207000	0.3	A	2	3	
52	E	Horz. Plate_Top_13	N	180	5400	8400	600	8						1												40,909	Steel	Steel	245	207000	0.3	A	2	3	
53	E	Horz. Plate_Top_14	N	180	4800	8400	600	8						1												40,909	Steel	Steel	245	207000	0.3	A	2	3	
54	E	Horz. Plate_Top_15	N	180	4200	8400	600	8						1												40,909	Steel	Steel	245	207000	0.3	A	2	3	
55	E	Horz. Plate_Top_16	N	180	3600	8400	600	8						1												40,909	Steel	Steel	245	207000	0.3	A	2	3	
56	E	Horz. Plate_Top_17	N	180	3000	8400	600	8						1												40,909	Steel	Steel	245	207000	0.3	A	2	3	
57	E	Horz. Plate_Top_18	N	180	2400	8400	600	8						1												40,909	Steel	Steel	245	207000	0.3	A	2	3	
58	E	Horz. Plate_Top_19	N	180	1800	8400	600	8						1												40,909	Steel	Steel	245	207000	0.3	A	2	3	
59	E	Horz. Plate_Top_20	N	180	1200	8400	600	8						1												40,909	Steel	Steel	245	207000	0.3	A	2	3	
60	E	Horz. Plate_Top_21	N	180	600	8400	600	8						1												40,909	Steel	Steel	245	207000	0.3	A	2	3	
61	E	Vert. Plate_Left_1	N	270	0	8400	600	10						1												40,909	Steel	Steel	245	207000	0.3	A	2	4	
62	E	Vert. Plate_Left_2	N	270	0	7800	600	10						1												40,909	Steel	Steel	245	207000	0.3	A	2	4	
63	E	Vert. Plate_Left_3	N	270	0	7200	600	10						1												40,909	Steel	Steel	245	207000	0.3	A	2	4	
64	E	Vert. Plate_Left_4	N	270	0	6600	600	10						1												40,909	Steel	Steel	245	207000	0.3	A	2	4	
65	E	Vert. Plate_Left_5	N	270	0	6000	600	10						1												40,909	Steel	Steel	245	207000	0.3	A	2	4	
66	E	Vert. Plate_Left_6	N	270	0	5400	600	10						1												40,909	Steel	Steel	245	207000	0.3	A	2	4	
67	E	Vert. Plate_Left_7	N	270	0	4800	600	10						1												40,909	Steel	Steel	245	207000	0.3	A	2	4	
68	E	Vert. Plate_Left_8	N	270	0	4200	600	10						1												40,909	Steel	Steel	245	207000	0.3	A	2	4	
69	E	Vert. Plate_Left_9	N	270	0	3600	600	10						1												40,909	Steel	Steel	245	207000	0.3	A	2	4	
70	E	Vert. Plate_Left_10	N	270	0	3000	600	10						1												40,909	Steel	Steel	245	207000	0.3	A	2	4	
71	E	Vert. Plate_Left_11	N	270	0	2400	600	10						1												40,909	Steel	Steel	245	207000	0.3	A	2	4	
72	E	Vert. Plate_Left_12	N	270	0	1800	600	10						1												40,909	Steel	Steel	245	207000	0.3	A	2	4	
73	E	Vert. Plate_Left_13	N	270	0	1200	600	10						1												40,909	Steel	Steel	245	207000	0.3	A	2	4	
74	E	Vert. Plate_Left_14	N	270	0	600	600	10						1												40,909	Steel	Steel	245	207000	0.3	A	2	4	
75	E	bottom_stif_1	N	0	600	0			113.6	6.65	63.5	13.4	1													17,318	Steel	Steel	245	207000	0.3	A	2	1	
76	E	bottom_stif_2	N	0	1200	0			113.6	6.65	63.5	13.4	1													17,318	Steel	Steel	245	207000	0.3	A	2	1	
77	E	bottom_stif_3	N	0	1800	0			113.6	6.65	63.5	13.4	1													17,318	Steel	Steel	245	207000	0.3	A	2	1	
78	E	bottom_stif_4	N	0	2400	0			113.6	6.65	63.5	13.4	1													17,318	Steel	Steel	245	207000	0.3	A	2	1	
79	E	bottom_stif_5	N	0	3000	0			113.6	6.65	63.5	13.4	1													17,318	Steel	Steel	245	207000	0.3	A	2	1	
80	E	bottom_stif_6	N	0	3600	0			113.6	6.65	63.5	13.4	1													17,318	Steel	Steel	245	207000	0.3	A	2	1	
81	E	bottom_stif_7	N	0	4200	0			113.6	6.65	63.5	13.4	1													17,318	Steel	Steel	245	207000	0.3	A	2	1	
82	E	bottom_stif_8	N	0	4800	0			113.6	6.65	63.5	13.4	1													17,318	Steel	Steel	245	207000	0.3	A	2	1	
83	E	bottom_stif_9	N	0	5400	0			113.6	6.65	63.5	13.4	1													17,318	Steel	Steel	245	207000	0.3	A	2	1	
84	E	bottom_stif_10	N	0	6000	0			113.6	6.65	63.5	13.4	1													17,318	Steel	Steel	245	207000	0.3	A	2	1	
85	E	bottom_stif_11	N	0	6600	0			113.6	6.65	63.5	13.4	1													17,318	Steel	Steel	245	207000	0.3	A	2	1	
86	E	bottom_stif_12	N	0	7200	0			113.6	6.65	63.5	13.4	1													17,318	Steel	Steel	245	207000	0.3	A	2	1	
87	E	bottom_stif_13	N	0	7800	0			113.6	6.65	63.5	13.4	1													17,318	Steel	Steel	245	207000	0.3	A	2	1	
88	E	bottom_stif_14	N	0	8400	0			113.6	6.65	63.5	13.4	1													17,318	Steel	Steel	245	207000	0.3	A	2	1	
89	E	bottom_stif_15	N	0	9000	0			113.6	6.65	63.5	13.4	1													17,318	Steel	Steel	245	207000	0.3	A	2	1	
90	E	bottom_stif_16	N	0	9600	0			113.6	6.65	63.5	13.4	1													17,318	Steel	Steel	245	207000	0.3	A	2	1	
91	E	bottom_stif_17	N	0	10200	0			113.6	6.65	63.5	13.4	1													17,318	Steel	Steel	245	207000	0.3	A	2	1	
92	E	bottom_stif_18	N	0	10800	0			113.6	6.65	63.5	13.4	1													17,318	Steel	Steel	245	207000	0.3	A	2	1	
93	E	bottom_stif_19	N	0	11400	0			113.6	6.65	63.5	13.4	1													17,318	Steel	Steel	245	207000	0.3	A	2	1	
94	E	bottom_stif_20	N	0	12000	0			113.6	6.65	63.5	13.4	1													17,318	Steel	Steel	245	207000	0.3	A	2	1	
95	E	rightside_stif_1	N	90	12600	600			113.6	6.65	63.5	13.4	1													17,318	Steel	Steel	245	207000	0.3	A	2	2	
96	E	rightside_stif_2	N	90	12600	1200			113.6	6.65	63.5	13.4	1													17,318	Steel	Steel	245	207000	0.3	A	2	2	
97	E	rightside_stif_3	N	90	12600	1800			113.6	6.65	63.5	13.4	1													17,318	Steel	Steel	245	207000	0.3	A	2	2	
98	E	rightside_stif_4	N	90	12600	2400			113.6	6.65	63.5	13.4	1													17,318	Steel	Steel	245	207000	0.3	A	2	2	
99	E	rightside_stif_5	N	90	12600	3000			113.6	6.65	63.5	13.4	1													17,318	Steel	Steel	245	207000	0.3	A	2	2	
100	E	rightside_stif_6	N	90	12600	3600			113.6	6.65	63.5	13.4	1													17,318	Steel	Steel	245	207000	0.3	A	2	2	
101	E	rightside_stif_7	N	90	12600	4200			113.6	6.65	63.5	13.4	1													17,318	Steel	Steel	245	207000	0.3	A	2	2	

##
ProColl Template
##
Filename Length Units
Box Girder A 1800 mm
##

##	ELEMENT DESCRIPTORS		COORDINATES:				PLATE DIMRIMARY LONGITUDINAL DIMENSIONS:							FRAME DIMENSIONS:									MATERIAL DEFINITIONS:							LOAD SHORTENING CURVE:			
ID	Type	Description	Mirror	angle	ycoord	zcoord	b	tp	hwx	twx	bfx	tfx	nsx	loop	hwx2	twx2	bfx2	tfx2	nsx2	hwy	twy	bfy	tfy	ramespacin	nsy	HA2	Pmat	Smat	str0eq	E	v	Imp	LSCurve	Clone	Sname
102	E	rightside_stif_8	N	90	12600	4800			113.6	6.65	63.5	13.4	1													17.318	Steel	Steel	245	207000	0.3	A	2	2	
103	E	rightside_stif_9	N	90	12600	5400			113.6	6.65	63.5	13.4	1													17.318	Steel	Steel	245	207000	0.3	A	2	2	
104	E	rightside_stif_10	N	90	12600	6000			113.6	6.65	63.5	13.4	1													17.318	Steel	Steel	245	207000	0.3	A	2	2	
105	E	rightside_stif_11	N	90	12600	6600			113.6	6.65	63.5	13.4	1													17.318	Steel	Steel	245	207000	0.3	A	2	2	
106	E	rightside_stif_12	N	90	12600	7200			113.6	6.65	63.5	13.4	1													17.318	Steel	Steel	245	207000	0.3	A	2	2	
107	E	rightside_stif_13	N	90	12600	7800			113.6	6.65	63.5	13.4	1													17.318	Steel	Steel	245	207000	0.3	A	2	2	
108	E	top_stif_1	N	180	12000	8400			113.6	6.65	63.5	13.4	1													17.318	Steel	Steel	245	207000	0.3	A	2	3	
109	E	top_stif_2	N	180	11400	8400			113.6	6.65	63.5	13.4	1													17.318	Steel	Steel	245	207000	0.3	A	2	3	
110	E	top_stif_3	N	180	10800	8400			113.6	6.65	63.5	13.4	1													17.318	Steel	Steel	245	207000	0.3	A	2	3	
111	E	top_stif_4	N	180	10200	8400			113.6	6.65	63.5	13.4	1													17.318	Steel	Steel	245	207000	0.3	A	2	3	
112	E	top_stif_5	N	180	9600	8400			113.6	6.65	63.5	13.4	1													17.318	Steel	Steel	245	207000	0.3	A	2	3	
113	E	top_stif_6	N	180	9000	8400			113.6	6.65	63.5	13.4	1													17.318	Steel	Steel	245	207000	0.3	A	2	3	
114	E	top_stif_7	N	180	8400	8400			113.6	6.65	63.5	13.4	1													17.318	Steel	Steel	245	207000	0.3	A	2	3	
115	E	top_stif_8	N	180	7800	8400			113.6	6.65	63.5	13.4	1													17.318	Steel	Steel	245	207000	0.3	A	2	3	
116	E	top_stif_9	N	180	7200	8400			113.6	6.65	63.5	13.4	1													17.318	Steel	Steel	245	207000	0.3	A	2	3	
117	E	top_stif_10	N	180	6600	8400			113.6	6.65	63.5	13.4	1													17.318	Steel	Steel	245	207000	0.3	A	2	3	
118	E	top_stif_11	N	180	6000	8400			113.6	6.65	63.5	13.4	1													17.318	Steel	Steel	245	207000	0.3	A	2	3	
119	E	top_stif_12	N	180	5400	8400			113.6	6.65	63.5	13.4	1													17.318	Steel	Steel	245	207000	0.3	A	2	3	
120	E	top_stif_13	N	180	4800	8400			113.6	6.65	63.5	13.4	1													17.318	Steel	Steel	245	207000	0.3	A	2	3	
121	E	top_stif_14	N	180	4200	8400			113.6	6.65	63.5	13.4	1													17.318	Steel	Steel	245	207000	0.3	A	2	3	
122	E	top_stif_15	N	180	3600	8400			113.6	6.65	63.5	13.4	1													17.318	Steel	Steel	245	207000	0.3	A	2	3	
123	E	top_stif_16	N	180	3000	8400			113.6	6.65	63.5	13.4	1													17.318	Steel	Steel	245	207000	0.3	A	2	3	
124	E	top_stif_17	N	180	2400	8400			113.6	6.65	63.5	13.4	1													17.318	Steel	Steel	245	207000	0.3	A	2	3	
125	E	top_stif_18	N	180	1800	8400			113.6	6.65	63.5	13.4	1													17.318	Steel	Steel	245	207000	0.3	A	2	3	
126	E	top_stif_19	N	180	1200	8400			113.6	6.65	63.5	13.4	1													17.318	Steel	Steel	245	207000	0.3	A	2	3	
127	E	top_stif_20	N	180	600	8400			113.6	6.65	63.5	13.4	1													17.318	Steel	Steel	245	207000	0.3	A	2	3	
128	E	leftside_stif_1	N	270	0	7800			113.6	6.65	63.5	13.4	1													17.318	Steel	Steel	245	207000	0.3	A	2	4	
129	E	leftside_stif_2	N	270	0	7200			113.6	6.65	63.5	13.4	1													17.318	Steel	Steel	245	207000	0.3	A	2	4	
130	E	leftside_stif_3	N	270	0	6600			113.6	6.65	63.5	13.4	1													17.318	Steel	Steel	245	207000	0.3	A	2	4	
131	E	leftside_stif_4	N	270	0	6000			113.6	6.65	63.5	13.4	1													17.318	Steel	Steel	245	207000	0.3	A	2	4	
132	E	leftside_stif_5	N	270	0	5400			113.6	6.65	63.5	13.4	1													17.318	Steel	Steel	245	207000	0.3	A	2	4	
133	E	leftside_stif_6	N	270	0	4800			113.6	6.65	63.5	13.4	1													17.318	Steel	Steel	245	207000	0.3	A	2	4	
134	E	leftside_stif_7	N	270	0	4200			113.6	6.65	63.5	13.4	1													17.318	Steel	Steel	245	207000	0.3	A	2	4	
135	E	leftside_stif_8	N	270	0	3600			113.6	6.65	63.5	13.4	1													17.318	Steel	Steel	245	207000	0.3	A	2	4	
136	E	leftside_stif_9	N	270	0	3000			113.6	6.65	63.5	13.4	1													17.318	Steel	Steel	245	207000	0.3	A	2	4	
137	E	leftside_stif_10	N	270	0	2400			113.6	6.65	63.5	13.4	1													17.318	Steel	Steel	245	207000	0.3	A	2	4	
138	E	leftside_stif_11	N	270	0	1800			113.6	6.65	63.5	13.4	1													17.318	Steel	Steel	245	207000	0.3	A	2	4	
139	E	leftside_stif_12	N	270	0	1200			113.6	6.65	63.5	13.4	1													17.318	Steel	Steel	245	207000	0.3	A	2	4	
140	E	leftside_stif_13	N	270.00001	0	600			113.6	6.65	63.5	13.4	1													17.318	Steel	Steel	245	207000	0.3	A	2	4	

b. Box Girder B

##																																		
##	ProColl Template																																	
##																																		
Filename	Length	Units																																
Box Girder B	1800	mm																																
##																																		
##	ELEMENT DESCRIPTORS		COORDINATES:				PLATE DIMMARY LONGITUDINAL DIMENSIONS:													FRAME DIMENSIONS:						MATERIAL DEFINITIONS:							LOAD SHORTENING CURVE:			
ID	Type	Description	Mirror	angle	ycoord	zcoord	b	tp	hwx	twx	bfx	tfx	nsx	loop	hwx2	twx2	bfx2	tfx2	nsx2	hwy	twy	bfy	tfy	·amespacir	nsy	HAZ	Pmat	Smat	str0eq	E	v	Imp	LSCurve	Clone	Sname
1	LSC		N				600	8	113.6	6.65	63.5	13.4	4							227.2	13.3	127	26.8		5	40.909	Steel	Steel	245	207000	0.3	A	1		
2	LSC		N				600	8	113.6	6.65	63.5	13.4	10							227.2	13.3	127	26.8		5	40.909	Steel	Steel	245	207000	0.3	A	1		
3	LSC		N				600	8	113.6	6.65	63.5	13.4	2							227.2	13.3	127	26.8		5	40.909	Steel	Steel	245	207000	0.3	A	1		
4	LSC		N				600	8	113.6	6.65	63.5	13.4	2							227.2	13.3	127	26.8		5	40.909	Steel	Steel	245	207000	0.3	A	1		
5	LSC		N				600	8	113.6	6.65	63.5	13.4	4							227.2	13.3	127	26.8		5	40.909	Steel	Steel	245	207000	0.3	A	1		
6	LSC		N				600	10	113.6	6.65	63.5	13.4	4							227.2	13.3	127	26.8		5	40.909	Steel	Steel	245	207000	0.3	A	1		
7	LSC		N				600	10	113.6	6.65	63.5	13.4	10							227.2	13.3	127	26.8		5	40.909	Steel	Steel	245	207000	0.3	A	1		
8	LSC		N				600	10	113.6	6.65	63.5	13.4	4							227.2	13.3	127	26.8		5	40.909	Steel	Steel	245	207000	0.3	A	1		
9	LSC		N				600	10	113.6	6.65	63.5	13.4	2							227.2	13.3	127	26.8		5	40.909	Steel	Steel	245	207000	0.3	A	1		
10	LSC		N				600	10	113.6	6.65	63.5	13.4	10							227.2	13.3	127	26.8		5	40.909	Steel	Steel	245	207000	0.3	A	1		
11	LSC		N				600	8	113.6	6.65	63.5	13.4	20							227.2	13.3	127	26.8		5	40.909	Steel	Steel	245	207000	0.3	A	1		
12	LSC		N				600	10	113.6	6.65	63.5	13.4	10							227.2	13.3	127	26.8		5	40.909	Steel	Steel	245	207000	0.3	A	1		
13	LSC		N				600	10	113.6	6.65	63.5	13.4	2							227.2	13.3	127	26.8		5	40.909	Steel	Steel	245	207000	0.3	A	1		
14	E	Horz. Plate_1	N	0	0	0	600	8						1												40.909	Steel	Steel	245	207000	0.3	A	2	1	
15	E	Horz. Plate_2	N	0	600	0	600	8						1												40.909	Steel	Steel	245	207000	0.3	A	2	1	
16	E	Horz. Plate_3	N	0	1200	0	600	8						1												40.909	Steel	Steel	245	207000	0.3	A	2	1	
17	E	Horz. Plate_4	N	0	1800	0	600	8						1												40.909	Steel	Steel	245	207000	0.3	A	2	1	
18	E	Horz. Plate_5	N	0	2400	0	600	8						1												40.909	Steel	Steel	245	207000	0.3	A	2	1	
19	E	Horz. Plate_6	N	0	3000	0	600	8						2												40.909	Steel	Steel	245	207000	0.3	A	2	2	
20	E	V_db.Plate_L_1	N	90	3000	0	600	8						L1L2												40.909	Steel	Steel	245	207000	0.3	A	2	3	
21	E	V_db.Plate_L_2	N	90	3000	600	600	8						L1L2												40.909	Steel	Steel	245	207000	0.3	A	2	3	
22	E	V_db.Plate_L_3	N	90	3000	1200	600	8						L1L2												40.909	Steel	Steel	245	207000	0.3	A	2	3	
23	E	V_db.Plate_R_1	N	90	9600	0	600	8						L2L3												40.909	Steel	Steel	245	207000	0.3	A	2	4	
24	E	V_db.Plate_R_2	N	90	9600	600	600	8						L2L3												40.909	Steel	Steel	245	207000	0.3	A	2	4	
25	E	V_db.Plate_R_3	N	90	9600	1200	600	8						L2L3												40.909	Steel	Steel	245	207000	0.3	A	2	4	
26	E	Horz. Plate_7	N	0	3600	0	600	8						2												40.909	Steel	Steel	245	207000	0.3	A	2	2	
27	E	Horz. Plate_8	N	0	4200	0	600	8						2												40.909	Steel	Steel	245	207000	0.3	A	2	2	
28	E	Horz. Plate_9	N	0	4800	0	600	8						2												40.909	Steel	Steel	245	207000	0.3	A	2	2	
29	E	Horz. Plate_10	N	0	5400	0	600	8						2												40.909	Steel	Steel	245	207000	0.3	A	2	2	
30	E	Horz. Plate_11	N	0	6000	0	600	8						2												40.909	Steel	Steel	245	207000	0.3	A	2	2	
31	E	Horz. Plate_12	N	0	6600	0	600	8						2												40.909	Steel	Steel	245	207000	0.3	A	2	2	
32	E	Horz. Plate_13	N	0	7200	0	600	8						2												40.909	Steel	Steel	245	207000	0.3	A	2	2	
33	E	Horz. Plate_14	N	0	7800	0	600	8						2												40.909	Steel	Steel	245	207000	0.3	A	2	2	
34	E	Horz. Plate_15	N	0	8400	0	600	8						2												40.909	Steel	Steel	245	207000	0.3	A	2	2	
35	E	Horz. Plate_16	N	0	9000	0	600	8						2												40.909	Steel	Steel	245	207000	0.3	A	2	2	
36	E	Horz. Plate_17	N	0	9600	0	600	8						3												40.909	Steel	Steel	245	207000	0.3	A	2	5	
37	E	Horz. Plate_18	N	0	10200	0	600	8						3												40.909	Steel	Steel	245	207000	0.3	A	2	5	
38	E	Horz. Plate_19	N	0	10800	0	600	8						3												40.909	Steel	Steel	245	207000	0.3	A	2	5	
39	E	Horz. Plate_20	N	0	11400	0	600	8						3												40.909	Steel	Steel	245	207000	0.3	A	2	5	
40	E	Horz. Plate_21	N	0	12000	0	600	8						3												40.909	Steel	Steel	245	207000	0.3	A	2	5	
41	E	DB.Plate_1	N	0	0	1800	600	10						L1L4												40.909	Steel	Steel	245	207000	0.3	A	2	6	
42	E	DB.Plate_2	N	0	600	1800	600	10						L1L4												40.909	Steel	Steel	245	207000	0.3	A	2	6	
43	E	DB.Plate_3	N	0	1200	1800	600	10						L1L4												40.909	Steel	Steel	245	207000	0.3	A	2	6	
44	E	DB.Plate_4	N	0	1800	1800	600	10						L1L4												40.909	Steel	Steel	245	207000	0.3	A	2	6	
45	E	DB.Plate_5	N	0	2400	1800	600	10						L1L4												40.909	Steel	Steel	245	207000	0.3	A	2	6	
46	E	DB.Plate_6	N	0	3000	1800	600	10						L2L4												40.909	Steel	Steel	245	207000	0.3	A	2	7	
47	E	DB.Plate_7	N	0	3600	1800	600	10						L2L4												40.909	Steel	Steel	245	207000	0.3	A	2	7	
48	E	DB.Plate_8	N	0	4200	1800	600	10						L2L4												40.909	Steel	Steel	245	207000	0.3	A	2	7	
49	E	DB.Plate_9	N	0	4800	1800	600	10						L2L4												40.909	Steel	Steel	245	207000	0.3	A	2	7	
50	E	DB.Plate_10	N	0	5400	1800	600	10						L2L4												40.909	Steel	Steel	245	207000	0.3	A	2	7	
51	E	DB.Plate_11	N	0	6000	1800	600	10						L2L4												40.909	Steel	Steel	245	207000	0.3	A	2	7	
52	E	DB.Plate_12	N	0	6600	1800	600	10						L2L4												40.909	Steel	Steel	245	207000	0.3	A	2	7	
53	E	DB.Plate_13	N	0	7200	1800	600	10						L2L4												40.909	Steel	Steel	245	207000	0.3	A	2	7	
54	E	DB.Plate_14	N	0	7800	1800	600	10						L2L4												40.909	Steel	Steel	245	207000	0.3	A	2	7	
55	E	DB.Plate_15	N	0	8400	1800	600	10						L2L4												40.909	Steel	Steel	245	207000	0.3	A	2	7	
56	E	DB.Plate_16	N	0	9000	1800	600	10						L2L4												40.909	Steel	Steel	245	207000	0.3	A	2	7	
57	E	DB.Plate_17	N	0	9600	1800	600	10						L3L4												40.909	Steel	Steel	245	207000	0.3	A	2	8	
58	E	DB.Plate_18	N	0	10200	1800	600	10						L3L4												40.909	Steel	Steel	245	207000	0.3	A	2	8	
59	E	DB.Plate_19	N	0	10800	1800	600	10						L3L4												40.909	Steel	Steel	245	207000	0.3	A	2	8	
60	E	DB.Plate_20	N	0	11400	1800	600	10						L3L4												40.909	Steel	Steel	245	207000	0.3	A	2	8	
61	E	DB.Plate_21	N	0	12000	1800	600	10						L3L4												40.909	Steel	Steel	245	207000	0.3	A	2	8	
62	E	Vert. Plate_R_1	N	90	12600	0	600	10						3												40.909	Steel	Steel	245	207000	0.3	A	2	9	
63	E	Vert. Plate_R_2	N	90	12600	600	600	10						3												40.909	Steel	Steel	245	207000	0.3	A	2	9	
64	E	Vert. Plate_R_3	N	90	12600	1200	600	10						3												40.909	Steel	Steel	245	207000	0.3	A	2	9	
65	E	Vert. Plate_R_4	N	90	12600	1800	600	10						4												40.909	Steel	Steel	245	207000	0.3	A	2	10	
66	E	Vert. Plate_R_5	N	90	12600	2400	600	10						4												40.909	Steel	Steel	245	207000	0.3	A	2	10	
67	E	Vert. Plate_R_6	N	90	12600	3000	600	10						4												40.909	Steel	Steel	245	207000	0.3	A	2	10	
68	E	Vert. Plate_R_7	N	90	12600	3600	600	10						4												40.909	Steel	Steel	245	207000	0.3	A	2	10	
69	E	Vert. Plate_R_8	N	90	12600	4200	600	10						4												40.909	Steel	Steel	245	207000	0.3	A	2	10	
70	E	Vert. Plate_R_9	N	90	12600	4800	600	10						4												40.909	Steel	Steel	245	207000	0.3	A	2	10	
71	E	Vert. Plate_R_10	N	90	12600	5400	600	10						4												40.909	Steel	Steel	245	207000	0.3	A	2	10	
72	E	Vert. Plate_R_11	N	90	12600	6000	600	10						4												40.909	Steel	Steel	245	207000	0.3	A	2	10	
73	E	Vert. Plate_R_12	N	90	12600	6600	600	10						4												40.909	Steel	Steel	245	207000	0.3	A	2	10	
74	E	Vert. Plate_R_13	N	90	12600	7200	600	10						4												40.909	Steel	Steel	245	207000	0.3	A	2	10	
75	E	Vert. Plate_R_14	N	90	12600	7800	600	10						4												40.909	Steel	Steel	245	207000	0.3	A	2	10	
76	E	Horz. Plate_Top_1	N	180	12600	8400	600	8						4												40.909	Steel	Steel	245	207000	0.3	A	2	11	
77	E	Horz. Plate_Top_2	N	180	12000	8400	600	8						4												40.909	Steel	Steel	245	207000	0.3	A	2	11	
78	E	Horz. Plate_Top_3	N	180	11400	8400	600	8						4												40.909	Steel	Steel	245	207000	0.3	A	2	11	
79	E	Horz. Plate_Top_4	N	180	10800	8400	600	8						4												40.909	Steel	Steel	245	207000	0.3	A	2	11	
80	E	Horz. Plate_Top_5	N	180	10200	8400	600	8						4												40.909	Steel	Steel	245	207000	0.3	A	2	11	
81	E	Horz. Plate_Top_6	N	180	9600	8400	600	8						4												40.909	Steel	Steel	245	207000	0.3	A	2	11	

##
ProColl Template
##

Filename	Length	Units
Box Girder B	1800	mm

##

##	ELEMENT DESCRIPTORS		COORDINATES:				PLATE DIMMARY LONGITUDINAL DIMENSIONS:							FRAME DIMENSIONS:										MATERIAL DEFINITIONS:							LOAD SHORTENING CURVE:			
ID	Type	Description	Mirror	angle	ycoord	zcoord	b	tp	hwx	twx	bfx	tfx	nsx	loop	hwx2	twx2	bfx2	tfx2	nsx2	hwy	twy	bfy	tfy	amespacir	nsy	HAZ	Pmat	Smat	str0eq	E	v	Imp	LSCurve	Clone	Sname
82	E	Horz. Plate_Top_7	N	180	9000	8400	600	8						4												40.909	Steel	Steel	245	207000	0.3	A	2	11	
83	E	Horz. Plate_Top_8	N	180	8400	8400	600	8						4												40.909	Steel	Steel	245	207000	0.3	A	2	11	
84	E	Horz. Plate_Top_9	N	180	7800	8400	600	8						4												40.909	Steel	Steel	245	207000	0.3	A	2	11	
85	E	Horz. Plate_Top_10	N	180	7200	8400	600	8						4												40.909	Steel	Steel	245	207000	0.3	A	2	11	
86	E	Horz. Plate_Top_11	N	180	6600	8400	600	8						4												40.909	Steel	Steel	245	207000	0.3	A	2	11	
87	E	Horz. Plate_Top_12	N	180	6000	8400	600	8						4												40.909	Steel	Steel	245	207000	0.3	A	2	11	
88	E	Horz. Plate_Top_13	N	180	5400	8400	600	8						4												40.909	Steel	Steel	245	207000	0.3	A	2	11	
89	E	Horz. Plate_Top_14	N	180	4800	8400	600	8						4												40.909	Steel	Steel	245	207000	0.3	A	2	11	
90	E	Horz. Plate_Top_15	N	180	4200	8400	600	8						4												40.909	Steel	Steel	245	207000	0.3	A	2	11	
91	E	Horz. Plate_Top_16	N	180	3600	8400	600	8						4												40.909	Steel	Steel	245	207000	0.3	A	2	11	
92	E	Horz. Plate_Top_17	N	180	3000	8400	600	8						4												40.909	Steel	Steel	245	207000	0.3	A	2	11	
93	E	Horz. Plate_Top_18	N	180	2400	8400	600	8						4												40.909	Steel	Steel	245	207000	0.3	A	2	11	
94	E	Horz. Plate_Top_19	N	180	1800	8400	600	8						4												40.909	Steel	Steel	245	207000	0.3	A	2	11	
95	E	Horz. Plate_Top_20	N	180	1200	8400	600	8						4												40.909	Steel	Steel	245	207000	0.3	A	2	11	
96	E	Horz. Plate_Top_21	N	180	600	8400	600	8						4												40.909	Steel	Steel	245	207000	0.3	A	2	11	
97	E	Vert. Plate_Left_1	N	270	0	8400	600	10						4												40.909	Steel	Steel	245	207000	0.3	A	2	12	
98	E	Vert. Plate_Left_2	N	270	0	7800	600	10						4												40.909	Steel	Steel	245	207000	0.3	A	2	12	
99	E	Vert. Plate_Left_3	N	270	0	7200	600	10						4												40.909	Steel	Steel	245	207000	0.3	A	2	12	
100	E	Vert. Plate_Left_4	N	270	0	6600	600	10						4												40.909	Steel	Steel	245	207000	0.3	A	2	12	
101	E	Vert. Plate_Left_5	N	270	0	6000	600	10						4												40.909	Steel	Steel	245	207000	0.3	A	2	12	
102	E	Vert. Plate_Left_6	N	270	0	5400	600	10						4												40.909	Steel	Steel	245	207000	0.3	A	2	12	
103	E	Vert. Plate_Left_7	N	270	0	4800	600	10						4												40.909	Steel	Steel	245	207000	0.3	A	2	12	
104	E	Vert. Plate_Left_8	N	270	0	4200	600	10						4												40.909	Steel	Steel	245	207000	0.3	A	2	12	
105	E	Vert. Plate_Left_9	N	270	0	3600	600	10						4												40.909	Steel	Steel	245	207000	0.3	A	2	12	
106	E	Vert. Plate_Left_10	N	270	0	3000	600	10						4												40.909	Steel	Steel	245	207000	0.3	A	2	12	
107	E	Vert. Plate_Left_11	N	270	0	2400	600	10						4												40.909	Steel	Steel	245	207000	0.3	A	2	12	
108	E	Vert. Plate_Left_12	N	270	0	1800	600	10						1												40.909	Steel	Steel	245	207000	0.3	A	2	13	
109	E	Vert. Plate_Left_13	N	270	0	1200	600	10						1												40.909	Steel	Steel	245	207000	0.3	A	2	13	
110	E	Vert. Plate_Left_14	N	270	0	600	600	10						1												40.909	Steel	Steel	245	207000	0.3	A	2	13	
111	E	bottom_stif_1	N	0	600	0			113.6	6.65	63.5	13.4	1												17.318	Steel	Steel	245	207000	0.3	A	2	1	
112	E	bottom_stif_2	N	0	1200	0			113.6	6.65	63.5	13.4	1												17.318	Steel	Steel	245	207000	0.3	A	2	1	
113	E	bottom_stif_3	N	0	1800	0			113.6	6.65	63.5	13.4	1												17.318	Steel	Steel	245	207000	0.3	A	2	1	
114	E	bottom_stif_4	N	0	2400	0			113.6	6.65	63.5	13.4	1												17.318	Steel	Steel	245	207000	0.3	A	2	1	
115	E	L_V.db_stif_1	N	90	3000	600			113.6	6.65	63.5	13.4	1												17.318	Steel	Steel	245	207000	0.3	A	2	3	
116	E	L_V.db_stif_2	N	90	3000	1200			113.6	6.65	63.5	13.4	1												17.318	Steel	Steel	245	207000	0.3	A	2	3	
117	E	R_V.db_stif_1	N	270	9600	600			113.6	6.65	63.5	13.4	1												17.318	Steel	Steel	245	207000	0.3	A	2	4	
118	E	R_V.db_stif_2	N	270	9600	1200			113.6	6.65	63.5	13.4	1												17.318	Steel	Steel	245	207000	0.3	A	2	4	
119	E	bottom_stif_6	N	0	3600	0			113.6	6.65	63.5	13.4	1												17.318	Steel	Steel	245	207000	0.3	A	2	2	
120	E	bottom_stif_7	N	0	4200	0			113.6	6.65	63.5	13.4	1												17.318	Steel	Steel	245	207000	0.3	A	2	2	
121	E	bottom_stif_8	N	0	4800	0			113.6	6.65	63.5	13.4	1												17.318	Steel	Steel	245	207000	0.3	A	2	2	
122	E	bottom_stif_9	N	0	5400	0			113.6	6.65	63.5	13.4	1												17.318	Steel	Steel	245	207000	0.3	A	2	2	
123	E	bottom_stif_10	N	0	6000	0			113.6	6.65	63.5	13.4	1												17.318	Steel	Steel	245	207000	0.3	A	2	2	
124	E	bottom_stif_11	N	0	6600	0			113.6	6.65	63.5	13.4	1												17.318	Steel	Steel	245	207000	0.3	A	2	2	
125	E	bottom_stif_12	N	0	7200	0			113.6	6.65	63.5	13.4	1												17.318	Steel	Steel	245	207000	0.3	A	2	2	
126	E	bottom_stif_13	N	0	7800	0			113.6	6.65	63.5	13.4	1												17.318	Steel	Steel	245	207000	0.3	A	2	2	
127	E	bottom_stif_14	N	0	8400	0			113.6	6.65	63.5	13.4	1												17.318	Steel	Steel	245	207000	0.3	A	2	2	
128	E	bottom_stif_15	N	0	9000	0			113.6	6.65	63.5	13.4	1												17.318	Steel	Steel	245	207000	0.3	A	2	2	
129	E	bottom_stif_17	N	0	10200	0			113.6	6.65	63.5	13.4	1												17.318	Steel	Steel	245	207000	0.3	A	2	5	
130	E	bottom_stif_18	N	0	10800	0			113.6	6.65	63.5	13.4	1												17.318	Steel	Steel	245	207000	0.3	A	2	5	
131	E	bottom_stif_19	N	0	11400	0			113.6	6.65	63.5	13.4	1												17.318	Steel	Steel	245	207000	0.3	A	2	5	
132	E	bottom_stif_20	N	0	12000	0			113.6	6.65	63.5	13.4	1												17.318	Steel	Steel	245	207000	0.3	A	2	5	
133	E	rightside_stif_1	N	90	12600	600			113.6	6.65	63.5	13.4	1												17.318	Steel	Steel	245	207000	0.3	A	2	9	
134	E	rightside_stif_2	N	90	12600	1200			113.6	6.65	63.5	13.4	1												17.318	Steel	Steel	245	207000	0.3	A	2	9	
135	E	rightside_stif_4	N	90	12600	2400			113.6	6.65	63.5	13.4	1												17.318	Steel	Steel	245	207000	0.3	A	2	10	
136	E	rightside_stif_5	N	90	12600	3000			113.6	6.65	63.5	13.4	1												17.318	Steel	Steel	245	207000	0.3	A	2	10	
137	E	rightside_stif_6	N	90	12600	3600			113.6	6.65	63.5	13.4	1												17.318	Steel	Steel	245	207000	0.3	A	2	10	
138	E	rightside_stif_7	N	90	12600	4200			113.6	6.65	63.5	13.4	1												17.318	Steel	Steel	245	207000	0.3	A	2	10	
139	E	rightside_stif_8	N	90	12600	4800			113.6	6.65	63.5	13.4	1												17.318	Steel	Steel	245	207000	0.3	A	2	10	
140	E	rightside_stif_9	N	90	12600	5400			113.6	6.65	63.5	13.4	1												17.318	Steel	Steel	245	207000	0.3	A	2	10	
141	E	rightside_stif_10	N	90	12600	6000			113.6	6.65	63.5	13.4	1												17.318	Steel	Steel	245	207000	0.3	A	2	10	
142	E	rightside_stif_11	N	90	12600	6600			113.6	6.65	63.5	13.4	1												17.318	Steel	Steel	245	207000	0.3	A	2	10	
143	E	rightside_stif_12	N	90	12600	7200			113.6	6.65	63.5	13.4	1												17.318	Steel	Steel	245	207000	0.3	A	2	10	
144	E	rightside_stif_13	N	90	12600	7800			113.6	6.65	63.5	13.4	1												17.318	Steel	Steel	245	207000	0.3	A	2	10	
145	E	top_stif_1	N	180	12000	8400			113.6	6.65	63.5	13.4	1												17.318	Steel	Steel	245	207000	0.3	A	2	11	
146	E	top_stif_2	N	180	11400	8400			113.6	6.65	63.5	13.4	1												17.318	Steel	Steel	245	207000	0.3	A	2	11	
147	E	top_stif_3	N	180	10800	8400			113.6	6.65	63.5	13.4	1												17.318	Steel	Steel	245	207000	0.3	A	2	11	
148	E	top_stif_4	N	180	10200	8400			113.6	6.65	63.5	13.4	1												17.318	Steel	Steel	245	207000	0.3	A	2	11	
149	E	top_stif_5	N	180	9600	8400			113.6	6.65	63.5	13.4	1												17.318	Steel	Steel	245	207000	0.3	A	2	11	
150	E	top_stif_6	N	180	9000	8400			113.6	6.65	63.5	13.4	1												17.318	Steel	Steel	245	207000	0.3	A	2	11	
151	E	top_stif_7	N	180	8400	8400			113.6	6.65	63.5	13.4	1												17.318	Steel	Steel	245	207000	0.3	A	2	11	
152	E	top_stif_8	N	180	7800	8400			113.6	6.65	63.5	13.4	1												17.318	Steel	Steel	245	207000	0.3	A	2	11	
153	E	top_stif_9	N	180	7200	8400			113.6	6.65	63.5	13.4	1												17.318	Steel	Steel	245	207000	0.3	A	2	11	
154	E	top_stif_10	N	180	6600	8400			113.6	6.65	63.5	13.4	1												17.318	Steel	Steel	245	207000	0.3	A	2	11	
155	E	top_stif_11	N	180	6000	8400			113.6	6.65	63.5	13.4	1												17.318	Steel	Steel	245	207000	0.3	A	2	11	
156	E	top_stif_12	N	180	5400	8400			113.6	6.65	63.5	13.4	1												17.318	Steel	Steel	245	207000	0.3	A	2	11	
157	E	top_stif_13	N	180	4800	8400			113.6	6.65	63.5	13.4	1												17.318	Steel	Steel	245	207000	0.3	A	2	11	
158	E	top_stif_14	N	180	4200	8400			113.6	6.65	63.5	13.4	1												17.318	Steel	Steel	245	207000	0.3	A	2	11	
159	E	top_stif_15	N	180	3600	8400			113.6	6.65	63.5	13.4	1												17.318	Steel	Steel	245	207000	0.3	A	2	11	
160	E	top_stif_16	N	180	3000	8400			113.6	6.65	63.5	13.4	1												17.318	Steel	Steel	245	207000	0.3	A	2	11	
161	E	top_stif_17	N	180	2400	8400			113.6	6.65	63.5	13.4	1												17.318	Steel	Steel	245	207000	0.3	A	2	11	
162	E	top_stif_18	N	180	1800	8400			113.6	6.65	63.5	13.4	1												17.318	Steel	Steel	245	207000	0.3	A	2	11	

##
ProColl Template
##

Filename	Length	Units
Box Girder B	1800	mm

##

##	ELEMENT DESCRIPTORS		COORDINATES:				PLATE DIMMARY LONGITUDINAL DIMENSIONS:								FRAME DIMENSIONS:									MATERIAL DEFINITIONS:						LOAD SHORTENING CURVE:		
ID	Type	Description	Mirror	angle	ycoord	zcoord	b	tp	hwx	twx	bfx	tfx	nsx	loop	hwx2	twx2	bfx2	tfx2	nsx2	hwy	twy	bfy	tfy	amespacir	nsy	HAZ	Pmat	Smat	str0eq	E	v	lmp	LSCurve	Clone	Sname
163	E	top_stif_19	N	180	1200	8400			113.6	6.65	63.5	13.4	1													17.318	Steel	Steel	245	207000	0.3	A	2	11	
164	E	top_stif_20	N	180	600	8400			113.6	6.65	63.5	13.4	1													17.318	Steel	Steel	245	207000	0.3	A	2	11	
165	E	leftside_stif_1	N	270	0	7800			113.6	6.65	63.5	13.4	1													17.318	Steel	Steel	245	207000	0.3	A	2	12	
166	E	leftside_stif_2	N	270	0	7200			113.6	6.65	63.5	13.4	1													17.318	Steel	Steel	245	207000	0.3	A	2	12	
167	E	leftside_stif_3	N	270	0	6600			113.6	6.65	63.5	13.4	1													17.318	Steel	Steel	245	207000	0.3	A	2	12	
168	E	leftside_stif_4	N	270	0	6000			113.6	6.65	63.5	13.4	1													17.318	Steel	Steel	245	207000	0.3	A	2	12	
169	E	leftside_stif_5	N	270	0	5400			113.6	6.65	63.5	13.4	1													17.318	Steel	Steel	245	207000	0.3	A	2	12	
170	E	leftside_stif_6	N	270	0	4800			113.6	6.65	63.5	13.4	1													17.318	Steel	Steel	245	207000	0.3	A	2	12	
171	E	leftside_stif_7	N	270	0	4200			113.6	6.65	63.5	13.4	1													17.318	Steel	Steel	245	207000	0.3	A	2	12	
172	E	leftside_stif_8	N	270	0	3600			113.6	6.65	63.5	13.4	1													17.318	Steel	Steel	245	207000	0.3	A	2	12	
173	E	leftside_stif_9	N	270	0	3000			113.6	6.65	63.5	13.4	1													17.318	Steel	Steel	245	207000	0.3	A	2	12	
174	E	leftside_stif_10	N	270	0	2400			113.6	6.65	63.5	13.4	1													17.318	Steel	Steel	245	207000	0.3	A	2	12	
175	E	leftside_stif_12	N	270	0	1200			113.6	6.65	63.5	13.4	1													17.318	Steel	Steel	245	207000	0.3	A	2	13	
176	E	leftside_stif_13	N	270	0	600			113.6	6.65	63.5	13.4	1													17.318	Steel	Steel	245	207000	0.3	A	2	13	
177	E	D.B._stif_1	N	180	12000	1800			113.6	6.65	63.5	13.4	1													17.318	Steel	Steel	245	207000	0.3	A	2	8	
178	E	D.B._stif_2	N	180	11400	1800			113.6	6.65	63.5	13.4	1													17.318	Steel	Steel	245	207000	0.3	A	2	8	
179	E	D.B._stif_3	N	180	10800	1800			113.6	6.65	63.5	13.4	1													17.318	Steel	Steel	245	207000	0.3	A	2	8	
180	E	D.B._stif_4	N	180	10200	1800			113.6	6.65	63.5	13.4	1													17.318	Steel	Steel	245	207000	0.3	A	2	8	
181	E	D.B._stif_6	N	180	9000	1800			113.6	6.65	63.5	13.4	1													17.318	Steel	Steel	245	207000	0.3	A	2	7	
182	E	D.B._stif_7	N	180	8400	1800			113.6	6.65	63.5	13.4	1													17.318	Steel	Steel	245	207000	0.3	A	2	7	
183	E	D.B._stif_8	N	180	7800	1800			113.6	6.65	63.5	13.4	1													17.318	Steel	Steel	245	207000	0.3	A	2	7	
184	E	D.B._stif_9	N	180	7200	1800			113.6	6.65	63.5	13.4	1													17.318	Steel	Steel	245	207000	0.3	A	2	7	
185	E	D.B._stif_10	N	180	6600	1800			113.6	6.65	63.5	13.4	1													17.318	Steel	Steel	245	207000	0.3	A	2	7	
186	E	D.B._stif_11	N	180	6000	1800			113.6	6.65	63.5	13.4	1													17.318	Steel	Steel	245	207000	0.3	A	2	7	
187	E	D.B._stif_12	N	180	5400	1800			113.6	6.65	63.5	13.4	1													17.318	Steel	Steel	245	207000	0.3	A	2	7	
188	E	D.B._stif_13	N	180	4800	1800			113.6	6.65	63.5	13.4	1													17.318	Steel	Steel	245	207000	0.3	A	2	7	
189	E	D.B._stif_14	N	180	4200	1800			113.6	6.65	63.5	13.4	1													17.318	Steel	Steel	245	207000	0.3	A	2	7	
190	E	D.B._stif_15	N	180	3600	1800			113.6	6.65	63.5	13.4	1													17.318	Steel	Steel	245	207000	0.3	A	2	7	
191	E	D.B._stif_17	N	180	2400	1800			113.6	6.65	63.5	13.4	1													17.318	Steel	Steel	245	207000	0.3	A	2	6	
192	E	D.B._stif_18	N	180	1800	1800			113.6	6.65	63.5	13.4	1													17.318	Steel	Steel	245	207000	0.3	A	2	6	
193	E	D.B._stif_19	N	180	1200	1800			113.6	6.65	63.5	13.4	1													17.318	Steel	Steel	245	207000	0.3	A	2	6	
194	E	D.B._stif_20	N	180	600	1800			113.6	6.65	63.5	13.4	1													17.318	Steel	Steel	245	207000	0.3	A	2	6	

c. Box Girder C

##																																				
##	ProColl Template																																			
##																																				
Filename	Length	Units																																		
Box Girder C	1800	mm																																		
##																																				
##	ELEMENT DESCRIPTORS		COORDINATES:				PLATE DIMMARY LONGITUDINAL DIMENSIONS:												FRAME DIMENSIONS:						MATERIAL DEFINITIONS:								LOAD SHORTENING CURVE:				
ID	Type	Description	Mirror	angle	ycoord	zcoord	b	tp	hwx	twx	bfx	tfx	nsx	loop	hwx2	twx2	bfx2	tfx2	nsx2	hwy	twy	bfy	tfy	amespacir	nsy	HAZ	Pmat	Smat	str0eq	E	v	Imp	LSCurve	Clone	Sname		
1	LSC		N				600	8	113.6	6.65	63.5	13.4	4							227.2	13.3	127	26.8		5	40.909	Steel	Steel	245	207000	0.3	A	1				
2	LSC		N				600	8	113.6	6.65	63.5	13.4	10							227.2	13.3	127	26.8		5	40.909	Steel	Steel	245	207000	0.3	A	1				
3	LSC		N				600	8	113.6	6.65	63.5	13.4	2							227.2	13.3	127	26.8		5	40.909	Steel	Steel	245	207000	0.3	A	1				
4	LSC		N				600	8	113.6	6.65	63.5	13.4	4							227.2	13.3	127	26.8		5	40.909	Steel	Steel	245	207000	0.3	A	1				
5	LSC		N				600	8	113.6	6.65	63.5	13.4	5							227.2	13.3	127	26.8		5	40.909	Steel	Steel	245	207000	0.3	A	1				
6	LSC		N				600	8	113.6	6.65	63.5	13.4	2							227.2	13.3	127	26.8		5	40.909	Steel	Steel	245	207000	0.3	A	1				
7	LSC		N				600	8	113.6	6.65	63.5	13.4	4							227.2	13.3	127	26.8		5	40.909	Steel	Steel	245	207000	0.3	A	1				
8	LSC		N				600	8	113.6	6.65	63.5	13.4	5							227.2	13.3	127	26.8		5	40.909	Steel	Steel	245	207000	0.3	A	1				
9	LSC		N				600	8	113.6	6.65	63.5	13.4	4							227.2	13.3	127	26.8		5	40.909	Steel	Steel	245	207000	0.3	A	1				
10	LSC		N				600	10	113.6	6.65	63.5	13.4	4							227.2	13.3	127	26.8		5	40.909	Steel	Steel	245	207000	0.3	A	1				
11	LSC		N				600	10	113.6	6.65	63.5	13.4	10							227.2	13.3	127	26.8		5	40.909	Steel	Steel	245	207000	0.3	A	1				
12	LSC		N				600	10	113.6	6.65	63.5	13.4	4							227.2	13.3	127	26.8		5	40.909	Steel	Steel	245	207000	0.3	A	1				
13	LSC		N				600	10	113.6	6.65	63.5	13.4	4							227.2	13.3	127	26.8		5	40.909	Steel	Steel	245	207000	0.3	A	1				
14	LSC		N				600	10	113.6	6.65	63.5	13.4	4							227.2	13.3	127	26.8		5	40.909	Steel	Steel	245	207000	0.3	A	1				
15	LSC		N				600	10	113.6	6.65	63.5	13.4	2							227.2	13.3	127	26.8		5	40.909	Steel	Steel	245	207000	0.3	A	1				
16	LSC		N				600	10	113.6	6.65	63.5	13.4	4							227.2	13.3	127	26.8		5	40.909	Steel	Steel	245	207000	0.3	A	1				
17	LSC		N				600	10	113.6	6.65	63.5	13.4	5							227.2	13.3	127	26.8		5	40.909	Steel	Steel	245	207000	0.3	A	1				
18	LSC		N				600	8	113.6	6.65	63.5	13.4	4							227.2	13.3	127	26.8		5	40.909	Steel	Steel	245	207000	0.3	A	1				
19	LSC		N				600	8	113.6	6.65	63.5	13.4	10							227.2	13.3	127	26.8		5	40.909	Steel	Steel	245	207000	0.3	A	1				
20	LSC		N				600	8	113.6	6.65	63.5	13.4	4							227.2	13.3	127	26.8		5	40.909	Steel	Steel	245	207000	0.3	A	1				
21	LSC		N				600	10	113.6	6.65	63.5	13.4	5							227.2	13.3	127	26.8		5	40.909	Steel	Steel	245	207000	0.3	A	1				
22	LSC		N				600	10	113.6	6.65	63.5	13.4	4							227.2	13.3	127	26.8		5	40.909	Steel	Steel	245	207000	0.3	A	1				
23	LSC		N				600	10	113.6	6.65	63.5	13.4	2							227.2	13.3	127	26.8		5	40.909	Steel	Steel	245	207000	0.3	A	1				
24	E	Horz. Plate_1	N	0	0	0	600	8						1												40.909	Steel	Steel	245	207000	0.3	A	2	1			
25	E	Horz. Plate_2	N	0	600	0	600	8						1												40.909	Steel	Steel	245	207000	0.3	A	2	1			
26	E	Horz. Plate_3	N	0	1200	0	600	8						1												40.909	Steel	Steel	245	207000	0.3	A	2	1			
27	E	Horz. Plate_4	N	0	1800	0	600	8						1												40.909	Steel	Steel	245	207000	0.3	A	2	1			
28	E	Horz. Plate_5	N	0	2400	0	600	8						1												40.909	Steel	Steel	245	207000	0.3	A	2	1			
29	E	Horz. Plate_6	N	0	3000	0	600	8						2												40.909	Steel	Steel	245	207000	0.3	A	2	2			
30	E	V_db.Plate_L_1	N	90	3000	0	600	8						L1L2												40.909	Steel	Steel	245	207000	0.3	A	2	3			
31	E	V_db.Plate_L_2	N	90	3000	600	600	8						L1L2												40.909	Steel	Steel	245	207000	0.3	A	2	3			
32	E	V_db.Plate_L_3	N	90	3000	1200	600	8						L1L2												40.909	Steel	Steel	245	207000	0.3	A	2	3			
33	E	V_ds.Plate_L_1	N	90	3000	1800	600	8						L4L5												40.909	Steel	Steel	245	207000	0.3	A	2	4			
34	E	V_ds.Plate_L_2	N	90	3000	2400	600	8						L4L5												40.909	Steel	Steel	245	207000	0.3	A	2	4			
35	E	V_ds.Plate_L_3	N	90	3000	3000	600	8						L4L5												40.909	Steel	Steel	245	207000	0.3	A	2	4			
36	E	V_ds.Plate_L_4	N	90	3000	3600	600	8						L4L5												40.909	Steel	Steel	245	207000	0.3	A	2	4			
37	E	V_ds.Plate_L_5	N	90	3000	4200	600	8						L4L5												40.909	Steel	Steel	245	207000	0.3	A	2	4			
38	E	V_ds.Plate_L_6	N	90	3000	4800	600	8						L4L6												40.909	Steel	Steel	245	207000	0.3	A	2	5			
39	E	V_ds.Plate_L_7	N	90	3000	5400	600	8						L4L6												40.909	Steel	Steel	245	207000	0.3	A	2	5			
40	E	V_ds.Plate_L_8	N	90	3000	6000	600	8						L4L6												40.909	Steel	Steel	245	207000	0.3	A	2	5			
41	E	V_ds.Plate_L_9	N	90	3000	6600	600	8						L4L6												40.909	Steel	Steel	245	207000	0.3	A	2	5			
42	E	V_ds.Plate_L_10	N	90	3000	7200	600	8						L4L6												40.909	Steel	Steel	245	207000	0.3	A	2	5			
43	E	V_ds.Plate_L_11	N	90	3000	7800	600	8						L4L6												40.909	Steel	Steel	245	207000	0.3	A	2	5			
44	E	V_db.Plate_R_1	N	90	9600	0	600	8						L2L3												40.909	Steel	Steel	245	207000	0.3	A	2	6			
45	E	V_db.Plate_R_2	N	90	9600	600	600	8						L2L3												40.909	Steel	Steel	245	207000	0.3	A	2	6			
46	E	V_db.Plate_R_3	N	90	9600	1200	600	8						L2L3												40.909	Steel	Steel	245	207000	0.3	A	2	6			
47	E	V_ds.Plate_R_1	N	90	9600	1800	600	8						L4L8												40.909	Steel	Steel	245	207000	0.3	A	2	7			
48	E	V_ds.Plate_R_2	N	90	9600	2400	600	8						L4L8												40.909	Steel	Steel	245	207000	0.3	A	2	7			
49	E	V_ds.Plate_R_3	N	90	9600	3000	600	8						L4L8												40.909	Steel	Steel	245	207000	0.3	A	2	7			
50	E	V_ds.Plate_R_4	N	90	9600	3600	600	8						L4L8												40.909	Steel	Steel	245	207000	0.3	A	2	7			
51	E	V_ds.Plate_R_5	N	90	9600	4200	600	8						L4L8												40.909	Steel	Steel	245	207000	0.3	A	2	7			
52	E	V_ds.Plate_R_6	N	90	9600	4800	600	8						L4L7												40.909	Steel	Steel	245	207000	0.3	A	2	8			
53	E	V_ds.Plate_R_7	N	90	9600	5400	600	8						L4L7												40.909	Steel	Steel	245	207000	0.3	A	2	8			
54	E	V_ds.Plate_R_8	N	90	9600	6000	600	8						L4L7												40.909	Steel	Steel	245	207000	0.3	A	2	8			
55	E	V_ds.Plate_R_9	N	90	9600	6600	600	8						L4L7												40.909	Steel	Steel	245	207000	0.3	A	2	8			
56	E	V_ds.Plate_R_10	N	90	9600	7200	600	8						L4L7												40.909	Steel	Steel	245	207000	0.3	A	2	8			
57	E	V_ds.Plate_R_11	N	90	9600	7800	600	8						L4L7												40.909	Steel	Steel	245	207000	0.3	A	2	8			
58	E	Horz. Plate_7	N	0	3600	0	600	8						2												40.909	Steel	Steel	245	207000	0.3	A	2	2			
59	E	Horz. Plate_8	N	0	4200	0	600	8						2												40.909	Steel	Steel	245	207000	0.3	A	2	2			
60	E	Horz. Plate_9	N	0	4800	0	600	8						2												40.909	Steel	Steel	245	207000	0.3	A	2	2			
61	E	Horz. Plate_10	N	0	5400	0	600	8						2												40.909	Steel	Steel	245	207000	0.3	A	2	2			
62	E	Horz. Plate_11	N	0	6000	0	600	8						2												40.909	Steel	Steel	245	207000	0.3	A	2	2			
63	E	Horz. Plate_12	N	0	6600	0	600	8						2												40.909	Steel	Steel	245	207000	0.3	A	2	2			
64	E	Horz. Plate_13	N	0	7200	0	600	8						2												40.909	Steel	Steel	245	207000	0.3	A	2	2			
65	E	Horz. Plate_14	N	0	7800	0	600	8						2												40.909	Steel	Steel	245	207000	0.3	A	2	2			
66	E	Horz. Plate_15	N	0	8400	0	600	8						2												40.909	Steel	Steel	245	207000	0.3	A	2	2			
67	E	Horz. Plate_16	N	0	9000	0	600	8						2												40.909	Steel	Steel	245	207000	0.3	A	2	2			
68	E	Horz. Plate_17	N	0	9600	0	600	8						3												40.909	Steel	Steel	245	207000	0.3	A	2	9			
69	E	Horz. Plate_18	N	0	10200	0	600	8						3												40.909	Steel	Steel	245	207000	0.3	A	2	9			
70	E	Horz. Plate_19	N	0	10800	0	600	8						3												40.909	Steel	Steel	245	207000	0.3	A	2	9			
71	E	Horz. Plate_20	N	0	11400	0	600	8						3												40.909	Steel	Steel	245	207000	0.3	A	2	9			
72	E	Horz. Plate_21	N	0	12000	0	600	8						3												40.909	Steel	Steel	245	207000	0.3	A	2	9			
73	E	DB.Plate_1	N	0	0	1800	600	10						L1L5												40.909	Steel	Steel	245	207000	0.3	A	2	10			
74	E	DB.Plate_2	N	0	600	1800	600	10						L1L5												40.909	Steel	Steel	245	207000	0.3	A	2	10			
75	E	DB.Plate_3	N	0	1200	1800	600	10						L1L5												40.909	Steel	Steel	245	207000	0.3	A	2	10			
76	E	DB.Plate_4	N	0	1800	1800	600	10						L1L5												40.909	Steel	Steel	245	207000	0.3	A	2	10			
77	E	DB.Plate_5	N	0	2400	1800	600	10						L1L5												40.909	Steel	Steel	245	207000	0.3	A	2	10			
78	E	DB.Plate_6	N	0	3000	1800	600	10						L2L4												40.909	Steel	Steel	245	207000	0.3	A	2	11			
79	E	DB.Plate_7	N	0	3600	1800	600	10						L2L4												40.909	Steel	Steel	245	207000	0.3	A	2	11			
80	E	DB.Plate_8	N	0	4200	1800	600	10						L2L4												40.909	Steel	Steel	245	207000	0.3	A	2	11			
81	E	DB.Plate_9	N	0	4800	1800	600	10						L2L4												40.909	Steel	Steel	245	207000	0.3	A	2	11			

##
ProColl Template
##

Filename	Length	Units
Box Girder C	1800	mm

##

##	ELEMENT DESCRIPTORS		COORDINATES:				PLATE DIMMARY LONGITUDINAL DIMENSIONS:								FRAME DIMENSIONS:									MATERIAL DEFINITIONS:						LOAD SHORTENING CURVE:			
ID	Type	Description	Mirror	angle	ycoord	zcoord	b	tp	hwx	twx	bfx	tfx	nsx	loop	hwx2	twx2	bfx2	tfx2	nsx2	hwy	twy	bfy	tfy	·amespacir	nsy	HAZ	Pmat	Smat	str0eq	E	v	Imp	LSCurve	Clone	Sname
82	E	DB.Plate_10	N	0	5400	1800	600	10						L2L4												40.909	Steel	Steel	245	207000	0.3	A	2	11	
83	E	DB.Plate_11	N	0	6000	1800	600	10						L2L4												40.909	Steel	Steel	245	207000	0.3	A	2	11	
84	E	DB.Plate_12	N	0	6600	1800	600	10						L2L4												40.909	Steel	Steel	245	207000	0.3	A	2	11	
85	E	DB.Plate_13	N	0	7200	1800	600	10						L2L4												40.909	Steel	Steel	245	207000	0.3	A	2	11	
86	E	DB.Plate_14	N	0	7800	1800	600	10						L2L4												40.909	Steel	Steel	245	207000	0.3	A	2	11	
87	E	DB.Plate_15	N	0	8400	1800	600	10						L2L4												40.909	Steel	Steel	245	207000	0.3	A	2	11	
88	E	DB.Plate_16	N	0	9000	1800	600	10						L2L4												40.909	Steel	Steel	245	207000	0.3	A	2	11	
89	E	DB.Plate_17	N	0	9600	1800	600	10						L3L8												40.909	Steel	Steel	245	207000	0.3	A	2	12	
90	E	DB.Plate_18	N	0	10200	1800	600	10						L3L8												40.909	Steel	Steel	245	207000	0.3	A	2	12	
91	E	DB.Plate_19	N	0	10800	1800	600	10						L3L8												40.909	Steel	Steel	245	207000	0.3	A	2	12	
92	E	DB.Plate_20	N	0	11400	1800	600	10						L3L8												40.909	Steel	Steel	245	207000	0.3	A	2	12	
93	E	DB.Plate_21	N	0	12000	1800	600	10						L3L8												40.909	Steel	Steel	245	207000	0.3	A	2	12	
94	E	Deck.Plate_1	N	0	0	4800	600	10						L5L6												40.909	Steel	Steel	245	207000	0.3	A	2	13	
95	E	Deck.Plate_2	N	0	600	4800	600	10						L5L6												40.909	Steel	Steel	245	207000	0.3	A	2	13	
96	E	Deck.Plate_3	N	0	1200	4800	600	10						L5L6												40.909	Steel	Steel	245	207000	0.3	A	2	13	
97	E	Deck.Plate_4	N	0	1800	4800	600	10						L5L6												40.909	Steel	Steel	245	207000	0.3	A	2	13	
98	E	Deck.Plate_5	N	0	2400	4800	600	10						L5L6												40.909	Steel	Steel	245	207000	0.3	A	2	13	
99	E	Deck.Plate_6	N	0	9600	4800	600	10						L7L8												40.909	Steel	Steel	245	207000	0.3	A	2	14	
100	E	Deck.Plate_7	N	0	10200	4800	600	10						L7L8												40.909	Steel	Steel	245	207000	0.3	A	2	14	
101	E	Deck.Plate_8	N	0	10800	4800	600	10						L7L8												40.909	Steel	Steel	245	207000	0.3	A	2	14	
102	E	Deck.Plate_9	N	0	11400	4800	600	10						L7L8												40.909	Steel	Steel	245	207000	0.3	A	2	14	
103	E	Deck.Plate_10	N	0	12000	4800	600	10						L7L8												40.909	Steel	Steel	245	207000	0.3	A	2	14	
104	E	Vert. Plate_R_1	N	90	12600	0	600	10						3												40.909	Steel	Steel	245	207000	0.3	A	2	15	
105	E	Vert. Plate_R_2	N	90	12600	600	600	10						3												40.909	Steel	Steel	245	207000	0.3	A	2	15	
106	E	Vert. Plate_R_3	N	90	12600	1200	600	10						3												40.909	Steel	Steel	245	207000	0.3	A	2	15	
107	E	Vert. Plate_R_4	N	90	12600	1800	600	10						8												40.909	Steel	Steel	245	207000	0.3	A	2	16	
108	E	Vert. Plate_R_5	N	90	12600	2400	600	10						8												40.909	Steel	Steel	245	207000	0.3	A	2	16	
109	E	Vert. Plate_R_6	N	90	12600	3000	600	10						8												40.909	Steel	Steel	245	207000	0.3	A	2	16	
110	E	Vert. Plate_R_7	N	90	12600	3600	600	10						8												40.909	Steel	Steel	245	207000	0.3	A	2	16	
111	E	Vert. Plate_R_8	N	90	12600	4200	600	10						8												40.909	Steel	Steel	245	207000	0.3	A	2	16	
112	E	Vert. Plate_R_9	N	90	12600	4800	600	10						7												40.909	Steel	Steel	245	207000	0.3	A	2	17	
113	E	Vert. Plate_R_10	N	90	12600	5400	600	10						7												40.909	Steel	Steel	245	207000	0.3	A	2	17	
114	E	Vert. Plate_R_11	N	90	12600	6000	600	10						7												40.909	Steel	Steel	245	207000	0.3	A	2	17	
115	E	Vert. Plate_R_12	N	90	12600	6600	600	10						7												40.909	Steel	Steel	245	207000	0.3	A	2	17	
116	E	Vert. Plate_R_13	N	90	12600	7200	600	10						7												40.909	Steel	Steel	245	207000	0.3	A	2	17	
117	E	Vert. Plate_R_14	N	90	12600	7800	600	10						7												40.909	Steel	Steel	245	207000	0.3	A	2	17	
118	E	Horz. Plate_Top_1	N	180	12600	8400	600	8						7												40.909	Steel	Steel	245	207000	0.3	A	2	18	
119	E	Horz. Plate_Top_2	N	180	12000	8400	600	8						7												40.909	Steel	Steel	245	207000	0.3	A	2	18	
120	E	Horz. Plate_Top_3	N	180	11400	8400	600	8						7												40.909	Steel	Steel	245	207000	0.3	A	2	18	
121	E	Horz. Plate_Top_4	N	180	10800	8400	600	8						7												40.909	Steel	Steel	245	207000	0.3	A	2	18	
122	E	Horz. Plate_Top_5	N	180	10200	8400	600	8						7												40.909	Steel	Steel	245	207000	0.3	A	2	18	
123	E	Horz. Plate_Top_6	N	180	9600	8400	600	8						4												40.909	Steel	Steel	245	207000	0.3	A	2	19	
124	E	Horz. Plate_Top_7	N	180	9000	8400	600	8						4												40.909	Steel	Steel	245	207000	0.3	A	2	19	
125	E	Horz. Plate_Top_8	N	180	8400	8400	600	8						4												40.909	Steel	Steel	245	207000	0.3	A	2	19	
126	E	Horz. Plate_Top_9	N	180	7800	8400	600	8						4												40.909	Steel	Steel	245	207000	0.3	A	2	19	
127	E	Horz. Plate_Top_10	N	180	7200	8400	600	8						4												40.909	Steel	Steel	245	207000	0.3	A	2	19	
128	E	Horz. Plate_Top_11	N	180	6600	8400	600	8						4												40.909	Steel	Steel	245	207000	0.3	A	2	19	
129	E	Horz. Plate_Top_12	N	180	6000	8400	600	8						4												40.909	Steel	Steel	245	207000	0.3	A	2	19	
130	E	Horz. Plate_Top_13	N	180	5400	8400	600	8						4												40.909	Steel	Steel	245	207000	0.3	A	2	19	
131	E	Horz. Plate_Top_14	N	180	4800	8400	600	8						4												40.909	Steel	Steel	245	207000	0.3	A	2	19	
132	E	Horz. Plate_Top_15	N	180	4200	8400	600	8						4												40.909	Steel	Steel	245	207000	0.3	A	2	19	
133	E	Horz. Plate_Top_16	N	180	3600	8400	600	8						4												40.909	Steel	Steel	245	207000	0.3	A	2	19	
134	E	Horz. Plate_Top_17	N	180	3000	8400	600	8						6												40.909	Steel	Steel	245	207000	0.3	A	2	20	
135	E	Horz. Plate_Top_18	N	180	2400	8400	600	8						6												40.909	Steel	Steel	245	207000	0.3	A	2	20	
136	E	Horz. Plate_Top_19	N	180	1800	8400	600	8						6												40.909	Steel	Steel	245	207000	0.3	A	2	20	
137	E	Horz. Plate_Top_20	N	180	1200	8400	600	8						6												40.909	Steel	Steel	245	207000	0.3	A	2	20	
138	E	Horz. Plate_Top_21	N	180	600	8400	600	8						6												40.909	Steel	Steel	245	207000	0.3	A	2	20	
139	E	Vert. Plate_Left_1	N	270	0	8400	600	10						6												40.909	Steel	Steel	245	207000	0.3	A	2	21	
140	E	Vert. Plate_Left_2	N	270	0	7800	600	10						6												40.909	Steel	Steel	245	207000	0.3	A	2	21	
141	E	Vert. Plate_Left_3	N	270	0	7200	600	10						6												40.909	Steel	Steel	245	207000	0.3	A	2	21	
142	E	Vert. Plate_Left_4	N	270	0	6600	600	10						6												40.909	Steel	Steel	245	207000	0.3	A	2	21	
143	E	Vert. Plate_Left_5	N	270	0	6000	600	10						6												40.909	Steel	Steel	245	207000	0.3	A	2	21	
144	E	Vert. Plate_Left_6	N	270	0	5400	600	10						6												40.909	Steel	Steel	245	207000	0.3	A	2	21	
145	E	Vert. Plate_Left_7	N	270	0	4800	600	10						5												40.909	Steel	Steel	245	207000	0.3	A	2	22	
146	E	Vert. Plate_Left_8	N	270	0	4200	600	10						5												40.909	Steel	Steel	245	207000	0.3	A	2	22	
147	E	Vert. Plate_Left_9	N	270	0	3600	600	10						5												40.909	Steel	Steel	245	207000	0.3	A	2	22	
148	E	Vert. Plate_Left_10	N	270	0	3000	600	10						5												40.909	Steel	Steel	245	207000	0.3	A	2	22	
149	E	Vert. Plate_Left_11	N	270	0	2400	600	10						5												40.909	Steel	Steel	245	207000	0.3	A	2	22	
150	E	Vert. Plate_Left_12	N	270	0	1800	600	10						1												40.909	Steel	Steel	245	207000	0.3	A	2	23	
151	E	Vert. Plate_Left_13	N	270	0	1200	600	10						1												40.909	Steel	Steel	245	207000	0.3	A	2	23	
152	E	Vert. Plate_Left_14	N	270	0	600	600	10						1												40.909	Steel	Steel	245	207000	0.3	A	2	23	
153	E	bottom_stif_1	N	0	600	0			113.6	6.65	63.5	13.4	1													17.318	Steel	Steel	245	207000	0.3	A	2	1	
154	E	bottom_stif_2	N	0	1200	0			113.6	6.65	63.5	13.4	1													17.318	Steel	Steel	245	207000	0.3	A	2	1	
155	E	bottom_stif_3	N	0	1800	0			113.6	6.65	63.5	13.4	1													17.318	Steel	Steel	245	207000	0.3	A	2	1	
156	E	bottom_stif_4	N	0	2400	0			113.6	6.65	63.5	13.4	1													17.318	Steel	Steel	245	207000	0.3	A	2	1	
157	E	L_V.db_stif_1	N	90	3000	600			113.6	6.65	63.5	13.4	1													17.318	Steel	Steel	245	207000	0.3	A	2	3	
158	E	L_V.db_stif_2	N	90	3000	1200			113.6	6.65	63.5	13.4	1													17.318	Steel	Steel	245	207000	0.3	A	2	3	
159	E	L_V.ds_stif_1	N	90	3000	2400			113.6	6.65	63.5	13.4	1													17.318	Steel	Steel	245	207000	0.3	A	2	4	
160	E	L_V.ds_stif_2	N	90	3000	3000			113.6	6.65	63.5	13.4	1													17.318	Steel	Steel	245	207000	0.3	A	2	4	
161	E	L_V.ds_stif_3	N	90	3000	3600			113.6	6.65	63.5	13.4	1													17.318	Steel	Steel	245	207000	0.3	A	2	4	
162	E	L_V.ds_stif_4	N	90	3000	4200			113.6	6.65	63.5	13.4	1													17.318	Steel	Steel	245	207000	0.3	A	2	4	

##
ProColl Template
##

Filename	Length	Units
Box Girder C	1800	mm

##

##	ELEMENT DESCRIPTORS		COORDINATES:				PLATE DIMMARY LONGITUDINAL DIMENSIONS:								FRAME DIMENSIONS:									MATERIAL DEFINITIONS:							LOAD SHORTENING CURVE:			
ID	Type	Description	Mirror	angle	ycoord	zcoord	b	tp	hwx	twx	bfx	tfx	nsx	loop	hwx2	twx2	bfx2	tfx2	nsx2	hwy	twy	bfy	tfy	amespacir	nsy	HAZ	Pmat	Smat	str0eq	E	v	Imp	LSCurve	Clone	Sname
163	E	L_V.ds_stif_6	N	90	3000	5400			113.6	6.65	63.5	13.4	1													17.318	Steel	Steel	245	207000	0.3	A	2	5	
164	E	L_V.ds_stif_7	N	90	3000	6000			113.6	6.65	63.5	13.4	1													17.318	Steel	Steel	245	207000	0.3	A	2	5	
165	E	L_V.ds_stif_8	N	90	3000	6600			113.6	6.65	63.5	13.4	1													17.318	Steel	Steel	245	207000	0.3	A	2	5	
166	E	L_V.ds_stif_9	N	90	3000	7200			113.6	6.65	63.5	13.4	1													17.318	Steel	Steel	245	207000	0.3	A	2	5	
167	E	L_V.ds_stif_10	N	90	3000	7800			113.6	6.65	63.5	13.4	1													17.318	Steel	Steel	245	207000	0.3	A	2	5	
168	E	R_V.db_stif_1	N	270	9600	600			113.6	6.65	63.5	13.4	1													17.318	Steel	Steel	245	207000	0.3	A	2	6	
169	E	R_V.db_stif_2	N	270	9600	1200			113.6	6.65	63.5	13.4	1													17.318	Steel	Steel	245	207000	0.3	A	2	6	
170	E	R_V.ds_stif_1	N	270	9600	2400			113.6	6.65	63.5	13.4	1													17.318	Steel	Steel	245	207000	0.3	A	2	7	
171	E	R_V.ds_stif_2	N	270	9600	3000			113.6	6.65	63.5	13.4	1													17.318	Steel	Steel	245	207000	0.3	A	2	7	
172	E	R_V.ds_stif_3	N	270	9600	3600			113.6	6.65	63.5	13.4	1													17.318	Steel	Steel	245	207000	0.3	A	2	7	
173	E	R_V.ds_stif_4	N	270	9600	4200			113.6	6.65	63.5	13.4	1													17.318	Steel	Steel	245	207000	0.3	A	2	7	
174	E	R_V.ds_stif_6	N	270	9600	5400			113.6	6.65	63.5	13.4	1													17.318	Steel	Steel	245	207000	0.3	A	2	8	
175	E	R_V.ds_stif_7	N	270	9600	6000			113.6	6.65	63.5	13.4	1													17.318	Steel	Steel	245	207000	0.3	A	2	8	
176	E	R_V.ds_stif_8	N	270	9600	6600			113.6	6.65	63.5	13.4	1													17.318	Steel	Steel	245	207000	0.3	A	2	8	
177	E	R_V.ds_stif_9	N	270	9600	7200			113.6	6.65	63.5	13.4	1													17.318	Steel	Steel	245	207000	0.3	A	2	8	
178	E	R_V.ds_stif_10	N	270	9600	7800			113.6	6.65	63.5	13.4	1													17.318	Steel	Steel	245	207000	0.3	A	2	8	
179	E	Deck_Hor_stif_1	N	180	600	4800			113.6	6.65	63.5	13.4	1													17.318	Steel	Steel	245	207000	0.3	A	2	13	
180	E	Deck_Hor_stif_2	N	180	1200	4800			113.6	6.65	63.5	13.4	1													17.318	Steel	Steel	245	207000	0.3	A	2	13	
181	E	Deck_Hor_stif_3	N	180	1800	4800			113.6	6.65	63.5	13.4	1													17.318	Steel	Steel	245	207000	0.3	A	2	13	
182	E	Deck_Hor_stif_4	N	180	2400	4800			113.6	6.65	63.5	13.4	1													17.318	Steel	Steel	245	207000	0.3	A	2	13	
183	E	Deck_Hor_stif_5	N	180	10200	4800			113.6	6.65	63.5	13.4	1													17.318	Steel	Steel	245	207000	0.3	A	2	14	
184	E	Deck_Hor_stif_6	N	180	10800	4800			113.6	6.65	63.5	13.4	1													17.318	Steel	Steel	245	207000	0.3	A	2	14	
185	E	Deck_Hor_stif_7	N	180	11400	4800			113.6	6.65	63.5	13.4	1													17.318	Steel	Steel	245	207000	0.3	A	2	14	
186	E	Deck_Hor_stif_8	N	180	12000	4800			113.6	6.65	63.5	13.4	1													17.318	Steel	Steel	245	207000	0.3	A	2	14	
187	E	bottom_stif_6	N	0	3600	0			113.6	6.65	63.5	13.4	1													17.318	Steel	Steel	245	207000	0.3	A	2	2	
188	E	bottom_stif_7	N	0	4200	0			113.6	6.65	63.5	13.4	1													17.318	Steel	Steel	245	207000	0.3	A	2	2	
189	E	bottom_stif_8	N	0	4800	0			113.6	6.65	63.5	13.4	1													17.318	Steel	Steel	245	207000	0.3	A	2	2	
190	E	bottom_stif_9	N	0	5400	0			113.6	6.65	63.5	13.4	1													17.318	Steel	Steel	245	207000	0.3	A	2	2	
191	E	bottom_stif_10	N	0	6000	0			113.6	6.65	63.5	13.4	1													17.318	Steel	Steel	245	207000	0.3	A	2	2	
192	E	bottom_stif_11	N	0	6600	0			113.6	6.65	63.5	13.4	1													17.318	Steel	Steel	245	207000	0.3	A	2	2	
193	E	bottom_stif_12	N	0	7200	0			113.6	6.65	63.5	13.4	1													17.318	Steel	Steel	245	207000	0.3	A	2	2	
194	E	bottom_stif_13	N	0	7800	0			113.6	6.65	63.5	13.4	1													17.318	Steel	Steel	245	207000	0.3	A	2	2	
195	E	bottom_stif_14	N	0	8400	0			113.6	6.65	63.5	13.4	1													17.318	Steel	Steel	245	207000	0.3	A	2	2	
196	E	bottom_stif_15	N	0	9000	0			113.6	6.65	63.5	13.4	1													17.318	Steel	Steel	245	207000	0.3	A	2	2	
197	E	bottom_stif_17	N	0	10200	0			113.6	6.65	63.5	13.4	1													17.318	Steel	Steel	245	207000	0.3	A	2	9	
198	E	bottom_stif_18	N	0	10800	0			113.6	6.65	63.5	13.4	1													17.318	Steel	Steel	245	207000	0.3	A	2	9	
199	E	bottom_stif_19	N	0	11400	0			113.6	6.65	63.5	13.4	1													17.318	Steel	Steel	245	207000	0.3	A	2	9	
200	E	bottom_stif_20	N	0	12000	0			113.6	6.65	63.5	13.4	1													17.318	Steel	Steel	245	207000	0.3	A	2	9	
201	E	rightside_stif_1	N	90	12600	600			113.6	6.65	63.5	13.4	1													17.318	Steel	Steel	245	207000	0.3	A	2	15	
202	E	rightside_stif_2	N	90	12600	1200			113.6	6.65	63.5	13.4	1													17.318	Steel	Steel	245	207000	0.3	A	2	15	
203	E	rightside_stif_4	N	90	12600	2400			113.6	6.65	63.5	13.4	1													17.318	Steel	Steel	245	207000	0.3	A	2	16	
204	E	rightside_stif_5	N	90	12600	3000			113.6	6.65	63.5	13.4	1													17.318	Steel	Steel	245	207000	0.3	A	2	16	
205	E	rightside_stif_6	N	90	12600	3600			113.6	6.65	63.5	13.4	1													17.318	Steel	Steel	245	207000	0.3	A	2	16	
206	E	rightside_stif_7	N	90	12600	4200			113.6	6.65	63.5	13.4	1													17.318	Steel	Steel	245	207000	0.3	A	2	16	
207	E	rightside_stif_9	N	90	12600	5400			113.6	6.65	63.5	13.4	1													17.318	Steel	Steel	245	207000	0.3	A	2	17	
208	E	rightside_stif_10	N	90	12600	6000			113.6	6.65	63.5	13.4	1													17.318	Steel	Steel	245	207000	0.3	A	2	17	
209	E	rightside_stif_11	N	90	12600	6600			113.6	6.65	63.5	13.4	1													17.318	Steel	Steel	245	207000	0.3	A	2	17	
210	E	rightside_stif_12	N	90	12600	7200			113.6	6.65	63.5	13.4	1													17.318	Steel	Steel	245	207000	0.3	A	2	17	
211	E	rightside_stif_13	N	90	12600	7800			113.6	6.65	63.5	13.4	1													17.318	Steel	Steel	245	207000	0.3	A	2	17	
212	E	top_stif_1	N	180	12000	8400			113.6	6.65	63.5	13.4	1													17.318	Steel	Steel	245	207000	0.3	A	2	18	
213	E	top_stif_2	N	180	11400	8400			113.6	6.65	63.5	13.4	1													17.318	Steel	Steel	245	207000	0.3	A	2	18	
214	E	top_stif_3	N	180	10800	8400			113.6	6.65	63.5	13.4	1													17.318	Steel	Steel	245	207000	0.3	A	2	18	
215	E	top_stif_4	N	180	10200	8400			113.6	6.65	63.5	13.4	1													17.318	Steel	Steel	245	207000	0.3	A	2	18	
216	E	top_stif_6	N	180	9000	8400			113.6	6.65	63.5	13.4	1													17.318	Steel	Steel	245	207000	0.3	A	2	19	
217	E	top_stif_7	N	180	8400	8400			113.6	6.65	63.5	13.4	1													17.318	Steel	Steel	245	207000	0.3	A	2	19	
218	E	top_stif_8	N	180	7800	8400			113.6	6.65	63.5	13.4	1													17.318	Steel	Steel	245	207000	0.3	A	2	19	
219	E	top_stif_9	N	180	7200	8400			113.6	6.65	63.5	13.4	1													17.318	Steel	Steel	245	207000	0.3	A	2	19	
220	E	top_stif_10	N	180	6600	8400			113.6	6.65	63.5	13.4	1													17.318	Steel	Steel	245	207000	0.3	A	2	19	
221	E	top_stif_11	N	180	6000	8400			113.6	6.65	63.5	13.4	1													17.318	Steel	Steel	245	207000	0.3	A	2	19	
222	E	top_stif_12	N	180	5400	8400			113.6	6.65	63.5	13.4	1													17.318	Steel	Steel	245	207000	0.3	A	2	19	
223	E	top_stif_13	N	180	4800	8400			113.6	6.65	63.5	13.4	1													17.318	Steel	Steel	245	207000	0.3	A	2	19	
224	E	top_stif_14	N	180	4200	8400			113.6	6.65	63.5	13.4	1													17.318	Steel	Steel	245	207000	0.3	A	2	19	
225	E	top_stif_15	N	180	3600	8400			113.6	6.65	63.5	13.4	1													17.318	Steel	Steel	245	207000	0.3	A	2	19	
226	E	top_stif_17	N	180	2400	8400			113.6	6.65	63.5	13.4	1													17.318	Steel	Steel	245	207000	0.3	A	2	20	
227	E	top_stif_18	N	180	1800	8400			113.6	6.65	63.5	13.4	1													17.318	Steel	Steel	245	207000	0.3	A	2	20	
228	E	top_stif_19	N	180	1200	8400			113.6	6.65	63.5	13.4	1													17.318	Steel	Steel	245	207000	0.3	A	2	20	
229	E	top_stif_20	N	180	600	8400			113.6	6.65	63.5	13.4	1													17.318	Steel	Steel	245	207000	0.3	A	2	20	
230	E	leftside_stif_1	N	270	0	7800			113.6	6.65	63.5	13.4	1													17.318	Steel	Steel	245	207000	0.3	A	2	21	
231	E	leftside_stif_2	N	270	0	7200			113.6	6.65	63.5	13.4	1													17.318	Steel	Steel	245	207000	0.3	A	2	21	
232	E	leftside_stif_3	N	270	0	6600			113.6	6.65	63.5	13.4	1													17.318	Steel	Steel	245	207000	0.3	A	2	21	
233	E	leftside_stif_4	N	270	0	6000			113.6	6.65	63.5	13.4	1													17.318	Steel	Steel	245	207000	0.3	A	2	21	
234	E	leftside_stif_5	N	270	0	5400			113.6	6.65	63.5	13.4	1													17.318	Steel	Steel	245	207000	0.3	A	2	21	
235	E	leftside_stif_7	N	270	0	4200			113.6	6.65	63.5	13.4	1													17.318	Steel	Steel	245	207000	0.3	A	2	22	
236	E	leftside_stif_8	N	270	0	3600			113.6	6.65	63.5	13.4	1													17.318	Steel	Steel	245	207000	0.3	A	2	22	
237	E	leftside_stif_9		270	0	3000			113.6	6.65	63.5	13.4	1													17.318	Steel	Steel	245	207000	0.3	A	2	22	
238	E	leftside_stif_10		270	0	2400			113.6	6.65	63.5	13.4	1													17.318	Steel	Steel	245	207000	0.3	A	2	22	
239	E	leftside_stif_12		270	0	1200			113.6	6.65	63.5	13.4	1													17.318	Steel	Steel	245	207000	0.3	A	2	23	
240	E	leftside_stif_13		270	0	600			113.6	6.65	63.5	13.4	1													17.318	Steel	Steel	245	207000	0.3	A	2	23	
241	E	D.B._stif_1		180	12000	1800			113.6	6.65	63.5	13.4	1													17.318	Steel	Steel	245	207000	0.3	A	2	12	
242	E	D.B._stif_2		180	11400	1800			113.6	6.65	63.5	13.4	1													17.318	Steel	Steel	245	207000	0.3	A	2	12	
243	E	D.B._stif_3		180	10800	1800			113.6	6.65	63.5	13.4	1													17.318	Steel	Steel	245	207000	0.3	A	2	12	

##																																	
##	ProColl Template																																
##																																	
Filename	Length	Units																															
Box Girder C	1800	mm																															
##																																	
##	ELEMENT DESCRIPTORS		COORDINATES:				PLATE DIMMARY LONGITUDINAL DIMENSIONS:							FRAME DIMENSIONS:										MATERIAL DEFINITIONS:								LOAD SHORTENING CURVE:			
ID	Type	Description	Mirror	angle	ycoord	zcoord	b	tp	hwx	twx	bfx	tfx	nsx	loop	hwx2	twx2	bfx2	tfx2	nsx2	hwy	twy	bfy	tfy	amespacii	nsy	HAZ	Pmat	Smat	str0eq	E	v	Imp	LSCurve	Clone	Sname
244	E	D.B._stif_4		180	10200	1800			113.6	6.65	63.5	13.4	1													17.318	Steel	Steel	245	207000	0.3	A	2	12	
245	E	D.B._stif_6		180	9000	1800			113.6	6.65	63.5	13.4	1													17.318	Steel	Steel	245	207000	0.3	A	2	11	
246	E	D.B._stif_7		180	8400	1800			113.6	6.65	63.5	13.4	1													17.318	Steel	Steel	245	207000	0.3	A	2	11	
247	E	D.B._stif_8		180	7800	1800			113.6	6.65	63.5	13.4	1													17.318	Steel	Steel	245	207000	0.3	A	2	11	
248	E	D.B._stif_9		180	7200	1800			113.6	6.65	63.5	13.4	1													17.318	Steel	Steel	245	207000	0.3	A	2	11	
249	E	D.B._stif_10		180	6600	1800			113.6	6.65	63.5	13.4	1													17.318	Steel	Steel	245	207000	0.3	A	2	11	
250	E	D.B._stif_11		180	6000	1800			113.6	6.65	63.5	13.4	1													17.318	Steel	Steel	245	207000	0.3	A	2	11	
251	E	D.B._stif_12		180	5400	1800			113.6	6.65	63.5	13.4	1													17.318	Steel	Steel	245	207000	0.3	A	2	11	
252	E	D.B._stif_13		180	4800	1800			113.6	6.65	63.5	13.4	1													17.318	Steel	Steel	245	207000	0.3	A	2	11	
253	E	D.B._stif_14		180	4200	1800			113.6	6.65	63.5	13.4	1													17.318	Steel	Steel	245	207000	0.3	A	2	11	
254	E	D.B._stif_15		180	3600	1800			113.6	6.65	63.5	13.4	1													17.318	Steel	Steel	245	207000	0.3	A	2	11	
255	E	D.B._stif_17		180	2400	1800			113.6	6.65	63.5	13.4	1													17.318	Steel	Steel	245	207000	0.3	A	2	10	
256	E	D.B._stif_18		180	1800	1800			113.6	6.65	63.5	13.4	1													17.318	Steel	Steel	245	207000	0.3	A	2	10	
257	E	D.B._stif_19		180	1200	1800			113.6	6.65	63.5	13.4	1													17.318	Steel	Steel	245	207000	0.3	A	2	10	
258	E	D.B._stif_20		180	600	1800			113.6	6.65	63.5	13.4	1													17.318	Steel	Steel	245	207000	0.3	A	2	10	

d. Box Girder D

##																																		
##	ProColl Template																																
##																																	
Filename	Length	Units																															
Box Girder D	1800	mm																															
##																																	
##	ELEMENT DESCRIPTORS		COORDINATES:				PLATE DIMMARY LONGITUDINAL DIMENSIONS:												FRAME DIMENSIONS:					MATERIAL DEFINITIONS:							LOAD SHORTENING CURVE:			
ID	Type	Description	Mirror	angle	ycoord	zcoord	b	tp	hwx	twx	bfx	tfx	nsx	loop	hwx2	twx2	bfx2	tfx2	nsx2	hwy	twy	bfy	tfy	ramespacir	nsy	HAZ	Pmat	Smat	str0eq	E	v	Imp	LSCurve	Clone	Sname
1	LSC		N				600	8	113.6	6.65	63.5	13.4	4							227.2	13.3	127	26.8		5	40.909	Steel	Steel	245	207000	0.3	A	1		
2	LSC		N				600	8	113.6	6.65	63.5	13.4	10							227.2	13.3	127	26.8		5	40.909	Steel	Steel	245	207000	0.3	A	1		
3	LSC		N				600	8	113.6	6.65	63.5	13.4	2							227.2	13.3	127	26.8		5	40.909	Steel	Steel	245	207000	0.3	A	1		
4	LSC		N				600	8	113.6	6.65	63.5	13.4	4							227.2	13.3	127	26.8		5	40.909	Steel	Steel	245	207000	0.3	A	1		
5	LSC		N				600	8	113.6	6.65	63.5	13.4	5							227.2	13.3	127	26.8		5	40.909	Steel	Steel	245	207000	0.3	A	1		
6	LSC		N				600	8	113.6	6.65	63.5	13.4	2							227.2	13.3	127	26.8		5	40.909	Steel	Steel	245	207000	0.3	A	1		
7	LSC		N				600	8	113.6	6.65	63.5	13.4	4							227.2	13.3	127	26.8		5	40.909	Steel	Steel	245	207000	0.3	A	1		
8	LSC		N				600	8	113.6	6.65	63.5	13.4	5							227.2	13.3	127	26.8		5	40.909	Steel	Steel	245	207000	0.3	A	1		
9	LSC		N				600	8	113.6	6.65	63.5	13.4	4							227.2	13.3	127	26.8		5	40.909	Steel	Steel	245	207000	0.3	A	1		
10	LSC		N				600	10	113.6	6.65	63.5	13.4	4							227.2	13.3	127	26.8		5	40.909	Steel	Steel	245	207000	0.3	A	1		
11	LSC		N				600	10	113.6	6.65	63.5	13.4	10							227.2	13.3	127	26.8		5	40.909	Steel	Steel	245	207000	0.3	A	1		
12	LSC		N				600	10	113.6	6.65	63.5	13.4	4							227.2	13.3	127	26.8		5	40.909	Steel	Steel	245	207000	0.3	A	1		
13	LSC		N				600	10	113.6	6.65	63.5	13.4	4							227.2	13.3	127	26.8		5	40.909	Steel	Steel	245	207000	0.3	A	1		
14	LSC		N				600	10	113.6	6.65	63.5	13.4	4							227.2	13.3	127	26.8		5	40.909	Steel	Steel	245	207000	0.3	A	1		
15	LSC		N				600	10	113.6	6.65	63.5	13.4	2							227.2	13.3	127	26.8		5	40.909	Steel	Steel	245	207000	0.3	A	1		
16	LSC		N				600	10	113.6	6.65	63.5	13.4	4							227.2	13.3	127	26.8		5	40.909	Steel	Steel	245	207000	0.3	A	1		
17	LSC		N				600	10	113.6	6.65	63.5	13.4	5							227.2	13.3	127	26.8		5	40.909	Steel	Steel	245	207000	0.3	A	1		
18	LSC		N				600	8	113.6	6.65	63.5	13.4	4							227.2	13.3	127	26.8		5	40.909	Steel	Steel	245	207000	0.3	A	1		
19	LSC		N				600	8	113.6	6.65	63.5	13.4	4							227.2	13.3	127	26.8		5	40.909	Steel	Steel	245	207000	0.3	A	1		
20	LSC		N				600	10	113.6	6.65	63.5	13.4	5							227.2	13.3	127	26.8		5	40.909	Steel	Steel	245	207000	0.3	A	1		
21	LSC		N				600	10	113.6	6.65	63.5	13.4	4							227.2	13.3	127	26.8		5	40.909	Steel	Steel	245	207000	0.3	A	1		
22	LSC		N				600	10	113.6	6.65	63.5	13.4	2							227.2	13.3	127	26.8		5	40.909	Steel	Steel	245	207000	0.3	A	1		
23	E	Horz. Plate_1	N	0	0	0	600	8						1												40.909	Steel	Steel	245	207000	0.3	A	2	1	
24	E	Horz. Plate_2	N	0	600	0	600	8						1												40.909	Steel	Steel	245	207000	0.3	A	2	1	
25	E	Horz. Plate_3	N	0	1200	0	600	8						1												40.909	Steel	Steel	245	207000	0.3	A	2	1	
26	E	Horz. Plate_4	N	0	1800	0	600	8						1												40.909	Steel	Steel	245	207000	0.3	A	2	1	
27	E	Horz. Plate_5	N	0	2400	0	600	8						1												40.909	Steel	Steel	245	207000	0.3	A	2	1	
28	E	Horz. Plate_6	N	0	3000	0	600	8						2												40.909	Steel	Steel	245	207000	0.3	A	2	2	
29	E	V_db.Plate_L_1	N	90	3000	0	600	8						L1L2												40.909	Steel	Steel	245	207000	0.3	A	2	3	
30	E	V_db.Plate_L_2	N	90	3000	600	600	8						L1L2												40.909	Steel	Steel	245	207000	0.3	A	2	3	
31	E	V_db.Plate_L_3	N	90	3000	1200	600	8						L1L2												40.909	Steel	Steel	245	207000	0.3	A	2	3	
32	E	V_ds.Plate_L_1	N	90	3000	1800	600	8						5												40.909	Steel	Steel	245	207000	0.3	A	2	4	
33	E	V_ds.Plate_L_2	N	90	3000	2400	600	8						5												40.909	Steel	Steel	245	207000	0.3	A	2	4	
34	E	V_ds.Plate_L_3	N	90	3000	3000	600	8						5												40.909	Steel	Steel	245	207000	0.3	A	2	4	
35	E	V_ds.Plate_L_4	N	90	3000	3600	600	8						5												40.909	Steel	Steel	245	207000	0.3	A	2	4	
36	E	V_ds.Plate_L_5	N	90	3000	4200	600	8						5												40.909	Steel	Steel	245	207000	0.3	A	2	4	
37	E	V_ds.Plate_L_6	N	90	3000	4800	600	8						6												40.909	Steel	Steel	245	207000	0.3	A	2	5	
38	E	V_ds.Plate_L_7	N	90	3000	5400	600	8						6												40.909	Steel	Steel	245	207000	0.3	A	2	5	
39	E	V_ds.Plate_L_8	N	90	3000	6000	600	8						6												40.909	Steel	Steel	245	207000	0.3	A	2	5	
40	E	V_ds.Plate_L_9	N	90	3000	6600	600	8						6												40.909	Steel	Steel	245	207000	0.3	A	2	5	
41	E	V_ds.Plate_L_10	N	90	3000	7200	600	8						6												40.909	Steel	Steel	245	207000	0.3	A	2	5	
42	E	V_ds.Plate_L_11	N	90	3000	7800	600	8						6												40.909	Steel	Steel	245	207000	0.3	A	2	5	
43	E	V_db.Plate_R_1	N	90	9600	0	600	8						L2L3												40.909	Steel	Steel	245	207000	0.3	A	2	6	
44	E	V_db.Plate_R_2	N	90	9600	600	600	8						L2L3												40.909	Steel	Steel	245	207000	0.3	A	2	6	
45	E	V_db.Plate_R_3	N	90	9600	1200	600	8						L2L3												40.909	Steel	Steel	245	207000	0.3	A	2	6	
46	E	V_ds.Plate_R_1	N	90	9600	1800	600	8						8												40.909	Steel	Steel	245	207000	0.3	A	2	7	
47	E	V_ds.Plate_R_2	N	90	9600	2400	600	8						8												40.909	Steel	Steel	245	207000	0.3	A	2	7	
48	E	V_ds.Plate_R_3	N	90	9600	3000	600	8						8												40.909	Steel	Steel	245	207000	0.3	A	2	7	
49	E	V_ds.Plate_R_4	N	90	9600	3600	600	8						8												40.909	Steel	Steel	245	207000	0.3	A	2	7	
50	E	V_ds.Plate_R_5	N	90	9600	4200	600	8						8												40.909	Steel	Steel	245	207000	0.3	A	2	7	
51	E	V_ds.Plate_R_6	N	90	9600	4800	600	8						7												40.909	Steel	Steel	245	207000	0.3	A	2	8	
52	E	V_ds.Plate_R_7	N	90	9600	5400	600	8						7												40.909	Steel	Steel	245	207000	0.3	A	2	8	
53	E	V_ds.Plate_R_8	N	90	9600	6000	600	8						7												40.909	Steel	Steel	245	207000	0.3	A	2	8	
54	E	V_ds.Plate_R_9	N	90	9600	6600	600	8						7												40.909	Steel	Steel	245	207000	0.3	A	2	8	
55	E	V_ds.Plate_R_10	N	90	9600	7200	600	8						7												40.909	Steel	Steel	245	207000	0.3	A	2	8	
56	E	V_ds.Plate_R_11	N	90	9600	7800	600	8						7												40.909	Steel	Steel	245	207000	0.3	A	2	8	
57	E	Horz. Plate_7	N	0	3600	0	600	8						2												40.909	Steel	Steel	245	207000	0.3	A	2	2	
58	E	Horz. Plate_8	N	0	4200	0	600	8						2												40.909	Steel	Steel	245	207000	0.3	A	2	2	
59	E	Horz. Plate_9	N	0	4800	0	600	8						2												40.909	Steel	Steel	245	207000	0.3	A	2	2	
60	E	Horz. Plate_10	N	0	5400	0	600	8						2												40.909	Steel	Steel	245	207000	0.3	A	2	2	
61	E	Horz. Plate_11	N	0	6000	0	600	8						2												40.909	Steel	Steel	245	207000	0.3	A	2	2	
62	E	Horz. Plate_12	N	0	6600	0	600	8						2												40.909	Steel	Steel	245	207000	0.3	A	2	2	
63	E	Horz. Plate_13	N	0	7200	0	600	8						2												40.909	Steel	Steel	245	207000	0.3	A	2	2	
64	E	Horz. Plate_14	N	0	7800	0	600	8						2												40.909	Steel	Steel	245	207000	0.3	A	2	2	
65	E	Horz. Plate_15	N	0	8400	0	600	8						2												40.909	Steel	Steel	245	207000	0.3	A	2	2	
66	E	Horz. Plate_16	N	0	9000	0	600	8						2												40.909	Steel	Steel	245	207000	0.3	A	2	2	
67	E	Horz. Plate_17	N	0	9600	0	600	8						3												40.909	Steel	Steel	245	207000	0.3	A	2	9	
68	E	Horz. Plate_18	N	0	10200	0	600	8						3												40.909	Steel	Steel	245	207000	0.3	A	2	9	
69	E	Horz. Plate_19	N	0	10800	0	600	8						3												40.909	Steel	Steel	245	207000	0.3	A	2	9	
70	E	Horz. Plate_20	N	0	11400	0	600	8						3												40.909	Steel	Steel	245	207000	0.3	A	2	9	
71	E	Horz. Plate_21	N	0	12000	0	600	8						3												40.909	Steel	Steel	245	207000	0.3	A	2	9	
72	E	DB.Plate_1	N	0	0	1800	600	10						L1L5												40.909	Steel	Steel	245	207000	0.3	A	2	10	
73	E	DB.Plate_2	N	0	600	1800	600	10						L1L5												40.909	Steel	Steel	245	207000	0.3	A	2	10	
74	E	DB.Plate_3	N	0	1200	1800	600	10						L1L5												40.909	Steel	Steel	245	207000	0.3	A	2	10	
75	E	DB.Plate_4	N	0	1800	1800	600	10						L1L5												40.909	Steel	Steel	245	207000	0.3	A	2	10	
76	E	DB.Plate_5	N	0	2400	1800	600	10						L1L5												40.909	Steel	Steel	245	207000	0.3	A	2	10	
77	E	DB.Plate_6	N	0	3000	1800	600	10						2												40.909	Steel	Steel	245	207000	0.3	A	2	11	
78	E	DB.Plate_7	N	0	3600	1800	600	10						2												40.909	Steel	Steel	245	207000	0.3	A	2	11	
79	E	DB.Plate_8	N	0	4200	1800	600	10						2												40.909	Steel	Steel	245	207000	0.3	A	2	11	
80	E	DB.Plate_9	N	0	4800	1800	600	10						2												40.909	Steel	Steel	245	207000	0.3	A	2	11	
81	E	DB.Plate_10	N	0	5400	1800	600	10						2												40.909	Steel	Steel	245	207000	0.3	A	2	11	

##
ProColl Template
##

Filename	Length	Units
Box Girder D	1800	mm

##

##	ELEMENT DESCRIPTORS		COORDINATES:				PLATE DIMMARY LONGITUDINAL DIMENSIONS:							FRAME DIMENSIONS:										MATERIAL DEFINITIONS:						LOAD SHORTENING CURVE:			
ID	Type	Description	Mirror	angle	ycoord	zcoord	b	tp	hwx	twx	bfx	tfx	nsx	loop	hwx2	twx2	bfx2	tfx2	nsx2	hwy	twy	bfy	tfy	amespacir	nsy	HAZ	Pmat	Smat	str0eq	E	v	Imp	LSCurve	Clone	Sname
82	E	DB.Plate_11	N	0	6000	1800	600	10						2												40.909	Steel	Steel	245	207000	0.3	A	2	11	
83	E	DB.Plate_12	N	0	6600	1800	600	10						2												40.909	Steel	Steel	245	207000	0.3	A	2	11	
84	E	DB.Plate_13	N	0	7200	1800	600	10						2												40.909	Steel	Steel	245	207000	0.3	A	2	11	
85	E	DB.Plate_14	N	0	7800	1800	600	10						2												40.909	Steel	Steel	245	207000	0.3	A	2	11	
86	E	DB.Plate_15	N	0	8400	1800	600	10						2												40.909	Steel	Steel	245	207000	0.3	A	2	11	
87	E	DB.Plate_16	N	0	9000	1800	600	10						2												40.909	Steel	Steel	245	207000	0.3	A	2	11	
88	E	DB.Plate_17	N	0	9600	1800	600	10						L3L8												40.909	Steel	Steel	245	207000	0.3	A	2	12	
89	E	DB.Plate_18	N	0	10200	1800	600	10						L3L8												40.909	Steel	Steel	245	207000	0.3	A	2	12	
90	E	DB.Plate_19	N	0	10800	1800	600	10						L3L8												40.909	Steel	Steel	245	207000	0.3	A	2	12	
91	E	DB.Plate_20	N	0	11400	1800	600	10						L3L8												40.909	Steel	Steel	245	207000	0.3	A	2	12	
92	E	DB.Plate_21	N	0	12000	1800	600	10						L3L8												40.909	Steel	Steel	245	207000	0.3	A	2	12	
93	E	Deck.Plate_1	N	0	0	4800	600	10						L5L6												40.909	Steel	Steel	245	207000	0.3	A	2	13	
94	E	Deck.Plate_2	N	0	600	4800	600	10						L5L6												40.909	Steel	Steel	245	207000	0.3	A	2	13	
95	E	Deck.Plate_3	N	0	1200	4800	600	10						L5L6												40.909	Steel	Steel	245	207000	0.3	A	2	13	
96	E	Deck.Plate_4	N	0	1800	4800	600	10						L5L6												40.909	Steel	Steel	245	207000	0.3	A	2	13	
97	E	Deck.Plate_5	N	0	2400	4800	600	10						L5L6												40.909	Steel	Steel	245	207000	0.3	A	2	13	
98	E	Deck.Plate_6	N	0	9600	4800	600	10						L7L8												40.909	Steel	Steel	245	207000	0.3	A	2	14	
99	E	Deck.Plate_7	N	0	10200	4800	600	10						L7L8												40.909	Steel	Steel	245	207000	0.3	A	2	14	
100	E	Deck.Plate_8	N	0	10800	4800	600	10						L7L8												40.909	Steel	Steel	245	207000	0.3	A	2	14	
101	E	Deck.Plate_9	N	0	11400	4800	600	10						L7L8												40.909	Steel	Steel	245	207000	0.3	A	2	14	
102	E	Deck.Plate_10	N	0	12000	4800	600	10						L7L8												40.909	Steel	Steel	245	207000	0.3	A	2	14	
103	E	Vert. Plate_R_1	N	90	12600	0	600	10						3												40.909	Steel	Steel	245	207000	0.3	A	2	15	
104	E	Vert. Plate_R_2	N	90	12600	600	600	10						3												40.909	Steel	Steel	245	207000	0.3	A	2	15	
105	E	Vert. Plate_R_3	N	90	12600	1200	600	10						3												40.909	Steel	Steel	245	207000	0.3	A	2	15	
106	E	Vert. Plate_R_4	N	90	12600	1800	600	10						8												40.909	Steel	Steel	245	207000	0.3	A	2	16	
107	E	Vert. Plate_R_5	N	90	12600	2400	600	10						8												40.909	Steel	Steel	245	207000	0.3	A	2	16	
108	E	Vert. Plate_R_6	N	90	12600	3000	600	10						8												40.909	Steel	Steel	245	207000	0.3	A	2	16	
109	E	Vert. Plate_R_7	N	90	12600	3600	600	10						8												40.909	Steel	Steel	245	207000	0.3	A	2	16	
110	E	Vert. Plate_R_8	N	90	12600	4200	600	10						8												40.909	Steel	Steel	245	207000	0.3	A	2	16	
111	E	Vert. Plate_R_9	N	90	12600	4800	600	10						7												40.909	Steel	Steel	245	207000	0.3	A	2	17	
112	E	Vert. Plate_R_10	N	90	12600	5400	600	10						7												40.909	Steel	Steel	245	207000	0.3	A	2	17	
113	E	Vert. Plate_R_11	N	90	12600	6000	600	10						7												40.909	Steel	Steel	245	207000	0.3	A	2	17	
114	E	Vert. Plate_R_12	N	90	12600	6600	600	10						7												40.909	Steel	Steel	245	207000	0.3	A	2	17	
115	E	Vert. Plate_R_13	N	90	12600	7200	600	10						7												40.909	Steel	Steel	245	207000	0.3	A	2	17	
116	E	Vert. Plate_R_14	N	90	12600	7800	600	10						7												40.909	Steel	Steel	245	207000	0.3	A	2	17	
117	E	Horz. Plate_Top_1	N	180	12600	8400	600	8						7												40.909	Steel	Steel	245	207000	0.3	A	2	18	
118	E	Horz. Plate_Top_2	N	180	12000	8400	600	8						7												40.909	Steel	Steel	245	207000	0.3	A	2	18	
119	E	Horz. Plate_Top_3	N	180	11400	8400	600	8						7												40.909	Steel	Steel	245	207000	0.3	A	2	18	
120	E	Horz. Plate_Top_4	N	180	10800	8400	600	8						7												40.909	Steel	Steel	245	207000	0.3	A	2	18	
121	E	Horz. Plate_Top_5	N	180	10200	8400	600	8						7												40.909	Steel	Steel	245	207000	0.3	A	2	18	
122	E	Horz. Plate_Top_17	N	180	3000	8400	600	8						6												40.909	Steel	Steel	245	207000	0.3	A	2	19	
123	E	Horz. Plate_Top_18	N	180	2400	8400	600	8						6												40.909	Steel	Steel	245	207000	0.3	A	2	19	
124	E	Horz. Plate_Top_19	N	180	1800	8400	600	8						6												40.909	Steel	Steel	245	207000	0.3	A	2	19	
125	E	Horz. Plate_Top_20	N	180	1200	8400	600	8						6												40.909	Steel	Steel	245	207000	0.3	A	2	19	
126	E	Horz. Plate_Top_21	N	180	600	8400	600	8						6												40.909	Steel	Steel	245	207000	0.3	A	2	19	
127	E	Vert. Plate_Left_1	N	270	0	8400	600	10						6												40.909	Steel	Steel	245	207000	0.3	A	2	20	
128	E	Vert. Plate_Left_2	N	270	0	7800	600	10						6												40.909	Steel	Steel	245	207000	0.3	A	2	20	
129	E	Vert. Plate_Left_3	N	270	0	7200	600	10						6												40.909	Steel	Steel	245	207000	0.3	A	2	20	
130	E	Vert. Plate_Left_4	N	270	0	6600	600	10						6												40.909	Steel	Steel	245	207000	0.3	A	2	20	
131	E	Vert. Plate_Left_5	N	270	0	6000	600	10						6												40.909	Steel	Steel	245	207000	0.3	A	2	20	
132	E	Vert. Plate_Left_6	N	270	0	5400	600	10						6												40.909	Steel	Steel	245	207000	0.3	A	2	20	
133	E	Vert. Plate_Left_7	N	270	0	4800	600	10						5												40.909	Steel	Steel	245	207000	0.3	A	2	21	
134	E	Vert. Plate_Left_8	N	270	0	4200	600	10						5												40.909	Steel	Steel	245	207000	0.3	A	2	21	
135	E	Vert. Plate_Left_9	N	270	0	3600	600	10						5												40.909	Steel	Steel	245	207000	0.3	A	2	21	
136	E	Vert. Plate_Left_10	N	270	0	3000	600	10						5												40.909	Steel	Steel	245	207000	0.3	A	2	21	
137	E	Vert. Plate_Left_11	N	270	0	2400	600	10						5												40.909	Steel	Steel	245	207000	0.3	A	2	21	
138	E	Vert. Plate_Left_12	N	270	0	1800	600	10						1												40.909	Steel	Steel	245	207000	0.3	A	2	22	
139	E	Vert. Plate_Left_13	N	270	0	1200	600	10						1												40.909	Steel	Steel	245	207000	0.3	A	2	22	
140	E	Vert. Plate_Left_14	N	270	0	600	600	10						1												40.909	Steel	Steel	245	207000	0.3	A	2	22	
141	E	bottom_stif_1	N	0	600	0			113.6	6.65	63.5	13.4	1													17.318	Steel	Steel	245	207000	0.3	A	2	1	
142	E	bottom_stif_2	N	0	1200	0			113.6	6.65	63.5	13.4	1													17.318	Steel	Steel	245	207000	0.3	A	2	1	
143	E	bottom_stif_3	N	0	1800	0			113.6	6.65	63.5	13.4	1													17.318	Steel	Steel	245	207000	0.3	A	2	1	
144	E	bottom_stif_4	N	0	2400	0			113.6	6.65	63.5	13.4	1													17.318	Steel	Steel	245	207000	0.3	A	2	1	
145	E	L_V.db_stif_1	N	90	3000	600			113.6	6.65	63.5	13.4	1													17.318	Steel	Steel	245	207000	0.3	A	2	3	
146	E	L_V.db_stif_2	N	90	3000	1200			113.6	6.65	63.5	13.4	1													17.318	Steel	Steel	245	207000	0.3	A	2	3	
147	E	L_V.ds_stif_1	N	90	3000	2400			113.6	6.65	63.5	13.4	1													17.318	Steel	Steel	245	207000	0.3	A	2	4	
148	E	L_V.ds_stif_2	N	90	3000	3000			113.6	6.65	63.5	13.4	1													17.318	Steel	Steel	245	207000	0.3	A	2	4	
149	E	L_V.ds_stif_3	N	90	3000	3600			113.6	6.65	63.5	13.4	1													17.318	Steel	Steel	245	207000	0.3	A	2	4	
150	E	L_V.ds_stif_4	N	90	3000	4200			113.6	6.65	63.5	13.4	1													17.318	Steel	Steel	245	207000	0.3	A	2	4	
151	E	L_V.ds_stif_6	N	90	3000	5400			113.6	6.65	63.5	13.4	1													17.318	Steel	Steel	245	207000	0.3	A	2	5	
152	E	L_V.ds_stif_7	N	90	3000	6000			113.6	6.65	63.5	13.4	1													17.318	Steel	Steel	245	207000	0.3	A	2	5	
153	E	L_V.ds_stif_8	N	90	3000	6600			113.6	6.65	63.5	13.4	1													17.318	Steel	Steel	245	207000	0.3	A	2	5	
154	E	L_V.ds_stif_9	N	90	3000	7200			113.6	6.65	63.5	13.4	1													17.318	Steel	Steel	245	207000	0.3	A	2	5	
155	E	L_V.ds_stif_10	N	90	3000	7800			113.6	6.65	63.5	13.4	1													17.318	Steel	Steel	245	207000	0.3	A	2	5	
156	E	R_V.db_stif_1	N	270	9600	600			113.6	6.65	63.5	13.4	1													17.318	Steel	Steel	245	207000	0.3	A	2	6	
157	E	R_V.db_stif_2	N	270	9600	1200			113.6	6.65	63.5	13.4	1													17.318	Steel	Steel	245	207000	0.3	A	2	6	
158	E	R_V.ds_stif_1	N	270	9600	2400			113.6	6.65	63.5	13.4	1													17.318	Steel	Steel	245	207000	0.3	A	2	7	
159	E	R_V.ds_stif_2	N	270	9600	3000			113.6	6.65	63.5	13.4	1													17.318	Steel	Steel	245	207000	0.3	A	2	7	
160	E	R_V.ds_stif_3	N	270	9600	3600			113.6	6.65	63.5	13.4	1													17.318	Steel	Steel	245	207000	0.3	A	2	7	
161	E	R_V.ds_stif_4	N	270	9600	4200			113.6	6.65	63.5	13.4	1													17.318	Steel	Steel	245	207000	0.3	A	2	7	
162	E	R_V.ds_stif_6	N	270	9600	5400			113.6	6.65	63.5	13.4	1													17.318	Steel	Steel	245	207000	0.3	A	2	8	

##																																	
##	ProColl Template																																
##																																	
Filename	Length	Units																															
Box Girder D	1800	mm																															
##																																	
##	ELEMENT DESCRIPTORS		COORDINATES:				PLATE DIMMARY LONGITUDINAL DIMENSIONS:												FRAME DIMENSIONS:							MATERIAL DEFINITIONS:							LOAD SHORTENING CURVE:			
ID	Type	Description	Mirror	angle	ycoord	zcoord	b	tp	hwx	twx	bfx	tfx	nsx	loop	hwx2	twx2	bfx2	tfx2	nsx2	hwy	twy	bfy	tfy	amespacir	nsy	HAZ	Pmat	Smat	str0eq	E	v	Imp	LSCurve	Clone	Sname
163	E	R_V.ds_stif_7	N	270	9600	6000			113.6	6.65	63.5	13.4	1													17.318	Steel	Steel	245	207000	0.3	A	2	8	
164	E	R_V.ds_stif_8	N	270	9600	6600			113.6	6.65	63.5	13.4	1													17.318	Steel	Steel	245	207000	0.3	A	2	8	
165	E	R_V.ds_stif_9	N	270	9600	7200			113.6	6.65	63.5	13.4	1													17.318	Steel	Steel	245	207000	0.3	A	2	8	
166	E	R_V.ds_stif_10	N	270	9600	7800			113.6	6.65	63.5	13.4	1													17.318	Steel	Steel	245	207000	0.3	A	2	8	
167	E	Deck_Hor_stif_1	N	180	600	4800			113.6	6.65	63.5	13.4	1													17.318	Steel	Steel	245	207000	0.3	A	2	13	
168	E	Deck_Hor_stif_2	N	180	1200	4800			113.6	6.65	63.5	13.4	1													17.318	Steel	Steel	245	207000	0.3	A	2	13	
169	E	Deck_Hor_stif_3	N	180	1800	4800			113.6	6.65	63.5	13.4	1													17.318	Steel	Steel	245	207000	0.3	A	2	13	
170	E	Deck_Hor_stif_4	N	180	2400	4800			113.6	6.65	63.5	13.4	1													17.318	Steel	Steel	245	207000	0.3	A	2	13	
171	E	Deck_Hor_stif_5	N	180	10200	4800			113.6	6.65	63.5	13.4	1													17.318	Steel	Steel	245	207000	0.3	A	2	14	
172	E	Deck_Hor_stif_6	N	180	10800	4800			113.6	6.65	63.5	13.4	1													17.318	Steel	Steel	245	207000	0.3	A	2	14	
173	E	Deck_Hor_stif_7	N	180	11400	4800			113.6	6.65	63.5	13.4	1													17.318	Steel	Steel	245	207000	0.3	A	2	14	
174	E	Deck_Hor_stif_8	N	180	12000	4800			113.6	6.65	63.5	13.4	1													17.318	Steel	Steel	245	207000	0.3	A	2	14	
175	E	bottom_stif_6	N	0	3600	0			113.6	6.65	63.5	13.4	1													17.318	Steel	Steel	245	207000	0.3	A	2	2	
176	E	bottom_stif_7	N	0	4200	0			113.6	6.65	63.5	13.4	1													17.318	Steel	Steel	245	207000	0.3	A	2	2	
177	E	bottom_stif_8	N	0	4800	0			113.6	6.65	63.5	13.4	1													17.318	Steel	Steel	245	207000	0.3	A	2	2	
178	E	bottom_stif_9	N	0	5400	0			113.6	6.65	63.5	13.4	1													17.318	Steel	Steel	245	207000	0.3	A	2	2	
179	E	bottom_stif_10	N	0	6000	0			113.6	6.65	63.5	13.4	1													17.318	Steel	Steel	245	207000	0.3	A	2	2	
180	E	bottom_stif_11	N	0	6600	0			113.6	6.65	63.5	13.4	1													17.318	Steel	Steel	245	207000	0.3	A	2	2	
181	E	bottom_stif_12	N	0	7200	0			113.6	6.65	63.5	13.4	1													17.318	Steel	Steel	245	207000	0.3	A	2	2	
182	E	bottom_stif_13	N	0	7800	0			113.6	6.65	63.5	13.4	1													17.318	Steel	Steel	245	207000	0.3	A	2	2	
183	E	bottom_stif_14	N	0	8400	0			113.6	6.65	63.5	13.4	1													17.318	Steel	Steel	245	207000	0.3	A	2	2	
184	E	bottom_stif_15	N	0	9000	0			113.6	6.65	63.5	13.4	1													17.318	Steel	Steel	245	207000	0.3	A	2	2	
185	E	bottom_stif_17	N	0	10200	0			113.6	6.65	63.5	13.4	1													17.318	Steel	Steel	245	207000	0.3	A	2	9	
186	E	bottom_stif_18	N	0	10800	0			113.6	6.65	63.5	13.4	1													17.318	Steel	Steel	245	207000	0.3	A	2	9	
187	E	bottom_stif_19	N	0	11400	0			113.6	6.65	63.5	13.4	1													17.318	Steel	Steel	245	207000	0.3	A	2	9	
188	E	bottom_stif_20	N	0	12000	0			113.6	6.65	63.5	13.4	1													17.318	Steel	Steel	245	207000	0.3	A	2	9	
189	E	rightside_stif_1	N	90	12600	600			113.6	6.65	63.5	13.4	1													17.318	Steel	Steel	245	207000	0.3	A	2	15	
190	E	rightside_stif_2	N	90	12600	1200			113.6	6.65	63.5	13.4	1													17.318	Steel	Steel	245	207000	0.3	A	2	15	
191	E	rightside_stif_4	N	90	12600	2400			113.6	6.65	63.5	13.4	1													17.318	Steel	Steel	245	207000	0.3	A	2	16	
192	E	rightside_stif_5	N	90	12600	3000			113.6	6.65	63.5	13.4	1													17.318	Steel	Steel	245	207000	0.3	A	2	16	
193	E	rightside_stif_6	N	90	12600	3600			113.6	6.65	63.5	13.4	1													17.318	Steel	Steel	245	207000	0.3	A	2	16	
194	E	rightside_stif_7	N	90	12600	4200			113.6	6.65	63.5	13.4	1													17.318	Steel	Steel	245	207000	0.3	A	2	16	
195	E	rightside_stif_9	N	90	12600	5400			113.6	6.65	63.5	13.4	1													17.318	Steel	Steel	245	207000	0.3	A	2	17	
196	E	rightside_stif_10	N	90	12600	6000			113.6	6.65	63.5	13.4	1													17.318	Steel	Steel	245	207000	0.3	A	2	17	
197	E	rightside_stif_11	N	90	12600	6600			113.6	6.65	63.5	13.4	1													17.318	Steel	Steel	245	207000	0.3	A	2	17	
198	E	rightside_stif_12	N	90	12600	7200			113.6	6.65	63.5	13.4	1													17.318	Steel	Steel	245	207000	0.3	A	2	17	
199	E	rightside_stif_13	N	90	12600	7800			113.6	6.65	63.5	13.4	1													17.318	Steel	Steel	245	207000	0.3	A	2	17	
200	E	top_stif_1	N	180	12000	8400			113.6	6.65	63.5	13.4	1													17.318	Steel	Steel	245	207000	0.3	A	2	18	
201	E	top_stif_2	N	180	11400	8400			113.6	6.65	63.5	13.4	1													17.318	Steel	Steel	245	207000	0.3	A	2	18	
202	E	top_stif_3	N	180	10800	8400			113.6	6.65	63.5	13.4	1													17.318	Steel	Steel	245	207000	0.3	A	2	18	
203	E	top_stif_4	N	180	10200	8400			113.6	6.65	63.5	13.4	1													17.318	Steel	Steel	245	207000	0.3	A	2	18	
204	E	top_stif_17	N	180	2400	8400			113.6	6.65	63.5	13.4	1													17.318	Steel	Steel	245	207000	0.3	A	2	19	
205	E	top_stif_18	N	180	1800	8400			113.6	6.65	63.5	13.4	1													17.318	Steel	Steel	245	207000	0.3	A	2	19	
206	E	top_stif_19	N	180	1200	8400			113.6	6.65	63.5	13.4	1													17.318	Steel	Steel	245	207000	0.3	A	2	19	
207	E	top_stif_20	N	180	600	8400			113.6	6.65	63.5	13.4	1													17.318	Steel	Steel	245	207000	0.3	A	2	19	
208	E	leftside_stif_1	N	270	0	7800			113.6	6.65	63.5	13.4	1													17.318	Steel	Steel	245	207000	0.3	A	2	20	
209	E	leftside_stif_2	N	270	0	7200			113.6	6.65	63.5	13.4	1													17.318	Steel	Steel	245	207000	0.3	A	2	20	
210	E	leftside_stif_3	N	270	0	6600			113.6	6.65	63.5	13.4	1													17.318	Steel	Steel	245	207000	0.3	A	2	20	
211	E	leftside_stif_4	N	270	0	6000			113.6	6.65	63.5	13.4	1													17.318	Steel	Steel	245	207000	0.3	A	2	20	
212	E	leftside_stif_5	N	270	0	5400			113.6	6.65	63.5	13.4	1													17.318	Steel	Steel	245	207000	0.3	A	2	20	
213	E	leftside_stif_7	N	270	0	4200			113.6	6.65	63.5	13.4	1													17.318	Steel	Steel	245	207000	0.3	A	2	21	
214	E	leftside_stif_8	N	270	0	3600			113.6	6.65	63.5	13.4	1													17.318	Steel	Steel	245	207000	0.3	A	2	21	
215	E	leftside_stif_9		270	0	3000			113.6	6.65	63.5	13.4	1													17.318	Steel	Steel	245	207000	0.3	A	2	21	
216	E	leftside_stif_10		270	0	2400			113.6	6.65	63.5	13.4	1													17.318	Steel	Steel	245	207000	0.3	A	2	21	
217	E	leftside_stif_12		270	0	1200			113.6	6.65	63.5	13.4	1													17.318	Steel	Steel	245	207000	0.3	A	2	22	
218	E	leftside_stif_13		270	0	600			113.6	6.65	63.5	13.4	1													17.318	Steel	Steel	245	207000	0.3	A	2	22	
219	E	D.B._stif_1		180	12000	1800			113.6	6.65	63.5	13.4	1													17.318	Steel	Steel	245	207000	0.3	A	2	12	
220	E	D.B._stif_2		180	11400	1800			113.6	6.65	63.5	13.4	1													17.318	Steel	Steel	245	207000	0.3	A	2	12	
221	E	D.B._stif_3		180	10800	1800			113.6	6.65	63.5	13.4	1													17.318	Steel	Steel	245	207000	0.3	A	2	12	
222	E	D.B._stif_4		180	10200	1800			113.6	6.65	63.5	13.4	1													17.318	Steel	Steel	245	207000	0.3	A	2	12	
223	E	D.B._stif_6		180	9000	1800			113.6	6.65	63.5	13.4	1													17.318	Steel	Steel	245	207000	0.3	A	2	11	
224	E	D.B._stif_7		180	8400	1800			113.6	6.65	63.5	13.4	1													17.318	Steel	Steel	245	207000	0.3	A	2	11	
225	E	D.B._stif_8		180	7800	1800			113.6	6.65	63.5	13.4	1													17.318	Steel	Steel	245	207000	0.3	A	2	11	
226	E	D.B._stif_9		180	7200	1800			113.6	6.65	63.5	13.4	1													17.318	Steel	Steel	245	207000	0.3	A	2	11	
227	E	D.B._stif_10		180	6600	1800			113.6	6.65	63.5	13.4	1													17.318	Steel	Steel	245	207000	0.3	A	2	11	
228	E	D.B._stif_11		180	6000	1800			113.6	6.65	63.5	13.4	1													17.318	Steel	Steel	245	207000	0.3	A	2	11	
229	E	D.B._stif_12		180	5400	1800			113.6	6.65	63.5	13.4	1													17.318	Steel	Steel	245	207000	0.3	A	2	11	
230	E	D.B._stif_13		180	4800	1800			113.6	6.65	63.5	13.4	1													17.318	Steel	Steel	245	207000	0.3	A	2	11	
231	E	D.B._stif_14		180	4200	1800			113.6	6.65	63.5	13.4	1													17.318	Steel	Steel	245	207000	0.3	A	2	11	
232	E	D.B._stif_15		180	3600	1800			113.6	6.65	63.5	13.4	1													17.318	Steel	Steel	245	207000	0.3	A	2	11	
233	E	D.B._stif_17		180	2400	1800			113.6	6.65	63.5	13.4	1													17.318	Steel	Steel	245	207000	0.3	A	2	10	
234	E	D.B._stif_18		180	1800	1800			113.6	6.65	63.5	13.4	1													17.318	Steel	Steel	245	207000	0.3	A	2	10	
235	E	D.B._stif_19		180	1200	1800			113.6	6.65	63.5	13.4	1													17.318	Steel	Steel	245	207000	0.3	A	2	10	
236	E	D.B._stif_20		180	600	1800			113.6	6.65	63.5	13.4	1													17.318	Steel	Steel	245	207000	0.3	A	2	10	

e. OL185 Containership

##																																						
##	ProColl Template																																					
##																																						
Filename	Length	Units																																				
10000TEU	0.791	m																																				
##																																						
##	ELEMENT DESCRIPTORS			COORDINATES:			PLATE DIMMARY LONGITUDINAL DIMENSIONS:											FRAME DIMENSIONS:							MATERIAL DEFINITIONS:								LOAD SHORTENING CURVE:					
ID	Type	Description	Mirror	angle	ycoord	zcoord	b	tp	hwx	twx	bfx	tfx	nsx	loop	hwx2	twx2	bfx2	tfx2	nsx2	hwy	twy	bfy	tfy	'amespacir	nsy	HAZ	Pmat	Smat	str0eq	E	v	lmp	LSCurve	Clone	Sname			
1	LSC	Bottom_P_LSC_1	N	0	0	0	0.84425	0.025	0.5	0.022	0.2	0.03	1		0.5	0.025	0.2	0.03	1						54	0.025	Steel	Steel	355000000	2.04E+11	0.3	A	1					
2	LSC	Bottom_P_LSC_2	N	0	0	0	0.83	0.025	0.5	0.022	0.2	0.03	2												54	0.025	Steel	Steel	355000000	2.04E+11	0.3	A	1					
3	LSC	Bottom_P_LSC_3	N	0	0	0	0.83	0.025	0.5	0.022	0.2	0.03	2												54	0.025	Steel	Steel	355000000	2.04E+11	0.3	A	1					
4	LSC	Bottom_P_LSC_4	N	0	0	0	0.83	0.025	0.5	0.022	0.2	0.03	2												54	0.025	Steel	Steel	355000000	2.04E+11	0.3	A	1					
5	LSC	Bottom_P_LSC_5	N	0	0	0	0.868	0.025	0.5	0.022	0.2	0.03	2												54	0.025	Steel	Steel	355000000	2.04E+11	0.3	A	1					
6	LSC	Bottom_P_LSC_6	N	0	0	0	0.7718	0.025	0.5	0.022	0.2	0.03	4												54	0.025	Steel	Steel	355000000	2.04E+11	0.3	A	1					
7	LSC	Bilge_S	N	0	0	0	0.88	0.021																	54	0.025	Steel	Steel	355000000	2.04E+11	0.3	A	1					
9	LSC	Bilge_P	N	0	0	0	0.88702	0.025																	54	0.025	Steel	Steel	355000000	2.04E+11	0.3	A	1					
10	LSC	Bilge_P	N	0	0	0	0.88	0.021																	54	0.025	Steel	Steel	355000000	2.04E+11	0.3	A	1					
13	LSC	Bilge_S	N	0	0	0	0.8802	0.021																	54	0.025	Steel	Steel	355000000	2.04E+11	0.3	A	1					
14	LSC	Bilge_S	N	0	0	0	0.88677	0.021																	54	0.025	Steel	Steel	355000000	2.04E+11	0.3	A	1					
17	LSC	Bilge_P	N	0	0	0	0.8802	0.021																	54	0.025	Steel	Steel	355000000	2.04E+11	0.3	A	1					
18	LSC	Bilge_P	N	0	0	0	0.88677	0.021																	54	0.025	Steel	Steel	355000000	2.04E+11	0.3	A	1					
20	LSC	Side_P_LSC_20	N	0	0	0	0.97	0.0175	0.44	0.011	0.2	0.025	2		0.5	0.011	0.2	0.03	2						54	0.025	Steel	Steel	355000000	2.04E+11	0.3	A	1					
21	LSC	Side_P_LSC_21	N	0	0	0	0.97	0.0175	0.4	0.011	0.2	0.025	5												54	0.025	Steel	Steel	355000000	2.04E+11	0.3	A	1					
22	LSC	Tank_Top_P_22	N	0	0	0	0.84425	0.01651	0.24	0.012	0.37	0.0387	1		0.48	0.011	0.2	0.03	2						54	0.025	Steel	Steel	355000000	2.04E+11	0.3	A	1					
23	LSC	Step_Cell_18_P	N	0	0	0	0.97	0.0155	0.4	0.011	0.2	0.002	2												54	0.025	Steel	Steel	355000000	2.04E+11	0.3	A	1					
24	LSC	Inner_Side_P_LSC_24	N	0	0	0	0.97	0.01475	0.3	0.011	0.043	0.0453	1		0.48	0.011	0.2	0.02	3						54	0.025	Steel	Steel	355000000	2.04E+11	0.3	A	1					
25	LSC	Side_P_LSC_25	N	0	0	0	0.97	0.0175	0.4	0.011	0.15	0.02	2												54	0.025	Steel	Steel	355000000	2.04E+11	0.3	A	1					
26	LSC	Side_P_LSC_26	N	0	0	0	0.64857	0.06453	0.3	0.075	0	0	1		0.4	0.075	0	0	5						54	0.025	Steel	Steel	355000000	2.04E+11	0.3	A	1					
27	LSC	Tank_Top_P_27	N	0	0	0	0.7718	0.016	0.48	0.011	0.2	0.03	2		0.48	0.011	0.2	0.015	1						54	0.025	Steel	Steel	355000000	2.04E+11	0.3	A	1					
28	LSC	Tank_Top_P_28	N	0	0	0	0.868	0.016	0.48	0.011	0.2	0.03	2												54	0.025	Steel	Steel	355000000	2.04E+11	0.3	A	1					
29	LSC	Tank_Top_P_29	N	0	0	0	0.83	0.016	0.48	0.011	0.2	0.03	1		0.48	0.011	0.13	0.015	1						54	0.025	Steel	Steel	355000000	2.04E+11	0.3	A	1					
30	LSC	Tank_Top_P_30	N	0	0	0	0.83	0.016	0.48	0.011	0.2	0.03	2												54	0.025	Steel	Steel	355000000	2.04E+11	0.3	A	1					
31	LSC	Tank_Top_P_31	N	0	0	0	0.83	0.016	0.48	0.011	0.2	0.03	2												54	0.025	Steel	Steel	355000000	2.04E+11	0.3	A	1					
32	LSC	Inner_Side_P_LSC_32	N	0	0	0	0.97	0.01225	0.4	0.011	0.2	0.02	1		0.4	0.011	0.15	0.02	3						54	0.025	Steel	Steel	355000000	2.04E+11	0.3	A	1					
33	LSC	Inner_Side_S_LSC_33	N	0	0	0	0.64857	0.06453	0.3	0.075			1		0.4	0.075	0	0	5						54	0.025	Steel	Steel	355000000	2.04E+11	0.3	A	1					
34	LSC	DB_Web_St	N	0	0	0	0.7	0.0165	0.2	0.015			2												54	0.025	Steel	Steel	355000000	2.04E+11	0.3	A	1					
35	LSC	DB_Web_St	N	0	0	0	0.7	0.0165	0.24	0.011	0.15	0.015	2												54	0.025	Steel	Steel	355000000	2.04E+11	0.3	A	1					
36	LSC	DB_Web_St	N	0	0	0	0.7	0.0165	0.2	0.015			2												54	0.025	Steel	Steel	355000000	2.04E+11	0.3	A	1					
37	LSC	DB_Web_St	N	0	0	0	0.7	0.0165	0.2	0.015			2												54	0.025	Steel	Steel	355000000	2.04E+11	0.3	A	1					
38	LSC	DB_Web_St	N	0	0	0	0.7	0.0165	0.2	0.015			2												54	0.025	Steel	Steel	355000000	2.04E+11	0.3	A	1					
39	LSC	DB_Web_St	N	0	0	0	0.7	0.0165	0.2	0.015			1		0.24	0.012	0.037	0.0387	1						54	0.025	Steel	Steel	355000000	2.04E+11	0.3	A	1					
40	LSC	Side_Web_St	N	0	0	0	0.769	0.014	0.3	0.011	0.043	0.0453	1		0.3	0.012	0.043	0.0453	2						54	0.025	Steel	Steel	355000000	2.04E+11	0.3	A	1					
41	LSC	Side_Web_St	N	0	0	0	0.769	0.0115	0.26	0.01	0.037	0.0387	2												54	0.025	Steel	Steel	355000000	2.04E+11	0.3	A	1					
42	LSC	Side_Web_St	N	0	0	0	0.769	0.0115	0.34	0.012	0.049	0.052	2												54	0.025	Steel	Steel	355000000	2.04E+11	0.3	A	1					
43	LSC	Side_Web_St	N	0	0	0	0.76904	0.011	0.26	0.01	0.037	0.0387	2												54	0.025	Steel	Steel	355000000	2.04E+11	0.3	A	1					
44	LSC	Side_Web_St	N	0	0	0	0.769	0.073	0.4	0.075			2												54	0.025	Steel	Steel	355000000	2.04E+11	0.3	A	1					
45	LSC	DB_P_S_LSC_45	N	0	0	0	0.7718	0.025	0.5	0.022	0.2	0.03	4												54	0.025	Steel	Steel	355000000	2.04E+11	0.3	A	1					
46	LSC	DB_P_S_LSC_46	N	0	0	0	0.868	0.025	0.5	0.022	0.2	0.03	2												54	0.025	Steel	Steel	355000000	2.04E+11	0.3	A	1					
47	LSC	DB_P_S_LSC_47	N	0	0	0	0.83	0.025	0.5	0.022	0.2	0.03	2												54	0.025	Steel	Steel	355000000	2.04E+11	0.3	A	1					
48	LSC	DB_P_S_LSC_48	N	0	0	0	0.83	0.025	0.5	0.022	0.2	0.03	2												54	0.025	Steel	Steel	355000000	2.04E+11	0.3	A	1					
49	LSC	DB_P_S_LSC_49	N	0	0	0	0.83	0.025	0.5	0.022	0.2	0.03	2												54	0.025	Steel	Steel	355000000	2.04E+11	0.3	A	1					
50	LSC	DB_P_S_LSC_50	N	0	0	0	0.84425	0.025	0.5	0.022	0.2	0.03	1		0.5	0.025	0.2	0.03	1						54	0.025	Steel	Steel	355000000	2.04E+11	0.3	A	1					
51	LSC	Side_S_LSC_51	N	0	0	0	0.97	0.0175	0.44	0.011	0.2	0.025	1		0.5	0.011	0.2	0.03	2						54	0.025	Steel	Steel	355000000	2.04E+11	0.3	A	1					
52	LSC	Side_S_LSC_52	N	0	0	0	0.97	0.0175	0.4	0.011	0.2	0.025	5												54	0.025	Steel	Steel	355000000	2.04E+11	0.3	A	1					
53	LSC	Side_S_LSC_53	N	0	0	0	0.97	0.0175	0.4	0.011	0.15	0.02	2												54	0.025	Steel	Steel	355000000	2.04E+11	0.3	A	1					
54	LSC	Side_S_LSC_54	N	0	0	0	0.64857	0.06453	0.3	0.075			1		0.4	0.075	0	0	5						54	0.025	Steel	Steel	355000000	2.04E+11	0.3	A	1					
55	LSC	DB_P_S_LSC_55	N	0	0	0	0.7718	0.016	0.48	0.011	0.2	0.03	2		0.48	0.011	0.2	0.015	1						54	0.025	Steel	Steel	355000000	2.04E+11	0.3	A	1					
56	LSC	DB_P_S_LSC_56	N	0	0	0	0.868	0.016	0.48	0.011	0.2	0.03	2												54	0.025	Steel	Steel	355000000	2.04E+11	0.3	A	1					
57	LSC	DB_P_S_LSC_57	N	0	0	0	0.83	0.016	0.48	0.011	0.2	0.03	1		0.48	0.011	0.13	0.015	1						54	0.025	Steel	Steel	355000000	2.04E+11	0.3	A	1					
58	LSC	DB_P_S_LSC_58	N	0	0	0	0.83	0.016	0.48	0.011	0.2	0.03	2												54	0.025	Steel	Steel	355000000	2.04E+11	0.3	A	1					
59	LSC	DB_P_S_LSC_59	N	0	0	0	0.83	0.016	0.48	0.011	0.2	0.03	2												54	0.025	Steel	Steel	355000000	2.04E+11	0.3	A	1					
60	LSC	DB_P_S_LSC_60	N	0	0	0	0.84425	0.01651	0.48	0.011	0.2	0.03	1		0.5	0.011	0.2	0.03	1						54	0.025	Steel	Steel	355000000	2.04E+11	0.3	A	1					
61	LSC	Step_Cell_13_St	N	0	0	0	0.97	0.0155	0.4	0.011	0.2	0.02	2												54	0.025	Steel	Steel	355000000	2.04E+11	0.3	A	1					
62	LSC	Inner_Side_P	N	0	0	0	0.64857	0.06453	0.3	0.075			1		0.4	0.075	0	0	5						54	0.025	Steel	Steel	355000000	2.04E+11	0.3	A	1					
63	LSC	DB_Web_P	N	0	0	0	0.7	0.0165	0.24	0.011	0.15	0.015	2												54	0.025	Steel	Steel	355000000	2.04E+11	0.3	A	1					
64	LSC	DB_Web_P	N	0	0	0	0.7	0.0165	0.2	0.015	0	0	2												54	0.025	Steel	Steel	355000000	2.04E+11	0.3	A	1					
65	LSC	Side_Web_P	N	0	0	0	0.769	0.0115	0.26	0.01	0.037	0.0387	2												54	0.025	Steel	Steel	355000000	2.04E+11	0.3	A	1					
66	LSC	Side_Web_P	N	0	0	0	0.769	0.0115	0.34	0.012	0.049	0.052	2												54	0.025	Steel	Steel	355000000	2.04E+11	0.3	A	1					
67	LSC	Side_Web_P	N	0	0	0	0.76904	0.011	0.26	0.01	0.037	0.0387	2												54	0.025	Steel	Steel	355000000	2.04E+11	0.3	A	1					
68	LSC	Side_Web_P	N	0	0	0	0.769	0.073	0.4	0.075			2												54	0.025	Steel	Steel	355000000	2.04E+11	0.3	A	1					
69	LSC	DB_Web_CL	N	0	0	0	0.7	0.0165	0.2	0.015			2												54	0.025	Steel	Steel	355000000	2.04E+11	0.3	A	1					
70	LSC	Inner Side_P_LSC_70	N	0	0	0	0.97	0.01225	0.4	0.011	0.2	0.02	1		0.4	0.011	0.15	0.02	3						54	0.025	Steel	Steel	355000000	2.04E+11	0.3	A	1					
71	LSC	Step_Cell_13_St	N	0	0	0	0.8915	0.014	0.3	0.011	0.043	0.0453	1												54	0.025	Steel	Steel	355000000	2.04E+11	0.3	A	1					
72	LSC	Inner Side_P_LSC_72	N	0	0	0	0.97	0.011	0.32	0.011	0.13	0.015	2												54	0.025	Steel	Steel	355000000	2.04E+11	0.3	A	1					
73	LSC	DB_Web_P	N	0	0	0	0.7	0.0165	0.2	0.015			2												54	0.025	Steel	Steel	355000000	2.04E+11	0.3	A	1					
74	LSC	DB_Web_P	N	0	0	0	0.7	0.0165	0.2	0.015			2												54	0.025	Steel	Steel	355000000	2.04E+11	0.3	A	1					
75	LSC	DB_Web_P	N	0	0	0	0.7	0.0165	0.2	0.015			2												54	0.025	Steel	Steel	355000000	2.04E+11	0.3	A	1					
76	LSC	DB_Web_P	N	0	0	0	0.7	0.0165	0.2	0.015			2												54	0.025	Steel	Steel	355000000	2.04E+11	0.3	A	1					
77	LSC	Step_Cell_18_P	N	0	0	0	0.8915	0.014	0.3	0.011	0.043	0.0453	1												54	0.025	Steel	Steel	355000000	2.04E+11	0.3	A	1					
78	LSC	Side_Web_P	N	0	0	0	0.769	0.014	0.3	0.012	0.043	0.0453	2												54	0.025	Steel	Steel	355000000	2.04E+11	0.3	A	1					
79	LSC	Inner Side_S_LSC_79	N	0	0	0	0.97	0.01475	0.48	0.011	0.2	0.02	1		0.5	0.11	0.2	0.025	2						54	0.025	Steel	Steel	355000000	2.04E+11	0.3	A	1					
80	LSC	Inner Side_S_LSC_80	N	0	0	0	0.97	0.011	0.32	0.011	0.13	0.015	2												54	0.025	Steel	Steel	355000000	2.04E+11	0.3	A	1					
81	LSC	Bilge_P	N	0	0	0	0.87995	0.025																	54	0.025	Steel	Steel	355000000	2.04E+11	0.3	A	1					
82	LSC	Bilge_P	N	0	0	0	0.87978	0.021																	54	0.025	Steel	Steel	355000000	2.04E+11	0.3	A	1					
83	LSC	Bilge_P	N	0	0	0	0.88004	0.021																	54	0.025	Steel	Steel	355000000	2.04E+11	0.3	A	1					
84	LSC	Bilge_P	N	0	0	0	0.88	0.021																	54	0.025	Steel	Steel	355000000	2.04E+11	0.3	A	1					
86	LSC	Bilge_S	N	0	0	0	0.88702	0.025																	54	0.025	Steel	Steel	355000000	2.04E+11	0.3	A	1					
87	LSC	Bilge_S	N	0	0	0	0.88	0.021																	54	0.025	Steel	Steel	355000000	2.04E+11	0.3	A	1					
89	LSC	Bilge_S	N	0	0	0	0.87995	0.025																	54	0.025	Steel	Steel	355000000	2.04E+11	0.3	A	1					
90	LSC	Bilge_S	N	0	0	0	0.87978	0.021																	54	0.025	Steel	Steel	355000000	2.04E+11	0.3	A	1					
91	LSC	Bilge_S	N	0	0	0	0.88004	0.021																	54	0.025	Steel	Steel	355000000	2.04E+11	0.3	A	1					
92	E	Bottom P	N	0	4.09	0	0.876	0.025						1												0.025	Steel	Steel	355000000	2.04E+11	0.3	A	2	1				

##
ProColl Template
##

Filename	Length	Units
10000TEU	0.791	m

##

##	ELEMENT DESCRIPTORS		COORDINATES:				PLATE DIMMARY LONGITUDINAL DIMENSIONS:							FRAME DIMENSIONS:										MATERIAL DEFINITIONS:							LOAD SHORTENING CURVE:			
ID	Type	Description	Mirror	angle	ycoord	zcoord	b	tp	hwx	twx	bfx	tfx	nsx	loop	hwx2	twx2	bfx2	tfx2	nsx2	hwy	twy	bfy	tfy	ramespacir	nsy	HAZ	Pmat	Smat	str0eq	E	v	Imp	LSCurve	Clone	Sname
93	E	Bottom DB _P_LSC_1	N	0	4.966	0	0.841	0.025						1												0.025	Steel	Steel	355000000	2.04E+11	0.3	A	2	1	
94	E	Bottom DB _P_LSC_1	N	0	5.807	0	0.83	0.025						1												0.025	Steel	Steel	355000000	2.04E+11	0.3	A	2	1	
95	E	Bottom DB _P_LSC_1	N	0	6.637	0	0.83	0.025						1												0.025	Steel	Steel	355000000	2.04E+11	0.3	A	2	1	
96	E	Bottom Stiffener_P_LSC_1	N	0	4.966	0	0	0	0.5	0.025	0.2	0.03	1													0.025	Steel	Steel	355000000	2.04E+11	0.3	A	2	1	
97	E	Bottom Stiffener_P_LSC_1	N	0	5.807	0	0	0	0.5	0.022	0.2	0.03	1													0.025	Steel	Steel	355000000	2.04E+11	0.3	A	2	1	
98	E	Bottom Stiffener_P_LSC_1	N	0	6.637	0	0	0	0.5	0.022	0.2	0.03	1													0.025	Steel	Steel	355000000	2.04E+11	0.3	A	2	1	
99	E	Bottom DB _P_LSC_2	N	0	7.467	0	0.83	0.025						2												0.025	Steel	Steel	355000000	2.04E+11	0.3	A	2	2	
100	E	Bottom DB _P_LSC_2	N	0	8.297	0	0.83	0.025						2												0.025	Steel	Steel	355000000	2.04E+11	0.3	A	2	2	
101	E	Bottom DB _P_LSC_2	N	0	9.127	0	0.83	0.025						2												0.025	Steel	Steel	355000000	2.04E+11	0.3	A	2	2	
102	E	Bottom Stiffener_P_LSC_2	N	0	8.297	0	0	0	0.5	0.022	0.2	0.03	1													0.025	Steel	Steel	355000000	2.04E+11	0.3	A	2	2	
103	E	Bottom Stiffener_P_LSC_2	N	0	9.127	0	0	0	0.5	0.022	0.2	0.03	1													0.025	Steel	Steel	355000000	2.04E+11	0.3	A	2	2	
104	E	Bottom DB _P_LSC_3	N	0	9.957	0	0.83	0.025						3												0.025	Steel	Steel	355000000	2.04E+11	0.3	A	2	3	
105	E	Bottom DB _P_LSC_3	N	0	10.787	0	0.83	0.025						3												0.025	Steel	Steel	355000000	2.04E+11	0.3	A	2	3	
106	E	Bottom DB _P_LSC_3	N	0	11.617	0	0.83	0.025						3												0.025	Steel	Steel	355000000	2.04E+11	0.3	A	2	3	
107	E	Bottom Stiffener_P_LSC_3	N	0	10.787	0	0	0	0.5	0.022	0.2	0.03	1													0.025	Steel	Steel	355000000	2.04E+11	0.3	A	2	3	
108	E	Bottom Stiffener_P_LSC_3	N	0	11.617	0	0	0	0.5	0.022	0.2	0.03	1													0.025	Steel	Steel	355000000	2.04E+11	0.3	A	2	3	
109	E	Bottom DB _P_LSC_4	N	0	12.447	0	0.83	0.025						4												0.025	Steel	Steel	355000000	2.04E+11	0.3	A	2	4	
110	E	Bottom DB _P_LSC_4	N	0	13.277	0	0.83	0.025						4												0.025	Steel	Steel	355000000	2.04E+11	0.3	A	2	4	
111	E	Bottom DB _P_LSC_4	N	0	14.107	0	0.83	0.025						4												0.025	Steel	Steel	355000000	2.04E+11	0.3	A	2	4	
112	E	Bottom Stiffener_P_LSC_4	N	0	13.277	0	0	0	0.5	0.022	0.2	0.03	1													0.025	Steel	Steel	355000000	2.04E+11	0.3	A	2	4	
113	E	Bottom Stiffener_P_LSC_4	N	0	14.107	0	0	0	0.5	0.022	0.2	0.03	1													0.025	Steel	Steel	355000000	2.04E+11	0.3	A	2	4	
114	E	Bottom DB _P_LSC_5	N	0	14.937	0	0.868	0.025						5												0.025	Steel	Steel	355000000	2.04E+11	0.3	A	2	5	
115	E	Bottom DB _P_LSC_5	N	0	15.805	0	0.868	0.025						5												0.025	Steel	Steel	355000000	2.04E+11	0.3	A	2	5	
116	E	Bottom DB _P_LSC_5	N	0	16.673	0	0.868	0.025						5												0.025	Steel	Steel	355000000	2.04E+11	0.3	A	2	5	
117	E	Bottom Stiffener_P_LSC_5	N	0	15.805	0	0	0	0.5	0.022	0.2	0.03	1													0.025	Steel	Steel	355000000	2.04E+11	0.3	A	2	5	
118	E	Bottom Stiffener_P_LSC_5	N	0	16.673	0	0	0	0.5	0.022	0.2	0.03	1													0.025	Steel	Steel	355000000	2.04E+11	0.3	A	2	5	
119	E	Bottom DB_P_LSC_6	N	0	17.541	0	0.83	0.025						6												0.025	Steel	Steel	355000000	2.04E+11	0.3	A	2	6	
120	E	Bottom DB_P_LSC_6	N	0	18.371	0	0.83	0.025						6												0.025	Steel	Steel	355000000	2.04E+11	0.3	A	2	6	
121	E	Bottom DB_P_LSC_6	N	0	19.201	0	0.83	0.025						6												0.025	Steel	Steel	355000000	2.04E+11	0.3	A	2	6	
122	E	Bottom DB_P_LSC_6	N	0	20.031	0	0.623	0.025						6												0.025	Steel	Steel	355000000	2.04E+11	0.3	A	2	6	
123	E	Bottom DB_P_LSC_6	N	0	20.654	0	0.746	0.025						6												0.025	Steel	Steel	355000000	2.04E+11	0.3	A	2	6	
124	E	Bottom Stiffener_P_LSC_6	N	0	18.371	0	0	0	0.5	0.022	0.2	0.03	1													0.025	Steel	Steel	355000000	2.04E+11	0.3	A	2	6	
125	E	Bottom Stiffener_P_LSC_6	N	0	19.201	0	0	0	0.5	0.022	0.2	0.03	1													0.025	Steel	Steel	355000000	2.04E+11	0.3	A	2	6	
126	E	Bottom Stiffener_P_LSC_6	N	0	20.031	0	0	0	0.5	0.022	0.2	0.03	1													0.025	Steel	Steel	355000000	2.04E+11	0.3	A	2	6	
127	E	Bottom Stiffener_P_LSC_6	N	0	20.654	0	0	0	0.5	0.022	0.2	0.03	1													0.025	Steel	Steel	355000000	2.04E+11	0.3	A	2	6	
128	E	ink Top P_Bottom DB _P_LSC_	N	0	4.09	2.1	0.876	0.016						1												0.025	Steel	Steel	355000000	2.04E+11	0.3	A	2	22	
129	E	Bottom DB _P_LSC_1	N	0	4.966	2.1	0.841	0.016						1												0.025	Steel	Steel	355000000	2.04E+11	0.3	A	2	22	
130	E	Bottom DB _P_LSC_1	N	0	5.807	2.1	0.83	0.016						1												0.025	Steel	Steel	355000000	2.04E+11	0.3	A	2	22	
131	E	Bottom DB _P_LSC_1	N	0	6.637	2.1	0.83	0.016						1												0.025	Steel	Steel	355000000	2.04E+11	0.3	A	2	22	
132	E	Bottom Stiffener_P_LSC_1	N	-270	4.09	2.1	0	0	0.24	0.012	0.037	0.0387	1													0.025	Steel	Steel	355000000	2.04E+11	0.3	A	2	22	
133	E	Bottom Stiffener_P_LSC_1	N	180	4.966	2.1	0	0	0.5	0.011	0.2	0.03	1													0.025	Steel	Steel	355000000	2.04E+11	0.3	A	2	22	
134	E	Bottom Stiffener_P_LSC_1	N	180	5.807	2.1	0	0	0.48	0.011	0.2	0.03	1													0.025	Steel	Steel	355000000	2.04E+11	0.3	A	2	22	
135		Bottom Stiffener_P_LSC_1	N	180	6.637	2.1	0	0	0.48	0.011	0.2	0.03	1													0.025	Steel	Steel	355000000	2.04E+11	0.3	A	2	22	
136	E	Bottom DB _P_LSC_2	N	0	7.467	2.1	0.83	0.016						2												0.025	Steel	Steel	355000000	2.04E+11	0.3	A	2	31	
137	E	Bottom DB _P_LSC_2	N	0	8.297	2.1	0.83	0.016						2												0.025	Steel	Steel	355000000	2.04E+11	0.3	A	2	31	
138	E	Bottom DB _P_LSC_2	N	0	9.127	2.1	0.83	0.016						2												0.025	Steel	Steel	355000000	2.04E+11	0.3	A	2	31	
139	E	Bottom Stiffener_P_LSC_2	N	180	8.297	2.1	0	0	0.48	0.011	0.2	0.03	1													0.025	Steel	Steel	355000000	2.04E+11	0.3	A	2	31	
140	E	Bottom Stiffener_P_LSC_2	N	180	9.127	2.1	0	0	0.48	0.011	0.2	0.03	1													0.025	Steel	Steel	355000000	2.04E+11	0.3	A	2	31	
141	E	Bottom DB _P_LSC_3	N	0	9.957	2.1	0.83	0.016						3												0.025	Steel	Steel	355000000	2.04E+11	0.3	A	2	30	
142	E	Bottom DB _P_LSC_3	N	0	10.787	2.1	0.83	0.016						3												0.025	Steel	Steel	355000000	2.04E+11	0.3	A	2	30	
143	E	Bottom DB _P_LSC_3	N	0	11.617	2.1	0.83	0.016						3												0.025	Steel	Steel	355000000	2.04E+11	0.3	A	2	30	
144	E	Bottom Stiffener_P_LSC_3	N	180	10.787	2.1	0	0	0.48	0.011	0.2	0.03	1													0.025	Steel	Steel	355000000	2.04E+11	0.3	A	2	30	
145	E	Bottom Stiffener_P_LSC_3	N	180	11.617	2.1	0	0	0.48	0.011	0.2	0.03	1													0.025	Steel	Steel	355000000	2.04E+11	0.3	A	2	30	
146	E	Bottom DB _P_LSC_4	N	0	12.447	2.1	0.83	0.016						4												0.025	Steel	Steel	355000000	2.04E+11	0.3	A	2	29	
147	E	Bottom DB _P_LSC_4	N	0	13.277	2.1	0.83	0.016						4												0.025	Steel	Steel	355000000	2.04E+11	0.3	A	2	29	
148	E	Bottom DB _P_LSC_4	N	0	14.107	2.1	0.83	0.016						4												0.025	Steel	Steel	355000000	2.04E+11	0.3	A	2	29	
149	E	Bottom Stiffener_P_LSC_4	N	180	13.277	2.1	0	0	0.48	0.011	0.2	0.03	1													0.025	Steel	Steel	355000000	2.04E+11	0.3	A	2	29	
150	E	Bottom Stiffener_P_LSC_4	N	180	14.107	2.1	0	0	0.48	0.011	0.13	0.015	1													0.025	Steel	Steel	355000000	2.04E+11	0.3	A	2	29	
151	E	Bottom DB _P_LSC_5	N	0	14.937	2.1	0.868	0.016						5												0.025	Steel	Steel	355000000	2.04E+11	0.3	A	2	28	
152	E	Bottom DB _P_LSC_5	N	0	15.805	2.1	0.868	0.016						5												0.025	Steel	Steel	355000000	2.04E+11	0.3	A	2	28	
153	E	Bottom DB _P_LSC_5	N	0	16.673	2.1	0.868	0.016						5												0.025	Steel	Steel	355000000	2.04E+11	0.3	A	2	28	
154	E	Bottom Stiffener_P_LSC_5	N	180	15.805	2.1	0	0	0.48	0.011	0.2	0.03	1													0.025	Steel	Steel	355000000	2.04E+11	0.3	A	2	28	
155	E	Bottom Stiffener_P_LSC_5	N	180	16.673	2.1	0	0	0.48	0.011	0.2	0.03	1													0.025	Steel	Steel	355000000	2.04E+11	0.3	A	2	28	
156	E	Bottom DB_P_LSC_6	N	0	17.541	2.1	0.83	0.016						6												0.025	Steel	Steel	355000000	2.04E+11	0.3	A	2	27	
157	E	Bottom DB_P_LSC_6	N	0	18.371	2.1	0.83	0.016						6												0.025	Steel	Steel	355000000	2.04E+11	0.3	A	2	27	
158	E	Bottom DB_P_LSC_6	N	0	19.201	2.1	0.83	0.016						6												0.025	Steel	Steel	355000000	2.04E+11	0.3	A	2	27	
159	E	Bottom DB_P_LSC_6	N	0	20.031	2.1	0.623	0.016						6												0.025	Steel	Steel	355000000	2.04E+11	0.3	A	2	27	
160	E	Bottom DB_P_LSC_6	N	0	20.654	2.1	0.746	0.016						6												0.025	Steel	Steel	355000000	2.04E+11	0.3	A	2	27	
161	E	Bottom Stiffener_P_LSC_6	N	180	18.371	2.1	0	0	0.48	0.011	0.2	0.03	1													0.025	Steel	Steel	355000000	2.04E+11	0.3	A	2	27	
162	E	Bottom Stiffener_P_LSC_6	N	180	19.201	2.1	0	0	0.48	0.011	0.2	0.03	1													0.025	Steel	Steel	355000000	2.04E+11	0.3	A	2	27	
163	E	Bottom Stiffener_P_LSC_6	N	180	20.031	2.1	0	0	0.48	0.011	0.2	0.03	1													0.025	Steel	Steel	355000000	2.04E+11	0.3	A	2	27	
164	E	Bottom Stiffener_P_LSC_6	N	180	20.654	2.1	0	0	0.48	0.011	0.2	0.015	1													0.025	Steel	Steel	355000000	2.04E+11	0.3	A	2	27	
165	E	BOTTOM S__DB_P_S_LSC_45	N	0	21.4	0	0.746	0.025						7												0.025	Steel	Steel	355000000	2.04E+11	0.3	A	2	45	
166	E	DB_P_S_LSC_45	N	0	22.146	0	0.623	0.025						7												0.025	Steel	Steel	355000000	2.04E+11	0.3	A	2	45	
167	E	DB_P_S_LSC_45	N	0	22.769	0	0.83	0.025						7												0.025	Steel	Steel	355000000	2.04E+11	0.3	A	2	45	
168	E	DB_P_S_LSC_45	N	0	23.599	0	0.83	0.025						7												0.025	Steel	Steel	355000000	2.04E+11	0.3	A	2	45	
169	E	DB_P_S_LSC_45	N	0	24.429	0	0.83	0.025						7												0.025	Steel	Steel	355000000	2.04E+11	0.3	A	2	45	
170	E	DB_Stiffener_S_LSC_45	N	0	22.146	0	0	0	0.5	0.022	0.2	0.03	1													0.025	Steel	Steel	355000000	2.04E+11	0.3	A	2	45	
171	E	DB_Stiffener_S_LSC_45	N	0	22.769	0	0	0	0.5	0.022	0.2	0.03	1													0.025	Steel	Steel	355000000	2.04E+11	0.3	A	2	45	
172	E	DB_Stiffener_S_LSC_45	N	0	23.599	0	0	0	0.5	0.022	0.2	0.03	1													0.025	Steel	Steel	355000000	2.04E+11	0.3	A	2	45	
173	E	DB_Stiffener_S_LSC_45	N	0	24.429	0	0	0	0.5	0.022	0.2	0.03	1													0.025	Steel	Steel	355000000	2.04E+11	0.3	A	2	45	
174	E	DB_P_S_LSC_46	N	0	25.259	0	0.868	0.025						8												0.025	Steel	Steel	355000000	2.04E+11	0.3	A	2	46	
175	E	DB_P_S_LSC_46	N	0	26.127	0	0.868	0.025						8												0.025	Steel	Steel	355000000	2.04E+11	0.3	A	2	46	
176	E	DB_P_S_LSC_46	N	0	26.995	0	0.868	0.025						8												0.025	Steel	Steel	355000000	2.04E+11	0.3	A	2	46	

##
ProColl Template
##

Filename	Length	Units
10000TEU	0.791	m

##

##	ELEMENT DESCRIPTORS		COORDINATES:				PLATE DIMMARY LONGITUDINAL DIMENSIONS:							FRAME DIMENSIONS:										MATERIAL DEFINITIONS:						LOAD SHORTENING CURVE:			
ID	Type	Description	Mirror	angle	ycoord	zcoord	b	tp	hwx	twx	bfx	tfx	nsx	loop	hwx2	twx2	bfx2	tfx2	nsx2	hwy	twy	bfy	tfy	ramespacir	nsy	HAZ	Pmat	Smat	str0eq	E	v	Imp	LSCurve	Clone	Sname
177	E	DB_Stiffener_S_LSC_46	N	0	26.127	0	0	0	0.5	0.022	0.2	0.03	1													0.025	Steel	Steel	355000000	2.04E+11	0.3	A	2	46	
178	E	DB_Stiffener_S_LSC_46	N	0	26.995	0	0	0	0.5	0.022	0.2	0.03	1													0.025	Steel	Steel	355000000	2.04E+11	0.3	A	2	46	
179	E	DB_P_S_LSC_47	N	0	27.863	0	0.83	0.025						9												0.025	Steel	Steel	355000000	2.04E+11	0.3	A	2	47	
180	E	DB_P_S_LSC_47	N	0	28.693	0	0.83	0.025						9												0.025	Steel	Steel	355000000	2.04E+11	0.3	A	2	47	
181	E	DB_P_S_LSC_47	N	0	29.523	0	0.83	0.025						9												0.025	Steel	Steel	355000000	2.04E+11	0.3	A	2	47	
182	E	DB_Stiffener_S_LSC_47	N	0	28.693	0	0	0	0.5	0.022	0.02	0.03	1													0.025	Steel	Steel	355000000	2.04E+11	0.3	A	2	47	
183	E	DB_Stiffener_S_LSC_47	N	0	29.523	0	0	0	0.5	0.022	0.02	0.03	1													0.025	Steel	Steel	355000000	2.04E+11	0.3	A	2	47	
184	E	DB_P_S_LSC_48	N	0	30.353	0	0.83	0.025						10												0.025	Steel	Steel	355000000	2.04E+11	0.3	A	2	48	
185	E	DB_P_S_LSC_48	N	0	31.183	0	0.83	0.025						10												0.025	Steel	Steel	355000000	2.04E+11	0.3	A	2	48	
186	E	DB_P_S_LSC_48	N	0	32.013	0	0.83	0.025						10												0.025	Steel	Steel	355000000	2.04E+11	0.3	A	2	48	
187	E	DB_Stiffener_S_LSC_48	N	0	31.183	0	0	0	0.5	0.022	0.2	0.03	1													0.025	Steel	Steel	355000000	2.04E+11	0.3	A	2	48	
188	E	DB_Stiffener_S_LSC_48	N	0	32.013	0	0	0	0.5	0.022	0.2	0.03	1													0.025	Steel	Steel	355000000	2.04E+11	0.3	A	2	48	
189	E	DB_P_S_LSC_49	N	0	32.843	0	0.83	0.025						11												0.025	Steel	Steel	355000000	2.04E+11	0.3	A	2	49	
190	E	DB_P_S_LSC_49	N	0	33.673	0	0.83	0.025						11												0.025	Steel	Steel	355000000	2.04E+11	0.3	A	2	49	
191	E	DB_P_S_LSC_49	N	0	34.503	0	0.83	0.025						11												0.025	Steel	Steel	355000000	2.04E+11	0.3	A	2	49	
192	E	DB_Stiffener_S_LSC_49	N	0	33.673	0	0	0	0.5	0.022	0.2	0.03	1													0.025	Steel	Steel	355000000	2.04E+11	0.3	A	2	49	
193	E	DB_Stiffener_S_LSC_49	N	0	34.503	0	0	0	0.5	0.022	0.2	0.03	1													0.025	Steel	Steel	355000000	2.04E+11	0.3	A	2	49	
194	E	DB_P_S_LSC_50	N	0	35.333	0	0.83	0.025						12												0.025	Steel	Steel	355000000	2.04E+11	0.3	A	2	50	
195	E	DB_P_S_LSC_50	N	0	36.163	0	0.83	0.025						12												0.025	Steel	Steel	355000000	2.04E+11	0.3	A	2	50	
196	E	DB_P_S_LSC_50	N	0	36.993	0	0.841	0.025						12												0.025	Steel	Steel	355000000	2.04E+11	0.3	A	2	50	
197	E	DB_P_S_LSC_50	N	0	37.834	0	0.876	0.025						12												0.025	Steel	Steel	355000000	2.04E+11	0.3	A	2	50	
198	E	DB_Stiffener_S_LSC_50	N	0	36.163	0	0	0	0.5	0.022	0.2	0.03	1													0.025	Steel	Steel	355000000	2.04E+11	0.3	A	2	50	
199	E	DB_Stiffener_S_LSC_50	N	0	36.993	0	0	0	0.5	0.022	0.2	0.03	1													0.025	Steel	Steel	355000000	2.04E+11	0.3	A	2	50	
200	E	DB_Stiffener_S_LSC_50	N	0	37.834	0	0	0	0.5	0.022	0.2	0.03	1													0.025	Steel	Steel	355000000	2.04E+11	0.3	A	2	50	
201	E	Tank Top S__DB_P_S_LSC_55	N	0	21.4	2.1	0.746	0.016						7												0.025	Steel	Steel	355000000	2.04E+11	0.3	A	2	55	
202	E	DB_P_S_LSC_55	N	0	22.146	2.1	0.623	0.016						7												0.025	Steel	Steel	355000000	2.04E+11	0.3	A	2	55	
203	E	DB_P_S_LSC_55	N	0	22.769	2.1	0.83	0.016						7												0.025	Steel	Steel	355000000	2.04E+11	0.3	A	2	55	
204	E	DB_P_S_LSC_55	N	0	23.599	2.1	0.83	0.016						7												0.025	Steel	Steel	355000000	2.04E+11	0.3	A	2	55	
205	E	DB_P_S_LSC_55	N	0	24.429	2.1	0.83	0.016						7												0.025	Steel	Steel	355000000	2.04E+11	0.3	A	2	55	
206	E	DB_Stiffener_S_LSC_55	N	180	22.146	2.1	0	0	0.48	0.011	0.2	0.015	1													0.025	Steel	Steel	355000000	2.04E+11	0.3	A	2	55	
207	E	DB_Stiffener_S_LSC_55	N	180	22.769	2.1	0	0	0.48	0.011	0.2	0.03	1													0.025	Steel	Steel	355000000	2.04E+11	0.3	A	2	55	
208	E	DB_Stiffener_S_LSC_55	N	180	23.599	2.1	0	0	0.48	0.011	0.2	0.03	1													0.025	Steel	Steel	355000000	2.04E+11	0.3	A	2	55	
209	E	DB_Stiffener_S_LSC_55	N	180	24.429	2.1	0	0	0.48	0.011	0.2	0.03	1													0.025	Steel	Steel	355000000	2.04E+11	0.3	A	2	55	
210	E	DB_P_S_LSC_56	N	0	25.259	2.1	0.868	0.016						8												0.025	Steel	Steel	355000000	2.04E+11	0.3	A	2	56	
211	E	DB_P_S_LSC_56	N	0	26.127	2.1	0.868	0.016						8												0.025	Steel	Steel	355000000	2.04E+11	0.3	A	2	56	
212	E	DB_P_S_LSC_56	N	0	26.995	2.1	0.868	0.016						8												0.025	Steel	Steel	355000000	2.04E+11	0.3	A	2	56	
213	E	DB_Stiffener_S_LSC_56	N	180	26.127	2.1	0	0	0.48	0.011	0.2	0.03	1													0.025	Steel	Steel	355000000	2.04E+11	0.3	A	2	56	
214	E	DB_Stiffener_S_LSC_56	N	180	26.995	2.1	0	0	0.48	0.011	0.2	0.03	1													0.025	Steel	Steel	355000000	2.04E+11	0.3	A	2	56	
215	E	DB_P_S_LSC_57	N	0	27.863	2.1	0.83	0.016						9												0.025	Steel	Steel	355000000	2.04E+11	0.3	A	2	57	
216	E	DB_P_S_LSC_57	N	0	28.693	2.1	0.83	0.016						9												0.025	Steel	Steel	355000000	2.04E+11	0.3	A	2	57	
217	E	DB_P_S_LSC_57	N	0	29.523	2.1	0.83	0.016						9												0.025	Steel	Steel	355000000	2.04E+11	0.3	A	2	57	
218	E	DB_Stiffener_S_LSC_57	N	180	28.693	2.1	0	0	0.48	0.011	0.13	0.015	1													0.025	Steel	Steel	355000000	2.04E+11	0.3	A	2	57	
219	E	DB_Stiffener_S_LSC_57	N	180	29.523	2.1	0	0	0.48	0.011	0.2	0.03	1													0.025	Steel	Steel	355000000	2.04E+11	0.3	A	2	57	
220	E	DB_P_S_LSC_58	N	0	30.353	2.1	0.83	0.016						10												0.025	Steel	Steel	355000000	2.04E+11	0.3	A	2	58	
221	E	DB_P_S_LSC_58	N	0	31.183	2.1	0.83	0.016						10												0.025	Steel	Steel	355000000	2.04E+11	0.3	A	2	58	
222	E	DB_P_S_LSC_58	N	0	32.013	2.1	0.83	0.016						10												0.025	Steel	Steel	355000000	2.04E+11	0.3	A	2	58	
223	E	DB_Stiffener_S_LSC_58	N	180	31.183	2.1	0	0	0.48	0.011	0.2	0.03	1													0.025	Steel	Steel	355000000	2.04E+11	0.3	A	2	58	
224	E	DB_Stiffener_S_LSC_58	N	180	32.013	2.1	0	0	0.48	0.011	0.2	0.03	1													0.025	Steel	Steel	355000000	2.04E+11	0.3	A	2	58	
225	E	DB_P_S_LSC_59	N	0	32.843	2.1	0.83	0.016						11												0.025	Steel	Steel	355000000	2.04E+11	0.3	A	2	59	
226	E	DB_P_S_LSC_59	N	0	33.673	2.1	0.83	0.016						11												0.025	Steel	Steel	355000000	2.04E+11	0.3	A	2	59	
227	E	DB_P_S_LSC_59	N	0	34.503	2.1	0.83	0.016						11												0.025	Steel	Steel	355000000	2.04E+11	0.3	A	2	59	
228	E	DB_Stiffener_S_LSC_59	N	180	33.673	2.1	0	0	0.48	0.011	0.2	0.03	1													0.025	Steel	Steel	355000000	2.04E+11	0.3	A	2	59	
229	E	DB_Stiffener_S_LSC_59	N	180	34.503	2.1	0	0	0.48	0.011	0.2	0.03	1													0.025	Steel	Steel	355000000	2.04E+11	0.3	A	2	59	
230	E	DB_P_S_LSC_60	N	0	35.333	2.1	0.83	0.016						12												0.025	Steel	Steel	355000000	2.04E+11	0.3	A	2	60	
231	E	DB_P_S_LSC_60	N	0	36.163	2.1	0.83	0.016						12												0.025	Steel	Steel	355000000	2.04E+11	0.3	A	2	60	
232	E	DB_P_S_LSC_60	N	0	36.993	2.1	0.841	0.016						12												0.025	Steel	Steel	355000000	2.04E+11	0.3	A	2	60	
233	E	DB_P_S_LSC_60	N	0	37.834	2.1	0.876	0.016						12												0.025	Steel	Steel	355000000	2.04E+11	0.3	A	2	60	
234	E	DB_Stiffener_S_LSC_60	N	180	36.163	2.1	0	0	0.48	0.011	0.2	0.03	1													0.025	Steel	Steel	355000000	2.04E+11	0.3	A	2	60	
235	E	DB_Stiffener_S_LSC_60	N	180	36.993	2.1	0	0	0.48	0.011	0.2	0.03	1													0.025	Steel	Steel	355000000	2.04E+11	0.3	A	2	60	
236	E	DB_Stiffener_S_LSC_60	N	180	37.834	2.1	0	0	0.5	0.011	0.2	0.03	1													0.025	Steel	Steel	355000000	2.04E+11	0.3	A	2	60	
237	E	SIDE P__Side_P_LSC_20	N	90	0	5.01	0.97	0.0175						19												0.025	Steel	Steel	355000000	2.04E+11	0.3	A	2	20	
238	E	Side_P_LSC_20	N	90	0	5.98	0.97	0.0175						19												0.025	Steel	Steel	355000000	2.04E+11	0.3	A	2	20	
239	E	Side_P_LSC_20	N	90	0	6.95	0.97	0.0175						19												0.025	Steel	Steel	355000000	2.04E+11	0.3	A	2	20	
240	E	Side_P_LSC_20	N	90	0	7.92	0.97	0.0175						19												0.025	Steel	Steel	355000000	2.04E+11	0.3	A	2	20	
241	E	Side_P_LSC_20	N	90	0	8.89	0.97	0.0175						19												0.025	Steel	Steel	355000000	2.04E+11	0.3	A	2	20	
242	E	Side_P_LSC_20	N	90	0	9.86	0.97	0.0175						19												0.025	Steel	Steel	355000000	2.04E+11	0.3	A	2	20	
243	E	Side_Stiffener_P_LSC_20	N	-90	0	5.98	0	0	0.5	0.011	0.2	0.03	1													0.025	Steel	Steel	355000000	2.04E+11	0.3	A	2	20	
244	E	Side_Stiffener_P_LSC_20	N	-90	0	6.95	0	0	0.5	0.011	0.2	0.03	1													0.025	Steel	Steel	355000000	2.04E+11	0.3	A	2	20	
245	E	Side_Stiffener_P_LSC_20	N	-90	0	7.92	0	0	0.44	0.011	0.2	0.025	1													0.025	Steel	Steel	355000000	2.04E+11	0.3	A	2	20	
246	E	Side_Stiffener_P_LSC_20	N	-90	0	8.89	0	0	0.44	0.011	0.2	0.025	1													0.025	Steel	Steel	355000000	2.04E+11	0.3	A	2	20	
247	E	Side_Stiffener_P_LSC_20	N	-90	0	9.86	0	0	0.44	0.011	0.2	0.025	1													0.025	Steel	Steel	355000000	2.04E+11	0.3	A	2	20	
248	E	Side_P_LSC_21	N	90	0	10.83	0.97	0.0175						20												0.025	Steel	Steel	355000000	2.04E+11	0.3	A	2	21	
249	E	Side_P_LSC_21	N	90	0	11.8	0.97	0.0175						20												0.025	Steel	Steel	355000000	2.04E+11	0.3	A	2	21	
250	E	Side_P_LSC_21	N	90	0	12.77	0.97	0.0175						20												0.025	Steel	Steel	355000000	2.04E+11	0.3	A	2	21	
251	E	Side_P_LSC_21	N	90	0	13.74	0.97	0.0175						20												0.025	Steel	Steel	355000000	2.04E+11	0.3	A	2	21	
252	E	Side_P_LSC_21	N	90	0	14.71	0.97	0.0175						20												0.025	Steel	Steel	355000000	2.04E+11	0.3	A	2	21	
253	E	Side_P_LSC_21	N	90	0	15.68	0.97	0.0175						20												0.025	Steel	Steel	355000000	2.04E+11	0.3	A	2	21	
254	E	Side_Stiffener_P_LSC_21	N	-90	0	11.8	0	0	0.4	0.011	0.2	0.025	1													0.025	Steel	Steel	355000000	2.04E+11	0.3	A	2	21	
255	E	Side_Stiffener_P_LSC_21	N	-90	0	12.77	0	0	0.4	0.011	0.2	0.025	1													0.025	Steel	Steel	355000000	2.04E+11	0.3	A	2	21	
256	E	Side_Stiffener_P_LSC_21	N	-90	0	13.74	0	0	0.4	0.011	0.2	0.025	1													0.025	Steel	Steel	355000000	2.04E+11	0.3	A	2	21	
257	E	Side_Stiffener_P_LSC_21	N	-90	0	14.71	0	0	0.4	0.011	0.2	0.025	1													0.025	Steel	Steel	355000000	2.04E+11	0.3	A	2	21	
258	E	Side_Stiffener_P_LSC_21	N	-90	0	15.68	0	0	0.4	0.011	0.2	0.025	1													0.025	Steel	Steel	355000000	2.04E+11	0.3	A	2	21	
259	E	Side_P_LSC_25	N	90	0	16.65	0.97	0.0175						21												0.025	Steel	Steel	355000000	2.04E+11	0.3	A	2	25	
260	E	Side_P_LSC_25	N	90	0	17.62	0.97	0.0175						21												0.025	Steel	Steel	355000000	2.04E+11	0.3	A	2	25	

##
ProColl Template
##

Filename	Length	Units
10000TEU	0.791	m

##

##	ELEMENT DESCRIPTORS		COORDINATES:				PLATE DIMMARY LONGITUDINAL DIMENSIONS:													FRAME DIMENSIONS:					MATERIAL DEFINITIONS:							LOAD SHORTENING CURVE:			
ID	Type	Description	Mirror	angle	ycoord	zcoord	b	tp	hwx	twx	bfx	tfx	nsx	loop	hwx2	twx2	bfx2	tfx2	nsx2	hwy	twy	bfy	tfy	ramespacir	nsy	HAZ	Pmat	Smat	str0eq	E	v	Imp	LSCurve	Clone	Sname
261	E	Side_P_LSC_25	N	90	0	18.59	0.96	0.0175						21												0.025	Steel	Steel	355000000	2.04E+11	0.3	A	2	25	
262	E	Side_Stiffener_P_LSC_25	N	-90	0	17.62	0	0	0.4	0.011	0.15	0.02	1												0.025	Steel	Steel	355000000	2.04E+11	0.3	A	2	25	
263	E	Side_Stiffener_P_LSC_25	N	-90	0	18.59	0	0	0.4	0.011	0.15	0.02	1												0.025	Steel	Steel	355000000	2.04E+11	0.3	A	2	25	
264	E	Side_P_LSC_26	N	90	0	19.55	0.646	0.043						22												0.025	Steel	Steel	355000000	2.04E+11	0.3	A	2	26	
265	E	Side_P_LSC_26	N	90	0	20.196	0.636	0.043						22												0.025	Steel	Steel	355000000	2.04E+11	0.3	A	2	26	
266	E	Side_P_LSC_26	N	90	0	20.832	0.636	0.073						22												0.025	Steel	Steel	355000000	2.04E+11	0.3	A	2	26	
267	E	Side_P_LSC_26	N	90	0	21.468	0.636	0.073						22												0.025	Steel	Steel	355000000	2.04E+11	0.3	A	2	26	
268	E	Side_P_LSC_26	N	90	0	22.104	0.636	0.073						22												0.025	Steel	Steel	355000000	2.04E+11	0.3	A	2	26	
269	E	Side_P_LSC_26	N	90	0	22.74	0.636	0.073						22												0.025	Steel	Steel	355000000	2.04E+11	0.3	A	2	26	
270	E	Side_P_LSC_26	N	90	0	23.376	0.724	0.073						22												0.025	Steel	Steel	355000000	2.04E+11	0.3	A	2	26	
271	E	Side_Stiffener_P_LSC_26	N	-90	0	20.196	0	0	0.4	0.075			1												0.025	Steel	Steel	355000000	2.04E+11	0.3	A	2	26	
272	E	Side_Stiffener_P_LSC_26	N	-90	0	20.832	0	0	0.4	0.075			1												0.025	Steel	Steel	355000000	2.04E+11	0.3	A	2	26	
273	E	Side_Stiffener_P_LSC_26	N	-90	0	21.468	0	0	0.4	0.075			1												0.025	Steel	Steel	355000000	2.04E+11	0.3	A	2	26	
274	E	Side_Stiffener_P_LSC_26	N	-90	0	22.104	0	0	0.4	0.075			1												0.025	Steel	Steel	355000000	2.04E+11	0.3	A	2	26	
275	E	Side_Stiffener_P_LSC_26	N	-90	0	22.74	0	0	0.4	0.075			1												0.025	Steel	Steel	355000000	2.04E+11	0.3	A	2	26	
276	E	Side_Stiffener_P_LSC_26	N	-90	0	23.376	0	0	0.3	0.075			1												0.025	Steel	Steel	355000000	2.04E+11	0.3	A	2	26	
277	E	Inner_Side_P_LSC_24	N	90	2.307	5.01	0.97	0.0155						19												0.025	Steel	Steel	355000000	2.04E+11	0.3	A	2	24	
278	E	Side_P_LSC_24	N	90	2.307	5.98	0.97	0.0155						19												0.025	Steel	Steel	355000000	2.04E+11	0.3	A	2	24	
279	E	Side_P_LSC_24	N	90	2.307	6.95	0.97	0.0155						19												0.025	Steel	Steel	355000000	2.04E+11	0.3	A	2	24	
280	E	Side_P_LSC_24	N	90	2.307	7.92	0.97	0.014						19												0.025	Steel	Steel	355000000	2.04E+11	0.3	A	2	24	
281	E	Side_P_LSC_24	N	90	2.307	8.89	0.97	0.014						19												0.025	Steel	Steel	355000000	2.04E+11	0.3	A	2	24	
282	E	Side_P_LSC_24	N	90	2.307	9.86	0.97	0.014						19												0.025	Steel	Steel	355000000	2.04E+11	0.3	A	2	24	
283	E	Side_Stiffener_P_LSC_24	N	90	2.307	5.98	0	0	0.5	0.011	0.2	0.025	1												0.025	Steel	Steel	355000000	2.04E+11	0.3	A	2	24	
284	E	Side_Stiffener_P_LSC_24	N	90	2.307	6.95	0	0	0.5	0.011	0.2	0.025	1												0.025	Steel	Steel	355000000	2.04E+11	0.3	A	2	24	
285	E	Side_Stiffener_P_LSC_24	N	90	2.307	7.92	0	0	0.48	0.011	0.2	0.02	1												0.025	Steel	Steel	355000000	2.04E+11	0.3	A	2	24	
286	E	Side_Stiffener_P_LSC_24	N	90	2.307	8.89	0	0	0.48	0.011	0.2	0.02	1												0.025	Steel	Steel	355000000	2.04E+11	0.3	A	2	24	
287	E	Side_Stiffener_P_LSC_24	N	90	2.307	9.86	0	0	0.48	0.011	0.2	0.02	1												0.025	Steel	Steel	355000000	2.04E+11	0.3	A	2	24	
288	E	Side_Stiffener_P_LSC_24	N	-180	2.307	5.01	0	0	0.3	0.011	0.043	0.0453	1												0.025	Steel	Steel	355000000	2.04E+11	0.3	A	2	24	
289	E	Side_P_LSC_32	N	90	2.307	10.83	0.97	0.013						20												0.025	Steel	Steel	355000000	2.04E+11	0.3	A	2	32	
290	E	Side_P_LSC_32	N	90	2.307	11.8	0.97	0.013						20												0.025	Steel	Steel	355000000	2.04E+11	0.3	A	2	32	
291	E	Side_P_LSC_32	N	90	2.307	12.77	0.97	0.013						20												0.025	Steel	Steel	355000000	2.04E+11	0.3	A	2	32	
292	E	Side_P_LSC_32	N	90	2.307	13.74	0.97	0.0115						20												0.025	Steel	Steel	355000000	2.04E+11	0.3	A	2	32	
293	E	Side_P_LSC_32	N	90	2.307	14.71	0.97	0.0115						20												0.025	Steel	Steel	355000000	2.04E+11	0.3	A	2	32	
294	E	Side_P_LSC_32	N	90	2.307	15.68	0.97	0.0115						20												0.025	Steel	Steel	355000000	2.04E+11	0.3	A	2	32	
295	E	Side_Stiffener_P_LSC_32	N	90	2.307	11.8	0	0	0.4	0.011	0.2	0.02	1												0.025	Steel	Steel	355000000	2.04E+11	0.3	A	2	32	
296	E	Side_Stiffener_P_LSC_32	N	90	2.307	12.77	0	0	0.4	0.011	0.2	0.02	1												0.025	Steel	Steel	355000000	2.04E+11	0.3	A	2	32	
297	E	Side_Stiffener_P_LSC_32	N	90	2.307	13.74	0	0	0.4	0.011	0.15	0.02	1												0.025	Steel	Steel	355000000	2.04E+11	0.3	A	2	32	
298	E	Side_Stiffener_P_LSC_32	N	90	2.307	14.71	0	0	0.4	0.011	0.15	0.02	1												0.025	Steel	Steel	355000000	2.04E+11	0.3	A	2	32	
299	E	Side_Stiffener_P_LSC_32	N	90	2.307	15.68	0	0	0.4	0.011	0.15	0.02	1												0.025	Steel	Steel	355000000	2.04E+11	0.3	A	2	32	
300	E	Inner_Side_P_LSC_72	N	90	2.307	16.65	0.97	0.011						21												0.025	Steel	Steel	355000000	2.04E+11	0.3	A	2	72	
301	E	Side_P_LSC_72	N	90	2.307	17.62	0.97	0.011						21												0.025	Steel	Steel	355000000	2.04E+11	0.3	A	2	72	
302	E	Side_P_LSC_72	N	90	2.307	18.59	0.96	0.011						21												0.025	Steel	Steel	355000000	2.04E+11	0.3	A	2	72	
303	E	Side_Stiffener_P_LSC_72	N	90	2.307	17.62	0	0	0.32	0.011	0.13	0.015	1												0.025	Steel	Steel	355000000	2.04E+11	0.3	A	2	72	
304	E	Side_Stiffener_P_LSC_72	N	90	2.307	18.59	0	0	0.32	0.011	0.13	0.015	1												0.025	Steel	Steel	355000000	2.04E+11	0.3	A	2	72	
305	E	Inner_Side_P_LSC_62	N	90	2.307	19.55	0.646	0.043						22												0.025	Steel	Steel	355000000	2.04E+11	0.3	A	2	62	
306	E	Side_P_LSC_62	N	90	2.307	20.196	0.636	0.043						22												0.025	Steel	Steel	355000000	2.04E+11	0.3	A	2	62	
307	E	Side_P_LSC_62	N	90	2.307	20.832	0.636	0.073						22												0.025	Steel	Steel	355000000	2.04E+11	0.3	A	2	62	
308	E	Side_P_LSC_62	N	90	2.307	21.468	0.636	0.073						22												0.025	Steel	Steel	355000000	2.04E+11	0.3	A	2	62	
309	E	Side_P_LSC_62	N	90	2.307	22.104	0.636	0.073						22												0.025	Steel	Steel	355000000	2.04E+11	0.3	A	2	62	
310	E	Side_P_LSC_62	N	90	2.307	22.74	0.636	0.073						22												0.025	Steel	Steel	355000000	2.04E+11	0.3	A	2	62	
311	E	Side_P_LSC_62	N	90	2.307	23.376	0.724	0.073						22												0.025	Steel	Steel	355000000	2.04E+11	0.3	A	2	62	
312	E	Side_Stiffener_P_LSC_62	N	90	2.307	20.196	0	0	0.4	0.075			1												0.025	Steel	Steel	355000000	2.04E+11	0.3	A	2	62	
313	E	Side_Stiffener_P_LSC_62	N	90	2.307	20.832	0	0	0.4	0.075			1												0.025	Steel	Steel	355000000	2.04E+11	0.3	A	2	62	
314	E	Side_Stiffener_P_LSC_62	N	90	2.307	21.468	0	0	0.4	0.075			1												0.025	Steel	Steel	355000000	2.04E+11	0.3	A	2	62	
315	E	Side_Stiffener_P_LSC_62	N	90	2.307	22.104	0	0	0.4	0.075			1												0.025	Steel	Steel	355000000	2.04E+11	0.3	A	2	62	
316	E	Side_Stiffener_P_LSC_62	N	90	2.307	22.74	0	0	0.4	0.075			1												0.025	Steel	Steel	355000000	2.04E+11	0.3	A	2	62	
317	E	Side_Stiffener_P_LSC_62	N	90	2.307	23.376	0	0	0.3	0.075			1												0.025	Steel	Steel	355000000	2.04E+11	0.3	A	2	62	
318	E	Hatch_Side_P	N	90	2.307	24.1	1.74	0.073																	0.025	Steel	Steel	390000000	2.04E+11	0.3	A	EP		
319	E	Hatch_Side_P	N	0	1.607	25.84	0.7	0.073																	0.025	Steel	Steel	390000000	2.04E+11	0.3	A	EP		
320	E	SIDE S__Side_S_LSC_51	N	90	42.8	5.01	0.97	0.0175						14												0.025	Steel	Steel	355000000	2.04E+11	0.3	A	2	51	
321	E	Side_S_LSC_	N	90	42.8	5.98	0.97	0.0175						14												0.025	Steel	Steel	355000000	2.04E+11	0.3	A	2	51	
322	E	Side_S_LSC_	N	90	42.8	6.95	0.97	0.0175						14												0.025	Steel	Steel	355000000	2.04E+11	0.3	A	2	51	
323	E	Side_S_LSC_	N	90	42.8	7.92	0.97	0.0175						14												0.025	Steel	Steel	355000000	2.04E+11	0.3	A	2	51	
324	E	Side_S_LSC_	N	90	42.8	8.89	0.97	0.0175						14												0.025	Steel	Steel	355000000	2.04E+11	0.3	A	2	51	
325	E	Side_S_LSC_	N	90	42.8	9.86	0.97	0.0175						14												0.025	Steel	Steel	355000000	2.04E+11	0.3	A	2	51	
326	E	Side_Stiffener_S_LSC_	N	90	42.8	5.98	0	0	0.5	0.011	0.2	0.03	1												0.025	Steel	Steel	355000000	2.04E+11	0.3	A	2	51	
327	E	Side_Stiffener_S_LSC_	N	90	42.8	6.95	0	0	0.5	0.011	0.2	0.03	1												0.025	Steel	Steel	355000000	2.04E+11	0.3	A	2	51	
328	E	Side_Stiffener_S_LSC_	N	90	42.8	7.92	0	0	0.44	0.011	0.2	0.025	1												0.025	Steel	Steel	355000000	2.04E+11	0.3	A	2	51	
329	E	Side_Stiffener_S_LSC_	N	90	42.8	8.89	0	0	0.44	0.011	0.2	0.025	1												0.025	Steel	Steel	355000000	2.04E+11	0.3	A	2	51	
330	E	Side_Stiffener_S_LSC_51	N	90	42.8	9.86	0	0	0.44	0.011	0.2	0.025	1												0.025	Steel	Steel	355000000	2.04E+11	0.3	A	2	51	
331	E	Side_S_LSC_52	N	90	42.8	10.83	0.97	0.0175						15												0.025	Steel	Steel	355000000	2.04E+11	0.3	A	2	52	
332	E	Side_S_LSC_21	N	90	42.8	11.8	0.97	0.0175						15												0.025	Steel	Steel	355000000	2.04E+11	0.3	A	2	52	
333	E	Side_S_LSC_21	N	90	42.8	12.77	0.97	0.0175						15												0.025	Steel	Steel	355000000	2.04E+11	0.3	A	2	52	
334	E	Side_S_LSC_21	N	90	42.8	13.74	0.97	0.0175						15												0.025	Steel	Steel	355000000	2.04E+11	0.3	A	2	52	
335	E	Side_S_LSC_21	N	90	42.8	14.71	0.97	0.0175						15												0.025	Steel	Steel	355000000	2.04E+11	0.3	A	2	52	
336	E	Side_S_LSC_21	N	90	42.8	15.68	0.97	0.0175						15												0.025	Steel	Steel	355000000	2.04E+11	0.3	A	2	52	
337	E	Side_Stiffener_S_LSC_21	N	90	42.8	11.8	0	0	0.4	0.011	0.2	0.025	1												0.025	Steel	Steel	355000000	2.04E+11	0.3	A	2	52	
338	E	Side_Stiffener_S_LSC_21	N	90	42.8	12.77	0	0	0.4	0.011	0.2	0.025	1												0.025	Steel	Steel	355000000	2.04E+11	0.3	A	2	52	
339	E	Side_Stiffener_S_LSC_21	N	90	42.8	13.74	0	0	0.4	0.011	0.2	0.025	1												0.025	Steel	Steel	355000000	2.04E+11	0.3	A	2	52	
340	E	Side_Stiffener_S_LSC_21	N	90	42.8	14.71	0	0	0.4	0.011	0.2	0.025	1												0.025	Steel	Steel	355000000	2.04E+11	0.3	A	2	52	
341	E	Side_Stiffener_S_LSC_52	N	90	42.8	15.68	0	0	0.4	0.011	0.2	0.025	1												0.025	Steel	Steel	355000000	2.04E+11	0.3	A	2	52	
342	E	Side_S_LSC_53	N	90	42.8	16.65	0.97	0.0175						16												0.025	Steel	Steel	355000000	2.04E+11	0.3	A	2	53	
343	E	Side_S_LSC_25	N	90	42.8	17.62	0.97	0.0175						16												0.025	Steel	Steel	355000000	2.04E+11	0.3	A	2	53	
344	E	Side_S_LSC_25	N	90	42.8	18.59	0.96	0.0175						16												0.025	Steel	Steel	355000000	2.04E+11	0.3	A	2	53	

##
ProColl Template
##

Filename	Length	Units
10000TEU	0.791	m

##

##	ELEMENT DESCRIPTORS		COORDINATES:				PLATE DIMMARY LONGITUDINAL DIMENSIONS:												FRAME DIMENSIONS:						MATERIAL DEFINITIONS:							LOAD SHORTENING CURVE:			
ID	Type	Description	Mirror	angle	ycoord	zcoord	b	tp	hwx	twx	bfx	tfx	nsx	loop	hwx2	twx2	bfx2	tfx2	nsx2	hwy	twy	bfy	tfy	·amespacir	nsy	HAZ	Pmat	Smat	str0eq	E	v	Imp	LSCurve	Clone	Sname
345	E	Side_Stiffener_S_LSC_25	N	90	42.8	17.62	0	0	0.4	0.011	0.15	0.02	1													0.025	Steel	Steel	355000000	2.04E+11	0.3	A	2	53	
346	E	Side_Stiffener_S_LSC_53	N	90	42.8	18.59	0	0	0.4	0.011	0.15	0.02	1													0.025	Steel	Steel	355000000	2.04E+11	0.3	A	2	53	
347	E	Side_S_LSC_54	N	90	42.8	19.55	0.646	0.043						17												0.025	Steel	Steel	355000000	2.04E+11	0.3	A	2	54	
348	E	Side_S_LSC_26	N	90	42.8	20.196	0.636	0.043						17												0.025	Steel	Steel	355000000	2.04E+11	0.3	A	2	54	
349	E	Side_P_LSC_26	N	90	42.8	20.832	0.636	0.073						17												0.025	Steel	Steel	355000000	2.04E+11	0.3	A	2	54	
350	E	Side_P_LSC_26	N	90	42.8	21.468	0.636	0.073						17												0.025	Steel	Steel	355000000	2.04E+11	0.3	A	2	54	
351	E	Side_P_LSC_26	N	90	42.8	22.104	0.636	0.073						17												0.025	Steel	Steel	355000000	2.04E+11	0.3	A	2	54	
352	E	Side_P_LSC_26	N	90	42.8	22.74	0.636	0.073						17												0.025	Steel	Steel	355000000	2.04E+11	0.3	A	2	54	
353	E	Side_P_LSC_26	N	90	42.8	23.376	0.724	0.073						17												0.025	Steel	Steel	355000000	2.04E+11	0.3	A	2	54	
354	E	Side_Stiffener_P_LSC_26	N	90	42.8	20.196	0	0	0.4	0.075			1													0.025	Steel	Steel	355000000	2.04E+11	0.3	A	2	54	
355	E	Side_Stiffener_P_LSC_26	N	90	42.8	20.832	0	0	0.4	0.075			1													0.025	Steel	Steel	355000000	2.04E+11	0.3	A	2	54	
356	E	Side_Stiffener_P_LSC_26	N	90	42.8	21.468	0	0	0.4	0.075			1													0.025	Steel	Steel	355000000	2.04E+11	0.3	A	2	54	
357	E	Side_Stiffener_P_LSC_26	N	90	42.8	22.104	0	0	0.4	0.075			1													0.025	Steel	Steel	355000000	2.04E+11	0.3	A	2	54	
358	E	Side_Stiffener_P_LSC_26	N	90	42.8	22.74	0	0	0.4	0.075			1													0.025	Steel	Steel	355000000	2.04E+11	0.3	A	2	54	
359	E	Side_Stiffener_P_LSC_54	N	90	42.8	23.376	0	0	0.3	0.075			1													0.025	Steel	Steel	355000000	2.04E+11	0.3	A	2	54	
360	E	Inner_Side_S_LSC_79	N	90	40.493	5.01	0.97	0.0155						14												0.025	Steel	Steel	355000000	2.04E+11	0.3	A	2	79	
361	E	Side_S_LSC_24	N	90	40.493	5.98	0.97	0.0155						14												0.025	Steel	Steel	355000000	2.04E+11	0.3	A	2	79	
362	E	Side_S_LSC_24	N	90	40.493	6.95	0.97	0.0155						14												0.025	Steel	Steel	355000000	2.04E+11	0.3	A	2	79	
363	E	Side_P_LSC_24	N	90	40.493	7.92	0.97	0.014						14												0.025	Steel	Steel	355000000	2.04E+11	0.3	A	2	79	
364	E	Side_P_LSC_24	N	90	40.493	8.89	0.97	0.014						14												0.025	Steel	Steel	355000000	2.04E+11	0.3	A	2	79	
365	E	Side_P_LSC_24	N	90	40.493	9.86	0.97	0.014						14												0.025	Steel	Steel	355000000	2.04E+11	0.3	A	2	79	
366	E	Side_Stiffener_P_LSC_24	N	-90	40.493	5.98	0	0	0.5	0.011	0.2	0.025	1													0.025	Steel	Steel	355000000	2.04E+11	0.3	A	2	79	
367	E	Side_Stiffener_P_LSC_24	N	-90	40.493	6.95	0	0	0.5	0.011	0.2	0.025	1													0.025	Steel	Steel	355000000	2.04E+11	0.3	A	2	79	
368	E	Side_Stiffener_P_LSC_24	N	-90	40.493	7.92	0	0	0.48	0.011	0.2	0.02	1													0.025	Steel	Steel	355000000	2.04E+11	0.3	A	2	79	
369	E	Side_Stiffener_P_LSC_24	N	-90	40.493	8.89	0	0	0.48	0.011	0.2	0.02	1													0.025	Steel	Steel	355000000	2.04E+11	0.3	A	2	79	
370	E	Side_Stiffener_P_LSC_24	N	-90	40.493	9.86	0	0	0.48	0.011	0.2	0.02	1													0.025	Steel	Steel	355000000	2.04E+11	0.3	A	2	79	
371	E	Side_Stiffener_P_LSC_79	N	-180	40.493	5.01	0	0	0.3	0.011	0.043	0.0453	1													0.025	Steel	Steel	355000000	2.04E+11	0.3	A	2	79	
372	E	Side_S_LSC_70	N	90	40.493	10.83	0.97	0.013						15												0.025	Steel	Steel	355000000	2.04E+11	0.3	A	2	70	
373	E	Side_P_LSC_32	N	90	40.493	11.8	0.97	0.013						15												0.025	Steel	Steel	355000000	2.04E+11	0.3	A	2	70	
374	E	Side_P_LSC_32	N	90	40.493	12.77	0.97	0.013						15												0.025	Steel	Steel	355000000	2.04E+11	0.3	A	2	70	
375	E	Side_P_LSC_32	N	90	40.493	13.74	0.97	0.0115						15												0.025	Steel	Steel	355000000	2.04E+11	0.3	A	2	70	
376	E	Side_P_LSC_32	N	90	40.493	14.71	0.97	0.0115						15												0.025	Steel	Steel	355000000	2.04E+11	0.3	A	2	70	
377	E	Side_P_LSC_32	N	90	40.493	15.68	0.97	0.0115						15												0.025	Steel	Steel	355000000	2.04E+11	0.3	A	2	70	
378	E	Side_Stiffener_P_LSC_32	N	-90	40.493	11.8	0	0	0.4	0.011	0.2	0.02	1													0.025	Steel	Steel	355000000	2.04E+11	0.3	A	2	70	
379	E	Side_Stiffener_P_LSC_32	N	-90	40.493	12.77	0	0	0.4	0.011	0.2	0.02	1													0.025	Steel	Steel	355000000	2.04E+11	0.3	A	2	70	
380	E	Side_Stiffener_P_LSC_32	N	-90	40.493	13.74	0	0	0.4	0.011	0.15	0.02	1													0.025	Steel	Steel	355000000	2.04E+11	0.3	A	2	70	
381	E	Side_Stiffener_P_LSC_32	N	-90	40.493	14.71	0	0	0.4	0.011	0.15	0.02	1													0.025	Steel	Steel	355000000	2.04E+11	0.3	A	2	70	
382	E	Side_Stiffener_P_LSC_70	N	-90	40.493	15.68	0	0	0.4	0.011	0.15	0.02	1													0.025	Steel	Steel	355000000	2.04E+11	0.3	A	2	70	
383	E	Side_S_LSC_80	N	90	40.493	16.65	0.97	0.011						16												0.025	Steel	Steel	355000000	2.04E+11	0.3	A	2	80	
384	E	Side_P_LSC_25	N	90	40.493	17.62	0.97	0.011						16												0.025	Steel	Steel	355000000	2.04E+11	0.3	A	2	80	
385	E	Side_P_LSC_25	N	90	40.493	18.59	0.96	0.011						16												0.025	Steel	Steel	355000000	2.04E+11	0.3	A	2	80	
386	E	Side_Stiffener_P_LSC_25	N	-90	40.493	17.62	0	0	0.32	0.011	0.13	0.015	1													0.025	Steel	Steel	355000000	2.04E+11	0.3	A	2	80	
387	E	Side_Stiffener_P_LSC_80	N	-90	40.493	18.59	0	0	0.32	0.011	0.13	0.015	1													0.025	Steel	Steel	355000000	2.04E+11	0.3	A	2	80	
388	E	Inner_Side_S_LSC_33	N	90	40.493	19.55	0.646	0.043						17												0.025	Steel	Steel	355000000	2.04E+11	0.3	A	2	33	
389	E	Side_P_LSC_26	N	90	40.493	20.196	0.636	0.043						17												0.025	Steel	Steel	355000000	2.04E+11	0.3	A	2	33	
390	E	Side_P_LSC_26	N	90	40.493	20.832	0.636	0.073						17												0.025	Steel	Steel	355000000	2.04E+11	0.3	A	2	33	
391	E	Side_P_LSC_26	N	90	40.493	21.468	0.636	0.073						17												0.025	Steel	Steel	355000000	2.04E+11	0.3	A	2	33	
392	E	Side_P_LSC_26	N	90	40.493	22.104	0.636	0.073						17												0.025	Steel	Steel	355000000	2.04E+11	0.3	A	2	33	
393	E	Side_P_LSC_26	N	90	40.493	22.74	0.636	0.073						17												0.025	Steel	Steel	355000000	2.04E+11	0.3	A	2	33	
394	E	Side_P_LSC_26	N	90	40.493	23.376	0.724	0.073						17												0.025	Steel	Steel	355000000	2.04E+11	0.3	A	2	33	
395	E	Side_Stiffener_P_LSC_26	N	-90	40.493	20.196	0	0	0.4	0.075			1													0.025	Steel	Steel	355000000	2.04E+11	0.3	A	2	33	
396	E	Side_Stiffener_P_LSC_26	N	-90	40.493	20.832	0	0	0.4	0.075			1													0.025	Steel	Steel	355000000	2.04E+11	0.3	A	2	33	
397	E	Side_Stiffener_P_LSC_26	N	-90	40.493	21.468	0	0	0.4	0.075			1													0.025	Steel	Steel	355000000	2.04E+11	0.3	A	2	33	
398	E	Side_Stiffener_P_LSC_26	N	-90	40.493	22.104	0	0	0.4	0.075			1													0.025	Steel	Steel	355000000	2.04E+11	0.3	A	2	33	
399	E	Side_Stiffener_P_LSC_26	N	-90	40.493	22.74	0	0	0.4	0.075			1													0.025	Steel	Steel	355000000	2.04E+11	0.3	A	2	33	
400	E	Side_Stiffener_S_LSC_33	N	-90	40.493	23.376	0	0	0.3	0.075			1													0.025	Steel	Steel	355000000	2.04E+11	0.3	A	2	33	
401	E	Inner_Side_Hatch_S_LSC	N	90	40.493	24.1	1.74	0.073																		0.025	Steel	Steel	390000000	2.04E+11	0.3	A	EP		
402	E	Hatch_Side_S	N	0	40.493	25.84	0.7	0.073																		0.025	Steel	Steel	390000000	2.04E+11	0.3	A	EP		
403	E	D.B. WEBS St__DB_Web_S	N	90	25.259	0	0.7	0.0165						L7L8												0.025	Steel	Steel	355000000	2.04E+11	0.3	A	2	34	
404	E	DB_Web_S	N	90	25.259	0.7	0.7	0.0165						L7L8												0.025	Steel	Steel	355000000	2.04E+11	0.3	A	2	34	
405	E	DB_Web_S	N	90	25.259	1.4	0.7	0.0165						L7L8												0.025	Steel	Steel	355000000	2.04E+11	0.3	A	2	34	
406	E	DB_Web_Stiffener_S	N	-90	25.259	0.7	0	0	0.2	0.015			1													0.025	Steel	Steel	355000000	2.04E+11	0.3	A	2	34	
407	E	DB_Web_Stiffener_S	N	-90	25.259	1.4	0	0	0.2	0.015			1													0.025	Steel	Steel	355000000	2.04E+11	0.3	A	2	34	
408	E	DB_Web_S	N	90	27.863	0	0.7	0.0165						L8L9												0.025	Steel	Steel	355000000	2.04E+11	0.3	A	2	35	
409	E	DB_Web_S	N	90	27.863	0.7	0.7	0.0165						L8L9												0.025	Steel	Steel	355000000	2.04E+11	0.3	A	2	35	
410	E	DB_Web_S	N	90	27.863	1.4	0.7	0.0165						L8L9												0.025	Steel	Steel	355000000	2.04E+11	0.3	A	2	35	
411	E	DB_Web_Stiffener_S	N	-90	27.863	0.7	0	0	0.24	0.011	0.15	0.015	1													0.025	Steel	Steel	355000000	2.04E+11	0.3	A	2	35	
412	E	DB_Web_Stiffener_S	N	-90	27.863	1.4	0	0	0.24	0.011	0.15	0.015	1													0.025	Steel	Steel	355000000	2.04E+11	0.3	A	2	35	
413	E	DB_Web_S	N	90	30.353	0	0.7	0.0165						L9L10												0.025	Steel	Steel	355000000	2.04E+11	0.3	A	2	36	
414	E	DB_Web_S	N	90	30.353	0.7	0.7	0.0165						L9L10												0.025	Steel	Steel	355000000	2.04E+11	0.3	A	2	36	
415	E	DB_Web_S	N	90	30.353	1.4	0.7	0.0165						L9L10												0.025	Steel	Steel	355000000	2.04E+11	0.3	A	2	36	
416	E	DB_Web_Stiffener_S	N	-90	30.353	0.7	0	0	0.2	0.015			1													0.025	Steel	Steel	355000000	2.04E+11	0.3	A	2	36	
417	E	DB_Web_Stiffener_S	N	-90	30.353	1.4	0	0	0.2	0.015			1													0.025	Steel	Steel	355000000	2.04E+11	0.3	A	2	36	
418	E	DB_Web_S	N	90	32.843	0	0.7	0.0165						L10L11												0.025	Steel	Steel	355000000	2.04E+11	0.3	A	2	37	
419	E	DB_Web_S	N	90	32.843	0.7	0.7	0.0165						L10L11												0.025	Steel	Steel	355000000	2.04E+11	0.3	A	2	37	
420	E	DB_Web_S	N	90	32.843	1.4	0.7	0.0165						L10L11												0.025	Steel	Steel	355000000	2.04E+11	0.3	A	2	37	
421	E	DB_Web_Stiffener_S	N	-90	32.843	0.7	0	0	0.2	0.015			1													0.025	Steel	Steel	355000000	2.04E+11	0.3	A	2	37	
422	E	DB_Web_Stiffener_S	N	-90	32.843	1.4	0	0	0.2	0.015			1													0.025	Steel	Steel	355000000	2.04E+11	0.3	A	2	37	
423	E	DB_Web_S	N	90	35.333	0	0.7	0.0165						L11L12												0.025	Steel	Steel	355000000	2.04E+11	0.3	A	2	38	
424	E	DB_Web_S	N	90	35.333	0.7	0.7	0.0165						L11L12												0.025	Steel	Steel	355000000	2.04E+11	0.3	A	2	38	
425	E	DB_Web_S	N	90	35.333	1.4	0.7	0.0165						L11L12												0.025	Steel	Steel	355000000	2.04E+11	0.3	A	2	38	
426	E	DB_Web_Stiffener_S	N	-90	35.333	0.7	0	0	0.2	0.015			1													0.025	Steel	Steel	355000000	2.04E+11	0.3	A	2	38	
427	E	DB_Web_Stiffener_S	N	-90	35.333	1.4	0	0	0.2	0.015			1													0.025	Steel	Steel	355000000	2.04E+11	0.3	A	2	38	
428	E	DB_Web_S	N	90	38.71	0	0.7	0.0165						L12L13												0.025	Steel	Steel	355000000	2.04E+11	0.3	A	2	39	

##
ProColl Template
##

Filename	Length	Units
10000TEU	0.791	m

##

##	ELEMENT DESCRIPTORS		COORDINATES:				PLATE DIMMARY LONGITUDINAL DIMENSIONS:							FRAME DIMENSIONS:										MATERIAL DEFINITIONS:							LOAD SHORTENING CURVE:			
ID	Type	Description	Mirror	angle	ycoord	zcoord	b	tp	hwx	twx	bfx	tfx	nsx	loop	hwx2	twx2	bfx2	tfx2	nsx2	hwy	twy	bfy	tfy	amespacir	nsy	HAZ	Pmat	Smat	str0eq	E	v	Imp	LSCurve	Clone	Sname
429	E	DB_Web_S	N	90	38.71	0.7	0.7	0.0165						L12L13												0.025	Steel	Steel	355000000	2.04E+11	0.3	A	2	39	
430	E	DB_Web_S	N	90	38.71	1.4	0.7	0.0165						L12L13												0.025	Steel	Steel	355000000	2.04E+11	0.3	A	2	39	
431	E	DB_Web_Stiffener_S	N	-90	38.71	0.7	0	0	0.2	0.015			1													0.025	Steel	Steel	355000000	2.04E+11	0.3	A	2	39	
432	E	DB_Web_Stiffener_S	N	-90	38.71	1.4	0	0	0.2	0.015			1													0.025	Steel	Steel	355000000	2.04E+11	0.3	A	2	39	
433	E	DB_Web_Stiffener_S	N	-90	38.71	2.1	0	0	0.24	0.012	0.037	0.0387	1													0.025	Steel	Steel	355000000	2.04E+11	0.3	A	2	39	
434	E	D.B. WEBS CL__DB_Web_CL	N	90	21.4	0	0.7	0.0165						L6L7												0.025	Steel	Steel	355000000	2.04E+11	0.3	A	2	69	
435	E	DB_Web_CL	N	90	21.4	0.7	0.7	0.0165						L6L7												0.025	Steel	Steel	355000000	2.04E+11	0.3	A	2	69	
436	E	DB_Web_CL	N	90	21.4	1.4	0.7	0.0165						L6L7												0.025	Steel	Steel	355000000	2.04E+11	0.3	A	2	69	
437	E	DB_Web_Stiffener_CL	N	90	21.4	0.7	0	0	0.2	0.015			1													0.025	Steel	Steel	355000000	2.04E+11	0.3	A	2	69	
438	E	DB_Web_Stiffener_CL	N	90	21.4	1.4	0	0	0.2	0.015			1													0.025	Steel	Steel	355000000	2.04E+11	0.3	A	2	69	
439	E	D.B. WEBS P__DB_Web_P	N	90	17.541	0	0.7	0.0165		0				L5L6												0.025	Steel	Steel	355000000	2.04E+11	0.3	A	2	73	
440	E	DB_Web_P	N	90	17.541	0.7	0.7	0.0165		0				L5L6												0.025	Steel	Steel	355000000	2.04E+11	0.3	A	2	73	
441	E	DB_Web_P	N	90	17.541	1.4	0.7	0.0165		0				L5L6												0.025	Steel	Steel	355000000	2.04E+11	0.3	A	2	73	
442	E	DB_Web_Stiffener_P	N	90	17.541	0.7	0	0	0.2	0.015			1													0.025	Steel	Steel	355000000	2.04E+11	0.3	A	2	73	
443	E	DB_Web_Stiffener_P	N	90	17.541	1.4	0	0	0.2	0.015			1													0.025	Steel	Steel	355000000	2.04E+11	0.3	A	2	73	
444	E	DB_Web_P	N	90	14.937	0	0.7	0.0165						L4L5												0.025	Steel	Steel	355000000	2.04E+11	0.3	A	2	63	
445	E	DB_Web_P	N	90	14.937	0.7	0.7	0.0165						L4L5												0.025	Steel	Steel	355000000	2.04E+11	0.3	A	2	63	
446	E	DB_Web_P	N	90	14.937	1.4	0.7	0.0165						L4L5												0.025	Steel	Steel	355000000	2.04E+11	0.3	A	2	63	
447	E	DB_Web_Stiffener_P	N	90	14.937	0.7	0	0	0.24	0.011	0.15	0.015	1													0.025	Steel	Steel	355000000	2.04E+11	0.3	A	2	63	
448	E	DB_Web_Stiffener_P	N	90	14.937	1.4	0	0	0.24	0.011	0.15	0.015	1													0.025	Steel	Steel	355000000	2.04E+11	0.3	A	2	63	
449	E	DB_Web_P	N	90	12.447	0	0.7	0.0165						L3L4												0.025	Steel	Steel	355000000	2.04E+11	0.3	A	2	74	
450	E	DB_Web_P	N	90	12.447	0.7	0.7	0.0165						L3L4												0.025	Steel	Steel	355000000	2.04E+11	0.3	A	2	74	
451	E	DB_Web_P	N	90	12.447	1.4	0.7	0.0165						L3L4												0.025	Steel	Steel	355000000	2.04E+11	0.3	A	2	74	
452	E	DB_Web_Stiffener_P	N	90	12.447	0.7	0	0	0.2	0.015			1													0.025	Steel	Steel	355000000	2.04E+11	0.3	A	2	74	
453	E	DB_Web_Stiffener_P	N	90	12.447	1.4	0	0	0.2	0.015			1													0.025	Steel	Steel	355000000	2.04E+11	0.3	A	2	74	
454	E	DB_Web_P	N	90	9.957	0	0.7	0.0165						L2L3												0.025	Steel	Steel	355000000	2.04E+11	0.3	A	2	75	
455	E	DB_Web_P	N	90	9.957	0.7	0.7	0.0165						L2L3												0.025	Steel	Steel	355000000	2.04E+11	0.3	A	2	75	
456	E	DB_Web_P	N	90	9.957	1.4	0.7	0.0165						L2L3												0.025	Steel	Steel	355000000	2.04E+11	0.3	A	2	75	
457	E	DB_Web_Stiffener_P	N	90	9.957	0.7	0	0	0.2	0.015			1													0.025	Steel	Steel	355000000	2.04E+11	0.3	A	2	75	
458	E	DB_Web_Stiffener_P	N	90	9.957	1.4	0	0	0.2	0.015			1													0.025	Steel	Steel	355000000	2.04E+11	0.3	A	2	75	
459	E	DB_Web_P	N	90	7.467	0	0.7	0.0165						L1L2												0.025	Steel	Steel	355000000	2.04E+11	0.3	A	2	64	
460	E	DB_Web_P	N	90	7.467	0.7	0.7	0.0165						L1L2												0.025	Steel	Steel	355000000	2.04E+11	0.3	A	2	64	
461	E	DB_Web_P	N	90	7.467	1.4	0.7	0.0165						L1L2												0.025	Steel	Steel	355000000	2.04E+11	0.3	A	2	64	
462	E	DB_Web_Stiffener_P	N	90	7.467	0.7	0	0	0.2	0.015			1													0.025	Steel	Steel	355000000	2.04E+11	0.3	A	2	64	
463	E	DB_Web_Stiffener_P	N	90	7.467	1.4	0	0	0.2	0.015			1													0.025	Steel	Steel	355000000	2.04E+11	0.3	A	2	64	
464	E	DB_Web_P	N	90	4.09	0	0.7	0.0165						L1L18												0.025	Steel	Steel	355000000	2.04E+11	0.3	A	2	76	
465	E	DB_Web_P	N	90	4.09	0.7	0.7	0.0165						L1L18												0.025	Steel	Steel	355000000	2.04E+11	0.3	A	2	76	
466	E	DB_Web_P	N	90	4.09	1.4	0.7	0.0165						L1L18												0.025	Steel	Steel	355000000	2.04E+11	0.3	A	2	76	
467	E	DB_Web_Stiffener_P	N	90	4.09	0.7	0	0	0.2	0.015			1													0.025	Steel	Steel	355000000	2.04E+11	0.3	A	2	76	
468	E	DB_Web_Stiffener_P	N	90	4.09	1.4	0	0	0.2	0.015			1													0.025	Steel	Steel	355000000	2.04E+11	0.3	A	2	76	
469	E	Side Web St__Side_Web_S	N	0	40.493	5.01	0.769	0.014						L13L14												0.025	Steel	Steel	355000000	2.04E+11	0.3	A	2	40	
470	E	Side_Web_S	N	0	41.262	5.01	0.769	0.014						L13L14												0.025	Steel	Steel	355000000	2.04E+11	0.3	A	2	40	
471	E	Side_Web_S	N	0	42.031	5.01	0.769	0.014						L13L14												0.025	Steel	Steel	355000000	2.04E+11	0.3	A	2	40	
472	E	Side_Web_Stiffener_S	N	-180	40.493	5.01	0	0	0.3	0.011	0.043	0.0453	1													0.025	Steel	Steel	355000000	2.04E+11	0.3	A	2	40	
473	E	Side_Web_Stiffener_S	N	-180	41.262	5.01	0	0	0.3	0.012	0.043	0.0453	1													0.025	Steel	Steel	355000000	2.04E+11	0.3	A	2	40	
474	E	Side_Web_Stiffener_S	N	-180	42.031	5.01	0	0	0.3	0.012	0.043	0.0453	1													0.025	Steel	Steel	355000000	2.04E+11	0.3	A	2	40	
475	E	Side_Web_S	N	0	40.493	10.83	0.769	0.0115						L14L15												0.025	Steel	Steel	355000000	2.04E+11	0.3	A	2	41	
476	E	Side_Web_S	N	0	41.262	10.83	0.769	0.0115						L14L15												0.025	Steel	Steel	355000000	2.04E+11	0.3	A	2	41	
477	E	Side_Web_S	N	0	42.031	10.83	0.769	0.0115						L14L15												0.025	Steel	Steel	355000000	2.04E+11	0.3	A	2	41	
478	E	Side_Web_Stiffener_S	N	-180	41.262	10.83	0	0	0.26	0.01	0.037	0.0387	1													0.025	Steel	Steel	355000000	2.04E+11	0.3	A	2	41	
479	E	Side_Web_Stiffener_S	N	-180	42.031	10.83	0	0	0.26	0.01	0.037	0.0387	1													0.025	Steel	Steel	355000000	2.04E+11	0.3	A	2	41	
480	E	Side_Web_S	N	0	40.493	16.65	0.769	0.0115						L15L16												0.025	Steel	Steel	355000000	2.04E+11	0.3	A	2	42	
481	E	Side_Web_S	N	0	41.262	16.65	0.769	0.0115						L15L16												0.025	Steel	Steel	355000000	2.04E+11	0.3	A	2	42	
482	E	Side_Web_S	N	0	42.031	16.65	0.769	0.0115						L15L16												0.025	Steel	Steel	355000000	2.04E+11	0.3	A	2	42	
483	E	Side_Web_Stiffener_S	N	-180	41.262	16.65	0	0	0.34	0.012	0.049	0.052	1													0.025	Steel	Steel	355000000	2.04E+11	0.3	A	2	42	
484	E	Side_Web_Stiffener_S	N	-180	42.031	16.65	0	0	0.34	0.012	0.049	0.052	1													0.025	Steel	Steel	355000000	2.04E+11	0.3	A	2	42	
485	E	Side_Web_S	N	0	40.493	19.55	0.769	0.011						L16L17												0.025	Steel	Steel	355000000	2.04E+11	0.3	A	2	43	
486	E	Side_Web_S	N	0	41.262	19.55	0.769	0.011						L16L17												0.025	Steel	Steel	355000000	2.04E+11	0.3	A	2	43	
487	E	Side_Web_S	N	0	42.031	19.55	0.769	0.011						L16L17												0.025	Steel	Steel	355000000	2.04E+11	0.3	A	2	43	
488	E	Side_Web_Stiffener_S	N	-180	41.262	19.55	0	0	0.26	0.01	0.037	0.0387	1													0.025	Steel	Steel	355000000	2.04E+11	0.3	A	2	43	
489	E	Side_Web_Stiffener_S	N	-180	42.031	19.55	0	0	0.26	0.01	0.037	0.0387	1													0.025	Steel	Steel	355000000	2.04E+11	0.3	A	2	43	
490	E	Side_Web_S	N	0	40.493	24.1	0.769	0.073						17												0.025	Steel	Steel	355000000	2.04E+11	0.3	A	2	44	
491	E	Side_Web_S	N	0	41.262	24.1	0.769	0.073						17												0.025	Steel	Steel	355000000	2.04E+11	0.3	A	2	44	
492	E	Side_Web_S	N	0	42.031	24.1	0.769	0.073						17												0.025	Steel	Steel	355000000	2.04E+11	0.3	A	2	44	
493	E	Side_Web_Stiffener_S	N	-180	41.262	24.1	0	0	0.4	0.075			1													0.025	Steel	Steel	355000000	2.04E+11	0.3	A	2	44	
494	E	Side_Web_Stiffener_S	N	-180	42.031	24.1	0	0	0.4	0.075			1													0.025	Steel	Steel	355000000	2.04E+11	0.3	A	2	44	
495	E	Step Cell 13_Plate St	N	90	38.71	2.1	0.97	0.0155						13												0.025	Steel	Steel	355000000	2.04E+11	0.3	A	2	61	
496	E	Step Cell 13_Plate St	N	90	38.71	3.07	0.97	0.0155						13												0.025	Steel	Steel	355000000	2.04E+11	0.3	A	2	61	
497	E	Step Cell 13_Plate St	N	90	38.71	4.04	0.97	0.0155						13												0.025	Steel	Steel	355000000	2.04E+11	0.3	A	2	61	
498	E	Step Cell 13_Stiffener St	N	-90	38.71	3.07	0	0	0.4	0.011	0.2	0.02	1													0.025	Steel	Steel	355000000	2.04E+11	0.3	A	2	61	
499	E	Step Cell 13_Stiffener St	N	-90	38.71	4.04	0	0	0.4	0.011	0.2	0.02	1													0.025	Steel	Steel	355000000	2.04E+11	0.3	A	2	61	
500	E	Step Cell 13_Plate St	N	0	38.71	5.01	0.887	0.014						13												0.025	Steel	Steel	355000000	2.04E+11	0.3	A	2	71	
501	E	Step Cell 13_Plate St	N	0	39.597	5.01	0.896	0.014						13												0.025	Steel	Steel	355000000	2.04E+11	0.3	A	2	71	
502	E	Step Cell 13_Stiffener St	N	-180	39.597	5.01	0	0	0.3	0.011	0.043	0.0453	1													0.025	Steel	Steel	355000000	2.04E+11	0.3	A	2	71	
503	E	Side_Web_P	N	0	0	5.01	0.769	0.014						L18L19												0.025	Steel	Steel	355000000	2.04E+11	0.3	A	2	78	
504	E	Side_Web_P	N	0	0.769	5.01	0.769	0.014						L18L19												0.025	Steel	Steel	355000000	2.04E+11	0.3	A	2	78	
505	E	Side_Web_P	N	0	1.538	5.01	0.769	0.014						L18L19												0.025	Steel	Steel	355000000	2.04E+11	0.3	A	2	78	
506	E	Side_Web_Stiffener_P	N	-180	0.769	5.01	0	0	0.3	0.012	0.043	0.0453	1													0.025	Steel	Steel	355000000	2.04E+11	0.3	A	2	78	
507	E	Side_Web_Stiffener_P	N	-180	1.538	5.01	0	0	0.3	0.012	0.043	0.0453	1													0.025	Steel	Steel	355000000	2.04E+11	0.3	A	2	78	
508	E	Side_Web_P	N	0	0	10.83	0.769	0.0115						L19L20												0.025	Steel	Steel	355000000	2.04E+11	0.3	A	2	65	
509	E	Side_Web_P	N	0	0.769	10.83	0.769	0.0115						L19L20												0.025	Steel	Steel	355000000	2.04E+11	0.3	A	2	65	
510	E	Side_Web_P	N	0	1.538	10.83	0.769	0.0115						L19L20												0.025	Steel	Steel	355000000	2.04E+11	0.3	A	2	65	
511	E	Side_Web_Stiffener_P	N	-180	0.769	10.83	0	0	0.26	0.01	0.037	0.0387	1													0.025	Steel	Steel	355000000	2.04E+11	0.3	A	2	65	
512	E	Side_Web_Stiffener_P	N	-180	1.538	10.83	0	0	0.26	0.01	0.037	0.0387	1													0.025	Steel	Steel	355000000	2.04E+11	0.3	A	2	65	

##
ProColl Template
##

Filename	Length	Units
10000TEU	0.791	m

##

##	ELEMENT DESCRIPTORS		COORDINATES:				PLATE DIMMARY LONGITUDINAL DIMENSIONS:											FRAME DIMENSIONS:						MATERIAL DEFINITIONS:							LOAD SHORTENING CURVE:			
ID	Type	Description	Mirror	angle	ycoord	zcoord	b	tp	hwx	twx	bfx	tfx	nsx	loop	hwx2	twx2	bfx2	tfx2	nsx2	hwy	twy	bfy	tfy	amespacir	nsy	HAZ	Pmat	Smat	strOeq	E	v	Imp	LSCurve	Clone	Sname
513	E	Side_Web_P	N	0	0	16.65	0.769	0.0115						L20L21												0.025	Steel	Steel	355000000	2.04E+11	0.3	A	2	66	
514	E	Side_Web_P	N	0	0.769	16.65	0.769	0.0115						L20L21												0.025	Steel	Steel	355000000	2.04E+11	0.3	A	2	66	
515	E	Side_Web_P	N	0	1.538	16.65	0.769	0.0115						L20L21												0.025	Steel	Steel	355000000	2.04E+11	0.3	A	2	66	
516	E	Side_Web_Stiffener_P	N	-180	0.769	16.65	0	0	0.34	0.012	0.049	0.052	1													0.025	Steel	Steel	355000000	2.04E+11	0.3	A	2	66	
517	E	Side_Web_Stiffener_P	N	-180	1.538	16.65	0	0	0.34	0.012	0.049	0.052	1													0.025	Steel	Steel	355000000	2.04E+11	0.3	A	2	66	
518	E	Side_Web_P	N	0	0	19.55	0.769	0.011						L21L22												0.025	Steel	Steel	355000000	2.04E+11	0.3	A	2	67	
519	E	Side_Web_P	N	0	0.769	19.55	0.769	0.011						L21L22												0.025	Steel	Steel	355000000	2.04E+11	0.3	A	2	67	
520	E	Side_Web_P	N	0	1.538	19.55	0.769	0.011						L21L22												0.025	Steel	Steel	355000000	2.04E+11	0.3	A	2	67	
521	E	Side_Web_Stiffener_P	N	-180	0.769	19.55	0	0	0.26	0.01	0.037	0.0387	1													0.025	Steel	Steel	355000000	2.04E+11	0.3	A	2	67	
522	E	Side_Web_Stiffener_P	N	-180	1.538	19.55	0	0	0.26	0.01	0.037	0.0387	1													0.025	Steel	Steel	355000000	2.04E+11	0.3	A	2	67	
523	E	Side_Web_P	N	0	0	24.1	0.769	0.073						22												0.025	Steel	Steel	355000000	2.04E+11	0.3	A	2	68	
524	E	Side_Web_P	N	0	0.769	24.1	0.769	0.073						22												0.025	Steel	Steel	355000000	2.04E+11	0.3	A	2	68	
525	E	Side_Web_P	N	0	1.538	24.1	0.769	0.073						22												0.025	Steel	Steel	355000000	2.04E+11	0.3	A	2	68	
526	E	Side_Web_Stiffener_P	N	-180	0.769	24.1	0	0	0.4	0.075			1													0.025	Steel	Steel	355000000	2.04E+11	0.3	A	2	68	
527	E	Side_Web_Stiffener_P	N	-180	1.538	24.1	0	0	0.4	0.075			1													0.025	Steel	Steel	355000000	2.04E+11	0.3	A	2	68	
528	E	Step Cell 18_Plate St	N	90	4.09	2.1	0.97	0.0155						18												0.025	Steel	Steel	355000000	2.04E+11	0.3	A	2	23	
529	E	Step Cell 18_Plate P	N	90	4.09	3.07	0.97	0.0155						18												0.025	Steel	Steel	355000000	2.04E+11	0.3	A	2	23	
530	E	Step Cell 18_Plate P	N	90	4.09	4.04	0.97	0.0155						18												0.025	Steel	Steel	355000000	2.04E+11	0.3	A	2	23	
531	E	Step Cell 18_Stiffener P	N	90	4.09	3.07	0	0	0.4	0.011	0.2	0.02	1													0.025	Steel	Steel	355000000	2.04E+11	0.3	A	2	23	
532	E	Step Cell 18_Stiffener P	N	90	4.09	4.04	0	0	0.4	0.011	0.2	0.02	1													0.025	Steel	Steel	355000000	2.04E+11	0.3	A	2	23	
533	E	Step Cell 18_Plate P	N	0	3.203	5.01	0.887	0.014						18												0.025	Steel	Steel	355000000	2.04E+11	0.3	A	2	77	
534	E	Step Cell 18_Plate P	N	0	2.307	5.01	0.896	0.014						18												0.025	Steel	Steel	355000000	2.04E+11	0.3	A	2	77	
535	E	Step Cell 18_Stiffener P	N	-180	3.203	5.01	0	0	0.3	0.011	0.043	0.0453	1													0.025	Steel	Steel	355000000	2.04E+11	0.3	A	2	77	
536	E	Bilge_S	N	14.6699	38.71	0	0.88702	0.025						13												0.025	Steel	Steel	355000000	2.04E+11	0.3	A	2	86	
537	E	Bilge_S	N	25.0164	39.5681	0.22464	0.87995	0.025						13												0.025	Steel	Steel	355000000	2.04E+11	0.3	A	2	89	
538	E	Bilge_S	N	35.3297	40.3655	0.59675	0.8802	0.021						13												0.025	Steel	Steel	355000000	2.04E+11	0.3	A	2	7	
539	E	Bilge_S	N	45.6134	41.0836	1.10575	0.87978	0.021						13												0.025	Steel	Steel	355000000	2.04E+11	0.3	A	2	13	
540	E	Bilge_S	N	55.9224	41.699	1.73447	0.88004	0.021						13												0.025	Steel	Steel	355000000	2.04E+11	0.3	A	2	91	
541	E	Bilge_S	N	66.2299	42.1921	2.46339	0.88	0.021						13												0.025	Steel	Steel	355000000	2.04E+11	0.3	A	2	87	
542	E	Bilge_S	N	76.5356	42.5468	3.26874	0.88	0.021						13												0.025	Steel	Steel	355000000	2.04E+11	0.3	A	2	90	
543	E	Bilge_S	N	86.8777	42.7517	4.12455	0.88677	0.021						13												0.025	Steel	Steel	355000000	2.04E+11	0.3	A	2	14	
544	E	Step_5010_S	N	0	37.834	5.01	0.876	0.014																		0.025	Steel	Steel	355000000	2.04E+11	0.3	A	EP		
545	E	Step_5010_S	N	-90	37.834	5.01	0.8	0.015																		0.025	Steel	Steel	355000000	2.04E+11	0.3	A	EP		
546	E	Bilge_P	N	-86.8777	0	5.01	0.88677	0.021						18												0.025	Steel	Steel	355000000	2.04E+11	0.3	A	2	18	
547	E	Bilge_P	N	-76.5356	0.0483	4.12455	0.88	0.021						18												0.025	Steel	Steel	355000000	2.04E+11	0.3	A	2	84	
548	E	Bilge_P	N	-66.2299	0.2532	3.26874	0.88	0.021						18												0.025	Steel	Steel	355000000	2.04E+11	0.3	A	2	10	
549	E	Bilge_P	N	-55.9224	0.6079	2.46339	0.88004	0.021						18												0.025	Steel	Steel	355000000	2.04E+11	0.3	A	2	83	
550	E	Bilge_P	N	-45.6134	1.101	1.73447	0.87978	0.021						18												0.025	Steel	Steel	355000000	2.04E+11	0.3	A	2	82	
551	E	Bilge_P	N	-35.3297	1.7164	1.10575	0.8802	0.021						18												0.025	Steel	Steel	355000000	2.04E+11	0.3	A	2	17	
552	E	Bilge_P	N	-25.0164	2.4345	0.59675	0.87995	0.025						18												0.025	Steel	Steel	355000000	2.04E+11	0.3	A	2	81	
553	E	Bilge_P	N	-14.6699	3.2319	0.22464	0.88702	0.025						18												0.025	Steel	Steel	355000000	2.04E+11	0.3	A	2	9	
554	E	Step_5010_P	N	180	4.966	5.01	0.876	0.014																		0.025	Steel	Steel	355000000	2.04E+11	0.3	A	EP		
555	E	Step_5010_P	N	-90	4.966	5.01	0.8	0.015																		0.025	Steel	Steel	355000000	2.04E+11	0.3	A	EP		
556	E	EP_12358	N	-180	41.193	25.84			0.25	0.04			1													0.025	Steel	Steel	3.90E+08	2.04E+11	0.3	A	EP		
557	E	12359	N	25.0164	40.3655	0.59675			0.37	0.013			1													0.025	Steel	Steel	355000000	2.04E+11	0.3	A	EP		
558	E	12360	N	35.3334	41.0836	1.10575			0.37	0.013			1													0.025	Steel	Steel	355000000	2.04E+11	0.3	A	EP		
559	E	12361	N	55.9224	42.1921	2.46339			0.37	0.013			1													0.025	Steel	Steel	355000000	2.04E+11	0.3	A	EP		
560	E	12362	N	89.9956	42.7517	4.12455			0.37	0.013			1													0.025	Steel	Steel	355000000	2.04E+11	0.3	A	EP		
561	E	12383	N	-180	1.607	25.84			0.25	0.04			1													0.025	Steel	Steel	3.90E+08	2.04E+11	0.3	A	EP		
562	E	12385	N	0.00014	3.2319	0.22464			0.37	0.013			1													0.025	Steel	Steel	355000000	2.04E+11	0.3	A	EP		
563	E	12386	N	-66.2299	0.2532	3.26874			0.37	0.013			1													0.025	Steel	Steel	355000000	2.04E+11	0.3	A	EP		
564	E	12252	N	90	4.966	4.21			0.2	0.015			1													0.025	Steel	Steel	355000000	2.04E+11	0.3	A	EP		
565	E	12261	N	-25.0164	2.4345	0.59675			0.37	0.013			1													0.025	Steel	Steel	355000000	2.04E+11	0.3	A	EP		
566	E	12262	N	-35.3334	1.7164	1.10575			0.37	0.013			1													0.025	Steel	Steel	355000000	2.04E+11	0.3	A	EP		
567	E	12263	N	-55.9224	0.6079	2.46339			0.37	0.013			1													0.025	Steel	Steel	355000000	2.04E+11	0.3	A	EP		
568	E	12264	N	-89.9956	0.0483	4.12455			0.37	0.013			1													0.025	Steel	Steel	355000000	2.04E+11	0.3	A	EP		
569	E	12316	N	-90	37.834	4.21			0.2	0.015			1													0.025	Steel	Steel	355000000	2.04E+11	0.3	A	EP		
570	E	12407	N	-0.00014	39.5681	0.22464			0.37	0.013			1													0.025	Steel	Steel	355000000	2.04E+11	0.3	A	EP		
571	E	12408	N	66.2299	42.5468	3.26874			0.37	0.013			1													0.025	Steel	Steel	355000000	2.04E+11	0.3	A	EP		
572	E	12415	N	-45.6134	1.101	1.73447			0.37	0.013			1													0.025	Steel	Steel	355000000	2.04E+11	0.3	A	EP		
573	E	12417	N	45.6134	41.699	1.73447			0.37	0.013			1													0.025	Steel	Steel	355000000	2.04E+11	0.3	A	EP		

f. Intact Box Girder E (Chapter 7)

##																																	
##	ProColl Template																																
##																																	
Filename	Length	Units																															
Box Girder E	1800	mm																															
##																																	
##	ELEMENT DESCRIPTORS		COORDINATES:				PLATE DIMMARY LONGITUDINAL DIMENSIONS:												FRAME DIMENSIONS:					MATERIAL DEFINITIONS:								LOAD SHORTENING CURVE:			
ID	Type	Description	Mirror	angle	ycoord	zcoord	b	tp	hwx	twx	bfx	tfx	nsx	loop	hwx2	twx2	bfx2	tfx2	nsx2	hwy	twy	bfy	tfy	amespacir	nsy	HAZ	Pmat	Smat	str0eq	E	v	Imp	LSCurve	Clone	Sname
1	LSC		N				600	8	113.6	6.65	63.5	13.4	7							227.2	13.3	127	26.8	1800	5	50	Steel	Steel	245	207000	0.3	A	1		
2	LSC		N				600	10	113.6	6.65	63.5	13.4	6							227.2	13.3	127	26.8	1800	5	50	Steel	Steel	245	207000	0.3	A	1		
3	LSC		N				600	8	113.6	6.65	63.5	13.4	7							227.2	13.3	127	26.8	1800	5	50	Steel	Steel	245	207000	0.3	A	1		
4	LSC		N				600	10	113.6	6.65	63.5	13.4	6							227.2	13.3	127	26.8	1800	5	50	Steel	Steel	245	207000	0.3	A	1		
5	E	Horz. Plate_1	N	0	0	0	600	8						1												50	Steel	Steel	245	207000	0.3	A	2	1	
6	E	Horz. Plate_2	N	0	600	0	600	8						1												50	Steel	Steel	245	207000	0.3	A	2	1	
7	E	Horz. Plate_3	N	0	1200	0	600	8						1												50	Steel	Steel	245	207000	0.3	A	2	1	
8	E	Horz. Plate_4	N	0	1800	0	600	8						1												50	Steel	Steel	245	207000	0.3	A	2	1	
9	E	Horz. Plate_5	N	0	2400	0	600	8						1												50	Steel	Steel	245	207000	0.3	A	2	1	
10	E	Horz. Plate_6	N	0	3000	0	600	8						1												50	Steel	Steel	245	207000	0.3	A	2	1	
11	E	Horz. Plate_7	N	0	3600	0	600	8						1												50	Steel	Steel	245	207000	0.3	A	2	1	
12	E	Horz. Plate_8	N	0	4200	0	600	8						1												50	Steel	Steel	245	207000	0.3	A	2	1	
13	E	Vert. Plate_R_1	N	90	4800	0	600	10						1												50	Steel	Steel	245	207000	0.3	A	2	2	
14	E	Vert. Plate_R_2	N	90	4800	600	600	10						1												50	Steel	Steel	245	207000	0.3	A	2	2	
15	E	Vert. Plate_R_3	N	90	4800	1200	600	10						1												50	Steel	Steel	245	207000	0.3	A	2	2	
16	E	Vert. Plate_R_4	N	90	4800	1800	600	10						1												50	Steel	Steel	245	207000	0.3	A	2	2	
17	E	Vert. Plate_R_5	N	90	4800	2400	600	10						1												50	Steel	Steel	245	207000	0.3	A	2	2	
18	E	Vert. Plate_R_6	N	90	4800	3000	600	10						1												50	Steel	Steel	245	207000	0.3	A	2	2	
19	E	Vert. Plate_R_7	N	90	4800	3600	600	10						1												50	Steel	Steel	245	207000	0.3	A	2	2	
20	E	Horz. Plate_Top_1	N	180	4800	4200	600	8						1												50	Steel	Steel	245	207000	0.3	A	2	3	
21	E	Horz. Plate_Top_2	N	180	4200	4200	600	8						1												50	Steel	Steel	245	207000	0.3	A	2	3	
22	E	Horz. Plate_Top_3	N	180	3600	4200	600	8						1												50	Steel	Steel	245	207000	0.3	A	2	3	
23	E	Horz. Plate_Top_4	N	180	3000	4200	600	8						1												50	Steel	Steel	245	207000	0.3	A	2	3	
24	E	Horz. Plate_Top_5	N	180	2400	4200	600	8						1												50	Steel	Steel	245	207000	0.3	A	2	3	
25	E	Horz. Plate_Top_6	N	180	1800	4200	600	8						1												50	Steel	Steel	245	207000	0.3	A	2	3	
26	E	Horz. Plate_Top_7	N	180	1200	4200	600	8						1												50	Steel	Steel	245	207000	0.3	A	2	3	
27	E	Horz. Plate_Top_8	N	180	600	4200	600	8						1												50	Steel	Steel	245	207000	0.3	A	2	3	
28	E	Vert. Plate_Left_1	N	270	0	4200	600	10						1												50	Steel	Steel	245	207000	0.3	A	2	4	
29	E	Vert. Plate_Left_2	N	270	0	3600	600	10						1												50	Steel	Steel	245	207000	0.3	A	2	4	
30	E	Vert. Plate_Left_3	N	270	0	3000	600	10						1												50	Steel	Steel	245	207000	0.3	A	2	4	
31	E	Vert. Plate_Left_4	N	270	0	2400	600	10						1												50	Steel	Steel	245	207000	0.3	A	2	4	
32	E	Vert. Plate_Left_5	N	270	0	1800	600	10						1												50	Steel	Steel	245	207000	0.3	A	2	4	
33	E	Vert. Plate_Left_6	N	270	0	1200	600	10						1												50	Steel	Steel	245	207000	0.3	A	2	4	
34	E	Vert. Plate_Left_7	N	270	0	600	600	10						1												50	Steel	Steel	245	207000	0.3	A	2	4	
35	E	bottom_stif_1	N	0	600	0			113.6	6.65	63.5	13.4	1													25	Steel	Steel	245	207000	0.3	A	2	1	
36	E	bottom_stif_2	N	0	1200	0			113.6	6.65	63.5	13.4	1													25	Steel	Steel	245	207000	0.3	A	2	1	
37	E	bottom_stif_3	N	0	1800	0			113.6	6.65	63.5	13.4	1													25	Steel	Steel	245	207000	0.3	A	2	1	
38	E	bottom_stif_4	N	0	2400	0			113.6	6.65	63.5	13.4	1													25	Steel	Steel	245	207000	0.3	A	2	1	
39	E	bottom_stif_5	N	0	3000	0			113.6	6.65	63.5	13.4	1													25	Steel	Steel	245	207000	0.3	A	2	1	
40	E	bottom_stif_6	N	0	3600	0			113.6	6.65	63.5	13.4	1													25	Steel	Steel	245	207000	0.3	A	2	1	
41	E	bottom_stif_7	N	0	4200	0			113.6	6.65	63.5	13.4	1													25	Steel	Steel	245	207000	0.3	A	2	1	
42	E	rightside_stif_1	N	90	4800	600			113.6	6.65	63.5	13.4	1													25	Steel	Steel	245	207000	0.3	A	2	2	
43	E	rightside_stif_2	N	90	4800	1200			113.6	6.65	63.5	13.4	1													25	Steel	Steel	245	207000	0.3	A	2	2	
44	E	rightside_stif_3	N	90	4800	1800			113.6	6.65	63.5	13.4	1													25	Steel	Steel	245	207000	0.3	A	2	2	
45	E	rightside_stif_4	N	90	4800	2400			113.6	6.65	63.5	13.4	1													25	Steel	Steel	245	207000	0.3	A	2	2	
46	E	rightside_stif_5	N	90	4800	3000			113.6	6.65	63.5	13.4	1													25	Steel	Steel	245	207000	0.3	A	2	2	
47	E	rightside_stif_6	N	90	4800	3600			113.6	6.65	63.5	13.4	1													25	Steel	Steel	245	207000	0.3	A	2	2	
48	E	top_stif_1	N	180	4200	4200			113.6	6.65	63.5	13.4	1													25	Steel	Steel	245	207000	0.3	A	2	3	
49	E	top_stif_2	N	180	3600	4200			113.6	6.65	63.5	13.4	1													25	Steel	Steel	245	207000	0.3	A	2	3	
50	E	top_stif_3	N	180	3000	4200			113.6	6.65	63.5	13.4	1													25	Steel	Steel	245	207000	0.3	A	2	3	
51	E	top_stif_4	N	180	2400	4200			113.6	6.65	63.5	13.4	1													25	Steel	Steel	245	207000	0.3	A	2	3	
52	E	top_stif_5	N	180	1800	4200			113.6	6.65	63.5	13.4	1													25	Steel	Steel	245	207000	0.3	A	2	3	
53	E	top_stif_6	N	180	1200	4200			113.6	6.65	63.5	13.4	1													25	Steel	Steel	245	207000	0.3	A	2	3	
54	E	top_stif_7	N	180	600	4200			113.6	6.65	63.5	13.4	1													25	Steel	Steel	245	207000	0.3	A	2	3	
55	E	leftside_stif_1	N	270	0	3600			113.6	6.65	63.5	13.4	1													25	Steel	Steel	245	207000	0.3	A	2	4	
56	E	leftside_stif_2	N	270	0	3000			113.6	6.65	63.5	13.4	1													25	Steel	Steel	245	207000	0.3	A	2	4	
57	E	leftside_stif_3	N	270	0	2400			113.6	6.65	63.5	13.4	1													25	Steel	Steel	245	207000	0.3	A	2	4	
58	E	leftside_stif_4	N	270	0	1800			113.6	6.65	63.5	13.4	1													25	Steel	Steel	245	207000	0.3	A	2	4	
59	E	leftside_stif_5	N	270	0	1200			113.6	6.65	63.5	13.4	1													25	Steel	Steel	245	207000	0.3	A	2	4	
60	E	leftside_stif_6	N	270	0	600			113.6	6.65	63.5	13.4	1													25	Steel	Steel	245	207000	0.3	A	2	4	

g. Box Girder E, Trans. Damage Case I

##																																	
##	ProColl Template																																
##																																	
Filename	Length	Units																															
Trs.Dam. Case I	1800	mm																															
##																																	
##	ELEMENT DESCRIPTORS		COORDINATES:				PLATE DIMMARY LONGITUDINAL DIMENSIONS:												FRAME DIMENSIONS:					MATERIAL DEFINITIONS:								LOAD SHORTENING CURVE:			
ID	Type	Description	Mirror	angle	ycoord	zcoord	b	tp	hwx	twx	bfx	tfx	nsx	loop	hwx2	twx2	bfx2	tfx2	nsx2	hwy	twy	bfy	tfy	ramespacir	nsy	HAZ	Pmat	Smat	str0eq	E	v	Imp	LSCurve	Clone	Sname
1	LSC		N				600	8	113.6	6.65	63.5	13.4	7							227.2	13.3	127	26.8		5	50	Steel	Steel	245	207000	0.3	A	1		
2	LSC		N				600	10	113.6	6.65	63.5	13.4	6							227.2	13.3	127	26.8		5	50	Steel	Steel	245	207000	0.3	A	1		
3	LSC		N				600	8	113.6	6.65	63.5	13.4	6							227.2	13.3	127	26.8		5	50	Steel	Steel	245	207000	0.3	A	1		
4	LSC		N				600	10	113.6	6.65	63.5	13.4	6							227.2	13.3	127	26.8		5	50	Steel	Steel	245	207000	0.3	A	1		
5	E	Horz. Plate_1	N	0	0	0	600	8						0												50	Steel	Steel	245	207000	0.3	A	2	1	
6	E	Horz. Plate_2	N	0	600	0	600	8						0												50	Steel	Steel	245	207000	0.3	A	2	1	
7	E	Horz. Plate_3	N	0	1200	0	600	8						0												50	Steel	Steel	245	207000	0.3	A	2	1	
8	E	Horz. Plate_4	N	0	1800	0	600	8						0												50	Steel	Steel	245	207000	0.3	A	2	1	
9	E	Horz. Plate_5	N	0	2400	0	600	8						0												50	Steel	Steel	245	207000	0.3	A	2	1	
10	E	Horz. Plate_6	N	0	3000	0	600	8						0												50	Steel	Steel	245	207000	0.3	A	2	1	
11	E	Horz. Plate_7	N	0	3600	0	600	8						0												50	Steel	Steel	245	207000	0.3	A	2	1	
12	E	Horz. Plate_8	N	0	4200	0	600	8						0												50	Steel	Steel	245	207000	0.3	A	2	1	
13	E	Vert. Plate_R_1	N	90	4800	0	600	10						0												50	Steel	Steel	245	207000	0.3	A	2	2	
14	E	Vert. Plate_R_2	N	90	4800	600	600	10						0												50	Steel	Steel	245	207000	0.3	A	2	2	
15	E	Vert. Plate_R_3	N	90	4800	1200	600	10						0												50	Steel	Steel	245	207000	0.3	A	2	2	
16	E	Vert. Plate_R_4	N	90	4800	1800	600	10						0												50	Steel	Steel	245	207000	0.3	A	2	2	
17	E	Vert. Plate_R_5	N	90	4800	2400	600	10						0												50	Steel	Steel	245	207000	0.3	A	2	2	
18	E	Vert. Plate_R_6	N	90	4800	3000	600	10						0												50	Steel	Steel	245	207000	0.3	A	2	2	
19	E	Vert. Plate_R_7	N	90	4800	3600	600	10						0												50	Steel	Steel	245	207000	0.3	A	2	2	
20	E	Horz. Plate_Top_1	N	180	4800	4200	600	8						0												50	Steel	Steel	245	207000	0.3	A	2	3	
21	E	Horz. Plate_Top_2	N	180	4200	4200	600	8						0												50	Steel	Steel	245	207000	0.3	A	2	3	
22	E	Horz. Plate_Top_3	N	180	3600	4200	600	8						0												50	Steel	Steel	245	207000	0.3	A	2	3	
23	E	Horz. Plate_Top_4	N	180	3000	4200	568	8																		50	Steel	Steel	245	207000	0.3	A	2		
24	E	Horz. Plate_Top_5	N	180	2368	4200	568	8																		50	Steel	Steel	245	207000	0.3	A	2		
25	E	Horz. Plate_Top_6	N	180	1800	4200	600	8						0												50	Steel	Steel	245	207000	0.3	A	2	3	
26	E	Horz. Plate_Top_7	N	180	1200	4200	600	8						0												50	Steel	Steel	245	207000	0.3	A	2	3	
27	E	Horz. Plate_Top_8	N	180	600	4200	600	8						0												50	Steel	Steel	245	207000	0.3	A	2	3	
28	E	Vert. Plate_Left_1	N	270	0	4200	600	10						0												50	Steel	Steel	245	207000	0.3	A	2	4	
29	E	Vert. Plate_Left_2	N	270	0	3600	600	10						0												50	Steel	Steel	245	207000	0.3	A	2	4	
30	E	Vert. Plate_Left_3	N	270	0	3000	600	10						0												50	Steel	Steel	245	207000	0.3	A	2	4	
31	E	Vert. Plate_Left_4	N	270	0	2400	600	10						0												50	Steel	Steel	245	207000	0.3	A	2	4	
32	E	Vert. Plate_Left_5	N	270	0	1800	600	10						0												50	Steel	Steel	245	207000	0.3	A	2	4	
33	E	Vert. Plate_Left_6	N	270	0	1200	600	10						0												50	Steel	Steel	245	207000	0.3	A	2	4	
34	E	Vert. Plate_Left_7	N	270	0	600	600	10						0												50	Steel	Steel	245	207000	0.3	A	2	4	
35	E	bottom_stif_1	N	0	600	0			113.6	6.65	63.5	13.4	1													25	Steel	Steel	245	207000	0.3	A	2	1	
36	E	bottom_stif_2	N	0	1200	0			113.6	6.65	63.5	13.4	1													25	Steel	Steel	245	207000	0.3	A	2	1	
37	E	bottom_stif_3	N	0	1800	0			113.6	6.65	63.5	13.4	1													25	Steel	Steel	245	207000	0.3	A	2	1	
38	E	bottom_stif_4	N	0	2400	0			113.6	6.65	63.5	13.4	1													25	Steel	Steel	245	207000	0.3	A	2	1	
39	E	bottom_stif_5	N	0	3000	0			113.6	6.65	63.5	13.4	1													25	Steel	Steel	245	207000	0.3	A	2	1	
40	E	bottom_stif_6	N	0	3600	0			113.6	6.65	63.5	13.4	1													25	Steel	Steel	245	207000	0.3	A	2	1	
41	E	bottom_stif_7	N	0	4200	0			113.6	6.65	63.5	13.4	1													25	Steel	Steel	245	207000	0.3	A	2	1	
42	E	rightside_stif_1	N	90	4800	600			113.6	6.65	63.5	13.4	1													25	Steel	Steel	245	207000	0.3	A	2	2	
43	E	rightside_stif_2	N	90	4800	1200			113.6	6.65	63.5	13.4	1													25	Steel	Steel	245	207000	0.3	A	2	2	
44	E	rightside_stif_3	N	90	4800	1800			113.6	6.65	63.5	13.4	1													25	Steel	Steel	245	207000	0.3	A	2	2	
45	E	rightside_stif_4	N	90	4800	2400			113.6	6.65	63.5	13.4	1													25	Steel	Steel	245	207000	0.3	A	2	2	
46	E	rightside_stif_5	N	90	4800	3000			113.6	6.65	63.5	13.4	1													25	Steel	Steel	245	207000	0.3	A	2	2	
47	E	rightside_stif_6	N	90	4800	3600			113.6	6.65	63.5	13.4	1													25	Steel	Steel	245	207000	0.3	A	2	2	
48	E	top_stif_1	N	180	4200	4200			113.6	6.65	63.5	13.4	1													25	Steel	Steel	245	207000	0.3	A	2	3	
49	E	top_stif_2	N	180	3600	4200			113.6	6.65	63.5	13.4	1													25	Steel	Steel	245	207000	0.3	A	2	3	
50	E	top_stif_3	N	180	3000	4200			113.6	6.65	63.5	13.4	1													25	Steel	Steel	245	207000	0.3	A	2	3	
51	E	top_stif_5	N	180	1800	4200			113.6	6.65	63.5	13.4	1													25	Steel	Steel	245	207000	0.3	A	2	3	
52	E	top_stif_6	N	180	1200	4200			113.6	6.65	63.5	13.4	1													25	Steel	Steel	245	207000	0.3	A	2	3	
53	E	top_stif_7	N	180	600	4200			113.6	6.65	63.5	13.4	1													25	Steel	Steel	245	207000	0.3	A	2	3	
54	E	leftside_stif_1	N	270	0	3600			113.6	6.65	63.5	13.4	1													25	Steel	Steel	245	207000	0.3	A	2	4	
55	E	leftside_stif_2	N	270	0	3000			113.6	6.65	63.5	13.4	1													25	Steel	Steel	245	207000	0.3	A	2	4	
56	E	leftside_stif_3	N	270	0	2400			113.6	6.65	63.5	13.4	1													25	Steel	Steel	245	207000	0.3	A	2	4	
57	E	leftside_stif_4	N	270	0	1800			113.6	6.65	63.5	13.4	1													25	Steel	Steel	245	207000	0.3	A	2	4	
58	E	leftside_stif_5	N	270	0	1200			113.6	6.65	63.5	13.4	1													25	Steel	Steel	245	207000	0.3	A	2	4	
59	E	leftside_stif_6	N	270	0	600			113.6	6.65	63.5	13.4	1													25	Steel	Steel	245	207000	0.3	A	2	4	

h. Box Girder E, Trans. Damage Case II

##																																	
##	ProColl Template																																
##																																	
Filename	Length	Units																															
Trs. Dam. Case II	1800	mm																															
##																																	
##	ELEMENT DESCRIPTORS		COORDINATES:				PLATE DIMMARY LONGITUDINAL DIMENSIONS:												FRAME DIMENSIONS:						MATERIAL DEFINITIONS:							LOAD SHORTENING CURVE:			
ID	Type	Description	Mirror	angle	ycoord	zcoord	b	tp	hwx	twx	bfx	tfx	nsx	loop	hwx2	twx2	bfx2	tfx2	nsx2	hwy	twy	bfy	tfy	'amespacir	nsy	HAZ	Pmat	Smat	str0eq	E	v	Imp	LSCurve	Clone	Sname
1	LSC		N				600	8	113.6	6.65	63.5	13.4	7							227.2	13.3	127	26.8	1800	5	50	Steel	Steel	245	207000	0.3	A	1		
2	LSC		N				600	10	113.6	6.65	63.5	13.4	6							227.2	13.3	127	26.8	1800	5	50	Steel	Steel	245	207000	0.3	A	1		
3	LSC		N				600	8	113.6	6.65	63.5	13.4	2							227.2	13.3	127	26.8	1800	5	50	Steel	Steel	245	207000	0.3	A	1		
4	LSC		N				600	10	113.6	6.65	63.5	13.4	6							227.2	13.3	127	26.8	1800	5	50	Steel	Steel	245	207000	0.3	A	1		
5	E	Horz. Plate_1	N	0	0	0	600	8						0												50	Steel	Steel	245	207000	0.3	A	2	1	
6	E	Horz. Plate_2	N	0	600	0	600	8						0												50	Steel	Steel	245	207000	0.3	A	2	1	
7	E	Horz. Plate_3	N	0	1200	0	600	8						0												50	Steel	Steel	245	207000	0.3	A	2	1	
8	E	Horz. Plate_4	N	0	1800	0	600	8						0												50	Steel	Steel	245	207000	0.3	A	2	1	
9	E	Horz. Plate_5	N	0	2400	0	600	8						0												50	Steel	Steel	245	207000	0.3	A	2	1	
10	E	Horz. Plate_6	N	0	3000	0	600	8						0												50	Steel	Steel	245	207000	0.3	A	2	1	
11	E	Horz. Plate_7	N	0	3600	0	600	8						0												50	Steel	Steel	245	207000	0.3	A	2	1	
12	E	Horz. Plate_8	N	0	4200	0	600	8						0												50	Steel	Steel	245	207000	0.3	A	2	1	
13	E	Vert. Plate_R_1	N	90	4800	0	600	10						0												50	Steel	Steel	245	207000	0.3	A	2	2	
14	E	Vert. Plate_R_2	N	90	4800	600	600	10						0												50	Steel	Steel	245	207000	0.3	A	2	2	
15	E	Vert. Plate_R_3	N	90	4800	1200	600	10						0												50	Steel	Steel	245	207000	0.3	A	2	2	
16	E	Vert. Plate_R_4	N	90	4800	1800	600	10						0												50	Steel	Steel	245	207000	0.3	A	2	2	
17	E	Vert. Plate_R_5	N	90	4800	2400	600	10						0												50	Steel	Steel	245	207000	0.3	A	2	2	
18	E	Vert. Plate_R_6	N	90	4800	3000	600	10						0												50	Steel	Steel	245	207000	0.3	A	2	2	
19	E	Vert. Plate_R_7	N	90	4800	3600	600	10						0												50	Steel	Steel	245	207000	0.3	A	2	2	
20	E	Horz. Plate_Top_1	N	180	4800	4200	600	8						0												50	Steel	Steel	245	207000	0.3	A	2	3	
21	E	Horz. Plate_Top_2	N	180	4200	4200	600	8						0												50	Steel	Steel	245	207000	0.3	A	2	3	
22	E	Horz. Plate_Top_3	N	180	3600	4200	480	8																		50	Steel	Steel	245	207000	0.3	A	2		
23	E	Horz. Plate_Top_6	N	180	1680	4200	480	8																		50	Steel	Steel	245	207000	0.3	A	2		
24	E	Horz. Plate_Top_7	N	180	1200	4200	600	8						0												50	Steel	Steel	245	207000	0.3	A	2	3	
25	E	Horz. Plate_Top_8	N	180	600	4200	600	8						0												50	Steel	Steel	245	207000	0.3	A	2	3	
26	E	Vert. Plate_Left_1	N	270	0	4200	600	10						0												50	Steel	Steel	245	207000	0.3	A	2	4	
27	E	Vert. Plate_Left_2	N	270	0	3600	600	10						0												50	Steel	Steel	245	207000	0.3	A	2	4	
28	E	Vert. Plate_Left_3	N	270	0	3000	600	10						0												50	Steel	Steel	245	207000	0.3	A	2	4	
29	E	Vert. Plate_Left_4	N	270	0	2400	600	10						0												50	Steel	Steel	245	207000	0.3	A	2	4	
30	E	Vert. Plate_Left_5	N	270	0	1800	600	10						0												50	Steel	Steel	245	207000	0.3	A	2	4	
31	E	Vert. Plate_Left_6	N	270	0	1200	600	10						0												50	Steel	Steel	245	207000	0.3	A	2	4	
32	E	Vert. Plate_Left_7	N	270	0	600	600	10						0												50	Steel	Steel	245	207000	0.3	A	2	4	
33	E	bottom_stif_1	N	0	600	0			113.6	6.65	63.5	13.4	1													25	Steel	Steel	245	207000	0.3	A	2	1	
34	E	bottom_stif_2	N	0	1200	0			113.6	6.65	63.5	13.4	1													25	Steel	Steel	245	207000	0.3	A	2	1	
35	E	bottom_stif_3	N	0	1800	0			113.6	6.65	63.5	13.4	1													25	Steel	Steel	245	207000	0.3	A	2	1	
36	E	bottom_stif_4	N	0	2400	0			113.6	6.65	63.5	13.4	1													25	Steel	Steel	245	207000	0.3	A	2	1	
37	E	bottom_stif_5	N	0	3000	0			113.6	6.65	63.5	13.4	1													25	Steel	Steel	245	207000	0.3	A	2	1	
38	E	bottom_stif_6	N	0	3600	0			113.6	6.65	63.5	13.4	1													25	Steel	Steel	245	207000	0.3	A	2	1	
39	E	bottom_stif_7	N	0	4200	0			113.6	6.65	63.5	13.4	1													25	Steel	Steel	245	207000	0.3	A	2	1	
40	E	rightside_stif_1	N	90	4800	600			113.6	6.65	63.5	13.4	1													25	Steel	Steel	245	207000	0.3	A	2	2	
41	E	rightside_stif_2	N	90	4800	1200			113.6	6.65	63.5	13.4	1													25	Steel	Steel	245	207000	0.3	A	2	2	
42	E	rightside_stif_2	N	90	4800	1800			113.6	6.65	63.5	13.4	1													25	Steel	Steel	245	207000	0.3	A	2	2	
43	E	rightside_stif_2	N	90	4800	2400			113.6	6.65	63.5	13.4	1													25	Steel	Steel	245	207000	0.3	A	2	2	
44	E	rightside_stif_2	N	90	4800	3000			113.6	6.65	63.5	13.4	1													25	Steel	Steel	245	207000	0.3	A	2	2	
45	E	rightside_stif_6	N	90	4800	3600			113.6	6.65	63.5	13.4	1													25	Steel	Steel	245	207000	0.3	A	2	2	
46	E	top_stif_1	N	180	4200	4200			113.6	6.65	63.5	13.4	1													25	Steel	Steel	245	207000	0.3	A	2	3	
47	E	top_stif_2	N	180	3600	4200			113.6	6.65	63.5	13.4	1													25	Steel	Steel	245	207000	0.3	A	2	3	
48	E	top_stif_6	N	180	1200	4200			113.6	6.65	63.5	13.4	1													25	Steel	Steel	245	207000	0.3	A	2	3	
49	E	top_stif_7	N	180	600	4200			113.6	6.65	63.5	13.4	1													25	Steel	Steel	245	207000	0.3	A	2	3	
50	E	leftside_stif_1	N	270	0	3600			113.6	6.65	63.5	13.4	1													25	Steel	Steel	245	207000	0.3	A	2	4	
51	E	leftside_stif_2	N	270	0	3000			113.6	6.65	63.5	13.4	1													25	Steel	Steel	245	207000	0.3	A	2	4	
52	E	leftside_stif_3	N	270	0	2400			113.6	6.65	63.5	13.4	1													25	Steel	Steel	245	207000	0.3	A	2	4	
53	E	leftside_stif_4	N	270	0	1800			113.6	6.65	63.5	13.4	1													25	Steel	Steel	245	207000	0.3	A	2	4	
54	E	leftside_stif_5	N	270	0	1200			113.6	6.65	63.5	13.4	1													25	Steel	Steel	245	207000	0.3	A	2	4	
55	E	leftside_stif_6	N	270	0	600			113.6	6.65	63.5	13.4	1													25	Steel	Steel	245	207000	0.3	A	2	4	

i. Box Girder E, Trans. Damage Case III

##																																	
##	ProColl Template																																
##																																	
Filename	Length	Units																															
Trs. Dam. Case III	1800	mm																															
##																																	
##	ELEMENT DESCRIPTORS		COORDINATES:				PLATE DIMMARY LONGITUDINAL DIMENSIONS:												FRAME DIMENSIONS:					MATERIAL DEFINITIONS:							LOAD SHORTENING CURVE:			
ID	Type	Description	Mirror	angle	ycoord	zcoord	b	tp	hwx	twx	bfx	tfx	nsx	loop	hwx2	twx2	bfx2	tfx2	nsx2	hwy	twy	bfy	tfy	amespacir	nsy	HAZ	Pmat	Smat	str0eq	E	v	Imp	LSCurve	Clone	Sname
1	LSC		N				600	8	113.6	6.65	63.5	13.4	7							227.2	13.3	127	26.8		5	50	Steel	Steel	245	207000	0.3	A	1		
2	LSC		N				600	10	113.6	6.65	63.5	13.4	6							227.2	13.3	127	26.8		5	50	Steel	Steel	245	207000	0.3	A	1		
3	LSC		N				600	8	113.6	6.65	63.5	13.4	1							227.2	13.3	127	26.8		5	50	Steel	Steel	245	207000	0.3	A	1		
4	LSC		N				600	10	113.6	6.65	63.5	13.4	6							227.2	13.3	127	26.8		5	50	Steel	Steel	245	207000	0.3	A	1		
5	E	Horz. Plate_1	N	0	0	0	600	8						0												50	Steel	Steel	245	207000	0.3	A	2	1	
6	E	Horz. Plate_2	N	0	600	0	600	8						0												50	Steel	Steel	245	207000	0.3	A	2	1	
7	E	Horz. Plate_3	N	0	1200	0	600	8						0												50	Steel	Steel	245	207000	0.3	A	2	1	
8	E	Horz. Plate_4	N	0	1800	0	600	8						0												50	Steel	Steel	245	207000	0.3	A	2	1	
9	E	Horz. Plate_5	N	0	2400	0	600	8						0												50	Steel	Steel	245	207000	0.3	A	2	1	
10	E	Horz. Plate_6	N	0	3000	0	600	8						0												50	Steel	Steel	245	207000	0.3	A	2	1	
11	E	Horz. Plate_7	N	0	3600	0	600	8						0												50	Steel	Steel	245	207000	0.3	A	2	1	
12	E	Horz. Plate_8	N	0	4200	0	600	8						0												50	Steel	Steel	245	207000	0.3	A	2	1	
13	E	Vert. Plate_R_1	N	90	4800	0	600	10						0												50	Steel	Steel	245	207000	0.3	A	2	2	
14	E	Vert. Plate_R_2	N	90	4800	600	600	10						0												50	Steel	Steel	245	207000	0.3	A	2	2	
15	E	Vert. Plate_R_3	N	90	4800	1200	600	10						0												50	Steel	Steel	245	207000	0.3	A	2	2	
16	E	Vert. Plate_R_4	N	90	4800	1800	600	10						0												50	Steel	Steel	245	207000	0.3	A	2	2	
17	E	Vert. Plate_R_5	N	90	4800	2400	600	10						0												50	Steel	Steel	245	207000	0.3	A	2	2	
18	E	Vert. Plate_R_6	N	90	4800	3000	600	10						0												50	Steel	Steel	245	207000	0.3	A	2	2	
19	E	Vert. Plate_R_7	N	90	4800	3600	600	10						0												50	Steel	Steel	245	207000	0.3	A	2	2	
20	E	Horz. Plate_Top_1	N	180	4800	4200	600	8						0												50	Steel	Steel	245	207000	0.3	A	2	3	
21	E	Horz. Plate_Top_2	N	180	4200	4200	360	8																		50	Steel	Steel	245	207000	0.3	A	2		
24	E	Horz. Plate_Top_7	N	180	960	4200	360	8																		50	Steel	Steel	245	207000	0.3	A	2		
25	E	Horz. Plate_Top_8	N	180	600	4200	600	8						0												50	Steel	Steel	245	207000	0.3	A	2	3	
26	E	Vert. Plate_Left_1	N	270	0	4200	600	10						0												50	Steel	Steel	245	207000	0.3	A	2	4	
27	E	Vert. Plate_Left_2	N	270	0	3600	600	10						0												50	Steel	Steel	245	207000	0.3	A	2	4	
28	E	Vert. Plate_Left_3	N	270	0	3000	600	10						0												50	Steel	Steel	245	207000	0.3	A	2	4	
29	E	Vert. Plate_Left_4	N	270	0	2400	600	10						0												50	Steel	Steel	245	207000	0.3	A	2	4	
30	E	Vert. Plate_Left_5	N	270	0	1800	600	10						0												50	Steel	Steel	245	207000	0.3	A	2	4	
31	E	Vert. Plate_Left_6	N	270	0	1200	600	10						0												50	Steel	Steel	245	207000	0.3	A	2	4	
32	E	Vert. Plate_Left_7	N	270	0	600	600	10						0												50	Steel	Steel	245	207000	0.3	A	2	4	
33	E	bottom_stif_1	N	0	600	0			113.6	6.65	63.5	13.4	1													25	Steel	Steel	245	207000	0.3	A	2	1	
34	E	bottom_stif_2	N	0	1200	0			113.6	6.65	63.5	13.4	1													25	Steel	Steel	245	207000	0.3	A	2	1	
35	E	bottom_stif_3	N	0	1800	0			113.6	6.65	63.5	13.4	1													25	Steel	Steel	245	207000	0.3	A	2	1	
36	E	bottom_stif_4	N	0	2400	0			113.6	6.65	63.5	13.4	1													25	Steel	Steel	245	207000	0.3	A	2	1	
37	E	bottom_stif_5	N	0	3000	0			113.6	6.65	63.5	13.4	1													25	Steel	Steel	245	207000	0.3	A	2	1	
38	E	bottom_stif_6	N	0	3600	0			113.6	6.65	63.5	13.4	1													25	Steel	Steel	245	207000	0.3	A	2	1	
39	E	bottom_stif_7	N	0	4200	0			113.6	6.65	63.5	13.4	1													25	Steel	Steel	245	207000	0.3	A	2	1	
40	E	rightside_stif_1	N	90	4800	600			113.6	6.65	63.5	13.4	1													25	Steel	Steel	245	207000	0.3	A	2	2	
41	E	rightside_stif_2	N	90	4800	1200			113.6	6.65	63.5	13.4	1													25	Steel	Steel	245	207000	0.3	A	2	2	
41	E	rightside_stif_2	N	90	4800	1800			113.6	6.65	63.5	13.4	1													25	Steel	Steel	245	207000	0.3	A	2	2	
41	E	rightside_stif_2	N	90	4800	2400			113.6	6.65	63.5	13.4	1													25	Steel	Steel	245	207000	0.3	A	2	2	
41	E	rightside_stif_2	N	90	4800	3000			113.6	6.65	63.5	13.4	1													25	Steel	Steel	245	207000	0.3	A	2	2	
42	E	rightside_stif_6	N	90	4800	3600			113.6	6.65	63.5	13.4	1													25	Steel	Steel	245	207000	0.3	A	2	2	
43	E	top_stif_1	N	180	4200	4200			113.6	6.65	63.5	13.4	1													25	Steel	Steel	245	207000	0.3	A	2	3	
49	E	top_stif_7	N	180	600	4200			113.6	6.65	63.5	13.4	1													25	Steel	Steel	245	207000	0.3	A	2	3	
50	E	leftside_stif_1	N	270	0	3600			113.6	6.65	63.5	13.4	1													25	Steel	Steel	245	207000	0.3	A	2	4	
51	E	leftside_stif_2	N	270	0	3000			113.6	6.65	63.5	13.4	1													25	Steel	Steel	245	207000	0.3	A	2	4	
52	E	leftside_stif_3	N	270	0	2400			113.6	6.65	63.5	13.4	1													25	Steel	Steel	245	207000	0.3	A	2	4	
53	E	leftside_stif_4	N	270	0	1800			113.6	6.65	63.5	13.4	1													25	Steel	Steel	245	207000	0.3	A	2	4	
54	E	leftside_stif_5	N	270	0	1200			113.6	6.65	63.5	13.4	1													25	Steel	Steel	245	207000	0.3	A	2	4	
55	E	leftside_stif_6	N	270	0	600			113.6	6.65	63.5	13.4	1													25	Steel	Steel	245	207000	0.3	A	2	4	

j. Box Girder E, Long. Damage Case I & II

##
ProColl Template
##

Filename	Length	Units
Long. Dam. Case I	1800	mm

##

##	ELEMENT DESCRIPTORS		COORDINATES:				PLATE DIM	PRIMARY LONGITUDINAL DIMENSIONS:							FRAME DIMENSIONS:							MATERIAL DEFINITIONS:								LOAD SHORTENING CURVE:		
ID	Type	Description	Mirror	angle	ycoord	zcoord	b	tp	hwx	twx	bfx	tfx	nsx	loop	hwx2	twx2	bfx2	tfx2	nsx2	hwy	twy	bfy	tfy	ramespacir	nsy	HAZ	Pmat	Smat	str0eq	E	v	Imp	LSCurve	Clone	Sname
1	LSC		N				600	8	113.6	6.65	63.5	13.4	7							227.2	13.3	127	26.8	1800	5	50	Steel	Steel	245	207000	0.3	A	1		
2	LSC		N				600	10	113.6	6.65	63.5	13.4	6							227.2	13.3	127	26.8	1800	5	50	Steel	Steel	245	207000	0.3	A	1		
3	LSC		N				600	8	113.6	6.65	63.5	13.4	2							227.2	13.3	127	26.8	1800	5	50	Steel	Steel	245	207000	0.3	A	1		
4	LSC		N				600	10	113.6	6.65	63.5	13.4	6							227.2	13.3	127	26.8	1800	5	50	Steel	Steel	245	207000	0.3	A	1		
5	E	Horz. Plate_1	N	0	0	0	600	8						0												50	Steel	Steel	245	207000	0.3	A	2	1	
6	E	Horz. Plate_2	N	0	600	0	600	8						0												50	Steel	Steel	245	207000	0.3	A	2	1	
7	E	Horz. Plate_3	N	0	1200	0	600	8						0												50	Steel	Steel	245	207000	0.3	A	2	1	
8	E	Horz. Plate_4	N	0	1800	0	600	8						0												50	Steel	Steel	245	207000	0.3	A	2	1	
9	E	Horz. Plate_5	N	0	2400	0	600	8						0												50	Steel	Steel	245	207000	0.3	A	2	1	
10	E	Horz. Plate_6	N	0	3000	0	600	8						0												50	Steel	Steel	245	207000	0.3	A	2	1	
11	E	Horz. Plate_7	N	0	3600	0	600	8						0												50	Steel	Steel	245	207000	0.3	A	2	1	
12	E	Horz. Plate_8	N	0	4200	0	600	8						0												50	Steel	Steel	245	207000	0.3	A	2	1	
13	E	Vert. Plate_R_1	N	90	4800	0	600	10						0												50	Steel	Steel	245	207000	0.3	A	2	2	
14	E	Vert. Plate_R_2	N	90	4800	600	600	10						0												50	Steel	Steel	245	207000	0.3	A	2	2	
15	E	Vert. Plate_R_3	N	90	4800	1200	600	10						0												50	Steel	Steel	245	207000	0.3	A	2	2	
16	E	Vert. Plate_R_4	N	90	4800	1800	600	10						0												50	Steel	Steel	245	207000	0.3	A	2	2	
17	E	Vert. Plate_R_5	N	90	4800	2400	600	10						0												50	Steel	Steel	245	207000	0.3	A	2	2	
18	E	Vert. Plate_R_6	N	90	4800	3000	600	10						0												50	Steel	Steel	245	207000	0.3	A	2	2	
19	E	Vert. Plate_R_7	N	90	4800	3600	600	10						0												50	Steel	Steel	245	207000	0.3	A	2	2	
20	E	Horz. Plate_Top_1	N	180	4800	4200	600	8						0												50	Steel	Steel	245	207000	0.3	A	2	3	
21	E	Horz. Plate_Top_2	N	180	4200	4200	600	8						0												50	Steel	Steel	245	207000	0.3	A	2	3	
22	E	Horz. Plate_Top_3	N	180	3600	4200	480	8																		50	Steel	Steel	245	207000	0.3	A	2		
23	E	Horz. Plate_Top_6	N	180	1680	4200	480	8																		50	Steel	Steel	245	207000	0.3	A	2		
24	E	Horz. Plate_Top_7	N	180	1200	4200	600	8						0												50	Steel	Steel	245	207000	0.3	A	2	3	
25	E	Horz. Plate_Top_8	N	180	600	4200	600	8						0												50	Steel	Steel	245	207000	0.3	A	2	3	
26	E	Vert. Plate_Left_1	N	270	0	4200	600	10						0												50	Steel	Steel	245	207000	0.3	A	2	4	
27	E	Vert. Plate_Left_2	N	270	0	3600	600	10						0												50	Steel	Steel	245	207000	0.3	A	2	4	
28	E	Vert. Plate_Left_3	N	270	0	3000	600	10						0												50	Steel	Steel	245	207000	0.3	A	2	4	
29	E	Vert. Plate_Left_4	N	270	0	2400	600	10						0												50	Steel	Steel	245	207000	0.3	A	2	4	
30	E	Vert. Plate_Left_5	N	270	0	1800	600	10						0												50	Steel	Steel	245	207000	0.3	A	2	4	
31	E	Vert. Plate_Left_6	N	270	0	1200	600	10						0												50	Steel	Steel	245	207000	0.3	A	2	4	
32	E	Vert. Plate_Left_7	N	270	0	600	600	10						0												50	Steel	Steel	245	207000	0.3	A	2	4	
33	E	bottom_stif_1	N	0	600	0			113.6	6.65	63.5	13.4	1													25	Steel	Steel	245	207000	0.3	A	2	1	
34	E	bottom_stif_2	N	0	1200	0			113.6	6.65	63.5	13.4	1													25	Steel	Steel	245	207000	0.3	A	2	1	
35	E	bottom_stif_3	N	0	1800	0			113.6	6.65	63.5	13.4	1													25	Steel	Steel	245	207000	0.3	A	2	1	
36	E	bottom_stif_4	N	0	2400	0			113.6	6.65	63.5	13.4	1													25	Steel	Steel	245	207000	0.3	A	2	1	
37	E	bottom_stif_5	N	0	3000	0			113.6	6.65	63.5	13.4	1													25	Steel	Steel	245	207000	0.3	A	2	1	
38	E	bottom_stif_6	N	0	3600	0			113.6	6.65	63.5	13.4	1													25	Steel	Steel	245	207000	0.3	A	2	1	
39	E	bottom_stif_7	N	0	4200	0			113.6	6.65	63.5	13.4	1													25	Steel	Steel	245	207000	0.3	A	2	1	
40	E	rightside_stif_1	N	90	4800	600			113.6	6.65	63.5	13.4	1													25	Steel	Steel	245	207000	0.3	A	2	2	
41	E	rightside_stif_2	N	90	4800	1200			113.6	6.65	63.5	13.4	1													25	Steel	Steel	245	207000	0.3	A	2	2	
42	E	rightside_stif_2	N	90	4800	1800			113.6	6.65	63.5	13.4	1													25	Steel	Steel	245	207000	0.3	A	2	2	
43	E	rightside_stif_2	N	90	4800	2400			113.6	6.65	63.5	13.4	1													25	Steel	Steel	245	207000	0.3	A	2	2	
44	E	rightside_stif_2	N	90	4800	3000			113.6	6.65	63.5	13.4	1													25	Steel	Steel	245	207000	0.3	A	2	2	
45	E	rightside_stif_6	N	90	4800	3600			113.6	6.65	63.5	13.4	1													25	Steel	Steel	245	207000	0.3	A	2	2	
46	E	top_stif_1	N	180	4200	4200			113.6	6.65	63.5	13.4	1													25	Steel	Steel	245	207000	0.3	A	2	3	
47	E	top_stif_2	N	180	3600	4200			113.6	6.65	63.5	13.4	1													25	Steel	Steel	245	207000	0.3	A	2	3	
48	E	top_stif_6	N	180	1200	4200			113.6	6.65	63.5	13.4	1													25	Steel	Steel	245	207000	0.3	A	2	3	
49	E	top_stif_7	N	180	600	4200			113.6	6.65	63.5	13.4	1													25	Steel	Steel	245	207000	0.3	A	2	3	
50	E	leftside_stif_1	N	270	0	3600			113.6	6.65	63.5	13.4	1													25	Steel	Steel	245	207000	0.3	A	2	4	
51	E	leftside_stif_2	N	270	0	3000			113.6	6.65	63.5	13.4	1													25	Steel	Steel	245	207000	0.3	A	2	4	
52	E	leftside_stif_3	N	270	0	2400			113.6	6.65	63.5	13.4	1													25	Steel	Steel	245	207000	0.3	A	2	4	
53	E	leftside_stif_4	N	270	0	1800			113.6	6.65	63.5	13.4	1													25	Steel	Steel	245	207000	0.3	A	2	4	
54	E	leftside_stif_5	N	270	0	1200			113.6	6.65	63.5	13.4	1													25	Steel	Steel	245	207000	0.3	A	2	4	
55	E	leftside_stif_6	N	270	0	600			113.6	6.65	63.5	13.4	1													25	Steel	Steel	245	207000	0.3	A	2	4	

Appendix C

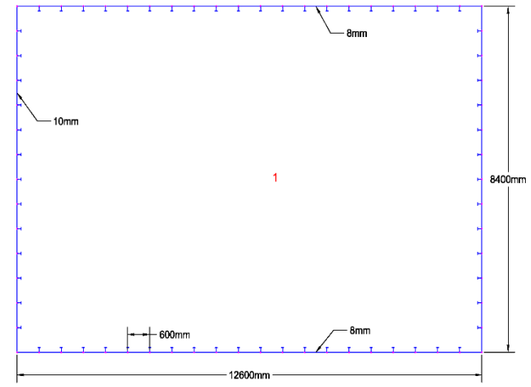

Cross section of Box Girder A

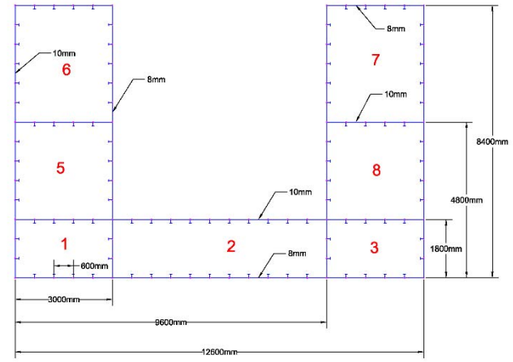

Cross section of Box Girder D

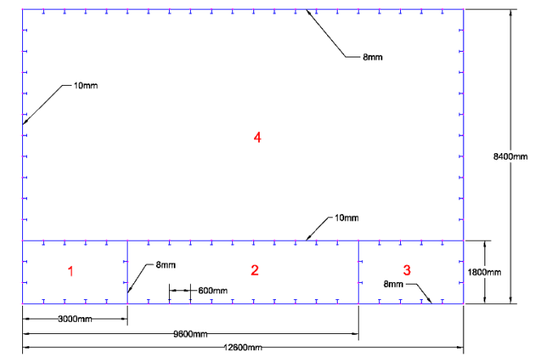

Cross Section of Box Girder B

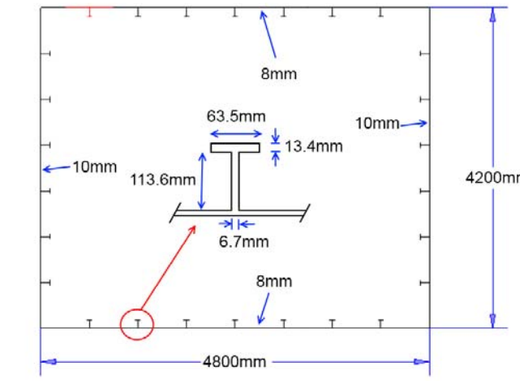

Cross Section of Box Girder E

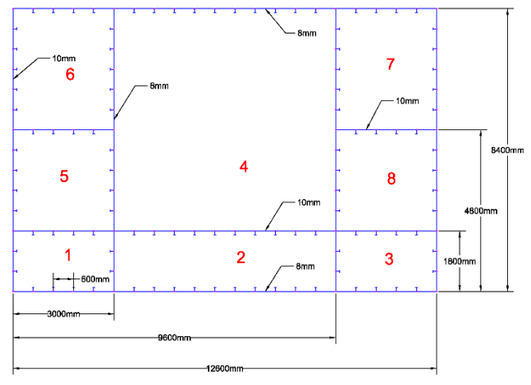

Cross Section of Box Girder C

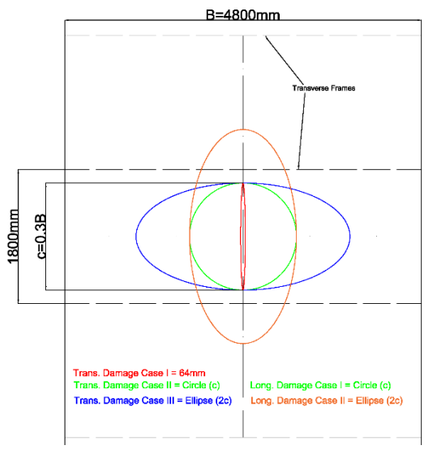

Trans. & Long. Damage Cases of Box Girder E